The 13th AUN/SEED-Net Regional Conference on Chemical Engineering 2020 (RCChE-2020)

Jointly held with

The 5th International Symposium on Conservation and Management of Tropical Lakes

PROCEEDINGS

INSIGHTS AND CHALLENGES TOWARD ACHIEVING SDGS

Institute of Technology of Cambodia, Phnom Penh, Cambodia
February 04-05, 2021

Contents

The 13th AUN/SEED-Net Regional Conference on Chemical Engineering 2020 (RCChE-2020)
Jointly held with
The 5th International Symposium on Conservation and Management of Tropical Lakes
"Insights and Challenges toward Achieving SDGs"

Rare Earth Elements and Yittrium (REYs) Precipitation From Solid Waste Coal Fly Ash Using Oxalic Acid: Study on Response Surface Methodology

Aulia Nur Rahmawati[1], Hotden Manurung[1,2*], I Made Bendiyasa[1,2], Himawan Tri Bayu Murti Petrus[1,2,*]

[1]*Departemen Teknik Kimia (Advanced Materials and* Sustainable Mineral Processing Research Group*), Fakultas Teknik, Universitas Gadjah Mada. Jalan Grafika No. 2 Daerah Istimewa Yogyakarta* 55281, Indonesia
[2]Unconventional Geo-resources Research Center, Faculty of Engineering. Universitas Gadjah Mada, Jl. Grafika No. 2, Yogyakarta, Indonesia
*bayupetrus@ugm.ac.id

Abstract

Rare earth elements and Yttrium called as REY become an important issue nowadays. REY is listed as a essential material in many industries such as catalyst, batteries, metal alloy, ceramics, electronic devices, magnet, glass and military defence system. In last decade, the supply and demand of REY is in disequilibrium due to the increasing demand annually. Currently, China is the largest producer of REY in the world with control over 95% from total world's production. Regarding to the Chinese goverment regulation about export restriction, including REY have created constrains in REY supply in many countries including Indonesia. Due to this condition, many researchers from various countries have been looking for the alternative source of REE such as red mud, zircon sand, spent catalyst, spent battries, coal and coal fly ash. Coal fly ash is listed as one of promising alternative sources of REY. In this presents study, coal fly ash as a raw material. REY precipitation is the last step for REY extraction from coal fly ash after conducting many steps such as physical separation (enrichment), alkaline leaching and acid leaching. In order to optimize the REY precipitation, the varible study were as temperature, pH levels and volume-to-volume ratio. Currently, several nano particle have been succesfully created after multilevel precipitation but still waiting for analysis using EDX and ICP-MS to indentify the REY concentration on the nano particle.

Keywords: *acid leaching, coal fly ash, precipitation, rare earth elements*

I. Introduction

In Indonesia, coal is still one of the main energy source to supply the ever-increasing demand for electricity. Based on data from the Ministry of Energy and Mineral Resources, almost 50% of the Steam Power Plant (PLTU) in Indonesia uses coal as its main fuel. This has resulted in the amount of coal demand continue to increase every year until it reached almost 50 million tons in 2016. In addition to its use as fuel, coal also produces solid waste in the form of fly ash. The production of fly ash continues to rise every year due to vast consumption of coal as a raw material in the Steam Power Plant (PLTU) industry.

According to Seredin and Finkelman (2008), coal combustion products (such as fly ash) are one of the sources of Rare earth elements and Yttrium (REY). REY is becoming an important issue and listed as an essential material in many industries such as catalyst, batteries, metal alloy, ceramics, electronic devices, magnet, glass and military defense system. Rare earth elements and Yttrium (REY) is an element whose demand continues to increase due to its use in various involvement in industrial sectors. REY contained in fly ash have economic value besides being

used in the construction sector. However, currently there are not many industrial-scale technologies that can take advantage of REY in flying ash. Therefore, It is necessary to do more in-depth research on the extraction of REY from fly ash waste to separate REY from fly ash waste using precipitation method.

This study aims to obtain optimal conditions in the separation of REY so that the highest levels of REY can be obtained from fly ash waste. This is the background of this research, so that in addition to being used as a source of REY collection, it is also a step in reducing environmental pollution.

II. Materials and Methods

2.1. Sampling sites

Raw material for fly ash was obtained from PT. Pembangkit Listrik Tanjung Awar-Awar Tuban Indonesia Corporation. This raw material is a type of sub-bituminous coal originating from Kalimantan.

2.2. Experimental set-up

Coal fly ash originating from the PLTU Tanjung Awar-Awar Tuban were pulverized to a size of 400 mesh and analyzed using ICP-MS and XRD. Furthermore, the resulting components of this process become non-magnetic components. This component is obtained through separation process using a wet magnetic separation device with a strong current of 2A. Magnetic wet separation aims to separate magnetic and non-magnetic fly ash using tools from the Mineral and Coal Technology Research and Development Center, Bandung. Next step is digest process the non-magnetic fly ash using 8 M concentration of NaOH, temperature 90 ºC. for 120 minutes.

The mixture was then filtered and washed using distilled water as much as 60 times the weight of the dry sample. Furthermore, the washing results were filtered and dried in the oven for 4 hours. The resulting fly ash was then leached with 3M concentration of HCl with a solid / liquid (S / L) ratio of 1:10, temperature 90 º C for 4 hours. The leaching results were then filtered to separate the leaching solution from the filtrate. The next step is the addition of CaCO3 until the pH of the mixture reaches 3.5 ± 0.2 with 2 hours stirring so that the mixture is stable, then filtered as a pH 3.5 leaching solution and the filtrate is dried. The pH 3.5 leaching solution is added with Ca (OH) 2 until the pH of the mixture reaches 5 ± 0.2 with 2 hours stirring so that the mixture is stable, then filtered as a pH 5 leaching solution and the filtrate was dried and then analyzed with EDX. The final stage is the precipitation of rare earth metals from the leaching solution pH 5 using oxalic acid (H2C2O4) with several variations, namely process temperature, concentration of oxalic acid and the ratio of the volume of the leaching solution to oxalic acid. REY sediment was then dried at 100 ºC for 3 hours and calcination at 1000 ºC for 4 hours.

2.3. Analytical methods

Fly ash from coal combustion solid waste, was analyzed using ICP-MS. The resulting solids were then analyzed by EDX to determine the percentage of REY that had been precipitated. The results of precipitation were then analyzed using the Response Surface Method (RSM). RSM functions is to develop, improve, and optimize the process of determining the optimum formulation for REY precipitation [3].

III. Results and Discussion

3.1. Fly Ash Raw Material Elements

Fly ash, which is the raw material for obtaining REY, was sieved first to smooth the granules until it passes 400 mesh. The Resulted Granules was then analyzed with ICP-MS. The results of the analysis of REY content with ICP can be seen in **Table 1**.

Tabel 1. Elemental compositions of industrial coal fly ash. (Concentrasions of major oxide given in %, REY in ppm).

Element	Tuban
SiO_2	50.9
Al_2O_3	28.7
Fe_2O_3	9.0
CaO	3.3
MgO	2.2
Na_2O	0.8
K_2O	0.9
TiO_2	1.0
La	42.3
Ce	84.9
Pr	9.7
Nd	37.4
Sm	7.7
Eu	1.7
Gd	7.7
Tb	1.3
Dy	7.8
Ho	1.8
Er	5.1
Tm	0.8

Yb	5.0
Lu	0.8
Y	46.4

Source: Rosita et. all [2]

Based on the results of the characterization, a Coutlock [4] calculation can be performed to determine the feasibility of REY extraction from coal fly ash at PLTU Paiton Tanjung Awar-Awar. The REY concentration value is shown in Equation 1.

$$Coutlook = \frac{((Nd+Eu+Tb+Dy+Er+Y)/\Sigma REY)}{((Ce+Hp+Tm+Yb+Lu)/\Sigma REY)} \quad (P1)$$

$$= \frac{((37.4 + 1.7 + 1.3 + 7.8 + 5.1 + 46.4)/\Sigma REY)}{((84.9 + 0 + 0.8 + 5.0 + 0.8)/\Sigma REY)}$$

$$= 1.091(> 0.7)$$

From the result of Equation 1, the Coutlook value is 1,091 (> 0.7) so it can be concluded that the coal fly ash from PLTU Tanjung Awar-Awar Tuban is suitable for extraction as a source of REY.

3.2. Hasil Pemisahan Wet Magnetik

Furthermore, fly ash was separated by a wet magnetic process, to obtain non-magnetic (NM) fly ash, with the results in accordance with Figure 1.

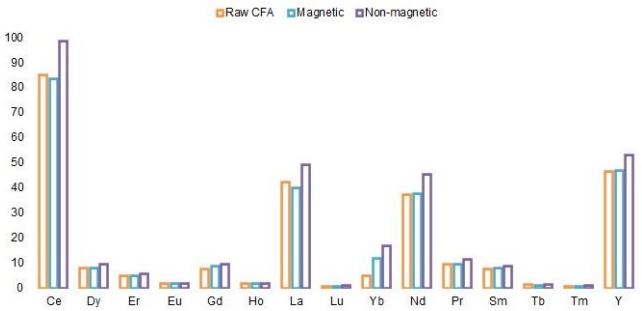

Figure 1. REY concentrations in raw materials, magnetic phase and non-magnetic phase.

Based on Figure 4.2, it can be seen that after separation with a magnetic separator, the REY elements experience enrichment in the non-magnetic phase.

3.3. Leaching Results

REY leaching of coal fly ash was carried out with 3 M HCl under operating conditions of 90 ° C for 240 minutes or 4 hours. According to Wang dkK [6] this condition is the optimum condition for REY leaching. During the leaching process, the stirring was carried out continuously for 4 hours.

3.4. Precipitation Results

In this deposition process, the purification process is first carried out by increasing the pH of the leaching solution to 5 ± 0.2 with the addition of 10% b/b $CaCO_3$ and $Ca(OH)_3$. During this process the mixture is stirred to keep the mixture suspended for 2 hours and then stored for 24 hours. The mixture was then filtered to separate the leaching solution and the residue was dried, calcined and analyzed using EDX. Purification purposes using $CaCO_3$ and $Ca(OH)_3$ was to be able to remove or reduce the levels of impurities in the REY solution such as Fe, P, Al and Th in the liquid $REE_2(Cl)_{3(liq)}$(Silva et.all, 2018).

The precipitation process is carried out using $C_2H_2O_4$ with variations in process temperature, variations in the concentration of $C_2H_2O_4$ and and variations in the volume ratio (v / v) of fluid $REE_2(Cl)_{3(liq)}$: $C_2H_2O_4$. The variation of process temperature used is 25°C, 60 °C and 80 °C. The variation in the concentration of $C_2H_2O_4$ was 5% and 10% . For variations in the volume ratio (v/v) $REE_2(Cl)_{3(liq)}$: $C_2H_2O_4$ was 2:1, 1:1 and 1:2. REE solution with a volume according to the variation then adjusted the temperature according to the variation of the $C_2H_2O_4$ slowly (2,5mL/minute) to prevent the formation of poor quality crystals. The EDX analysis results of precipitation with variations in temperature treatment can be seen in **Table 2.**

Table 2. Elemental compositions of industrial coal fly ash after precipitation (Oxide and REO given in %).

Volume oxalic acid : leaching (v:v)	Oxalic Acid (w/w)	Temperature	% (Percent) Precipitation							
			REO	Al	Si	Ca	Fe	Mn	Ni	Co
2:1	5%	25°C	-	28.73	71.06	-	-	-	-	0.22
		60°C	-	-	-	-	23.34	-	49.96	26.70
		80°C	-	-	-	-	44.98	-	-	55.02
	10%	25°C	-	-		-	28.43	29.55	-	-
		60°C	0.438	29.37	69.90	-	0.20	-	0.09	-
		80°C	21.52	-	-	-		-	24.95	53.50
1:1	5%	25°C	16.25	-	-	-	33.16	-	50.60	
		60°C	45.09	-	-	-	32.66	-	-	22.25
		80°C	59.59	-	-	-	40.42	-	-	-
	10%	25°C	70.13	-	-	-	12.25	-	-	17.62
		60°C	-	1.35	1.25	97.34	0.01	-	0.01	-
		80°C	33.83	-	-	-	18.58	-	20.96	26.62
1:2	5%	25°C	-	-	-	-	33.45	17.19	-	49.34
		60°C	-	99.33	-	-	0.67	-	-	-
		80°C	3.35	95.89	-	-	0.77	-	-	-
	10%	25°C	0.095	1.24	1.21	97.46	-	-	-	-
		60°C		-	-	-	29.24	-	40.75	30.01
		80°C	33.56	-	-	-	37.97	28.48	-	-

Based on Table 2, it can be seen that the highest REY deposition efficiency level is in the conditions of a volume ratio of 1:1, with 10% concentration of oxalic acid and an operating temperature of 25° C. amounting to 70.13%. There are several operating conditions where REY deposition does not occur, such as in the 2:1 volume ratio and 5% oxalic acid

concentration. This may occur due to excess oxalic acid which can cause the deposition of calcium and aluminum oxalate [7].

3.4. Analysis of Response Surface Methode

From the P-Value of Figure 3. The three variables do not have a significant effect on the percent yield of REO precipitation (P> 0.5).

Analysis of Variance

Source	DF	Adj SS	Adj MS	F-Value	P-Value
Model	8	5494.49	686.81	1.75	0.212
Linear	3	553.20	184.40	0.47	0.711
Temperature	1	458.25	458.25	1.16	0.309
Oxalic acid (%)	1	71.75	71.75	0.18	0.679
Volume	1	22.93	22.93	0.06	0.815
Square	2	4770.92	2385.46	6.06	0.021
Temperature*Temperature	1	784.08	784.08	1.99	0.192
Volume*Volume	1	4018.23	4018.23	10.21	0.011
2-Way Interaction	3	176.58	58.86	0.15	0.927
Temperature*Oxalic acid (%)	1	164.98	164.98	0.42	0.533
Temperature*Volume	1	10.24	10.24	0.03	0.875
Oxalic acid (%)*Volume	1	0.14	0.14	0.00	0.985
Error	9	3540.90	393.43		
Total	17	9035.38			

Figure 3. Analysis of Variance

Figure 4 shows the contour plot where each color shows the range of responses generated for each REY element. The maximum conditions for the plots are dark green with a value for REO of 50 %.

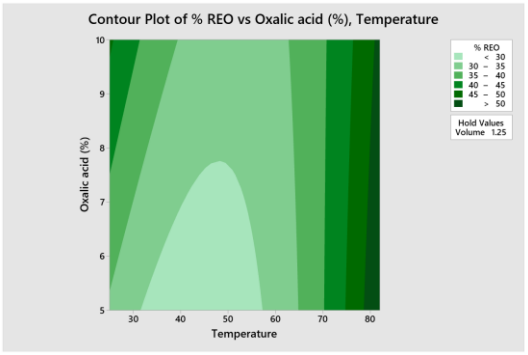

Figure 4. Contout plot of % REO vs Oxalic acid (%), Temperature

IV. Conclusion

From the results of precipitation using EDX, the largest percentage yield of precipitation is 70.13% REO. It can be seen that the impurity content is still high, so it must be separated first so that the resulting REO has a higher level of purity.

Acknowledgement

We are thankful to the Chemical Engineering Department (Advanced Materials and Sustainable Mineral Processing Research Group), Faculty of Engineering, Gadjah Mada University and Unconventional Geo-Resources Research Center, Faculty of Engineering. Gadjah Mada University.

References

[1] Seredin, V. V and Finkelman, R. B., 2018. International Journal of Coal Geology Metalliferous coals : A review of the main genetic and geochemical types, *International Journal of Coal Geology,*76(4), pp. 253–289. https://doi.org/10.1016/j.coal.2008.07.016.

[2] Rosita, Widya., Bendiyasa, I Made., Perdana, Indra., Anggara, Ferian., 2020. Sequential particle-size and magnetic separation for enrichmen of rare-earth elements and yttrium in Indonesia coal fly ash. *Journal of Environmental Chemical Engineering*, 2213-3437 https://doi.org/ 10.1016/j.jecel.2019.103575.

[3] Trihaditia, Riza., Syamsiah, Melissa., Awaliyah, Aliya., 2018. Penentuan formulasi optimum pembuatan cookies dari bekatul padi pandanwangi dengan penambahan tepung terigu menggunakan metode RSM (Response Surface Method), Agroscience Vol 8 No. 2 Tahun 2018, 1979-4661.

[4] Seredin, V V (2010): A New Method for Primary Evaluation of the Outlook for Rare Earth Element Ores, Geology of Ore Deposits, 52(5), 5-6. https://doi.org/10.1134/S1075701510050077

[5] Blissett, R. S., Samlley, N., and Rowson, N.A. (2014): An investigation into six coal fly ashes from United Kingdom and Poland to evaluate rare earth element content, FUEL, 119, 236-239. https://doi.org/10.1016/j.fuel.2013.11.053

[6] Wang, J. et al., 2017. Recovery of rare earths and aluminum from FCC waste slag by acid leaching and selective precipitation, *Journal of Rare Earths*. Elsevier Ltd, 35(11), pp. 1141–1148. https://doi.org/ 10.1016/j.jre.2017.05.011.

[7] Silva, R., Morais, C., Teixeira, L., & Oliveira, E. (2018). Selective removal of impurities from rare earth sulfuric liquor using different reagents. Miner Engineering, 238-246.

The 13th AUN/SEED-Net Regional Conference on Chemical Engineering 2020 (RCChE-2020)
Jointly held with
The 5th International Symposium on Conservation and Management of Tropical Lakes
"Insights and Challenges toward Achieving SDGs"

Adsorption Characteristics of Methylene Blue from Aqueous Solution by Amorphous Silica

Naing Min Tun[1*], Wai Hnin Phyu Phyu[2], Aung Than Htwe[3]

[1,3] *Department of Chemistry, University of Yangon, University Avenue Road., P.O. 11041, Yangon, Myanmar*
[2] *Department of Chemistry, Monywa University, Kyaukka Road., Monywa, Myanmar*
**nainglay20@gmail.com*

Abstract

This research was conducted to find the removal potential of amorphous silica from the source of agricultural by-product rice husk. Rice husk abundant agricultural by-product in Myanmar, it was used to produce amorphous silica in water rinsed and different acid-treated (HCl, H_2SO_4, H_3PO_4) by the sol-gel method. The as-prepared silica was characterized by energy dispersive X-ray fluorescence (EDXRF) analysis, X-ray differential (XRD) analysis, and Fourier transform infrared (FT IR) spectroscopy analysis. From the obtained results, all kinds of samples composed of amorphous silica and the silica content above 99 % by quantitatively. Continuously, the as-prepared silica was used as an adsorbent for the removal of methylene blue (MB) from aqueous solution. In the experimental investigations were carried out the effect of contact time, the effect of adsorbent dosage, and the initial dye concentration. The equilibrium data were fitted to the linear form of Langmuir and Freundlich isotherm. Langmuir isotherm model was the best R^2 value than the Freundlich isotherm. The maximum monolayer adsorption capacity of MB on silica was found in 17.5438 mg/g for Si-4 with the correlation coefficients R^2 value of 0.9987.

Keywords: *Adsorbent, amorphous silica, Langmuir isotherm, Freundlich isotherm, rice husk*

I. Introduction

The high silica content of rice husk has attracted increasing uses as a source of commercial production of silica. Recently, many researchers have reported the production of silica from rice husk by various methods, optimization by the synthesis of highly purified silica in the amorphous form [1], amorphous form of spherical silica nanoparticles by different acids treatment [2], the production of amorphous silica by hydrochloric acid leaching [3], and high surface area nanosilica extraction with hydrochloric treatment [4]. Sodium silicate produced by reacting the rice husk ash and aqueous sodium hydroxide in open and closed reaction systems [5]. The reaction variables have studied depend on the time, temperature, and composition of the reaction mixture. Furthermore, the rice husk has been used as a source of microbial nutrients for single-cell protein production [6], as a raw material for the production of ethanol and reducing sugar [7].

The removal of methylene blue from wastewater was investigated by the potential use of pretreated rice husk and rice husk ash [8]. Adsorption is one of the most effective techniques to remove heavy metals, organic and inorganic pollutants, and non-biodegradable pollutants (including dyes) from wastewater due to the simplicity as well as the availability to the choice of a wide range of adsorbents. The

purpose of this study is to remove the methylene blue from aqueous solution using a high purity of amorphous silica from rice husk as agricultural waste.

II. Materials and Methods

2.1. Preparation of silica particles

The preparation of silica particles was carried out according to the described method [1]. In this research, the procedure was modified the sonication of sodium silicate by addition of 5 mL of ethanol after refluxing with HCl. The as-prepared samples of SiO_2 were nominated for untreated or distilled water rinsed (Si-1), with hydrochloric acid-treated (Si-2), for sulphuric acid-treated (Si-3), and for phosphoric acid-treated sample (Si-4). The extraction process and purification of the silica occurred according to equations 1 and 2, respectively [1].

$$SiO_2(Ash) + 2NaOH \rightarrow Na_2SiO_3 + H_2O \quad \text{(Eq.1)}$$

$$Na_2SiO_3 + H_2SO_4 \rightarrow SiO_2 + Na_2SO_4 + H_2O \quad \text{(Eq.2)}$$

2.2. Experimental

2.2.1 Characterization of silica particles

The as-prepared silica powder was used for XRD analysis (Rigaku X-ray Diffractometer). The elemental composition of the obtained silica samples was determined by (EDXRF) (Shimadzu EDX 7000, EDXRF Spectrometer), and The binding of functional groups of silica was identified by FT IR analysis.

2.2.2 Removal of methylene blue (MB) by using amorphous silica

About 0.03 g of silica was mixed with 60 mL of methylene blue with a known concentration. The mixture was shaken with a linear shaker at 300 rpm at a specific time. The mixture was allowed to settle at definite times and was centrifuged at about 5000 rpm for 10 min. The separated phase of the aliquot was analyzed by PD-303 spectrophotometer with a wavelength of 665 nm.

III. Results and Discussion

The elemental composition of samples was identified by EDXRF there was found SiO_2 is the most abundant element in all samples. The silica content in all samples (Si-1, Si-2, Si-3, and Si-4) was found above 99 %. The minimum amount of silica content was found in Si-1 untreated sample. In addition, the presence of silica the other elements such as Fe, K, Ca, Cr, Cu, Zn, and Mn are also composed of the oxide form.

3.1 XRD Analysis

Fig. 1 shows the X-ray diffraction profiles of SiO_2 particles from rice husk Si-1 untreated, and different acid-treated samples Si-2, Si-3, and Si-4. As the X-ray diffractograms of all profiles are not having any sharp peaks, the following samples were amorphous in nature. In the diffractograms of all samples, a broad single peak appeared at the range of 20-23º (*2θ), i*t was indicated that the presence of only amorphous silica by [1, 9]. According to **Fig. 1**, all samples are observed the same amorphous nature pattern as each other.

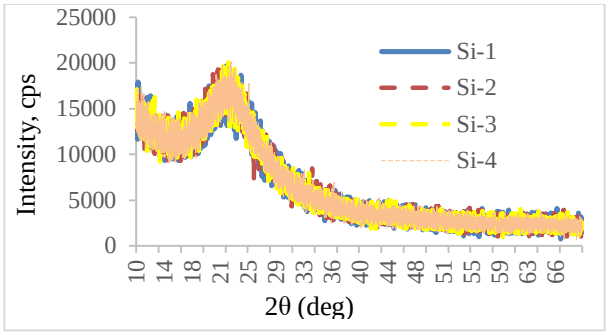

Fig 1. The XRD pattern of silica (Si-1, Si-2, Si-3, and Si-4)

3.2 FT IR analysis

The FT IR analysis of silica particle samples was carried out in the wave number 400-4000 cm^{-1}. **Fig. 2** shows the FT IR profiles untreated (Si-1) and acid-treated (Si-2, Si-3, and Si-4) silica particles. Normally, the FT IR spectra of all silica samples detected the typical bands of O-Si-O stretching at 1,065-1075 cm^{-1} and 797-799 cm^{-1} and the bending vibrations at 450-454 cm^{-1} [1].

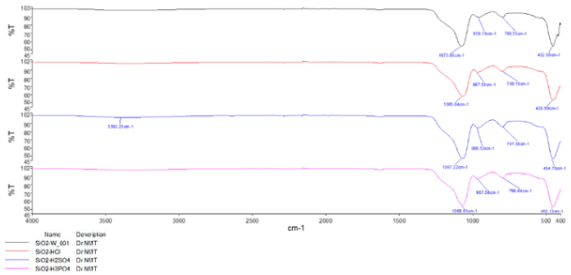

Fig 2. The FTIR profile of silica (Si-1, Si-2, Si-3, and Si-4)

3.3 Study on adsorption isotherm

The nature of the adsorption will depend on not only the physical or chemical characteristics of the adsorbent system

but also the taken times and the amount of dosage. **Fig. 3** shows the adsorption capacity of silica samples Si-1, Si-2, Si-3, and Si-4 depend on adsorption times with the same concentration of MB 10 mg/L at 32 °C. This figure shows that the adsorption efficiency of MB by Si-1, Si-2, Si-3, and Si-4 gradually increases by the time until 7 h. For the first time, the adsorption capacity was reached at a minimum of 7 mg/g for Si-2 to a maximum of 16 mg/g for Si-4 at 20 min.

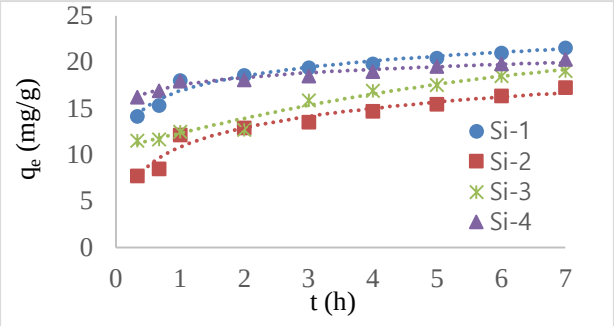

Fig 3. The variation of adsorption capacity with time

3.4 Adsorption isotherm

Adsorption equilibrium isotherms are important to describe the mechanism and interaction of methylene blue onto the adsorbent surface. In this experiment, the Langmuir and Freundlich isotherms were used for the methylene blue adsorbed onto silica particles of Si-1, Si-2, Si-3, and Si-4. The amount of removal efficiency (R, %) and the amount of q_e (mg/g) at adsorption equilibrium was calculated by the following equations [10].

$$q_e = \frac{(C_0 - C_e)V}{m} \quad \text{(Eq.3)}$$

$$R = \frac{(C_0 - C_e)}{C_0} \times 100 \quad \text{(Eq.4)}$$

The generalized Langmuir isotherm can be represented by the following equation [11]:

$$q_e = \left[\frac{X_m K_L C_e}{1 + K_L C_e}\right] \quad \text{(Eq.5)}$$

Its linear form can be expressed as:

$$\frac{C_e}{q_e} = \frac{1}{X_m K_L} + \frac{1}{X_m} C_e \quad \text{(Eq.6)}$$

Where C_e is the equilibrium concentration (mg L^{-1}) of MB in the solution after adsorption, X_m is the amount of MB adsorption capacity on the adsorbent (mg g^{-1}) and K_L is the equilibrium constant related to the energy of adsorption (L mg^{-1}). The Langmuir isotherm model of Si-1, Si-2, Si-3, and Si-4 are shown in **Fig. 4.**

On the other hand, the Freundlich isotherm assumes to describe the equilibrium of heterogeneous surfaces and hence does not assume monolayer capacity. In which the energy term of the Langmuir equation varies as a function of the surface coverage [12]. The empirical equation of Freundlich isotherm is given as follows [13]:

$$q_e = K_f (C_e)^{1/n} \quad \text{(Eq.7)}$$

The Freundlich equation can be linearized in logarithmic form described as following:

$$\log\ q_e = \log\ K_f + \frac{1}{n} \log C_e \quad \text{(Eq.8)}$$

Where C_e is the equilibrium concentration of the adsorbate (mg/L), q_e is the amount of adsorbate adsorbed per unit mass of adsorbent (mg/g), K_f and n are the Freundlich isotherm constants.

The value of 1/n possible ranging between 0 and 1, if the value is closer to zero become more favourable the heterogeneous system [14]. The Freundlich isotherm model data fitting of Si-1, Si-2, Si-3, and Si-4 are shown in **Fig. 5.**

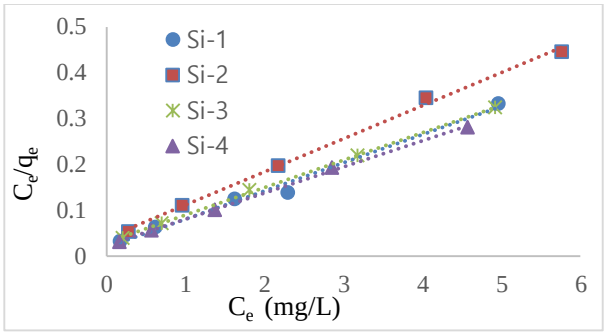

Fig. 4. Langmuir adsorption isotherm of methylene blue onto silica samples (Si-1, Si-2, Si-3, and Si-4).

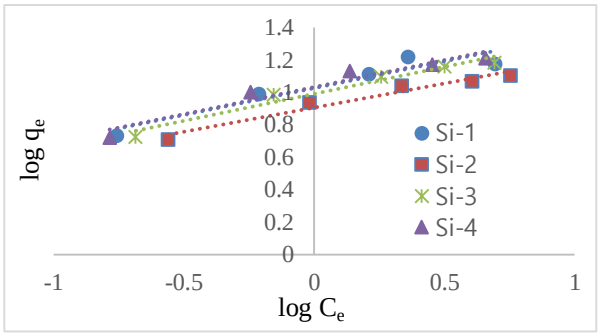

Fig. 5. Freundlich adsorption isotherm of methylene blue onto silica particles (Si-1, Si-2, Si-3, and Si-4)

The isotherm parameters and correlation coefficients (R^2) were obtained from linear fitting. **Tables 3** and **4** show the maximum amount of X_m of MB onto sample Si-4 were conducted about 17.5438 mg g^{-1} and for Si-2 was found 13.8696 mg g^{-1}. According to the obtained results, the correlation coefficients of Langmuir isotherm are more relevant than Freundlich isotherm.

Table 3. Langmuir isotherm constants and correlation coefficients for adsorption of methylene blue onto silica

Sample	Langmuir isotherm parameters			
	X_m (mg g^{-1})	K_L (L g^{-1})	R^2	R_L
Si-1	16.2601	3.2190	0.9885	0.9688
Si-2	13.8696	1.8115	0.9971	0.9822
Si-3	16.6944	1.9966	0.9991	0.9804
Si-4	17.5438	2.4152	0.9987	0.9764

Table 4. Freundlich isotherm constants and correlation coefficients for adsorption of methylene blue onto silica

Sample	Freundlich isotherm parameters		
	K_f	n	R^2
Si-1	10.6316	3.0312	0.8991
Si-2	8.0612	3.3749	0.9551
Si-3	9.7836	3.0184	0.9594
Si-4	10.8118	3.0075	0.9368

IV. Conclusions

The characterization of silica by EDXRF, XRD, and FT IR analysis was confirmed the quantitative presence of SiO_2 above 99 % and the amorphous silica. The adsorption of MB onto silica was investigated favorable and represented by Langmuir and Freundlich isotherm. Langmuir isotherm showed that the better fitting the experimental data than Freundlich isotherm. The linear correlation coefficients R^2 of Langmuir isotherm showed above the range of 0.9885 to 0.9991experimental data and for the Freundlich isotherm from 0.8991 to 0.9594 varying depending on the sample nature.

Acknowledgments

I would like to thanks Dr Ni Ni Than, Professor (Head), Department of Chemistry, University of Yangon, for her suggestion and comments. I would like to also express my deep gratitude to organizers of RCChE2020 and AUN/SEED-Net for submitting of research paper to present at "The 13th AUN/SEED-Net Regional Conference on Chemical Engineering 2020".

References

[1] Rafiee, E., Shahebrahimi, S., Feyzi, M., Shaterzadeh, M., 2012. Optimization of synthesis and characterization of nanosilica produced from rice husk (a common waste material). *International Nano Letters* 2(1), 1-8.

[2] Ghorbani, F., Sanati, A. M., Maleki, M., 2015. Production of silica nanoparticles from rice husk as agricultural waste by environmental friendly technique. *Environmental Studies of Persian Gulf* 2(1), 56-65.

[3] Chakraverty, A., Kaleemullah, S., 1991. Conver-sion of rice husk into amorphous silica and combu-stible gas. *Energy Convers. Mgmt*. 32, 565-570.

[4] Liou, T. -H., Yang C. -C., 2011. Synthesis and surface characteristics of nanosilica produced from alkali-extracted rice husk ash. *Materials Science and Engineering* 176(7), 521-529.

[5] Foletto, E. L., Gratieri, E., Oliveira, L. H. de, Jahn, S. L., 2006. Conversion of rice hull ash into soluble sodium silicate. *Materials Research* 9(3), 335–338.

[6] Hussein, A. M., El-Saied, H., Yasin, M. H., 1992. Bioconversion of hemicelluloses of rice hull black liquor into single-cell protein. *Journal of Chemical Technology and Biotechnology* 53, 147-152.

[7] Singh, A., Das, K., Sharma, D. K., 1984. Produ-ction of reducing sugars from bagasse and rice husk by acid hydrolysis. *Agricultural Wastes* 9, 131-145.

[8] Sharma, P., Kaur, R., Baskar, C., Chung, W.-J., 2010. Removal of methylene blue from aqueous waste using rice husk and rice husk ash. *Desalination* 259(1-3), 249–257.

[9] Hassan, A. F., Abdelghny, A. M., Elhadidy H., Youssef. A. M., 2014. Synthesis and character-rization of high surface area nanosilica from rice husk ash by surfactant-free sol-gel method. *Journal of Sol-Gel Science and Technol*ogy 69, 465-472.

[10] Ge, X., Liu, J., Song, X., Wang, G., Zhang, H., Zhang, Y., Zhao, H., 2016. Hierarchical iron containing γ-MnO 2 hollow microspheres: A facile one-step synthesis and effective removal of As(III) via oxidation and adsorption. *Chemical Engineering Journal 301, 139–148.*

[11] Langmuir, L., 1918. Adsoption of gases on plane surfaces of glass, mica and platinum. *Journal of American Chemical Society* 40, 1361–1403.

[12] Weber, T. W., Chakkravorti, R. K., 1974. Pore and solid diffusion models for fixed-bed adsorbers, AlChE Journal 20(2), 228-238.

[13] Freundlich, H. M. F., 1906. Over the adsorption in solution. *The Journal of Physical Chemistry* 57A, 385–471.

[14] Haghseresht, F., Lu, G., 1998. Adsorption characteristics of phenolic compounds onto coal-reject-derived adsorbents. *Energy Fuels* 12, 1100–1107.

The 13th AUN/SEED-Net Regional Conference on Chemical Engineering 2020 (RCChE-2020)
Jointly held with
The 5th International Symposium on Conservation and Management of Tropical Lakes
"Insights and Challenges toward Achieving SDGs"

Removal of Cr (VI) from Wastewater Using Chitosan-Activated Carbon Composite as Adsorbent: Study of the Adsorption Equilibrium

Faridatuz Zuhroh [*], Agus Prasetya [2] and Wahyudi Budi Sediawan [2]

[1] *Department of Chemical Engineering, Faculty of Engineering, Gadjah Mada University, 55381 Sleman, Yogyakarta, Indonesia*

** profesifarida@gmail.com*

Abstract

One of alternative treatment that mostly used to reduce the level of wastewater problem is adsorption. This research focuses on the finding of the capacity of adsorption which represent maximum removal of Cr from water. The used adsorbent was a composite of chitosan and activated carbon. Started with 20 grams of activated carbon poured into 1000 ml of chitosan solution. Medium heating and constant stirring make this solution changed its viscosity and gradually looked like gel. Bead formation had been obtained by slowly pumped the gel into the solution of NaOH 0,7 M. Finally, the adsorbent needed to be neutralized and dried at temperature of 50^{o}C. The adsorption experiment used a Chromium solution 20 ppm with variation of adsorbent mass arranged as 0.5gram, 1 gram, and 1.5 gram at temperature of 298 K, 308 K, and 318 K. The concentration of Cr in wastewater solution were measured every 10, 20, 40, 60, 120, 180, and 210 minutes. The adsorbent characteristics were analysed using XRD, BET, SEM, and FTIR for its crystallinity, surface area, surface morphology and functional groups. XRD graphic showed the adsorbent was an amorphous solid. Currently, the adsorbent characteristics were being analysed. BET result will informs whether the surface area on its pores were increased or not than its original material. Data of Cr (VI) that dispersed onto the bead composite could be determined by SEM or EDX analysis. Then, FTIR data analysis will gives information about its functional group, it will confirm whether chitosan is really coated on the activated carbon's surface or not. Generally, by gathering all the experiment data will inform the result of the adsorption process in term of its adsorption equilibrium.

Keywords: *Activated Carbon, Adsorption, Bead Composite, Chitosan and Cr (VI) ion*

I. Introduction

Heavy metals present in the water as contaminants is a problem and a threat to human and ecosystem in various countries. Many considerable methods and efforts are being made to decrease the concentration of heavy metals in the effluent wastewater to permissible discharge levels set by pollution control and regulatory authorities of each country. A wide range of processes such as chemical precipitation, ion exchange, membrane filtration, electrolytic method, coagulation, reverse osmosis and adsorption are being used for the removal of heavy metal ions from industrial effluents. Among these processes, the most promising efficient technique has been identified as adsorption with a suitable adsorbent.[1] This is really a serious environmental issue related to wastewater treatment.

Reported that Cr is used on a large scale in many different industries as plating, alloying, tanning of animal hides, inhibition of water corrosion, textile dyes and mordants, pigments, ceramic glazes, refractory bricks, and pressure-treated lumber.[2] If the effluent wastewater from these industries did not met the standard authorized by

pollution control and regulatory authorities, some pollution problem may occurred as the negative impact.

Actually, chromium has several oxidation states ranging from Cr(−II) to Cr(+VI). The trivalent and hexavalent states are the most stable, although Cr with valences of I, II, IV and V have also been shown to exist in a number of compounds.[3]

Generally the trivalent Cr is considered not harmful. It is needed by human for metabolism, but only in a little amount. But in contrast, the hexavalent Cr is considered the most toxic forms of chromium, as it presents high oxidizing potential, high solubility, and mobility across the membranes in living organisms and in the environment.

In recent years, contamination of the environment by Chromium (Cr), especially hexavalent Cr, has become a major area of concern. Because of that, constant monitoring and analysis of chromium becomes a necessity. [3,4]

In the aquatic environment, the toxicity of Cr(VI) has been shown to be greater than Cr(III).[4] Other problem is that Cr(III) can be oxidized and changed became Cr(VI).

Cr(III) in the forms of oxides, hydroxides, and sulphates is less toxic as it is relatively insoluble in water, presents lower mobility, and is mainly bound to organic matter in soil and aquatic environments. Moreover, Cr(III) forms tend to form hydroxide precipitates with Fe at typical ground water pH values. At high concentrations of oxygen or Mn oxides, Cr(III) can be oxidized to Cr(VI).[5,6] Oxidation of Cr(III) to Cr(VI) represents a significant environmental hazard because a relatively nontoxic species is transformed into a more toxic one.[2]

Chitosan is good adsorbent because of its active group and widely used in the removal process of heavy metal in wastewater. And activated carbons are unique and versatile adsorbents because of the availability of extensive surface area, its micro porous structure and high adsorption capacity.[1]

The objective of this study was to demonstrate the adsorption performance where the adsorbent is a bead composite for the removal of Cr (VI) ion in water. The bead composite was a modified of activated carbon and chitosan.

II. Materials and Methods

2.1. Materials

Active Carbon was purchased from Alfa Kimia (Yogyakarta, Indonesia) and for the Chitosan was from Monodon Group (Lampung, Indonesia).

2.2. Preparation of Adsorbent

The preparation of adsorbent was started with preparing the materials. The raw material used were active carbon and chitosan. Each material needs some pre-treatment in order to make a good composite.

Particle size is an important factor to make a good composite. The active carbon used in this experiment was the active carbon with its particle size was 100mesh. And for the chitosan, it was 80mesh.

After the particle size was determined, about 40gram of active carbon need to be soaked in oxalic acid 250ml 0.2M for 4 hours. This step was done for keeping the activation of the carbon. After neutralized with distilled water, the activated carbons need to be dried to eliminate the water inside.

Same solution for the chitosan, oxalic acid 1000ml 0.2M was also needed to dissolve 20gram of chitosan. This step was done for making the chitosan viscous gel. The form of gel can be obtained by heating and stirring the solution in the same time.

The dried activated carbon need to be poured into the chitosan solution after its viscosity became higher. Constant stirring still need to be maintained. The mixture was also heated at 40-50ºC to facilitate mixing. It was important to the homogeneity of the compositing process between activated carbon and chitosan.

For the best condition, it was used the magnetic stirrer tools that had a temperature controller on its side because the heating and stirring were supposed to be held in the same time.

The next step was slowly pumping the gel into some solution to gain the bead formation. The needed solution was NaOH 0,7M. Soon after the pumped gel dropped and contacted with the solution, its form was changed into some spherical bead of solid that moved to the ground of the solution. It took some time to let the bead composite formation was stabilized.

The beads were still needed to be neutralized with distilled water and then dried at the temperature of 50ºC so the beads were ready to be characterized and used as the adsorbent in the adsorption process.

2.3. Experimental set-up

Adsorption experiments were carried out in the batch contact method. The used media was a water bath shaker where some erlenmeyers can be arranged in it.

The adsorption experiment used a Chromium soluti

on 20 ppm with the independent variables were adsorb ent mass, time and temperature.

Variation of adsorbent mass arranged as 0.5gram, 1 gram, and 1.5 gram at temperature of 298 K, 308 K, and 318 K. The concentration of Cr in wastewater sol ution were measured every 10, 20, 40, 60, 120, 180, and 210 minutes.

2.4. Analytical methods

X-Ray Diffraction (XRD) analysis

X-Ray Diffraction analysis were performed in order to define the change of microstructure in the adsorbent material. XRD result analysis also contain of information on amorphous and crystalline nature of particles.

Fourier transforms infrared (FTIR) spectroscopy

The prepared samples were prepared from the bead composite and bead composite after adsorption. The FTIR analysis were performed to compare the functional group. So the result will confirm whether chitosan is really coated on the activated carbon's surface or not.

BET analysis

The prepared samples were tested and recorded on a Quantachrome NovaWin - Data Acquisition and Reduction for NOVA instruments 1994-2013, Quantachrome Instruments version 11.03.

Samples for the BET analysis were prepared from the raw material (chitosan) and the bead composite adsorbent. BET analysis was performed to compare the surface area and pore volume.

SEM analysis

A scanning electron microscope inter-phased with an electron dispersive X-ray spectrometer was used to study the surface morphologies and elemental analysis of the bead composite before and after adsorption. The result of SEM analysis will show the data of Cr (VI) that dispersed on-to the bead composite. The result also can be confirm ed with conduct the EDX analysis.

Adsorption Equilibrium

Adsorption equilibrium is obtained when the solid adsorbent has contact with the adsorbate molecule and then there is movement from the solution to the solid adsorbent make both concentration in solution and solid is equal. In other words, the adsorption rate and the desorption rate are equal.

Equation of equilibrium in adsorption is usually performed as adsorption isotherm. This equation defines the connection between the concentration of ion in a liquid phase with the concentration that adsorbed in the surface of adsorbent. In aqueous system, there are Langmuir Isotherm and Freundlich Isotherm.

Langmuir Isotherm is usually used for the adsorption model which the adsorbate molecule is adsorbed in one layer (monolayer) in the surface of adsorbent. It means that all the adsorbed molecule does not have interaction each other and all the surface area of the adsorbent have the same affinity level to the adsorbate. Contrarily, Freundlich Isotherm is used when the adsorption model was multilayer. It means that there is a possibility that each surface of the adsorbent may have different functional group.

$$qe = \frac{qm\, K_l C_e}{1 + K_l C_e} \quad \text{(Eq.1)}$$

$$\frac{C_e}{qm} = \frac{1}{qm\, K_l} + \frac{1}{qm} C_e \quad \text{(Eq.2)}$$

$$qe = K_f C_e^{\left(\frac{1}{n}\right)} \quad \text{(Eq.3)}$$

$$Logqe = LogK_f + \frac{1}{n} LogC_e \quad \text{(Eq.4)}$$

where qe is amount of ion that adsorbed when equilibrium, qm is the maximum adsorption capacity of ion, K_l is the constant of Langmuir Isotherm, K_f is the constant of Freundlich Isotherm, C_e is the concentration of solution when equilibrium.

The equations above are used to determine the favorability of the adsorption system. (Eq.1) and (Eq.2) for the Langmuir isotherm, (Eq.3) and (Eq.4) for the Freundlich isotherm.

I. Results and Discussion

Result of the X-Ray Diffraction (XRD) analysis for the bead composite adsorbent is shown in **Table 1**. As shown in **Table 1** and imagined in **Fig. 1**, the strongest peak of adsorbent samples were 2θ = 25.9800°, 27.2443°, and 28.1800°.

Table 1. Strongest Peak X-Ray Diffraction Analysis

No	Peak Number	2Theta (deg)
1	29	25.9800
2	31	27.2443
3	32	28.1800

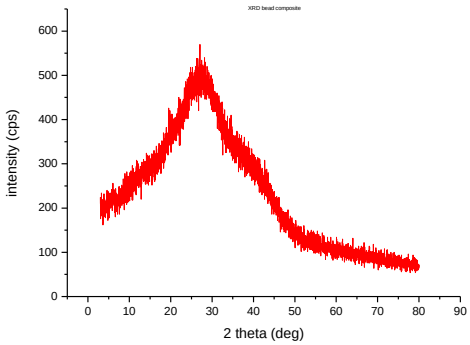

Fig. 1. X-Ray Diffraction Graphic Analysis

Table 2. BET Analysis

Ads.	Surface Area (m^2/g)	Pore Volume (cc/g)	Pore Radius (A°)
1	9.491	0.017	26.966
2	12.047	0.037	26.895
3	12.314	0.038	26.742
4	18.392	0.040	26.970

As shown in **Table 2**, the BET result informs that there is an increasement in the surface area on its pores than its original material.

Currently, the adsorbent characteristics were still being analyzed in lab for the rest analysis, so there is not any data result of FTIR and SEM analysis yet.

IV. Conclusion

It is very possible to combine the chitosan adsorbent with activated adsorbent to make a composite adsorbent because of each good properties. Chitosan is good in its mechanical properties but lack in acid solution, and it is covered with activated carbon which is good in its pore structure and surface area. The form of bead composite is actually a stable form of modification composite, it is easy to mobile in the solution and easy to be investigated in the process of removal of Cr(VI) in water. But actually the initial diameter or size of the spherical bead should be made in bigger size, because after the drying treatment, the size will decreased as the water inside the bead is eliminated. The size of spherical bead composite will influence the amount of adsorbent uses in every adsorption experiment.

Acknowledgement

We are thankful to the Energy Conservation and Pollution Prevention Lab (KEPP) and Instrumental Analysis Lab (ANINS) for their laboratory equipment and analysis support.

References

Journal Papers

[1] T. Anirudhan, S. Sreekumari., 2011. Adsorptive removal of heavy metal ions from industrial effluents using activated carbon derived from waste coconut buttons. *Journal of Environmental Sciences.* 1989-1998.

[2] A. Zayed, N. Terry., 2003. Chromium in The Environment: Factors Affecting Biological Remediation. *Journal of Plant and Soil.* 139-156.

[3] S. Avudainayagam, M. Megharaj, G. Owens, R. S. Kookana, D. Chittleborough, R. Naidu., 2003. Chemistry of chromium in soils with emphasis on tannery waste sites. *Reviews of Environmental Contamination and Toxicology*. 53–91.

[4] R. Rakhunde, L. Deshpande, H. Juneja., 2012. Chemical Speciation of Chromium in Water: A Review. *Journal of Critical Reviews in Environmental Science and Technology.* 776-810.

[5] T. Becquer, C. Quantin, M.Sicot et al., 2003. Chromium Availibility in Ultramafic Soils from New Caledonia. *Journal of Science of the Total Environment.* 251-261.

[6] J. Peralta-Videa, M.Lopez, M.Narayan et al., 2009. The Biochemistry of Environmental Heavy Metal Uptake by Plants: Implications for The Food Chain. *Journal of Biochemistry and Cell Biology.* 1665-1677.

The Extraction of lignin from Sugarcane Bagasse Using Urea Based Hydrotropic Process

Ulfia Al Rahma[1], Muslikhin Hidayat[1], Wahyudi Budi Sediawan[1*], Indah Hartati[2]

[1] *Chemical Engineering Department, Faculty of Engineering, Gadjah Mada University, jln.Grafika No.2, Yogyakarta 55281, Indonesia*
[2] *Department of Chemical Engineering, Faculty of Engineering, Universitas Wahid Hasyim, 50236, Indonesia*

**wbsediawan@ugm.ac.id*

Abstract

Lignin is one of the largest reservoirs of aromatic compound that can be used in various applications while *hydrotropes* have been explored as new green chemical for lignin separation. The objective of this study was to recover lignin from filtrate of sugarcane bagasse microwave-assisted hydrotropic extraction process. The lignin extraction were performed at a fixed solid and liquid ratio of 1:20, agitation speed of 900 rpm, urea concentration 30%, while temperature and extraction duration were varied between 70 -90 ^{o}C, and 30-150 minutes, respectively. The soluble lignin was precipitated from the hydrotropic extraction filtrate by adding 5 times of water and bringing the pH of the solution to pH 4-5. The research showed that the higher the *hydrotrope* concentration applied, the higher the recovery of lignin would be. The profile of the lignin recovery of hydrotropic extraction conducted on higher temperatures also showed a similar trend as the one the application of higher *hydrotrope* concentration. The optimum condition obtained from the research was at a temperature of 90^{o}C, 30% of concentration urea *hydrotropes*, and in the time of 120 minutes, the % lignin extracted 13.45 %.
Keywords: *Lignin, hydrotropes, extraction, urea*

I. Introduction

Bagasse is a solid residue obtained from sugarcane processing in sugar and ethanol industry [1]. Generally, 280 kg of bagasse is produced from the processing of 1 ton of sugarcane [2]. Lignocellulosic materials consist of three main polymers which are cellulose, lignin, and hemicellulose [3]. The cellulose, hemicellulose, and lignin content of sugarcane bagasse are 41-55%, 20-22.5%, and 18-26.3%, respectively [4].

Lignin, the most abundant natural aromatic polymer on earth, has been regarded as a potential raw material for various higher values of fuels and chemicals [3]. Type of biomass sources, extraction methods, and extraction severity are some factors affecting the lignin isolation efficiency. Lignin extraction process is intended to separate and recover both cellulose and lignin from lignocellulose biomass. Kraft, sulfate, organosolv, soda, and hydrothermal are common processes applied in biomass pretreatment [5]. Lignin from Kraft, sulfate, and soda process are still contains chemicals. Lignin from organosolv and hydrothermal processes are having good quality as it has low molecular weight and good solubility in organic solvents. However, both of organosolv and hydrothermal processes are expensive. The utilization of harsh chemicals and operation condition are the other back draws of the above processes [5].

The application of friendly extraction process including the utilization of green chemicals and application of mild operation condition will be beneficial. Hydrotropic extraction is considered as an environmentally friendly water-based method with a simple recovery of hydrotropic solutions to obtain several products. Several hydrotropes

have been applied in lignin and cellulose separation from various biomasses. Devendra and Pandey [6] reported that sodium cumene sulfonate was able to remove up to 50% of lignin from rice straw. Urea is one of potential hydrotrope agent since it is safe and low-price product [6].

In this work we reported the application of urea as the hydrotropic agent in microwave assisted lignin extraction from sugarcane bagasse.

II. Materials and Methods

2.1. Material

Bagasse was acquired from sugar factory Geneng, Ngawi regency. Sugarcane bagasse was air dried, milled and then sieved with a sieve size of 70 mesh (210 µm). The cellulose, hemicellulose and lignin content of sugarcane bagasse was tabulated on Table 1.

Table 1. Chemical composition of sugarcane bagasse

Component	Values (%)
Cellulose	24.317
Hemicellulose	45.588
Lignin	18.249

Urea was from PT. Kujang Indonesia and sulfuric acid in which used to control the pH of the reaction mixture was from Merck.

2.2. Lignin Extraction Procedure

20 grams of bagasse and 400 ml of 30% urea hydrotropes solution were put into glass tube. The reaction mixture was subjected to microwave heating (70-90^{0}C) for 30-150 minutes at 900 rpm. After completing the extraction process, the suspension was filtered and rinsed using 500 ml of hot water (90ºC) to remove the remaining hydrotropes attached to the solid residue. After filtration, the solid residue was dried in an oven at 90ºC until constant weight and the lignin-containing filtrate was treated for further processing. Series of experiments were carried out in same way to determine the effect of temperature, hydrotropes concentration and time on lignin extraction.

The dissolved lignin contained in the hydrotropic filtrate was recovered by water precipitation. 200 ml of the filtrate was added with distilled water up to 4x the original volume. The pH of the solution was set to pH 4-5 by utilized 5 N of sulphuric acid [7]. The precipitated lignin was then vacuum-filtered by using Whatman filter paper no. 42. The precipitated lignin obtained was then heated in an oven at 100ºC until its constant weight. The lignin extraction % on solute was calculated based on its initial lignin content of raw material sugarcane bagasse [8].

2.3. Analytical methods

The lignin content was determined by using Chesson method. One gram of dry sample (a) was refluxed for 2 hours with 150 ml H_2O at 100ºC. The residue was filtered, washed with 300 mL of hot water and oven-dried to constant weight (b). The residual powder obtained was then added with 150 mL of 0.5 M H_2SO_4 and then refluxed for 2 hours at 100 ºC. The residue was filtered and washed with 300 ml of water until neutral condition. The residue was dried to a constant weight (c). The dry residue was added with 10 mL of 72% (v/v) H_2SO_4 and soaked at room temperature for 4 hours. 150 mL of 0.5 M H_2SO_4 was added and refluxed at 100 ºC for 2 hours. The residue was filtered and washed with 400 mL of distilled water until neutral condition. The residue obtained was weighted (d). The solid residue was then ashed in a furnace, and the ash was weighted (e). The lignin content was calculated by:

$$\text{Lignin (\%)} = \frac{d-e}{a} x100\% \qquad \text{(Eq.1)}$$

The lignin solids analysis was carried out using FTIR at room temperature of 298 K in region 4000-400 cm $^{-1}$ on Thermo Scientific Nicolet iS10.

III. Results and Discussion

During urea based hydrotropic extraction of lignin from sugarcane bagasse, the color of the filtrate solution became dark (Figure 1a). The darkening of the hydrotropic solution during pretreatment of biomass was also reported in alkyl benzene sulfonates based hydrotropic processing of cotton stalk Karthyani et al., [9]. It was believed that the darkening solution indicates that biomass components were solubilized into the hydrotropic solution. Karthyani et al., [9] mentioned that due to hydrophobic interactions of the aromatic ring of phenolic lignin with the aromatic ring of the hydrotrope, lignin solublization was more preferential than cellulose and hemicelluloses [8].

The hydrotropic lignin was precipitated from the filtrate by water dilution under acidic condition and the obtained lignin was brown colored powder (Figure 1b). Brown colored powder of sugarcane bagasse lignin was also obtained from alkyl benzene sulfonate based hydrotropic treatment. Ansari et al., [10] as mentioned by

Jingjing [11] that most isolated lignin are brown powder.

(a) (b)

Figure 1. Filtrate solution of hydrotropic delignification and (b) hydrotropic lignin

3.1. Effect of Temperature and Time

Lignin extraction from sugarcane bagasse was carried out by utilized urea solution (30%) in temperature range of 70-90 ^{o}C and time range of 30-150 minutes with time interval of 30 minutes. The profile of lignin extraction percentage was illustrated on Figure 2. It was shown that temperature is significantly affecting the dissolution of lignin in hydrotropic extraction. The lignin extracted was increase with the increase of temperature in lignin extraction from 30 minutes to 120 minutes. The lignin extraction performed at 120 minutes and at temperature of 70, 80 and 90^{0}C gave lignin extraction percentage of 9.70, 12.05 and 13.45%, respectively. Gabov [8] stated that at higher temperatures, hydrotropic molecules aggregate and the hydrogen bonds between water molecules become unstable resultin in excess hydration and in increased surface activity. The rise of temperature can cause a significant change in the structure of the aggregate, thereby causing more solute to dissolve in the hydrotrope solution. Increasing temperature can raise the amount of aggregation and thus create more hydrotrope aggregates, each of which can interact with solute molecules [8].

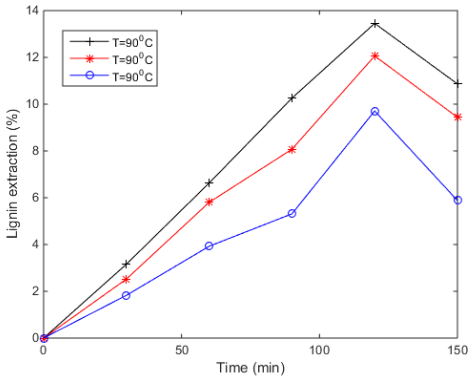

Figure 2. Lignin extraction percentage of hydrotropic extraction of lignin from sugarcane bagasse

The optimum temperature and time of the hydrotropic lignin extraction were achieved at 90^{o}C and time of 120 minutes. This increasing of time, the % extracted lignin also increases at various temperatures. Based on the graph above, the optimum % extracted lignin at 120 minutes reached 13.45%, while at 150 minutes there was a decrease, where the percentage of lignin extracted was only 10.86%.The decreased lignin extraction yield at 150 minutes was due to the inhibition of mass transfer of the hydrotrope solution which entered the sugarcane baggage matrix due to the degradation of urea as hydrotropes.

3.1.2. Lignin Characterization

FTIR analysis was performed on lignin powder obtained from hydrotropic extraction conducted at temperature of 90 ^{o}C and time of 120 minutes.

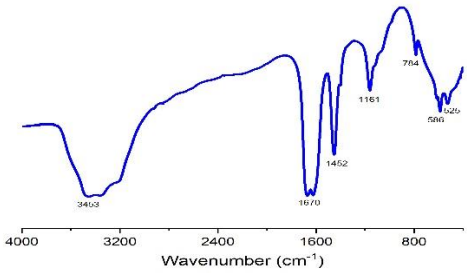

Fig.3. FTIR Lignin

Lignin is a complex aromatic heteropolymer that is composed of three main monolignols, namely, pcoumaryl, coniferyl, and synapyl alcohol, with different degrees of methoxylation. When incorporated into lignin polymers, monolignol produces p-hydroxyphenyl (H), guaiacyl (G), and syringyl (S), each of which has a structural variation in the polymer. Based on the literature for soft-stemmed plants such as bagasse, the most dominant lignin components are Guacyl and p-hydroxyphenyl minor [12]. Based on the FTIR results presented in Figure 3, it shows that the wavenumber 1161.35 cm-1 indicates the presence of a p-hydroxyphenyl group which is one of the components of lignin.

IV. Conclusion

Urea based hydrotropic solution was proved as a good hydrotropic agent for lignin extraction. Temperature an time lignin, the higher the temperature of the extracted lignin also increases, the optimum temperature is at 90 ^{o}C. Meanwhile, the longer the time used for extraction, the

decreasing of the extraction results, the best optimum time to obtain lignin extraction is 120 minutes**.**

Acknowledgement

The authors are grateful for Author greatly acknowledge The ministry of Research, Technology and Higher Education of Republic of Indonesia which support this work through PDUPT research grant of 2020, with contract number of 2845/UN1/DITLIT/DIT-LIT/2020.

References

[1] Chandel, Anuj K.da Silva., Silvio S. Carvalho., Walter Singh., Om V., 2012. **Sugarcane Bagasse and leaves: Foreseeable Biomass of Biofuel and Bio-Products**. *Journal of Chemical Technology and Biotechnology* 87, 11-20.

[2] Spiridon, Iuliana. 2018., **Biological and Pharmaceutical Applications of Lignin and Its Derivatives: a Mini-Review.** *CELLULOSE CHEMISTRY AND TECHNOLOGY Cellulose Chem. Technol* 52, 543-550.

[3] Yunpu, Wang, Leilei., D A I, Liangliang., F A NShaoqi., Shan Yuhuan, L I U., 2016. **Journal of Analytical and Applied Pyrolysis Review of Microwave-Assisted lignin Conversion for Renewable Fuels and Chemicals**. *Journal of Analytical and Applied Pyrolysis* 119, 104-103.

[4] Mokhena, C Teboho., Mochane, J Mokgotsa., Moutang, E Tshwafo., Linganiso, Z Linda., Thekisoe, M Oriel., Songca, P Sandile., 2018. **Sugarcane Bagasse and Cellulose Polymer Composites**. Intechopen, 71497.

[5] Chung, Hoyong.,Washburn, Newell, R., 2016. **Extraction and Types of Lignin**. *Lignin in Polymer Composites*, 13-25.

[6] Devendra, Leena P., Pandey, Ashok., 2015. **Hydrotropic pretreatment on rice straw for bioethanol production**. *Renewable Energy* 98, 2-8.

[7] Watkins, Dereca., Nurudin, Md., Hosur, Mahesh., Tcherbi-Narteh, Alfred., Jaelani, Saek., 2014., Exctraction and Characterization of Lignin from different biomass Resources. Journal of Materials Research and Technology, 4(1): 26-32.

[8] Gabov, Konstantin. 2018., **Hydrotropic Process for Green Biorefinery Applications applications.** Finlad, United state.

[9] Karthyani, S., Pandey, Ashok., Devendra, P Leena., 2017. **Delignification of Cotton Stalk Using Sodium Cumene Sulfonat for Bioethanol Production**. Biofuels, 1759-7269.

[10] Ansari, Khursheed B., Gaikar, Vilas G. 2013., **Green hydrotropic Extraction Technology for Delignification of Sugarcane Bagasse by Using Alkybenzene Sulfonates As Hydrotropes**. *Chemical Engineering Science*, 1-10.

[11] Jingjing, Li., 2011. **Isolation Lignin From Wood**. Saima University of Applied Science, Imatra.

[12] Van Maris, Antonius., Abbott, A Derek., Bellismi, Eleonara., deen Brink, Van Joost., Kuyper, Marko., H Luttik, A Marijke., Wisselink, Woufer H., Scheffers, Alexander W., Van Dijken, Johanes P., 2006. **Alcoholic Fermentation of Carbon Source in Biomasss Hydrolysates by Saccaromyces Cerevisiae, Current Status**. Springer Science 90, 391-418.

The 13th AUN/SEED-Net Regional Conference on Chemical Engineering 2020 (RCChE-2020)
Jointly held with
The 5th International Symposium on Conservation and Management of Tropical Lakes
"Insights and Challenges toward Achieving SDGs"

Bleaching of Rice Straw Hydrotropic Pulp with Hydrogen Peroxide

Rara Ayu Lestary [1], Moh. Fahrurrozi [1], Wahyudi Budi Sediawan[1*] and Indah Hartati[1, 2]

[1] *Departement of Chemical Engineering, Faculty of Engineering, Universitas Gadjah Mada, Jl. Grafika No. 2, Yogyakarta 55281, Indonesia*
[2] *Departement of Chemical Engineering, Faculty of Engineering, Universitas Wahid Hasyim, Jl. Menoreh Tengah X No 22 Semarang, Indonesia*
** wbsediawan@ugm.ac.id*

Abstract

One of the potential lignocellulose resources from agriculture biomass residue is rice straw. Cellulose, the main component of lignocellulose can be processes into various products. Hydrotropic treatment and peroxide bleaching can be considered as an environmentally friendly pretreatment for lignocellulose. Bleaching plays an important role in removing both hemicellulose and lignin resulting in producing high cellulose purity and brightness. This research aimed to study the rice straw hydrotropic pulp bleaching with hydrogen peroxide. Hydrotropic treatment of rice straw was conducted with 30% w/v of urea solution at 80ºC for 60 minutes and the chelation stage was conducted with EDTA at 70ºC for 60 minutes. Bleaching of rice straw hydrotropic pulp was investigated under various time and concentration of hydrogen peroxide (2%, 4%, and 6%) at 90ºC with microwave heating. Lignocellulose content, chemical composition, brightness, and yield of bleached pulp were evaluated. The results showed that the maximum value of bleached pulp brightness was obtained with 4% hydrogen peroxide concentration at temperature 90ºC for 120 minute reaction time with the cellulose content was 52.41% and the lignin content was 14.45%.

Keywords: *Bleaching, Hydrotropic Pulp, Hydrogen Peroxide, Rice Straw*

I. Introduction

Rice straw, one of the potential lignocellulose resources from agriculture biomass residue, is usually being disposed of by burning it in an open field, plowing it into the field, or using it as animal feed [2]. One of the main components in rice straw cell walls is cellulose, a versatile polymer, in which utilized for fibre, films, membranes, excipient, and composites [3].

Cellulose and its derivatives can be obtained from lignocellulose treatment, fractionation and conversion processes. Pretreatment of lignocellulose materials is an essential step for hemicelluloses and lignin removal because cellulose is embedded in hemicelluloses and lignin matrix [4]. Hydrotropic treatment followed by peroxide bleaching are considered as an environmentally friendly lignocellulose pretreatment.

Hydrotropic treatment has several attractive features that make it a remarkable alternative for biomass fractionation. Hydrogen peroxide is considered as an environmentally friendly bleaching agent because it decomposes into oxygen and water only. The effectiveness of hydrogen peroxide as a bleaching agent is greatly influenced by the presence of metal ions in pulp. Chelation stage prior the bleaching process is useful in removing pulp metal ions and in increasing the bleaching efficiency [5]. Bleaching plays an important role to remove remaining hemicellulose and lignin, so cellulose is expected to have high cellulose purity and high brightness. In the present work, rice straw hydrotropic pulp has been used to investigate the effect of concentration and time of bleaching on brightness, yield, and chemical compositional of unbleached pulp.

II. Materials and Methods

2.1. Materials

Rice straw was obtained from a local rice field in Blitar, East Java. Urea was produced and supplied by PT Pupuk Kujang, Hydrogen Peroxide H_2O_2 30% Solution (Merck), Sodium Hydroxide NaOH (Merck), Sulfuric Acid H_2SO_4 95-97% (Merck), EDTA (Merck), and distilled water.

2.2. Experimental set-up

2.2.1 Hydrotropic Treatment and Chelation Stage

Rice straw was chopped, grounded into powder and 60 mesh sieved. Rice straw powder was inserted in glass jar followed by the addition of urea solution 30% w/v. Hydrotropic treatment was conducted in a glass jar with microwave heating at 80°C for 60 minutes and agitating speed was set at 300 rpm. The pulp was separated by filtration process and oven-dried at 105°C.

The rice straw hydrotropic pulp was then chelated with EDTA 2% w/w at adjusted pH 4-5, temperature of 70°C for 60 minutes. The chelation residue was separated by a filtration process then it was oven-dried at 105°C.

2.2.2 Bleaching stage

The bleaching process was performed at various reaction times and H_2O_2 concentration with 1.5% NaOH in a glass jar with microwave heating. The microwave temperature was set to 90°C and the agitation speed was set at 300 rpm. The bleached pulp was separated, washed with distilled water and oven dried at 105°C.

2.2.3 Compositional analysis

Cellulose and lignin content in unbleached and bleached pulp were determined by Chesson-Datta Analysis [6]. 1 gr of sample (a) and 150 ml distilled water were refluxed at temperature of 100°C for 2 hours. The sample was then oven-dried at 105°C (b). The dried sample and 150 mL of 1 N H_2SO_4 solution were refluxed at temperature of 100°C for 2 hours to quantify the hemicellulose content. The sample was then oven-dried at 105°C (c). Furthermore, the sample was immersed in 10 mL of 72% H_2SO_4 solution at room temperature then it was refluxed using 150 mL of 1 N H_2SO_4 solution at temperature of 100°C for 2 hours to quantify the cellulose content (d). The sample was burned in a furnace and lignin content was measured as the difference between the sample weight before and the sample weight after burning (e). The percentage of hemicellulose, cellulose, and lignin can then be calculated by Eq. 1, 2, and 3.

$$\text{Hemicellulose } \% = \frac{\text{b-c}}{\text{a}} \quad \text{(Eq.1)}$$

$$\text{cellulose } \% = \frac{\text{c-d}}{\text{a}} \quad \text{(Eq.2)}$$

$$\text{Lignin } \% = \frac{\text{d-e}}{\text{a}} \quad \text{(Eq.3)}$$

2.2.4 Chemical analysis

Residual H_2O_2 was determined by iodometric method. The filtrate sample from the bleaching stage was inserted into Erlenmeyer flask and added with 50 mL distilled water, 3 drops of ammonium molybdate solution, 4 mL of 4N H_2SO_4 solution, and 10 mL of 10% KI solution. The mixture was titrated with 0.1 N $Na_2S_2O_3$ solution until the brown tri iodide color has been reduced to a light straw color then a few drops of the starch solution was added to the mixture. Subsequently, the titration was performed until the color of the solution changes to colorless. The concentration of H_2O_2 in the sample can then be calculated by equation 4, where A is the titration volume for sample, B is titration volume for blank, and N is normality of $Na_2S_2O_3$.

$$H_2O_2 \text{ \% w/w} = \frac{(\text{A-B})(\text{N})(1.7007)}{\text{Sample weight}} \quad \text{(Eq.4)}$$

2.2.5 Colour Measurement

Colour measurement of sample was conducted with Chroma meter Minolta. The L, a, and b parameter value were measured. The brightness can then be calculated by Eq. 5.

$$\text{Brightness } \% = 100\text{-}[(100\text{-L})^2+(a^2+b^2)]^{0.5} \quad \text{(Eq.5)}$$

III. Results and Discussion

Rice straw hydrotropic pulp obtained by hydrotropic pretreatment and chelation stage. The cellulose, hemicellulose, and lignin composition of rice straw before hydrotropic pretreatment was 31.14%, 28.90%, and 21.10% respectively. The chemical composition of rice straw after the chelation

stage was 37.42%, 25.80%, 18.06% respectively. The hydrotropic pretreatment and chelation stage were able to increase the cellulose content of rice straw by up to 6.28% from the initial composition.

Rice straw hydrotropic pulp was subjected to peroxide bleaching. The effect of increased bleaching reaction time and concentration of hydrogen peroxide on chemical composition in rice straw is shown in **Fig.1** and **Fig.2**. **Fig.1** shows that the application of higher concentration of hydrogen peroxide results in the increase of the cellulose content, in which the highest cellulose content was found in 6% hydrogen peroxide concentration (53.33%). The partial elimination of hemicellulose and lignin causes cellulose content to increase. Bleaching with hydrogen peroxide under alkaline conditions will produce perhydroxyl anion, which is believed to be the main active species in the elimination of chromophore in lignin, especially the conjugated carbonyl structures that react easily with perhydroxyl anion. This reaction will cause the lignin dissolution so that the amount of lignin in the pulp decrease [5]. This phenomenon is characterized by decreasing lignin content with increasing reaction time. Similar results were obtained for cellulose extraction with alkaline peroxide treatment by Fitriana *et al* (2020). The higher hydrogen peroxide concentration used, the higher cellulose content obtained [7].

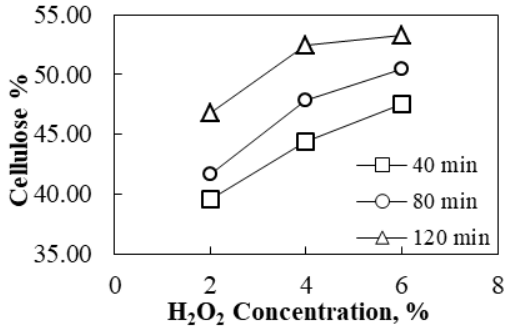

Fig 1. Cellulose % in Rice Straw Hydrotropic Pulp

The hydrotropic treatments, chelation, and bleaching stage not only impact on the changes of the chemical composition of rice straw but also affect the optical properties. The effects of the increased reaction time and concentration of hydrogen peroxide on the brightness of the unbleached pulp are shown in **Fig.3**. Pulp brightness reached the maximum value at 4% hydrogen peroxide concentration for 120 minute reaction time. The brightness of the unbleached pulp was 54,23%, while the brightness of the bleached pulp obtained from bleaching process with 4% hydrogen peroxide concentration for 40, 80, and 120 minutes were 76.29%, 77.28%, and 80.78% respectively.

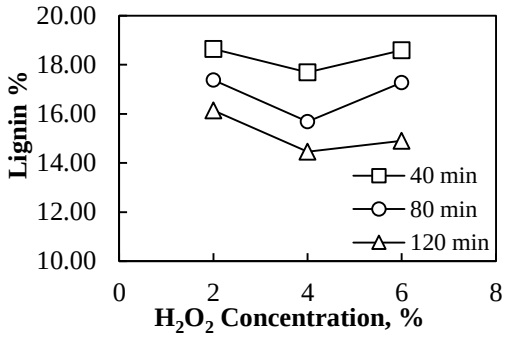

Fig 2. Lignin % in Rice Straw Hydrotropic Pulp

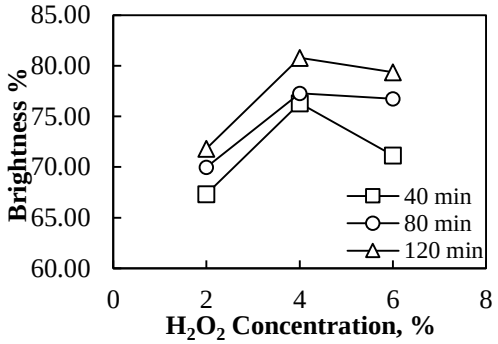

Fig 3. Brightness % Rice Straw Hydrotropic Pulp

Table 1. Yield and H_2O_2 Consumption

No.	H_2O_2 (%)	Time (min)	Yield (%)	H_2O_2 Consumption (%)
1	2	40	61.66	73.13
2	2	80	57.79	88.77
3	2	120	56.15	87.20
4	4	40	60.04	70.16
5	4	80	58.54	79.63
6	4	120	58.47	90.25
7	6	40	65.88	84.21
8	6	80	60.73	88.02
9	6	120	59.10	92.57

The brightness of the rice straw hydrotropic pulp at various times of the bleaching process increased as the hydrogen peroxide concentration increased from 2% to 4%. The increase in brightness of rice straw hydrotropic pulp is caused by the high formation of

perhydroxyl anion, which causes lignin to dissolved [8]. Similar results were obtained for alkaline peroxide bleaching by Tutus *et al* (2014), the brightness of the pulp increases with increasing hydrogen peroxide concentration [9].

The brightness of the rice straw pulp at 6% hydrogen peroxide concentration is lower than 4%. It occurs caused by the use of excess hydrogen peroxide so that some hydrogen peroxide does not react with ion hydroxide to produce perhydroxyl anion but decomposes to oxygen and water [8]. It can be seen in **Table 1,** the consumption of hydrogen peroxide is expressed as the percentage of the residual hydrogen peroxide to the initial amount of hydrogen peroxide added. Consumption of hydrogen peroxide at a concentration of 6% is greater than 4% meanwhile the lignin content of 6% is higher than 4%.

IV. Conclusion

Hydrogen peroxide bleaching of rice straw hydrotropic pulp was able to produce bleached pulp brightness value of 67-80%. Hydrogen peroxide concentration and bleaching time give significant effect on cellulose content, lignin content and brightness of the bleached pulp. The maximum value of bleached pulp brightness was obtained from the bleaching process with 4% hydrogen peroxide concentration at temperature 90^{o}C for 120 minute reaction time with the cellulose content was 52.41% and the lignin content was 14.45%.

Acknowledgement

The authors are thankful to The Ministry of Research, Technology, and Higher Education of Republic of Indonesia for their support this work through PDUPT research grant of 2020 with contract number of 2845/UN1/DITLIT/DIT-LIT/2020.

References

[1] Abraham, A., Mathew, A.K., Sindhu, R., Pandey, A. and Binod, P., 2016. Potential of rice straw for bio-refining: An overview. *Bioresource Technology*, *215*, pp.29-36.,

[2] Matsumura, Y., Minowa, T. and Yamamoto, H., 2005. Amount, availability, and potential use of rice straw (agricultural residue) biomass as an energy resource in Japan. *Biomass and Bioenergy*, *29*(5), pp.347-354.

[3] Ibrahim, M.M., El-Zawawy, W.K., Jüttke, Y., Koschella, A. and Heinze, T., 2013. Cellulose and microcrystalline cellulose from rice straw and banana plant waste: preparation and characterization. *Cellulose*, *20*(5), pp.2403-2416.

[4] Ramos, L.P., 2003. The chemistry involved in the steam treatment of lignocellulosic materials. *Química Nova*, *26*(6), pp.863-871.

[5] Dence, C.W. and Reeve, D.W., Pulp Bleaching: Principles and Practice,(1996).

[6] Datta, R., 1981. Acidogenic fermentation of lignocellulose-acid yield and conversion of components. *Biotechnol. Bioeng.;(United States)*, *23*(9).

[7] Fitriana, N.E., Suwanto, A., Jatmiko, T.H., Mursiti, S. and Prasetyo, D.J., 2020. Cellulose extraction from sugar palm (Arenga pinnata) fibre by alkaline and peroxide treatments. *E&ES*, *462*(1), p.012053.

[8] Fuadi, A.M. and Sediawan, P.P.I.W.B., 2009. Pemakaian hidrogen peroksida sebagai bahan pemutih pulp (Doctoral dissertation, [Yogyakarta]: Universitas Gadjah Mada).

[9] Tutus, A., 2004. Bleaching of rice straw pulps with hydrogen peroxide. *Pakistan Journal of Biological Sciences*, *7*(8), pp.1327-1329.

The 13th AUN/SEED-Net Regional Conference on Chemical Engineering 2020 (RCChE-2020)
Jointly held with
The 5th International Symposium on Conservation and Management of Tropical Lakes
"Insights and Challenges toward Achieving SDGs"

Different Effectiveness of disinfectants on Virus and Bacteria Removal on Surface

Chakriya Kong[1] , Dariya Sek [1], Monychot Tepy Chanto[1,2], Sokly Siev[1,3] , Chanthol Peng [1,3*], Reasmey Tan[2] , Thavarith Chunhieng[1] , Romny Om[4], Phen Sieng[1], San Penh[1]

[1] *Faculty of Chemical and Food Engineering, Institute of Technology of Cambodia, Russian Federation Blvd., P.O. Box 86, 12156 Phnom Penh, Cambodia*
[2] *Food Technology and Nutrition Research Unit, Research and Innovation Center, Institute of Technology of Cambodia, Russian Federation Blvd., P.O. Box 86, 12156 Phnom Penh, Cambodia*
[3] *Water and Environment Research Unit, Research and Innovation Center, Institute of Technology of Cambodia, Russian Federation Blvd., P.O. Box 86, 12156 Phnom Penh, Cambodia*
[4] *Department of Electrical and Energy Engineering,*
**peng@itc.edu.kh*

Abstract

The infectious diseases caused by virus and bacteria have posed serious threats to public health worldwide. The rapid community spread of infection and the lack of sanitization could pose major human health problem. The diseases are often transmitted by close human-to-human contact or by contacting contaminated surface. In prevention, the disinfection of surface is essential to reduce the transmission. In this study, different disinfectant such as ethanol (75% v/v and 90% v/v), hydrogen peroxide (3%) and calcium hypochlorite (2 ppm and 4 ppm) were evaluated their effectiveness under various application conditions to disinfect virus and bacteria on the surface. The virus, bacteriophage T4 and the bacteria, *Escherichia coli* K-12 were used as a model strains in this study. The disinfectants were applied on the virus and bacteria laying on the surface by spraying method for 5 and 10 times with 30s and 60s of contact time. The effectiveness of those disinfectants was evaluated based on the survival of virus and bacteria through plaque assay and spread plate method. As a result, hydrogen peroxide showed the most promising effective disinfectant compared to other. For instance, at spraying for 10 times in 60s, the bacteria are completely reduced and the highest virus reduction was 90%. While ethanol at concentration of 90% showed 85% reduction for virus and around 98% for bacteria, the rest showed reduction less than 50%. This implies that the effectiveness of disinfectant depends on the type, contact time and the concentration.

Keywords: *Disinfectant, Bacteriophage, E. coli, Contacting Time*

I. Introduction

The health center and community acquired infection caused by virus and bacteria have become a majority concern. In prevention, the chemical disinfectants are used to eliminate the contaminated surface. There are many types of disinfectants such as calcium hypochlorite ($Ca(OCL)_2$), ethanol (C_2H_5OH) and hydrogen peroxide (H_2O_2) which are used in different application. Calcium hypochlorite is used as disinfection of water treatment, surface area, etc. Its activity was reported to be effective against *Staphylococcus. aureus*, *Salmonella choleraesuis*, and *Pseudomonas. aeruginosa* with just contact time less than10 minutes [1]. Ethanol is used for hospital pagers, scissors, and stethoscopes, surface and hand sanitation. Ethanol has

antimicrobial activity against with *P. aeruginosa, Serratia marcescens, Escherichia coli* and *Salmonella typhosa,* rotavirus, echovirus, and astrovirus [2]. Hydrogen peroxide used to remove pollutants from waste water and from air and treat pollutions that can be easily oxidized. Hydrogen peroxide is active against *E. coli, Streptococcus species, and Pseudomonas species* [1]. However, it is essential to understand their effectiveness including the safety and killing time in order to choose the right disinfectant to inactivate bacteria and virus for disease prevention.

In review, *E. coli* is a gram negative bacteria which the peptidoglycan layer is relatively thin and it is found at the inside of the outer membrane. *E. coli* is found in the intestine of men and animals and it is released into the environment through fecal material [3]. One of the *E. coli* strain K-12 which is generally used in experimental and considered as nonpathogenic.

The bacteriophage T4 which is one of the strain of bacteriophages that infects *E. coli* K-12 was used as a model virus in this research. T4 phage infection of *E. coli* has been one of the most thoroughly studied model systems in molecular biology and microbiology for over 60 years due to harmless for human [4]. In order to multiply their quantity, they need to get into a bacterium where they break the bacterial cell to release the new viruses[5].

Most of studies focus on the activity of disinfection suspension but little is known about their activity when spraying on the surface application. Recently, the use of various disinfectant on the cabin spray has been emerged. Yet, the study of the effectives of the spray application of disinfectant is unknown. Therefore, the aims of this study is to investigate the effectiveness of different disinfections on model strain of bacteria and virus by spray application. Calcium hypochlorite at 2ppm and 4 ppm, ethanol concentration at 75% and 90%, hydrogen peroxide concentration 3% were carried out to identify their effectiveness against on the bacteria (*E. coli* K-12) and virus (T4 phage) with different contacting time, 30 and 60 second on surface.

II. Materials and Methods

2.1 *Escherichia coli* K-12 preparation

To use *E. coli* K-12 as a model bacterium, the host cell solution was prepared from pure culture *E. coli* K-12's mother stock. The preparation of bacteria was started by selecting a single colony from mother stock to cultivate in 2 ml of Luria- Bertani (LB) liquid media at 37℃ for 18-20h using BR-21UM Bio-shaker at the speed of 120 rpm [6]. The overnight culture of *E. coli* K-12 was probably 1.00E+09 CFU/ml.

2.2. T4 phage Preparation

To prepare this virus, a single plaque of T4 from mother stock was used for propagation with host cell, *E. coli* K-12 using the double layer agar method and incubated at 37 ºC overnight. T4 phage purification was conducted by repeated plating and picking of single plaques, followed by plate lysate and the polyethylene glycol (PEG) # 6000 – NaCl precipitation method [7].The concentration of daughter phage was determined by using plaque essay method.

2.3. Disinfectant Preparation

The stock solution of calcium hypochlorite $Ca(OCL)_2$ was prepared from $\mathrm{Ca(OCL)_2}$ powder by dissolving 0.1g of $Ca(OCL)_2$ in 100ml distilled water. The stock solution was stirred on the magnetic stirrer until they are completely dissolved. The concentration of $Ca(OCL)_2$ were identified using Colorimeter C401. The used concentrations of ethanol were archived by the dilution of absolute ethanol solution 99,9%(v/v) with distilled water. The 3% hydrogen peroxide is purchased from the market. The disinfectant conditions were summarized in **Error! Reference source not found.** .

2.4 Disinfectant Spray Treatment Method

Spreading method is a popular procedure to identify the amount colony of bacteria. In this method, 0.1ml of *E. coli* K-12 overnight culture was pipetted to spread on the layer of Chromocult agar in plastic plate. Then, the plates were transferred to incubator at 37 °C for overnight before counting [8].

Plaque assay is one of the widespread approaches used to determine the amount of infectious virus in a sample. The virus T4 phage stock was vortexed and pipetted 110μ to the 0.5ml eppendorf. After that, 110 µl of host cell *E. coli* K-12 were added. Then, 200 µl of the solution were pipetted and transferred into the 3 ml of LB soft agar which was the complex mixture of tryptone, yeast extraction, Sodium Chloride, Magnesium Sulphate (1M, 0.5% (w/v)) and Calcium Chloride (1M, 0.5% (w/v)). Next, it was poured on the top layer of LB agar. The solution was winded to homogenize and left until it was dried. The culture of bacteriophage was incubated at 37 °C for overnight before counting [9]. The removal effectiveness of disinfectant on

bacteria and virus were calculated by equation below:

$$Removal = \frac{(N_i - N_f) \times 100}{N_i} \qquad \text{(E.q.1)}$$

Where N_i is the number of total colony or plaque without spraying disinfectant, and N_f is the number of colony or plaque after spraying with disinfectant.

Table 1: The spaying condition of disinfectant

Disinfectant	Concentration	Spraying (time)	Contact time (second)
H_2O_2	3%	5, 10	30, 60
$C_5H_5O_6$	75%, 90%	5, 10	30, 60
$Ca(OCl)_2$	2ppm,4ppm	5, 10	30, 60

The spraying treatment on bacteria *E. coli* K-12 was performed duplicate by dropping 5µl of *E. coli* K-12 overnight culture solution (≈1.00E+06 CFU/ml) on the sterilized glass plate. Then the disinfectant was sprayed in 5 time and 10 time on the bacteria surface within contacting time 30 second and 60 second. After that, 5ml of PBS were added and shaken until the solution was homogenous. Then, 0.1ml of that solution was pipetted to conduct spread plate method to determine the bacteria colony.

The spraying treatment on bacteriophage was performed triplicate by dropping 5µl of T4 phage (≈1.00E+06 PFU/ml) on the sterilized glass plate. Then, 5 times and 10 times of disinfectant were sprayed on the T4 phage within contacting time 30 second and 60 second. After that, 5ml of SM buffer were added and shaken until homogenous. Then, plaque essay method was used to identify the plaque of virus.

III. Results and Discussion

The Bacteria (*E. coli* K-12) was removed by the effectiveness of disinfectant under various application conditions. In spraying test, the most effective disinfectants were hydrogen peroxide (3%), ethanol (75% and 90%) spaying 10 times in 60s which the bacteria were completely removed. Furthermore, spraying 10 times in 30s of the same disinfectants revealed the reduction around 98%, while the highest effectiveness of calcium hypochlorite (4ppm) showed only 92% of reduction within spraying 10 times in 60s as have showed in Fig. 1.

In spray treatment test, the effectiveness of T4 phage plaque reduction of disinfectant was noticeable. As have shown in Fig. 2, the most effective disinfectant with the highest removal efficiency is hydrogen peroxide spaying 10 times which was able to remove 90% and 87% of T4 phage with 60s and 30s contacting time respectively. On the other hand, ethanol concentration 90% spraying for 10 times is permitted to reduce 85% in 60s and 70% in 30s. Calcium Hypochlorite 2ppm and 4ppm achieved the lowest effectiveness against bacteria as its efficiency was around 50%.

According to **Error! Reference source not found.** and **Error! Reference source not found.**, the effectiveness of disinfectants on bacteria were higher than the effectiveness of disinfectant on virus. It can be assumed that hydrogen peroxide (3%) and ethanol 90% were the most effective disinfectants against microorganism growth while calcium hypochlorite seemed to be the least effective one compared to other disinfectants.

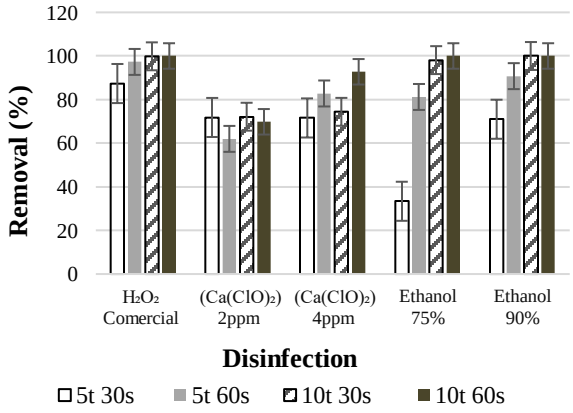

Fig. 1: The removal efficiency of disinfectants on *E. coli* K-12. 5t, 10t: 5, 10 times spry of disinfectants.

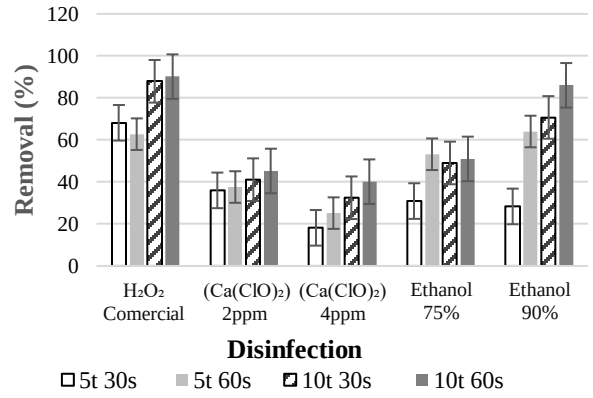

Fig. 2: The removal efficiency of disinfectants on T4 phage

Base on the duration and number of spray, it was shown

that the removal efficiency of bacteria and virus were decrease as the number of spray and contacting time were reduced while increasing the contacting time and number of spray lead to high removal results. Additionally, ethanol 90% and hydrogen peroxide (3%) seemed to be effective for surface disinfection while Calcium Hypochlorite (2ppm) and (4ppm) did not work effectively in this experiment.

The safety level of disinfectants was limited to avoid any unexpected health hazard. The permitted level of hydrogen peroxide is between 6-3% which is commonly used to remove surface contaminated, pollutants from wastewater and, teeth, hair and produced food [1]. Commercially available 3% hydrogen peroxide is a stable and effective disinfection for using on inanimate surfaces. Hydrogen peroxide is poorly absorbed by skin; however, it is mildly irritating to the skin and mucous membranes in the concentration more than 3% [10].

The USA Food and Drug Administration (FDA) classified Ethanol 60-95% was safe and effective active agent to use in antiseptic and hygiene hand wash products [11]. Ethanol is widely used in all kinds of products with direct exposure to the human skin. The higher concentration of Ethanol have been describe to be a higher removal efficiency [12].

The toxic effects of calcium hypochlorite are primarily due to the corrosive properties of hypochlorite. Ingesting a small amount of household bleaches (3-6% hypochlorite) can cause the gastrointestinal irritation and if ingesting more concentrated commercial bleach 10% or higher hypochlorite may suffer severe corrosive injuries to the mouth, throat, esophagus and stomach with bleeding, perforation, and eventually death. Contacting of strong hypochlorite solutions with your skin may cause burning pain, inflammation, and blisters [13].

Surface disinfectant products are used for surface disinfection, which refers to the application of chemical disinfectants to surfaces in order to sanities them. This disinfection differs from aerosol/dry-fogging and water disinfection in terms of the requirements for the disinfectant as well as the mode of application. [14]. Clean and disinfect high-touch surfaces daily in household common areas (e.g. tables, hard-backed chairs, doorknobs, light switches, phones, tablets, touch screens, remote controls, keyboards, handles, desks, toilets, sinks) this type of disinfection primarily involves treating easy-to-clean, washable and chemical-resistant surfaces [15].

IV. Conclusion

The most effective disinfectants for removing bacteria and virus were H_2O_2 concentration 3% and ethanol 90% at 10times 60s which showed 98% removal for bacteria and 90% for virus reduction while the effectiveness of Ca $(OCl)_2$ on bacteria and virus were less than 50%. However, the effectiveness of disinfectants includes calcium hypochlorite, ethanol, and hydrogen peroxide against bacteria and virus depended on the concentration of disinfectants, contacting time and number of spraying.

Although some tested disinfectants showed a promising antibacterial and antiviral on the model strain, in term of dose and safety in spray application is not yet known. The further study is necessary to investigate on health toxicity associated with cabin and disinfectant spray system.

Acknowledgement

We are thankful to the Institute of Technology of Cambodia for the financial support of this study.

References

[1] Rutal,W.A., Weber. D. J. (2019). Guidline for Disinfectant and Sterilization in Healthcare Fecilities, 2008. Center for Disease Control and prevention. University of North Carolina Health Care System pp 40

[2] Kampf, G., Grotheer,D.,Steinmann, J., 2019. Efficacy of three ethanol-based hand rubs against feline calicivirus , *a surrogate virus for norovirus,* pp. 144–149.

[3] Siva,B.,Storms,J.,Sauvageau,Z.,and Dominic,S.,2016. Host receptors for bacteriophage adsorbtion.*FEMS Microbiology letters,*363,1-11.

[4] Bryan,D., El-shibiny,A., Hobbs,Z.,Porter,J., Kutter, E.M., 2016. Bacteriophage T4 Infection of Stationary Phase E . coli. *Life after Log from a Phage Perspective,* vol. 7, no. September, pp. 1–12.

[5] Gutiérrez,D., Fernádez, L., Maetínez, B., Rodríguez, A.,García, P., 2016. Bacteriophage. The Enemies of Bad Bacteria Are Our Friends. Frontiers for Young Minds,vol.4.

[6] Karen,L.,Roger,B.,(2018) Growth of E.coli in liquid media. Current protocol in molecules biology vol 125, pp81

[7] Synnott. A. J., Kuang.Y., Kurimoto. M.,Yamamichi. K., Iwano. H., Tanji.Y. (2009). Isolation from

sewage influent and characterization of novel Staphylococcus aureus bacteriophages with wide host ranges and potent lytic capabilities. *Appled Environ Microbiology*

[8] Spread plate technique; principles,procedure and advance,(2019).Microbe Noted. https//microbenotes .com/spread-plate-technique/. Assesed 05 December 2020

[9] Acharya,T.,(2018). Medical Micrology Guid. Bacteriophage plaque Assay Principle, Procedure and Results. https://microbeonline.com/phage-plaque-assay-principle-procedure-results/.Assesed 05 December 2020.

[10] Agency for Toxic Substances and Disease Registry 4770 Buford Hwy NE Atlanta, GA30341: Toxic Substance Portal-Hydrogen Peroxide

[11] Food and Drug Administration: Tentative final monograph for healthcare antiseptic drug products; proposed rule. Federal Register. 1994, 59: 31441-31452.

[12] Kramer A, Rudolph P, Kampf G,Pittet D: Limited efficacy of alcohol-based hand gels. Lancet. 2002, 359: 1489-1490. 10.1016/S0140-6736(02)08426-X.

[13] Agency for Toxic Substances and Disease Registry (ATSDR). 2002. Managing Hazardous Materials Incidents. Volume III – Medical Management Guidelines for Acute Chemical Exposures: Calcium Hypochlorite/Sodium Hypochlorite Atlanta, GA: U.S. Department of Health and Human Services, Public Health Service.

[14] Eichtalstrasse 49 CH-8634 Homebrechtikon., 2020 Sanosil LTD. All Rights Reserved.

[15] CDC Home Care Guidance for people pets., Centers for Disease control and prevention., July10, 2020: Detail Disinfection Guidan.

The 13th AUN/SEED-Net Regional Conference on Chemical Engineering 2020 (RCChE-2020)
Jointly held with
The 5th International Symposium on Conservation and Management of Tropical Lakes
"Insights and Challenges toward Achieving SDGs"

Identification and Quantitative Analysis of Alternative Diesel from Waste Plastic Pyrolysis

Zin Thu Aung [1], Chinda Charoenphonphanich[1*], Hidenori Kosaka [2], Pop-Paul Ewphun[2], Prathan Srichai[3]

[1]*School of Engineering, Department of Mechanical Engineering, King Mongkut's of Institute of Technology Ladkrabang, Soi chalongkrung1, Ladkrabang, Bangkok 10520 Thailand*
[2]*School of Engineering, Department of System and Control Engineering, Tokyo Institute of Technology, Ishikawadai 6th Building, Room 323-2-12-1 Ookayama, Meguro-ku, Tokyo, 152-8552, Japan*
Department of Mechanical Engineering, Princess of Naradhiwas University, Naradhiwas 96000 Thailand
**Corresponding author: kmitl.chinda@gmail.com*

Abstract

Plastic is a synthetic material made from a wide range of organic polymers, facilitating the human life and helping promote the global economy. The use of plastics, however, has been associated with significant environmental problems due to their accumulation in landfills, as plastic waste does not degrade or degrades at very low pace. Nowadays, fast pyrolysis of waste plastic into valuable fuels is main platform method in the waste disposal but also could be used as alternative fuel for internal combustion engines. The purpose of this study was to identify, quantify and compare the composition of waste plastic diesel (WPD) with the commercial diesel (CD) of Thailand. Simulated distillation (GC-FID) and n-d-M method were used for finding the composition of both fuels. Results indicated that the content of naphtha, kerosene, diesel, and heavy oil were determined quantitatively and also identified the paraffin, naphthenes, and aromatic contents for both fuels. Naphtha and heavy oil contents of WPD were 9.2 and 8.9wt% higher than those of CD but kerosene and diesel contents were 0.7and 17.4wt% less than those of commercial diesel. After that, paraffin, naphthenes and aromatic contents of WPD from hydrocarbon type analysis were 80.42, 14.54 and 5.04wt% and these hydrocarbon contents of CD were 60.61, 25.91 and 13.48wt% respectively. By knowing them, the appropriate method can be determined for fuel upgrading and interpret correctly the combustion and emissions results.

Keywords: *Fast pyrolysis, Simulated distillation, n-d-M method, Waste plastic diesel, Commercial diesel*

I. Introduction

Plastics are essential materials due to their numerous applications in daily life. Consequently, a huge number of plastic products accumulate as waste in the environment. Plastic waste is a big issue in the world including Thailand, because the amount of recycled plastic remains low due to recycling problems [1]. One of the recycling problems is economy as they need to be collected separately or sorted before the process can begin [2]. Most plastics are not compatible with each other and hence they cannot be processed together during recycling.

For instance, a polyvinyl chloride (PVC) bottle in polyethylene terephthalate (PET) recycle can ruin the entire batch by becoming yellowish and brittle [3].Unlike recycling, pyrolysis does not require a keen sorting of different plastics. Therefore, fast pyrolysis of waste plastic into valuable fuels is main platform method the waste disposal but also could be used as alternative fuel for internal combustion engines.

Previous studies found that individual type of waste plastics or mixed waste plastic, which were used to produce alternative fuel, identify the chemical compounds and carbon number, and investigate the physical properties [4-6]. There are no or few studies to quantify the boiling fractions and hydrocarbon type of waste plastic fuel.

Therefore, the purpose of this study is to identify and

quantify the composition of waste plastic diesel (WPD) from real mixed waste plastic pyrolysis, and compare with commercial diesel (CD).

II. Materials and Methods

2.1. Materials

The waste plastic diesel utilized in this study was derived from catalytic fast pyrolysis of real mixed waste plastic (mostly PVC) and commercial diesel (B10) were purchased from PTT fuel station in Thailand. **Table 1** shows the comparison of physical properties of WPD and CD.

Table 1. Physical properties of fuels

Property	ASTM Method	CD	WPD
Density@15℃ (kg/m^3)	D4052	824	805
Viscosity@40℃ (Cst)	D445	3.24	2.9
Cetane Index	D976	56.43	67.93
Energy Content (MJ/kg)	D240	45.86	46.29
Sulfur Content (wt.%)	D5453	0.003	0.014

2.2. Simulated Distillation Method

The identification and quantitative analysis of WPD and CD were done by simulated distillation (ASTM D2887). Simulated distillation is a Gas Chromatographic technique for determining the boiling point distribution of fuels by Flame Ionization Detection (GC-FID). Two standard solutions were used for quantification of waste plastic diesel and commercial diesel: normal alkanes ranging from n-C_5 to n-C_{10} and n-C_{10} to n-C_{40}. **Table 2** shows the testing condition of GC-FID. In simulated distillation method, the analyse retention times are directly related to the boiling points of various hydrocarbons. A calibration curve is generated from standard solution, where the retention time of each n-alkane is plotted against its boiling point. Calculating the area of each time interval allows the proportion of elution weight (%) in each time interval. The elution weight (%) in each boiling point range can be determined from calibration curve and used to obtain the relationship between the elution weight (%) and boiling point to create the distillation curve of fuel samples.

Table 2. Experimental conditions for ASTM D2887

Column	DB-10,10mx0.53mm,2.65µm
Column temperature	40℃ to 350℃
Carrier gas flow rate	13.989 L/min (helium)
Injection temperature	350℃
FID temperature	375℃
Gas flow rate	
Nitrogen (makeup)	45 mL/min
Hydrogen	40 mL/min
Air flow	450 mL/min
Injection volume	0.1 µL

2.3. n-d-M Method (PNA composition Analysis)

This method requires three physical properties of refractive index (n_{20}), density (d_{20}), and molecular weight (M). For this reason, the method is called n-d-M method. The method is included in the ASTM manual under ASTM D3238. It calculates the distribution of carbon in paraffin (%C_P), naphthenes (%C_N), and aromatics (%C_A) using equations 1 to 5. The refractive index and density at 20℃ and molecular weight are used as input data, which are estimated from correlations that are adopted in API-TDB [7].

$$v = 2.51(n - 1.475) - (d - 0.851) \quad \text{(Eq.1)}$$

$$a = 430 \; if \; v > 0 \; and \; 670 \; if \; v < 0$$

$$\%C_A = av + 3660/M \quad \text{(Eq.2)}$$

$$w = (d - 0.851) - 1.11(n - 1.475) \quad \text{(Eq.3)}$$

$$\%C_R = 1440w - 3\%S + \frac{10600}{M} if \; w < 0 \quad \text{(Eq.4)}$$

$$\%C_R = \%C_N + \%C_A \quad \text{(Eq.5)}$$

$$\%C_P = 100 - \%C_R \quad \text{(Eq.6)}$$

III. Results and Discussion

` The simulated distillation curve represents the boiling points of compounds in a fuel mixture at atmospheric pressure. Simulated distillation curve is presented in term of boiling point versus wt% of mixture vaporized because composition is measured in terms of wt% or weight fractions in gas chromatography. Simulated distillation curve is very close to actual or true boiling point curve. The distillation curve obtained applying the ASTM D2887 method allow the quantification of fuel composition such as naphtha, kerosene, diesel and heavy oil as shown in **Fig. 1**. The composition of CD and WPD are listed in **Table 2**.

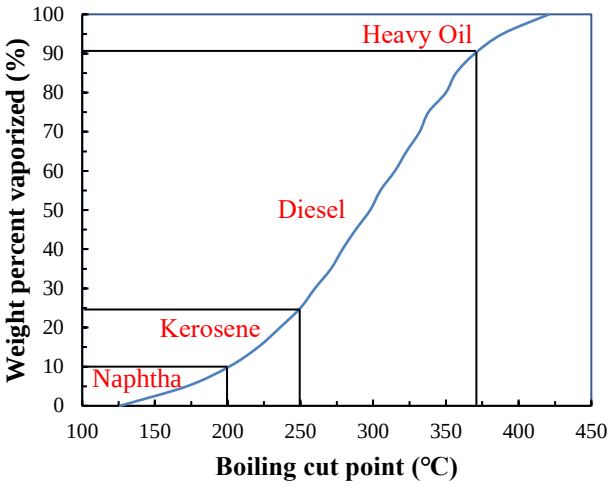

Fig. 1. Distillation curve with cut points

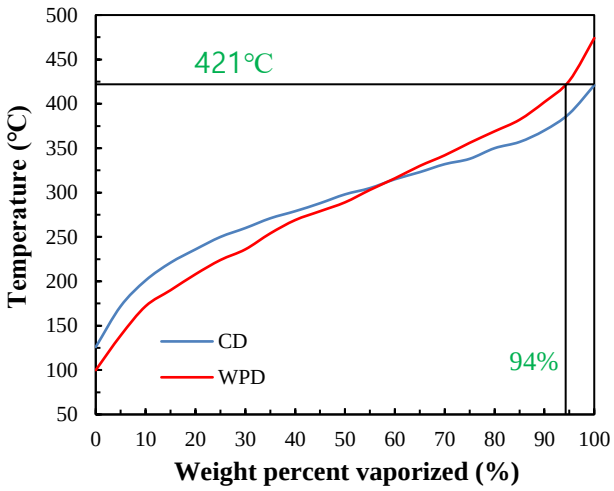

Fig. 2. Comparison distillation curves of CD and WPD

Table 2. Fuel compositions of WPD and CD

Composition	Cut point range	CD wt.%	WPD wt.%
Naphtha	IBP-200℃	9.6	18.8
Kerosene	200-250℃	15.4	14.7
Diesel	250-370℃	65.2	47.8
Heavy Oil	370-FBP	9.8	18.7

It can be seen that naphtha and heavy oil contents of WPD were 9.2 and 8.9 wt% higher than those of CD but kerosene and diesel contents were 0.7 and 17.4% wt% less than those of commercial diesel.

A comparison of the distillation curve between CD and WPD is shown in **Fig. 2** and distillation temperatures of WPD and CD are provided in **Table 3**. In **Fig. 2**, initial boiling range of WPD is almost 60% lower and final boiling range is almost 40% higher than those of CD. Therefore, the WPD can be called as wide distillation fuel (WDF) because it is included lighter and heavier compounds than those of CD. In fact, the lighter and heavier compounds can be removed to match the initial boiling point and final boiling point of WPD and CD fuels by distillation. Nowadays, gasoline-diesel blended or wide distillation fuels have potential to reduce soot emission and increase thermal efficiency but HC emission of these fuels are slightly higher than that of diesel because of low cetane number [8]. Remarkably, cetane index of WPD is much higher than that of CD, although it contains almost 60% of lighter compounds. Paraffin and aromatic ratio of WPD is higher than that CD as shown in **Table 4** of WPD

Table 3. Boiling points of WPD and CD

Distillation Wt.%	ASTM	CD (℃)	WPD (℃)
IBP:0.5%		126	100
10%		201	172
20%		236	208
30%		260	236
50%		298	289
60%	2887	315	316
70%		332	342
80%		350	369
90%		370	402
95%		389	426
FBP:99.5%		421	474

For low temperature combustion of modern diesel engine, desirable fuel characteristics are low aromatic and high cetane index (high normal paraffin) but high cetane index and end boiling point can lead to high smoke for hot temperature combustion of normal diesel. **Table 5** shows that all detected carbon number concentrations of WPD are greater than that of CD. That is why WPD has high cetane index and paraffin contents. The C_{28}-C_{40} are not detected for both fuels but three peaks are detected between C_{24} and C_{28} in WPD. Therefore, end fractions 6% of WPD should be removed to achieve the same end point as shown in **Fig. 2** and **Table 5**.

Table 4. PNA concentration of fuels

Carbon Content	CD	WPD
Paraffin (%C_P)	60.61	80.41
Naphthenes (%C_N)	25.91	14.54
Aromatic (%C_A)	13.48	5.05

Table 5. Constituents (area%) identified by GC-FID

Carbon Content	CD	WPD
C6	2.1457	3.38784
C7	Not detected	1.71151
C8	Not detected	2.35746
C10	Not detected	1.41769
C11	1.38791	3.71853
C14	2.84199	4.32735
C15	1.7203	4.77871
C16	1.07963	5.20978
C17	2.42153	5.19759
C18	3.68398	6.00175
C20	3.59628	5.52902
C24	1.47851	3.10487
-	Not detected	2.52215
-	Not detected	2.06772
-	Not detected	1.61383
C28	Not detected	Not detected
C32	Not detected	Not detected
C36	Not detected	Not detected
C40	Not detected	Not detected

IV. Conclusion

In this work, the composition of WPD are identified and quantified using simulated distillation and n-d-M methods. Some conclusions can be drawn as follows.

1. Naphtha and heavy oil contents of WPD were 9.2 a nd 8.9wt% higher than those of CD but kerosene and diesel contents were 0.7and 17.4wt% less than those of commercial diesel.

2. Initial boiling range of WPD is almost 60% lower and final boiling range is almost 40% higher than those of CD. Therefore, the WPD can be called as wide distillation fuel (WDF) because it is included lighter and heavier compounds than those of CD.

3 All detected carbon number concentration of WPD are greater than that of CD. That is why WPD has high cetane index and paraffin contents. Then, the C_{28}-C_{40} are not detected for both fuels but three peaks are detected between C_{24} and C_{28} in WPD. Therefore, end fractions 6% of WPD should be removed to achieve the same end point.

Acknowledgement

This work was supported by ASEAN University Network/Southeast Asia Engineering Education Development Network (AUN/SEED-Net). The authors would like to thank Assoc. Prof. Dr Kanit Wattanavichien, Center of Fuel and Energy from Biomass (Chulalongkorn University) for his contribution in this work.

References

[1] W Khatha., S Ekarong., M Somkiat., S Jiraphon.,2020. Fuel properties, performance and emission of alternative fuel from pyrolysis of waste plastic. IOP Conf. Series: Materials Science and Engineering 717.

[2] Fazal Mabood., M.R.Jan Jasmin Shah., Farah Jabeen., 2012. Catalytic pyrolysis of waste plastic and tyres. LAP LAMBERT academic publishing, U.S.A.

[3] Anandhu, V., Jilse, S., 2018. Pyrolysis process to produce fuel from different types of plastic- a review. IOP Conf. Series: Materials Science and Engineering 396.

[4] Brajendra, K.S., Bryan, R.M., Karl, E.V., Kenneth, M.D., Nandakishore, R., 2014. Production, characterization and fuel properties of alternative diesel fuel from pyrolysis of waste plastic grocery bags. Fuel processing technology 122, 79-90.

[5] A.M. Motawie., Hala. B.I., Hasabo, M.A., Sahar, M.A., R.M, Abualsoud., 2016. Fractional distillation of fuel from mixed plastic waste. Conference paper.

[6] Z.T, Aung., C, Charoenphonphanich., H, Kosaka., P, Ewphum., P, Srichai., 2019. Investigation on physical properties and measurement of bulk modulus of waste plastic diesel. The 10th AUN/SEED-NET RCMEManuE,129-132.

[7] M. R, Riazi., 2005. Characterization and properties of petroleum fractions. 1st ed. ASTM, U.S.A.

[8] J, Wang., Z, Wang., H, Liu., 2015. Combustion and emission characteristics of direct injection compression ignition engine fueled with full distillation fuel. Journal of fuel 140, 561-567

The 13th AUN/SEED-Net Regional Conference on Chemical Engineering 2020 (RCChE-2020)
Jointly held with
The 5th International Symposium on Conservation and Management of Tropical Lakes
"Insights and Challenges toward Achieving SDGs"

Hydrothermal Technology for Wastewater Treatment Plants Sludge Treatment Into Potential Organic Liquid Fertilizer

Farida Crisnaningtyas[1*], Mohammad Fahrurrozi[1], Arif Sosiawan[2], Chandra Wahyu Purnomo[1,3]

[1]*Department of Chemical Engineering, Faculty of Engineering, Universitas Gadjah Mada Jl. Grafika No. 2 Sleman, Yogyakarta 55381, Indonesia*
[2]*PT. Sarihusada Generasi Mahardhika, Yogyakarta Factory, Yogyakarta Indonesia*
[3]*Agrotechnology Innovation Center, PIAT-UGM, Sleman, Yogyakarta, Indonesia*
**farida2018@mail.ugm.ac.id*

Abstract

Wastewater Treatment Plants (WWTP) sludge can be converted into liquid fertilizer using hydrothermal treatment (HT). This conversion technology utilizes high temperature and pressure with the presence of water as a solvent as well as reactant. Treatment temperature of 180ºC, 200 ºC, 220 ºC, with water-sludge ratio of 1:3, 1:5, 1:7, and a residence time of 30 minutes were used in this research. The sludge was mixed with zeolite as catalyst, with ratio of 20% (w/w) of the sludge. Liquid product was analyzed for the content of macronutrients (i.e. N, P, K) using the Kjeldahl method, Phosphate High Range Portable Photometer, and Pottasium High Range Portable Photometer, respectively. The content of micronutrients was analyzed by using Inductively Coupled Plasma (ICP). The results showed that the liquid product has concentration of 4000-16000 ppm of total N, 300-800 ppm of P, and 3000-5000 ppm of K. Result shows that there was a potential application to utilize the liquid as organic fertilizer. The solid product was become more stable and safer to be disposed.

Keywords: *hydrothermal, sludge, liquid fertilizer, waste treatment*

I. Introduction

Dairy industry generates a large amount of solid waste which is easily to decomposed that causes an unpleasant odor in the environment [1]. Several methods to treat solid waste including sludge from wastewater treatment plants (WWTP) are composting, fermentation, fortification, pyolysis, hydrothermal, and so on [2]. The method used is focused on decreasing the growth rate of bacteria, thereby inhibiting further digestion of sludge, making it more stable in the environment. Fermentation and composting methods take a longer time, more than one day or even weeks to get the results [2]. Meanwhile, pyrolysis method requires pretreatment before being put into the reactor. On the other hand, hydrothermal offers effective and economical sludge treatment by thermal method with rapid process. It is require high temperature and pressure surrounded by water during the reaction time. In hydrothermal process, the solid material is bounded by water during reaction, which is kept in liquid state by allowing the pressure to rise with the steam pressure in high-pressure

reactors [3]. After hydrothermal process, waste sludge becomes more stable. If the raw materials contain organic materials, the characteristic of the hydrothermal product would slightly different, but with more stable and safe properties, so we can use it into something more valuable such as fertilizer, both solid and liquid compounds such as N,P,K, and micronutrients.

Research on hydrothermal has been done a lot. Yuan et al. used hydrothermal technology with an operating temperature of 110ºC to 200ºC; reaction time 0, 10, 30, 60 minutes; stirring 60 rpm to study the fertilizer potential of liquid product from hydrothermal treatment of swine manure [4]. Jambaldorj states that the concentrations of N and K decrease when the temperature is increased, but that the concentration of P increases when the temperature is increased [5]. Shao et al, said about the advantage of hydrochar from the hydrothermal process and it can be used as an adsorbent material and solid fuel by using an operating temperature of 130-190ºC, *holding time* 1 hour, and the ratio of liquid and solid is 8:1 [6].

Publications on the processing of dairy waste using the hydrothermal method are still rare. Research on this shows that organic waste from the dairy industry can be used to recover nutrient elements which can be used as raw material for fertilizer production.

II. Materials and Methods

2.1. Materials

Sludge was collected from a wastewater treatment plant of a dairy milk factory located in Jogjakarta. Sludge has moisture content of 89,03% and pH of 6,94. Composition of N, P and K was 1.96, 0.71, 0.14 respectively, meanwhile, for Ca, Mg, Fe, Mn, Cu, and Zn were 0.51, 0.09, 0.77, 0.09. 0.01, 0.05 respectively. Natural zeolite (3 mesh) for the experiment was taken from Klaten, Central Java.

2.2. Experimental set-up

Hydrothermal treatments were carried out in a 2 L batch reactor. The reactor was equipped with a stirrer, a pressure sensor, and a temperature controller as shown in Figure 1.

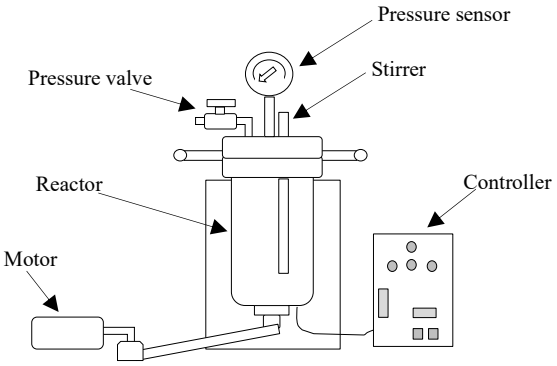

Figure 1. Scematic view of small scale hydrothermal reactor

The sludge was mixed with distilled water with the ratio of 1:3, 1:5, and 1:7. Natural zeolite was added to the reactor with 20% of sludge. Reactor was sealed, then heated with the average heating rate of 6°C/min to targeted temperatures (180, 200, and 220 °C) and kept for 30 min (the holding time). Once the holding time was completed, the reactor was cooled down (< 60°C) and depressurized. The treated mixture was taken out. Solid and liquid were separated. The solid phase was oven-dried (105°C for 4-8 hours) meanwhile liquid phase was filtered through sterile analytical filter units (Whatman 42). A schematic diagram of the experimental setup is shown in Figure 2.

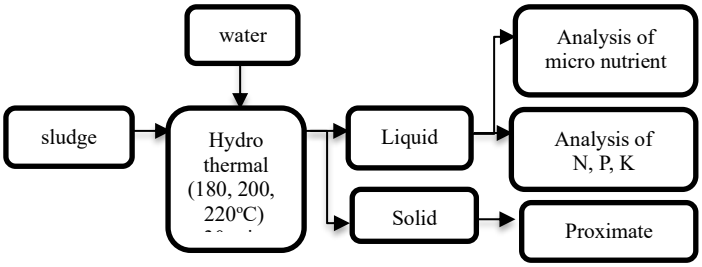

Figure 2. Schematic diagram of experimental

2.3. Analyses

The macro and micronutrients were analyzed after product separation. The total-N was measured using the Kjeldahl method while potassium (K) and Phosphate (P) were analyzed with HANNA portable high range spectrophotometer (HI96717, HANNA, USA). The micronutrient and other heavy metals were determined using the ICP emission spectroscopy (8300, Perkin Elmer, USA).

.

III. Results and Discussion

The hydrothermal treatment produces three products i.e liquid, solid and gas products. The distribution of those products was shown in Table 2. Experiments showed when temperature increased, the yield of liquid product also increased. When the temperature raised, the solid production decreased gradually and the liquid product increased [8]. In Table 2, the amount of liquid product has increased as well as temperature increase. The highest amount of liquid produced at 220°C. This happened because biomass conversion needed the role of temperature to provide heat to disintegrate the fragmentation of biomass bonds [8]. Temperature is the most influential parameter for bio-oil from hydrothermal liquefaction process with raw materials for several types of biomass [9]. High temperature causes a higher reaction speed and affects the number of hydrolyzed compounds [10]. The same results were observed for the reaction of cellulose in water at 190°C in the absence of pressurized H_2, suggesting that the solubilization ratio appears to be temperature-dependent only [11].

Table 2. Distribution of solid and liquid product after hydrothermal process

Ratio	Temp, (°C)	Liquid (ml)	Solid (g)
1:3	180	500	174
	200	504	130
	220	505	131
1:5	180	700	169
	200	705	121
	220	750	97
1:7	180	800	119
	200	860	67
	220	865	68

Besides temperature, the water-sludge ratio had an important effect on the production of liquid products from hydrothermal process. The higher ratio of water/sludge, the higher quantity of liquid product was generated. Water becomes the solvent of hydrothermal process. It has an important role to enhance the stability and solubility of decomposition compounds. As reported previously, the increase of water in the ratio, enhance the yield of liquid and gas [12]. On the other hand, the highest amount of solid product was in the lowest temperature.

Effects of temperature on the nutrient components

The concentration of nutrients in the liquid product of hydrothermal was shown in Table 3 and Table 4. The macronutrients in liquid product were Nitrogen (N), phosphate (P), and potassium (K).

Table 3. The concentration of macronutrients in the liquid product of hydrothermal

Ratio	Temp, (°C)	N (mg/L)	P (mg/L)	K (mg/L)
1:3	180	16223	680	4200
	200	12236	810	5400
	220	9032	860	6800
1:5	180	9339	550	4000
	200	8357	740	5200
	220	7073	810	5400
1:7	180	5360	480	3400
	200	5115	550	4200
	220	4322	700	4800

The effects of temperature on the nutrient component produced from hydrothermal treatment were shown in table 3. The higher the temperature, the higher the P and K obtained. The result shows that the highest concentration of P and K was achieved at 220°C. On the other hand, the concentration of N decreased when the temperature increased. The reason is that the steam supply increased as well as the temperature increase and make the dilution happened.

But among the other compounds that were produced in this experiment, Nitrogen was found to be in the highest concentration. This merely because the initial concentration of Nitrogen in the sludge's raw material was also high. Before treatment, nitrogen was present in the form of macromolecular organic nitrogen in the solid phase of the sludge.

Beside the macronutrient, there was micronutrient content from the sludge that we want to gain as the potential materials for fertilizer. Table 4 shows that the contents of micronutrient in the liquid product from 180°C to 200°C, most of the elements were increased as well as the temperature increase, but the micronutrients decrease when the temperature increase from 200°C to 220°C.

Table 4. The concentration of micronutrients in the liquid product of hydrothermal

Ratio	Temp (°C)	Fe (%)	Al (%)	Mn (%)	Ca (%)	Na (%)	Si (%)
1:3	180	0.006	0.001	6.9E-05	0.195	0.023	0.013
	200	0.007	0.005	9.41E-05	0.190	0.027	0.014
	220	0.006	0.004	5.76E-05	0.198	0.027	0.016
1:5	180	0.004	0.001	9.05E-05	0.143	0.018	0.019
	200	0.004	0.004	4.48E-05	0.099	0.018	0.020
	220	0.003	0.003	5.96E-05	0.121	0.016	0.021
1:7	180	0.002	0.001	3.08E-05	0.100	0.011	0.016
	200	0.003	0.002	4.64E-05	0.110	0.013	0.018
	220	0.002	0.002	2.47E-05	0.084	0.013	0.017

After separated the liquid and solid product of hydrothermal treatment, and dried the solid product, the proximate analysis was carried out by using several standards: ASTM D3173 for water content, ASTM D3174 for ash content, ASTM D3175 for volatile content, and ASTM D3172 for fixed carbon content. The result of the proximate analysis is shown in Table 5.

Table 5. Proximate analysis of solid product

Temp (°C)	Moisture (%)	Ash (%)	volatile matter (%)	fixed carbon (%)
Raw	9.62	52.00	31.38	7.00
180	5.31	46.59	28.69	19.41
200	4.95	44.90	37.77	12.38
220	6.93	41.18	33.66	17.24

Table 5 indicates that the carbon content of sludge increase after hydrothermal treatment. The fixed carbon content is influenced by moisture, ash, and volatile matter. If the ash and volatile content increase, the combustion efficiency will reduce [13].

IV. Conclusion

The liquid product of hydrothermal treatment from wastewater treatment plant sludge contained the main nutrient elements (N, P, K) and the micronutrient needed by plants. The results showed that liquid products had conc entrations of 4000-16000 ppm Nitrogen, 400-800 ppm P hosphate, and 3000-6000 ppm Potassium. The optimum concentration of macronutrients (N, P, K) is produced at 180°C and 1:3 ratio of sludge/water. Considering the res ult from the liquid product, hydrothermal could be a pro mising technology for producing potential liquid fertilize r from the sludge waste.

References

[1] B. S. S. and N. P. Shinkar, "Dairy Industry Wastewater Sources , Characteristics & its Effects on Environment," *Int. J. Curr. Eng. Technol.*, vol. Vol.3, No., pp. 1611–1615, 2013.

[2] S. Rana, P. Mishra, R. Gupta, and L. Singh, *solid-wastes to useful products*. Elsevier B.V., 2020.

[3] J. A. Libra *et al.*, "Hydrothermal carbonization of biomass residuals: a comparative review of the chemistry, processes and applications of wet and dry pyrolysis," *Biofuels*, vol. 2, no. 1, pp. 71–106, 2010.

[4] T. Yuan *et al.*, "Fertilizer potential of liquid product from hydrothermal treatment of swine manure," *Waste Manag.*, vol. 77, pp. 166–171, 2018.

[5] G. Jambaldorj, M. Takahashi, and K. Yoshikawa, "Liquid Fertilizer Production from Sewage Sludge by Hydrothermal Treatment," *Proc. Int. Symp. EcoTopia Sci. 2007*, vol. 07, pp. 605–608, 2007.

[6] Y. Shao, Y. Long, H. Wang, D. Liu, D. Shen, and T. Chen, "Hydrochar derived from green waste by microwave hydrothermal carbonization," *Renew. Energy*, 2018.

[7] Q. Mo, J. Liao, L. Chang, A. L. Cha, and W. Bao, "Transformation behaviors of C , H , O , N and S in lignite during hydrothermal dewatering process," vol. 236, no. August 2018, pp. 228–235, 2019.

[8] S. Nizamuddin *et al.*, "An overview of effect of process parameters on hydrothermal carbonization of biomass," vol. 73, no. December 2016, pp. 1289–1299, 2017.

[9] B. De Caprariis, P. De Filippis, A. Petrullo, and M. Scarsella, "Hydrothermal liquefaction of biomass : Influence of temperature and biomass composition on the bio-oil production," *Fuel*, vol. 208, pp. 618–625, 2017.

[10] Z. Robbiani, "Hydrothermal carbonization of biowaste / fecal sludge Conception and construction of a HTC prototype," ETH Zurich, 2013.

[11] M. T. Reza, M. H. Uddin, J. G. Lynam, S. K. Hoekman, and C. J. Coronella, "Hydrothermal carbonization of loblolly pine : reaction chemistry and water balance," *Biomass Convers. Biorefinery*, vol. 4, pp. 1–11, 2014.

[12] M. K. et al Jindal, "Effect Of Process Conditions On Hydrothermal Liquefaction Of Biomass 1*," *IJCBS Res. Pap.*, vol. 2, no. 8, pp. 8–18, 2015.

[13] A. A. Khan, W. De Jong, P. J. Jansens, and H. Spliethoff, "Biomass combustion in fluidized bed boilers : Potential problems and remedies," *Fuel Process. Technol.*, vol. 90, no. 1, pp. 21–50, 2008.

The 13th AUN/SEED-Net Regional Conference on Chemical Engineering 2020 (RCChE-2020)
Jointly held with
The 5th International Symposium on Conservation and Management of Tropical Lakes
"Insights and Challenges toward Achieving SDGs"

Fate and Transport of Antibiotics from Pig Farms along the Bang Pakong River, Thailand

Rathborey Chan [1,2,3*], Ratboren Chan[1,2], Sirinthrar Wandee[2], Manna Wang[3], Wilai Chiemchaisri[2], Chart Chiemchaisri[2] and Chihiro Yoshimura[3]

[1]*Faculty of Hydrology and Water Resource Engineering, Institute of Technology of Cambodia, Russian Federation Blvd., P.O. Box 86, 12156 Phnom Penh, Cambodia*
[2]*Department of Environmental Engineering, Faculty of Engineering, Kasetsart University, Bangkhen, Bangkok, 10900 Thailand*
[3]*Department of Civil and Environmental Engineering, Tokyo Institute of Technology, Ookayama, Meguro-ku, Tokyo 152-8552, Japan*
**Corresponding author: chanrathborey@itc.edu.kh*

Abstract

This study was investigated the impact of different season (dry and rainy seasons) in 2018 on the fate and transport of antibiotics drained from pig farms along the Bang Pakong River, Thailand. Twenty-one residual and antibiotics were detected in pig farm effluent, drainages, and the river in both seasons. Amoxicillin, tetracycline, chlortetracycline, and tiamulin were detected as dominant compounds in pig farm effluent, showing detection ratio of 83–100%. Maximum residual concentrations of those antibiotics were 0.12–5.20 in the dry season and 0.12–16.10 µg/L in the rainy season. Tetracycline (15.1 µg/L) and chlortetracycline (16.1 µg/L) were found at the highest concentration in the rainy season. We the applied multiple linear regression and random forest to residual antibiotics from pig farm effluents and the river in both seasons in order to model dilution and removal processes of antibiotics drained in river. Beside dilution, removal processes of antibiotics were defined by their partition coefficients, solubility, biodegradability, and volatility. Compared to multiple linear regression, random forest models better helped us to identifying the removal processes of pig farm antibiotics drained to river (R^2: 0.77 in the dry season, 0.35 in the rainy season).

Keywords: *Residual Antibiotics, Pig Farm, Random Forest, Molecular Property*

I. Introduction

Pig farms in Thailand were developed in the 1960s when the first commercial pig feeds were imported from the United Kingdom and the United Stage. Antimicrobial drugs for prevention pig diseases and growth promoter was take into consideration in this development. Common antibiotics uses in pig farms were in classes of β-lactam, tetracyclines, sulfonamides, lincosamides, macrolides, and quinolones[1]. Those antibiotics are given to pigs through feeds, drinking water, and others as injection. But dosages and consumption pattern of those compounds are varied across regions and countries worldwide. Due to low adsorption of antibiotics in pig's gut, 30%–90% of antibiotics were estimated to excrete to the environment through manure and urine. Then, those compounds consisting in wastes could then enter the stream or river via runoff or direct pig farm effluent discharged. Additionally, residual antibiotics in the surface water, even at the low concentration, could also exert selective pressure to the bacterial population to acquire antibiotic resistant, which is more harmful to human and animal.

When antibiotics reached river from pig farms and other sources, their removal processes during transport along the river depended on dilution and their molecular properties [2]. The rate disappearance of antibiotics through dilution was clearly shown to associate with seasonal variation (i.e., dry and rainy season) and movement of antibiotics drained along the river. In contrast, the information about all significant molecular properties that could affect removal processes of antibiotics drained along the river have never mentioned in one study area. Moreover, statistical methods that can make more evident the relationship between one response variable and two or more explanatory variables are rarely used. Since it is currently not possible to quantitatively describe removal processes of antibiotics, we aim to study impact of seasonal variation on fate and transport of pig farm antibiotics drained long the river. Multiple linear regressing and random forest models were applied to residual antibiotics from the pig farm effluent and river in both seasons to model the dilution and their molecular properties, which possibly effect removal processes of antibiotics drained in the river.

II. Materials and Methods

2.1. Study area and sample collection

The site investigation was conducted at Chachoengsao Province, which is in the eastern Thailand and known as one of intensive pig production areas. Water consumed in most pig farms is commonly Bang Pakong River water. Typical wastewater treatment used in pig farms is lagoon treatment in series, but additional anaerobic digestion is mostly found at large farms. Fig.1a shows all sampling locations and flow direction of six farm (F1-F6), nine drainage water sampling location (D1-D9), and nine river sampling locations (R1-R9). Pig farm F2, F4, and F6 are classified into small farms while F1, F3, and F5 are medium farms.

2.2. Antibiotic determination

Pig farm effluents, drainage water, river water, and pig feed samples were analyzed for twenty-one antibiotics i.e., penicillin G (PEN G), ampicillin (AMP), amoxicillin (AMX), neomycin (NEO), gentamicin (GEN), tetracycline (TE), chlortetracycline (CTC), doxycycline (DOX), oxytetracycline (OXY), erythromycin (ERY), tylosin (TYL), timicosin (TIL), norfloxacin (NOR), enrofloxacin (ENR), sulfadiazine (SDZ), trimethoprim (TMP), sulfamethoxazole (SXZ), colistin (CLS), lincomycin (LIN), tiamulin (TIA), and florfenicol (FCC). The extraction method was followed the EPA 2007[3], whereas their concentration were detected by using LC-MS/MS.

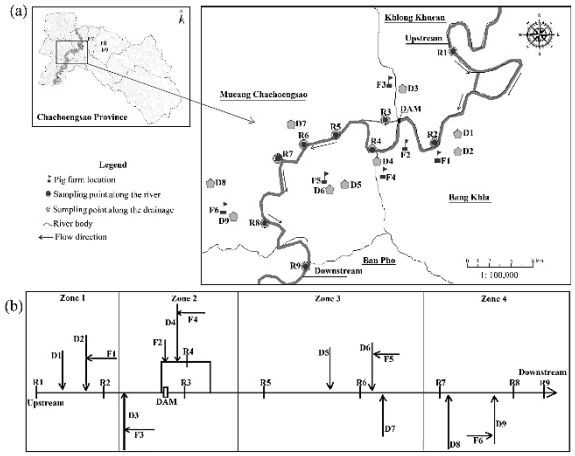

Fig. 1. The location of sampling sites along the Bang Pakong River (a) and the flow directions of pig farm effluent, drainages and the river (b)

2.3. Modelling fate and transport of antibiotics

The study area was divided into four zones (Fig.1b). Multiple linear regressing and random forest models were applied to residual antibiotics from the pig farm effluent and the river in both seasons to model the dilution and their molecular properties i.e., biodegradability (Biowin1 and 2), partition coefficient ($LogK_{ow}$), solubility (LogSol), and volatility (LogVol), which possibly effect removal processes of antibiotics drained in the river. All calculation methods and modelling processes were detailed in our current paper publication [4].

III. Results and Discussion

3.1. Residual antibiotics

In small farms, the major residual compounds in pig farm effluent were TC, CTC, AMX, TIA, and FCC. In addition, those dominant compounds were also detected in effluent from medium farms while FCC was found at the highest concentration with 272.5 µg/L at Farm F5. The maximum concentration of AMX was 32.5 µg/L while maximum concentrations of TE and CTC were 20.4 µg/L, 11.2 µg/L, respectively. Furthermore, the maximum concentration of TIA was 11.7 µg/L while others were detected at the level lower than 1.9 µg/L. TC, CTC and AMX were confirmed in pig feeds with maximum concentrations of 1.7 mg/kg, 8.3 mg/kg, and 0.53 mg/kg. Other antibiotics (i.e., TMP, FCC, OXY, NEO, TIA, NOR, DOX, and SDZ) also presented in the pig feed, showing residual concentrations of 0.0003–0.033 mg/kg. The results revealed that most antibiotics in the effluent were residual compounds from the pig feed.

The concentrations of antibiotics detected in drainages and the river in dry and rainy seasons are shown in Fig. 2. In

drainages, AMX was detected at most of the sampling sites with the maximum concentration of 0.12 µg/L in the dry season while it was detected only at the site D3 and D9 in the rainy season, showing the maximum concentration of 0.71 µg/L. TE and CTC were also a dominant compounds in drainage water. The maximum concentration TE was 0.063 µg/L in the dry season and 15.1 µg/L in the rainy season while CTC was 5.2 µg/L and 16.1 µg/L. TIA presented at all sampling sites, but its maximum concentration decreased from 0.23 µg/L in the dry season to 0.12 µg/L in the rainy season. Furthermore, TMP and SDZ were detected at most of the sampling sites in the dry season (max. 0.14 µg/L), but it only detected at the site D1, D3 and D9 in the rainy season (max.4.42 µg/L). Other antibiotic compounds were detected of lower than 0.05 µg/L except for LIN at the site D9 in the dry season (max. 2.3 µg/L). All dominant antibiotics in drainages also presented at most of sampling sites in the river. AMX was detected at most of sampling sites in the dry season with the maximum concentration of 0.12 µg/L, but it was only detected at the site R3 in the rainy season (max. 0.02 µg/L). TE and CTC were detected at higher levels in the rainy season with maximum concentrations of 4.7 µg/L and 1.1 µg/L, compared to those of 0.14 µg/L and 0.18 µg/L in the dry season. TIA was detected at all sampling sites (max. 0.003 µg/L). Moreover, maximum concentration of sulfonamides (TMP and SDZ) increase form 0.087 µg/L in the dry season to 10.32 µg/L in the rainy season. Other antibiotics were also detected at some sampling sites, showing their maximum concentration of 0.17 µg/L in the dry season and 0.0036 µg/L in the rainy season.

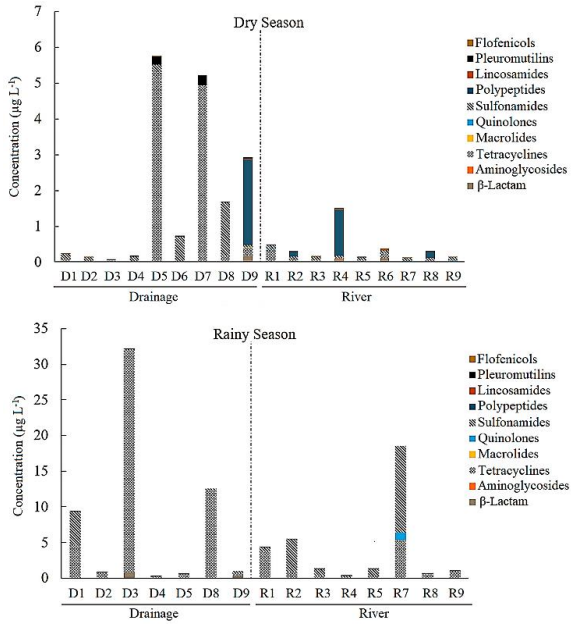

Fig. 2. The concentrations of antibiotic classes detected at each sampling site in the drainage and the river dry and rainy seasons

Overall, AMX, TC, CTC and TIA were the dominant antibiotics in pig farm effluents, which were also dominant in drainages and the river except for TMP and SDZ. Thus, the antibiotic contamination in the aquatic environment is likely caused by the residual antibiotics from the pig farm. Furthermore, the application of the pig manure to farmland as organic fertilizer should be another source for residual antibiotics in the aquatic environment [5]. Residual antibiotics in effluent may be firstly disposed to the drainage system and then further distributed to the river. Likewise, SDZ and TMP in this study were investigated as dominant antibiotics used in urban areas. However, the rainy season and surface runoff in October (176 mm rainfall/month) should dilute residual antibiotics much more than dry season (54 mm rainfall/month), higher concentrations of tetracyclines and sulfonamides in drainages and river water were still detected in rainy season, indicating the higher release of antibiotics from wastewater sources including pig farms at that period.

3.2. Modelling fate and transport of antibiotics

In the dry season, dilution factor (D) in Zone 1 was estimated to be 217.9 while D factors in Zone 2 were 8.8 in the west flow and 1.4 in the south flow. In addition, D factor in Zone 3 was 0.51, whereas Zone 4 showed a negative D factor. The negative D factor in zone, where is located at the urban areas, might be caused by the release of wastewater contamination from many sources including pig farms to the river. In addition, the hydraulic retention time of the river water was short in this season. Thus, those processes were the possible cause for the high fluctuation of EC (954 µS/cm) at Site R7. In the rainy season, D factor in all targeted zones varied from 5.83 to 187, respectively. Most D factors were higher in most targeted zones in rainy season than those in the dry season except for the Zone 1 due to rich rainfall precipitation in the rainy season.

For the MLR model in the dry season, Biowin2 showed the highest t-value of 2.8, followed by LogVol (t-value: 1.58). The percentage of variance explained by this model was 19.2% (overall R^2: 0.17, residual standard error: 22.4 on DF of 69, and F-statistic: 7.1). Likewise, the *p*-value of Biowin2 was lower than 0.05 while the *p*-value of LogVol was only 0.1. Identically, Biowin2 was the most relevant in the model, corresponding to 10.7% of total contribution. For the MLR model in the rainy season, t-values of all variables were in acceptable range (t-value>1.6). The percentage of variance explained by this model was 19.8% (overall R^2: 0.2, residual standard error: 10.1 on DF 74, and F-statistic: 3.6). Variables shown percentage of relative important ranging from 1.5% to 6.1%.

For the RF model in the dry season, the percentage of variance explained by the model was 92.5% with the mean squared residuals of 16.6. The highest percentage decrease accuracy (%IncMSE) was presented by Biwon2 following by $LogK_{ow}$, LogVol, LogSol, and Biowin1. In the rainy

season, the percentage of variance explained by the model was 92.4% with the mean squared residuals of 3.6. In both seasons, all variables presented significance in the models, showing %IncMSE of 3.8%–24.7%.

Based on AIC, RF models in both seasons indicated the lower prediction error than MLR models. Fig. 3 shows the plots of actual and modelled concentrations in dry and rainy seasons. The coefficient of determination of MLR and RF models accounted for 0.06 and 0.14, respectively in the dry season while they were 0.43 and 0.51 in the rainy season. RF models showed better fitness between modelled and actual concentrations than MLR models. Lower %IncMSEs of all variables in the RF model in the dry season may imply the low effluent flux from pig farms due to no hydraulic overload in the retention lagoon. Moreover, due to the longer hydraulic retention in the drainages system in this season, residual antibiotics were not transported well from drainages to the river.

Overall, major removal processes of residual antibiotics in this area during dry and rainy seasons were determined by their partition coefficients, solubilities, biodegradability and volatility. Partition coefficient and solubilities of antibiotics could define their adsorption affinity to suspend particles or sediment in the river[6]. Antibiotics with low $LogK_{ow}$ and high solubility are defined to low adsorption affinity while those with the high $LogK_{ow}$ and the low solubility are defined to high adsorption affinity. Likewise, antibiotics with Biowin1 and Biowin2 values of higher than 0.5 are defined as high biodegradation in surface water. In this case, AMX may be highly removed in the river water by biodegradation because its Biowin1 and Biowin 2 values are above 0.5. Likewise, substantial removal of TIA drained along the river may be occurred by adsorption because its $LogK_{ow}$ and solubility are 4.75 and 0.6 mg/L. TE, CTC, SDZ, and TMP, were still high in drainages and the river because both antibiotics are more stable and persistence in biotransformation. Moreover, TE and CTC persistence in aquatic environment may be also associated with low volatility in water.

IV. Conclusion

We investigated the fate and transport of antibiotics along Bang Pakong River and found that residual antibiotics in the river are discharged from pig farms especially in the rainy season. In this target area, TE, CTC and TIA were dominant antibiotics in the pig farm effluent and were determined as major antibiotics in the drainages and the river. In addition, the removal processes of antibiotics during such transportation to the river were modeled as functions of their partition coefficients, their solubilities, biodegradability and volatility.

Acknowledgement

Authors are grateful to Kurita Water and Environment Foundation (KWEF), Japan for funding this research under 20th anniversary KWEF commemorative research project. The study was also carried out under the scheme of collaborative research (CR) and PhD Sandwich Program of AUN/SEED-Net that is supported by the Japan International Cooperation Agency (JICA).

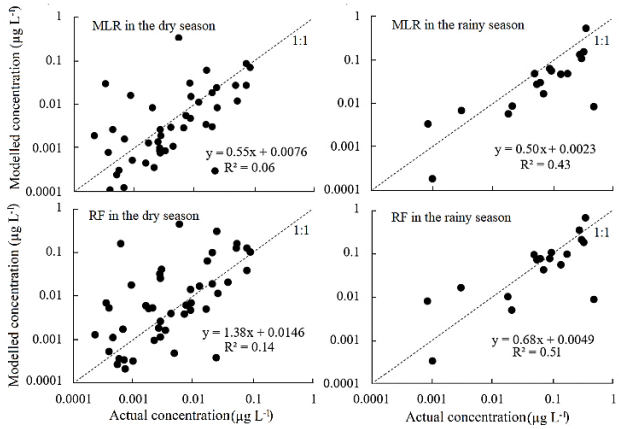

Fig. 3. Comparison of multiple linear regression (MLR) and random forest (RF) models performance on test data in dry and rainy seasons

References

[1] Lekagul, A., Tangcharoensathien, V., Mills, A., Rushton, J. and Yeung, S., 2020. How antibiotics are used in pig farming: a mixed-methods study of pig farmers, feed mills and veterinarians in Thailand. *BMJ Global Health*, *5*(2), p.e001918.

[2] Selvam, A., Kwok, K., Chen, Y., Cheung, A., Leung, K.S. and Wong, J.W., 2017. Influence of livestock activities on residue antibiotic levels of rivers in Hong Kong. *Environmental Science and Pollution Research*, *24*(10), pp.9058-9066.

[3] EPA., 2007. Method 1694 : Pharmaceuticals and Personal Care Products in Water , Soil , Sediment , and Biosolids by HPLC / MS / MS. *EPA Method*.

[4] Chan, R., Wandee, S., Wang, M., Chiemchaisri, W., Chiemchaisri, C. and Yoshimura, C., 2020. Fate, transport and ecological risk of antibiotics from pig farms along the bang pakong River, Thailand. *Agriculture, Ecosystems & Environment*, *304*, p.1071235.

[5] Kemper, N., 2008. Veterinary antibiotics in the aquatic and terrestrial environment. *Ecological indicators*, *8*(1), pp.1-13.

[6] Boy-Roura, M., Mas-Pla, J., Petrovic, M., Gros, M., Soler, D., Brusi, D. and Menció, A., 2018. Towards the understanding of antibiotic occurrence and transport in groundwater: Findings from the Baix Fluvià alluvial aquifer (NE Catalonia, Spain). *Science of the total environment*, *612*, pp.1387-1406.

The 13th AUN/SEED-Net Regional Conference on Chemical Engineering 2020 (RCChE-2020)
Jointly held with
The 5th International Symposium on Conservation and Management of Tropical Lakes
"Insights and Challenges toward Achieving SDGs"

Microcrystalline Cellulose Production from Acid Hydrolysis of Rice Straw's Hydrotropic Pulp

Frita Dewi Damayanti [1], Wahyudi Budi Sediawan [1,*], Muhammad Mufti Azis [1], Indah Hartati [1, 2]

[1] *Department of Chemical Engineering, Faculty of Engineering, Universitas Gadjah Mada, 55281 Indonesia*
[2] *Department of Chemical Engineering, Faculty of Engineering, Universitas Wahid Hasyim, 50236, Indonesia*
**Corresponding author: wbsediawan@ugm.ac.id*

Abstract

As one of the largest rice producers in Asia, Indonesia has huge of biomass resources such as rice straw. The objective of this work was to find the highest cellulose content from hydrolysis of rice straw's hydrotropic pulp with hydrochloric acid and sulfuric acid. The rice straw was successively pretreated with hydrotropic delignification and bleaching before hydrolysis. The hydrotropic delignification and bleaching were able to remove significant amount of lignin, hemicellulose, and other extractive substances. In this study, the hydrotropic delignification was performed at 80ºC for 60 minutes with urea solution 30% and bleaching was performed at 70ºC for 60 minutes with hydrogen peroxide. The hydrolysis of rice straw hydrotropic pulp was carried out in a reactor under microwave irradiation, where the hydrolysis reaction times (10-50 minutes) were examined. The result shows that the highest cellulose content found at the optimum of observed conditions (2 M, 80ºC, 30 minutes) for hydrochloric acid and sulfuric acid hydrolysis were 64.44% and 56.93% respectively.

Keywords: *hydrolysis, hydrotropic pulp, microcrystal cellulose, rice straw*

I. Introduction

Nowadays, the research of sustainable and environmentally friendly processes involves the use of alternatives lignocellulosic materials. Indonesia is an agricultural country where most of the population has a livelihood in agriculture or farming. As one of the largest rice producers in Asia, Indonesia has huge amount of biomass resources such as rice straw. Rice straw is the residue of rice processing that has not been fully utilized. Most of the rice straw was burnt on site, generating large amounts of heavy smoke as well as carbon dioxide and resulting in environmental pollution [1]. Lignocellulosic materials are abundant, cheap, and renewable and may be used for the production of microcrystalline cellulose (MCC). MCC has various applications in pharmaceutical, chemical, food industries, etc. It is meaningful to use rice straw as raw material for MCC production. Rice straw is mainly composed of three major polymers like cellulose, hemicellulose, and lignin which is contains 35-50%, 20-35%, and 10-25% respectively [2] .Conversion of rice straw is a very complicated process due to the presence of complex structure of lignin and hemicelluloses with cellulose. A pretreatment process is required as it can remove significant amount of lignin, hemicellulose, and other extractive substances [3].

There are three important processes for MCC production, namely the delignification, bleaching, and hydrolysis process. Pretreatments are required for increasing accessibility of surface area of cellulose for reducing sugar production by removing components such as hemicellulose and lignin from the complex structure. Many researches have been carried out to develop an environmentally friendly chemical pretreatment process such as the use of hydrotropic solution on delignification process. Urea solution is considered as a green chemical for lignin removal due to its non-corrosiveness, its lower risk to human health,

and less impact on other lignocellulose component [4]. Bleaching is a process using chemical substances to remove stains or dirt attached to the material. One of the commonly used as a bleaching agent is hydrogen peroxide. Hydrogen peroxide is an oxidizing agent that can be used as an environmentally friendly pulp bleach [5].

The hydrolysis reaction in dilute acid is very complex, mainly because the substrate is in a solid phase and the catalyst in a liquid phase. Various factors (particle size, liquid to solid ratio, type and concentration of acid used, temperature, and reaction time) influence monomer yield [6]. Hydrochloric and sulfuric acids have been used to catalyst the hydrolysis of rice straw. For other raw materials hydrofluoric and acetic acids were also employed as a catalyst.

Microwave irradiation has been widely used in many areas because of its high heating efficiency and easy operation [7]. Microwave heats the target object directly by applying an electromagnetic field to dielectric molecules as compared to conduction or convection heating which is based on intramolecular heat transfer. It can significantly increase the hydrolysis of rice straw. Several researcher have used microwave as a potential method for treatment of various lignocellulosic materials and to damage the recalcitrant lignin [3].

The objective of this work is to study the hydrolysis of rice straw's hydrotropic pulp with hydrochloric acid and sulfuric acid to find the highest cellulose content.

II. Materials and Methods

2.1. Raw Materials

Rice straw was obtained from local farm around Yogyakarta city (Yogyakarta, Indonesia). Other reagents were purchased from Merck Chemicals and Life Sciences (Jakarta, Indonesia); they were analytically pure and applied without pretreatment.

The rice straw was cut into pieces of size of 1-2 cm and washed with water to remove dirty and aqueous soluble substances. The washed rice straw was then dried under sunlight for 2 days. The rice straw was then crushed until it becomes a powder. The powder was sieved using a 60 Mesh sieve, and the undersize was dried. The chemical compositions of rice straw before hydrolysis are presented in **Table 1**.

2.2. Isolation of Cellulose from Rice Straw

Hydrotropic Treatment of Rice Straw. Forty grams of rice straw powder and 1200 ml 30% urea solution were put into 1500 ml flask. The mixture was then heated at 80ºC for 60 minutes in a microwave heater. The mixture was then filtered. The solid residue collected was washed thoroughly by distilled water until became neutral and then dried at 80ºC for 6 h. Finally, the rice straw's hydrotropic pulp was weighed to determine the yield.

Bleaching of Rice Straw's Hydrotropic Pulp. Twenty grams of rice straw's hydrotropic pulp was put into a flask, and mixed with hydrogen peroxide (5% concentration) and distilled water to obtain a solid to liquid ratio of 1:10. The bleaching process is carried out in alkaline condition (pH = 11) by addition of aqueous sodium hydroxide (2%). The mixture was then heated in a microwave at 70ºC for 60 minutes. After that, the mixture was filtered and washed using distilled water until the filtrate became neutral. The solid obtained was then dried in an oven until constant weight.

Acid Hydrolysis of Rice Straw's Hydrotropic Pulp. Samples of 10 g bleached pulp were mixed with 200 ml solutions of acid (sulfuric and hydrochloric acid). For this study, both sulfuric and hydrochloric acid concentrations of 2 M were applied. The hydrolysis was carried out at 80ºC in a microwave oven with temperature control. To prevent water loss by evaporation, the reactor was equipped with a reflux system. Mild agitation was also applied. On completion of the hydrolysis reaction (10, 20, 30, 40, 50 minutes), the reactor contents were filtered and washed thoroughly by distilled water until the residue became neutral. The samples were dried at 80ºC for 6 h before further analysis.

Table 1. Chemical composition of rice straw using Chesson Method

Number	Components	Values (%)
1	Cellulose	37.56
2	Hemicellulose	35.37
3	Lignin	14.45
4	Ash	11.29

2.3. Analysis

The contents of cellulose, hemicellulose, lignin, and ash were determined by using Chesson analysis method [8]. One g of dry sample (a) was added with 150 ml of aquadest, then refluxed at 100ºC in water bath for 1 h. The resultant solution was filtered, and the residue was washed with hot water (300 ml). The residue was then dried in an oven until

constant weight (b). After that, the residue was added with 150 ml of 1 N H_2SO_4 then refluxed in a water bath at the temperature of 100ºC for 1 h. The obtained solids were filtered and washed with aquadest (300 ml) to neutral condition, dried and weighed (c). The dried residue was then added with 10 ml of 72% H_2SO_4 and soaked at room temperature for 4 h. The residue was then mixed with 150 ml of 1 N H_2SO_4 and refluxed on a water bath for 1 h. After that, the residue was filtered and washed with aquadest (400 ml) until neutral condition and then heated in an oven at temperature of 105ºC until constant weight. The solid obtained was weighed (d). Finally, the solid residue was ashes in a furnace, and the ash was weighed (e).

The composition of the pulp was calculated by:

$$Hemicellulose\ content\ (\%) = \frac{b-c}{a} \times 100 \quad (1)$$

$$Cellulose\ content\ (\%) = \frac{c-d}{a} \times 100 \quad (2)$$

$$Lignin\ content\ (\%) = \frac{d-e}{a} \times 100 \quad (3)$$

$$Ash\ content\ (\%) = \frac{e}{a} \times 100 \quad (4)$$

The yields of MCC from rice straw were calculated according to equation (Eq. 5) as follows:

$$Yield\ (\%) = \frac{m'}{m_o} \times 100 \quad (5)$$

where m' and m_o are the mass of product and raw material of the hydrolysis process, respectively.

III. Results and Discussion

For acid hydrolysis, both sulfuric and hydrochloric acid concentrations were 2 M, the temperature of reaction was 80ºC, and reaction time was varied from 10 to 50 minutes. The cellulose and lignin content obtained from the solid phase at various reaction time are presented in **Table 2**.

Based on **Table 2**, the yield of MCC slightly decreased from 88.60 to 82.25% for sulfuric acid hydrolysis and decreased from 82.96 to 78.36% for hydrochloric acid hydrolysis. The MCC yield decreased steadily with increasing reaction time in the range from 10 to 50 minutes. This is probably due to the excessive hydrolysis of cellulose to glucose.

Table 2 shows that rice straw before hydrolysis contained 47.42% of cellulose and 10.89% of lignin. Sulfuric acid hydrolysis for 10 minutes was the lowest for cellulose content and the highest of lignin content among others. Hydrolysis for 10 minutes has been able to increase cellulose by 13.01% and to decrease the lignin content by 2.38%. Meanwhile, for 30 minutes of hydrolysis, the cellulose became 56.93% or increased 20.05% and lignin decreased by 20.57%. Hydrochloric acid hydrolysis for 10 minutes was the lowest for cellulose content and the highest lignin content among others. Hydrolysis for 10 minutes has been able to increase cellulose by 14.15% and to decrease the lignin content by 3.86%. Meanwhile, for 30 minutes of hydrolysis, the cellulose became 64.44% or increased 35.89 % and lignin decreased by 20.47%. For 40 – 50 minutes, both sulfuric and hydrochloric acid, the cellulose content decreased with reaction time. From this data, it can be seen that if the cellulose content increased higher, the lignin content will also decreased more. This may be due to production of sugar. The level and composition of the sugar released depend on the type of the acid in the reaction mixture. Acid treatment with sulfuric acid mainly releases xylose [9]. It can also be seen that the using of hydrochloric acid was more effective to increase cellulose content than the using of sulfuric acids for hydrolysis of rice straw.

This study was compared to the traditional heating method by Fan, G [7], especially sharp decrease in treatment time. The time of delignification and acid treatment decreased from 12 h to 60 minutes and 5 h to 30 minutes, respectively. Thus it is reasonable to conclude that microwave assist is an effective methodology to prepare MCC from rice straw as raw material.

Characterizations of rice straw before and after hydrolysis have been examined by applied X-ray Diffraction (XRD) analysis technique. The result is presented in **Fig.1**. The XRD pattern of rice straw before hydrolysis, after

Table 2. Acid Hydrolysis of Rice Straw

Entry	Time (min)	Sulfuric Acid			Hydrochloric Acid		
		Cellulose content (wt %)	Lignin content (wt %)	Yield (%)	Cellulose content (wt %)	Lignin content (wt %)	Yield (%)
1	0	47.42	10.89	100	47.42	10.89	100
2	10	53.59	10.63	88.60	54.13	10.47	82.96
3	20	54.22	10.61	88.31	61.08	9.70	81.42
4	30	56.93	8.65	85.95	64.44	8.66	80.36
5	40	54.29	8.32	84.11	63.95	8.55	79.93
6	50	53.35	7.28	82.25	63.42	7.26	78.36

hydrolysis with sulfuric acid, and after hydrolysis with hydrochloric acid are shown in **Fig. 1**. The peak around 22.3° is contributed to the typical crystal lattice of cellulose I_β [10]. The shoulder peak at 15.8° is also assigned to the typical crystal lattice of cellulose I_α [11]. The diffraction peak at 22.3° is wide and round in the curve of rice straw before hydrolysis **(Fig. 1-C)** but becomes relatively sharper and narrower after hydrolysis **(Fig. 1-D1 and 1-D2)**, indicating the removal of amorphous components such as lignin, hemicellulose, and silica. It is well known that cellulose consist of both crystalline and amorphous regions. In biomass, hemicellulose and lignin are amorphous in nature while cellulose is crystalline [12]. The sharper diffraction peak indicates higher crystallinity degree. The crystallinity increases from 53.75% to 65.32% in hydrolysis with sulfuric acid and 63.46% in hydrolysis with hydrochloric acid. The result showed that removal of amorphous parts of rice straw, that is lignin and hemicellulose, was more in sample treated with sulfuric acid than hydrochloric acid.

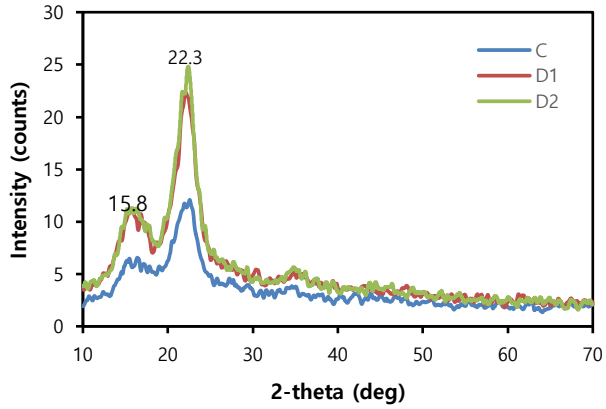

Fig. 1 XRD pattern of rice straw before hydrolysis (C), after hydrolysis with sulfuric acid (D1), and after hydrolysis with hydrochloric acid (D2)

V. Conclusion

Optimum result for hydrolysis of rice straw was obtained by using hydrochloric acid of 2 M for 30 minutes. The percentage of cellulose content obtained after hydrolysis using hydrochloric acid is higher (64.44%) than the one using sulfuric acid (56.93%).

Acknowledgement

The authors are grateful to The Ministry of Research, Technology and Higher Education of Republic of Indonesia which support this work through PDUPT research grant of 2020, with contract number of 2845/UN1/DITLIT/DIT-LIT/LT/2020.

References

[1] J. Domínguez-Robles, R. Sánchez, P. Díaz-Carrasco, E. Espinosa, M. T. García-Domínguez, and A. Rodríguez, 2017. Isolation and characterization of lignins from wheat straw: Application as binder in lithium batteries. *Int. J. Biol. Macromol.*, vol. 104, 909–918.

[2] B. C. Saha, 2004. Lignocellulose Biodegradation and Applications in Biotechnology. *U.S Gov. Work. Am. Chem. Soc.*, 2–34.

[3] R. Singh, S. Tiwari, M. Srivastava, and A. Shukla, 2014. Microwave Assisted Alkali Pretreatment of Rice Straw for Enhancing Enzymatic Digestibility, vol. 2014.

[4] M. Pulcer, 2006. Displacement Washing of Pulp with Urea Solutions, vol. 60, 365–370.

[5] A. Tutus, 2004. Bleaching Rice straw with hydrogen Peroxide, 1327–1329.

[6] M. J. Taherzadeh, C. Niklasson, and G. Lidn, 1997. Acetic acid friend or foe in anaerobic batch conversion of glucose to ethanol by Saccharomyces cerevisiae, vol. 52, no. 15.

[7] S. Zhu, Y. Wu, Z. Yu, J. Liao, and Y. Zhang, 2005. Pretreatment by microwave/alkali of rice straw and its enzymic hydrolysis, *Process Biochem.*, vol. 40, no. 9, 3082–3086.

[8] A. Fermentation and L. Yield, 1981. Acidogenic Fermentation of Lignocellulose-Acid Yield and Conversion of Components, vol. XXIII, 2167–2170.

[9] C. J. Israilides, G. A. Grant, and Y. W. Han, 1978. Sugar level, fermentability, and acceptability of straw treated with different acids, *Appl. Environ. Microbiol.*, vol. 36, no. 1, 43–46.

[10] M. L. Nelson and R. T. O'Connor, 1964. Relation of Certain Infrared Bands to Cellulose Crystallinity and Crystal Lattice Type . Part II . A New Infrared Ratio for Estimation of Crystallinity in Celluloses I and II *, *J. Appl. Polym. Sci.*, vol. 8, 1325–1341.

[11] H. S. Barud *et al.*, 2008. Thermal behavior of cellulose acetate produced from homogeneous acetylation of bacterial cellulose, *Thermochim. Acta*, vol. 471, no. 1–2, 61–69.

[12] J. P. O'Dwyer, L. Zhu, C. B. Granda, and M. T. Holtzapple, 2007. Enzymatic hydrolysis of lime-pretreated corn stover and investigation of the HCH-1 Model: Inhibition pattern, degree of inhibition, validity of simplified HCH-1 Model, *Bioresour. Technol.*, vol. 98, no. 16, 2969–2977.

The 13th AUN/SEED-Net Regional Conference on Chemical Engineering 2020 (RCChE-2020)
Jointly held with
The 5th International Symposium on Conservation and Management of Tropical Lakes
"Insights and Challenges toward Achieving SDGs"

Effect of Temperature and Airflow Rates on Design Parameters for Drying of Natural Tannin Extracts From *Rhizophora apiculata* Bark Waste

Edia Rahayuningsih [1*], Aswati Mindaryani [1], Mukmin Sapto Pamungkas 1, Dwi Tyaningsih Adriyanti [2], Chandra Wahyu Purnomo [1], and Joshua Bagaskara [1]

[1] *Department of Chemical Engineering, Faculty of Engineering, Universitas Gadjah Mada, 55381 Sleman, Yogyakarta, Indonesia*
[2] *Faculty of Forestry, Universitas Gadjah Mada, Yogyakarta, Indonesia*
**edia_rahayu@ugm.ac.id*

Abstract

PT Bintuni Utama Murni Wood Industries (PT BUMWI) produces bark waste for the *Rhizophora apiculata* type in the form of chips (small pieces) reaching 250-500 tons per month. Based on previous research results, the bark has a natural dye content of 0.2101 grams per gram of dry solid with a tannin content of up to 0.0531 grams per gram of solid. In this study, the bark waste's concentrated extract was dried in an open system using a hotplate on a metal plate with airflow. The drying temperature was varied at 60, 70, and 80 ºC, and the airflow rates was adjusted to variations of 1, 2, and 3 m/s. Drying was carried out for the extract thickness of 1 mm. The mass of the material was weighed every 2 minutes. The optimum drying was found by using response surface methodology (RSM) and obtained at a temperature of 80 ºC, airflow rates 1.75 m/s with drying design parameters were mass transfer coefficient (K_ya) at 65.77 kg H_2O m^{-2} hour $^{-1}\Delta y^{-1}$, a constant drying rate (R_c) at 9.01 kg H_2O $hour^{-1}$ m^{-2}, and critical time (t_c) for 0.5 hours. This optimization can be used to design appropriate technology for processing bark waste as a source of natural dyes on a more massive scale.

Keywords: *Rhizophora apiculata, natural dye, drying design parameters*

I. Introduction

PT Bintuni Utama Murni Wood (PT BUMWI) produces bark waste from the *Rhizophora apiculata* type in chips (small pieces) reaching 250-500 tons per month. In addition, based on the results of previous identification, PT BUMWI's *Rhizophora apiculata* bark has a natural dye content of 0.2101 grams per gram of solid with a tannin content of up to 0.0531 grams per gram of solid. Tannin is a natural dye in textiles that can give a yellow-brown colour [1]. The tannin content in bark waste is relatively high and can be used as a potential source of mordant dyes. Tannin powder can be produced from the bark by extraction, followed by evaporation, and drying processes [2].

This research focuses on the drying process of the concentrated extract. The drying system commonly used is energy from sunlight. Drying with this method is done by contacting the material directly under the sun or indirectly. The resulting water vapor is removed from the drying area through an airstream by free or forced convection [3].

The drying process needs to be studied to obtain a dye powder that is more applicable and more efficient. The experimental design is carried out with an appropriate technology reference frame to suit conditions in a remote area. Therefore, this present research was conducted to

obtain the optimum drying process by varying airflow rates and heating temperatures.

II. Materials and Methods

2.1. Materials

The material used in this research was concentrated extract (ρ = 1.084 g/mL). This material was obtained from the extraction of *Rhizophora apiculata* bark powder from PT BUMWI then evaporated up to 8x concentrations.

2.2. Methods

The drying tray with dimensions of 10 x 10 cm was dried in a 105 ºC oven for 15 minutes. The tray was kept in the desiccator for 5 minutes. The empty tray was weighed on a digital analytical balance. A total volume of 10 mL of concentrated extract was poured into the drying tray. The tray containing concentrated extract was weighed initially. Drying begins by placing the tray on the hotplate with airflow through on it. The tray was weighed every 2 minutes for 1 hour. Optimization of the drying process was carried out using a 2^k factorial design shown in **Table 1.**

Table 1. Experimental Range and Level Design

Independent Variable	Range and Level		
	-1	0	+1
Temperature [T], ºC	60	70	80
Airflow rate [v], m/s	1	2	3

2.3. Analytical methods

Unsteady state mass balance was applied to the drying process and the rate of change in moisture content ($\frac{dx}{dt}$) follows (Eq.1)

$$\frac{dx}{dt} = \frac{(x_{i+1} - x_i)}{\Delta t} \qquad \text{(Eq.1)}$$

The design parameters of the dryer were found by using the numerical method was performed to obtain the constant drying rate (R_c), mass transfer coefficient ($K_y a$), and constant drying time (t_c) using the following equation:

$$Rc_{i \to i+1} = \frac{Ls}{A}\frac{(x_{i+1} - x_i)}{\Delta t} \qquad \text{(Eq.2)}$$

$$K_y a = \frac{Rc}{(y's - y')} \qquad \text{(Eq.3)}$$

$$tc = \frac{Ls}{A}\frac{\Delta x}{Rc} \qquad \text{(Eq.4)}$$

Where, R_c is constant drying rate in kg H_2O $hour^{-1}$ m^{-2}, Ls is mass of the sample in kg, A is effective drying surface area in m^2, x_{i+1} is water content at t = t+1, x_i is water content at t = t, Δt is the time interval in an hour, $K_y a$ is overall mass transfer coefficient in kg H_2O m^{-2} $hour^{-1}$ Δy^{-1}, y's is moisture saturates on the surface of the material at wet bulb temperature, y is drying gas humidity in kg H_2O per kg dry solids, t_c is constant drying time in an hour, and Δx is change in water content in solids.

Optimization of the drying process from each independent variable (*X*; T and v) on the dependent variable (*Y*; $K_y a$ and R_c) was carried out using Response Surface Methodology in Minitab 16 Statistical Software. The experimental design model is a second-order polynomial model, presented in the following equation [4].

$$Y_i = \beta_0 + \sum_{i=1}^{k}\beta_i X_i + \sum_{i=1}^{k}\beta_{ii} X^2 + \sum\sum_{i<j}\beta_{ij} X_i X_j + \varepsilon \qquad \text{(Eq.5)}$$

III. Results and Discussion

In designing the appropriate technology, drying aims to extend shelf life and facilitate handling during sales [5]. Dyes products in powder form will be easy to distribute and easy to apply in their use. After conducting research on the effect of variations in airflow rates and drying temperature in the hotplate system, different results were obtained.

From **Fig. 1** it can be seen that the higher the airflow rates, at the same time, the higher the sample moisture content will be obtained. This result shows that the drying process was affected by airflow rates. **Fig. 1(b) and (c)** shows that drying at a temperature of 70 ºC and 80 ºC produces a moisture content that is relatively the same with speed variations. The difference can be observed in the gradient of the decrease in mass of the sample. The change in the sample's water content at a temperature of 80 ºC with a speed of 2 m/s is the fastest.

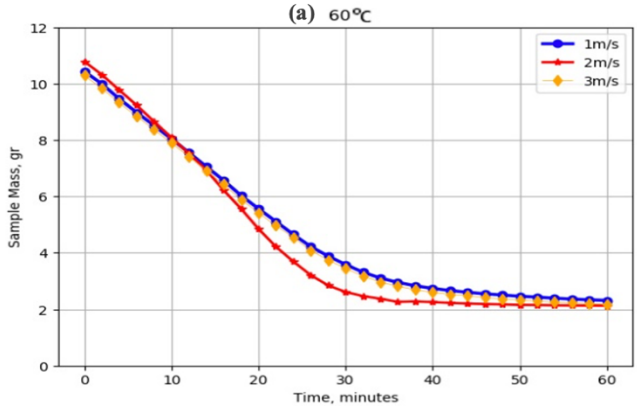

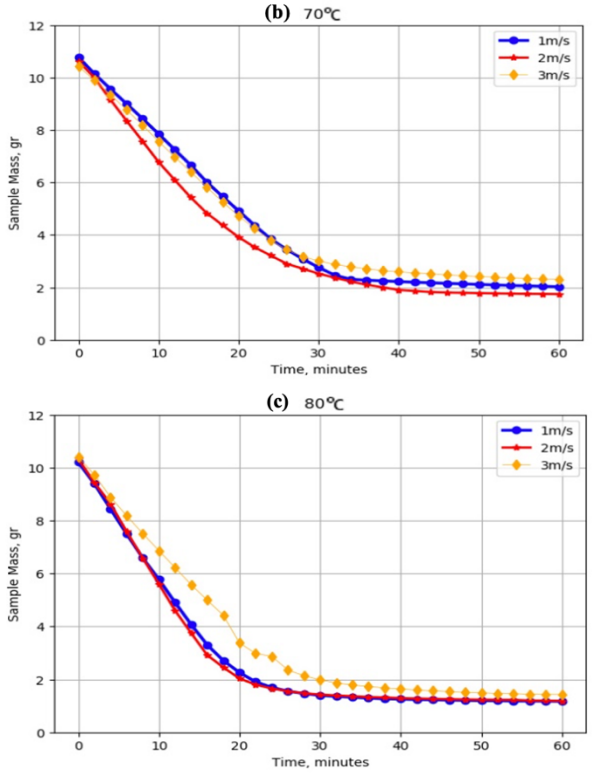

Fig. 1. Sample Mass vs. Time

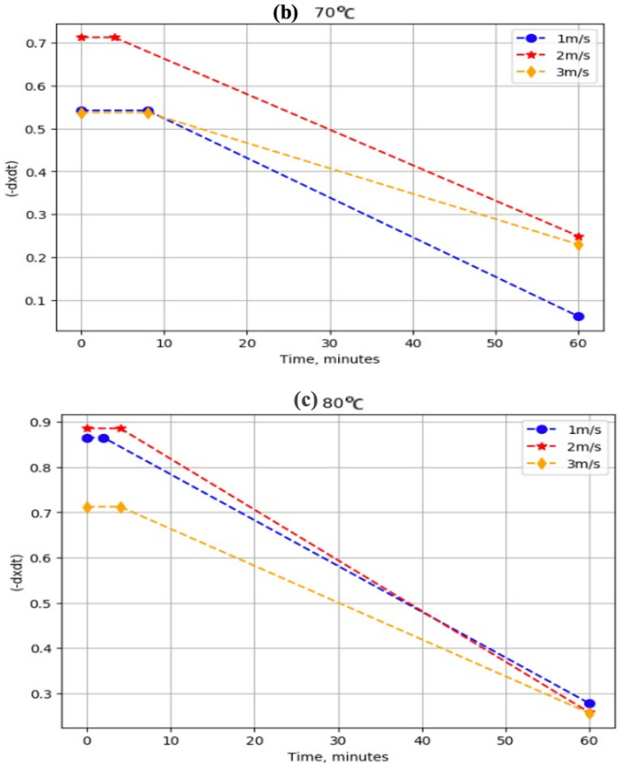

Fig. 2. Drying Rate vs. Time

The drying rate (-dx/dt) was determined by processing the sample's water content against time using the calculus method, dividing the graph of moisture content against time into three parts. Part 1, which is the part that forms a straight line, is carried out by linear regression until the maximum correlation coefficient (R^2) is obtained. Part 2 is the part that includes the curved line and is subjected to polynomial regression. Part 3 is the one that forms a horizontal line, which indicates that the drying process has stopped. The relationship curve between the rate of reduction in water content with time is presented in **Fig. 2.**

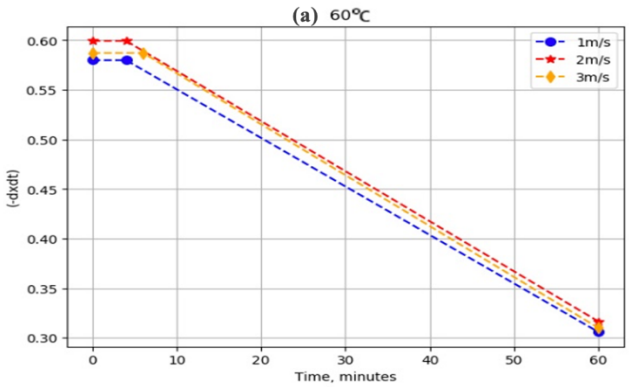

Based on **Fig. 2,** The drying rate profile has increased from 60 to 80 ºC. It can be seen that the lowest water content produced at the end of drying occurs at drying 70 ºC, an airflow rate of 1 m/s with a water content of 6.2 %. Airflow rates affect the temperature distribution at the time of drying. The drying rate increases for a speed of 1 m/s to 2 m/s. However, at the highest airflow rates, heat transferred to the hotplate decrease.

Airflow rates at 3 m/s cause the surface temperature to be the same as air flowed temperature so that the heat transfer for drying is reduced. The drying operation at a temperature of 80 ℃ with a 2 m/s is the highest drying rate achieved, which is 0.8858 grams/minute in 4 minutes.

A summary of the design parameters for drying is presented in **Table 2**. It can be concluded that the mass transfer coefficient and rate of drying value will increase with increasing drying temperature at the same airflow rates. High temperatures will provide more heat energy. When viewed for variations in airflow rates, an increase in airflow rates will encourage the fluid's tendency to flow turbulently. With the turbulent flow, the film layer formed during the mass transfer process will become thinner so that the mass

transfer process (diffusion) between water compounds takes place more intensely. However, in the drying process with a hotplate system flowed by air, it will cause a decrease in the temperature on the hotplate surface at high speeds so that the heat energy for drying and $K_y a$ value will decrease.

Table 2. Drying Design Parameter

[T], ^{O}C	[v], m/s	Rc	$K_y a$	tc, hours
60	1	3.71	37.27	1.20
70	1	2.78	38.23	0.83
80	1	7.97	59.40	0.60
60	2	4.81	48.32	1.20
70	2	6.69	52.28	0.50
80	2	8.79	65.46	0.50
60	3	3.72	37.37	1.20
70	3	3.79	38.13	0.93
80	3	5.96	44.37	0.50

Rc (kg H_2O hour^{-1} m^{-2}); $K_y a$ (kg H_2O m^{-2} hour $^{-1}\Delta y^{-1}$)

Optimization was carried out by Response Surface Methodology (RSM). Contour plot and optimization of $K_y a$ and R_c value are shown in **Fig. 1.**

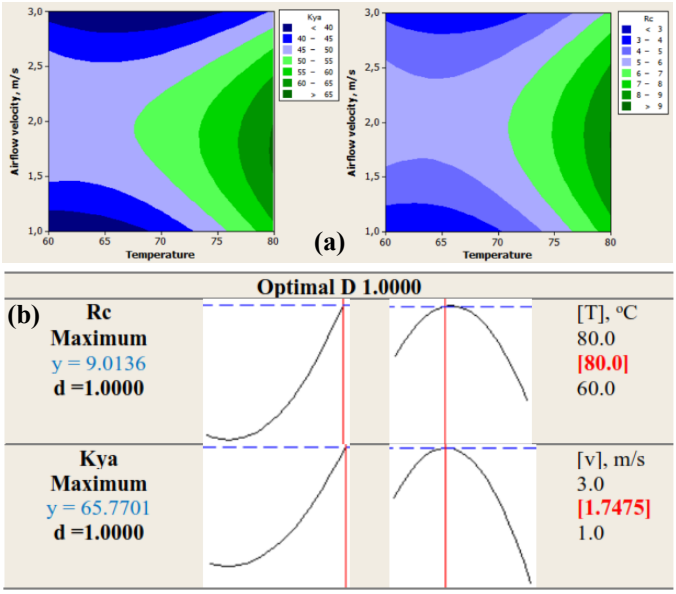

Fig. 1. (a) Contour Plot **(b)** Optimization Curve Showing The Effects of Independent Variables on $K_y a$ and R_c Value

The model equations for $K_y a$ and R_c are presented in (Eq.6) and (Eq.7) with the coefficient of determination R^2 value at 97.51% and 90.98%.

$$K_y a = 183.1 - 6.62\,T + 75.3v + 0.06T^2 - 12.89\,v^2 - 0.38\,T.v \quad \text{(Eq.6)}$$

$$Rc = 47.35 - 1.69T + 11.8v + 0.014T^2 - 2.11\,v^2 - 0.051\,T.v \quad \text{(Eq.7)}$$

The optimum results were obtained at a temperature of 80 ºC with airflow rates at 1.75 m/s. The maximum value of $K_y a$ and R_c were 65.770 kg H_2O m^{-2} hour $^{-1}\Delta y^{-1}$ and 9.013 kg H_2O hour^{-1} m^{-2}. Critical time (t_c) was obtained at 0.5 hours.

IV. Conclusion

The optimum condition for drying of concentrated extract from *Rhizophora apiculata* bark occurred at a temperature of 80 ºC with an airflow rates of 1.75 m/s. The drying design parameters were constant drying rate at 9.01 kg H_2O hour^{-1} m^{-2}, mass transfer coefficient ($K_y a$) at 65.77 kg H_2O m^{-2} hour $^{-1}\Delta y^{-1}$, and critical time (t_c) for 0.5 hours.

Acknowledgment

We would like to thank The Direktorat Penelitian UGM for their financial support in this research.

References

[1] Park, C., 2007, A Dictionary of Environment and Conservation 1st, Oxford University Press, New York.

[2] Rahayuningsih, E., Mindaryani, A., Adriyanti, D.T., Prihastiwi, L.P., Adina, P., Ayu, E. D., 2020, Conceptual Design of a Process Plant for the Production of Natural Dye from Merbau *(Intsia bijuga)* Bark, *Regional Symposium* on *Chemical Engineering (RSCE) 26th*, Kuala Lumpur

[3] Earle, R. L., 2004, Unit Operations in Food Processing Web. Edition, The New Zealand Institute of Food Science & Technology (Inc.), Terrace End.

[4] Montgomery, D. C., Myers, R.H., Anderson, C.M., 2012, Response Surface Methodology: Process and Product Optimization Using Designed Experiments, New York: John Wiley & Sons.

[5] Chowdury, K., Khan, S., Karim, R., Hasan, A., and Obaid, M., 2011, Effect of Moisture, Water Activity and Packaging Materials on Quality and Shelf Life of Some Locally Packed Chanachur, Bangladesh Journal of Scientific and Industrial Research 46, 33-40.

The Assessment of Concentration of Particulate Matter Emitted from Vehicles in Phnom Penh City

Rany You[1], Chanto Chea[1], Tomoki Nakayama[2], Rithy Kan[3], Chanmoly Or[3], Mitsuhiko Hata[4], Masami Furuuchi[4], Chanreaksmey Taing[1,5,] *

[1] *Faculty of Food and Chemical Engineering, Institute of Technology of Cambodia*
Russian Federation Blvd., P.O. Box 86, 12156 Phnom Penh, Cambodia
[2] *Faculty of Environmental Science, Nagasaki University*
1-14 Bunkyomachi, Nagasaki, 852-8521, Japan
[3] *Research and Innovation Center, Institute of Technology of Cambodia*
Russian Federation Blvd., P.O. Box 86, 12156 Phnom Penh, Cambodia
[4] *Graduate School of Natural Science and Technology, Kanazawa University, Kanazawa, Japan*
Kakumamachi, Kanazawa, Ishikawa 920-1164, Japan
[5] *Research Unit Water and Environment, Institute of Technology of Cambodia*
Russian Federation Blvd., P.O. Box 86, 12156 Phnom Penh, Cambodia
* *tsmey16@gmail.com*

Abstract

Ambient air pollution is a mix of chemicals, particulate matter, and biological materials that react with each other to form tiny hazardous particles. It causes breathing problems, chronic diseases, increased hospitalization, and premature mortality. One of the air pollutant generators is traffic activities. Therefore, the purposes of this study are to assess the concentration of Total Suspended Particulate (TSP), correlation of TSP with the number of vehicles, and Particulate Matter (PM) fraction emitted from traffic along with the road sites in Phnom Penh city to the atmosphere. The experiment was conducted in 4 sites including Kim Il Sung Blvd (KISB), Chroy Changvar Cross-intersection (CCV), Stung Mean Chey Cross-intersection (SMC), and Russian Federation Blvd (RFB). High-Volume air sampler was used for TSP measurement, Nano sampler for PM fraction, and Low-cost sensor for PM2.5 detection. As the result, at four sampling sites the concentrations of TSP and PM2.5 reached the maximum at 1072µg/m^3 and 41.35±1.37µg/m^3, 234.09µg/m^3 and 28.33±1.79µg/m^3, 151.27µg/m^3 and 15.88±1.57µg/m^3, and 161.64µg/m^3 and 14.24±1.65µg/m^3, respectively at 5-7 pm. The correlation between traffic and TSP at SMC has r^2=0.82, shows that traffic was the main source that contributes to the concentration of TSP. However, the traffic movement was not merely a source of the pollutants at RFB (r^2=0.03) while the other two sites, KISB and CCV had the moderate effect with r^2=0.56 and 0.64, respectively. The concentration of PM fraction was found the highest in coarse particles size at KISB, SMC, and RFB while the concentration of PM0.1 reached the maximum,116.79µg/m3 at CCV. Thus, this study indicates that the atmospheric particle concentration in Phnom Penh city is affected by the air pollutants emitted from vehicles.

Keywords: *Total suspended particulate, Particulate Matter, Low-cost sensor, PM2.5*

I. Introduction

The development of Phnom Penh, the capital city of Cambodia, is particularly important. On the other hand, this urbanization invigorates people to immigrate from rural areas to urban. Due to this, the number of vehicles has been increased and the congestion happened almost every part of the city [1]. Ambient air pollution is a mix of chemicals, particulate matter, and biological materials that react with each other to form tiny hazardous particles called Particulate Matter (PM), a mixture of solid, liquid, or solid and liquid particles suspended in the air [2]. It causes breathing problems, chronic diseases, increased hospitalization, and premature mortality. To simplify the assessment of PM levels and facilitate the implementation of PM pollution control policies, it is common to categorize PM levels by the aerodynamic diameter such as total suspended particulate (TSP) (PM<30μm), PM10 (PM<10μm), PM2.5 (PM<2.5μm), coarse particles (2.5μm<PM<10μm), and ultrafine particles (UF) (PM<0.1μm) [3]. However, traffic movement produces road dust and air turbulence that can re-entrain road dust [4], which are the dominant sources of air pollution. Therefore, the purposes of this study are to assess the concentration of TSP, correlation of TSP with the number of vehicles, and PM fraction emitted from traffic along with the road sites in Phnom Penh city to the atmosphere.

II. Materials and Methods

2.1. Sampling sites

The experiment of this project was conducted in Phnom Penh, the capital city of Cambodia. The four main cross-intersection such as Kim Il Sung Boulevard (KISB), Chroy Changvar cross-intersection (CCV), Stung Mean Chey cross-intersection (SMC), and Russian Federation Boulevard (RFB) were selected as shown in **Fig. 1.**

2.2. Method of Sampling

In each sampling site, the data has been collected for 2 days that must be included one weekday and one weekend day. However, the duration of the experiment was 12 hours per day for all instruments. Throughout the monitoring period, traffic volume at every site described above has been recorded for 12 hours during the experiment. Since there were many vehicles, we cannot count directly while they travel on the road, then we use the camera to record for counting at another time. We recorded 5 minutes at the beginning of time and 5 minutes of the end of time, then we added the number of vehicles from these two periods together and multiplied by 6 to represent for 1 hour. TSP was measured every 2-hour so the filter used with a high-volume air sampler (HV) model (SHIBATA HV-500F) must be changed every 2-hour. Whereas Nano sampler (NS) model KANOMAX 3180 is used for measuring the concentration of PM fraction. Low-Cost Sensor (LCS) was used to detect the amount of PM2.5.

2.3. Analytical methods

The concentration of TSP and PM were calculated by the following formula:

$$C_{TSP} = \frac{m_f - m_i}{V} \times 10^3 \quad \text{(Eq.1)}$$

$$C_{PM} = \frac{m_f - m_i}{t \times q} \times 10^6 \quad \text{(Eq.2)}$$

Where C_{TSP} , C_{PM} are the concentration of TSP and PM particularly (μg/m^3), m_i , m_f are the mass filter before an d after sampling (mg), V is the total volume of an air s ample shown on HV, (m^3), t is sampling period (min), and q is the flow rate (L/min).

III. Results and Discussion

3.1. Pollutants Concentration

At KISB in the rush hours, 5-7pm, the mass concentration of TSP and PM2.5 rose to the peak at 1072μg/m^3 and 41.35±1.37μg/m^3, respectively as shown in **Fig. 2(a)**. Also, during 5-7 pm has released by far the greatest mass concentration of TSP, approximately greater than twice as much as during 9-11 am, which is the time that received the next largest amount of TSP concentration. Whereas **Fig. 2(b)** clearly shows that at CCV, the amount of PM2.5 reached the peak of 22.79±1.28μg/m^3 and 28.32±1.79μg/m^3 in rush hours, 7-9am and 5-7pm, respectively while it tended to the minimum about 14.59±0.97μg/m^3 during 1-3 pm. As represented in **Fig. 2(c)**, the peaks of TSP concentration reached 151.27μg/m^3 and 148.89μg/m^3 in the rush hours during 7-9am and 5-7pm, individually whereas between 9am to 5pm, the concentration of TSP seems a bit fluctuated. Moreover, the concentration of PM2.5 in the rush hours, 7-9 am and 5-7 pm, also reached the peak at 15.88±1.30μg/m3 and 12.30±1.57μg/m3, respectively while the others remained in a low concentration. Lastly, at RFB, during rush hours the concentration of TSP reached the highest at 161.64μg/m^3 while PM2.5 also reached a maximum of 14.24±1.65μg/m^3 as seen in **Fig. 2(d)**.

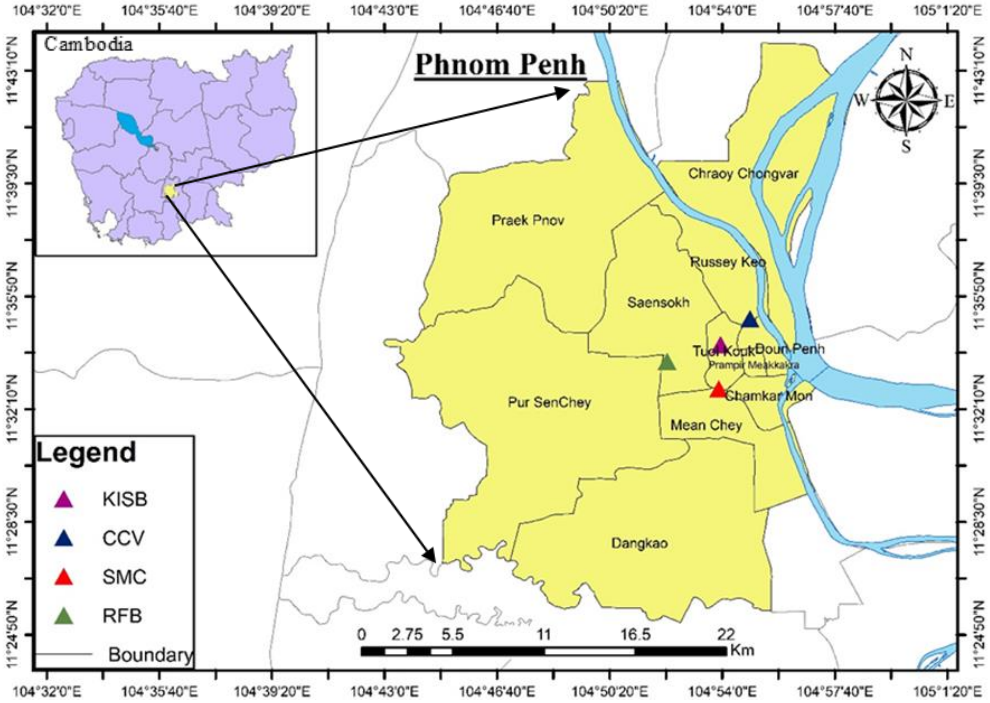

Figure1. Study area in Phnom Penh city**.**

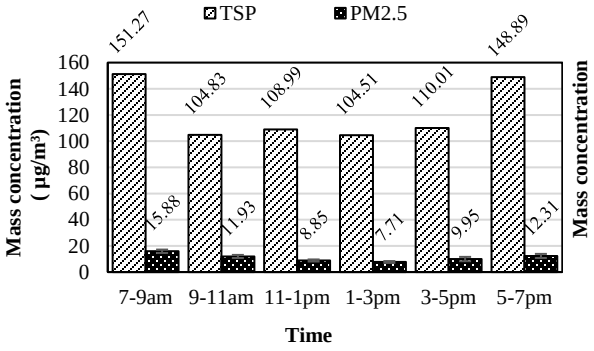

Fig. 2(a). The concentration of TSP and PM at KISB

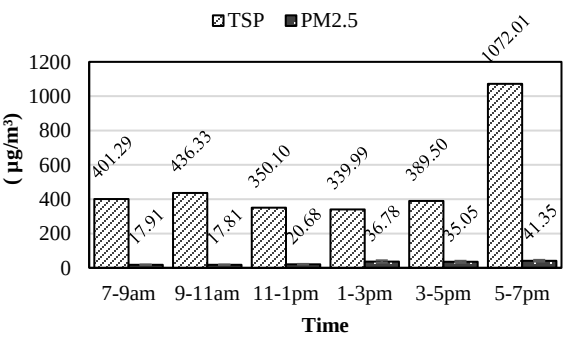

Fig. 2(b). The concentration of TSP and PM at CCV

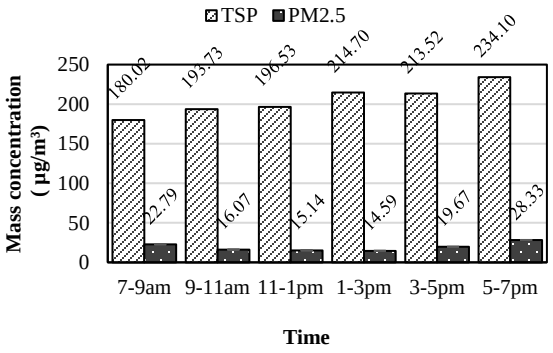

Fig. 2(c). The concentration of TSP and PM at SMC

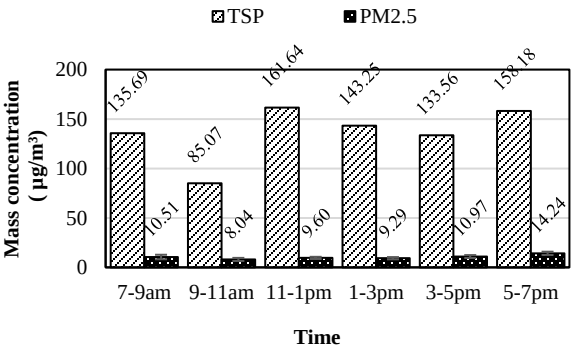

Fig. 2(d). The concentration of TSP and PM at RFB

3.2. Correlation between TSP and number of Vehicles

At KISB, there is a clear correlation according to the coefficient of determination R-squared (R^2) was 0.567 which means that there is about 56.7% possibility of TSP link to the amount of traffic while at CCV reveals that traffic count explained 64.41%. However, the traffic responses 82.76% of the variation in TSP concentration. This can be assumed that it is the main source that contributes to the mass concentration of TSP. At RFB, the traffic counted explained 3.8% of the variation in the TSP level meaning that traffic was not merely a source of TSP concentration as shown in **Fig. 3.**

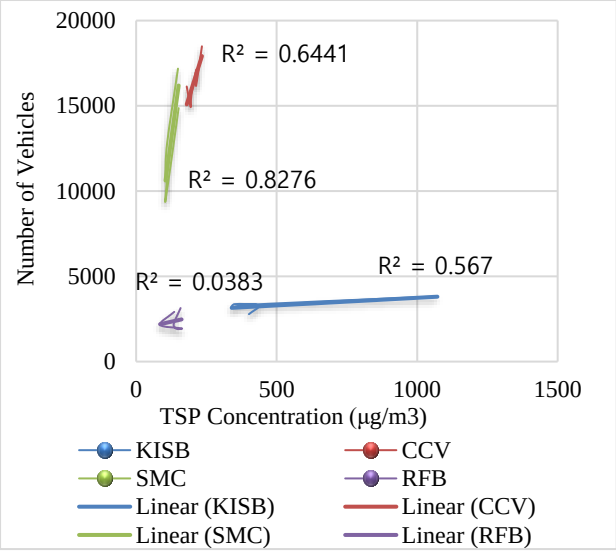

Fig. 3. The relation between Number of Vehicles and TSP

3.3. Particulate Matter Fraction Concentration

Table 1. The concentration of PM fraction.

Particle size (µm)	The Concentration of PM (µg/m^3)			
	KISB	CCV	SMC	RFB
>10	90.46	116.48	152.60	49.18
2.5-10	100.17	113.50	160.98	63.89
1-2.5	69.98	101.34	152.00	44.59
0.5-1	69.98	102.14	145.08	42.77
0.1-0.5	14.07	3.95	4.00	7.16
<0.1	66.59	116.79	160.45	48.84

From **Table.1** the concentration of PM fraction at KISB, SMC, and RFB were found in coarse particles, 2.5-10µm, with the amount of 100.17µg/m^3, 160.98µg/m^3, and 63.89µg/m^3, respectively. Coarse particles come from road dust, construction, and traffic activities[5]. However, at CCV the concentration of PM<0.1 µm (UF) and PM>10µm were the highest, 116.79µg/m^3 and 116.48µg/m^3 if compared to the total concentration.

IV. Conclusion

To sum up, the concentrations of TSP measured by HV and PM2.5 reached the maximum at all sites during 5-7 pm. Moreover, the highest concentration of TSP was found at KISB. The correlation between TSP and the number of vehicles shows that the number of vehicles can be the main source that contributes to the mass concentration of TSP at SMC while it was not merely a source at RFB. The UF was found the highest at CCV while the other 3 sampling sites were found in coarse particles. Thus, this study exactly indicates that the atmospheric particle concentration in Phnom Penh city is affected by the air pollutants emitted from traffic along with the road sites.

The chemical composition of PM such as carbonaceous, heavy metal, and water-soluble ionic compounds should be analyzed for the future study to determine the emission sources.

Acknowledgement

The authors would like to thank Dr. OR Chanmoly and Mr. KAN Rithy for giving us the permission to use the Biomass Energy Laboratory for the sample storage and analysis. We also thank the sampling sites' owners for allowing us do the experiment.

References

[1] Ung P, Sroy S. Effect of traffic and construction on air quality of Phnom Penh City, Cambodia. 2016;(September):0–2.

[2] Brunekreef B, Holgate ST. Air pollution and health. 2002;360:1233–42.

[3] Englert N. Fine particles and human health - A review of epidemiological studies. Toxicol Lett. 2004;149(1–3):235–42.

[4] WHO. Particulate Matter. Encycl Met. 2013;(1):1663–1663.

[5] Srivastava A, Gupta S, Jain VK. Source apportionment of total suspended particulate matter in coarse and fine size ranges over delhi. Aerosol Air Qual Res. 2008;8(2):188–200.

The 13th AUN/SEED-Net Regional Conference on Chemical Engineering 2020 (RCChE-2020)
Jointly held with
The 5th International Symposium on Conservation and Management of Tropical Lakes
"Insights and Challenges toward Achieving SDGs"

Synthesis of Ni-CaO/Activated Carbon (AC) Catalyst for Cooking Oil Conversion to Green Diesel

Desy Septriana [1], Joko Wintoko [1], Muhammad Mufti Azis[1,*]

[1]*Department of Chemical Engineering, Faculty of Engineering, Universitas Gadjah Mada, 55281 Indonesia*
**muhammad.azis@ugm.ac.id*

Abstract

Herein, we report the synthesis procedure of promising Ni-CaO/Activated Carbon (AC) catalyst for cooking oil conversion to green diesel. The Ni-CaO/AC catalyst was synthesized using wetness impregnation method over commercial AC. The Ni and Ca precursors were 20% of $Ni(NO_3)\cdot 6H_2O$ and 15% $Ca(NO_3)\cdot 4H_2O$. After impregnation step, the solid catalyst was calcined in a horizontal tubular furnace under N_2 flow at 700°C. To detect the presence of Ni and Ca, we have characterized the catalyst with energy dispersive X-ray spectroscopy (EDX). The result showed that the Ni and Ca content were 64 and 34%, respectively. Surface area of Ni-CaO/AC is 19.129 m^2/g. Then, pore volume of Ni-CaO/AC is 5.61 $.10^{-2}$ cc/g. The catalyst powder was then modified to form a catalyst pellet by mixing it with phenolix resin and plasticizer. Our result shows that the use of 40 wt% of phenolix resin and 6% of plasticizer could form a stable catalyst pellet. Evaluation of catalyst performance in decarboxylation reaction was conducted in a batch autoclave with variation in operation temperature of 300, 330, 350 and 370 °C. The results showed that the largest percentage removal of carboxylic acid was obtained at 350 ^OC with estimated conversion of 96.95%. However, the target product of decarboxylation reaction over Ni-CaO/AC pellet was still low and hence requires further improvement.

Keywords: *cooking oil, decarboxylation, impregnation, Ni-CaO/AC, pellet*

I. Introduction

Green Diesel / renewable diesel is an important transportation fuel as it may replace diesel fuel derived from fossil. For large scale production green diesel is produced by converting fatty acids or fatty oils from abundant source of biomass. Green Diesel has similar properties with diesel fuel which contains low oxygenate component. It is important as oxygenate component could lower the chemical stability and energy content in fuel as commonly found in biodiesel. For this reason, it is necessary to remove the oxygenate component in fatty acids or fatty oil from biomass to become Green Diesel. The process for removing oxygen components is called a deoxygenation process which includes: hydrodeoxygenation, decarboxylation and decarbonylation.

Decarboxylation is one of promising route for green diesel production. Even though the decarboxylation process does not require H_2, it still requires inert gases with atmospheric conditions such as Ar, N_2, and He, because these inert gases can spontaneously change the route of the carboxyl groups in oil or fatty acids, for example it can prevent dehydration. Among four gases as a deoxygenation reaction medium, N_2 is commonly used as it is easy to handle and to analyze [1].

The oxygen group on the carbon surface determines the hydrophilic / hydrophobic properties of the carbon support thereby making it alkaline, acidic or neutral from the surface of the catalyst. The oxygen group affects the acidity of carbon surface, thereby reducing the hydrophobic properties of the carbon. This surface group plays an important role in the dispersion of the active phase, and in catalytic activity [2]. The acidity of the support gives a total

number of acid sites. The number of acid sites of activated carbon is very high. The amount of acid on the support site can be calculated by the NH_3 adsorbs method. The number of acid sites of activated carbon is higher than ZrO_2 and H-ZSM-5 [2]. The acidity of activated carbon comes from the acidity or functional group of surface oxygen such as carboxylates and phenols. A high acid site number is preferred in the decarboxylation reaction.

The incorporation of acid-base metals to give acid-base properties can promote a decarboxylation reaction with low coke formation. The effectiveness of metal promoters can be increased by the addition of different functional groups incorporated with a metal promoter which is preferably more highly reducible. Metal-supported catalysts can be made in the hydrogen-free state. The acid-base property can enhance oxygenate transfer by decarboxylation and decarbonylation reactions. The use of a single active site that is alkaline is not favored by the deoxygenation reaction because there is a breakdown of carbon-carbon bonds which will reduce the fraction of diesel range hydrocarbons [3]. Because of that, Ca metals was used as promotor and give basic properties. CaO facilitates oxygen removal by absorbing more CO_2 in gas phase. Transition metal oxides (TMOs) is a good promotor in catalyst synthesis, because they can alternate noble metals such as Pt and Pd in the field of catalytic cracking activity [4].

The objective of present work is to synthesize Ni-CaO/AC catalyst to convert conventional palm based cooking oil to green diesel. The reaction was conducted in a batch reactor and conversion of palmitic and oleic acid will be evaluated under different operation temperatures.

II. Materials and Methods

2.1. Materials

The feedstock of this work, palm oil-Cooking Oil was obatained from mini market namely Bimoli. $Ni(NO_3)_2{\cdot}6H_2O$ (>98.0% purity), $(Ca(NO_3)_2{\cdot}4H_2O)$ with 99.0% purity were obtained from Merck and N-Hexane (GC grade) with purity > 98% was used for dilution that obatained from Merck. The N_2 gas, with 99.9% purity, was supplied by Samator gas industri. Powdered activated charcoal Darco were purchased from Merck. Deionized water was prepared in our laboratory. Composition of used cooking oil available in **table 1.**

Table 1. Fatty Acid Composition of Cooking Oil

Components	Values (%)
Myristic Acid	2.41
Palmitic Acid	32.74
Stearic Acid	3.41
Oleic Acid	61.43

2.2. Catalyst Synthesis

The catalyst for decarboxylation of Cooking Oil is Ni-CaO/AC catalyst. The catalyst was prepared by wet impregnation method. Two precursor solutions, 20% Ni $(NO_3)_2.6H_2O$ and 15% $Ca(NO_3)_2{\cdot}4H_2O$ were used. Furthermore, two these solutions are impregnated into activated carbon continuously for 5 hours under vacuum pressure. Subsequently, the impregnation solution was left overnight, then followed by evaporation, filtering and drying at 105 ^oC to obtain a dry powder [5]. Later, the resulting dry impregnation solution is called a Ni-CaO / AC catalyst which was calcined at temperature of 700 ^oC for 4 hours with N_2 gas flowing at atmospheric pressure in a tubular furnace [6]. Then, the resulting powder of Ni-CaO/AC was modified to pellets with the aid of 40 wt% of phenolix resin and 6% of plasticizer.

2.3. Catalyst Characterization

Volume/size analysis of the catalyst was carried out with a NOVA 2000e surface area and pore size analyzer (Quantachrome Instruments). The samples were degassed at 120 °C with a continuous flow of nitrogen and helium at 10 psi overnight prior to the analysis. Liquid nitrogen was used as an adsorbent during the measurements. The Multi-Point Brunauer−Emmett−Teller (BET) method was used to determine the surface area and the BarretJoyner-Halenda (BJH) method was used as the most common and accurate method to compute the average pore volume and pore size of the samples.

Energy dispersive X-ray was carried out to determine the presence of metals on the activated carbon that might contribute to the hydrogenation/deoxygenation catalysis.

2.4. Experimental set-up

The decarboxylation tests were performed in a customized autoclave reactor (250 ml) operating in a batch mode as displayed in **Fig.1**. A multi-blade impeller was equipped for mixing of liquid reactant and solid catalyst. The temperature was measured with a K-type

thermocouple. In a typical batch experiment, 90 g of cooking oil as a model compound of vegetable oils, and 4.5 g of catalysts were placed in the reactor. After loading Cooking Oil and catalyst, the reactor was flushed with nitrogen in order to remove the remaining oxygen. Then, the reactor was heated to 300^{O}C and maintained for 105 minutes at that temperature. The stirring speed was maintained to 100 rpm during reaction. The reactor was subsequently cooled down to room temperature. The liquid products were collected after filtering solid phase catalyst. The final products was further analysed using GC–MS. This experiment was repeated for the other temperatures at 330, 350, 370 ^{O}C.

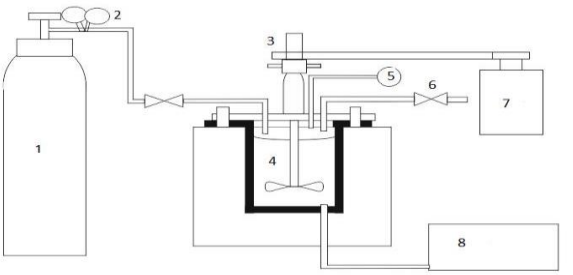

Fig.1. Schematic of Batch Reactor Setup: (1) N_2 Tube, (2) regulator, (3) mixer, (4) reactor, (5) pressure sensor, (6) purge valve, (7) motor, (8) temperature controller

2.5. Analytical methods

Liquid products were analyzed by a gas chromatograph–mass spectrometer system (Shimadzu GC-MS QP-2010) equipped with Rtx-5MS column. The carrier gas was helium and the flow rate was 1.0 ml/min. The column temperature was programmed to increase from 80 to 300 °C at 5 °C/min. The final temperature was 300 °C and held for 12 min. The sample was diluted by hexane before injection in GC-MS. For data analysis, percentage removal of carboxylic acid can be computed as:

$$\% \text{ Removal of –COOH group} = \frac{\sum n_i - \sum n_p}{\sum n_i} \times 100 \qquad \text{(Eq.1)}$$

Where n_i is initial peak area of –COOH group in Cooking Oil, n_p is peak area of –COOH group in the liquid product.

III. Results and Discussion

Catalyst characterization

The surface area as well as the pore volume of Ni-CaO/AC catalyst is presented in **Table 2**.

Table 2. Characterisation of Ni-CaO/AC Catalyst

Parameter	Value
Surface Area (m^2/g) BET	19.129
Pore Volume (cc/g) BJH	5.61×10^{-2}

Both Surface area and Pore Volume of Ni-CaO/AC catalyst in pellets were relatively small. This is probably due to the strong influence of phenolix resin and plasticizer which was added to the catalyst.

Table 3. Elemental Analysis of Ni-CaO/AC Catalyst with EDX

Analyte	Composition (%)
Ni	64.314
Ca	34.783
Si	0.683
K	0.195
S	0.024

The EDX mapping of the catalyst is presented in **Table 3**. It is important to note that carbon was not included as it is undetectable with the EDX. As seen here, the impregnation of Ni and Ca has been recorded well with the Ni and Ca content of 64.314 and 34.783 %, respectively.

Catalyst evaluation in a batch reactor

The result from catalyst evaluation of Ni-CaO/AC Catalyst in decarboxylation of cooking oil is presented in **Fig. 2**.

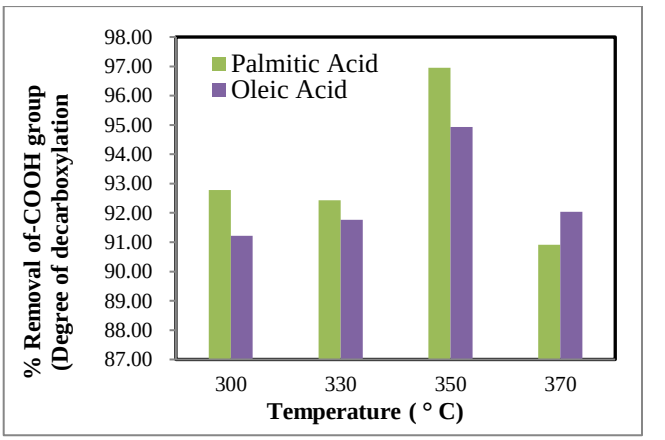

Fig.2. Degree of decarboxylation of Palmitic Acid and Oleic Acid over Ni-CaO/AC Catalysts

As seen in Figure 2, it showed that in general the catalyst facilitates high conversion of Palmitic and Oleic Acid with area based conversion higher than 90%. The percentage removal of carboxylic acid was obtained at 350^{O}C with conversion of 96.95%. Hence, it can be concluded that the optimum temperature in this experiment was 350 ^{O}C.

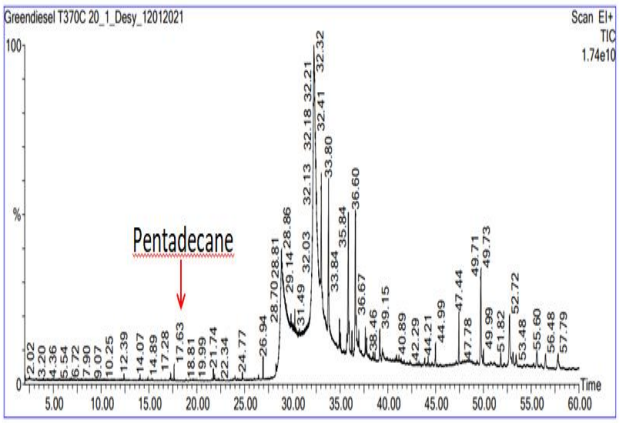

Fig.3. Peak Area of GCMS result for Decarbocylation Product at 370 ^{O}C

The desired product like pentadecane (green diesel) was only detected at 370^{O}C with less than 1% w/w as be seen in **Fig.3**. Evaluation of GC-MS products revealed that the target product of green diesel which lies in the range of paraffin C14-C22 was not fully detected. Most of deoygenated product was still carboxylic group, while a small compositions were in the form of ketones, alcohols and alkanes. The low selectivity to green diesel is probably due to the reduced active surface area and pore volume in the presence of phenolic resin and plasticizer.

Existence of acid sites support oxygen removal via hydrolysis of carboxylic ester to acid and then dehydration pathway. Both oxygen and hydrogen content can be removed in the reaction pathway.. The Ni-CaO/AC pellets is also fragile under the environment used in this reaction. From literature, the catalytic deoxygenation of triolein to green diesel over modified CaO-based catalyst powder showed optimum deoxygenation conditions of 5 wt% of catalyst, 340^{O}C within 105 minutes. Ni-CaO catalyst can give a hydrocarbon compound yield (C8-C20) of about 90% [4].

IV. Conclusion

Decarboxylation of cooking oil over Ni-CaO/AC catalyst has been investigated in the present work using batch reactor at various temperature of 300, 330, 350 and 370 ^{O}C. In general, the catalyst gave high conversion of palmitic and oleic acid, above 90% area based conversion. The apparent optimum condition was 350 ^{O}C with 96.95% conversion. Inspection on green diesel products from GC-MS results did not give any significant fraction of C14-C22 compounds. This might be due to the reduced surface area of the catalyst as a result of binder addition to form pellet. Hence, further investigation is still needed to improve the selectivity of cooking oil to green diesel.

Acknowledgement

We are thankful to Gadjah Mada University for the financial support through research grant of Department of Chemical Engineering.

References

[1] S.Ying, P. Lv, C. Zhao, M. Li, L. Yang, Z. Wang, Y. Chen, and S. Liu, "Solvent-free catalytic deoxygenation of oleic acid via nano-Ni/HZSM-5: Effect of reaction medium and coke characterization", *Fuel Processing Technology*. Elsevier, 179(June), pp. 324–333, 2018

[2] N. Hongloi, P. Prapainainar, A. Seubsai, K. Sudsakorn, and C. Prapainainar, "Nickel catalyst with different supports for green diesel production", *Energy*. Elsevier Ltd, 182, pp. 306–320, 2019

[3] G.A.Alsultan, N.A. Mijan, H.V. Lee, U. Rashid, A. Islam, and Y.H. Taufiq-Yap*, "*Review on thermal conversion of plant oil (Edible and inedible) into green fuel using carbon-based nanocatalyst", *Catalysts*, 9(4), pp. 1–25, 2019

[4] N.A. Mijan, H.V. Lee, J.C. Juan, A.R. Noorsaadah, and Y.H.Taufiq-Yap, "Catalytic deoxygenation of triglycerides to green diesel over modified CaO-based catalyst " , *The Royal Society of Chemistry, pp.* 46445-4640, 2017

[5] Md. Z. Hossain, M.B.I. Chowdhury, A.K. Jhawar, W.Z. Xu, "Continuous low pressure decarboxylation of fatty acids to fuel-range hydrocarbons with in situ hydrogen production", *Fuel*. Elsevier, 212 (June 2017), pp. 470–478, 2017

[6] G.A. Alsultan, N.A. Mijan, H.V. Lee, A.S. Albazzaz, and Y.H. Taufiq-Yap*, "*Deoxygenation of waste cooking to renewable diesel over walnut shell-derived nanorode activated carbon supported CaO-La2O3 catalyst", *Energy Conversion and Management*, 151(May), pp. 311–323, 2017

Packing of NiO Nanoparticles into the SBA-15 Support by Ethylene Glycol Assisted Impregnation Method

Nway Nay Hlaing[1,*], Tay Zar Lin[2], Aye Mya Thu[1], Osamu Nakagoe[3], Shuji Tanabe[3]

[1]*Chemical Engineering Department, Yangon Technological University, Yangon 095-11011, Myanmar*
[2] *Mechanical Engineering Department, Technological University (Thanlyin), Thanlyin 095-11291, Myanmar*
[3]*Division of Chemistry and Material Science, Graduate School of Engineering, Nagasaki University, 1-14 Bunkyo-machi, Nagasaki 852-8521, Japan*
* *nwaynayhlaing@ytu.edu.mm*

Abstract

Production of hydrogen from biomass by gasification is a practical way for energy substitution. Tar formation is a primary problem in the gasification process and catalytic tar steam reforming is an effective process due to 100% tar conversion. Almost all reported tar steam reforming catalysts are prepared by the conventional method that the active metal's particle size is usually large. In this work, the catalysts were prepared by the ethylene glycol (EG) assisted impregnation method. Firstly, large pore SBA-15 materials were synthesized using a P123 surfactant and Hexane. The structural properties were accessed by N_2 physisorption. The material with a BET surface area, BJH pore volume, and BJH desorption pore size of 666 m^2/g, 1.27 m^3/g, and 9 nm were obtained at the aging temperature of 333 K and aging time of 2 days. 10Ni/SBA-15 catalysts were synthesized by EG assisted impregnation method. The characteristics were analyzed by N_2 physisorption, X-ray diffraction, and TEM observation. The catalyst prepared by 1:10 molar ratio of EG to metal specie showed favorable properties. The particle sizes of the NiO in the synthesized catalyst were smaller than 5 nm and the particles are highly dispersed in the mesoporous framework of SBA-15 support. The particle sizes in the conventional catalyst showed greater than 14 nm. The activity of the catalysts will examine in the catalytic tar reforming.

Keywords: *10Ni/SBA-15 catalysts, ethylene glycol assisted impregnation, NiO nanoparticle, SBA-15 material, tar steam reforming catalyst*

I. Introduction

Hydrogen is an environmentally friendly fuel and the generation of hydrogen from biomass can be accomplished by biological or thermochemical process [1, 2]. Thermochemical conversions have higher efficiency than biological processes and the process options in the thermochemical conversion of biomass are combustion, gasification, pyrolysis, and liquification. The product components produced by the gasification or pyrolysis of biomass include the gaseous mixture, char, and tar. Removal of tar from the gas stream is required and fabrication of downstream components raises the cost. Therefore, conventional gasification processes are used to operate at high temperatures (> 1073 K) to remove tar from the product

gas stream [3]. The process can operate at a lower temperature (< 1073 K) by the utility of catalyst and catalytic steam reforming of tar was an effective way to carry out the process at low temperature and also improved carbon efficiency by reforming of tar into synthesis gas [4]. Accordingly, the development of tar steam reforming catalyst is an impressive research topic for scientists and researchers.

Ni-based catalyst is the most promising due to its high catalytic activity and low cost compared to novel metal catalysts [2]. It had already been known that a catalyst with a high surface area could provide the more available active sites. Therefore, the choice of catalyst support with a high surface area is important to disperse active metal species into it. Mesoporous structure SBA-15 material was recognized to be favorable catalyst support due to their great advantages of large surface area and pore volumes, tunable mesoporous size, and highly ordered mesostructure which allows diffusion and adsorption of large molecules [5, 6]. M. Kruk and L. Cao synthesized large pore SBA-15 in the presence of Hexane and they reported that tailorable pore size was as large as 16.5 nm [7].

Supported Ni catalysts were commonly prepared by impregnation or precipitation method [8, 9]. By using the conventional techniques, NiO particles were decomposed on the outer surface of the support, resulting in large particle size by agglomeration during calcination. Fortunately, it was reported that the double-solvent approach can deliver metal particles into the channel of the porous support [10-13]. S. Qiu et. al. recently reported that EG can assist to pack the metal particles into the porous structure of the SBA-15 support [14].

In this work, firstly, large pore SBA-15 materials were synthesized by the soft template procedure. Structural properties of SBA-15 materials were analyzed by N_2 physisorption. 10wt% Ni loaded SBA-15 supported catalysts were synthesized by EG assisted impregnation method. NiO particle size and the characteristics of the 10Ni/SBA-15 catalysts were accessed by XRD, TEM, and N_2 physisorption measurement.

II. Materials and Methods

2.1. Synthesis of large pore SBA-15 and 10Ni/SBA-15 catalyst

Large pore mesoporous structure SBA-15 materials were synthesized by following the procedure of Sun et al. [15]. 1:0.0168:4.02:0.295:4.42:133 molar composition of chemicals (P123:TEOS:C_6H_{14}:NH_4F:HCl: H_2O) was used in this synthesis. P123 and NH_4F have dissolved in HCl (conc. 35%) solution and stirred at room temperature until the solution becomes clear. The solution was then transferred to a water batch, set at 288±1 K, and stirred for 1 h. A mixture of TEOS and Hexane was added and continued stirring at 288±1 K for 24 h. Follow by aging were performed at 333 K or 353 K for 2 days or 5 days. The product was collected by centrifugation and washing with water and dried in an oven at 343 K overnight. Large pore SBA-15 was obtained after calcination in air at 773 K with a heating rate of 1 K/min for 6 h.

The preparation of Ni/SBA-15 catalyst was performed by an EG assisted impregnation technique and the metal loading was set 10 wt %. The molar ratio of metal species to EG was used 1 or 10. In a typical catalyst preparation, EG and $Ni(NO_3)_2 \cdot 6H_2O$ were dissolved in ultra-pure and mixed with SBA-15 support material. The resultant slurry was pre-stirred for 2 h or 12 h. The mixture was impregnated at 353 K in a water bath with intermittent stirring and kept at this temperature until all the water was evaporated. The catalyst precursor powder was then dried at 373 K in an oven overnight and calcined at 723 K for 2 h in a furnace.

2.2. Characterization of Catalyst

The specific surface area, pore diameter and pore volume of the SBA-15 and 10Ni/SBA-15 catalysts were measured using a Micromeritics Tristar 3000 by N_2 adsorption at 77 K. The crystalline structure and crystallite size of the catalysts were accessed using Miniflex 600, Rigaku with Cu K_α radiation (wavelength = 1.54ºA). TEM images of the catalysts were taken by JEOL, JEM-2010.

III. Results and Discussion

N_2 adsorption-desorption isotherms, and BJH desorption pore size distributions of the large pore SBA-15 support and 10Ni/SBA-15 catalysts are shown in **Fig. 1** and **2**. BET surface area (S_{BET}), BJH pore volume (V_P), and pore size (D_{BJH}) are listed in **Table 1**.

The N_2 adsorption isotherms of the SBA-15 materials are typical type IV isotherm with H1 hysteresis loops, representing the characteristic for mesoporous materials according to IUPAC classification [16]. The isotherms of the SBA-15 synthesized at 333 K (SBA-15;333/2D and SBA-15;333/5D) showed a thinner and narrow hysteresis loop than that of the SBA-15 synthesized at 353 K. Consequently,

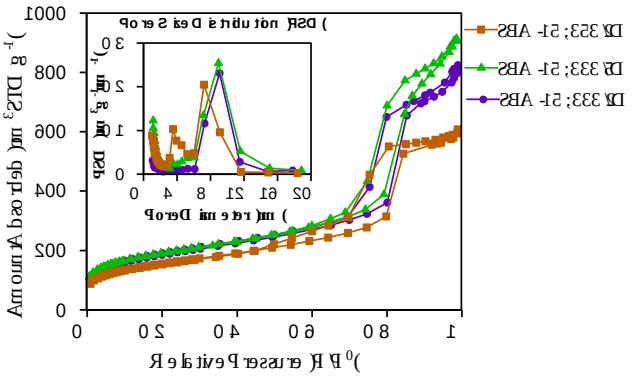

Fig. 1. Structural properties of the large pore SBA-15.

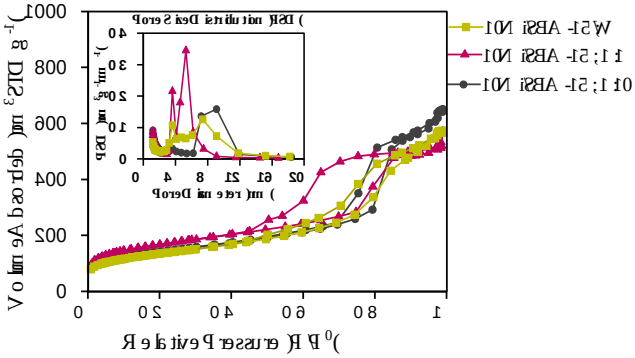

Fig. 2. Structural properties of the 10Ni/SBA-15 catalysts.

pore size distributions in SBA-15;333/2D and SBA-15;333/5D catalysts were narrow pore diameter range (6-12 nm) and pore diameter at a maximum point were 9 nm and 9.1 nm, respectively. In contrast, SBA-15;353/2D catalyst had dual pore size distribution in which the new pore size region appeared at 3-6 nm. These small pore sizes were probably due to the evaporation of hexane during aging at 353 K.

The hysteresis loop of the 10Ni/SBA-15;W catalyst (**Fig. 2**) become wider significantly and resulted in dual pore size distribution with 3-5 nm and 5-12 nm by Ni impregnation. In the EG assisted 10Ni/SBA-15;1:1 catalyst, the hysteresis loop enlarged and the pore size distribution range moved to a lower pore size region with a dual pore size distribution range of 3-4 nm and 4-9 nm. Fortunately, significant deformation was not observed in the 10Ni/SBA-15;1:10 catalyst by Ni impregnation. Pore size distribution range also similar to the pure SBA-15 support. However, the amount of pore volume was less than the pure SBA-15 support, associated with the placement of Ni particles into the porous structure of the SBA-15 support.

Table 1. Characteristic of the SBA-15 materials and 10Ni/SBA-15 catalysts

Material	S_{BET} m^2/g	V_P cm^3/g	V_{MP} cm^3/g	D_{BJH} nm	D_{NiO}^/* nm
S; 353/2D	545	0.935	0.036	3.4/6.7	-
S; 333/5D	670	1.41	0.053	9.1	-
S; 333/2D	666	1.27	0.045	9	-
10Ni/S;W	478	0.889	0.028	7.4/3.6	15^ / 20*
10Ni/S;1:1	596	0.885	0.047	5.3/3.6	3.2^ / 4*
10Ni/S;1:10	629	0.817	0.042	9.1	4.8^ / 4.5*

S: SBA-15, S_{BET}: BET specific surface area, V_P: total pore volume, V_{MP}: micro-pore volume, D_{BJH}: BJH pore diameter (taken as a maximum point), D_{NiO}^ crystallite size of NiO (calculated from XRD result),D_{NiO}^ average particle size of NiO (calculated from 70-100 particles of TEM images)

S_{BET} and V_P of the SBA-15;333 were higher than SBA-15;353. Both SBA-15;333 materials exhibited high S_{BET}, large V_P, and favorable pore diameter. Consideration from the energy usage, SBA-15; 333/2D required shorter aging time that it was chosen as a support for the synthesizing of the 10Ni/SBA-15 catalysts.

S_{BET} and V_P of the SBA-15 support were lost by Ni impregnation. S_{BET} lose in 10Ni/SBA-15;W, 10Ni/SBA-15;1:1 and 10Ni/SBA-15;1:10 catalysts were 28%, 11% and 6%. In the same way, V_P losses were 30%, 30%, and 45%, respectively. Among them, 10Ni/SBA-15;1:10 catalysts have the smallest loss in S_{BET} and V_P.

X-ray diffraction patterns and TEM images can be seen in **Fig. 3** and **4**. The particle size of the NiO (D_{NiO}) of the 10Ni/SBA-15 catalysts is presented in **Table 1**.

In 10Ni/SBA-15;W catalyst, the sharp diffraction peaks were identified at 2θ of 37.18, 43.21, and 62.7, attributed to the crystalline NiO phase. In 10Ni/SBA-15;1:1 and 10Ni/SBA-15;1:10 catalysts, the diffraction peaks of NiO are weak and diffused, associating to small NiO nanoparticles with high dispersion. The crystallite sizes of the NiO were calculated from 2θ of 43.21 degrees and it was 14.86 nm in the 10Ni/SBA-15;W catalyst while the crystallite sizes were smaller than 5 nm in the 10Ni/SBA-15;1:1 and10Ni/SBA-15;1:10 catalysts.

The dispersion of NiO particles in the SBA-15 support can be seen in TEM images. In 10Ni/SBA-15;W catalyst (**Fig. 4 (a)**), large NiO particles are deposited on the surface of the SBA-15 support. In 10Ni/SBA-15;1:1 and 10Ni/SBA-15;1:10 catalysts (**Fig. 4 (b)** and **(c)**), very small NiO single

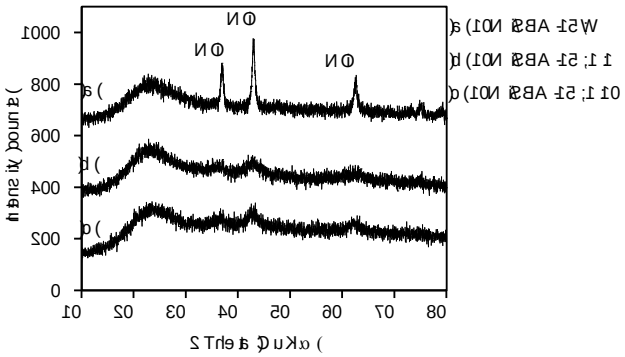

Fig. 3. XRD patterns of the 10Ni/SBA-15 catalysts.

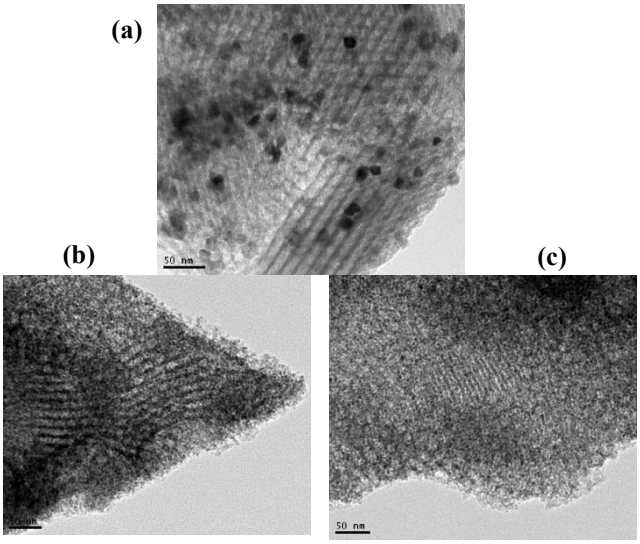

Fig. 4. TEM images of the catalysts (a) 10Ni/SBA-15;W, (b) 10Ni/SBA-15;1:1 and (c) 10Ni/SBA-15;1:10.

particles are highly dispersed in the mesoporous SBA-15 support. 10Ni/SBA-15; 1:10 catalysts showed better dispersion than 10Ni/SBA-15;1:1 catalyst. According to TEM results, the particle size of NiO in 10Ni/SBA-15;W catalyst was 20 nm while that in 10Ni/SBA-15;1:1 and10Ni/SBA-15;1:10 catalysts were 4 and 4.5 nm.

IV. Conclusion

Mesoporous SBA-15 material with a narrow pore size distribution, 6-12 nm, with pore size (at maximum volume point), 9 nm, was obtained by aging at 333 K and aging time for 2 days using soft template method. The catalyst with small NiO nanoparticles (< 5nm) was obtained by synthesizing EG assisted impregnation method while the conventional method resulted in large NiO particles (19.9 nm). As determined by N_2 physisorption, it can be expected that NiO nanoparticles are delivered into the porous structure of SBA-15 support in 10Ni/SBA-15;1:10 catalyst. Therefore, 10Ni/SBA-15; 1:10 catalyst will the most possible candidate for tar steam reforming catalyst, and catalytic activity will be confirmed by the catalytic steam reforming experiments in our future study.

References

[1] L. Wanga, L. Wellerb Curtis, D. Jonesb David, A. Hannab Milford, *Biomass and Bioenergy* 2008, 32: 573-581.

[2] Behdad Moghtaderi, *Fuel*, 2007, 86: 2422–2430.

[3] D. Li, Y. Nakagawa and K. Tomishige, *Chin. J. Catal.*, 2012, 33: 583–594.

[4] M. Yung Matthew, S. Jablonski Whitney, and A. Magrini-Bair Kimberly, *Energy & Fuels,* 2009, 23: 1874–1887.

[5] E. Ahmadi, N. Dehghannejad, S. Hashemikia, M.Ghasemnejad, and H. Tabebordbar, *Drug Deliv*, 2014, 21(3): 164–172.

[6] N. Rahmat, A. Z. Abdullah, A.R. Mohamed, *Am. J. Applied Sci.*, 2010, 7(12): 1579-1586.

[7] M. Kruk and L. Cao, *Langmuir,* 2007, 23, 7247-7254.

[8] M. Campanati, G. Fornasari and A. Vaccari, *Catalysis Today*, 2003, 77: 299–314.

[9] P. van Beurden*, ECN-I--04-003*, December 2004.

[10] Q. Zhu and Q. Xu, *Chem 1*, 2016, 220-245.

[11] Q. Zhu, J. Li, and Q. Xu, *J. Am. Chem. Soc.,* 2013, 135:10210−10213.

[12] A. Aijaz, A. Karkamkar, Y. J. Choi, N. Tsumori, E. R. Nnebro, T. Autrey, H. Shioyama, and Q. Xu, *J. Am. Chem. Soc*. 2012, 134:13926−13929.

[13] Arshad Aijaz and Qiang Xu, *J. Phys. Chem. Lett.,* 2014, 5: 1400−1411.

[14] S. Qiu, Q. Zhang, W. Lv, T. Wang, Q. Zhang and L. Ma, *RSC Adv.*, 2017, 7: 24551–24560.

[15] M. Kruk and L. Cao, *Langmuir*, 2007, 23:7247-7254.

[16] K. S. W. SING, *Pure & Appl.Chem.,* 1982, 54: 2201-2218.

The 13th AUN/SEED-Net Regional Conference on Chemical Engineering 2020 (RCChE-2020)
Jointly held with
The 5th International Symposium on Conservation and Management of Tropical Lakes
"Insights and Challenges toward Achieving SDGs"

Effect of Temperature and pH on Lanthanum Precipitation from Spent Catalysts Using Oxalic Acid

Fellicia Kartika Sari [1], Himawan Tri Bayu Murti Petrus [1*] and Widi Astuti [2]

[1] *Department of Chemical Engineering (Sustainable Mineral Processing Research Group), Universitas Gadjah Mada Jl. Grafika 2, Yogyakarta 55281, Indonesia*
[2] *Research Division for Mineral Technology, Indonesian Institute of Sciences (LIPI) Jl. Ir. Sutami Km. 15, Tanjung Bintang, Lampung Selatan, Indonesia*
**E-mail : bayupetrus@ugm.ac.id*

Abstract

Currently, REE is categorized as a critical mineral where there are few underground sediment reserves and occurs in small concentrations in many locations. The increasing use of REE globally has a vital function in the high technology industry to produce superior products. Indirectly unwanted by-products are also produced as a waste of spent catalysts. Interestingly, spent catalysts as secondary resources are mostly done to extract valuable minerals using reagents. This research is the basis for studying the precipitation of one of the REE minerals (i.e., lanthanum) from spent catalysts using oxalic acid at various temperatures and pH. Begins with a leaching process of 125 grams of used lanthanum catalyst using 500 mL of 1 M citric acid, followed by precipitation using 0.5 M oxalic acid by varying the temperature (60; 80; 90) and pH (1.0; 1.5; 2.0). Based on the analyzed results using the response surface method (RSM), to find the optimal value of several independent variables that affect a response variable on precipitation characteristics. A second-order polynomial equation was used to correlate response and independent variables. The coefficient of determination (R^2) shows a satisfactory result of 98.86%, and the standard probability plot ensures the model's adequacy.

Keywords: *lanthanum, oxalic acid, precipitation, REE, RSM (Response Surface Method), spent catalysts*

I. Introduction

Technological advances and industrial growth will produce desired products, but unwanted by products are also produced as waste from spent catalysts with different types, namely liquid, gas, and solid waste[1].

Minimizing waste not only demonstrates an ability to tre at waste from an economic perspective but is also an im portant part of environmental management responsibility. Many of the wasteby-products of spent catalysts, which management methods are widely used by industry, are t he disposal of land (land disposal)[2].

Precipitation reaction is a method of separating rare eart h elements which are widely used precipitating substanc e in a solution due to a chemical reaction. This is by ad ding certain chemicals that can change the compounds c ontained in the liquid into solids.

The choice of acid greatly influences the precipitation yield. In previous studies, most of the precipitation process used oxalic acid, which in Indonesia always increases every year. Currently, Indonesia is still importing oxalic acid from abroad to fulfil some of the domestic needs for oxalic acid. Oxalic acid is widely used as a neutralizing or acidifying agent, a material for celluloid and rayon, explosives, glycerol purifiers, stearin, tanneries, dyestuffs and for laboratory purposes[3].

Oxalic acid is an example of an organic acid that will be used in the precipitation process. Meanwhile, the spent catalyst lanthanum used was the result of leaching that had been carried out in previous studies. The use of oxalic acid is to obtain high levels of lanthanum from spent catalysts and

minimize waste of spent catalysts.

II. Materials and Methods

2.1. Raw material

The initial raw material for precipitation is a solution of leaching spent catalyst lanthanum with citric acid ($C_6H_8O_7$) 0.1 M. For the leaching process using a hot plate stirrer equipped with an Erlenmeyer, magnetic stirrer, thermometer, and laboratory meters for pH. The leaching solution was heated to a temperature of 90°C and stirred at a speed of 400 rpm for 8 hours in pH 2. Table 1 and Fig. 1 are the analysis of the leaching solution using XRF and XRD

Table 1. XRF result of spent catalyst

Constituents	%Mass
Al	24.109
Si	57.464
Ni	8.569
Fe	2.351
Ti	2.246
La	**1.912**
P	1.001
Ca	0.625
Mn	0.451
Co	0.353
K	0.22
Zn	0.151

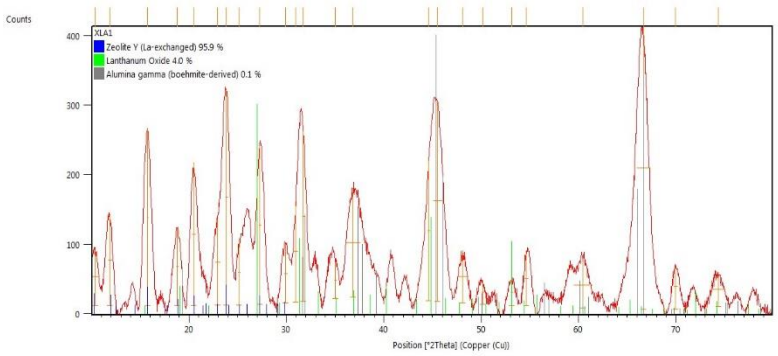

Fig. 1. XRD pattern of the spent catalyst

2.2. Precipitation process

The precipitation process is carried out using a hot plate stirrer. The immediate solution (leaching results) of 100 ml was put into Erlenmeyer, then added 0.5 M oxalic acid ($C_2H_2O_4$) until it reached pH 1. The process was carried out for 2 hours at 60^0C, 80^0C, and 90^0C. The experiment was repeated at pH 1.5 and pH 2 with the same temperature and time. The precipitate is then filtered using filter paper and dried in an oven at 90^0C. After drying, the solids are then weighed. The filtered liquid (filtrate) was then analyzed using ICP-OES. The weighed solid was analyzed using XRF and XRD. Table 2 is the analysis result using ICP-OES solution of precipitation spent catalyst lanthanum using oxalic acid.

Table 2. ICP-OES Result for Lantahnum Precipitation

Temperature (^{0}C)	pH	Concentrate (ppm)
60	1	0.071
	1.5	0.222
	2	0.735
80	1	0.075
	1.5	0.221
	2	0.742
90	1	0.066
	1.5	0.236
	2	0.453

2.3. Recovery Analysis of Precipitate

The result of the precipitation process will produce sediment in the form of wet solids and a filtrate solution. The wet solids are dried and weighed, then analyzed using XRF to determine the elemental composition in these solids and XRD to identify the crystalline phase in the material.

In the filtrate solution, using ICP-OES analysis to determine the concentration that is reduced during the precipitation process. Therefore, the recovery calculation must be done using a constant denominator, not the total Mass. It can be seen in the following formula :

$$\%R = \frac{M_0 - M_l}{M_0} \qquad \text{(Eq.1)}$$

Where % R is the recovery percentage, M_0 and M_l are the weight of lanthanum after precipitation and after the leaching process, where the Mass after leaching is 1.0703 in gr.

2.4. Design Response Surface Method of Experiment

This study aims to understand the role of the response surface method in determining the value of the independent variables and response variable. The selection of a suitable experimental design and analysis for the response surface is essential. A full three-level factorial design was used with two independent variables, pH and temperature. The response variable must be the precipitation of lanthanum[4].

The design is shown in Table 3 :

Table 3. Experimental range and level of independent variables

Independent variables	Range Level		
	+1	0	-1
pH (X_1)	1	1.5	2
Temperature, ^{0}C (X_2)	60	80	90

With the second-order polynomial equation, written as following [5] :

$$y = \beta_0 + \sum_{i=0}^{k} \beta_i x_i + \sum_{i=1}^{k} \beta_{ii} x_i^2 + \sum\sum \beta_{ij} x_i x_j + \varepsilon \qquad \text{(Eq.2)}$$

Where x_1 and x_2 represent the coded value of the input factor that determines the response (y). In addition, β_0, β_i , β_{ii} , and β_{ij} represents the regression equation, and the last a symbol is ε is the error[6]. The model's RSM accuracy was analyzed using the coefficient of determination (R^2). The value R^2 has ranged from 0 to 1. If R^2 is close 1, it shows that the model is highly accurate[7].

III. Results and Discussion

3.1. Analysis of Variance (ANOVA)

Based on research conducted using ICP-OES analysis and recalculating to get the grams contained in the filtrate solution from the precipitated results. The results are in Table 4. It can be seen that at a temperature of 60°C with a pH of 2, the result of lanthanum recovery is 98.78%. This calculation uses the formula previously described and precipitate which is only produced at a temperature of 60°C with a pH of 2.

Table 4. The Filtrate Solution from The precipitated

Temperature (^{0}C)	pH	Precipitate (gr)	La Recovery %
60	1	1.056	98.67
	1.5	1.055	98.60
	2	1.057	98.78
80	1	1.037	96.89
	1.5	1.037	96.90
	2	1.035	96.69
90	1	0.986	92.10
	1.5	0.964	90.04
	2	0.940	87.83

The estimation results of the model equation coefficient from the Minitab 18 output are shown in the following equation:

$$\text{Precipitation (gr)} = 0{,}728 + 0{,}3418\ X_1 + 0{,}00380\ X_2 - 0{,}1067\ X_1^2 - 0{,}000014\ X_2^2 - 0{,}001493\ X_1X_2$$

The data satisfactoriness and the model's fitness were assessed by regression and analysis of variance (ANOVA). It can be concluded that the second-order model for this case is the right model. The results can be seen in Table 5. This can be seen from the P-value for the model is greater than α = 5% while for the second-order model, the P-value is less than α. The P-value = 0.001 is smaller than the degree of significance α = 5%, and this means that the independent variables xi make a significant contribution to the model. As it can be seen from the table, the P-value for all linear independent variables were practically smaller than the square or 2-way interaction mode.

Table 5. Analysis of Variance from Minitab 18

Source	DF	Adj SS	Adj MS	F-Value	P-Value
Model	5	0,015191	0,003038	52,05	0,004
Linear	2	0,012352	0,006176	105,82	0,002
X_1	1	0,011984	0,011984	205,33	0,001
X_2	1	0,000368	0,000368	6,31	0,087
Square	2	0,001437	0,000719	12,31	0,036
X_1* X_1	1	0,001422	0,001422	24,37	0,016
X_2* X_2	1	0,000015	0,000015	0,25	0,648
2-Way Interaction	1	0,000520	0,000520	8,91	0,058
X_1* X_2	1	0,000520	0,000520	8,91	0,058
Error	3	0,000175	0,000058		
Total	8	0,015366			

For the model summary, from the result using Minitab 18, R^2 square in the precipitation resul 0,98 and the prediction 0,84. The results can be seen in Table 6

Table 6. Model Summary Precipitation vs pH;Temperature

S	R-sq	R-sq(adj)	R-sq(pred)
0,0076398	98,86%	96,96%	84,61%

IV. Conclusion

In this study, from the experimental results it can be concluded that oxalic acid (C2H2O4) can be used as a depositing agent for a solution of precipitation spent catalyst lanthanum and the maximum presentation of lanthanum is obtained at 60 ° C at pH 2 with a large percentage of recovery of 98.67%.

Acknowledgement

The authors are very thankful to the Department of Chemical Engineering (Sustainable Mineral Processing Research Group), Universitas Gadjah Mada and Research Division for Mineral Technology, Indonesian Institute of Sciences (LIPI) Lampung support.

References

[1] O. Sidjabat, "Effect of the Element Lanthanum (La) on Fe-Zeolite Catalyst in the Treatment of Liquid Waste Containing Phenol," vol. 41, no. 3, pp. 43–51, 2007.

[2] P. Studi and T. Lingkungan, "Utilization of Waste as Oil Processing Catalyst," pp. 182–188, 2008.

[3] N. Nurul, S. Chadijah, and K. Ramadani, "Optimal Time And Temperature In The Production Of Oxalic Acid (H2c2o4) From HVS Waste With Alkali Melting Method," *Al-Kimia*, vol. 5, no. 1, pp. 39–47, 2017, DOI: 10.24252/al-Kimia.v5i1.2847.

[4] H. Tri *et al.*, "Study on Temperature and Molarity Effect on Lanthanum Extraction From Spent Catalyst Using," no. May, pp. 2–5, 2018.

[5] R. Faulina, S. Andari, and D. Anggraeni, "Response surface methodology (RSM) dan aplikasinya," *Magister Stat. Its*, pp. 152–175, 2011.

[6] A. Yulandra, I. Trisnawati, I. M. Bendiyasa, W. Rachmi pusparini, and H. T. B. M. Petrus, "Optimasi Presipitasi Logam Tanah Jarang dari Campuran Konsentrat Logam Tanah Jarang dengan Metode "Response Surface Methodology"," *Met. Indones.*, vol. 42, no. 1, p. 28, 2020, doi: 10.32423/jmi.2020.v42.28-34.

[7] N. Vedaraman *et al.*, "Ultrasonic extraction of natural dye from Rubia Cordifolia, optimization using response surface methodology (RSM) & comparison with artificial neural network (ANN) model and its dyeing properties on different substrates," *Chem. Eng. Process. - Process Intensif.*, vol. 114, pp. 46–54, 2017, doi: 10.1016/j.cep.2017.01.008.

Synthesis Zeolit X and Zeolit A from Geothermal Sludge

Reny Oktavianti [1*], Chandra Wahyu Purnomo [1] and Rochmadi [1]

[1] *Department of Chemical Engineering (Sustainable Mineral Processing Research Group), Universitas Gadjah Mada*
Jl. Grafika 2, Yogyakarta 55281, Indonesia
**E-mail : reny.oktavianti@mail.ugm.ac.id*

Abstract

Geothermal sludge was a waste from Geothermal Power Plant Dieng, produced about 165 tons per month. An alternative way to reduce waste accumulation is to utilize it for zeolite synthesis. Based on EDX analysis carried of day geothermal sludge it contains 98% silica. Geothermal sludge has the potential to be processed into zeolite base material which has high economic value. Zeolite synthesis was carried out by hydrothermal at various operating temperatures 100^0C with a processing time of 7 hours, and variations molar ratio of Si/Al was 1, 1.5, 2. The characterization of synthetic products was carried out using XRD. Zeolite X and zeolite A synthesis have the highest crystallinity at ratio Si/Al of 1.5 at 77.62 % and 22.38 % respectively. Crystallite size of zeolite X molar ratio Si/Al 1, 1.5, and 2 is a 137.120 nm, 122.898 nm, and 146.914 nm respectively.

Keywords: *synthesis, geothermal sludge, hydrothermal, zeolite A, zeolite X*

I. Introduction

Indonesia has the potential source of silica from geothermal solid waste. Geothermal waste, a by-product of steam power plants that use underground geothermal resources. The use of geothermal energy as a Geothermal Power Plant positively impacts national development because geothermal energy is abundant [1]. However, the negative impact of using geothermal energy as an energy source is that geothermal energy production produces waste. For example, the deposition column's resulting sludge at power plant Dieng-Wonosobo reaches around 165 tons per month [2].

One alternative to prevent environmental pollution from waste accumulation is to process the geothermal sludge waste at the power plant into synthetic zeolite raw materials. Geothermal dry contains approximately 98% silica after energy dispersive X-ray analysis. From previous research, experiments with a geothermal waste composition of silica sand elements from power plant Dieng were mostly SiO2 of 77.7748% [3].

Zeolite is a porous material widely used in research and industry and has high commercial value. Zeolite has the form of alumina -silicate crystals that are very regular with cavities interconnected in all directions which cause the zeolite surface area to be quite large. The formation of zeolite is influenced by temperature, time, hydroxide concentration, Si/Al ratio, reaction pressure, ageing, and stirring [4]. In this research, zeolite will be synthesized hydrothermally with the primary material of geothermal sludge obtained from power plant Dieng owned by PT. Geo Dipa Energy. The final result of this research aims to get zeolite X and A in the zeolite synthesis.

II. Materials and Methods

2.1. Raw material

This study's raw materials were geothermal solid waste obtained from PT GEO DIPA, Dieng-Wonosobo, Central Java, Indonesia (98% silica), Sodium Hydroxide and Aluminium Hydroxide powder were purchased from Merck (UN 1283), and demineralized water.

2.2. Zeolite Synthesis

Geothermal sludge is cleaned of impurities and then dried using an oven until it forms a powder and sieving into 100 mesh. The geothermal powder is then calcined by igniting in a furnace at a temperature of 650ºC for 6 hours. X-Ray Diffraction analyzed geothermal solid waste to determine the chemical and its mineralogical. The geothermal powder (50 gram) and mixed with NaOH solution 3.5M then heated followed by stirring (300 rpm) at 90˚C for 60 minutes until homogenous was obtained.

Component	Element %	
	Before Furnace	After Furnace
SiO_2	94.727	98.138
SO_3	2.648	0.732
K_2O	1.033	0.509
Fe_2O_3	0.825	0.416
CaO	0.601	0.129
Sb_2O_3	0.057	0.025
As_2O_3	0.040	0.020
CuO	0.038	0.009
MnO	0.001	0.007
Br	0.013	0.005
Rb_2O	0.009	0.005
ZnO	0.007	0.001

Based on the analysis of the EDX results in Table 1, Si (silica) 's elemental content in the geothermal powder before calcination was 94.727% and after calcining was 98.138%. This shows that after calcined geothermal powder at a temperature of 650^0C for 6 hours can reduce the metal content in it to increase the percentage of silica element content in geothermal powder.

Table 2 is the analysis result using ICP solution of extraction silica.

The zeolite formation is carried out by adding Al powder (in grams) to the sodium silicate solution with the calculated Si/Al ratio (1; 1.5; 2). The solution was put into an autoclave reactor and heated at 100 °C for 7 hours. The hydrothermal output of the zeolite was then washed by using demineralized water.

2.3. Catalyst characterization

The catalysts were analyzed in term of crystallinity, specific surface area, and morphology. The crystallite was determined by using X-ray Diffraction (XRD).

III. Results and Discussion

3.1. Characteristics of Geothermal Powder Raw Materials

The raw material can use in geothermal powder. The composition of geothermal sludge can be seen in Table 1. Where the silica content is the largest component compared to other components.

Table 1. Composition Geothermal Sludge

Based on the analysis of the EDX results in Table 1, Si (silica) 's elemental content in the geothermal powder before calcination was 94.727% and after calcining was 98.138%. This shows that after calcined geothermal powder at a temperature of 650^0C for 6 hours can reduce the metal content in it to increase the percentage of silica element content in geothermal powder.

Table 2. ICP-OES Result for Synthesis Zeolite

Component	Element (ppm)	
	Furnace Method	Leaching Method
Si	7,098	20,371
Al	209	209
Na	1,205	1,602

In table 4.2, the results of the ICP (Inductively Coupled Plasma) analysis from silica extraction using the tube furnace method are shown, the components of silica, alumina, sodium are 7,098 ppm; 209 ppm; 1,205 ppm and the leaching method each obtained 20,371 ppm; 209 ppm; 1,602 ppm. Of the two approaches, the most extensive silica extract is the leaching method. This is because the silica leaching method has high solubility. Compared to using the tube furnace method, the solubility of silica is lower because it is carried out in the solid-solid phase with the addition of NaOH as a solvent.

Any factor that increases diffusivity and solubility in the above steps will facilitate extraction. Extraction of silica from geothermal powders yields a percent yield of 90-95% [17]. And taking silica from geothermal powders using the tube furnace method yields a percent yield of 70-75%. The percent yield also strengthens that the leaching method of

silica removal results in a relatively large silica solubility compared to the tube furnace method.

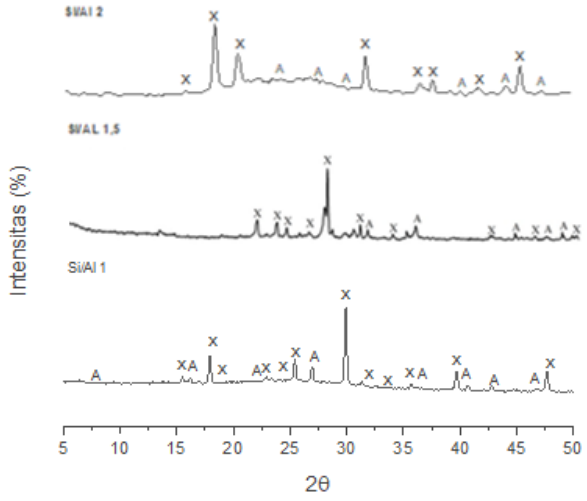

3.2. Synthesis of Zeolite X

Zeolite synthesis is carried out by dissolving the ingredients with distilled water. The material dissolved with water is then mixed with NaOH solution to form a sodium aluminate and sodium silicate solution. NaOH functions in zeolite synthesis as an activator during smelting to form a water-soluble solution of sodium aluminate and sodium silicate, then mixed and stirred using a stirrer for 60 minutes until the mixture is homogeneous.

The next stage of the sol-gel method is polycondensation; at this stage, the transition process from sol to gel occurs. To produce the maximum gel, a curing/ripening stage of the gel is required, carried out for 30 minutes. In the ageing stage, a gel tissue formation is stiff, strong and shrinks in solution. This stage plays an essential role in zeolite synthesis because it includes a gel formation process that is the beginning of nucleation and crystal growth [14]. In mixing these materials, the following reactions occur [14]. The reaction that occurs in silica removal:

$$SiO_{2\,(s)} + 2NaOH_{(aq)} \longrightarrow Na_2SiO_{3\,(aq)} + H_2O_{(l)}$$

The reaction of making aluminate:

$$Al_2O_{3\,(s)} + 2NaOH_{(aq)} \longrightarrow Na_2Al_2O_{4\,(aq)} + H_2O_{(l)}$$

Overall reaction:

$$NaOH_{(aq)} + {}_x\,Al_2O_3.\,ySiO_2\; Na_2SiO_{3\,(aq)} + Na_2Al_2O_{4\,(aq)}$$
$$\longrightarrow NaOH_{(aq)} + Na_2Al_2\,(OH)_{4\,(aq)} + Na_2SiO_{3\,(aq)}$$
$$\longrightarrow Na_x\,(AlO_2)_{\,y}\,(SiO_2)_{\,p}\,(SiO_2)_{\,z}.NaOH.H_2O_{(gel)}$$
$$Na_p\,(AlO_2)_{\,p}\,(SiO_2)_{\,p.\,h}\,H_2O_{(gel)}$$

The final stage of the hydrothermal sol-gel method is drying (drying) to remove unwanted water and liquid in zeolite X, to expand zeolite X's surface.

Product Zeolit	Component (%)	
	Zeolit A	Zeolit X
Ratio 1	28.17	71.83
Ratio 1.5	22.38	77.62
Ratio 2	27.32	72.68

3.3. Charactesization of synthetic zeolite, Si/Al ratio 1; 1.5; 2 with X-Ray Diffraction (XRD)

Figure 1. Zeolite X and A Molar Ratio Si / Al diffractogram

Zeolite X is the most dominant phase formed in each synthetic zeolite ratio. The number of zeolite X peaks started decreases with increasing Si/Al molar ratio. The number of zeolite peaks X at the rate 1; 1.5; and 2, respectively 12, 10, and 8. The height of zeolite A also decreases in intensity as the Si/Al molar ratio increases. However, the ratio of 1.5 has the least amount of zeolite A mixture, so that the purest zeolite X is obtained at a ratio of 1.5.

The crystallinity of zeolite X was higher with increasing Si/Al molar ratio. However, zeolite X's highest crystallinity occurs at a ratio of 1.5 so that the crystallinity of zeolite X is 1.5 > ratio 2 > ratio 1. This difference in crystallinity occurs because the number of crystalline fields produced in each ratio is different. Samples that can reflect more rays will produce high intensity so that the crystallinity of zeolite X increases [12].

The qualitative analysis of synthetic zeolites is related to the number of zeolite peaks formed. The more zeolite X peaks formed and the less zeolite A peaks, the greater the purity of zeolite X. Meanwhile, quantitative analysis was carried out to determine the synthetic zeolite's percentage composition. Based on the XRD results, it was found that all synthetic products were formed of two types of zeolites, namely zeolites X and A. The quantitative analysis of the composition of synthetic zeolites is shown in Table 3. Synthesis Zeolite Products Synthesis Zeolite Composition (%)

Table 3. Results of Quantitative Analysis

Based on Table 3. that the highest percentage of zeolite X purity was found at a ratio of 1.5 compared to synthetic

zeolite with other ratios of 77.62%. In general, the percentage of zeolite X purity decreases with increasing Si/Al ratio. This is due to the decreasing number of zeolite X peaks formed. However, at a ratio of 1.5, the highest percentage of zeolite X is found at a ratio of 1.5.

Table 4. Distance between Crystal

Table 4. shows that the distance between crystal planes from the smallest is zeolite X ratio 1.5 < zeolite X ratio 2 < zeolite X ratio 1. The smaller the distance between the crystal planes, the denser and more stable the crystal structure is. This causes the crystal structure formed to have high crystallinity. The highest crystallinity is zeolite X at a ratio of 1.5.

Table 5. Size of Synthesized Zeolite X Crystals

Zeolit	Crystal Size (nm)
Si/Al 1	137.120
Si/Al 1.5	122.495
Si/Al 2	146.914

The XRD analysis data can also be used to determine the crystal size. The crystal size of synthetic zeolite X based on calculations using the Debye Scherrer equation is presented in Table 5. Based on these results, it is known that the crystal size of synthetic zeolite X is in the range of 100-200 nm.

The distance between particles in zeolite crystals is directly proportional to the crystal size [6]. The small crystal size causes the distance between the particles to be short so that the crystal structure formed becomes even tighter and more regular. The denser and more stable crystal structure causes the degree of crystallinity to be high, therefore according to the XRD results from the highest crystallinity of zeolite X, it is at a ratio of 1.5 the smallest crystal size compared to zeolite X ratios 1 and 2, which is 122.495 nm.

IV. Conclusion

Synthesis of zeolite X and A using the hydrothermal autoclave method produces crystalline zeolites, and the oven hydrothermal method has amorphous zeolites. According to the XRD analysis shown. Geothermal waste can be used as a raw material for making zeolite to increase the economic value of the waste.

Analysis using XRD shows that at each molar ratio Si / Al 1; 1.5 and 2 produce a mixture of zeolites X and A. The difference in Si/Al ratio affects the crystal structure formed. With the most extensive zeolite synthesis X and zeolite A composition, the Si/Al molar ratio of 1.5 reached 77.62% and 22.38%. Zeolite crystal size X Si/Al molar ratio 1; 1.5 and 2 are 137.120 nm; 122.495 nm and 146.914 nm.

Acknowledgement

Zeolit	Distance between Crystal (Å)
Si/Al 1	3.984
Si/Al 1.5	3.165
Si/Al 2	4.848

The authors are very thankful to the Department of Chemical Engineering (Sustainable Mineral Processing Research Group), Universitas Gadjah Mada.

References

[1] Saptadji, N.M. (2009). “Teknik Panas Bumi”. Departemen Teknik Perminyakan Fakultas Ilmu Kebumian dan Teknologi Mineral Institut Teknologi Bandung, Bandung.

[2] Suprapto, S. J. (2009). “Panas Bumi Sebagai Sumber Energi dan Penghasil Emas”. Warta Geologi Volume 4 No. 2, Bandung.

[3] Syakur, A., Tumiran, Berahim, H., Rochmadi, 2011, “Pengujian Karakteristik Limbah Pasir PLTP Dieng Sebagai Bahan Pengisi Isolator Resin Epoksi Silane”, Jurnal Rekayasa Elektrika Vol. 9, No. 4..

[4] Payra, Pramatha and Dutta, Prabir K. (2003). "Handbook of Zeolite Science and Technology". The Ohio State University Columbus.

[5] Hamdan, H., 1992, Introduction to Zeolites: Synthesis, characterization, and modifications, University Teknologi Malaysia, Kuala Lumpur.

[6] Ramirez, M., Garcia, T., Camacho, R., Badillo, L., Mojica, M., Gomez, M. (2020). Simple Synthesis of Hierarchically Structured X Zeolit from Geothermal Nanosilika and Its Evaluation in the Dehydration of Aqueous Solutions of Ethanol.

[7] Nikmah, R. A. Syukuri., Widiastuti, N., dan Fansuri, H. 2008. Pengaruh Waktu dan Perbandingan Si/Al Terhadap Pembentukan Zeolit A dari Abu Dasar Bebas Karbon dari PLTU PT. IPMOMI dengan Metode Hidrotermal. Journal of Indonesia Zeolites. Vol. 7 No. 1. Mei 2008 ISSN: 1411-6723.

The 13th AUN/SEED-Net Regional Conference on Chemical Engineering 2020 (RCChE-2020)
Jointly held with
The 5th International Symposium on Conservation and Management of Tropical Lakes
"Insights and Challenges toward Achieving SDGs"

Studying of Particulate Matter Concentrations in the Ambient Air during National Holidays and Special Events

Pothiphimean Chhheang [1], Chinda Haing [1], Chanreaksmey Taing [1,2,*], Rithy Kan [3], Chanmoly Or [3], Mitsuhiko Hata [4], Masami Furuuchi [4]

[1] *Faculty of Chemical and Food Engineering, Institute of Technology of Cambodia, Russian Federation Blvd., P.O. Box 86, 12156 Phnom Penh, Cambodia*
[2] *Research Unit Water and Environment, Institute of Technology of Cambodia Russian Federation Blvd., P.O. Box 86, 12156 Phnom Penh, Cambodia*
[3] *Research and Innovation Center, Institute of Technology of Cambodia, Russian Federation Blvd., P.O. Box 86, 12156 Phnom Penh, Cambodia*
[4] *Graduate School of Natural Science and Technology, Kanazawa University, Kakuma-machi, Kanazawa, Ishikawa, 920-1192, Japan*
* *tsmey16@gmail.com*

Abstract

Cambodian has many public holidays and special events. Annual movement of population in urban area during holidays affects the ambient air quality in Phnom Penh. Due to these reasons, the aim of this study is to determine the particulate matter (PM) concentrations during four special events, including Pchum Ben's Day, Water Festival, Year-end event, and Chinese New Year's Day and the influence of each event on the ambient air quality in Phnom Penh. The sampling point was conducted at the rooftop of Institute of Technology of Cambodia, building H (10 meter above the ground), three times a month and during studying occasions. The PM and Total Suspended Particles (TSP) mass concentrations were measured by gravimetric method, whilst Carbonaceous Aerosol (CA) were measured by IMPROVE-TOR protocol. According to the results, PM and TSP was generally higher during short-term events like year-end compared to long events like Chinese New Year. The average mass concentration of total carbon (TC) accounted for about 20% of TSP atmosphere during all the events. Meanwhile, PM concentrations were all lower than the WHO Air Quality Guideline ($PM_{2.5}$: 25 µg/m^3 PM_{10}: 50 µg/m^3) during all the events, except on the year-end celebration with the concentration of 55.694 µg/m^3 for PM_{10} and 37.282 µg/m^3 for $PM_{2.5}$. According to the result, the ambient air quality in Phnom Penh was mainly polluted on year-end, moderately effect on the Pchum Ben's Day and Water Festival. Surprisingly, the ambient air has not been severely polluted during Chinese New Year's Day as expected.

Keywords: *Anthropogenic sources, carbonaceous aerosols, particulate matter, public holidays, total suspended particles.*

I. Introduction

Population growth, industrialization, and socioeconomic development are the factors contributing to air pollution. The pollution may come from both natural and man-made sources. Fuel combustion is considered as an important source in lower-income countries, whilst motor vehicles in higher-income countries [1].

During the last decade, as a developing country, Cambodia undergoes through rapid economic and population growth. As a result, the numbers of vehicles and constructions have been significantly increased which leads to major environmental issues, including air, water, soil and solid wastes pollution. According to [2] , vehicle emission is considered as the critical source of air pollution in Phnom

Penh. The level of pollution from vehicles may vary from day by day, especially during special events and national holidays. Interestingly, during the holidays and religious-related event, the human activities and population flow in and out of the city fluctuate. On some occasions, people leave the city and go back to their homeland, while people from other provinces come to visit Phnom Penh during the events. For instance, during Water Festival, people from other provinces come to celebrate this event in Phnom Penh. Meanwhile, during Pchum Ben's day, people left the city and back to their hometown. It is interesting to discover the pollution level during these events on ambient air quality in Phnom Penh. Therefore, the objective of this study was to evaluate the impact of the events on the ambient air quality by determining PM, TSP, and CA concentration on the before, during and after the event in comparison to monthly concentration.

II. Materials and Methods

2.1. Sampling sites

The sampling point was located at the rooftop of building H of Institute of Technology of Cambodia, which is situated on the Russian Confederation Boulevard, Phnom Penh, Cambodia. The equipment was set at the geographical longitude of 104°53'48.19" and latitude of 11°34'14.18". The sampling point is approximately 10 meters above the ground level. There is no big building around to block the air circulation and it is surrounded by resident building, laboratories, and canteen. The high-volume air sampler (SHIBATA HV-500F) was used to collect the TSP. The sampler was operated at the constant flow rate of 500 L/min. Meanwhile for PM, Nano sampler designed by [3] was used with the constant flow rate of 40L/min.

2.2. Sampling period

The **Table 2.1.** represented the summary of sampling periods during the events. The sampling was conducted for.

Table 1. Summary of sampling periods

Events/holidays	Start date	Stop date
Pchum Ben (PB)	07/10/18	11/10/18
Water Festival (WF)	20/11/18	24/11/18
Year-end (YE)	30/12/18	01/01/19
Chinese New Year (CNY)	03/02/19	08/02/19

24 hours a day and only one sample was collected. At the same time, the sampling was conducted periodically 3 times a month or every ten days and were used as control.

2.3. Analytical methods

TSP and PM mass concentration

The mass concentration of Total Suspended Particle and Particulate Matter in samples were determined by the following formula.

$$TSP\ or\ PM = \frac{(M_f - M_i)}{V_T} \times 10^3 \qquad \text{(Eq. 1)}$$

The TSP and PM were expressed as $\mu g/m^3$ where; M_f was the final mass of filter and M_i was the blank filter mass (mg), and V_T was the sampling volume (m^3).

Carbonaceous aerosol mass concentration

The carbonaceous aerosol (CA) in the collected samples were determined via the protocol of IMPROVE TOR [4], [5] by using Carbon Thermo-Optical Analyzer. Firstly, the filter is cut into $0.5cm^2$ circular segment. Then this segment is insert into a heating zone where temperature is continuously increased in stepwise under two conditions, non-oxidizing (100% helium) and oxidizing (98%, 2% of helium and oxygen, respectively). During this heating stage, the carbonaceous aerosols on the sample is volatized, pyrolyzed, and combusted into gas-phase compounds which is oxidized into CO_2 as they pass through an oxidizer (MnO_2) at and reduced to CH_4 as they pass through nickel catalyst at approximately The CH_4 concentration is then determined by a flame-ionization detector (FID).

For 100% helium condition, the temperature is 120°C (OC1), 250°C (OC2), 450°C (OC3), and 550°C (OC4). As temperature increases to the next level, the response from FID might return to baseline or remain constant for 30 sec. The residence time is varied according to the sample loads, the longer time it takes for more heavily loaded samples. As for 98% helium and 2% oxygen condition, temperature plateaus are 550°C (EC1), 700°C (EC2), and 800°C (EC3). OC, EC, and TC are determined from eight carbon fractions as describe below [6]:

$$OC = OC1 + OC2 + OC3 + OC4 + OP \qquad \text{(Eq. 2)}$$
$$EC = EC1 + EC2 + EC3 - OP \qquad \text{(Eq. 3)}$$
$$TC = OC + EC \qquad \text{(Eq. 4)}$$

Table 2. Summary of TSP and Carbonaceous mass concentration

Event	TC (μg/m^3)	TSP (μg/m^3)	TC/TSP (%)	OC (μg/m^3)	EC (μg/m^3)	OC/EC	Char-EC (μg/m^3)	Soot-EC (μg/m^3)	Char-EC /Soot-EC
PB	18.7±4.0	106.4±20.6	17.5±1.8	13.4±2.7	5.2±2.0	2.8±0.8	2.6±1.2	2.6±0.9	1.0±0.2
Oct	17.8±7.3	106.0±27.2	16.8±3.4	12.2±4.2	5.6±3.1	2.4±0.7	3.1±0.7	2.5±0.5	1.1±0.2
WF	20.3±5.9	137.8±39.9	15.5±4.8	14.5±4.1	5.8±2.0	2.6±0.5	3.1±1.6	2.7±0.5	1.0±0.5
Nov	19.9±10.1	122.0±69.8	16.9±2.6	13.9±6.9	6.0±3.3	2.4±0.1	2.9±1.0	2.7±0.3	1.9±1.0
YE	28.0±2.2	149.4±8.3	17.8±5.0	21.9±1.3	6.1±0.8	3.6±0.3	3.0±0.1	3.0±1.0	2.6±1.1
Dec	21.2±3.3	111.9±21.9	19.1±1.2	15.2±2.5	6.0±0.8	2.5±0.1	1.5±0.8	3.0±0.2	2.1±0.8
CNY	25.2±3.8	149.7±16.3	16.5±1.9	19.2±2.8	6.0±1.2	3.2±0.3	3.9±1.0	2.2±0.6	1.9±0.8
Feb	31.8±8.4	152.8±18.2	17.2±1.5	23.9±6.4	7.9±2.0	3.0±0.2	2.2±2.0	3.0±02	1.6±0.7

Char-EC = EC1 – OP (Eq. 5)
Soot-EC = EC2 + EC3 (Eq. 6)

III. Results and Discussion

The concentration of TSP, TC, OC, EC, Char-EC and Soot-EC were summarized in **Table 1**. As shown in **Table 1**, all the parameters, except TSP and Char-EC, shared the same trend, the highest concentration of pollutants was found on YE followed by CNY, WF and PB. As for TSP, the highest concentration was found during CNY, following by YE, 149.7±16.3 μg/m^3 and 149.4±8.3 μg/m^3, respectively. The TSP level continuously rose from 106.4±20.6 μg/m^3 in PB and reached the highest on CNY with 149.7±16.3 μg/m^3. During December to early February, this period is considered as the coldest month of the year. Normally, people, especially in rural and suburb areas, practice open burning to against the cold weather. This might be the factor contributing to higher concentration during the last two events. Despite the rise of TSP level during studying period, the concentrations were still under the standard (330 μg/m^3) according to the Sub-decree on The Control of Air Pollution and Noise Disturbance by the Royal Government of Cambodia [7].

For CA, the average mass concentration of TC accounted for 18.7±4.0 μg/m^3, 20.3±5.9 μg/m^3, 28.0±2.2 μg/m^3, 25.2±3.8 μg/m3, individually. OC fractions were almost three-fold higher than EC fractions in all the events. Among all events, carbon composition made up of 15-20% of total TSP mass concentration. The average mass concentration of total carbon (TC) accounted for 17.5 %, 15.5%, 17.8%, 16.5% of average mass concentration in TSP in the atmosphere for PB, WF, YE, and CNY, respectively. The ratio of OC/EC in all the event exceeded 2.0,2.8±0.8, 2.6±0.5, 3.6±0.3, 3.2±0.3, orderly. High OC/EC ratio might be the contribution from OC-rich source emission to long-range transportation [8]. Some studies suggested the particles generated from the exhaust emission of diesel and gasoline motor vehicles when the ratios between 1.0 and 4.2 [9].The result is parallel to the report by [10] The ratios of OC/EC larger than 2.0 has been used as an indicator presence of SOC formation [11]. The OC fraction was found the highest concentration during YE (21.9±1.3 μg/m^3) and moderately greater than Dec (15.2±2.5 μg/m^3). Generally, people celebrate this event heavily, especially in Phnom Penh. At the midnight, there is also firework cracker and firework burning to welcome new year. All the temporary activities contribute to air pollution. As evident by [12], firework burning is considered as a short-term anthropogenic sources of air pollution since it emits a large amount of particulates and other toxic gases.

Overall, EC are made up of approximately 50% Char-EC and 50% of Soot-EC. It was reported by [4] that the ratio (<1) indicated motor vehicular exhaust, a ratio of 1.31 indicated coal combustion and ratio of 22.6 indicated biomass combustion. In this study, the highest ratio was found on CNY (3.8±1.5), suggesting that a great contribution from coal combustion process. The lowest concentration was observed on PB (1.9±0.4), indicating a greater generation of EC from the exhaust of vehicular emissions.

The **Table 3** described the PM mass concentration in comparison to WHO standard. Both PM¬10 (55.7±5.8 µg/m3) and PM2.5 (37.3±5.6 µg/m3) concentration on YE exceeded the WHO standard, 50 µg/m3 for PM10 and 25 µg/m3 for $PM_{2.5}$. As for PB and WF, the PM_{10} was still in allowance range, while $PM_{2.5}$ was over the standard. Surprisingly, both PM_{10} and $PM_{2.5}$ were under the standard on CNY. According to the comparison between the mean concentration of individual event with the standard by one sample t-test using SPSS program, all the mean concentrations were not statistically significant from the standard, except the PM_{10} on PB and CNY. This result indicated that YE was the most polluted event among all the studying events, following by WF, PB and CNY.

Table 3. Comparison of PM mass concentration to WHO Standard

Event	PM_{10}	$PM_{2.5}$
PB	24.74±9.06	17.29±6.90
WF	41.51±11.94	26.46±5.91
YE	55.44±6.83	37.12±6.77
CNY	35.21±9.86	18.32±2.97
Standard	50.00 ±0.00	25.00±0.00

IV. Conclusion

The TSP, PM and carbonaceous aerosol mass concentrations on PB, WF, YE and CNY were studied. For further studies, it is important to focus on temporal trends of PM, TSP and carbonaceous aerosol during Water Festival and year-end. In these two events, there is firework burning which is known to temporarily degrade air quality as it emits a large amount of air pollutants. In addition, it is also essential to extend sampling periods on pre-event and post-event. The evidence from this study is not strong enough to evaluate the effect of holidays and events on ambient air quality in PP by collecting the samples a day before and a day after event. Moreover, gases pollutants like NOx, O_3 and other heavy metals determination should be considered.

Acknowledgement

This work was supported by the Atmospheric Environment and Air Pollution Control at Kanazawa University.

References

[1] J. Cramer, "Population growth and local air pollution: methods, models, and results," *Popul. Dev. Rev.*, vol. 28, pp. 22–52, 2002.

[2] P. Ung and S. Sroy, "Effect of traffic and construction on air quality of Phnom Penh City, Cambodia," no. September, pp. 0–2, 2016.

[3] M. Furuuchi *et al.*, "Development and performance evaluation of air sampler with inertial filter for nanoparticle sampling," *Aerosol Air Qual. Res.*, vol. 10, no. 2, pp. 185–192, 2010.

[4] J. C. Chow, J. G. Watson, L. W. A. Chen, W. P. Arnott, H. Moosmüller, and K. Fung, "Equivalence of elemental carbon by thermal/optical reflectance and transmittance with different temperature protocols," *Environ. Sci. Technol.*, vol. 38, no. 16, pp. 4414–4422, 2004.

[5] J. G. Watson, J. C. Chow, and L.-W. A. Chen, *Summary of Organic and Elemental Carbon/Black Carbon Analysis Methods and Intercomparisons*, vol. 5, no. 1. 2005.

[6] J. C. Chow *et al.*, "The IMPROVE_A temperature protocol for thermal/optical carbon analysis: Maintaining consistency with a long-term database," *J. Air Waste Manag. Assoc.*, vol. 57, no. 9, pp. 1014–1023, 2007.

[7] Sub-Decree No 42, 2000. "ANUKRET on The Control of Air Pollution and Noise Disturbance. https://static1.squarespace.com/static/593a250a15d5dbd460e153ad/t/59784a59bf629a80c566ddce/1501055578125/The+Control+of+Air+Pollution+and+Noise+Disturbances+%282000%29.pdf Accessed on on 15 November 2020.

[8] W. Phairuang, M. Inerb, M. Furuuchi, M. Hata, S. Tekasakul, and P. Tekasakul, "Size-fractionated carbonaceous aerosols down to PM0.1 in southern Thailand: Local and long-range transport effects," *Environ. Pollut.*, vol. 260, p. 114031, 2020.

[9] J. J. Schauer, M. J. Kleeman, G. R. Cass, and B. R. T. Simoneit, "Measurement of emissions from air pollution sources. 5. C1 - C32 organic compounds from gasoline-powered motor vehicles," *Environ. Sci. Technol.*, vol. 36, no. 6, pp. 1169–1180, 2002.

[10] EANET, "MYANMAR: Policies and Practices Concerning Acid Deposition," no. 2, pp. 40–43, 2019.

[11] R. Zhang *et al.*, "Characterization of atmospheric organic and elemental carbon of PM2.5 in a typical semi-arid area of northeastern China," *Aerosol Air Qual. Res.*, vol. 12, no. 5, pp. 792–802, 2012.

[12] S. F. Kong *et al.*, "The impacts of firework burning at the Chinese Spring Festival on air quality: Insights of tracers, source evolution and aging processes," *Atmos. Chem. Phys.*, vol. 15, no. 4, pp. 2167–2184, 2015.

The 13th AUN/SEED-Net Regional Conference on Chemical Engineering 2020 (RCChE-2020)
Jointly held with
The 5th International Symposium on Conservation and Management of Tropical Lakes
"Insights and Challenges toward Achieving SDGs"

Identification and Quantitative Analysis of Alternative Diesel from Waste Plastic Pyrolysis

Zin Thu Aung [1], Chinda Charoenphonphanich[1*], Hidenori Kosaka [2], Pop-Paul Ewphun[2], Prathan Srichai[3]

[1]*School of Engineering,Department of Mechanical Engineering, King Mongkut's of Institute of Technology Ladkrabang, Soi chalongkrung1, Ladkrabang, Bangkok 10520 Thailand*
[2]*School of Engineering, Department of System and Control Engineering, Tokyo Institute of Technology, Ishikawadai 6th Building, Room 323-2-12-1 Ookayama, Meguro-ku, Tokyo, 152-8552, Japan*
Department of Mechanical Engineering, Princess of Naradhiwas University, Naradhiwas 96000 Thailand
**kmitl.chinda@gmail.com*

Abstract

Plastics are an essential part of the human life and the global economy. However, the use of plastics has been associated with significant environmental problems due to their accumulation in landfills, as plastic waste does not degrade or degrades at very low pace. Nowadays, fast pyrolysis of waste plastic into valuable fuels is main platform method in minimizing not only the waste disposal but also could be used as an alternative fuel for internal combustion engines. The purpose of this study was to identify, quantify and compare the composition of waste plastic diesel (WPD) with the commercial diesel (CD) of Thailand. Simulated distillation (GC-FID) and n-d-M method were used to find the composition of both fuels. Results indicated that the content of naphtha, kerosene, diesel, and long residue were determined quantitatively and also identified the paraffin, naphthenes, and aromatic contents for both fuels. Naphtha and heavy oil contents of WPD were 9.2 and 8.9wt% higher than that of CD but kerosene and diesel contents were 0.7and 17.4wt% less than that of commercial diesel. After that, paraffin, naphthenes and aromatic contents of WPD from PNA analysis were 80.42, 14.54 and 5.04wt% and these hydrocarbon contents of CD were 60.61, 25.91 and 13.48wt% respectively. By knowing them, the appropriate method can be determined for fuel upgrading and interpret correctly of combustion and emissions results.

Keywords: *Fast pyrolysis, Simulated distillation, n-d-M method, Waste plastic diesel, Commercial diesel*

I. Introduction

Plastic have essential materials due to their numerous applications in normal life. Consequently, a huge number of plastic products accumulate as waste in the environment. Plastic waste is a big issue in Thailand, because the amount of recycled plastic remains low due to recycling problems [1]. One of the recycling problems is economy as they need to be collected separately or sorted before the process can begin [2]. Most plastics are not compatible with each other and hence cannot be processed together during recycling. For instance, a PVC bottle in PET recycle can ruin the entire batch by becoming yellowish and brittle [3]. Unlike recycling, pyrolysis does not require a keen sorting of different plastics. Therefore, fast pyrolysis of waste plastic into valuable fuels is main platform method in minimizing not only the waste disposal but also could be used as an alternative fuel for internal combustion engines.

Previous studies found that individual type of waste plastics or mixed waste plastic, which were used to produce alternative fuel, identify the chemical compounds and carbon number, and investigate on physical properties

[4][5][6]. There are no or few studies to quantity the boiling fractions and hydrocarbon type of waste plastic fuel.

Therefore, the purpose of this study is to identify and quantify the composition of waste plastic diesel (WPD) from real mixed waste plastic pyrolysis, and compare with commercial diesel (CD).

II. Materials and Methods

2.1. Materials

The waste plastic diesel utilized in this study were derived from catalytic fast pyrolysis of real mixed waste plastic (mostly PVC) and commercial diesel (B10) were purchased from PTT fuel station in Thailand. **Table 1** shows the comparison of physical properties of WPD and CD.

Table 1. Physical properties of fuels

Property	ASTM Method	CD	WPD
Density@15℃ (kg/m^3)	D4052	824	805
Viscosity@40℃ (Cst)	D445	3.24	2.9
Cetane Index	D976	56.43	67.93
Energy Content (MJ/kg)	D240	45.86	46.29
Sulfur Content (wt.%)	D5453	0.003	0.014

2.2. Simulated Distillation Method

The identification and quantitative analysis of WPD and CD were done by simulated distillation (ASTM D2887). Simulated distillation is a Gas Chromatographic technique for determining the boiling point distribution of fuels by Flame Ionization Detection (GC-FID). Two standard solutions were used for quantification of waste plastic diesel and commercial diesel: normal alkanes ranging n-C_5 to n-C_{10} and n-C_{10} to n-C_{40}. **Table 2** shows the testing condition of GC-FID. In simulated distillation method, the analyte retention times are directly related to the boiling points of the various hydrocarbons. A calibration curve is generated from standard solution, where the retention time of each n-alkane is plotted against its boiling point. And calculating the area of each time interval which is divided by total area allows the proportion of elution weight (%) in each time interval. The elution weight (%) in each boiling point range can be determine from calibration curve and used to obtain the relationship between the elution weight (%) and boiling point, that is, to create the distillation curve of fuel samples.

Table 2. Experimental conditions for ASTM D2887

Column	DB-10,10mx0.53mm,2.65µm
Column temperature	40℃ to 350℃
Carrier gas flow rate	13.989 L/min (helium)
Injection temperature	350℃
FID temperature	375℃
Gas flow rate	
Nitrogen (makeup)	45 mL/min
Hydrogen	40 mL/min
Air flow	450 mL/min
Injection volume	0.1 µL

2.3. n-d-M Method (PNA composition Analysis)

This method requires three physical properties of refractive index(n_{20}), density(d_{20}), and molecular weight(M). For this reason, the method is called n-d-M method. The method is included in the ASTM manual under ASTM D3238. It calculates the distribution of carbon in paraffins($\%C_P$), naphthenes($\%C_N$), and aromatics($\%C_A$) using equation 1 to 5. The refractive index and density at 20℃ and molecular weight are used as input data, which are estimated from correlations that are adopted in API-TDB [7].

$$v = 2.51(n - 1.475) - (d - 0.851) \quad \text{(Eq.1)}$$

$$a = 430 \; if \; v > 0 \; and \; 670 \; if \; v < 0$$

$$\%C_A = av + 3660/M \quad \text{(Eq.2)}$$

$$w = (d - 0.851) - 1.11(n - 1.475) \quad \text{(Eq.3)}$$

$$\%C_R = 1440w - 3\%S + \frac{10600}{M} \; if \; w < 0 \quad \text{(Eq.4)}$$

$$\%C_R = \%C_N + \%C_A \quad \text{(Eq.5)}$$

$$\%C_P = 100 - \%C_R \quad \text{(Eq.6)}$$

III. Results and Discussion

` The simulated distillation curve represents the boiling points of compounds in a fuel mixture at atmospheric pressure. Simulated distillation curve is presented in term of boiling point versus wt% of mixture vaporized because composition is measured in terms of wt% or weight fractions in gas chromatography. And simulated distillation curve is very close to actual or true boiling point curve. The distillation curve obtained applying the ASTM D2887 method allow the quantification of fuel composition such as

naphtha, kerosene, diesel and heavy oil as shown in **Fig. 1.** And the composition of CD and WPD are listed in **Table 2.**

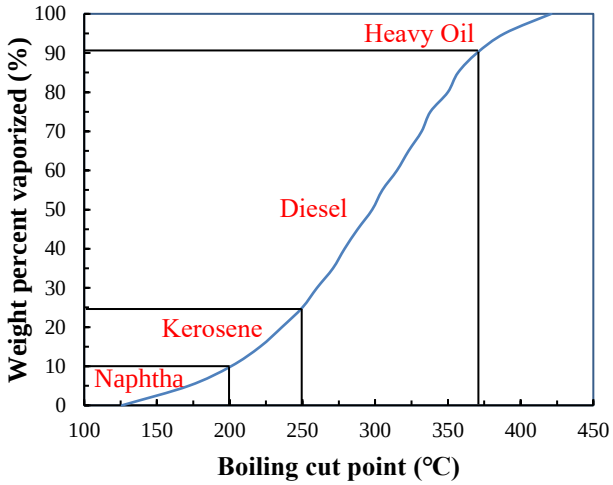

Fig. 1. Distillation curve with cut points

Table 2. Fuel compositions of WPD and CD

Composition	Cut point range	CD wt.%	WPD wt.%
Naphtha	IBP-200℃	9.6	18.8
Kerosene	200-250℃	15.4	14.7
Diesel	250-370℃	65.2	47.8
Heavy Oil	370-FBP	9.8	18.7

It can be seen that naphtha and heavy oil contents of WPD were 9.2 and 8.9 wt% higher than those of CD but kerosene and diesel contents were 0.7and 17.4 wt % less than those of commercial diesel.

A comparison of the distillation curve between CD and WPD is shown in **Fig. 2** and distillation temperature of WPD and CD are provided in **Table 3**. In **Fig. 2**, initial boiling range of WPD is almost 60% lower and final boiling range is almost 40% higher than those of CD. Therefore, the WPD can be called as wide distillation fuel (WDF) because it is included lighter and heavier compounds than those of CD. In fact, the lighter and heavier compounds can be removed to match the initial boiling point and final boiling point of WPD and CD fuels by distillation. Nowadays, gasoline-diesel blended or wide distillation fuels have potential to reduce soot emission and to increase thermal efficiency but HC emission of these fuels are slightly higher than that of diesel because of low cetane number [8]. Interestingly, cetane index of WPD is much higher than that of CD, although it contains almost 60% of lighter compounds. And paraffin and aromatic ratio of WPD is higher than that CD as shown in **Table 4**.

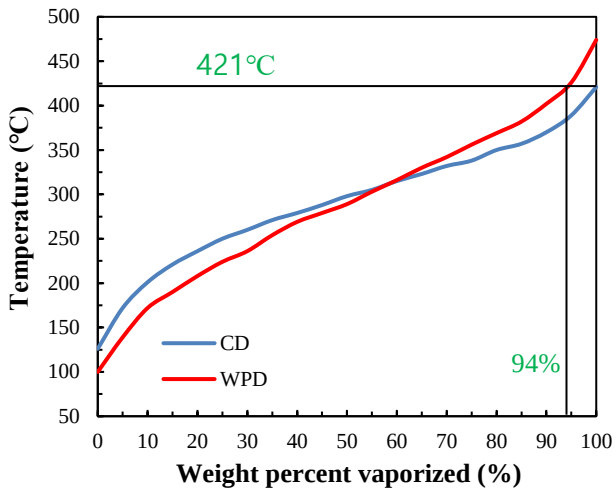

Fig. 2. Comparison distillation curves of CD and WPD

Table 3. Boiling points of WPD and CD

Distillation Wt.%	ASTM	CD (℃)	WPD (℃)
IBP:0.5%		126	100
10%		201	172
30%		260	236
50%	2887	298	289
70%		331	342
90%		370	402
95%		389	426
FBP:99.5%		421	474

For low temperature combustion of modern diesel engine, desirable fuel characteristics are low aromatic and high cetane index (high normal paraffin) but high cetane index and end boiling point can lead to high smoke for hot temperature combustion of normal diesel. **Table 5** can be shown that all detected carbon number concentration of WPD are greater than that of CD. That's why WPD have high cetane index and paraffin contents. The C_{28}-C_{40} are not detected for both fuels but three peaks are detected between C_{24} and C_{28} in WPD. Therefore, end fractions 6% of WPD should be removed to achieve the same end point as shown in **Fig. 2** and **Table 5**.

Table 4. PNA concentration of fuels

Carbon Content	CD	WPD
Paraffin (%C_P)	60.61	80.41
Naphthenes (%C_N)	25.91	14.54
Aromatic (%C_A)	13.48	5.05

Table 5. Constituents(area%) identified by GC-FID

Carbon Content	CD	WPD
C6	2.1457	3.38784
C7	Not detected	1.71151
C8	Not detected	2.35746
C10	Not detected	1.41769
C11	1.38791	3.71853
C14	2.84199	4.32735
C15	1.7203	4.77871
C16	1.07963	5.20978
C17	2.42153	5.19759
C18	3.68398	6.00175
C20	3.59628	5.52902
C24	1.47851	3.10487
-	Not detected	2.52215
-	Not detected	2.06772
-	Not detected	1.61383
C28	Not detected	Not detected
C32	Not detected	Not detected
C36	Not detected	Not detected
C40	Not detected	Not detected

IV. Conclusion

In this work, the composition of WPD are identified and quantified using simulated distillation and n-d-M methods. Some conclusions can be drawn as follows.

1. Naphtha and heavy oil contents of WPD were 9.2 a nd 8.9wt% higher than those of CD but kerosene and diesel contents were 0.7and 17.4wt% less than those of commercial diesel.

2. Initial boiling range of WPD is almost 60% lower and final boiling range is almost 40% higher than those of CD. Therefore, the WPD can be called as wide distillation fuel (WDF) because it is included lighter and heavier compounds than those of CD.

3 All detected carbon number concentration of WPD are greater than that of CD. That's why WPD have high cetane index and paraffin contents. Then, the C_{28}-C_{40} are not detected for both fuels but three peaks are detected between C_{24} and C_{28} in WPD. Therefore, end fractions 6% of WPD should be removed to achieve the same end point

Acknowledgement

This work was supported by ASEAN University Network/Southeast Asia Engineering Education Development Network (AUN/SEED-Net). The authors would like to thank Asso Prf: Dr Kanit Wattanavichien, Center of Fuel and Energy from Biomass (Chulalongkorn University) for his contribution in this work.

References

[1] W Khatha., S Ekarong., M Somkiat., S Jiraphon.,2020. Fuel properties, performance and emission of alternative fuel from pyrolysis of waste plastics. IOP Conf. Series: Materials Science and Engineering 717.

[2] Fazal Mabood., M.R.Jan Jasmin Shah., Farah Jabeen., 2012. Catalytic pyrolysis of waste plastic and tyres. LAP LAMBERT academic publishing, U.S.A.

[3] Anandhu, V., Jilse, S., 2018. Pyrolysis process to produce fuel from different types of plastic- a review. IOP Conf. Series: Materials Science and Engineering 396.

[4] Brajendra, K.S., Bryan, R.M., Karl, E.V., Kenneth, M.D., Nandakishore, R., 2014. Production, characterization and fuel properties of alternative diesel fuel from pyrolysis of waste plastic grocery bags. Fuel processing technology 122, 79-90.

[5] A.M. Motawie., Hala. B.I., Hasabo, M.A., Sahar, M.A., R.M, Abualsoud., 2016. Fractional distillation of fuel from mixed plastic waste. Conference paper.

[6] Z.T, Aung., C, Charoenphonphanich., H, Kosaka., P, Ewphum., P, Srichai., 2019. Investigation on physical properties and measurement of bulk modulus of waste plastic diesel. The 10th AUN/SEED-NET RCMEManuE,129-132.

[7] M.R, Riazi., 2005. Characterization and properties of petroleum fractions. 1st ed. ASTM, U.S.A.

[8] J, Wang., Z, Wang., H, Liu., 2015. Combustion and emission characteristics of direct injection compression ignition engine fueled with full distillation fuel. Journal of fuel 140, 561-567.

The 13th AUN/SEED-Net Regional Conference on Chemical Engineering 2020 (RCChE-2020)
Jointly held with
The 5th International Symposium on Conservation and Management of Tropical Lakes
"Insights and Challenges toward Achieving SDGs"

Assessment of Water Quality and Soil Salinity in the Coastal Area of Cambodia

Kongkea Phan[1, 2, *], Huy Sieng[1, 3] Sotha Chek[1, 3], Kyoung Woong Kim[4], Chheng Y Seng[2], Sophanith Hoeng[2]

[1]*Cambodian Chemical Society, Street 598, Phnom Penh, Cambodia*
[2]*Faculty of Science and Technology, International University, Phnom Penh 12101, Cambodia*
[c]*Royal Academy of Cambodia, Russian Blvd, Phnom Penh, Cambodia*
[d]*School of Earth Sciences and Environmental Engineering, Gwangju Institute of Science and Technology, Gwangju 500-712, Republic of Korea*
[*]*Corresponding author: kongkeaphan@gmail.com*

Abstract

In the present study, we investigate water quality and soil salinity in the coastal area of Cambodia. A total number of 59 water samples were collected from Kampot; 23 water samples were collected from Kep and 50 Water sample of are collected from Koh Kong provinces. On-site measurements were conducted for pH, ORP, EC, TDS, salinity and DO using respective Hanna field instruments. Concurrently, agricultural soils in Koh Kong are collected from each site using a grab sampling technique. Soil salinity is determined by soil/water extract method following a standard protocol. All chemical measurements were performed using Spectrophotometry methods. Analytical results reveal that 28.6% of tube well, 28.6% of dug well and 40% of ponds are saline in Kep and Kampot. Chemical analysis reveals that 2.6 % of tube well and 17.9% of dug well have As > 10 ppb, exceeded the WHO's Drinking Water Quality Guideline. Approximately, 29.3% of tube well, 28.6% and 60% of pond have Fe > 0.3 mg L^{-1} whereas 47.5% of tube well, 45.7% of dug well and 20% of pond has Mn > 0.1 mg L^{-1}. Moreover, 2.5 % tube well has F^- > 1.5 mg L^{-1}; 5.7% of tube well and 14.3% of dug well have NO_3^- > 50 mg L^{-1}. However, 12.5% of tube well and 6.2% of dug well have F^- > 0.8 mg L^{-1}, Japanese Drinking Water Quality Standard. In Koh Kong, analytical results reveal that approximately 12.5% of tube well, 4% of dug well and 20% pond water are saline. Fe and Mn are the common contaminants for most of the water sources in Koh Kong coastal area. Our current data show that most of agricultural soils in Koh Kong coastal area are non-salinity, but the agricultural fields which are close to coastline and/or in the estuarine are considered as high and server salinity. This study suggests that appropriate water treatment technologies are needed to provide safe drinking water to people residing in Cambodian coastal areas. Moreover, adaptation actions should be further promoted in order to cope with the potential impacts of the climate change in this coastal zone.

Keywords: *Water quality; climate change; salinity; coastal area; Cambodia*

I. Introduction

The coastal shoreline of Cambodia is approximately 435 km along the Gulf of Thailand covering four provinces namely Koh Kong, Sihanoukville, Kampot and Kep with an estimated area between 17,791km² and 18,477km² [1]. Urbanization and industrialization in the coastal zone of Cambodia are of a relatively small scale. Most urban and industrial developments are located along the coast of Sihanoukville and Kampot Province [2]. Cement factories are located in Kampot and breweries, handicraft manufacturing, petrol storage, local and international ports, hotels and restaurants are being increasingly developed in Sihanoukville [2]. The coastal water is considered to be of fairly good quality in terms of total suspended solids, dissolved oxygen, biochemical oxygen demand, total nitrogen and total phosphorous [3]. However, various pollution sources such as untreated wastewater from

manufacturing and mining, service and tourism industries, solid and liquid wastes discharged from slaughterhouses and livestock farms, as well as transportation by waterways, have a major impact on water quality in the country [3]. For instance, the domestic and municipal waste from the provincial town of Kampot has been discharged through the poor draining system to open manmade canals or natural streams and then to the coastal water without treatment [4]. The impacts of the discharge of sewage in costal water could increase in oligotrophic, coastal water pollution, eutrophication, and public health deterioration [2]. All the rivers that flow into the Gulf of Thailand are relatively small and very short with varying water levels depending upon rainfall. They have their sources in hills about 500 to 600 m in altitude which are located 15 to 20 km from the sea [4]. The ecological communities and living organisms in receiving water are affected by direct discharge of the effluents from various industries [5]. In addition, trace metals in drinking water and foodstuffs cultivated in the contaminated soil can pose significant health effect to their consumers [6-7]. There is a little known about environmental pollution in Cambodian coastal areas. The marine water and sediment quality and biological samples of Cambodian coastal zones were documented in 2003 [4]. There is no a regular monitoring program which has been well established in the coastal areas of Cambodia, except Sihanoukville [8]. It is of significance to investigate water quality and salinity susceptibility in the coastal areas of Cambodia.

II. Materials and Methods

2.1. Sampling sites

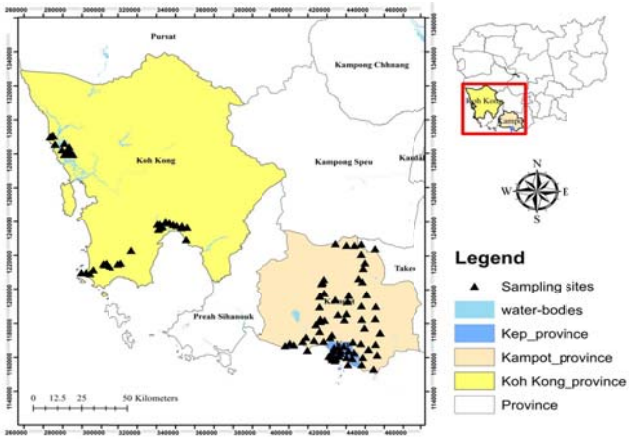

Fig. 1 Map of sampling sites

2.2. Field sampling

Water sample was collected from tube well, dug well and pond in Kampot, Kep and Koh Kong provinces (**Fig. 1**). In total, 59 water samples (tube water n = 31, dug well n = 23 and pond n = 5) were collected from Kampot province while 23 water samples (tube well n = 11 and dug well n = 12) were collected from Kep province. Water sample of tube well (n = 80), dug well (n = 25), canal (n = 7), pond (n = 5) and rain water (n = 5) were collected across the Koh Kong coastal area of Cambodia. Groundwater was collected tube well after pumping out about 5-10 min to flush the standing water out of the tube. Water sample was then filled into two bottles for different purposes of analyses. One was filled into a 500ml acid-cleaned polyethylene bottle which was used to analyze cations and anions concentrations. Another was filled into a 250 ml acid-cleaned polyethylene bottle and acidified to pH < 2 for measuring arsenic and heavy metal concentrations. Concurrently, on-site measurement of physicochemical properties was conducted at each site during the field sampling. pH and ORP was measured by Hanna HI 98191 pH/ORP meter (Hanna, Italy). Conductivity, TDS and salinity were measured by HI 98192 EC/TDS/NaCl/ Resistivity meter (Hanna, Italy) while DO was measured by HI9147 DO meter (Hanna, Italy). All field equipment and instruments were checked and calibrated with the respective standard solutions prior to each field trip. Water from dug well was collected and treated in the same manner as groundwater. One was filled into the 500ml acid-cleaned polyethylene bottle and another was filled into the 250ml acid-cleaned polyethylene bottle after which was acidified with HNO_3 (65%) to pH less than 2. Pond water were collected using grab sampling method at depth about 0-30 cm. A composite sample was filled into the respective polyethylene bottles. All water samples were kept in a cooler after field and transferred to a fridge at laboratory where they were stored at 4 ^{0}C until analysis.

2.3. Sample preparation and analysis

All chemical measurements were performed at Food Chemistry Laboratory of the Faculty of Science and Technology, International University, Phnom Penh. All water samples were taken out of the fridge and allowed to reach to a room temperature before analysis. Arsenic was tested with an arsenic test kit (Hach, USA). The concentrations of Cr, Cu, F, Fe and Mn were measured by

Spectrophotometer DR 1900 (Hach, USA). Hach DR 1900 was also used to measure nitrate, nitrite, sulfate, fee chlorine and total chlorine. Al, Ca, K and phosphate were analyzed by Hanna HI 83099 (Hanna, Italy) using the respective reagents obtained from Hanna company. All analytical methods and procedures of Hach are compliant with U.S.EPA. Likewise, as soon as agricultural soil samples are delivered to a laboratory, the samples are air-dried in thin layer and continuously turned over and mixed to avoid fungal development. After that, the dried soil samples are ground with a mortar and a pestle and passed through 0.2 mm (80 meshes) sieve. In the laboratory, soil salinity is measured as the electrical conductivity at 25°C from an unfiltered 1:5 soil : distilled water suspension ($EC_{1:5}$) following a method described by Hardie and Doyle [9]. In brief, 1: 5 soil/water suspension is prepared by weighing 20.0 g air-dry soil into a vial and add 100 mL deionized water which is then mechanically shaken (end-over-end preferred) at 25°C in a closed system for 30 min to dissolve soluble salts. It is then allowed about 15 min for the soil to settle. The measurement of EC is performed by Hanna HI 98192 dipping the conductivity cell into the supernatant, moving it up and down slightly without disturbing the settled soil.

III. Results and Discussion

Table 1 Summary of chemical measurements of water sources in Kep province

Parameters	Tube Well (n = 11)					Dug Well (n = 12)					WHO's DWQ Guideline	CDWQS
	Mean	Median	SD	Min	Max	Mean	Median	SD	Min	Max		
As (ppb)	4.00	0.00	9.66	n.d	30.00	4.44	0.00	10.14	n.d	30.00	10	50
Cu (µg L^{-1})	227.55	141.33	289.62	n.d	930.00	147.75	49.17	189.89	1.33	570.00	2,000	1,000
Fe (mg L^{-1})	0.30	0.10	0.50	n.d	1.71	0.46	0.05	0.94	0.01	3.30	-	0.3
Mn (mg L^{-1})	0.19	0.08	0.25	n.d	0.73	0.60	0.31	0.73	n.d	2.07	-	0.1
Cr (mg L^{-1})	0.01	0.01	0.01	n.d	0.02	0.01	0.01	0.01	n.d	0.03	0.05	0.05
Al (mg L^{-1})	0.04	0.02	0.05	n.d	0.15	0.02	0.02	0.01	0.01	0.03	-	0.2
Ca (mg L^{-1})	4.60	0.01	15.06	n.d	50.00	17.24	0.01	50.94	n.d	176.66	-	-
K^+ (mg L^{-1})	22.78	20.00	6.31	18.33	30.00	26.67	25.84	7.07	20.00	35.00	-	-
F^- (mg L^{-1})	0.39	0.05	0.60	n.d	1.68	0.12	0.10	0.14	n.d	0.44	1.5	1.5
NO_3^- (mg L^{-1})	0.65	0.29	0.78	n.d	1.93	0.73	0.00	1.04	n.d	2.50	50	50
NO_2^- (mg L^{-1})	0.00	0.00	0.00	n.d	0.01	0.00	0.00	0.01	n.d	0.02	3	3
PO_4^{3-}(mg L^{-1})	0.61	0.67	0.44	n.d	1.27	0.33	0.17	0.40	n.d	1.07	-	-
SO_4^{2-} (mg L^{-1})	13.09	4.00	18.14	n.d	58.33	27.42	9.50	29.13	n.d	68.33	-	250
Cl_2 (mg L^{-1})	0.30	0.01	0.92	n.d	3.07	0.02	0.01	0.02	n.d	0.07	-	-
Tot Cl_2(mg L^{-1})	0.06	0.05	0.05	0.01	0.15	0.23	0.05	0.48	0.01	1.40	5	0.2-0.5

DWQ, Drinking water quality; CDWQS, Cambodian drinking water quality standard; SD, Standard deviation; Min, Minimum; Max, Maximum; n.d, not detectable

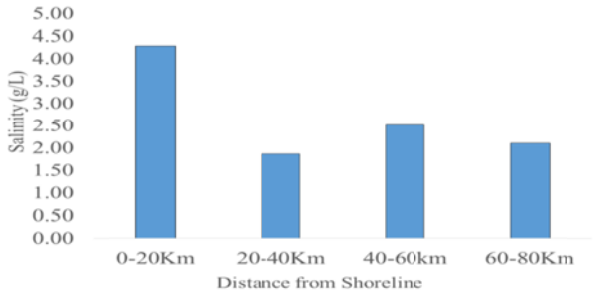

Fig. 2 Water salinity level from shoreline

The Summary of chemical measurements of water sources in Kep province is presented in **Table 1**. In Kampot and Kep, approximately 28.6% of tube well, 28.6% of dug well and 40% of pond are saline and 45.2% of tube well, 45.7% of dug well and 100% of pond are turbid. Chemical analysis reveals that 2.6 % of tube well and 17.9% of dug well have As > 10 ppb, exceeded the WHO's Drinking Water Quality Guidelines. Concurrently, 29.3% of tube well, 28.6% and 60% of pond have Fe greater than 0.3 mg L^{-1} whereas 47.5% of tube well, 45.7% of dug well and 20% of pond has Mn > 0.1 mg L^{-1}. Concurrently, 5.7% of tube well and 14.3% of dug well have nitrate greater than 50 mg L^{-1}, exceeded CDWQS and WHO's DWQ Guidelines. In Koh Kong, analytical results reveal that approximately 12.5% of tube well, 4% of dug well and 20% pond water are saline. Fe and Mn are the common contaminants for most of the water sources in Koh Kong coastal area. The water salinity decreases while the distance from the shoreline increases (**Fig. 2**).

Table 2 The summary of pH and salinity (µS cm^{-1}) of soil in Koh Kong coastal area

	KMP(n=15)		KRS(n = 13)		BSK (n = 17)	
Statistics	EC	pH	EC	pH	EC	pH
Mean	40.43	5.18	73.58	5.78	130.01	4.83
Median	39.36	5.23	31.11	5.95	32.81	4.49
SD	18.82	0.86	153.81	1.05	356.69	0.73
Min	13.44	4.10	6.65	4.25	22.70	3.79
Max	72.53	6.83	583.57	7.44	1510.67	6.16

KMP, Khemarak Pumin; KRS, Kirisakor; BSK, Botumsakor
SD, Standard deviation; Min, Minimum; Max, Maximum; Salinity is measured by 1:5 dilution $EC_{1:5}$ method

The summary of pH and salinity (µS cm^{-1}) of soil in Koh Kong coastal area is presented in **Table 2**. The mean salinity of soil in Khemarak Pumin, Kirisakor and Botimsakor are less than 150 µS cm-1 which is considered non-salinity by Australian soil salinity classification for sandy soil (**Table 3**).

Table 3 Australian salinity class based on saturated paste equivalent with corresponding 1:5 dilution value

	Saturated paste EC_{eq} or EC_{sp}	1:5 Dilution $EC_{1:5}$		
Salinity class	All soils (dS m^{-1})	Sand (dS m^{-1})	Loam (dS m^{-1})	Clay (dS m^{-1})
Non-salinity	0-2	0-0.14	0-0.18	0-0.25
Low	2.0-4.0	0.15-0.28	0.19-0.36	0.26-0.50
Moderate	4.0-8.0	0.29-0.57	0.37-0.72	0.51-1.00
High	8.0-16.0	0.58-1.14	0.73-1.45	1.01-2.00
Severe	16.0-32.0	1.15-2.28	1.46-2.90	2.01-4.00
Extreme	> 32.0	> 2.28	> 2.90	> 4.00

Adapted from Hardie and Doyle [9]; 1 dS m^{-1} = 1,000 µS cm^{-1}

Statistical data analysis indicates that soil salinity in Khemarak Pumin does not significantly differ from those in Kirisakor (*t*-test, $p > 0.05$) and Botumsakor (*t*-test, $p > 0.05$). Likewise, there is no significant difference in soil salinity in Kirisakor and Botumsakor (*t*-test, $p > 0.05$). However, upper range of soil salinity in Kirisakor and Botumsakor are considered as high and server, respectively, for sandy soil (Table 3). This could reflect seawater intrusion in Koh Kong coastal area, especially the agricultural fields close to coastline or in the estuarine.

IV. Conclusion

The present study reveals that water sources near shoreline are saline. Water salinity decrease as distance from shoreline increases. Fe and Mn are the common contaminants for most of the water sources in Cambodian coastal area. Soil pH in Koh Kong coastal area is acidic; most of the agricultural soil in the Koh Kong coastal area is considered non-salinity, but some areas which are close to coastline or in the estuarine is considered high and server salinity, respectively. This study suggests that appropriate treatment technologies are necessary for residents in the coastal area to access to clean water and minimize their potential health risks. Moreover, adaptation actions should be further promoted in order to cope with the potential impacts of the climate change in this coastal area.

Acknowledgements

This work was supported by GIST Research Institute (GRI) grant funded by the Gwangju Institute of Science and Technology (GIST) in 2020. The authors thank students in Food Chemistry Lab, Faculty of Science and Technology, IU for their field and lab assistance.

References

[1] Johnsen, S., Munford, G. (2012). European Union Delegation to Cambodia. "Country Environment Profile." https://eeas.europa.eu/archives/delegations/cambodia/documents/publications/country_env_profile_cam_april_2012_en.pdf Accessed: 15 December 2020.
[2] Rizvi, A.R. and Singer, U. (2011). Cambodia Coastal Situation Analysis, Gland, Switzerland: IUCN. 58 pp
[3] Water Environment Partnership in Asia (WEPA). 2015. WEPA Outlook on Water Environmental Management in Asia, Ministry of the Environment, Japan
[4] Water Environment Partnership in Asia (WEPA). 2020. The state of water environment, Cambodia. http://www.wepa-db.net/policies/state/cambodia/seaarea.htm Accessed: 15 December 2020
[5] Krishna, A.K., Satyanarayanan, M., Govil, P.K., 2009. Assessment of heavy metal pollution in water using multivariate statistical techniques in an industrial area: A case study from Patancheru, Medak District, Andhra Pradesh, India. Journal of Hazardous Materials 167, 366-373.
[6] Kavcar, P., Sofuoglu, A., Sofuoglu, S.C., 2009. A health risk assessment for exposure to trace metals via drinking water ingestion pathway. International Journal of Hygiene and Environmental Health 212, 216-227.
[7] Huang, M.L., Zhou, S.L., Sun, B., Zhao, Q.G., 2008. Heavy metals in wheat grain: Assessment of potential health risk for inhabitants in Kunshan, China. Science of the Total Environment 405, 54-61.
[8] Vorng, S. 2016. Water and Wastewater Management Cambodia. Conference on Watershed Management for Controlling Municipal Wastewater in South East Asia, 28 July 2016, Nagoya, Japan
[9] Hardie, M., Doyle, R. 2012. Measuring Soil Salinity: In Sergey Shabala, S and Cuin, T.A. (Edit). Plant Salt Tolerance, Methods and Protocols, Springer New York Heidelberg Dordrecht London

The 13th AUN/SEED-Net Regional Conference on Chemical Engineering 2020 (RCChE-2020)
Jointly held with
The 5th International Symposium on Conservation and Management of Tropical Lakes
"Insights and Challenges toward Achieving SDGs"

Application of Statistical Downscaling for Seasonal Rainfall Forecasts in Cambodia: A Comparison between Constructed Analogue and Bias Correction Methods

Thean THOEURN [1, 2, *], Tri Wahyu Hadi [1], Rattana CHHIN [2, 3]

[1] *Earth Sciences Study Program, Faculty of Earth Sciences and Technology, Bandung Institute of Technology, Jalan Ganesa No. 10 Bandung 40132, Jawa Barat Indonesia*
[2] *Faculty of Water Resources and Hydrology, Institute of Technology of Cambodia, Russian Federation Blvd., P.O. Box 86, 12156 Phnom Penh, Cambodia*
[3] *Water and Environment Unit, Research and Innovation Center, Institute of Technology of Cambodia, Russian Federation Blvd., P.O. Box 86, 12156 Phnom Penh, Cambodia*
** thoeurn.thean@gmail.com*

Abstract

Seasonal rainfall prediction is very important product for various purposes, especially agriculture application. The forecast of the rain in Cambodia contains a high value of uncertainty due to high rainfall variability and complex geography. The level of uncertainty can be delivered quantitatively using probability. This study aims (1) to apply and evaluate two statistical downscaling methods; Constructed Analogue (CA) and Bias Correction (BC) Methods based on the Climate Forecast System version 2 (CFSv2) output for seasonal rainfall forecasts and (2) to assess the probabilistic forecasting skills of the forecasted rainfall over Cambodia. The predictors used for CA method include stream function (ψ), velocity potential (χ) and geopotential height at 850 hPa level (z850), whereas the predictand is rainfall quantity. Two statistical indicators are used to evaluate the performance of each method in downscaling rainfall in Cambodia, namely Correlation Coefficient and Brier Score. Based on the Correlation Coefficient, the predicted rainfall of CA method shows higher correlation with observation compared to BC method. However, BS used to evaluate the seasonal extreme showed that the CA method was not able to capture the extreme rainfall events. The area-averaged BS over Cambodia is 0.26 and 0.33 for CA and BC method (lower BS, better prediction skill), respectively. Thus, CA method is recommended for climate downscaling in Cambodia.

Keywords: *Bias Correction, Brier Score, CFSv2, Constructed Analogue*

I. Introduction

Seasonal forecast of rainfall in Cambodia is important for various purposes, especially agricultural management and practices. Seasonal rainfall forecast is available globally from National Center of Environmental Prediction (NCEP) and Climate Forecast System version 2 (CFSv2); however, downscaling is needed to obtain forecast data with higher spatial resolution that is necessary for climate impact assessment. There are a number of statistical downscaling methods for the prediction of rainfall but two statistical methods, namely Constructed Analogue (CA) and Bias Correction (BC), are considered to be potentially applicable for Cambodia. The CA method has been shown to have significant skill in reproducing the variability of daily precipitation over the United States (US), especially in the western coast, while the BC method provides downscaling capabilities comparable to other statistical and dynamical methods in the context of hydrologic impacts [1]. However, performance of these methods for application in Cambodia

have not been thoroughly assessed. Moreover, CFSv2 provides ensemble rainfall prediction that needs to be processed and delivered as probabilistic forecast products. Specific methods are needed to assess the skill of the probabilistic rainfall forecast in quantifying the uncertainty of spatially varying seasonal rainfall patterns across Cambodia due to complex topography. The objectives of this study are as the following:

1. To apply and evaluate the performance of two statistical methods, CA and BC, applied for downscaling CFSv2 output for seasonal rainfall forecasts in Cambodia

2. To assess the probabilistic forecasting skills of seasonal rainfall forecast in Cambodia.

II. Materials and Methods

2.1. Dataset

Rainfall data with long records are needed to implement the CA method but gauge observations that meet such specification are not obtainable for this study. Therefore, Asian Precipitation—Highly Resolved Observational Data Integration Towards Evaluation of Water Resources (APHRODITE) gridded secondary dataset is used because it covers Cambodia and available from 1951 to present. APHRODITE dataset covers Asian continent and contains daily rain gauge data from a dense network derived from the Global Telecommunication System (GTS) and consists of gridded rainfall data with 0.25°×0.25° spatial resolution [2]. APHRODITE is regarded as a proper dataset for climate study over Indochina Region [3].

Other most important dataset for this study is the database of global model output, for which the Climate Forecast System Reanalysis (CFSR) dataset with 1979−2010-time span is used. In addition, archives of CFSv2 operational predictions model output from 2012 to 2015 are also collected. These databases actually contain many variables but for the purpose of this study, only horizontal wind vector and geo-potential height *z* at 850 hPa level from the CFSR dataset are selected. The wind vectors are then transformed into two scalar variables namely stream function ψ and velocity potential χ. These two variables are already available in the CFSv2 data, so further calculations are not needed. More detailed discussions about the use of the variables in CA method implementation is given in the following sections.

2.2. Constructed Analogue Method

Constructed analogue (CA) is a method of statistical downscaling which is stimulated by analog weather forecasting. CA should be basically implemented in two steps: diagnosis, and prognostic processes. Diagnosis process is performed to find relationships between patterns of predictor that are similar in two different times (usually the past and future). The measure of similarity of analogue for two vectors $\vec{a}(u)$ and $\vec{a}(t)$ can be identified by using, cosine similarity as given by the following expression:

$$S(u) = \frac{\vec{a}(u).\vec{a}(t)}{|\vec{a}(u)||\vec{a}(t)|} \quad \text{(Eq.1)}$$

In the diagnosis process, both vectors represent same predictor variable; in this case, one of previously mentioned three variables ψ, χ, or z at 850hPa. For target time *t*, an analog predictor in the database is searched and selected based on the similarity value, $S(u)$ which is valid for a past time *u*. Different from original analogue method, where only single analogue is searched, 30 best analogues are selected by the rank of $S(u)$ in this CA implementation. The relationship between those 30 analogues and the predictor value at target time *t* can be established by several methods like linear regression or weighted averaging. Herein, a weighted averaged model is employed to get the constructed value by:

$$Z_{CA}(t) = \sum_{i=1} W_i P_i \quad \text{(Eq.2)}$$

Where P_i is a database predictor of each 30 best analogue and Z_{CA} is a target predictor value at target time *t*.

The prognosis process aims to form one analogue rainfall (constructed analogue) at every target time *t*, based on the best analog group (subset) obtained from the process diagnosis. In this study we used a weighted averaging method in the prognosis process. The weight (W) of each member of the analog subset of predictors was determined based on the correlation coefficient and RMSE on target predictors.

This weight is used in the formation of constructed analogues at the target time t:

$$R_{CA}(t) = \sum_{i=1} W_i R_i \quad \text{(Eq.3)}$$

Where R_i is a predictand analog subset that pairs with an analog subset of predictors and R_{CA} is a predicted rainfall of CA. In this study, the training period starts from 1979 to 2010, while the target period starts from 2012 to 2015.

2.3. Bias Correction Method

The first step of statistical Bias Correction is to find the ratio for each quintile (α_q) between data rainfall observation (in this research, APHRODITE data used as secondary data) with database of rainfall estimation based on CFSv2. α_q is considered a correction factor for each quantile and a multiplier for estimated values CFSv2 in the same quantile ($CFSV2\_pred_q$) to obtain corrected rainfall (P_pred_q). The correction factor for each quantile is as follows.

$$\alpha_q = \frac{database\_Aphrodite_q}{database\_CFSv2_q} \qquad \text{(Eq.4)}$$

After obtaining correction factor of each quantile, the correction factor will be used to correct rainfall in the testing period with the equation as following.

$$P\_pred_q = \alpha_q \times CFSV2\_pred_q \qquad \text{(Eq.5)}$$

2.3. Deterministic Forecast Verification

Correlation Coefficient (CC) is a measure of linear correlation of two variables. It indicates how well observation and forecast value fit a line. This can be estimated by:

$$CC = \frac{n\sum_{s=1}^{n} RF_s OBS_s - \sum_{s=1}^{n} RF_s \sum_{s=1}^{n} OBS_s}{\sqrt{[n\sum_{s=1}^{n} RF_s^2 - (\sum_{s=1}^{n} RF_s)^2][n\sum_{s=1}^{n} OBS_s^2 - (\sum_{s=1}^{n} OBS_s)^2]}} \qquad \text{(Eq.6)}$$

Where OBS is the value of observed rainfall, and RF is rainfall forecast. CC is ranged from -1 (poorest skill) to 1 (highest skill).

2.4. Probabilistic Forecast Verification

Brier Score (BS) is used to evaluate the accuracy of probabilistic predictions. BS is a measure of mean square error of probability of prediction for two categories such as rain event and no rain event. BS is calculated as follows;

$$BS = \frac{1}{N}\sum_{i=1}^{N}(p_i - a_i)^2 ; \quad 0<BS<1 \qquad \text{(Eq.7)}$$

Where; N is the number of samples p_i is the probability of prediction and a_i is that of observation (a_i is 1 if the event occurs and 0 if the event does not occur). BS ranged from 0 (highest skill) to 1 (poorest skill).

(a) (b)

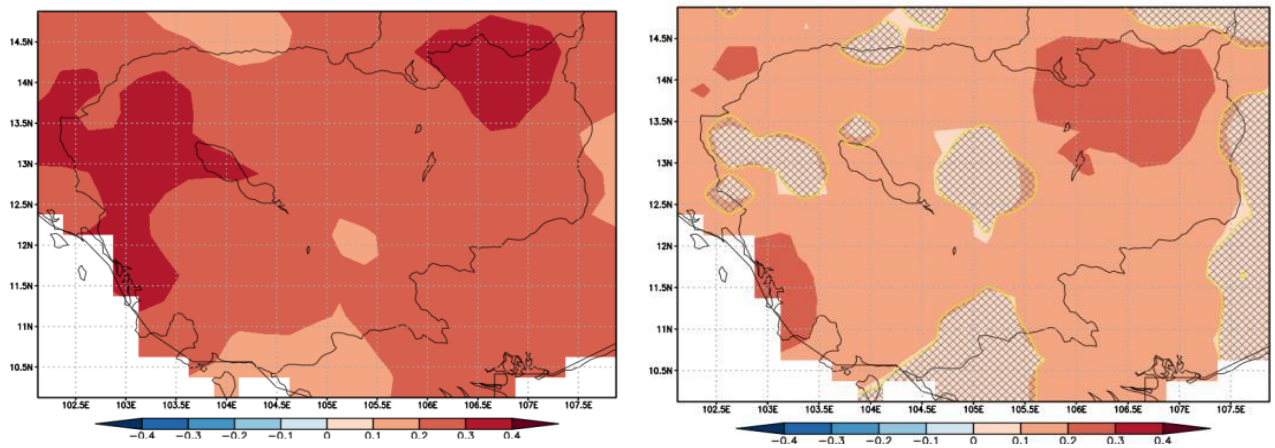

Fig. 1. Correlation between observed rainfall and predicted rainfall of Constructed Analogue (a) and Bias Correction (b) with each grid cell over Cambodia region. The correlation is significant at 99% confident interval based on student t-test. The cross-hatched and the yellow contours indicate that the test is failed

III. Results and Discussion

3.1. A Comparison of Statistical Performance between the CA and BC Methods

Figure 1 illustrates the correlation of daily rainfall of ensemble mean between the downscaled rainfalls with observation. Based on the result, it can be seen that the CA (Fig. 1a) method showed higher correlation compared to BC Method (Fig. 1b). This indicates that BC method is not well perform compared to CA method. The CA method exhibits slightly higher correlations over certain regions such as the western part of Cambodia, while BC method show limited

skill over some regions, i.e., hatched areas in Fig. 1b (correlation is not significant).

3.2. Verification of the Probabilistic Seasonal Rainfall Forecast

In this study, the probability of seasonal rainfall which is more than 66 percent is used to define seasonal rainfall above normal. BS is one of the probabilistic verification methods used for verifying the seasonal prediction skill of climate model result. Technically, the lower BS indicates that the probability of the forecast is close to the observed event and vice versa for the higher BS. The result of BS for seasonal rainfall above normal is illustrated in Fig. 2. The area-averaged BS over Cambodia is 0.26 and 0.33 for CA and BC method, respectively. It is noted that the BS as a result of the CA method over the south-western part of Cambodia is higher than that of BS method. This is because this region is the coastline area which frequently experienced higher rainfall. Moreover, the prediction of the CA method was not able to capture extremely low and high observed rainfall values. For the BC method, certain parts of Cambodia have higher BS due to a large uncertainty produced by the BC method. However, the BC method shows higher skill than the CA method in several locations such as the north-eastern part of Cambodia.

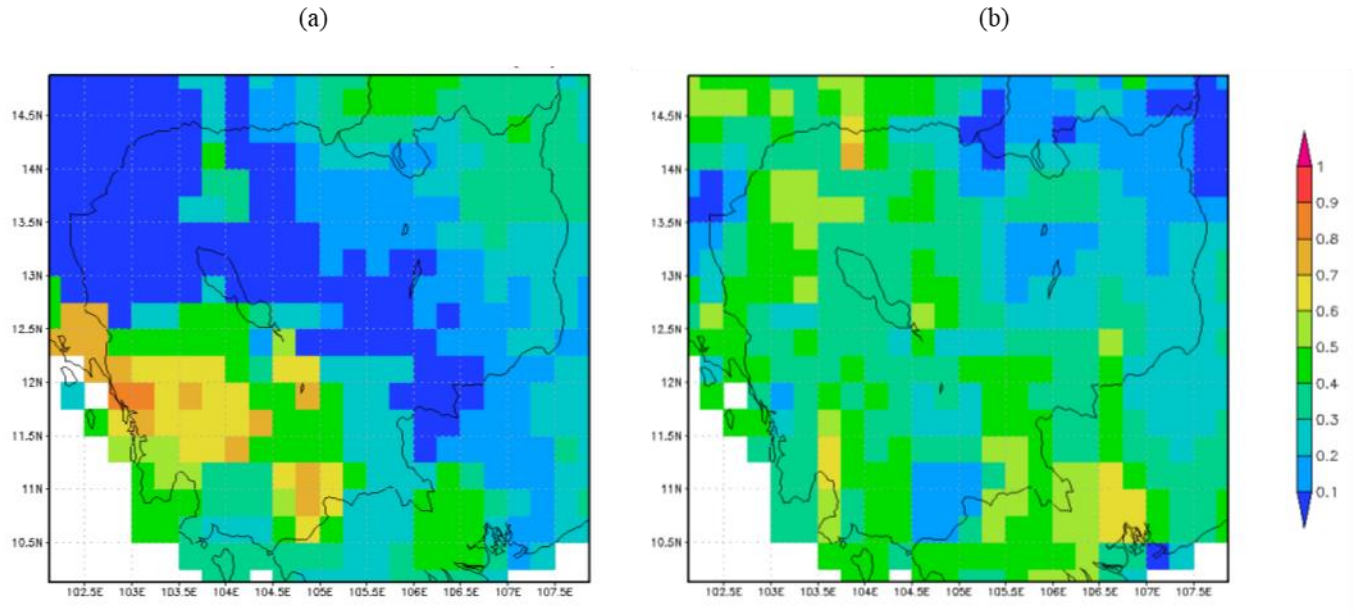

Fig. 2. Brier Score of seasonal above normal of Constructed Analogue (a) and Bias Correction method (b) for May-July (MJJ). The correlation is significant at 99% confident interval based on student t-test. The cross-hatched and the yellow contours indicate that the test is failed

IV. Conclusion

Based on statistical performance analysis, Bias Correction (BC) method shows lower correlation compared to Constructed Analogue (CA) method. Brier Score (BS) using to evaluate probabilistic forecast of the seasonal rainfall above normal showed that the CA method was not able to capture the extreme event. The area-averaged BS over Cambodia is 0.26 and 0.33 for CA and BC method (lower BS, better prediction skill), respectively. Thus, CA method is recommended for climate downscaling in Cambodia.

References

[1] Wood, A.W., Leung, L.R., Sridhar, V., Lettenmaier, D.P., 2004. Hydrologic implications of dynamical and statistical approaches to downscaling climate model outputs. *Climatic Change* 62, 189.

[2] Yatagai, A., Kamiguchi, K., Arakawa, O., Hamada, A., et al., 2012. Aphrodite constructing a long-term daily gridded precipitation dataset for Asia based on a dense network of rain gauges. *Bulletin of the American Meteorological Society* 93, 1401–1415.

[3] Chhin, R., Bui, H.-H., Yoden, S., 2017. Characterization of monthly precipitation over Indochina region to evaluate CMIP5 historical runs. *DPRI Annuals* 60B, 502–522.

The 13th AUN/SEED-Net Regional Conference on Chemical Engineering 2020 (RCChE-2020)
Jointly held with
The 5th International Symposium on Conservation and Management of Tropical Lakes
"Insights and Challenges toward Achieving SDGs"

A Survey of Household Water Use and Groundwater Quality Index Assessment in a Rural Community of Cambodia for Studying Potential Water Treatment Plant

Sreymao Sek [1,2], Borin Heang [1,2], Pisut Painmanakul [3], Chantha Oeurng [2] and Saret Bun [2,*]

[1] *Water and Environmental Engineering, Graduate School, Institute of Technology of Cambodia, Phnom Penh 12156, Cambodia*
[2] *Faculty of Hydrology and Water Resources Engineering, Institute of Technology of Cambodia, Phnom Penh 12156, Cambodia*
[3] *Department of Environmental Engineering, Faculty of Engineering, Chulalongkorn University, Bangkok 10330, Thailand*
* *Corresponding author: saret@itc.edu.kh*

Abstract

The objective of this assessment is to estimate the household domestic water use and groundwater quality index in a small rural community of Preyveng province. About household water use, 100 respondents in Preal commune were randomly selected as the participants for field survey questionnaire. Average daily water consumption in Preal is about 71 liters per capita. From this value, it was estimated that more than 80% of the households in study area is facing the water scarcity in terms of water quantity, which may consider as a serious concern for health promoting in the study area. All households in Preal heavily relies on groundwater wells for household domestic water use. The household used raw groundwater as drinking water was found up to 56% without a proposer treatment system. Hence, their perception about groundwater was studied in order to acknowledge their knowledge on quality of water. As the result, more than haft of the household indicated that their current water use is safe while other 19% considered not safe and still directly accessed to that raw water in a reason of no choice. About water price investigation, the results demonstrated that the price of domestic water use in Preal commune is about 0.228 USD/m^3, which is more expensive than clean water supply of Phnom Penh Water Supply Authority. In terms of water quality, about 75% of groundwater wells in Preal commune presented in poor conditions and unsuitable for drinking purpose. Arsenic, fluoride, and iron were defined as the main associated contaminants in groundwater on water quality index. Consequently, the presence of these three contaminants has been considered as one of the major challenges associating to water scarcity in Preal commune as well as many rural communities of Southeast Asia countries.

Keywords: *Cambodia, Groundwater quality index, Household water use, Survey questionnaire*

I. Introduction

Over past few decades, water scarcity has been experienced as the serious problem than ever from local to global scale. Groundwater can be considered as the suitable alternative water source due to its quantity, quality, and accessibility in community level, where faces high water scarcity. It advances as the key resource of drinking water. Withdrawal of groundwater was estimated about 982 km^3 annually as the most extracted raw material in the world [1]. More than half has been used for domestic water supply in

many counties and generally provides more than 45% of drinking water in the world, especially in the small towns and rural communities where rely for domestic supplies [2,3]. Groundwater is an optional resource where pipe water supply is not accessible.

In Cambodia, groundwater roles as the main source for drinking water supply, which used up to 53% of Cambodian households in dry season. It is currently used for a small community water supply and expected to be trend more for industrial and agricultural irrigation use. Main issues and challenges, groundwater contents high level of arsenic, iron, manganese, fluorides, and salt in Mekong and Tonle Sap river basin, particularly along the river and some areas [4]. Not only Cambodia, the neighboring countries including Laos, Thailand, and Vietnam have reported about the serious arsenic, iron, fluoride, etc. contamination in groundwater.

To propose an efficient system for addressing the water scarcity, the information on water consumption and groundwater contamination related to the water quantity and quality are essential for estimating the optimal preparation of the comprehensive water system including groundwater treatment processes design and supply system. Such type of investigation assumes importance for satisfying the growing needs of the people in the community. This study aimed to estimate the household domestic water consumption and groundwater quality index in a small rural community of Preyveng province, Cambodia, for proposing a quantitative information for designing groundwater treatment processes and supply system. Moreover, the results and findings of the present study with respect to Preal commune in Kanhchriech district of Preyveng province would be practical, beneficial and meaningful and will act as a model for the rural sector water resource managers in rural or semi-urban area of Cambodia as well as in other parts of the globe.

II. Materials and Methods

2.1. Study area

This study has been carried out in a small scale of Preyveng province in Preal commune of Kanhchriech district (see **Fig. 1**). Preal is one of the communes among 8 in Kanhchriech district, where located at the south of Phnom Penh capital about 45 kilometers, along the coordinate 11º 39'N latitude and 105º 37'E longitude. Coverage area of Preal commune is about 66.5 km^2 to group 16 villages. Based on commune database online (CDB) of national committee for sub-national democratic development (NCDD) [5], more than 1,100 groundwater wells were used for household potable water and other 77 wells used as irrigation or agriculture wells (about 65 families). It is divided into three types of groundwater well including pump or mixed, ring, and unprotected dug wells.

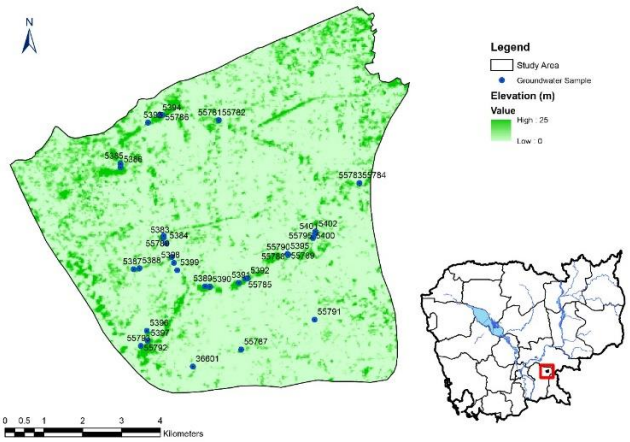

Fig. 1. Study area of Preal commune in Preyveng province

2.2. Data collection and analysis on water use

A survey was conducted at the individual household level in the study area. Basic information of sample size selecting for data collection is crucial importance related to resource and time consuming as well as result accuracy. Determination sample size mainly depend on three parameters: level of precision (e), level of confidence or risk, and degree of variability in attribute [6]. In this study, sample size of the respondents was determined amount of family need to conduct interview with prepared questionnaires. The 95% of confidence level, 50% of variability degree, and 5% of precision level was selected to estimate the sample size. Maximum sample size for infinite population is 100. Hence, 100 respondents were collected for conducting an analysis.

Methodology of water use analysis is based on an interdisciplinary, descriptive, intergraded, and cross-sectional analysis approaches. Survey questionnaires contained both closed and open-ended question included the questions on domestic and drinking water consumption and source, respondent perception on water quality, and level of awareness about safe water accessibility. It was conducted through direct face-to-face interview at the household of respondents. Various types and sizes of vessels used in each household were measured the volume. Amount of household domestic and drinking water use was asked in terms of usage duration per each vessel in which convenient for respondent and data accuracy. It was therefore used to determine daily

water consumption for overall household and drinking only.

2.3. Socio-economic classification

Annual household income was selected for socio-economic classification in this study since it is easy to operate and understand, as indicated by Singh and Turkiya (2013) [7]. A collected annual income data from each surveyed household was classified into five socio-economic groups. These five groups are Group 1 (< USD 500), Group 2 (USD 500 - 1,000), Group 3 (USD 1,000 - 2,000), Group 4 (USD 2,000 - 4,000), and Group 5 (> USD 4,000).

2.4. Groundwater quality index method

Groundwater quality was mainly based on the secondary data source. Available groundwater quality data of a total 21 accessible wells (see **Fig. 1.**) sampled and analyzed between 2007 and 2008 was collected (MRD-Cambodia, 2010). Water quality index (WQI) is the method for investigating the influence of individual water quality parameter on the overall water quality. Procedure for WQI calculation was divided into three steps. First, all nine parameters were assigned as weight based on their perceived effects on primary health. Assigned weight of each parameter was referred to the previous studies of Ramakrishnaiah, Sadashivaiah, and Ranganna (2009) [8] and Sadat-Noori, Ebrahimi, and Liaghat (2014) [9], as shown in **Table 1**. Secondly, a relative weight (W_i) of each parameter was determined by using **Eq. (1)**, where w_i is the weight each parameter, n is number of parameters investigated, W_i is the relative weight. WHO standard level, weight (w_i), and relative weight (W_i) were provided in Table 1.

$$W_i = \frac{w_i}{\sum_{i=1}^{n} w_i} \quad \text{(Eq.1)}$$

$$q_i = \frac{C_i}{S_i} \times 100 \quad \text{(Eq.2)}$$

$$SI_i = W_i \times q_i \quad \text{(Eq.3)}$$

$$WQI = \sum SI_i \quad \text{(Eq.4)}$$

Last step, a quality rating scale (q_i) was determined using **Eq. (2)**, where q_i is quality ranking, C_i is concentration of each parameter (mg/L), and S_i is WHO standard level (mg/L). Value of q_i was used for determining sub-index (SI_i) before calculating WQI using **Eq. (3)**, and **(4)**, respectively.

Table 1. Weight (w_i) and relative weight (W_i) of each water quality parameter

Parameter	Unit	WHO Std.	w_i	W_i
pH	-	6.5 - 8.5	4	0.125
Iron	mg/L	0.3	4	0.125
Arsenic	µg/L	10	5	0.156
Fluoride	mg/L	1.5	4	0.125
Hardness	mg/L*	100	2	0.063
Chloride	mg/L	250	3	0.094
Manganese	mg/L	0.05	4	0.125
Nitrate	mg/L	50	5	0.156
Turbidity	NTU	1	1	0.031

*as $CaCO_3$

Estimated values of WQI were classified into five levels described water condition, as presented in **Table 2**.

Table 2. Water quality classification based on WQI

WQI range	Water quality
< 50	Excellent water
50 – 100	Good water
100 – 200	Poor water
200 – 300	Very poor water
> 300	Unsuitable water for drinking purpose

III. Results and Discussion

3.1. Daily water consumption

Total domestic water consumption in daily of Preal commune were estimated about 31,303 liters. Maximum domestic water was taken by Group 4 households followed by Group 5 and 3 households. These three socio-economic groups constituted more than 70% of total consumption. For maximum water consumption by Group 4 represented the socio-economic group with the annual income between USD 2,000 and 4,000 is in a good agreement with the finding of Singh and Turkiya (2013) [7] that maximum water consumption was observed at a socio-economic class with annual income USD 2,000 – 4,000.

Table 3. Daily water consumption (litter per capita)

Socio-economic	Mean value	SD
Group 1	76.8	69.0
Group 2	65.8	45.2
Group 3	68.6	46.4
Group 4	76.0	64.1
Group 5	66.2	44.3
Mean	70.7	53.8

Table 3 presented the domestic water consumption per capita in Preal commune. Average daily water consumption per household in the study area is 313.0 litters whereas per capita is around 70.7 litters. It is quite low, almost two times compared to the minimum water quantity (150 L/day.capita) recommended by WHO. More than 80% of the households in Preal commune is facing water scarcity in terms of water quantity. The value found is such as a serious concern for health promoting in the study area which instantly required a suitable and sustainable solution.

3.2. Sources of water use

Information of water sources for domestic water was also investigated during field survey. It showed that 93% of the households heavily relies on groundwater wells only, while other 6% are using both groundwater wells and rain water storage. There is only 1% of the households depend on groundwater wells with surface water.

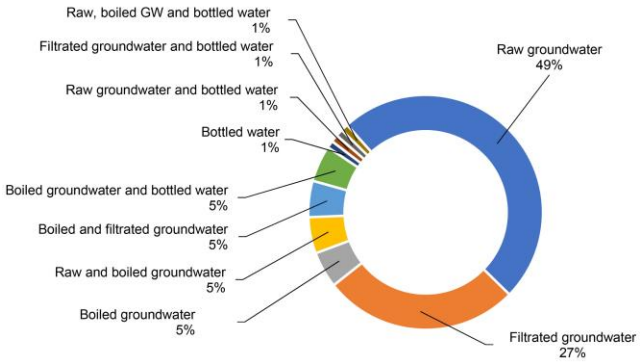

Fig. 2. Number of households in different drinking waters

Based on **Fig. 2**, 49% of households in Preal commune directly drank raw groundwater without any treatment processes and other 37% used groundwater as the source for drinking water with additional processes including boiling (5%), water filter unit (27%), and both (5%). Moreover, only 1% of residents was found using only bottled water as the drinking water while other 8% used bottled water with boiled groundwater (5%), with raw groundwater (1%), with filtrated groundwater (1%), and with raw and boiled groundwater (1%). It indicated that a majority of households in Preal commune consumed raw groundwater directly without treatment processes (49%), followed by filtrated groundwater using household filtration unit (27%), and mixed four types of drinking water (13%). Boiled groundwater (5%) and bottled water (1%) were found in low consumption possibly due to the higher cost required.

3.3. Perception of water quality

Perception of water users on current water use quality is another important information should be acknowledged even there is a water quality standard set, especially, for a rural community of developing country. Approximate 40% of household in Preal commune responded that they did not concern about their current water use quality. Moreover, it was noticed during the field survey that few people simplified that their water was traditionally used long time ago without any serious problems observed while other few people mentioned that raw groundwater is more favorite and tastier compared to boiled or filtrated or bottled waters. More than haft of household in Preal commune believe that their current water use is safe while other 19% considered not safe, but still directly accessed to that raw water. From this result, the water quality assessment becomes more and more important in order to clarify the safety level of their current water use.

3.4. Estimated current price of water use

The price of current water used in Preal commune was estimated for both total domestic water and drinking water across socio-economic groups. It should be noted that the price of water was determined from the cost of the related payment for water supply, for example, the cost of petroleum or electric city used for pump, maintenance cost of the pump, cost of the heating energy for boiling water, maintenance cost of household filtration unit, cost of bottled water, etc. Summary and calculation were done for this price of water estimation and the result was illustrated in **Fig. 3**.

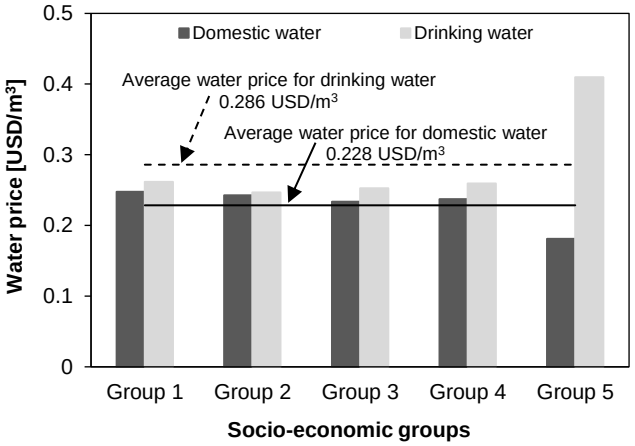

Fig. 3. Estimated water price of each water use

The results demonstrated that the price of domestic water use in Preal commune is about 0.228 USD/m^3 whereas drinking water is about 0.286 USD/m^3. This result is very important for future estimation on water use development as well as water economic analysis in the study area. By the way, assuming that a single household monthly consumed about 10 m^3 of water, the price of water use in Preal commune (0.228 USD/m^3) is more expensive than that of clean water supply of Phnom Penh Water Supply Authority. It is expected the people living condition as well as local GDP should be better after a qualified water was supplied with a reasonable price due to the payment on water sector, consequently resulted on health concern as well as human productivity, etc.

3.5. Groundwater quality assessment

Based on the result from previous part, all households in Preal commune mainly relies on groundwater wells for their domestic activities and more than haft of households directly consumed raw groundwater as drinking water without any treatments. Therefore, this groundwater quality assessment is very important in order to clarify the potential effect of contaminants in groundwater as well as on human health. This part aims to assess the quality of groundwater in Preal commune mainly based on the secondary data source.

Table 4. Statistical analysis of groundwater quality parameters in Preal commune

Parameter	Unit	Min	Mean	Max	SD
pH	-	5.30	6.80	7.42	0.47
Iron	mg/L	0.00	2.70	9.00	3.01
Arsenic	µg/L	0.00	6.00	25.00	8.00
Fluoride	mg/L	0.35	2.46	5.33	2.23
Hardness	mg/L*	18.0	131.0	198.0	54.0
Chloride	mg/L	0.29	4.32	14.00	3.68
Manganese	mg/L	0.01	0.10	0.15	0.03
Nitrate	mg/L	0.00	1.38	10.54	2.87
Turbidity	NTU	0.42	10.82	106.0	23.84

*as $CaCO_3$

Statistical analysis results were presented in **Table 4**. Based on the results, it indicated that groundwater in Preal commune mainly contaminated by iron, arsenic, fluoride, and manganese, which are mainly associated on human health effect from daily consumption. Additionally, water quality index should be estimated in order to understand the water condition of each groundwater wells in the study area as well as to find out the main associated contaminants on water quality index. Water quality index was determined in order to check if groundwaters in Preal commune is suitable for drinking purpose or not. Water quality index of each groundwater well was estimated and the result showed that there is no groundwater can be categorized as 'Excellent water' while only 5 wells are classed in 'Good water' and the rest fall below this range. It means that 75% of the groundwater wells in study area presents in poor conditions and unsuitable for drinking purpose. Moreover, water quality index was mainly distributed by four contaminants including arsenic, iron, fluoride, and manganese. It indicated that the presence of these contaminants is the barer for accessing to the qualified water use in daily life of the people in Preal commune and may distribute the nearby communities as well.

IV. Conclusion

This study aimed to estimate the household domestic water consumption and assess the groundwater quality in a small rural community of Preyveng province, Cambodia. In average, daily water consumption in Preal commune is about 71 liters per capita. Related to daily water use, all residents in this community heavily relies only on groundwater wells for household domestic water use and the household used raw groundwater as drinking water was found up to 56% without treatment process. Due to the importance of groundwater used in Preal commune and their accessibility without treatment, the assessment of its water quality is very necessary for a protection and solution preparation. Based on water quality index method, about 75% of groundwater wells in Preal commune presented in poor conditions and unsuitable for drinking purpose. Arsenic, fluoride, and iron were defined as the main associated contaminants in groundwater on water quality index. Based on the result of this study, a removal of iron, arsenic, and fluoride from groundwater is very necessary for addressing water scarcity through groundwater use.

Acknowledgement

We are thankful to Project for Strengthening Engineering Education and Research for Industrial Development in Cambodia of JICA through LBE Research Grant for financial support.

References

[1] Margat, J., Van der Gun, J., 2013. Groundwater around the world: a geographic synopsis. CRC Press.

[2] National Groundwater Association, 2016. Facts about global groundwater usage.

[3] UNESCO, 2009. The united nations world water development report 3–water in a changing world. United Nations Educational Scientific and Cultural Organization, Paris.

[4] Ha, K., Ngoc, N. T. M., Lee, E., Jayakumar, R., 2015. Current Status and Issue of Groundwater in the Mekong River Basin. KIGAM, CCOP & UNESCO, Bangkok.

[5] CDB Online, 2010. Commune Database Online.

[6] Miaoulis, G., Michener, R. D, 1976. An introduction to sampling, Kendall.

[7] Singh, O., Turkiya, S. 2013. A survey of household domestic water consumption patterns in rural semi-arid village, India. *GeoJournal* 78(5), 777-790.

[8] Ramakrishnaiah, C., Sadashivaiah, C., Ranganna, G., 2009. Assessment of water quality index for the groundwater in Tumkur Taluk, Karnataka State, India. *Journal of Chemistry* 6(2) (2009), 523-530.

[9] Sadat-Noori, S., Ebrahimi, K., Liaghat, A., 2014. Groundwater quality assessment using the Water Quality Index and GIS in Saveh-Nobaran aquifer, Iran. *Environmental Earth Sciences* 71(9), 3827-3843.

Calcination of Raw Ferralsols for Enhancing Its Adsorptive Removal of Phosphorus from Aqueous Solutions

Thi An Hang Nguyen [1*], Thi Van Le [2], Keisuke Sato [1,2], and Ngoc Duy Vu [3]

[1] *Vietnam Japan University, Vietnam National University, Hanoi, Luu Huu Phuoc St., Nam Tu Liem Dist., Hanoi 101000, Vietnam*
[2] *Graduate School of Science and Engineering, Ritsumeikan University, Biwako-Kusatsu Campus, Shiga 525-8577, Japan*
[3] *University of Science (VNU-HUS), Vietnam National University, Hanoi, 334 Nguyen Trai Rd., Thanh Xuan Dist., Hanoi 120106, Vietnam*
* *Corresponding author : nta.hang@vju.ac.vn*

Abstract

It is well recognized that high levels of phosphorus (P) in water bodies can cause eutrophication, adversely influencing the aquatic life and ecosystem sustainability. Thus, the decontamination of P-rich wastewater before discharging it into the surrounding environment is essential. This article investigates the feasibility of calcination of natural ferralsols to intensify its adsorptive removal of P from aqueous solutions. First, the best calcination temperature was determined. Next, a comparative study between the natural ferralsols (NF) and ferralsols calcined at the selected temperature (CF500) in terms of both physicochemical properties and adsorptive behaviors was performed. Then, SEM, XRD, XRF, and FTIR analyses were performed to clarify the effects of calcination. It was found that among three examined calcination temperatures, 500°C resulted in the highest P sorption capacity and most neutral pH value in the post-adsorption solution. CF500 produced by lab-scale furnace and commercial scale one were quite similar with respect to P binding capacity. CF500 exhibited better P sorption capacity and rate (19.38 mg/g and 0.23 min^{-1}) than NF (12.09 mg/g and 0.12 min^{-1}). Additionally, CF500 possessed higher porosity (51%), more neutral pH_{H2O} (6.18), lower organic matter (< 0.08%), lower available P (0.86 mg P_2O_5/100 g soil), higher $F_{eoxalate}$ (2.296 mg/g) and $Al_{oxalate}$ (2.167 mg/g) as compared to NF, which were considered to favor the P retention ability of CF500. These findings were consistent with the changes in morphology, mineral and metal oxide composition as well as the functional groups of NF after calcination. Due to simple procedure, significant improvement in P treatment performance, and no secondary pollution, calcination can be a promising method for fabrication of the P adsorbent from naturally occurring and locally abundant ferralsols. The favorable characteristics of CF500 enable its actual application as the potential filter materials in constructed wetlands for purification of P-rich wastewater.

Keywords: *Adsorption, Calcination, Ferralsols, Phosphorus removal, Phosphorus rich wastewater*

I. Introduction

It is well recognized that excessive levels of phosphorus in the aquatic medium can cause eutrophication and adversely impact the aquatic life. Thus, the decontamination of P-rich wastewater is urgent. There is an increasing trend to use naturally occurring materials as P adsorbents. However, their wide application is usually

restricted by low P sorption capacity, thus requiring the modification. Among several methods used for this purpose, thermal treatment also known as calcination is preferred because of its simplicity and lack of secondary pollution. This study aims at improving the P sorption capacity of natural ferralsols by calcination by (i) selection the best calcination temperature, (ii) characterization of NF and CF500, and (iii) investigation of adsorptive behaviors of NF and CF500.

II. Materials and Methods

2.1. Sampling sites

Collection of NF in Dak Nong province in Vietnam.

2.2. Experimental set-up

Calcination of NF was first done with lab-scale furnace at 3 types of temperatures (300, 500, and 700°C) to select the best one, which will be applied to the commercial furnace.

NF and CF500 were investigated in aspects to physicochemical properties and adsorptive behaviors according to the standard methods.

2.3. Analytical methods

NF and CF500 was characterized using analyses of SEM (JSM-IT100, Jeol, Japan), XRD (Empyrean, PANalytical, Netherlands), XRF (S4 Pioneer, BrukerE AXS, Germany), and FTIR (FT/IR-4600typeA, Jasco, Germany) at the VNU Key Laboratory of Advanced Materials for Green Growth.

Physicochemical properties of NF and CF500 were analyzed at the Lab of Pedology and Soil Environment, Faculty of Environmental Sciences (FES), VNU University of Science (HUS) using the respective analysis methods of TCVN 5979:2007, TCVN 8941:2011, TCVN 8941:2011, TCVN 5256:2009, and oxalate extraction.

The concentrations of ortho-P in aqueous solutions were measured according to Method 365.3 (EPA) using UV/Vis Diode Array Spectrophotometer (S2100 UV, Unico, USA) at the wavelength number of 710 nm. The pH values were monitored with SevenCompact pH/Ion meter (S220-Kit, Mettler Toledo, China).

2.3. Calculation

$$\text{Removal efficiency (\%)} = \frac{(C_i - C_e)}{C_i} \times 100\% \quad \text{(Eq.1)}$$

where C_i is the initial P concentration (mg/L), C_e is the equilibrium P concentration (mg/L).

$$q_e = \frac{C_i - C_e}{m} \times V \quad \text{(Eq.2)}$$

where q_e is adsorption capacity at the equilibrium (mg/g); C_i is the initial P concentration (mg/L); C_e is the equilibrium P concentration (mg/L); and m is the mass of the adsorbent (g).

III. Results and Discussion

3.1. Calcination

Table 1. Comparison of ferralsols before and after calcination at different temperatures

Materials	P adsorption capacity (mg/g)	pH of post-adsorption solution
NF	2.58	6.05
CF300	3.83	6.67
CF500	4.68	6.95
CF700	4.25	6.76

3.2. Characterization

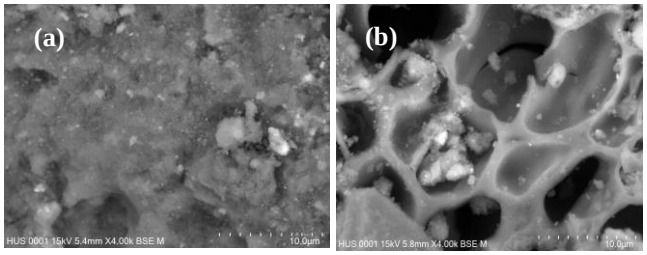

Fig. 1. SEM observation of a) NF and b) CF500

It is demonstrated in **Fig. 1** that calcination of NF resulted in the porous structure on the surface of CF500 with much greater pore diameters, thus improving the P sorption on CF500.

Table 2. Mineral composition of NF and CF500

Materials	NF (%)	CF500 (%)
Kaolinite $Al_2O_3.2SiO_2.2H_2O$	37	81

Hematite, Fe_2O_3	5	13
Gibbsite, $Al(OH)_3$	50	0
Goethite, FeO(OH)	8	6

It can be seen from **Table 2** that after calcination, the Gibbsite and Goethite in NF were mostly converted into Kaolinite and Hematite, which were proven to favor P sorption [1].

Table 3. Metal oxide composition of NF and CF500

Composition	NF (%)	CF500 (%)
Al_2O_3	30.54	35.44
Fe_2O_3	21.83	22.92
TiO_2	4.15	4.40
Na_2O	<0.01	<0.01
K_2O	0.03	0.03
CaO	0.02	0.02
MnO	0.09	0.10

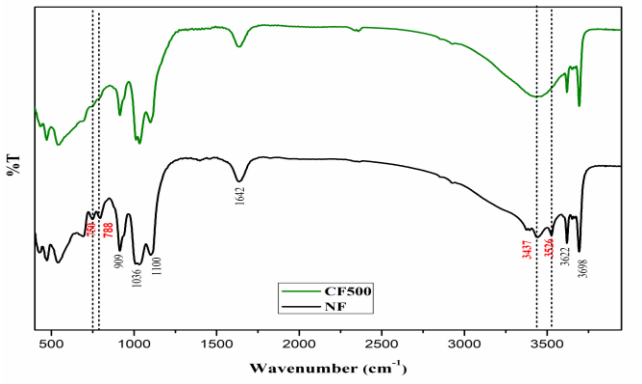

Fig. 2. FTIR spectra of NF and CF500

It can be seen from **Fig. 2** that some negative functional groups (e.g. $-OH^-$) disappeared on the surface of CF500. Consequently, the binding of PO_4^{3-} anions on CF500 was intensified due to the electrostatic attraction [2].

Physicochemical properties

Table 4. Physicochemical properties of NF and CF500

Parameters	Unit	NF	CF500
pH_{H2O}	-	5.14	6.18
Organic matter	%	0.62	<0.08
Density	g/cm^3	2.79	3.56
Soil texture	% sand	9.28	74.56
	% limon	46.8	17.28
	% clay	43.92	8.16
Total P	$\%P_2O_5$	0.09	0.08
Available P	Mg P_2O_5/ 100 g soil	3.44	0.86
$Fe_{Oxalate}$	g/kg	0.728	2.296
$Al_{Oxalate}$	g/kg	0.848	2.167

Table 4 indicates that CF 500 resulted in the near neutral pH values, had extremely low contents of organic matter, total P, available P but high levels of $Fe_{oxalate}$ and $Al_{oxalate}$. These enable its P elimination ability.

3.2. Adsorption tests

Influential factors

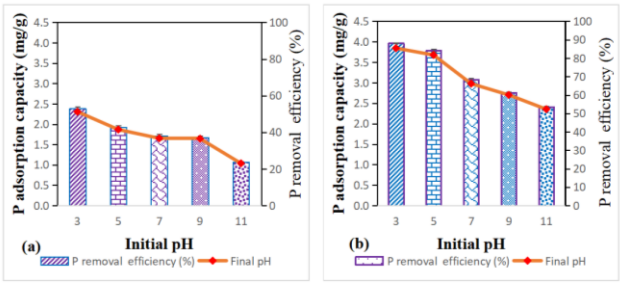

Fig. 3. Effect of pH on P adsorption of a) NF and b) CF500

Effect of pH on P sorption of NF and CF500 is displayed in **Fig. 3**. As shown in **Fig. 3**, the optimal pH values for both NF and CF500 were 3.

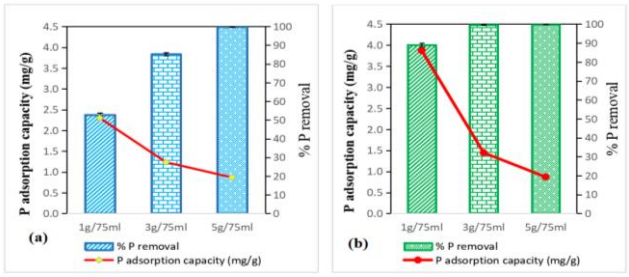

Fig. 4. Effect of adsorbent dose on P sorption of a) NF and b) CF500

In **Fig. 4**, the P adsorption capacity of NF and CF500 reached the highest values at adsorbent dose of 1g/75 mL. Therefore, this will be used as the optimal adsorbent dose for next experiments.

Isotherm and kinetic studies

Table 5. Isotherm parameters for P sorption of NF and CF500

Isotherm model	Isotherm parameters	NF	CF500
Langmuir	q_m (mg/g)	12.09	19.38
	K_L	0.005	0.008
	R^2	0.910	0.982
Freundlich	n	1.91	2.35
	K_f	0.34	1.10
	R^2	0.980	0.980

Table 5 shows that CF500 (19.38 mg/g) exhibited a significantly higher q_{max} value as compared to NF (12.09 mg/g), suggesting that calcination was efficient in enhancing P binding ability of NF. Langmuir model was better in describing experimental isotherm data of CF500, indicating that the P sorption by CF500 was mono-layer.

Table 6. Kinetic parameters for P sorption of NF and CF500

Kinetic model	Kinetic parameters	NF	CF500
Pseudo-first-order	q_e (mg/g)	1.75	1.96
	k_1 (min^{-1})	0.12	0.25
	R^2	0.840	0.932
Pseudo-second-order	q_e (mg/g)	1.87	1.99
	k_2 (g/mg.min)	0.025	0.164
	R^2	0.880	0.949

It can be observed from **Table 6** that the kinetic data of both NF and CF500 matched the Pseudo-second-order kinetic model better than the Pseudo-first-order model, implying that the main pathway for P removal by NF and CF500 was via chemisorption [3]. Also, the P sorption rate of CF500 (k_2 = 0.164 min^{-1}) was substantially higher than that of NF (k_2 = 0.025 min^{-1}).

Table 7. Thermodynamic parameters for P sorption of CF500

Temperature (K)	303	313	323
q_m (mg/g)	19.58	21.29	23.51
K_d	1.017	1.227	1.553
△G (J/mol)	-41.47	-533.20	-1181.40
△H (J/mol)		20642	
△S (J/mol/K)		51	

It is evident from **Table 7** that the P sorption by CF500 was spontaneous and feasible (△G <0), had endothermic nature (△H >0) with high affinity (△S >0) [4,5].

IV. Conclusion

Calcination of raw ferralsols favored its P retention capacity. This was resulted from the changes in the surface morphology, functional groups, and mineral composition of the material under high temperature. The optimal calcination temperature was 500°C. The P sorption on CF500 was characterized by mono-layer and chemisorption.

Acknowledgement

This research was funded by Vietnam National Foundation for Science and Technology Development (NAFOSTED) [grant number 105.99-2018.13, 2018]. We are thankful to the Japan International Cooperation Agency (JICA) for the financial support to attend the Conference.

References

[1] Almasri, D. A., Saleh, N. B., Atieh, M. A., McKay, G., Ahzi, S., 2019. Adsorption of phosphate on iron oxide doped halloysite nanotubes. *Scientific reports*, 9(1), 1-13.

[2] Wu, B., Lo, I. M., 2020. Surface Functional Group Engineering of CeO2 Particles for Enhanced Phosphate Adsorption. *Environmental Science & Technology*, 54(7), 4601-4608.

[3] Kumar, P. S., Vincent, C., Kirthika, K., Kumar, K. S., 2010. Kinetics and equilibrium studies of Pb^{2+} in removal from aqueous solutions by use of nano-silversol-coated activated carbon. *Brazilian Journal of Chemical Engineering*, 27(2), 339-346.

[4] Peng, L., Qin, P., Lei, M., Zeng, Q., Song, H., Yang, J., … Gu, J., 2012. Modifying Fe_3O_4 nanoparticles with humic acid for removal of Rhodamine B in water. *Journal of Hazardous Materials*, 209-210, 193–198.

[5] Mezenner, N. Y., & Bensmaili, A., 2009. Kinetics and thermodynamic study of phosphate adsorption on iron hydroxide-eggshell waste. *Chemical Engineering Journal*, 147(2-3), 87-96.

Oxidation-Precipitation of Iron (II) in Groundwater using Modified Airlift Reactor: Kinetics and Influence of Process Conditions

Saret Bun [1], Fumiyuki Nakajima [2], Tomohiro Tobino [3] and Pisut Painmanakul [4,*]

[1] *Water and Environmental Engineering, Faculty of Hydrology and Water Resources Engineering, Institute of Technology of Cambodia, Phnom Penh 12156, Cambodia*
[2] *Environmental Science Center, The University of Tokyo, Tokyo 113-0033, Japan*
[3] *Department of Urban Engineering, Graduate School of Engineering, The University of Tokyo, Tokyo 113-8656, Japan*
[4] *Department of Environmental Engineering, Faculty of Engineering, Chulalongkorn University, Bangkok 10330, Thailand*
* *Corresponding author: saret@itc.edu.kh*

Abstract

The objective of this work is to study the influence of operation parameters on ferrous iron oxidation kinetic under batch conditions using enhanced aeration efficiency reactor, modified airlift reactor (MALR). It presented as a rectangular internal-loop column for containing 6.6 litter total working volume. The influence of process conditions, i.e., initial pH (between 6.5 and 8.0), gas flow rate (between 0.5 and 2 L/min), initial ferrous iron concentration (3 and 20 mg/L), and insoluble ferric hydroxide particle (between 0 and 20 mg/L) were investigated. As the result, iron oxidation is strongly dependent on pH which emphasizes a good ability to maintain a constant pH of gas-liquid reactor such as MALR. Around neutral pH should be considered for controlling iron oxidation reaction. For the study of different initial concentrations of ferrous iron, it indicates that higher ferrous initial concentration (>10 mg/L), the kinetic constant was influenced by heterogeneous reaction. Therefore, the kinetic constant values estimated are possibly exceed than the actual value as it is the combination of homogeneous and heterogeneous reaction kinetic constants. It also found that dissolved oxygen supplied to an aeration system has a pronounced effect on ferrous iron oxidation performance when it was provided in low condition, however, it does not influent if excess amount of oxygen was provided or oxygen concentration reached the saturation. However, air flow rate may not only significant impact only on dissolved oxygen level in diffused aerator, but also the hydrodynamic characteristics which resulted in heterogeneous mechanism based on ferrous adsorption on ferric hydroxide particles. The study showed that the rate of ferrous iron oxidation was significantly affected by the presence of ferric hydroxide and proportionally increased with its concentration. Ferric hydroxide acts as an effective catalyst for the oxygenation. Heterogenous reaction occurred through adsorption mechanism highlights the good mixing ability in multi-phase reactor including MALR. In practical aspect, this effective catalyst can be enhanced by recirculating the ferric hydroxide particles from ferrous oxidation byproducts in a slurry phase, consequently, possible saving on reactor size through the decreasing residence time.

Keywords: *Ferrous iron, Groundwater, Kinetic, Oxidation-precipitation*

I. Introduction

Groundwater is a key resource of drinking water. In Cambodia, more than haft of the population relies heavily on groundwater resources to deal with water shortages in dry season when surface water is not available. Even it is looked so clear and clean, some contaminants, i.e., iron, arsenic, fluoride, etc., are commonly found. Since it is often mildly acidic and devoid of dissolved oxygen, iron presents in groundwater mostly in a form of soluble ferrous iron [1]. Its presence results an unpleasantness of taste in mouth and anesthetic red or brown stains on clothes and sanitary facilities or even foods. Therefore, the presence of iron likely the most common water problem faced by consumers and water treatment operators [1]. A recommendation of World Health Organization for maximum iron in drinking water is 0.3 mg/L as guideline in order to avoid aesthetic and organoleptic problems. However, a range between 0.7 and 80 mg/L have been reported as a ferrous iron concentration in groundwater [2]. Seriously, iron concentration in groundwater of Cambodia up to 100 mg/L was documented by RDI-Cambodia (2016) [3]. Consequently, removal of iron from water is really necessary.

Iron removal from water can be done through physicochemical or biological process of a conventional water treatment. Oxidation-precipitation process followed by sedimentation or/and filtration is the most common treatment pathway. Soluble iron (Fe^{2+}) will be oxidized to insoluble iron (Fe^{3+}). Among all oxidation processes, aeration process is usually considered for ferrous iron oxidation in water with high concentration (higher than 5 mg/L) and it also could avoid costs on chemicals used.

Based on technological application, water can be saturated by oxygen through various ways, i.e., diffused aerator [4], orifice spay reactor [5], and open-air cascades or trays [6]. In the last decade, gas-liquid reactors including bubble column and airlift reactors have been used as diffused aerators for ferrous iron oxidation [1,2] and manganese oxidation [7] due to its benefits such as good mixing, low energy consumption, gas-liquid mass transfer, and pH control properties.

The objective of this work is to study the influence of operation parameters, i.e., ferrous initial concentration, initial pH, supplied gas flow, and additional ferric hydroxide particles on ferrous iron oxidation kinetic under batch conditions using Modified Airlift Reactor (MALR).

II. Materials and Methods

2.1. Experimental set-up

MALR presented as a rectangular internal-loop column for containing 6.6 litter total working volume was used in this study. Compressed air pump and nitrogen gas tank were connected to rigid stone air spargers at the riser bottom of the reactor controlled by the mass flow meter, as shown in **Fig. 1**. A DO probe meter was installed in the middle of downcomer compartment for measuring dissolved oxygen concentration in aquatic solution. A pH meter was used to measure pH and temperature values in aquatic solution as the gas separation zone. The samples were sampled from the gas separation zone of the reactor before preparing for analysis. All experiments were conducted at the room temperature.

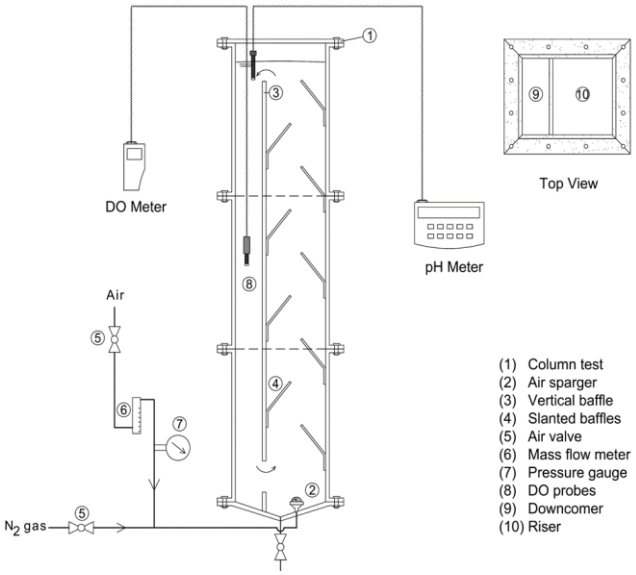

Fig. 1. Experimental set-up of MALR for ferrous oxidation

2.2. Experimental procedure

Experiment was carried out in the 6.6 liter working volume of MALR under semi-batch conditions at room temperature. The influence of process conditions, i.e., initial pH (between 6.5 and 8.0), gas flow rate (between 0.5 and 2 L/min), initial ferrous iron concentration (3 and 20 mg/L), and insoluble ferric hydroxide particle (between 0 and 20 mg/L). Values of pH, dissolved oxygen, and ferrous concentration were measured along the time.

The synthetic waters were prepared by deoxygenated tap water with ferrous sulphate. Nitrogen gas was used for reducing the initial oxygen concentration in tap water to less

than 1 mg/L and for mixing during the synthetic and pH adjustment. Diluted acid and base were prepared for pH adjustment in aquatic solution. For the effective study of additional ferric hydroxide particles on ferrous oxidation, ferric particle in sludge appearance was used. Ferrous samples were recovered from the gas separator zone within every 5 minutes for analysis. After sampling immediately, it was mixed with HCl in order to limit future ferrous oxidation; then, it was added 1,10-phenanthroline to react with ferrous iron and resulted in a color. Last, its concentration was measured by UV spectrophotometer.

III. Results and Discussion

3.1. Effect of initial pH

Ferrous oxidation performance in different initial pH was examined in semi-batch experiments using 10 mg/L of ferrous initial concentration and gas flow 1 L/min without pH constant maintaining. The result showed that 47% removal efficiency was obtained at the lowest initial pH within 45 minutes aeration. Time required to achieve more than 90% removal efficiency for initial pH 7.0 and 8.0 are 40 and 20 minutes, respectively. **Fig. 2** presents the evolution of ferrous iron with time for different initial pH values. The result of ferrous iron followed an exponential decrease demonstrated a first-order removal mechanism. It can be therefore written as **Eq. (1)** below, where k is pseudo-first-order constant presented in min^{-1} unit.

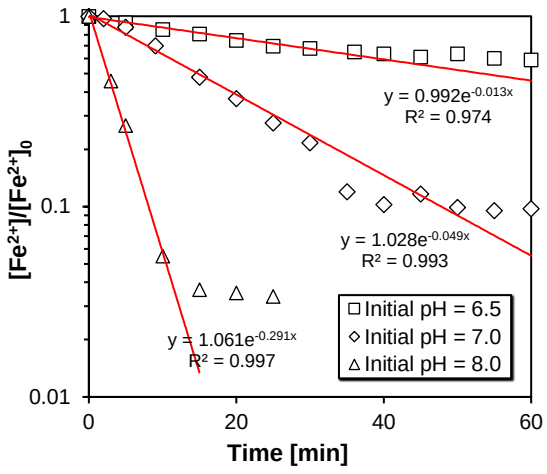

Fig. 2. Semi-logarithmic plot of ferrous iron concentration with aeration time in function of initial pH value

$$-\frac{d[Fe^{2+}]}{dt} \approx k\,[Fe^{2+}] \qquad \text{(Eq.1)}$$

Fitting experimental result into **Eq. (1)**, k values for each condition can be estimated from the slopes of **Fig. 2**. The k values for initial pH 6.5, 7.0, and 8.0 are 0.013, 0.049, and 0.291 min^{-1}, respectively. In conclusion as practical aspect, iron oxidation is strongly dependent on pH which emphasizes a good ability to maintain a constant pH of gas-liquid reactor such as MALR. Last, around neutral pH should be considered for controlling iron oxidation reaction.

3.2. Effect of ferrous initial concentration

A slightly drop of aquatic pH approximate 0.2 was observed for low initial concentration of ferrous iron (≤ 10 mg/L) within 15 minutes before subsequent increase at the end (data not shown). However, a significant decrease of pH value was observed for the highest ferrous initial concentration from for an hour aeration time. Experimental results obtained in semi-batch experiments for an initial ferrous concentration equal 3, 10, and 20 mg/L, keeping all other experimental conditions identical with initial pH 7.0 are reported in **Fig 3**. Result showed ferrous concentration decreases along an aeration and its oxidation is much slower when its initial concentration increases. It can be explained based on the strong pH-dependency of ferrous iron oxidation by air. Only initial pH adjustment before starting the experiment without pH constant controlling was performed in this experiment.

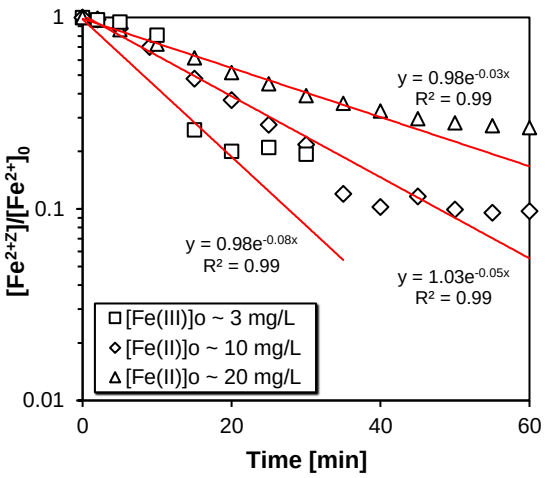

Fig. 3. Semi-logarithmic plot of ferrous iron concentration with aeration time in function of initial concentration

Consequently, higher concentration of ferrous iron must particularly drop aquatic pH value than lower ones along the same aeration time, followed ferrous oxidation stoichiometry equation. Lower aquatic pH surely resulted in lower oxidation performance as higher pH could faster oxidize ferrous iron as aforementioned. Even increasing initial concentration of ferrous iron could not enhance its conversion yield due to the strong effect of aquatic pH, it was confirmed in many researches that iron oxidation byproducts, ferric iron has a contribution on ferrous oxidation rate through catalytic effect as a heterogeneous mechanism which allows ferrous iron adsorption on ferric hydroxide particles together with homogeneous mechanism.

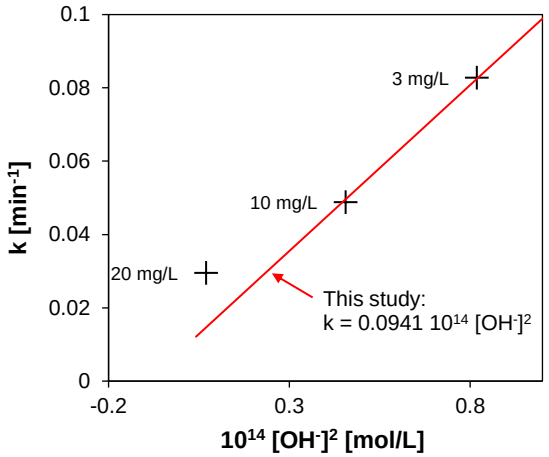

Fig. 4. Comparison of aquatic pH presented in $[OH^-]^2$ on kinetic constant values

A comparative plot of the aquatic pH and aquatic pH represented for different ferrous initial concentrations influence on k value were illustrated in **Fig. 4**. If there is only a homogeneous reaction in the system, experimental data sets must follow the model line constructed from the previous section results. Based on the results, it clearly indicates that at higher ferrous initial concentration (>10 mg/L), the kinetic constant was influenced by heterogeneous reaction. Therefore, the k values estimated in **Fig. 3** are possibly exceed than the actual value as it is the combination of kinetic constant between homogeneous and heterogeneous reactions. Kinetic equation can be derived to **Eq. 2**, where k_1 and k_2 represented kinetic constant of homogeneous and heterogeneous reactions, respectively.

$$-\frac{d\,[Fe^{2+}]}{dt} = k\,[Fe^{2+}] = (k_1 + k_2\,[Fe^{3+}])\,[Fe^{2+}] \qquad \text{(Eq.2)}$$

In order to investigate the other constants of Eq. (2), the additional experiments will be examined for validating the proposed expression. A study of additional ferric hydroxide particles dispersed in the system will be analyzed in order to clarify heterogeneous reaction. Moreover, since the effect of ferric iron particles was occurred through adsorption of ferrous iron on surface of iron particle, liquid flow pattern as well as recirculating ferric particles should be considered. Therefore, different gas flow rates will be investigated in order to study not only the effect of oxygen distribution on ferrous oxidation through homogeneous reaction, but also effect mixing condition on ferrous removal through heterogeneous reaction.

3.3. Effect of supplied gas flow rate

Evolution of ferrous iron removal as a function of supplied gas flow rate was studied in semi-batch experiments in order to evaluate the effect of gas flow with 10 mg/L ferrous initial concentration and initial pH 7.0. Effect of supplied air flow on ferrous oxidation was demonstrated in **Fig. 5**. The plots were started until 35-50 minutes aeration. The experimental result indicates that higher air flow increases ferrous oxidation yield. Aeration time to achieve at least 90% removal efficiency for gas flow 0.5, 1.0, and 2.0 L/min are 60, 40, and 35 minutes, respectively.

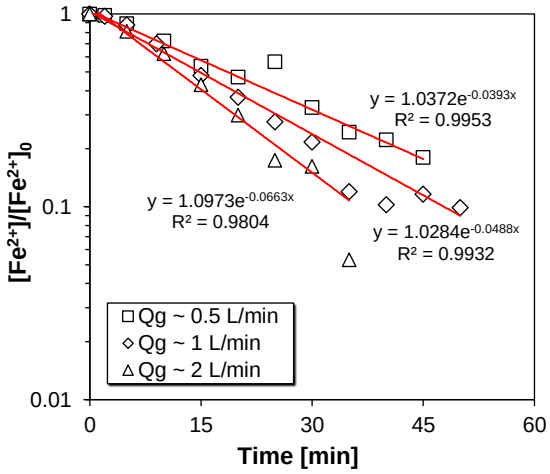

Fig. 5. Semi-logarithmic plot of ferrous iron concentration with aeration time in function of supplied gas flow rate

There are two possible reasons caused a better ferrous oxidization after increasing air flow rate supplied to diffused aerator. Based on the pattern of dissolved oxygen at each gas

flow, an extensive difference can be remarkable at the first 10-30 minutes after aerating from a very low concentration. This time step is the log yield period for ferrous oxidation as well. Between this time range, the dissolved oxygen might not yet sufficient for oxidizing ferrous iron, consequently, higher air flow resulted in faster oxidation yield compared to the lower ones. This finding is in a good confirmation with M. Ghosh (1962) [8], who found that dissolved oxygen supplied for aeration does have a significant influence on ferrous oxidation reaction kinetics at certain amount. Other possible pathway is influence of mixing behaviors on heterogeneous reaction. Using initial concentration of ferrous iron 10 mg/L may result in a catalytic effect of ferric hydroxide particles roleplay as an adsorbent for ferrous iron adsorption as found in previous section. Therefore, higher slurry mixing characteristic could advance better adsorption performance resulted a faster ferrous removal.

3.4. Effect of additional $Fe(OH)_3$ particles

Prepared ferric hydroxide concentration between 0 and 20 mg/L were added into the ferrous iron water sample. In order to obtain a constant concentration of ferric hydroxide in the process, 5 mg/L of ferrous initial concentration was selected as this level was expected that there is no significant influence of autocatalytic effect caused by ferric iron precipitated from ferrous oxidation [1]. Therefore, kinetic equation can be written as **Eq. (3)**.

$$-\frac{d\,[Fe^{2+}]}{dt} = (k_1 + k_2\,[Fe^{3+}])\,[Fe^{2+}] = k_{cat}\,[Fe^{2+}] \qquad \text{(Eq.3)}$$

Experimental results from semi-batch condition with gas flow 2 L/min were reported in **Fig. 6**. Result indicates that higher additional concentration of ferric hydroxide increases ferrous oxidation yield. Aeration time to achieve more than 90% removal efficiency when adding ferric hydroxide concentration 0, 10, and 20 mg/L are 30, 22, and 17 minutes, respectively. To remove ferrous iron from 0.3 mg/L to < 0.3 mg/L, adding 20 mg/L of ferric hydroxide could decrease aeration time almost two times, from 40 to 22 minutes compared to non-additional condition. Aquatic pH decreased while increase additional ferric hydroxide, however, the kinetic constant increased with ferric hydroxide additional. It means that the rate of ferrous iron oxidation was significantly affected by the presence of ferric hydroxide and increased with its concentration.

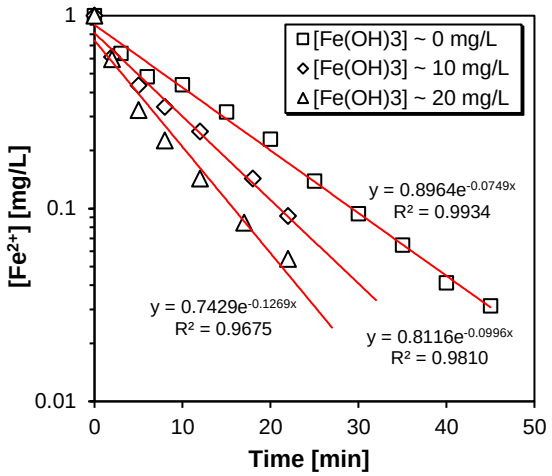

Fig. 6. Semi-logarithmic plot of ferrous iron concentration with aeration time in function of ferric hydroxide addition

For aquatic pH value 6.76 ± 0.18, the k_{cat} values at different additional ferric hydroxide particles were estimated. The k_1 and k_2 constants could be calculated for a certain process condition, as written in **Eq. (4)**.

$$-\frac{d\,[Fe^{2+}]}{dt} = (0.0745 + 0.0026\,[Fe^{3+}])\,[Fe^{2+}] \qquad \text{(Eq.4)}$$

IV. Conclusion

The present part aims to study the influence of process conditions on ferrous iron oxidation kinetic under batch conditions of MALR. Iron oxidation is strongly dependent on pH which emphasizes a good ability to maintain a constant pH of gas-liquid reactor such as MALR. Around neutral pH should be considered for controlling iron oxidation reaction. For different initial concentrations of ferrous iron, it indicates that higher ferrous initial concentration (>10 mg/L), kinetic constant was influenced by heterogeneous reaction. Therefore, the kinetic constant values estimated are possibly exceed than the actual value as it is the combination of homogeneous and heterogeneous reaction kinetic constants. It also found that dissolved oxygen supplied to an aeration system has a pronounced effect on ferrous iron oxidation performance when it was provided in low condition, however, it does not influent if excess amount of oxygen was provided or oxygen concentration reached the saturation. However, air flow rate may not only significant impact only on dissolved oxygen level in diffused aerator, but also the hydrodynamic characteristics which resulted in heterogeneous mechanism

based on ferrous adsorption on ferric hydroxide particles.

The study showed that the rate of ferrous iron oxidation was significantly affected by the presence of ferric hydroxide and proportionally increased with its concentration. Ferric hydroxide acts as an effective catalyst for the oxygenation. Heterogenous reaction occurred through adsorption mechanism highlights the good mixing ability in multi-phase reactor including MALR. In practical aspect, this effective catalyst can be enhanced by recirculating the ferric hydroxide particles from ferrous oxidation byproducts in slurry phase, consequently, possible saving on reactor size through decreasing residence time.

Acknowledgement

This research has been supported by AUN/SEED-Net Program of JICA through Collaborative Research. Authors also acknowledge Project for Strengthening Engineering Education and Research for Industrial Development in Cambodia of JICA through LBE Research Grant.

References

[1] El Azher, N., Gourich, B., Vial, C., Soulami, M. B., and Ziyad, M. 2008. Study of ferrous iron oxidation in Morocco drinking water in an airlift reactor. *Chemical Engineering and Processing: Process Intensification* 47(9-10), 1877-1886.

[2] Stiriba, Y., Gourich, B., and Vial, C. 2017. Numerical modeling of ferrous iron oxidation in a split-rectangular airlift reactor. *Chemical Engineering Science* 170, 705-719.

[3] RDI-Cambodia. (2016). Summary of Groundwater Data. http://www.rdic.org. Accessed 2017.

[4] Roustan, M. 2003. Transferts gaz-liquide dans les procédés de traitement des eaux et des effluents gazeux. *TEC&DOC.*

[5] Klein, D. B., and Neufeld, R. D. 2005. Use of a multiple orifice spray reactor to accelerate ferrous iron oxidation in acidic mine water. *Mine Water and the Environment* 24(4), 186-193.

[6] Rathinakumar, V., Dhinakaran, G., and Suribabu, C. 2014. Assessment of aeration capacity of stepped cascade system for selected geometry. *International Journal of ChemTech Research* 6(1), 254-262.

[7] Kouzbour, S., et al. 2017. Removal of manganese (II) from drinking water by aeration process using an airlift reactor. *Journal of water process engineering* 16, 233-239.

[8] Ghosh, M. 1962. A study of the rate of oxidation of iron in aerated ground waters. *Sanitary Engineering Series* 012.

The 13th AUN/SEED-Net Regional Conference on Chemical Engineering 2020 (RCChE-2020)
Jointly held with
The 5th International Symposium on Conservation and Management of Tropical Lakes
"Insights and Challenges toward Achieving SDGs"

Evaluation of Wastewater Treatment Efficiency Utilizing Coconut Fiber as Filter Media

Chenda Lai[1*], Thary Vorn[2], Boreborey Ty[3]

[1]*Water and Environmental Engineering, Institute of Technology of Cambodia, Russian Federation Blvd, P.O. Box 86, 12156 Phnom Penh, Cambodia*
[2]*SUDrain, Impact Hub Phnom Penh, St 306 #17, Phnom Penh, Cambodia*
[3]*Faculty of Chemical and Food Engineering, Institute of Technology of Cambodia, Russian Federation Blvd., P.O. Box 86, Phnom Penh, Cambodia.*
*Correspoding author: chendalai7@gmail.com

Abstract

The system using coconut fiber as filter media (CFFM) was developed for wastewater treatment in this study. The aim of this experiment is overall to estimate the efficiency of CFFM with various media ratios and hydraulic retention time (HRT) for wastewater pollutant reduction. Two reactor tanks were designed with 14cm^3 and complied with low media ratio (LMR V/V=15%) and high media ratio (HMR V/V =30%). All parameters were measured after treated 24 hours, 3 days, 1 week, 2 weeks, and 4 weeks called Phase-1, and the process was repeated in Phase-2 using the old media from Phase-1. Nutrient compositions such as NO_3^-, NH_4^+, SO_4^{2-}, and PO_4^{3-} were determined by IC while heavy metals were determined by ASS. The results showed that HMR had no significant effect on the removal while the volume increased 2 times (15%-30%). It is noticed that LMR of V/V=15% with 2 x 2 cm and 0. 19g/cm^3 density was a good condition for this wastewater pollutant load. The percentage removals of COD, Cu, Cd, NO_3^-, NH_4^+, andSO_4^{2-} were only slightly increased between 1 day and 3 days of HRT but it showed a remarkable change at 1week of HRT with 7.2% (SO_4^{2-}) minimum and 25 % maximum (COD) of increasing. The maximum removal of COD in Phase-1 was 78.01% and 93.68% in Phase-2 while Cu was considered as the highest (about 80%) among heavy metals. Besides that, SO_4^{2-} was the best removal (81.25%) of nutrient compositions, whereas Fe was the lowest one among all studied parameters. It was proved that the removals were related to the HRT; however, 1week of HRT is the better choice for pollutants reduction in terms of efficiency, time, and space-saving.

Keywords: *Coconut fiber, Heavy metals, Media ratio, Nutrient compositions*

I. Introduction

Poor environmental conditions and the lack of pollution control lead to disease and poor sanitation contributes to environmental degradation [1]. Coconut fiber is noticeable to be one of the potential filtering media for pollutant reduction [2]. The chemical components of coconut fiber are lignin (about 45.8%), cellulose (43.4%), pectin and related compound (3%), water soluble(5%), ash and other compound (7.8%) [3]. Sato (2017) did the microsomes experiment with the bundle of coconut fiber 0.2m length. The maximum removals in synthetic sewage were (30.5%) of BOD, 10.2% of COD, 30.8% of TN, and 21.8% of TP while in synthetic leachate, the maximum removal were 45.2% of BOD, 46.5% of COD, 41.2% of TP, and 32.9% of TN [4].

The aim of this study is to evaluate the efficiency of coconut fiber for wastewater pollutant reduction, whereas two specific objectives are taken into account: (1) designing, and (2) optimizing lab-scale of wastewater treatment (WWT) using biological filter from recycling coconut waste as a filter media and evaluating the efficient removal of wastewater treatment utilizing coconut fiber in different media ratios (MRs) and hydraulic retention times (HRTs).

II. Materials and Methods

2.1. Sampling Sites

Wastewater was collected from the wastewater treatment system at Phnom Penh Special Economic Zone. The wastes are mainly from the small medium enterprises (SME) and factories in that zone.

2.2. Experimental set-up

In order to set up the experiment, two acrylic rectangular tanks shaped with an operation volume of 14cm^3 were designed and complied with the coconut fiber media ratio of low media ration. The specification set-up of the coconut fiber filter media (CFFM) system is shown in **Table 1.**

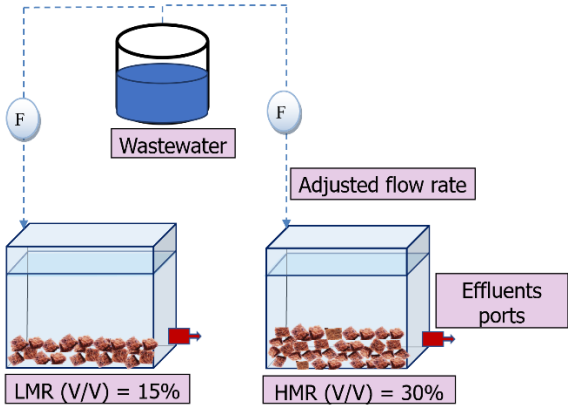

Fig. 1. Experimental set-up

Table 1. Specification set-up of coconut fiber

Modeling	Unit	Condition
Media Shape and Size	cm	Rectangular Surface: 2 x 2 Height: 1
Density	g/cm^3	0.19
HRT	-	24h, 3 days, 1 week, 2 weeks, 4 weeks
Flow rate	cm^3/h	24h HRT: 500

2.3. Analytical methods

2.3.1. pH, Temperature, EC, and Turbidity

pH and EC were measured using pH meter HM-30P and EC meter(hold) respectively while Turbidity was measured with Turbidity meter model HI98703.

2.3.2. Total Suspended Solid

Cellulose Nitrate Filter Papers with pore size 0.45µm were used to separate liquid and solid following the method 2540 of Eaton *et al*. (2005). The formula for TSS calculation was followed as in **Eq. 1** below

$$\text{TSS mg/L} = \frac{(\text{F-I})(\text{g}) \text{ x } 1000\text{mg/L}}{\text{sample volume in L}} \qquad \text{(Eq. 1)}$$

Where

F= final dried weight of the filter (mg)

I = Initial weight of the filter (mg)

2.3.3. Chemical Oxygen Demand (COD)

There are COD low range (LR) capacity with 0-150mg/L, and COD high range (HR) capacity with 20-1500mg/L following the method of 5220-COD/SM. They were added with 2mL of the reagent test tube, heated in HATCH DRB-200 for 2h and 150 oC, and cool down it before analysis with HATCH DR 1000 by COD LR and COD HR method.

2.3.4. Heavy Metal Analysis

The samples were filtered with 0.45µm filer paper using auto air pumps. The standard condition of each metal was prepared by Fe (0ppm, 0.1ppm, 0.5ppm, 1ppm, and 2ppm), Pb (0ppm, 0.5ppm, 1ppm, 2ppm, and 5ppm), Cd (0 ppm, 0.05ppm, 0.1ppm, 0.2ppm, and 0.5ppm), and Cu (0ppm, 0.1ppm, 0.5ppm, 1ppm and 2ppm). The samples were analyzed with AAS model AA-7000 SHIMADZU.

2.3.5. Nutrient Composition Analysis

Nutrients composition in terms of the cation (NH_4^+) and anion ($SO4^{2-}$, PO_4^3, and NO_3^-,) were determined by Ion Chromatography (IC) model IC CTO-20A. The samples

need to be filtered to remove particles larger than 0.45µm before analysis (Eaton, 2017).

III. Results and Discussion

Influent wastewater was analyzed in terms of physical and chemical parameters and its characteristic is shown in **Table 2**.

Table 2. The characteristic of influent wastewater

Parameters	Unit	Value	MoE. Std (1)
pH	-	7.88 ± 0.16	5-9
Temperature	^{o}C	27.82 ± 0.21	<45
TSS	mg/L	404.33 ± 4.24	<50
Turbidity	NTU	85.03 ± 2.78	None
EC	mS/cm	912.33 ± 130	None
TDS	ppm	582.33 ± 8.48	<1000
COD	mg/L	425.50 ± 15.32	<50
Cd	ppm	2.61 ± 0.31	<0.1
Cu	ppm	2.90 ± 0.14	<0.2
Fe	ppm	0.13 ± 0 .033	<1.0
Pb	ppm	2.66 ± 0.32	<0.1
NO_3^-	ppm	11.58 ± 1.52	<10
NH_4^+	ppm	24.22 ± 3.36	None
SO_4^{2-}	ppm	341.50 ± 28	<300
PO_4^{3-}	ppm	140.01 ± 43.36	<3.0

3.1. Evaluation of Treatment Performance in Phase-1 and Effect of Media Ratio

The removal efficiency of COD **(Fig.5.)** indicates that in 1 day of treatment the percentage removal started from 40.18% of LMR and 41.63% of HMR. It is not a significant difference between LMR and HMR. Dharmarathne *et al*. (2013b) also reported that HFD (high fiber density) and LFD (low fiber density) treatment tank showed a very parallel trend in the COD removal [5]. The removal of COD is related to the biofilm which grows on the surface of media.

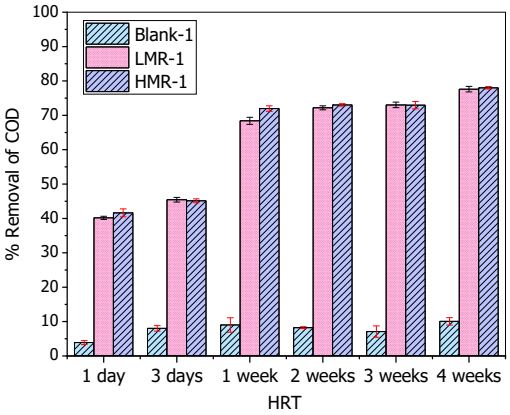

Fig.2. % Removal of COD in Phase-1

The media provided a good treatment of SO_4^{2-} since the first HRT (67.43% and 69.40% for LMR and HMR). As shown in **8**, there was no significant difference in removal efficiency between LMR and HMR. The removal involves with the biofilm and H_2S transform in anaerobic condition.

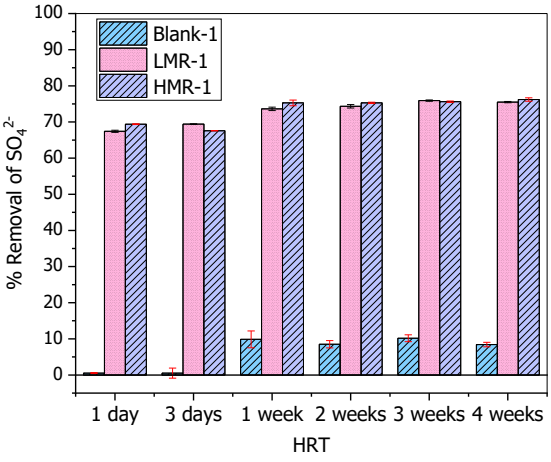

Fig.3. % Removal of Fe in Phase-1

3.2. Summary of All Percentage Removals and Parameters Comparatives

Turbidity in Phase-1 provided the best removal in terms of the physical parameters in LMR-1 condition which showed the maximum reduction of about 98% at 4 weeks HRT. The performance was the same in LMR-2 condition. However, in terms of chemical parameters, Cu was the best parameter in LMR-1, whereas COD was the best one for LMR-2. Irons provided the lowest removal among all heavy metals in both phases while PO_4^{3-} was the lowest one in terms of nutrient compositions.

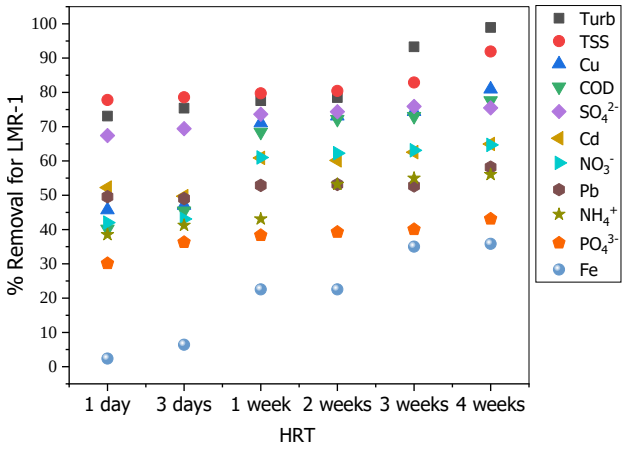

Fig.4. % Removal in all condition for LMR-1

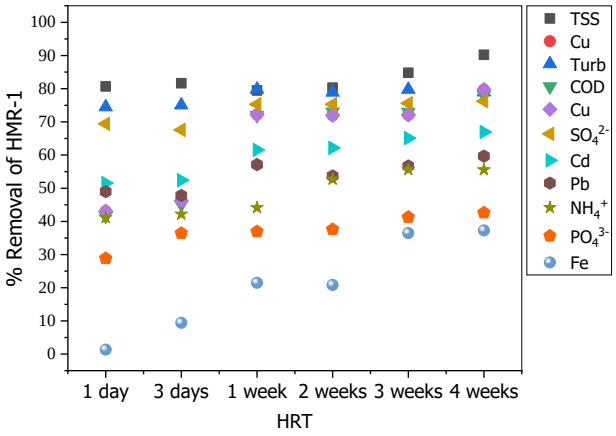

Fig.5. % Removal in all condition for HMR-1

The summary of percentage removals in both phases of HMRs were shown in **Fig. 5.** Cu was the best element among chemical parameters in HMR-1, whereas COD became the best for HMR-2 with maximum removal of 91.68%. It was also observed that there was no difference between HMR and LMR on the iron performances which provided the lowest removal among heavy metals parameters while PO_4^{3-} was the lowest one among nutrient compositions.

IV. CONCLUSIONS

Based on the results from the CFFM system, the finding of this study can be summarized as follows: The CFFM could be successfully operated by LMR (V/V=15%) with this type of wastewater. The higher MR did not show better results while the volume increased 2 times. The maximum removal of COD in Phase-1 was 78.01% and 93.68% in Phase-2, whereas Fe was the lowest removal among all studied parameters. This study is beneficial for the further research as it provided the data of treatment by using coconut fiber which is the low-cost materials as the filter media.

ACKNOWLEDGMENTS

This research was financially supported by AFD-EU; laboratory support by SATREPS lab, Ministry of Environment lab, Phnom Penh Special Economic Zone.

References

[1] Tyagi, S., Garg, N., & Paudel, R. (2014). Environmental Degradation: Causes and Consequences. *European Researcher*, *81*, 1491.

[2] Islam, T., Islam, S., Saifullah, I., Datta, D., & Ahmed, A. (2017). *Suitability of Recycled Coconut Fiber as Filter Media for the Treatment of Wastewater*. Proceedings of 5th International Conference on Solid Waste Management in the Developing Countries, Wastesafe-2017, Khulna, Bangladesh.

[3] Sagar, S. S., Chavan, R. P., Patil, C. L., Shinde, D. N., & Kekane, S. S. (2015). Physico-chemical parameters for testing of water-A review. *International Journal of Chemical Studies*, *3*(4): 24-28.

[4] Sato, N. (2017). Microcosm Experiments on a Coconut-Fibre Biofilm Treatment System to Evaluate Waste Water Treatment Efficiencies. S., Garg, N., & Paudel, R. (2014). Environmental Degradation: Causes and Consequences. *European Researcher*, *81*, 1491.

[5] Dharmarathne, N., Sato, N., Kawamoto, K., Sato, H., & Tanaka, N. (2013, November 1). *Evaluation of Wastewater Treatment Efficiency Using Coconut Fiber Biofilm Reactor System with Synthetic Leachate*.

Current Presence and Possible Repercussions of UV Filters in Coral Reef in Okinawa Prefecture

Jorge Garcia-Hernandez*, Rajendra Khanal and Chihiro Yoshimura

Department of Civil and Environmental Engineering
School of Environment and Society
Tokyo Institute of Technology
2-12-1-M1-4, Ookayama, Meguro-ku, Tokyo, 152-8552, Japan
** garcia.j.aa@m.titech.ac.jp*

Abstract

Ultra-violet (UV) filters are pollutants of arising concern due to its persistence in water environment. In previous researches, UV filters have been reported in pristine coral environment in Okinawa, Japan. The main objective of this research is to review the spatiotemporal variation of 12 of the 16 UV filters, categorized as 3 groups by the Food and Drug Administration (FDA) on the Act to Modernize the Regulation of Sunscreen Products in the United States proposed in 2019. The target area is the Japanese coral reef environment in Ryukyu Trench, Ryukyu Islands, and Okinawa trough, for highlighting its toxicological and bioaccumulating impacts on coral reefs ecosystems. The web of science database from 2000 to 2020 was searched with the key words: anthropogenic activities, persistent organic pollutants, sunscreens, UV filters, UV protection, sunblock, UV stabilizer, coral, Japan, and Okinawa. Most of the studies agreed that organic UV filters such as oxybenzone, octinoxate or octocrylene significantly degrade the water quality, which may have potential risk to coral ecosystems. In addition, the wide spread of UV filters has shown a perceivable presence in some Okinawa beaches, containing around 1.4 µg/L oxybenzone during summer season. Nevertheless, oxybenzone at some reef sites have been found to be around 0.01 µg/L which is almost 500 times lower than the LC50 range of 5.4 to 14.5 µg/ for *Acropora cervicornis* larvae. More toxicological and bioaccumulate studies on coral reef bleaching by UV filters have to be performed to support this statement and re-evaluate their ecological risks in coral reef ecosystems at different season and complex environmental exposure.

Keywords: *UV filters, Okinawa, UV protection, coral, Oxybenzone*

I. Introduction

In recent years, the concern about micropollutants and their impact in the environment have increased. Sunscreens and other Persistent Organic Pollutants (PPPs) have received particular attention from several researchers around the world due to the concern about their potential impact in the environment. Several studies have focused on the ecotoxicological effects of sunscreen pollutants in marine biodiversity, potential bioaccumulation problems and possible coral bleaching. Nevertheless, a few studies have focused on the Japanese coral reefs impact due to the use of sunscreen chemicals.

Japanese coral reefs are located along the boundary of the Philippine sea plate and is composed by the Ryukyu Trench, Ryukyu Islands and Okinawa Trough in the Okinawa prefecture [1]. Each reef is characterized by the property of the island, such as the soil type, land-use land cover, and precipitation regime. The climatic conditions and the crystalline water create a perfect place to receive

thousands of tourists each year with Okinawa islands being the most visited one. Coral reefs around the main island in Okinawa is located a few meters off the coast.

Several activities such as scuba diving and snorkeling are popular and it attracts tourists to discover the beauty of the Japanese coral reefs. According to the tourism minister of Japan, in 2017 over 9 million people visited Okinawa and the trend tends to increase year by year possibly to 12 million people by 2021 [2]. However, there are several environmental issues to face as the tourism is expanding such as coastal development and construction, land reclamation and degradation of coral reefs.

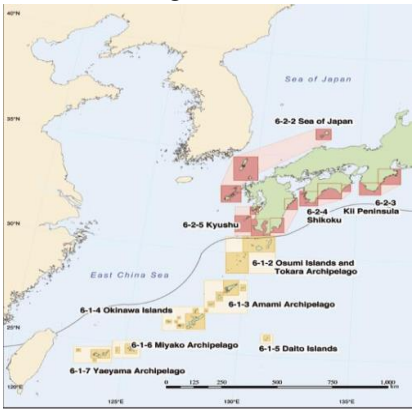

Fig. 1. Japanese coral reefs. Provided by Marine Biotic Environment Survey.

Coral reefs declining has been reported in the 1980's where approximately 40% of the coral bleached and 10% died in Sesoko and Okinawa Island [1]. The main stressors that influence in coral bleaching are solar irradiance, global warming and anthropogenic activities like municipal and industrial wastewater effluent and micro-pollution.

Micropollutants directly and indirectly enter the aquatic environment via industrial or municipal wastewater effluents, stormwater runoff, or recreational activities. Several studies have focused on the ecotoxicological effects of sunscreen pollutants in marine biodiversity, proving the presence of Oxybenzone (BP-3) in *Scrobicularia plana*, an indicator species for assessing the health statues of estuarine and coastal ecosystems [3]. Furthermore, in situ and laboratory experiments in several tropical regions have shown coral bleaching of communities, such as *Zooxanthella*, where the organic ultraviolet filters induce the lytic viral cycle with latent infections [4].

UV-filters are widely popular to offer protection to human skin against deleterious effects of UV radiation. These are substances with almost null absorption of visible radiation but important light absorption in the UVA (315-400nm) and UVB (280-315nm) [7], moreover, regarding their mechanism of action, can be classified into organic (chemical) absorbers and inorganic (physical) blockers.

A detailed sunscreen classification has been done by the FDA (Food and Drugs Administration) in 2019 in the United States, where sunscreen products for over-the-counter human use are classified in three main categories called GRASE (Generally Recognized as Safe and Effective).

The main objective of this research is to review the spatiotemporal variation of 12 of the 16 UV filters (Avobenzone, Cinoxate, Dioxybenzone, Ensulizole, Homosalate, Meradimate, Octinoxate, Octisalate, Octocrylene, Oxybenzone, Padimate O, Sulisobenzone), categorized as 3 groups by the FDA on the Act to Modernize the Regulation of Sunscreen Products in the United States proposed in 2019.

II. Methodology

We conducted this review using the web of science, filtering data from 2000 to 2020 using the keywords: anthropogenic activities, persistent organic pollutants, sunscreens, UV filters, UV protection, sunblock, UV stabilizer, coral, Japan, and Okinawa.

From this screening process, 40 different articles were identified to highlight the presence of persistent organic pollutants in Japanese marine environment. Nevertheless, just 2 of them reported concentrations and affectations in Japanese coral reefs by sunscreen UV filters [5,6].

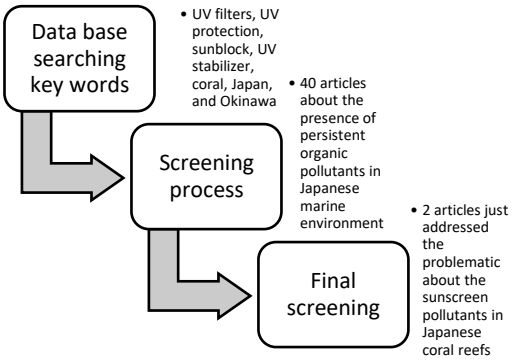

Fig. 2. Screening process of literature review.

III. Results

3.1. UV filters presence in coral reefs in Okinawa Prefecture

High level of organic pollutants (Organo-tin compounds

(OTCs), organochlorine pesticides (OCPs) and polychlorinated biphenyls (PCBs) were detected in surface water and sediments of some rivers and coastal waters of Okinawa [6]. OTCs were found at considerable concentrations in sediments that could be a possible threat to marine life including coral communities around Okinawa Island. This study refers to a large number of chemical groups and non-sunscreen chemical was detected or consider in this study. Nevertheless, this study set the ball rolling for further investigations and monitoring of coral reef ecosystem to elucidate the effects of toxic organic pollutants on the subtropical marine life around Okinawa Island.

Yutaka Tashiro performed a constant sampling once a month in Okinawa main Island for analyzing the occurrence of UVFs and UVLs in seawater [5]. The results varied due to the fact that the distribution of the chemical in the beach water is not uniform and is strongly affected by water movement. The maximum concentration of BP-3 (1.34 µg/L) detected at Sunset beach in July was one fifth of its PNEC value (6 µg/L). In fact, the concentration of UV chemicals at the reefs were much lower that the estimated lethal concentration, however it was suggested that more studies over the range of concentrations detected and exposure time are strongly necessary to prevent impact in coral ecosystems. In this same investigation, the wide spread of UV filters has shown a perceivable presence in some Okinawa most visited beaches, containing around 1.4 µg/L oxybenzone during summer season. Nevertheless, oxybenzone at some reef sites have been found to be around 0.01 µg/L which is almost 500 times lower than the LC50 range of 5.4 µg/L to 14.5 µg/L for *Acropora cervicornis larvae*.

IV. Discussion

4.1. Importance of UV filters

Based on the production and consumption of cosmetic sun products, commonly people applied around 65-130mg of sunscreen each time. In Germany, annually 7,900 tons of sunscreen are consumed assuming that 20,000 tons are released in the northern Mediterranean [9]. According to some estimations, 10% of the sunscreens produced in the world are normally used in tropical areas with coral reefs [9]. Nevertheless, this statement was done in 2004, and based on the gradual increase of sunscreen products sales, the amount of these chemicals entering to the environment is unknown.

A novel report [10] was released in 2019 in Hawaii, where UV-filters were reported in coral tissue in Hawaiian coral reefs. Octinoxate, Homosalate, Octocrylene and Oxybenzone were detected in coral tissue from three important tourist sports at Oahu island (Ka'a'awa, Waikiki beach and Kaneohe Bay). The detection frequencies of the four chemicals were 100%, 100%, 96% and 82%, showing a the presence of those compounds in Hawaiian coral reefs.

In this same study [10], eight different UV filters were detected in marine environments, especially in Kaneohe bay, where the concentration of BP-3 was higher before water-users arrived at this site, than later in the morning after people arrived. The first sample at 8am contained 6.6 ± 0.7 ng/L BP-3 and 2.8 ± 0.1 ng/L of OC, then around 10 am and with more than 120 people around the coral reefs another sample was taken showing an increased to 27.0± 18.4 ng/L and 23.6 ± 19.0 ng/L, respectively [10], assuming that sunscreen primary source in coastal water is due to the increased of swimmers around the area, causing different fluctuations in the final exposure in coral reefs.

The two research articles from the Okinawa prefecture are considered the pioneers for addressing the environmental impacts of sunscreen pollutants this field in Japan. More research has to be performed based on the UV filters are the most consumed in the Japanese sunscreen market. It can be inferred that, according the investigations addressed in this review paper, the main impacts of chemical filters are bleaching of hard corals, damage of coral larvae, and possible biomagnification and bioaccumulation issues.

Coral bleaching in Okinawa prefecture have occurred before in 1998, 2001, 2008 and recently 2016 [12]. The Ministry of the Environment Government of Japan have reported that in 2016 in Sekisei Lagoon around 90% of the reef presented damage from coral beaching, including 70% that died by the bleaching phenomenon" [12]. Several investigations on Japanese coral reefs damage have been shown that temperature rising and ocean acidification are the main factors leading to the stress and decline of the coral communities. Nevertheless, Persistent Organic Pollutants such as sunscreen UV filters in Japanese coral reefs can contribute to the bleaching problem.

As the consumption of this products increases, the concern about the possible repercussions of UV filters in the environment raises up. Japanese cultural background about skin protection is an influential factor to consider in the consumption, especially when the skin beauty is important for some sectors of the society. The cultural background and the desire for a white and spot free skin is coming from the *Bihaku* or skin whitening culture which is a common practice by the majority of the Japanese woman. Bihaku

products sales have been increased gradually year by year generated revenue of around 62 billion ¥ in 2018 [14]. Pharmaceutical industries find the Japanese skin care market as reliable and demanding.

V. Conclusion

Although Oxybenzone was found in Okinawa corals with a concentration of 1.4 µg/L, the potential harm for larvae species such as *Acropora cervicornis* is lower than the LC50 range. However, further investigations should be done to prove potential ecotoxicological risks by prolonged exposure of UV filters under real conditions, to refuse or affirm, any affectation to the coral ecosystem. The main motivation to elaborate this review paper is to highlight investigations and actions other countries are taking already to face coral declining, and review the presence of 12 sunscreen chemicals stated in the FDA list published in 2019.

Probable data of the presence of sunscreen chemicals in Japanese coral reefs will bring more investigations to this field and consequently find alternatives to mitigate any potential risk. Spatial-temporal variation of UV filters in Japanese marine environment and ecotoxicological studies in coral reef biota, are necessary to know the affectation of sunscreen chemicals in coral ecosystems.

Acknowledgement

Authors would like to express gratitude to Asia-Pacific Network for Global Change Research for funding this project - "Collaborative Research Platform to Manage Risk and Enhance Resilience of Coral Reef in Southeast Asia, CRRP2019-08MY-Khanal".

References

[1] Nakano Y (2004) Index map for Chapter 6. In: Tsuchiya M, Nadaoka K, Kayanne H, Yamano H (eds) Coral reefs of Japan. Ministry of the Environment, Tokyo, pp 155.

[2] The Japan times., 2018. Okinawa Tourist Numbers Top Those of Hawaii For First Time: https://www.japantimes.co.jp/news/2018/02/09/national/okinawa-tourist-numbers-top-hawaii-first-time/. Accessed 16 December 2020.

[3] O'Donovan, S., Mestre, N., Abel, S., Fonseca, T., Carteny, C., Willems, T., Prinsen, E., Cormier, B., Keiter, S. and Bebianno, M., 2020. Effects of the UV filter, oxybenzone, adsorbed to microplastics in the clam Scrobicularia plana. *Science of The Total Environment*, 733, 139102.

[4] Danovaro, R., Bongiorni, L., Corinaldesi, C., Giovannelli, D., Damiani, E., & Astolfi, P. et al., 2008. Sunscreens Cause Coral Bleaching by Promoting Viral Infections. *Environmental Health Perspectives*, 116(4), 441-447.

[5] Tashiro, Y., & Kameda, Y. 2013., Concentration of organic sun-blocking agents in seawater of beaches and coral reefs of Okinawa Island, Japan. *Marine Pollution Bulletin*, 77(1-2), 333-340.

[6] Imo, S., Sheikh, M., Sawano, K., Fujimura, H., & Oomori, T. 2008,. Distribution and Possible Impacts of Toxic Organic Pollutants on Coral Reef Ecosystems around Okinawa Island, Japan. *Pacific Science*, 62(3), 317-326.

[7] Giokas, D., Salvador, A., & Chisvert, A. 2007., UV filters: From sunscreens to human body and the environment. *Trac Trends In Analytical Chemistry*, 26(5), 360-374.

[8] Tsui, M., Leung, H., Wai, T., Yamashita, N., Taniyasu, S., & Liu, W. et al. 2014., Occurrence, distribution and ecological risk assessment of multiple classes of UV filters in surface waters from different countries. *Water Research*, 67, 55-65.

[9] Danovaro, R., & Corinaldesi, C. 2003., Sunscreen Products Increase Virus Production Through Prophage Induction in Marine Bacterioplankton. *Microbial Ecology*, 45(2), 109-118.

[10] Mitchelmore, C., He, K., Gonsior, M., Hain, E., Heyes, A., & Clark, C. et al. (2019). Occurrence and distribution of UV-filters and other anthropogenic contaminants in coastal surface water, sediment, and coral tissue from Hawaii. *Science Of The Total Environment*, 670, 398-410.

[11] Schaap, I., & Slijkerman, D. 2018., An environmental risk assessment of three organic UV-filters at Lac Bay, Bonaire, Southern Caribbean. *Marine Pollution Bulletin*, 135, 490-495.

[12] Kayanne, H., Suzuki, R., Liu, G. 2017., Bleaching in the Ryukyu Islands in 2016 and associated Degree Heating Week threshold., *Journal Of Coral Reef Studies*, 19(1), 17-18.

[13] Tokyoesque (2017)., Beauty, Grooming & Skincare Market in Japan. https://tokyoesque.com/industries-japan-market/skincare-market-in-japan/. Accessed 24 November 2020.

The 13th AUN/SEED-Net Regional Conference on Chemical Engineering 2020 (RCChE-2020)
Jointly held with
The 5th International Symposium on Conservation and Management of Tropical Lakes
"Insights and Challenges toward Achieving SDGs"

Prediction of Future Land Use Change in the basin of Tonle Sap Lake Using Scenario Analysis in CLUMondo

Sreykeo Puok*, Kong Chhuon

Faculty of Hydrology and Water Resources Engineering, Institute of Technology of Cambodia ,Russian Ferderation Blvd., P.O. Box 86, Phnom Penh, Cambodia.

**Corresponding author: sreykeo.puok12@gmail.com*

Abstract

Land-Use and Land-Cover (LULC) is an important factor for maintaining healthy ecosystem. The change in LULC responses to different socio-ecological system and regime shifts. Due to the significant change of LULC in Tonle Sap Lake (TSL) of Cambodia in last decade, it puts more concern on the consequence impacts to the surrounding environment while it lacks of scientific study on how LULC in this area will be change in the future. The aim of this study is to assess the future land use change in the basin of TSL using CLUMondo model over the period 2015-2045 based on the recent land use update. Four scenarios were simulated based on the government policy and commitment: The Economic Land Concession scenario, the Moderate Conservation scenario, the Conservation scenario, and the SDG-2030 scenario. All scenarios show an increase in the urban area, annual crop, wood plantation, and agricultural land while the flooded forest remain constant. The economic land concession or business as usual scenario cause highly change of LULC. Particularly, until 2045, the forest cover in the basin of TSL will change differently from each scenario which are -10%, -8%, -6%, -6% for ELC, Moderate Conservation, Conservation and SDG-2030 respectively. The shifting cultivation declines dramatically and will all disappear by 2030 for all scenarios while grassland will be completely transferred to annual crop, wood plantation, urban area, and agricultural land by 2045 to compensate the need of land for food production in the scenario of conservation and SDG2030. The result of this study can guide and support future land use planning, management, and policy formulation in the basin of TSL.

Keywords: *CLUMondo model, Tonle Sap Lake, Land-Use, Scenario,*

I. Introduction

Land use and land cover change is an important factor in the study of environmental change [1]. Land use is thus a central component of biophysical, social, and economic systems acting across various scales. Therefore, the study of land use and land cover change becomes very important to address the environmental issues.

The basin of the Tonlé Sap Lake (TSL) is a unique basin where the fluvial water flows in two directions during the year as a result of the rain season. This interesting catchment is influenced by the surrounding environment where land use changes impact the hydrological processes such as surface runoff generation, groundwater recharge and soil erosion. However, some studies have assessed the land cover but not the prediction for the future change. The study on the drivers of deforestation and agricultural transformations in

the Northwestern uplands of Cambodia by analyzing historical rejection of land use/ cover changes using a chronological series of Landsat data and the investigated of land cover and land use Change in Stung Chrey Bak Catchment [3,4]. Recently, there are many studies have been conduct on the impact of land use change on water supply for the Angkor temple and the surrounding population and the impact of land use and climate change on water resources and remand in Srepok River Basin [5,6]. The objective of this paper is to systematically study of land use change with different changing scenarios using CLUMondo model over Tonle Sap basin. This study is intended to integrate together ArcMap (GIS) and CLUMondo model approach to identify a change in land use pattern in the basin of Tonle Sap Lake during 2015 to 2045.

II. Materials and Methods

2.1. Study area

The area of the basin of Tonle Sap Lake is located in the northwest of Cambodia (102°00'-106°00' E, 11°30'-14°30' N), with a total land area of 81,372 Km2. The basin consists of the Tonle Sap lake and 12 sub-basin which covered on 10 provinces [7]. The average annual rainfall is from 1000-1500mm with, the daily mean temperatures between 21-25 °C (minimum) and 30-35 °C (maximum). The average humidity varies from 70% (March) to 85% (September) [8]. The main land system divided into five classifications: Forest (48.5%), Agricultural land (25.6%), Barren land (13.3%), Aquatic ecosystems (12.7%), and Urban area (0.1%) [7].

2.2. Data Sources

The existing data included the land use/cover (2015) were obtained from the National Institute Statistic (NIS). These land use datasets separated into 9 categories (water, urban area, annual crop, flooded forest, wood plantation, grass land, forest, agricultural, and shifting cultivation). The climate and topographic got from Mekong river commission (MRC) and SRTM, the socioeconomic and soil data were obtained from NIS.

2.3. Model implementation

To simulate the land system, change until 2045, we applied CLUMondo model with the spatial resolution of 2 × 2 km to simulate the future scenarios land system in TLS. This model determines the global spatial allocation of land system through the allocated the land system change based on the demand of goods, services for difference land system[1]. The overall flowchart was described in **Fig. 1.**

The demands considered in this study included cash crop, wood production, subsistence crop, and built-up area. The driving factor indicate the factors that can affect land use change. In this report, these driving factors were characterized into 4 categories included, Climate, Socioeconomic, Soil type, and Topographic. We estimate the conversion order base on the realities of land use services with the land use types. The conversion order is a technical parameter that tells the model how to change land use to fulfill demand while, the values that do not supply a good or service get a 0, and all land-uses that do supply a good or service get a value from 1 onwards.

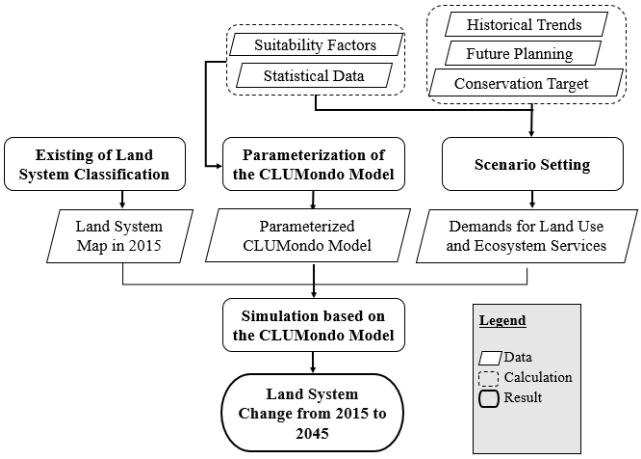

Fig. 1. Flowchart of land system simulation

The conversion resistance factor for each land system estimated base on the costs of conversion, information on local policies on land use, and scenarios setup. In the model we have assigned each land-use type a dimensionless factor that represents the relative elasticity to conversion, ranging from 0 (easy conversion) to 1 (irreversible change).

The conversion matrix was estimated by the model which indicates what types of land use conversions are allowed. We have assigned each land-use type based on the reality of the land policy and scenario setup which 0 (no conversion allowed) and 1 (conversion is allowed).

2.4. Scenario setting

To capture land system change under different levels of socioeconomic development and environmental conservation, four scenarios were developed according to the historical trend of land system change, the land use planning from 2015 to 2045, and the biodiversity conservation targets. These differences reflect the importance given to different land system functions under different scenarios. The first scenario Economic Land

Concessions (ELC) is a scenario based on only demand, population, and economic. it's long-term to clear land in order to develop industrial scale agriculture and can be granted for various activities. Second, The Moderate Conservation (MCO) is a scenario based on demand, increasing rate of population and economic, with moderate conservation of forest. It is balancing between demand and supply. Third, Strong Conservation (SCO) is a scenario based on the limit conservation of forest. The limit must be high to preserve the biodiversity or to put in the conservation area. The last one, Sustainable Development Goals 2030 (SDG-2030) is a scenario that based on the restoration to achieve the 60% of forest cover over Cambodia in 2030.

III. Results and Discussion

The results from the four scenarios are presented in terms of the simulated land system changes in TLS basin.

Fig. 2 shows the resulting land system maps in 2045 under the four future scenarios which three quite different land system changes, even though the demands for most land system commodities and services are similar across all scenarios. The percentage of land system change between 2015-2045 under different scenario shows in **Fig. 3**. In this case study, the water and flooded forest remained unchanged for all the scenarios, when the other land system is strongly changing. The total amount of agricultural land, urban area, annual crop land, and wood plantation approximately increase to 30.5%, 8.75%, 28.85%, and 3.1% in 2045. However, three types of land system will be takeover in grassland(0%), shifting cultivation(0%), and forest land (21%) in Conservation and SDG 2030 scenario. For both scenario Economic land concessions and Moderate conservation, the shifting cultivation land decrease to 0% since 2030, when the grassland remains less than 4.5% and 19% for forest land in 2045.

The model simulation presented the land system change that is a major driver of change in the spatial pattern and overall provision of ecosystem service. Four scenarios show that, while the demand for cash crop, wood product, subsistence crop, and built-up area can be provided by both smallholders and large-scale land acquisition (LSLAs), but as the result “Water” and “Flooded forest” area would remain constant for an area of 353,200 ha (4.34%) and 277,200 ha (3.41%). Even though, the urban area, annual crop, wood plantation, and agricultural land are similar to increase until 2045, but other types of land system are very different changing. In the ELC and Moderate Conservation scenario, most of the increasing of the urban area and annual crop land take a place of forest cover and shifting cultivation. However, we see the increasing of the urban area and annual crop take a place of grassland and shifting cultivation than the forest in the Conservation and SDG-2030 scenario. As can be seen, all the changes of each land use type are almost linear except the type of water and flooded forest that remains stable.

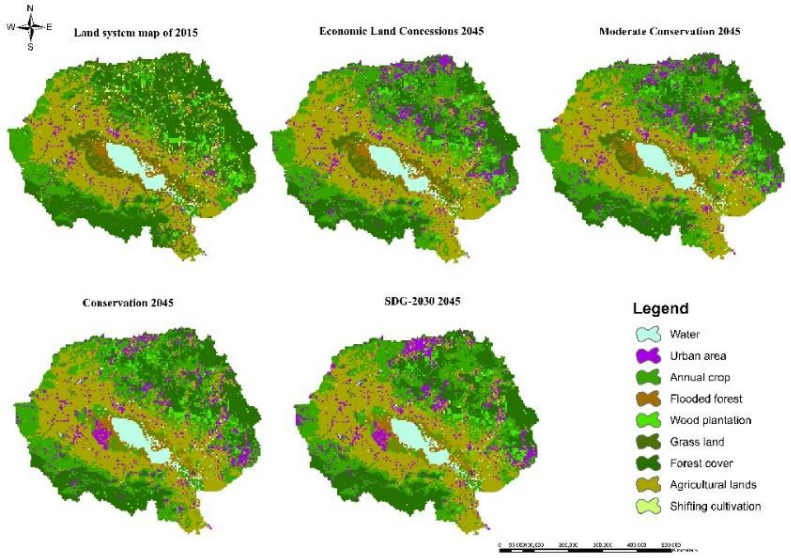

Fig. 2. Land system changes in case study under the four scenarios

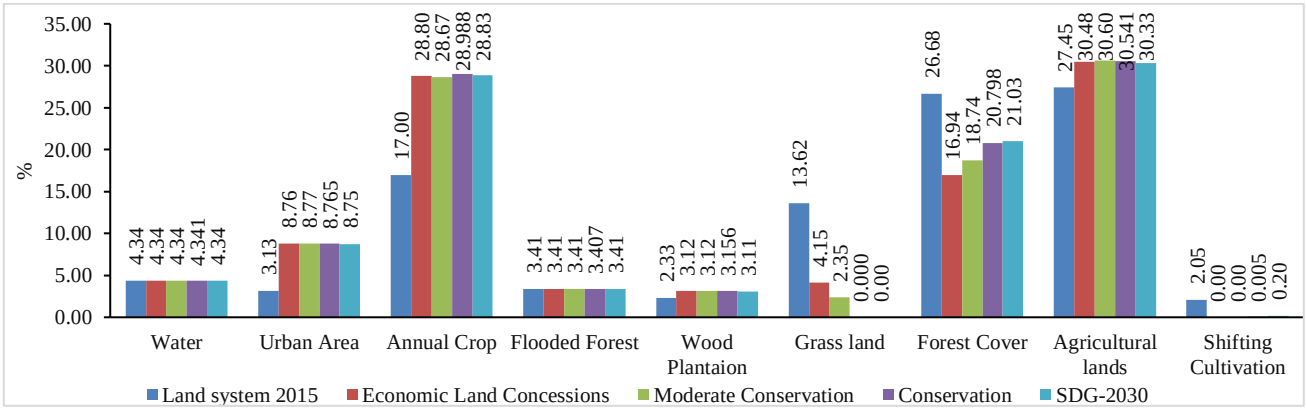

Fig. 3 The percentage of land system change from 2015 to 2045

The main reason that produces the results performing like this is that all data of scenario including cash crop production, wood production, subsistence crops production, and built-up land were defined annually by a linear increase.

IV. Conclusion

LULC change is closely related to the socio-economic development of an area and local planning and policy. In this study four scenarios, which considered multiple demands for commodities and services, representing different pathways of managing TLS's land resources, were using CLUMondo simulation demonstrated that land-use change between 2015 and 2045. The result from the analysis in CLUMondo model can serve as an indicator of the direction and magnitude of change in the future. CLUMondo tool can conveniently explore the possible patterns of multiple land-use changes under the influence of both human and natural effects. These results of land-use models are important to evaluate policy options and assess the impact of land-use change on natural and socio-economic conditions.

Acknowledgement

This work was supported by the Science and Technology Research Partnership for Sustainable Development (SATREPS), the Japan Science and Technology Agency (JST)/Japan International Cooperation Agency (JICA).

References

[1] S. Van Asselen and P. H. Verburg, "Land cover change or land-use intensification: Simulating land system change with a global-scale land change model," *Glob. Chang. Biol.*, vol. 19, no. 12, pp. 3648–3667, 2013, doi: 10.1111/gcb.12331.

[2] E. F. Lambin, H. J. Geist, and E. Lepers, " D Ynamics of L and -U Se and L and -C Over C Hange in T Ropical R Egions ," *Annu. Rev. Environ. Resour.*, vol. 28, no. 1, pp. 205–241, 2003, doi: 10.1146/annurev.energy.28.050302.105459.

[3] R. Kong *et al.*, "Understanding the drivers of deforestation and agricultural transformations in the Northwestern uplands of Cambodia," *Appl. Geogr.*, vol. 102, no. April 2018, pp. 84–98, 2019, doi: 10.1016/j.apgeog.2018.12.006.

[4] S. Chann, N. Wales, and T. Frewer, "An Investigation of Land Cover and Land Use Change in Stung Chrey Bak Catchment, Cambodia," no. 53, 2011.

[5] K. Chim, J. Tunnicliffe, A. Shamseldin, and T. Ota, "Land use change detection and prediction in upper Siem Reap River, Cambodia," *Hydrology*, vol. 6, no. 3, 2019, doi: 10.3390/hydrology6030064.

[6] T. Van Ty, K. Sunada, Y. Ichikawa, and S. Oishi, "Scenario-based Impact Assessment of Land Use/Cover and Climate Changes on Water Resources and Demand: A Case Study in the Srepok River Basin, Vietnam-Cambodia," *Water Resour. Manag.*, vol. 26, no. 5, pp. 1387–1407, 2012, doi: 10.1007/s11269-011-9964-1.

[7] C. O. Project, M. Committee, M. Committee, T. H. E. M. Project, O. F. Mekong, and R. Commission, "Learning from the lakes : IWRM implementation in Tonle Sap Lake of Cambodia and Songkhla Lake Basin of Thailand," no. August, pp. 1–89, 2013.

[8] C. Oeurng, T. A. Cochrane, S. Chung, M. G. Kondolf, T. Piman, and M. E. Arias, "Assessing climate change impacts on river flows in the Tonle Sap Lake Basin, Cambodia," *Water (Switzerland)*, vol. 11, no. 3, 2019, doi: 10.3390/w11030618.

Water Quality Mapping Using High Resolution Satellite Image Sentinel-2

Vattanakvichea NHEM[1], Sokly SIEV*[1,3,7], Rattana CHHIN[2], Porsry UNG[1,4], Hideto FUJII[5], Chihiro YOSHIMURA[6]

[1] *Faculty of Chemical and Food Engineering, Institute of Technology of Cambodia Russian Federation Blvd., P.O. Box 86, 12156 Phnom Penh, Cambodia,*
[2]*Faculty of Hydrology and Water Resource Engineering, Institute of Technology of Cambodia, Russian Federation Blvd., P.O. Box 86, 12156 Phnom Penh, Cambodia*
[3]*Water and Environmental Research Unit, Research and Innovation Center, Institute of Technology of Cambodia, Russian Federation Blvd, P.O. Box 86, 12156 Phnom Penh, Cambodia*
[4]*Department of Science, Technology & Innovation Promotion and development, National Institute of Science, Technology & Innovation, Ministry of industry, Science, Technology & Innovation*
[5]*Yamagata University, Japan*
[6]*Department of Civil and Environmental Engineering, Tokyo Institute of Technology, Tokyo, Japan*
[7]*Department of Science, Technology & Innovation Policy, General Department of Science, Technology & Innovation, Ministry of industry, Science, Technology & Innovation*

**sievsokly@yahoo.com*

Abstract

Water quality of Tonle Sap Lake have been investigated for many years. However, the applicability of high-resolution satellite images for monitoring spatial variations of water quality has not been studied. Therefore, this study aimed to explore the spatial variation based on field observation and the remote sensing as a mean of water quality mapping. Water quality including temperature, electrical conductivity (EC), total dissolved solids (TDS), salinity, and total bacteria concentration were sampled during the dry season (March 2018) at 19 points in Chhuk Tru area and statistically fitted by the reflectance of Sentinel-2's bands with the central wavelength between 665 nm to 1610 nm. As the result, the coefficient of determination (R^2) of temperature and Band 8A at 865nm was 0.83. EC (R^2= 0.80), TDS (R^2=0.79), and Salinity (R^2=0.79) were best fitted with Band 11 at 1610 nm. Total bacteria concentration in water and sediment (R^2= 0.87 and R^2= 0.55) were fitted with Band 11 at 1610 nm and band 4 at 665 nm, respectively. Those correlations are possibly due to light absorption and reflecting properties of each water quality parameter. Those results showed potential applicability of Sentinel-2 for monitoring the water quality, especially in the large area (e.g., floating village and Tonle Sap Lake) using fitted equations and reflectance bands. The output of this research may provide benefits to decision makers for water quality management in floating villages.

Keywords: *High-resolution image, Sentinel-2, Tonle Sap Lake, Water quality*

I. Introduction

Water quality is a general descriptor of water properties in terms of physical, chemical, and biological characteristics. Water quality parameters can be measured by direct sampling of water which consuming and is the only representative of a limited spatial and temporal domain [1]. Since it is difficult to define a single water quality standard to satisfy all kinds of uses and users, monitoring water quality at a local to global scale is needed [2]. In the late 1970s, satellite remote sensing for monitoring water quality was set back because of a lack of appropriate sensors such as a lack of a sufficient number of spectral bands as well as relatively low radiometric sensitivity and low spatial and temporal resolution. However, with the availability of new satellites with a higher spatial and temporal resolution like Sentinel-2, water quality retrieval and mapping from the orbit has become more reachable. Researchers showed that Sentinel-2 is not only can improve global inland water mapping but can offer useful rage information for monitoring certain water quality indicators [3]. Like, Toming et al. (2016) [4] have shown the suitability of Sentinel-2 data to map different water quality such as Chl-a, Water color, CDOM, and DOC for small inland water. But there are not many applications of high-resolution satellite image for monitoring water quality has been studied yet, especially at Tonle Sap Lake. Hence, the spatial variation base of field observation and remote sensing as a means of water quality mapping has been used to determine the best-fitted equations and reflectance bands. It is an effective tool for synoptic water and water level monitoring, water demand modelling, and water quality monitoring.

The purpose of this study is to test the suitability of Sentinel-2 data for mapping different water quality parameters, namely temperature, electrical conductivity (EC), total dissolved solids (TDS), salinity, and bacteria concentration on both water and sediment with the reflectance of Sentinel-2's bands with a central wavelength between 665nm and 1610nm.

II. Materials and Methods

2.1. Study Area

Chhuk Tru, the selected area for this study, is one of the biggest villages on the Tonle Sap Lake that has abundant in natural resource, so the local have more opportunities to develop a stable life style [5]. In this study, water samples were collected during dry season (March 7, 2018) at 19 points in Chhuk areas as shown in **Figure 1**.

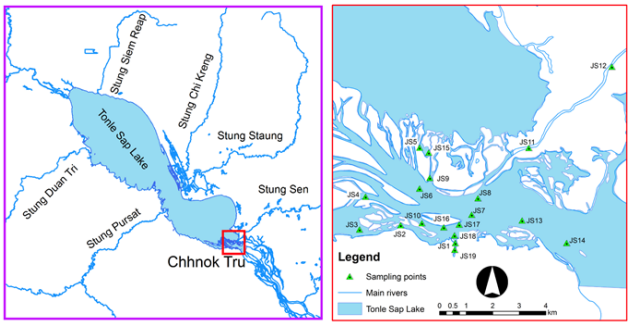

Figure 1. The Location of Chhuk Tru Area

2.2. Water quality and bacteria monitoring

A lake water sample was collected near the rear of the floating house and a storage water sample was collected from the storage tank of a floating house. The concentration of the bacteria on both water and sediment was measured following the method of previous work [6]. Water depth and other water quality such as temperature, EC, TDS, Salinity and bacteria concentration of the lake was conducted in-situ measurement using YSI EXO Water Quality Sonders [7]. Descriptive statistics have been applied to show the central to delineate the spatial distribution of important basic water quality parameters in order to tendency and variation of water quality parameters for highlighting the specific characteristics.

2.3. Relating reflectance to water quality

Image for water quality measuring were selected from a dry season (March 2018). Since it was the best period for remote sensing of water quality in Chhuk Tru area. Sentinel-2 image were available on 07 March 2018. The 19 sampling points was conducted surrounding the Chhuk Tru floating villages. The cloud coverage can cause misleading results in the analyses of surface and atmospheric parameter [9]. The downloaded Sentinel-2 image from was treated to mask the cloud cover by thresholding the reflectance band. In order to extract and map the water line, the Normalized Difference Water Index (NDWI) was applied on the image, then water bodies can be mapped. The correlation and regression analysis technique have been used in order to investigate and study the relationship between water quality parameters and the bands of Sentinel-2 by light absorption and reflectance of each parameters. The regression analysis develops the mathematical equation which express each relation. The R^2 equation can be expressed as the following:

$$R^2 = 1 - \frac{\sum_i (y_i - \hat{y}_i)^2}{\sum_i (y_i - \bar{y}_i)^2} \qquad \text{(Eq 1.)}$$

Where y_i is actual observation, $\bar{y}_i$ is mean of actual observation and $\hat{y}_i$ is predicted observation.

The height of the reflectance peak around 820nm has been used for capturing the temperature of the water from 30°C to 35°C [8]. Therefore, Band 8A was chosen to capture the image for estimating the temperature of the water in Chhnuk Tru areas. In the other hand, Band 11 was used

for capture the image for EC, TDS, and Salinity at 1610nm. The image of bacteria concentration in water was capture by band 11 which is the same as other parameters. But, for bacteria concentration in sediment with the high spatial resolution 10m and wavelength 665nm, band 4 was used to mature the image for monitoring bacteria concentration in sediment. By reflectance measurement and in-situ measurement, it gives the suitable values from water quality parameter and its reflectance.

III. Results and Discussion

3.1. Temperature

Daily temperature at TSL about 20℃ and 36℃ in dry season that the weather is influence by monsoon. In this study, the temperature of water was around 30 to 31℃ **(Figure 2)** with the coefficient of determination R^2= 0.83 (**Figure 3**), while the highest temperature from those 19 points was around 34℃.

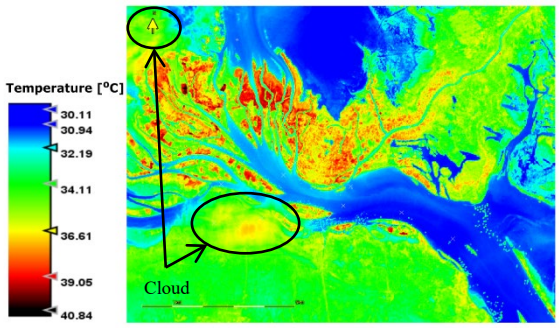

Figure 2. Map of Temperature

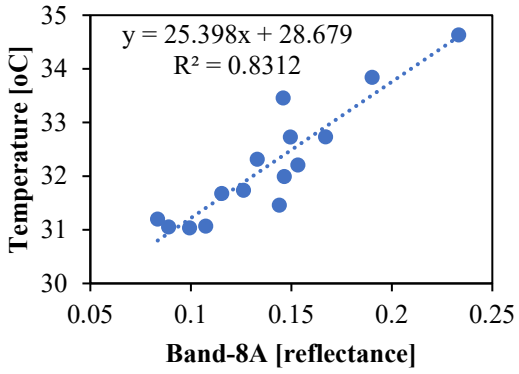

Figure 3. Correlation between Temperature and B8A reflectance

3.2. Conductivity, Total dissolved solid and Salinity

Electrical conductivity is the measure of water capacity to conduct electrical current. It illustrated significant correlation with TDS and Salinity. Band 11 was used for analyzing the data of EC, TDS and salinity. The spatial distribution of water that is used to estimate those parameters are generally increase from solid surface to water surface. As a result, EC value was around 100µS/cm, TDS was around 50mg/L and Salinity was 0.025psu with R^2= 0.80, R^2=0.79 and R^2=0.79 (**Table 1**), respectively. Band 11, with the wavelength 1610nm (SWIR), give the best potential for salinity detection and discrimination [10] the same for electrical conductivity and total dissolve solid. Since the bands found in SWIR were associate with information related to salt content differences.

3.3. Bacteria concentration

For bacteria concentration, two different bands were used to determine the bacteria concentration. Band 11 was used to analyze bacteria concentration in water and Band 4 was used for estimating sediment. The mean value of bacteria concentration in water and sediment was around 70.37 CFU and 1075 CFU with R^2= 0.87 and R^2= 0.55, respectively as shown in **Table 1.** bacteria concentration in sediment, Band 4 (Visible) is needed for monitoring it because the sediment in suspension present in the bodies of water are visibly seen by their coloring, which are varies depending on the concentration of sediments from dark brown to yellowish green. The correlation of between sedimentary bacteria and B-4 reflectance is very low due to the cause of turbidity in the low water depth. Since turbidity is a measured of the cloudiness in water.

Table 1. Parameter of water quality, types of bands value range and R^2

Parameter	Types of Bands	Value range	R^2
Temperature	B8A	31-34℃	0.83
EC	B11	47-735 µS/cm	0.80
TDS	B11	27-408 mg/L	0.79
Salinity	B11	0.02-0.3 psu	0.79
Bac-wat	B11	5.19-467-86	0.87
Bac-sed	B4	0-0.0041	0.55

The results of this study were suitable compare to other study, in term of correlation from the reflecting properties of each parameters. except the bacteria concentration in sediment. due to the reflecting value is bigger than other parameters. It is also give the possible to measuring another water quality parameter such as turbidity an Chlorophyll a via Sentinel-2 since it is also related to the water quality parameters that we already study.

	Temperature	EC	TDS	Salinity	Bac_wat	Bac_sed
Temperature	1	0.38	0.39	0.38	0.47	0.3
EC	0.38	1	1	1	0.96	0
TDS	0.39	1	1	1	0.96	0.01
Salinity	0.38	1	1	1	0.96	0
Bac_wat	0.47	0.96	0.96	0.96	1	0.04
Bac_sed	0.3	0	0.01	0	0.04	1

Figure 4. The coefficient of correlation (R) between water quality parameters

The corresponding goodness of fit statistical parameters of the water quality is shown in **Figure 4** The correspondence between Temperature and other parameters is not good with R between 0.3 to 0.47 since the difference band of Sentinel-2 was used. But it gives the best fit between EC, TDS, Salinity, and Bac-wat because these parameters using the same Sentinel-2 bands. While the coefficient of correlation (R) between the Bac-sed and other parameters is too low which is close to zero.

IV. Conclusion

Satellite sensing technology has been developed over the past few decades that make it possible for experts in monitoring the large area on the earth. Those results have shown that the mean value from the raster data gave a better correlation with the reflectance from the bands, but there are some errors from reflectance due to the cloudiness around that area during the study. Furthermore, besides the promising technical feature of sentinel-2, it is worth monitoring the public availability of its imagery. It has a wide range of useful application in monitoring water quality, yet still there is room for improvement.

Acknowledgement

We are thankful to the Science and Technology Research Partnership for Sustainable Development (SATREPS), the Japan Science and Technology Agency (JST)/Japan International Cooperation Agency (JICA) for their financial support. (Grant No: JPMJSA1503)

References

[1] Salama, M., Radwan, M. and van der Velde, R., 2012. A hydro-optical model for deriving water quality variables from satellite images (HydroSat): A case study of the Nile River demonstrating the future Sentinel-2 capabilities. *Physics and Chemistry of the Earth*, 50(52), pp.224-232.

[2] Ritchie, J., Zimba, P. and Everitt, J., 2003. Remote Sensing Techniques to Assess Water Quality. *Photogrammetric Engineering & Remote Sensing*, 69(6), pp.695-704.

[3] Saberioon, M., Brom, J., Nedbal, V., Souček, P. and Císar, P., 2020. Chlorophyll-a and total suspended solids retrieval and mapping using Sentinel-2A and machine learning for inland waters. *Ecological Indicators*, 113, pp.1-11.

[4] Toming, K., Kutser, T., Laas, A., Sepp, M., Paavel, B. and Nõges, T., 2016. First Experiences in Mapping Lake Water Quality Parameters with Sentinel-2 MSI Imagery. *Remote Sensing*, 8(8), p.640.

[5]. Weber, E., 2020. *MEKONG RIVER EXPERIENCE*. [online] Travel-inspirations.lu. Available at: https://travel-inspirations.lu/fr/inspiration/60. Accessed 26 October 2020.

[6] Ung, P., Un, S., Chheun, S., Aun, S., Penh, S., Sann, S., Tan, R., Miyanaga, K. and Tanji, Y., 2018. Analysis of Total Bacterial Concentration and Microbial Community in Waters Used by Floating Villagers, Tonle Sap Lake. In: *ENHANCING SUSTAINABILITY AND RESILIENCE UNDER ANTHROPOGENIC PRESSURE AND CLIMATE CHANGE*. Phnom Penh: Porsry Ung, pp.320-324.

[7] Kaing, V., Sok, T., Ich, I., Oeurng, C., Song, L., Siev, S., Uk, S., Mong, M., Hak, D., Khanal, R. and Chihiro, Y., 2018. In: *ENHANCING SUSTAINABILITY AND RESILIENCE UNDER ANTHROPOGENIC PRESSURE AND CLIMATE CHANGE*. Phnom Penh: Vinhteang Kaing, pp.303-306.

[8]. Rizwan Salwwm, M., Honkanen, S. and Turunen, J., 2012. Partially athermalized waveguide gratings. *Proceedings of SPIE*, 8428(17), pp.1-9.

[9]. Coluzzi, R., Imbrenda, V., Lanfredi, M. and Simoniello, T., 2018. A first assessment of the Sentinel-2 Level 1-C cloud mask product to support informed surface analyses. *Remote Sensing of Environment*, 217, pp.426-443.

[10]. Bannari, A., El-Battay, A., Bannari, R. and Rhinane, H., 2018. Sentinel-MSI VNIR and SWIR Bands Sensitivity Analysis for Soil Salinity Discrimination in an Arid Landscape. *Remote Sensing*, 10(6), p.855

The 13th AUN/SEED-Net Regional Conference on Chemical Engineering 2020 (RCChE-2020)
Jointly held with
The 5th International Symposium on Conservation and Management of Tropical Lakes
"Insights and Challenges toward Achieving SDGs"

Optimization of Electrocoagulation Reactor Integrated Sedimentation for Turbidity and Color Removal from Industrial Wastewater

Sreynich Pang [1], Sreyla Vet [1], Penghour Hong [1], Pisut Painmanakul [2] and Saret Bun [1,*]

[1] *Water and Environmental Engineering, Faculty of Hydrology and Water Resources Engineering, Institute of Technology of Cambodia, Phnom Penh 12156, Cambodia*
[2] *Department of Environmental Engineering, Faculty of Engineering, Chulalongkorn University, Bangkok 10330, Thailand*
* *Corresponding author: saret@itc.edu.kh*

Abstract

This study aimed to optimize electrode configuration and operation condition of electrocoagulation reactor for removing color and turbidity from synthetic textile wastewater. The experiment was firstly conducted in the small batch column for investigating the performance of different electrode types, arrangements, gaps, and current density. The result showed that the arrangement of electrodes as monopolar and bipolar with 1.5 cm inner gap and 1.5 mA/cm^2 current density provided the optimal performance in terms of gas flow and electrode loss. Monopolar was found as optimum level in terms of energy consumption while comparable treatment efficiency was observed. Hence, the experiments for color and turbidity removal kinetic under optimal condition were conducted for defining the sufficient hydraulic retention time and overflow rate of continues electrocoagulation reactor integrated sedimentation. Bentonite and reactive dye were used for preparing turbidity and color wastewater, respectively. To archive 95% removal efficiency of both pollutants, the detention time about 25 to 30 minutes using 4.5 mA/cm^2 current density are required. Plus, overflow rate 2.1 m/hr was found as the effective condition for gravity settling to design sedimentation compartment. Therefore, integrated system in continues operation was constructed as semi-industrial scale, 141 litters, for performance evaluation study. Approximate 95% and 97% removal efficiency of both pollutants was obtained under the optimal condition found (13.5 mA/cm^2 current density) with liquid flow rate 3 and 1 L/min, respectively. However, 2 L/min was found as the optimum liquid flow for simultaneous removal of both pollutants.

Keywords: *Color, Electrocoagulation, Industrial wastewater, Turbidity*

I. Introduction

As the increasing of industrial sector, amount of wastewater enter to the water body has risen. Most of the industrial wastewater effluence contains high amount of color and turbidity. Discharge untreated wastewaters from industries are the main source of adding substantial coloration to water. A highly colored water could not sustain aquatic life, which could lead to the long-term impairment of the ecosystem. Therefore, removal of turbidity and color from wastewater are occasionally required.

Various technologies have been employed for dye effluent treatment including conventional biological processes (aerobic and anaerobic), coagulation, and adsorption [1]. Since the effluence contains toxic dyes in nature as mentioned, it may also impact on the bacteria development in biological process. Furthermore, chemical

coagulation requires an addition of chemicals, which leads to generate huge quantity of sludge.

Electrocoagulation (EC) process has been interested for studying with different types of effluents from the industries. EC has been employed successfully for the reduction dyes using a direct current source between metal or aluminum electrodes immersed in polluted water. It has the capacity to treat wastewater more efficient comparing to conventional coagulant, about 10 – 15% [2]. This study aims to develop and evaluate the electrocoagulation reactor combining both EC and sedimentation units in terms of design criteria and operation condition in batch and continue modes for color and turbidity removal from wastewater of textile industry.

II. Materials and Methods

2.1. Experimental set-up

Batch column was constructed from clear acrylic material in cylinder shape with 3 cm-diameter for containing 4 litters of water sample, as illustrated in **Fig. 1**. At the bottom, it was connected to the drainage port for discharging the sludge and sample after conducting the experiments. The electrode plates (20 cm × 5 cm × 0.2 cm) were installed in the reactor and connected to the direct current (DC) generator for supplying the current. Aluminum electrode plates were used in this study. At the top, an acrylic cap was covered for collecting the generated gas from the system to the soap film meter. Tap water was firstly used as liquid phase at room temperature (25 ± 3°C) for optimization study of EC configuration and operation condition.

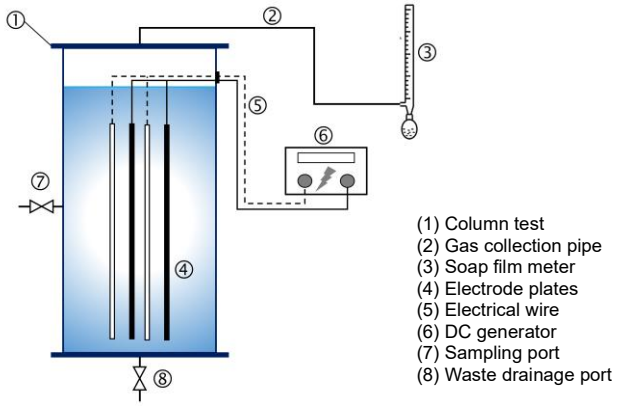

Fig. 1. Experimental set-up in batch column reactor

2.2. Synthetic wastewater

To synthesize turbidity and color wastewater, bentonite and reactive dye were prepared with tap water. For synthetic turbidity, bentonite was rapidly mixed with water at 300 rpm for 5 minutes, followed by slow mixing at 40 rpm for 30 minutes, and let it settle down 35 minutes. Moreover, synthetic color wastewater was prepared by dissolving the reactive dye in tap water for 5 minutes with 300 rpm.

2.3. Electrode optimization

Configuration and operation condition of electrodes were initially investigated to define the optimum condition in the batch column experiment in terms of generated gas flow and electrode corrosive loss ratio (Qg/E_{loss}). Generated gas flow (Qg) was directly measured using soap film meter captured from the reactor cap covering (see **Fig. 1**). It can be estimated by using **Eq. (1)**, where Qg is gas flow rate [mL/s], $\Delta V = V_2 - V_1$ is the different volume of gas (mL), and $\Delta t = t_2 - t_1$ is the different time of gas moved (sec.). Electrode loss (E_{loss}) presented in percentage was defined the different weights of electrode used before and after the experimental work, as expressed in **Eq. (2)**. Electrode configuration and operation condition parameters included electrode gap (1 – 2 cm), electrode arrangement (monopolar and bipolar), and current density (1.5 – 2.5 mA/cm^2). The initial turbidity and color concentration in this part were 250 NTU and 6,000 ADMI, respectively.

$$Q_g = \frac{\Delta V}{\Delta t} \quad \text{(Eq.1)}$$

$$E_{loss} = \frac{\text{initial weight - final weight}}{\text{initial weight}} \quad \text{(Eq.2)}$$

2.4. Settling column test

Setting test was examined in batch column to determine the over flow rate (OFR) as the design criteria of settling performance for design the sedimentation tank as the separation process after the EC treatment. This sedimentation experiment was conducted within 100 minutes with 4 ports, i.e., 13, 18, 23, and 28 cm, from the water surface for water sampling. The initial concentration of turbidity and color prepared for this part were 250 NTU and 6,000 ADMI, respectively.

III. Results and Discussion

3.1. Optimize EC configuration and operation condition

This part aimed to optimize the electrocoagulation condition including electrode configuration, arrangement,

and current density. Electrode configuration, i.e., gap, arrangement, and current density, was initially investigated in terms of Qg/E_{loss}. It was investigated between monopolar and bipolar, inner electrode gap (1.0 – 2.5 cm), and current density (1.5 – 2.5 mA/cm^2). It was found that the optimum electrode in monopolar and bipolar arrangement were 1.5 mA/cm^2 of current density with 1.5 cm and 2 cm of electrode gap, respectively (data not shown). These conditions were therefore used to conduct under synthetic wastewater of 250 NTU turbidity and 6,000 ADMI color.

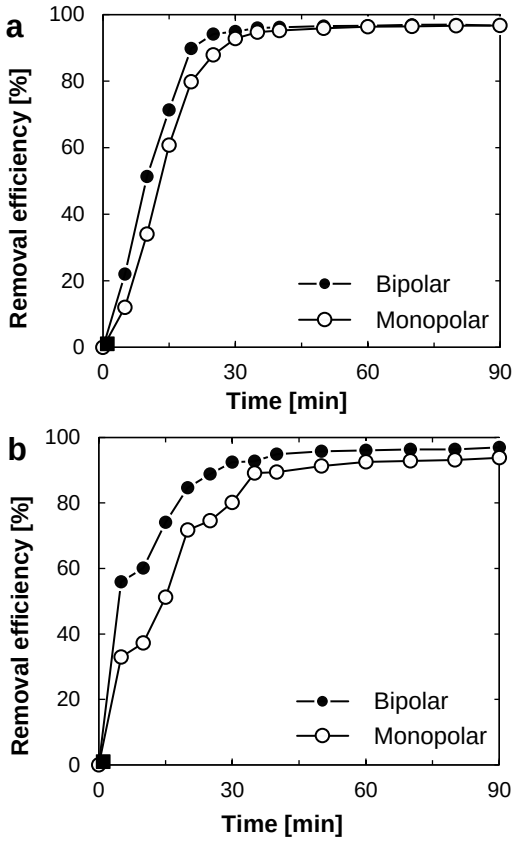

Fig. 2. Removal efficiency under optimum condition and electrode arrangements for: (a) turbidity, and (b) color

The result was shown in **Fig. 2**. Bipolar connection consumed high voltage than monopolar one to increase temperature for promoting electrode plate to generate more coagulants and gas bubble at the early stage. However, a similar performance was observed at the stable stage. At 35 minutes treatment time, monopolar could remove turbidity and color up to 95 % and 89%, respectively; while bipolar could treat up to 96% and 93% for respective turbidity and dye. Since the treatment performance of both electrode arrangement were comparable, other evaluation factor, treatment cost, was used to select the optimum one. Based on the energy consumption estimation, bipolar required approximate $US 0.31 to remove one kilogram of dye from 1 m^3 of wastewater, while $US 0.05 was paid by using monopolar electrode. Hence, aluminum electrode in monopolar arrangement with 1.5 cm gap was selected as the economize condition in terms of turbidity and color removal. Therefore, it will be designed for investigating under different current density.

Current density plays an important role in EC process. In this study, it was then varied in 5 levels, i.e., 1.5, 2.5, 3.5, 4.5, and 5.5 mA/cm^2 for turbidity and color removal from wastewater. The result showed that the current density of 4.5 mA/cm^2 was the optimal condition and the operation time of steady stage was 30 minutes for both turbidity and color removal (data not shown).

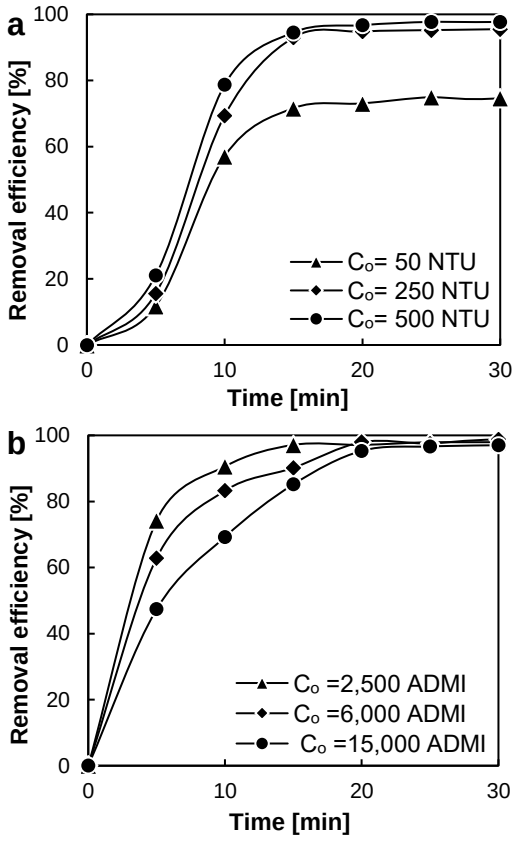

Fig. 3. Removal kinetic at different initial concentration of: (a) turbidity, and (b) color

3.2. Turbidity and color removal kinetic

Effect of different initial concentrations on the treatment

performance was kinetically studied in this part. The initial turbidity and color concentrations were examined in range of 50 to 500 NTU, and 2,500 to 15,000 ADMI, respectively. The result was shown in **Fig. 3**. Initial concentration of 50 NTU needed electrolysis time about 25 minutes to dissolve aluminum ion to improve the lag stage until reaching the stable stage, which provided removal efficiency around 75%. For 250 NTU and 500 NTU, it was required electrolysis time only 20 minutes with removal efficiency 96% and 98%, respectively (see **Fig. 3 (a)**). Low concentration of color consumed less electrolysis time and provided higher treatment efficiency than the high concentration at lag stage. At stable stage, removal efficiency of three initial concentrations were very similar, 98% ± 1% after 20 minutes (see **Fig. 3 (b)**).

3.3. Settling performance

Settling test was studied in a batch column containing 4-litter sample with 33-cm height. Four sampling ports, 13, 18, 23, and 28 cm from water surface, were designed for samples collection. It was investigated after operating EC of optimum condition previously found with 250 NTU and 6,000 ADMI as initial concentrations. The results showed that 2.1 and 1.7 m/hr of overflow rate (OFR) can separate turbidity (~ 87%) and color (~ 90%), respectively (data not shown). This finding will be used as the design criteria of the settling separation process.

3.4. Performance of ECR integrated sedimentation

Based on the result separately found, each design criteria were used for constructing the new ECR, which was included EC (4 units of EC) and separation compartments. The experiment was conducted for individual pollutants with 13.5 mA/cm^2. Under initial concentration 250 NTU and 6,000 ADMI, turbidity and color can be removed to less than 20 NTU and 300 ADMI after using liquid flow 3 and 1 L/min, respectively (data not shown).

Then, a simultaneous removal of both pollutants was conducted to define the optimum liquid flow. Under 3 L/min flow, color cannot be completely removed to the target level, 300 ADMI (data not shown). The simultaneous removal under the flow 2 L/min was conducted and the result was shown in **Fig. 4**. Removal efficiency was reached to 90% for both turbidity and color after 60 minutes operation as the stable stage. At 150 minutes, color removal reaches 97%, (residual color 213 ADMI), and 94% removal efficiency for turbidity (residual turbidity 14.2 NTU). It can be explained that after decreasing the liquid flow to 2 L/min, the removal efficiency increased due to the higher hydraulic retention time allowing the coagulant and particles attached to each other to form floc for settle down.

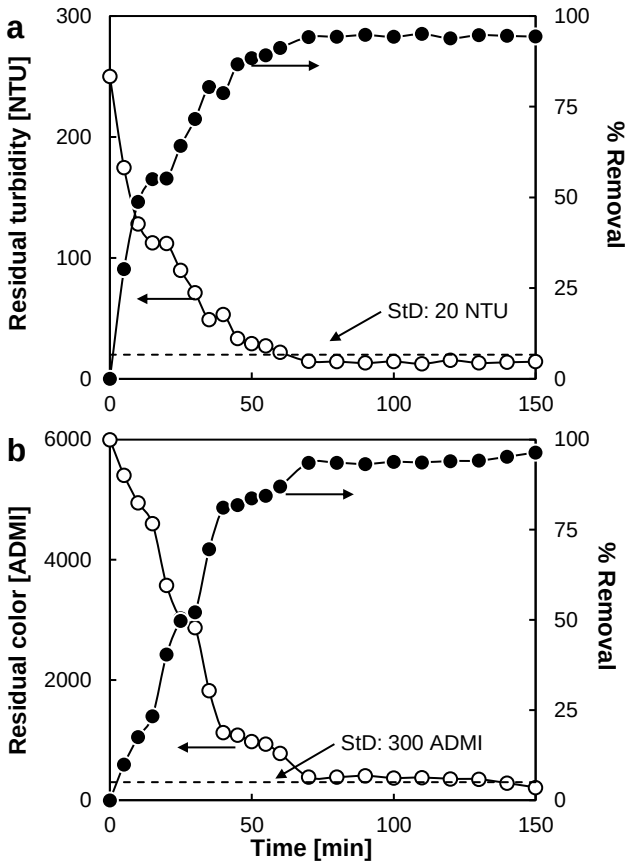

Fig. 4. Treatment performance in continuous EC integrated sedimentation (2 L/min) for: (a) turbidity, and (b) color

IV. Conclusion

The objective of the present study is to optimize the electrode configuration and operation condition of electrocoagulation reactor integrated sedimentation for removing color and turbidity from synthetic textile wastewater. In order to confirm the effect of the new reactor design, several parameters in batch and continue reactor was evaluated. It was firstly examined in a small batch column for different electrode types, arrangements, gaps, and current density. Monopolar with 1.5 cm inner gap and 1.5 mA/cm^2 current density was found as the optimum condition in terms of Qg/E_{loss} ratio and energy consumption, while monopolar and bipolar resulted comparable treatment performance. Therefore, color and turbidity removal kinetic under optimal

condition were conducted for defining the sufficient hydraulic retention time and overflow rate of continues ECR integrated sedimentation. Approximate 95% removal efficiency was obtained under the detention time about 25 to 30 minutes using 4.5 mA/cm^2 current density. Moreover, 2.1 m/hr of overflow rate was found as the effective condition for gravity settling to design sedimentation compartment. Integrated system in continues operation was constructed to evaluate treatment performance. A simultaneous removal of turbidity and color can be completely removed to be lower than effluent wastewater standard under the optimum condition found with 13.5 mA/cm^2 current density with 2 L/min liquid flow.

Acknowledgement

Authors acknowledges Project for Strengthening Engineering Education and Research for Industrial Development in Cambodia of JICA through LBE Research Grant for financial support.

References

[1] Verma, A., Bhunia, P., and Dash, R., 2014. Reclamation of wastewater using composite coagulants: A sustainable solution to the textile industries. *Chem. Eng. Trans*. 42, 175-180.

[2] Zaleschi, L., Teodosiu, C., Cretescu, I., Rodrigo, M. A., 2012. A comparative study of electrocoagulation and chemical coagulation processes applied for wastewater treatment. *Environmental Engineering & Management Journal*. 11(8).

The 13th AUN/SEED-Net Regional Conference on Chemical Engineering 2020 (RCChE-2020)
Jointly held with
The 5th International Symposium on Conservation and Management of Tropical Lakes
"Insights and Challenges toward Achieving SDGs"

Biodegradation of Perfluorooctanesulfonate (PFOS) and Perfluorooctanoic Acid (PFOA) by Acclimated Sludge

Sovannlaksmy Sorn [1], Hiroe Hara-Yamamura [2] and Ryo Honda [2,*]

[1] *School of Natural Science and Technology, Kanazawa University, Kakuma-machi, Kanazawa City, Ishikawa Prefecture 920-1192, Japan*
[2] *Faculty of Geosciences and Civil Engineering, Kanazawa University, Kakuma-machi, Kanazawa City, Ishikawa Prefecture 920-1192, Japan*
* *Corresponding author: rhonda@se.kanazawa-u.ac.jp*

Abstract

Perfluorooctanesulfonate (PFOS) and Perfluorooctanoic acid (PFOA) have been strictly regulated due to their high bioaccumulation and potential toxicity to human health. PFOS and PFOA are commonly found in the environment; however, knowledge of biodegradation of PFOS and PFOA is still limited. The aim of this research is to investigate PFOS and PFOA biodegradability using environmental microbes from acclimated sludges. The return sludge from a local wastewater treatment plant was cultured in synthetic wastewater with a stepwise increase of PFOS or PFOA dose at 0, 5, 10, 20 µg/L in every 5 days under aerobic condition. After 20-days, acclimated sludge with each concentration of PFOS or PFOA were utilized as inoculum in Kirk liquid media for batch biodegradation experiment. The mixture of 20 µg/L PFOS and 20 µg/L PFOA was spiked in glass vials with a rubber stopper and seal crimp in triplication. These vials were then incubated at 30°C under orbital shaking at 170-180 rpm and their headspaces were replaced with ambient air every 2-4 days to supply oxygen. Liquid samples were taken after 6 hours, and days 1, 2, 7. PFOS and PFOA were measured by LC-MS/MS after solid phase extraction. With PFOS-acclimated sludge, PFOS was decomposed approximately 40% after 7 days of incubation. On the contrary, significant biodegradation was not observed for PFOA with PFOA- nor PFOS-acclimated sludges. Thus, this study could contribute to the biodegradation of PFOS using microbial communities derived from wastewater sludge.

Keywords: *Bioremediation, LC-MS/MS, Perfluoroalkyl and Polyfluoroalkyl substances (PFASs), Perfluorooctanoic acid (PFOA), Perfluorooctanesulfonate (PFOS)*

I. Introduction

Perfluoroalkyl and Polyfluoroalkyl substances (PFASs) are a large group of synthetic substances with more than 5000 subclasses. PFASs have a great ability to repel fire, water, oil, and stains. Therefore, they are widely used in variety of products such as the stain and water resistance fabrics, nonstick pans, protecting sprays, firefighting foams, food packaging materials, cleaning products and so on. Possessed the stable chemistry, PFASs are very persistent and hard to biodegrade in environment. PFASs have potential toxic to human health after exposure to contaminated water, agricultural and aquacultural products. They accumulated long term in human bodies and frequently detected in blood serum of human, wildlife nearby contaminated sites. Therefore, PFASs were regulated in several countries. The US Environmental Protection Agency

(EPA) has set the safety consumption dose in drinking water up to 70 ppt and banned PFASs production since 2000s [1]. However, the legacy of PFASs still existed in environment these days.

PFASs have been commonly detected as high concentration in wastewater treatment plants, industrial producing or using PFASs, and firefighter training sites [2]. PFASs are hardly to remove using existed treatment technologies, therefore; residue of PFASs have still found in downstream even at low concentrations. The US reported the median of total 17 PFASs in source of water is 21.4 ng/L, and 19.5 ng/L in treated drinking water [3]. PFASs were also reported in drinking water and bottle waters at range of 116-140ng/L according to an assessment of PFASs in Brazil, France, and Spain [4]. Regarding the numbers of survey by French Overseas Territories, PFOS and PFOA were founded as the most frequently existed compounds in surface water [5].

Previous studies have shown their great efforts on PFASs remediation using various technologies in both physical and chemical approaches such as absorption, photocatalytic, electrochemical oxidation, and reverse osmosis [6]. These treatment technologies have limitations for their application on high operational cost and may also produce perfluorocarbons wastes (PFCs). The PFCs waste are potentially more harmful to health and even more persistence in future.

Microbial approach for remediation is a key to eliminate the harmful pollutants from environment. It has gained the interest of researchers to combat PFASs in the last decades. PFASs degradable microbes enriched from environmental samples have been applied as one of affordable bioremediation treatment technologies. Previously, loam soil from an agronomy farm was used as microcosms on 8:2 Fluorotelomer Stearate Monoester biodegradation [7], aerobic and anaerobic river sediment also performed for 6:2 fluorotelomer sulfonate treatment [8], and marine sediment from False Creek used for N-Ethyl Perfluorooctane Sulfonamido Ethanol (EtFOSE) and EtFOSE-Based Phosphate biodegradation [9]. Lab scale acclimation has also been performed to enrich biodegrading bacteria strain from soil samples, and Pseudomonas parafulva was reported as PFOA-degrading bacteria strain [10]. Some studies draw their attention on pure culture isolation which were isolated from PFASs contaminated environment that commonly known as potential inoculum sources for stronger degradability microbial cultivation. Groundwater and soil samples from Aqueous film forming foam utilized sites were employed as seeding for fungi isolation by American research group to degrade 6:2 FTOH [11]. PFOS degradable Pseudomonas aeruginosa strain was enriched from activated sludge of PFCs contaminated municipal wastewater treatment plants in Korea [12]. These studies suggested the potential of enrichment and isolation PFASs degradable microbes from historically PFASs contaminated sites and effectiveness of acclimation processes. It also reflected the development on bioremediation technologies that are expected to increase the efficiency of treatment PFAS in real polluted environment. The aim of this research is to investigate PFOS and PFOA biodegradability using environmental microbes from acclimated sludges.

II. Materials and Methods

2.1. Sludge acclimatation

The return sludge was taken from a local wastewater treatment plant and used as inoculum. It was cultured in synthetic wastewater by ratio 1:2 which prepared according to OECD recipe [13]. New synthetic wastewater has been replacing every 2-3 days with stepwise increase of PFOS or PFOA dose at 0, 5, 10, 20 μg/L in every 5 days under aerobic condition.

2.2. Batch biodegradation experiment

After 20-days, sludge acclimatized with each of PFOS and PFOA, and non-acclimated sludge were utilized as inoculum in Kirk liquid media as described by Ramírez and co-workers [14] for batch biodegradation experiment. Deactivated sludge by autoclaving non-acclimated sludge has also been examined to reveal the sludge absorption of PFOS and PFOA. A mixture of 20 μg/L PFOS and 20 μg/L PFOA was spiked in 50 mL glass vials with a rubber stopper and seal crimp in triplication. These vials were then incubated at 30°C under orbital shaking at 170-180 rpm and their headspaces were replaced with ambient air every 2-4 days to supply oxygen.

Mix liquor in each glass vial was transferred into a sterile 50 mL polypropylene (PP) centrifuge tubes after 6 hours and days 1, 2, 7. The samples were centrifuged at 13,000 ×g for 5 min to separate supernatant and pallet. Then, the used glass vials, and sludge have been rinsed using Phosphate-buffered saline to collect all attachment PFOS and PFOA. After rinsing, all liquid samples were collected at final volume 40 mL and stored at 4°C till extraction.

2.4. Analytical determination of PFOS and PFOA

Each liquid sample was spiked with 50 µL of isotopically labeled 1 mg/L $^{13}C_4$-PFOS and 1 mg/L $^{13}C_4$-PFOA standards. PFOS and PFOA were enriched on Oasis WAX (150mg, 6cc) cartridge (Waters, U.S.A.) according to manufacturer's instruction [15]. Briefly, sample was the cartridges were preconditioned by 4 mL of 0.1% ammonia/methanol, 4 mL of methanol and 4 mL of Milli Q water. Samples were loaded at the frow rate of 5 ml/min or slower, and washed with 4 mL of ammonium acetate buffer. Subsequently, the cartridges were dried under vacuum for 2 min before elution into 15 mL PP conical tubes using 4 mL of methanol and 4 mL of 0.1% ammonia/methanol. The eluent was evaporated to dryness under gentle nitrogen stream at temperature 40°C. The extracts were reconstituted in 0.5 mL of 50% methanol and Milli Q water before being transferred to PP vial for LC-MS/MS analysis.

PFOS and PFOA were analyzed on a Nexera X2 HPLC (Shimadzu, Japan) using a 2.1×100 mm Inertsil ODS-4 column (3µm) (GL Science, Japan) coupled to a Sciex 3200 triple quadruple spectrometer in multiple reaction monitoring and negative electrospray ionization mode. 5 µL of extracts were injected via an autosampler and eluted with 50% of 10 mM ammonium acetate and 50 % of acetonitrile as mobile phase. The flow rare was set at 0.2 mL/min.

III. Results and Discussion

3.1. PFOS biodegradation

The trend of the PFOS biodegradation experiments performed with non-acclimated sludge (AS), deactivated sludge (AS), PFOS acclimated sludge (PFOS-AS), and PFOA acclimated sludge (PFOA-AS) is shown in **Fig.1**. PFOS concentration is gradually decreased after incubation 2 days about 20%, and successively up to 40% after 7 days in PFOS-AS and followed by AS, however, no significant degradation observed under PFOA-AS condition. This result suggested that PFOS is degradable using microbial communities in PFOS-AS or AS even at low concentration, but not PFOA-AS. Moreover, there is no significant decrease observed under DS tested. The complete sterilization of the control could be responsible for the conclusive biodegradation in PFOS-acclimated test. Thus, it indicated that PFOS biodegradation using acclimated sludge can be effective at low dose and short degradation time, compared to previous studies [7,8,9].

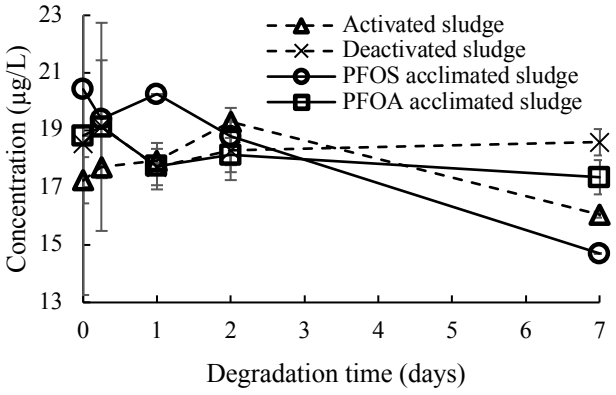

Fig. 1. Biodegradation of PFOS using non acclimated sludge, deactivated sludge, PFOS-acclimated sludge and PFOA acclimated sludge.

Results of the experiments set up under four different types of sludge conditions are presented in **Fig.2**. None of the tested conditions showed a significant decrease in the concentration of PFOA during experiment 7 days. Thus, microbial communities in PFOA-AS are likely unable to degrade PFOA nor PFOS. These results supported the highly tolerant nature of PFOA in microbial communities derived from wastewater sludge. At the same time, it indicated that microbial profile in PFOS-AS might differ to PFOA-AS.

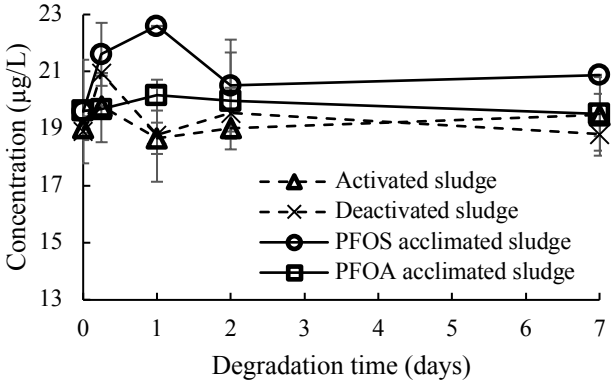

Fig. 2. Biodegradation of PFOA using non acclimated sludge, deactivated sludge, PFOS-acclimated sludge and PFOA acclimated sludge.

IV. Conclusion

This study showed the biodegradability of PFOS by PFOS-acclimated sludge. It was found that the decomposition was approximately 40% after 7 days of incubation. On the contrary, significant biodegradation was

not observed for PFOA with PFOA-AS nor PFOS-AS. Thus, this study could contribute to the biodegradation of PFOS using microbial communities derived from wastewater sludge. Further study should be focused on microbial community with high degradation capacity acclimated sludge by 16S rRNA sequencing.

Acknowledgement

We are thankful to Prof. Shaily Mahendra of Department of Civil and Environmental Engineering, University of California in Los Angeles for her experiences on this field of research on bioremediation and documentary supports.

References

[1] EPA, 2017. Technical Fact Sheet- Perfluorooctane Sulfonate (PFOS) and Perfluorooctanoic acid (PFOA).

[2] Dauchy, X., 2019. Per- and polyfluoroalkyl substances (PFASs) in drinking water: Current state of the science. *Current Opinion in Environmental Science & Health*, 7, 8–12.

[3] Boone, J. S., Vigo, C., Boone, T., Byrne, C., Ferrario, J., Benson, R., Donohue, J., Simmons, J. E., Kolpin, D. W., Furlong, E. T., & Glassmeyer, S. T., 2019. Per- and polyfluoroalkyl substances in source and treated drinking waters of the United States. *Science of the Total Environment*, 653, 359–369.

[4] Schwanz, T. G., Llorca, M., Farré, M., & Barceló, D., 2016. Perfluoroalkyl substances assessment in drinking waters from Brazil, France and Spain. *Science of the Total Environment*, 539, 143–152.

[5] Munoz, G., Labadie, P., Botta, F., Lestremau, F., Lopez, B., Geneste, E., Pardon, P., Dévier, M. H., & Budzinski, H., 2017. Occurrence survey and spatial distribution of perfluoroalkyl and polyfluoroalkyl surfactants in groundwater, surface water, and sediments from tropical environments. *Science of the Total Environment*, 607–608, 243–252.

[6] Kucharzyk, K.H., Darlington, R., Benotti, M., Deeb, R., Hawley, E., 2017. Novel treatment technologies for PFAS compounds: A critical review. *Environmental Management*, 204 (2),757-764.

[7] Dasu, K., Liu, J., & Lee, L. S., 2012. Aerobic soil biodegradation of 8:2 fluorotelomer stearate monoester. *Environmental Science and Technology*, 46(7), 3831–3836.

[8] Zhang, S., Lu, X., Wang, N., & Buck, R. C., 2016. Biotransformation potential of 6:2 fluorotelomer sulfonate (6:2 FTSA) in aerobic and anaerobic sediment. *Chemosphere*, 154, 224–230.

[9] Benskin, J. P., Ikonomou, M. G., Gobas, F. A. P. C., Begley, T. H., Woudneh, M. B., & Cosgrove, J. R., 2013. Biodegradation of N-ethyl perfluorooctane sulfonamido ethanol (EtFOSE) and EtFOSE-based phosphate diester (SAmPAP diester) in marine sediments. *Environmental Science and Technology*, 47(3), 1381–1389.

[10] Yi, L. B., Chai, L. Y., Xie, Y., Peng, Q. J., & Peng, Q. Z., 2016. Isolation, identification, and degradation performance of a PFOA-degrading strain. *Genetics and Molecular Research*, 15(2), 1–12.

[11] Merino, N., Wang, M., Ambrocio, R., Mak, K., O'Connor, E., Gao, A., Hawley, E. L., Deeb, R. A., Tseng, L. Y., & Mahendra, S., 2018. Fungal biotransformation of 6:2 fluorotelomer alcohol. *Remediation*, 28(2), 59–70.

[12] Kwon, B. G., Lim, H. J., Na, S. H., Choi, B. I., Shin, D. S., & Chung, S. Y., 2014. Biodegradation of perfluorooctanesulfonate (PFOS) as an emerging contaminant. *Chemosphere*, 109, 221–225.

[13] OECD, 2010. OECD Guidelines for the Testing of Chemicals (Technical Report 209). Activated Sludge, Respiration Inhibition Test (Carbon and Ammonium Oxidation. Guideline 16.

[14] Ramírez, D. A., Muñoz, S.V., Atehortua, L., Michel, F. C., Jr., 2010. Effects of different wavelengths of light on lignin peroxidase production by the white-rot fungi *Phanerochaete chrysosporium* grown in submerged cultures. *Bioresource Technology*, 101 (23), 9213-9220.

[15] Waters. (2009). PFOS/PFOA extraction method using Oasis WAX. https://www.waters.com/waters/promotionDetail.htm?id=10108600&locale=145. Accessed 26 Oct 2020.

.

Effect of Crop Growth through Improving Drip Irrigation Uniformity

Channtola SOT[1*], Vouchleang SREANG[1], Mengheak PHOL[1], Sophanith THA[1], Makara SOY[1], Somnang SRIM[1], Seum MAO[1], Chanthan HEL[2], Chantha OEURNG[1], Pinnara KET[1]

[1]*Faculty of Hydrology and Water Resource Engineering, Institute of Technology of Cambodia, Russian Federation Blvd., P.O. Box 86, 12156 Phnom Penh, Cambodia.*
[2]*Faculty of Telecommunication, Electronic, and Network Engineering, Institute of Technology of Cambodia, Russian Federation Blvd., P.O. Box 86, 12156 Phnom Penh, Cambodia*
** Corresponding author: tolasot25@gmail.com*

Abstract

Crop production experiments of three crops, such as, Red Oakleaf, Red Lettuce and Bok Choy with different system uniformities and field scales controlled by driplines were conducted in a greenhouse in 2020. The Christiansen uniformity coefficients were evaluated. The uniformity of systems was established with nominal emitter discharge rates along a dripline. For all of the system uniformities tested, dry matter above ground uptake displayed high uniformity coefficients throughout the entire growing season. The effects of system uniformity on the crop growth was evaluated. The crop growth experiment of 3 plants, such as, Red Oakleaf (R1), Red Lettuce (R2) and Bok Choy (R3) in the new system installed presented the excellent crop growth with the uniformity of 70-90%. The yields obtained R1 7000kg/ha, R2 6500kg/ha, R3 14000kg/ha. However, the crop growth uniformity of Bok Choy was affected by insects so that lead to lower uniformity despites the irrigation uniformity.

Keywords: *Drip Irrigation, irrigation uniformity, crop growth uniformity*

I. Introduction

Water use efficiency (WUE) in irrigation is the factor that saves water to increase crop yields. WUE can be enhanced through improving water distribution uniformity in irrigation system (Phengphaengsy and Okudaira 2008; Li 1998).

Actually, in drip irrigation system, the uniformity is considered as a key parameter to design a proper system. Improper determination of the parameter, it leads to nonuniform and lower yields (Bralts and Kesner 1983), (Zhao et al. 2012). Some previous scientific studies prove that a good design of the water pressurize by using the software to increase the system performance and water efficiency obtained energy saving was (34.23 ; 29.54%) with slope 2% by using lateral length 30m for drip irrigation(Attia et al. 2019).

This knowledge of irrigation uniformity is important for Cambodian farmers. Currently, there is emerge and increase of using drip irrigation for vegetable production in Cambodia. Therefore, there is a need to prove this knowledge to the farmers.

The purpose of this study was to investigate the effect of drip irrigation uniformity to crop growth uniformity of lettuce growth in greenhouse.

II. Materials and Methods

II.1. Sampling sites

Field experiment was conducted in greenhouse at Institute of Technology of Cambodia, Phnom Penh, Cambodia. The area of greenhouse equaled to 10mx8m. There are total amount of 16 raised bed boxes. Only 10 boxes were used for testing. Dimension of each box was 1.3mx1.9m =2.47m^2.

Growing the plants started in rainy season with temperature around 30 ℃ at day and 27 ℃ at night. Planting was spent 43 days with three types of crops, Red Oak leaf, Red Lettuce and Bok Choy. They were selected to transplant in the greenhouse on 17 October 2020. The crops were planted in the raised bed boxes as indicated in ***Figure 1***. Worm compost was selected for nutrient and not allow other chemical fertilizers for nutrient, so food safety was achieved from this condition. In a box, we cropped 12 plants and irrigated the same amount of water, nutrient, temperature at the same time.

Planting and transplanting dates are presented in **Table 1**.

Table 1: Date of each growing step

Planting date	Transplanting date	Harvesting date
25.09.2020	17.10.2020	18.11.2020

Soil properties were measured as indicated in the **Table 2**

Table 2. Soil properties

Parameters	Value
Soil Texture	Loam
pH	6.63

Figure 1. Three selected crops planted in the greenhouse.
A) Red lettuce, B) Red Oakleaf C) Bok Choy

II.2. Experimental set-up

There were two events of installation of the drip system. The first event (F1) presented the improper uniformity of the drip system installed in August. The second event (F2) presented the proper uniformity of the drip system after consideration of quality of the drip line, emitters and soil moisture distribution. There were different materials used in the both events.

II.3. Data collection

In the first event, there are 24 emitters with 4 laterals for testing, space of emitter was 317mm and space of lateral was 325mm. The pressure of pump was 2.5bar (***Figure 2***).

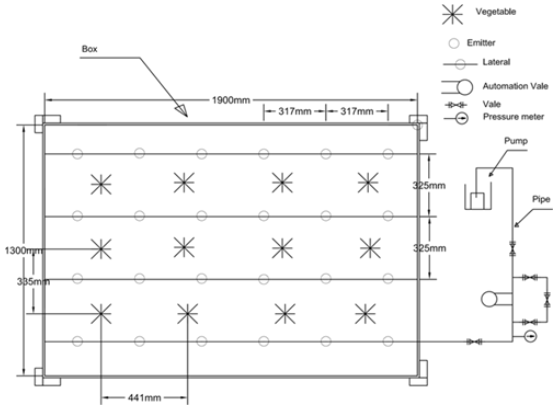

Figure 2. Schema of drip system at the first event

After measured wet area was designed the spacing emitters and laterals in the same shape of box which had 48 emitters with 6 laterals in order to get the water uniformly cover the soil and the root length will get water enough for growing according to the graph shown ***(Figure 3)***.

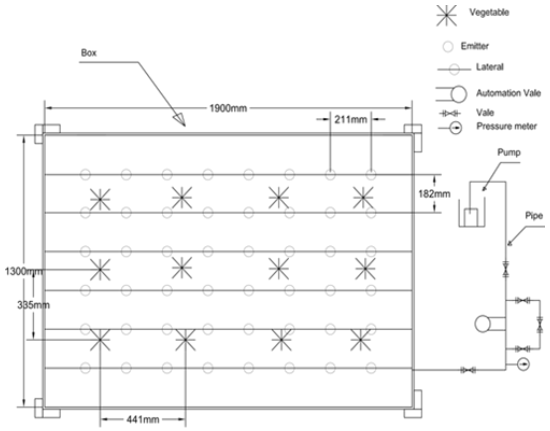

Figure 3. The schema of drip irrigation installed at the second event.

Emitters flow rates measured in the boxes using plastic glass as indicated in the ***Figure 4***. The flow rates were measured for a minute

Figure 4. Emitter flow rate measurement in the box of soil.

A) first event of drip system installation, B) Second event of drip system installation.

Biomass of plants were collected for 3-weeks and those plants were dried in oven at 70°C in 48h. In each plant type, the three-difference types of biomasses were collected.

II.4. Analytical methods

The Christiansen uniformity coefficient (CU) (Chinese

Standard, 1995) uses for determine quality uniformity of discharge and yield of planting.

$$CU = 100 \times (1 - \frac{\sum_{i=1}^{n}|x_i - \overline{x}|}{n\overline{x}})$$

Where x_i parameter of discharge each emitter (ml/min), $\overline{x}$ is the average of all discharge in the emitter, n is the total emitter.

(Zhao et al. 2012) suggests a design Christiansen uniformity coefficient (CU) got greater than 80%. However,

Using the same principle of Christiansen uniformity to calculate the uniformity of crop growth

$$CU_{crop} = 100 \times (1 - \frac{\sum_{i=1}^{n}|b_i - \overline{b}|}{n\overline{b}})$$

Where b_i parameter of biomass of each plant (g/plant), $\overline{b}$ is the average of weight's plant, n is the total emitter.

III. Results and discussion

III.1. Improvement of drip irrigation uniformity

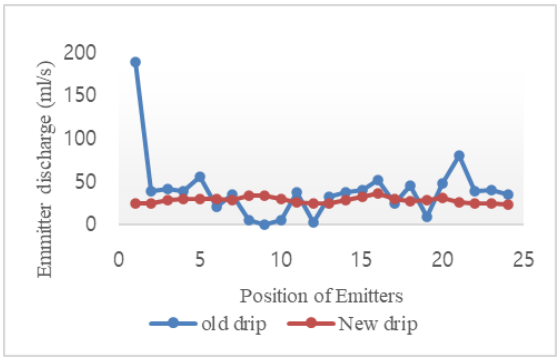

Figure 5. Emitter flow rates of the 2 installation events

Figure 5. shows the flow rate variation in the growing boxes. The first event of drip installation presented the large variation within the box. This means that there were nonuniformity of the irrigation water supply in the box that impacted the crop growth. The new event of installation presented the small graduation of the flow rate in the box.

Table 3: CU Analysis

	Flow rate of old emitter (F1) (ml/min)	Flow rate of new emitter (F2) (ml/min)
Average	36.73	27.75
CU	54%	91%

For F1 CU reached 54% but CU F2 reached 91% (**Table 1**). input discharge from pump, pressure and method of measurement was similar to F1 CU level 54% it's was nonuniformity so planting wouldn't get water enough to profit themselves then it's made low the yield, but level CU of F2 91% its uniformity so we can control the flow rate to planting and it's an important to saving the water and it's a part to get the high yield.

Drip F1 and F2 was design the similar physical so ***Figure 3*** can describe F1 and F2. For F1, the specification of embitter and lateral are 2.4L/h, whereas F2 is 2.2L/h. we used 24 emitters with 4 laterals, space of each emitter was 317mm and space of lateral was 325mm. we used pump that has pressure 2.5bar.

Comparison between old drip system with new drip system. Acording to measuring in greenhouse, The old water system had different discharge and pressure that caused drip irrigation nonuniformly. In addition, using unproper excavating emmitter made different flow rate in each lateral and provided nonuniform water supply. Wheareas, installing new drip, we calibrated by measuring flow rate. Following the graphic above, the result is uniform compared to old drip

III.2. Crop growth

Figure 6. Presents the crop growth during the second event, F2. Getting uniformity of water, we can see the varied growth of difference plants. Between 7 to 18 days of those plants weigh were similar, yet the weight started extremely changes after 29 days because these various plants absorbed different fertilizer and amount of water. After 3 months, the yields obtained R1 7000kg/ha, R2 6500kg/ha, R3 14000kg/ha. Each plant was healthier and got higher yield than general types of plant because some condition like uniformity of water, temperature is enough for plant growing, soil type of loam mix with worm compost and in a greenhouse no longer allow bad inset to destroy.

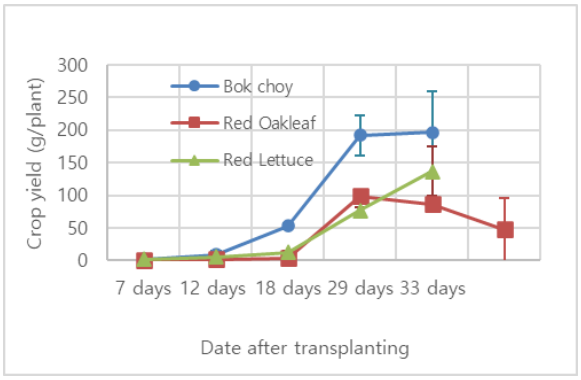

Figure 6. Variation of crop yields planting in the greenhouse after improving the irrigation uniformity

III.3. Crop growth uniformity

The ***Figure 7*** illustrated the crop growth uniformity from transplanting until harvesting.

The results shown that both lettuce crops presenting the high uniformity of the corp growth within 70 to 90%. However, the crop growth of Bok Choy presented lowest uniformity due to the fact that it is sensitive to destruction from insects such as worms.

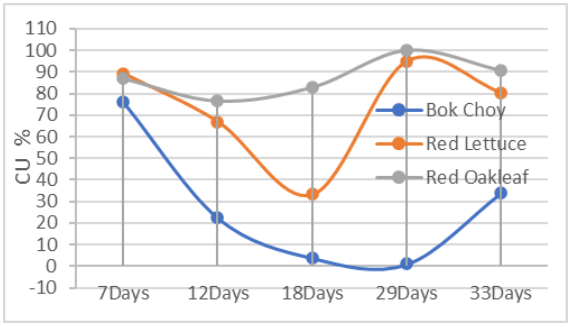

Figure 7: Crop growth uniformity during the plantation

IV. Conclusion

The study has shown the differences between old drip and new drip experiment effect crop yield. After installing a new irrigation system, there are two main factors: first, the selection of a new emitter and the use of the CU Method to calculate the results.

1. The Christiansen uniformity coefficient (CU): For old drip, F1 CU reach 54%, the crop yield is lower flow rate. For new drip set up, level of CU reaches 91%. The new drip system setup presented the successful of irrigation uniformity.
2. The crop growth experiment of 3 plants, such as, Red Oakleaf (R1), Red Lettuce (R2) and Bok Choy (R3) in the new system installed presented the excellent crop

growth with the uniformity of 70-90%. The yields obtained R1 7000kg/ha, R2 6500kg/ha, R3 14000kg/ha. However, the crop growth uniformity of Bok Choy is affected by insects so that lead to lower uniformity despites the irrigation uniformity.

Acknowledgement

We are thankful to ARES-CCD for financial support for this research.

References

Attia, Samir S., Abdel Ghany M. El-Gindy, Hani A. Mansour, Soha E. Kalil, and Yasser E. A rafa. 2019. “Performance Analysis of Pressur ized Irrigation Systems Using Simulation Mo del Technique.” Plant Archives 19:721–31.

Bralts, Vincent F., and Charles D. Kesner. 1983. “Drip Irrigation Field Uniformity Estimation. ” Transactions of the American Society of A gricultural Engineers 26(5):1369–74. doi: 10. 13031/2013.34134.

Li, Jiusheng. 1998. “Modeling Crop Yield as Affe cted by Uniformity of Sprinkler Irrigation Sy stem.” 38:135–46.

Phengphaengsy, Fongsamuth, and Hiroshi Okudair a. 2008. “Assessment of Irrigation Efficienci es and Water Productivity in Paddy Fields in the Lower Mekong River Basin.” Paddy an d Water Environment 6(1):105–14. doi: 10.1 007/s10333-008-0108-z.

Zhao, Weixia, Jiusheng Li, Yanfeng Li, and Jianfe ng Yin. 2012. “Effects of Drip System Unifo rmity on Yield and Quality of Chinese Cabb age Heads.” Agricultural Water Management 110:118–28. doi: 10.1016/j.agwat.2012.04.00 7.

(Phengphaengsy and Okudaira 2008)

Attia, Samir S., Abdel Ghany M. El-Gindy, Hani A. Mansour, Soha E. Kalil, and Yasser E. A rafa. 2019. “Performance Analysis of Pressur ized Irrigation Systems Using Simulation Mo del Technique.” Plant Archives 19:721–31.

Bralts, Vincent F., and Charles D. Kesner. 1983. “Drip Irrigation Field Uniformity Estimation. ” Transactions of the American Society of A gricultural Engineers 26(5):1369–74. doi: 10. 13031/2013.34134.

Li, Jiusheng. 1998. “Modeling Crop Yield as Affe cted by Uniformity of Sprinkler Irrigation Sy stem.” 38:135–46.

Phengphaengsy, Fongsamuth, and Hiroshi Okudair a. 2008. “Assessment of Irrigation Efficienci es and Water Productivity in Paddy Fields in the Lower Mekong River Basin.” Paddy an d Water Environment 6(1):105–14. doi: 10.1 007/s10333-008-0108-z.

The 13th AUN/SEED-Net Regional Conference on Chemical Engineering 2020 (RCChE-2020)
Jointly held with
The 5th International Symposium on Conservation and Management of Tropical Lakes
"Insights and Challenges toward Achieving SDGs"

Groundwater Quality Assessment in the coastal area of Preah Sihanouk and Kampot province, Cambodia

Sovandy Sem[1], Ech Chin[2], Thida Khoeun[2], Ratha Doung[2], Kong Chhuon[2], Sambo Lun[2], Sytharith Pen[2], Ratino Sith[2], Sylvain Massuel[3], Khy Eam Eang[2*]

[1] *Master of UWE, Graduate School, Institute of Technology of Cambodia, Russian Federation Blvd., P.O. Box 86, Phnom Penh, Cambodia*
[2] *Faculty of Hydrology and Water Resources Engineering, Institute of Technology of Cambodia, Russian Federation B lvd., P.O. Box 86, Phnom Penh, Cambodia*
[3] *UMR G-EAU, IRD, Institute of Technology of Cambodia, Russian Federation Blvd., P.O. Box 86, Phnom Penh, Cambodia*

**Corresponding author: khyeam_eang@yahoo.com*

Abstract

An attempt has been made to assess the water quality within the fast-growing coastal zone of Sihanoukville and Kampot area. Groundwater samples were collected from the coastal areas of Sihanouk Ville and Kampot and analyzed for major physicochemical parameters. Experimental results appear that the well water in Kampot was strong acidic to slightly alkaline. In comparison to Sihanouk Ville, the pH was slightly acidic to neutral in the range of 4.83 to 7.1, respectively. The ORP value higher, and then in comparison the ORP value in Kampot from -42 to 211.3 mV higher than in Sihanouk Ville from -31.4 to 173.4 mV. Otherwise, the concentrations of manganese probably released from the manganese-bearing rock into the wells due to having ORP negative. The value of TDS in Kampot (660.66 mg/L) is higher than in Sihanouk Ville (295.33 mg/L). The concentration of TDS in this study site slightly fluctuated between Sihanouk Ville and the Kampot location. For the result of alkalinity from Sihanouk Ville, water samples contained higher alkalinity may be affected by the presence of bicarbonate and carbonate. The alkalinity of water samples from Sihanouk Ville province was mean and dramatically fluctuated gradually varied. Heavy metals distributed in all water samples from Sihanouk Ville within two wells, F3W13 and F3W18, the value over standard, and the other samples resulted in exceeding the DWS and while significantly lowest the WHO guideline. For the Fe, almost well water samples were found acceptable with the standard of drinking water and few samples in Sihanouk Ville had Fe much lower than the standard drinking water. So, related to drinking water quality evaluation resulted that almost all water samples from Sihanouk Ville and Kampot were observed unsuitable for drinking purpose in terms of pH, turbidity, alkalinity, TDS, ORP, and Mn.

Keywords: *Groundwater quality, Drinking water*

I. Introduction

Groundwater resources are beneath seriously anthropogenic activities and the constant risk of contamination. Human activities such as agriculture, urbanization, and industry have caused irreversible degradation of groundwater quality; in this manner, protection is the foremost suitable technique within the battle against groundwater contamination [1]. Cambodia's coastal regions inferring from resource-dependent activities, there are advanced pressures caused by urbanization and industrialization along the coastline. Most urban and industrial developments are found along the coast of Sihanoukville and Kampot Province with the fastest-growing regions and are powering the economic growth. Moreover, the coastal aquifer at Sihanoukville is stressed by households increasingly depending on tube wells to counterbalance the undersized dispersion network [2]. So far, in a coastal area, no environmental observation networks exist in these areas and barely any data are available preventing the assessment of the situation and its potential evolution, especially for groundwater. The quality of water is basically affected by pollution from different sources. Sectoral approaches partition the total accessible water,

leading to a shortage. Within the coastal zone, the major cause of groundwater pollution is seawater intrusion. Over-exploitation may be an extreme issue that affects the potability of water. Hydrogeochemical processes are controlling components of water chemistry [3]. The present study was carried out in the coastal area (Sihanoukville) in order to analyze water quality. The seawater intrusion was reported from this area by international organizations [2]. Essentially, a few groundwaters actually contain constituents of well-being concern, and a few well waters at Sihanouk Ville which is used for the household is sometimes not known whether its quality is fulfilled with the standard of drinking water. Subsequently, understanding the effect of groundwater on public health is exceptionally valuable. It is exceptionally useful to be known all these specified issues. So, the present study was conducted with an objective to evaluate groundwater chemistry and water quality in the coastal area of Preah Sihanouk and Kampot province which focuses on the current status of the integration of groundwater with seawater intrusion and the suitability of drinking water quality compared to WHO standard.

II. Materials and Methods

2.1. Study Area

The study was conducted along the Cambodia's coastal aquifers **(Fig. 1)** which include Preah Sihanouk and Kampot province. There are 51 groundwater samples were collected from tube wells and dug wells with several sources like household, community, and rural supply well by 39 locations in Sihanouk Ville and 12 locations in Kampot.

Fig. 1. Map of study area

2.2. Experimental set-up

Physicochemical properties include TDS, ORP, Temp, pH, Turbidity and Conductivity were analyzed in-situ using YSI EXO2 multi-parameter instrument. Then, well water sample were analyzed in SATREPS laboratory of Institute of Technology of Cambodia. Alkalinity was determined by 0.01M sulfuric acid titration, harmful substances [Arsenic (As), Iron (Fe), and Manganese (Mn)] were analyzed by atomic absorption spectrophotometer (AAS, Shimadzu AA-7000).

2.3. Analytical methods

In this study, the groundwater was taken from the well by pumping or drawing water with a bucket/container in case of no pumping machine. At the same time, four parameters such as pH, ORP, conductivity, and temperature were measured at situ by EXO Sondes YSI.

The alkalinity was analyzed only with water samples that had pH greater than 4.5, while water with pH lower than 4.5 was assumed that no alkalinity in the water [4]. The measurement was divided into 4 steps including: Sulfuric acid preparation, calibration of pH meter, alkalinity measurement, and alkalinity calculation.

+ AAS analysis for the heavy metals: Each water sample was filtered 0.45 µm membrane after adding 0.05 ml of nitric acid (65% of HNO_3). The accuracy of the AAS result was confirmed by maintaining the r^2 value of the calibration curve at least 0.99.

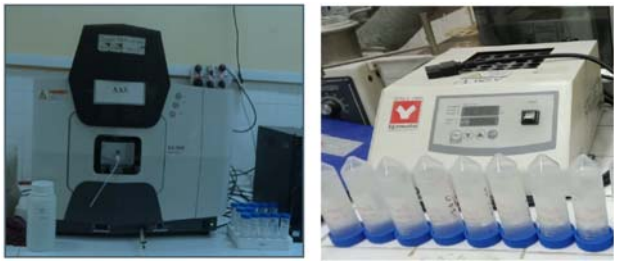

Fig. 2. AAS machine used for Fe, Mn, and As analyses

Straightway, to survey drinking water this study has utilized the current information to compare with Cambodia Drinking Water Quality Standard (DWS) and World Health Organization (WHO) as shown in **Table 1**.

III. Results and Discussion

3.1. Current status of water quality

In-situ measurement of the groundwater quality conducted by EXO shows that **pH** value ranged out of the allowable limit of DWS and WHO of drinking water (**Fig. 3** and **Table 2).** Well water in Kampot was strongly acidic to slightly alkaline with the pH. In comparison to Sihanouk Ville, the pH was slightly acidic to neutral in the pH range of 4.83 to 7.1, respectively. According to Appelo and Postma (2005), the pH ranges <6.3 resulted in abundant carbonic acid (H_2CO_3), indicating that wells from Sihanouk Ville and Kampot contained H_2CO_3. In comparison, dug/tube wells from Sihanouk Ville obtained higher HCO_3- due to pH ranged from 4.83 to 7.1. The concentration of Fe and Mn perhaps elevated in well water from Kampot due to acidic water [5].

Electrical Conductivity: The value of each well water sample in both areas slightly fluctuated. Also, the twelve

sampling in Sihanouk Ville and Kampot location have high EC especially found in well F2W2, F3W2, F1W12, F1W15, F3W14, and F3W20. The other sampling was exceeded the desirable limit in drinking water of WHO, 250 µS/cm.

Oxidation-reduction potential (ORP): In Sihanouk Ville, the ORP value ranged from -49 to 207.2 mV with a mean is 95.83 mV. In Kampot, the ORP varied from -42 to 211.3 mV with average is 112.76mV. The ORP value the higher than in Sihanouk Ville. Perhaps, the concentrations of manganese probably released from the manganese rock into the wells due to having ORP negative [6]. So, other well numbers may obtain more manganese concentration than other wells.

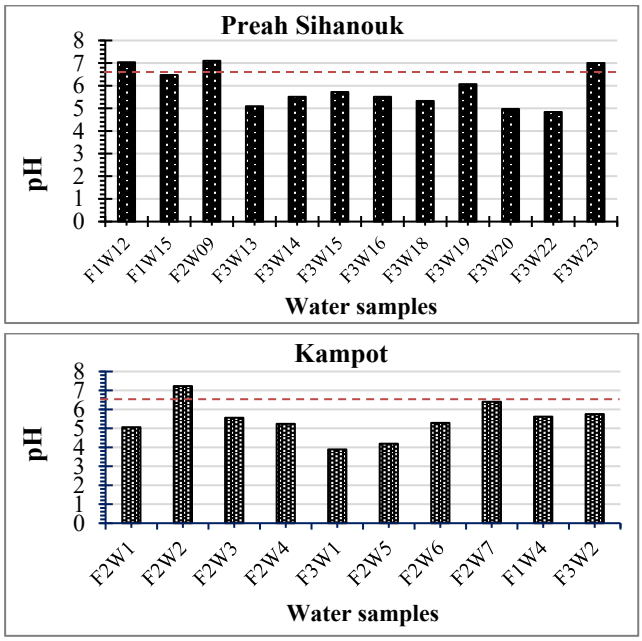

Fig. 3. The result of pH at Sihanouk and Kampot collection dash-red line means maximum value of Cambodia drinking Standard

Turbidity: The value of turbidity in Sihanouk Ville higher than in Kampot. **Fig.4**, referring to the result in Kampot, five sampling points such as F2W6, F1W4, and F3W3. In Sihanouk Ville, there were six locations such as F3W14, F3W15, F3W16, F3W18, F3W19 and F3W23 were accounted for turbidity seriously higher than standard.

Total Dissolved Solids: The TDS distribution in Sihanouk Ville exhibited of a minimum 44 mg/L, a maximum of 1390 mg/L and a mean of 295.33 mg/L. The value of TDS in Kampot ranged from 17 mg/L to 3212 mg/L with a mean of 660.66 mg/L. In Kampot, the TDS values were higher than in Sihanouk Ville. The concentration of TDS in this study site slightly fluctuated between Sihanouk Ville and the Kampot location.

Alkalinity: The wells contain low alkalinity with low pH, indicating corrosive concern. **Fig.5.** illustrated the detailed result of alkalinity from Sihanouk Ville. Water samples contained higher alkalinity may be affected by the presence of bicarbonate and carbonate.

3.2. Heavy metals

Manganese (Mn): The manganese for drinking purposes was recommended by the Cambodia standard and WHO, 0.1 mg/L and 0.5 mg/L, respectively. **Fig.6.** illustrated the concentration of Mn distributed in all water samples from Sihanouk Ville. In this study, two wells the value over standard as F3W13 and F3W18, and the other samples resulted in exceeding the DWS and while significantly lowest the WHO guideline.

Iron (Fe): The iron for drinking water was recommended by the WHO and DWS in Cambodia, 0.3 mg/l almost all well water samples were found in the standard of drinking water except few samples in Sihanouk Ville that were not in the standard of drinking water. So, the result of Fe in Sihanouk is good for household use. In addition, the amount of iron in water causes a stain on laundry, materials, and vegetables.

Table 1. Drinking Water Quality Standard [7, 8]

Parameters	Unit	Cambodia	WHO
pH	-	6.5-8.5	6.5-8.5
Turbidity	NTU	5	≤5
TDS	mg/L	800	-
EC	µS/cm	-	250
Hardness	mg/L	-	300
Alkalinity	mg/L	-	-
Arsenic (As)	mg/L	0.05	0.01
Iron (Fe)	mg/L	0.3	-
Manganese (Mn)	mg/L	0.1	0.5

-: not mentioned

Table 2. Ranges of physicochemical parameters and their comparison with MIME and WHO standards for drinking water

Site		Temp (°C)	Cond (µS/cm)	TDS (mg/L)	pH	ORP (mV)	Turbidity (FUN)
Preah	Min	27.5	16.1	11	3.82	-49	-4.69
Sihanouk	Mean	29.2	304.85	187.52	5.94	95.83	61.35
	Max	40.1	2294.4	1390	7.61	207.2	1202.4
Kampot	Min	28.8	28.1	17	3.89	-42	-3.65
	Mean	29.6	294.12	660.66	5.42	112.76	2.99
	Max	30.7	1390.5	3212	7.23	211.3	24.73
MIME/WHO		-	250	800	6.5-8.5	-	5

-: not mentioned

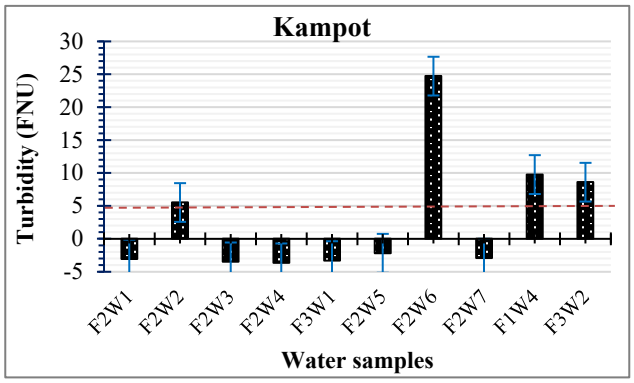

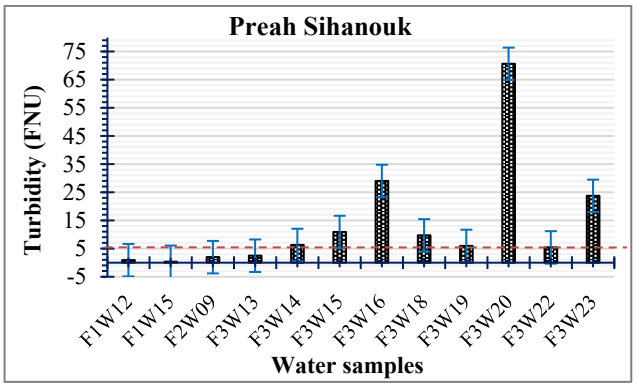

Fig. 4. Result of turbidity in Kampot and Preah Sihanouk, dash-red line means maximum value of Cambodia drinking standard

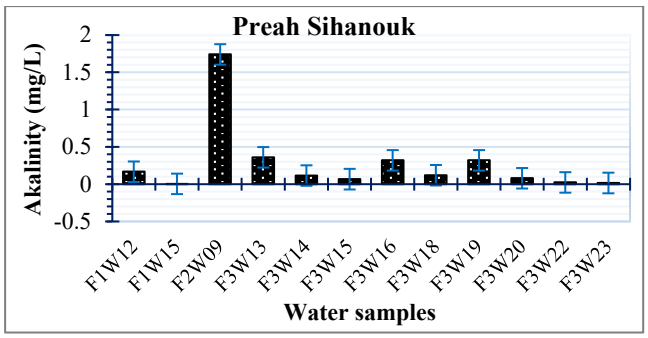

Fig. 5. Result of alkalinity at Sihanouk

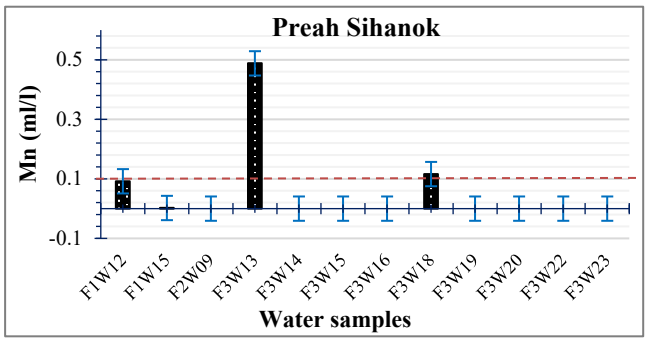

Fig. 6. The result of Mn dash-red line means maximum value of Cambodia drinking

IV. Conclusion

Water from the dug/tube well is an important source for various uses; however, related to drinking water quality, assessment resulted that almost all water samples from Sihanouk Ville and Kampot were observed unsuitable for drinking purpose in terms of pH, turbidity, alkalinity, TDS, ORP, and Mn. The result of Fe and temperature from Sihanouk Ville is lower than the standard. Kampot has only 4 wells and Sihanouk Ville have 9 wells that stay in the water quality. Parameters in the wells are exceeding the limited standard especially pH and EC. There are only 2 wells in Sihanouk Ville have Mn above the drinking standard.

Acknowledgement

We are thankful to the Science and Technology Research We are thankful to the 4-C water project for the financial support under the management of Institut de Recherche pour le Développement (IRD).

References

[1] Kazakis, N., Voudouris, K. S. (2015). Groundwater vulnerability and pollution risk assessment of porous aquifers to nitrate: Modifying the DRASTIC method using quantitative parameters. Journal of Hydrology, 525, 13-25.

[2] Rizvi, A. R., Singer, U. (2011). Cambodia Coastal Situation Analysis. Education, 2(2), 3.

[3] Kumar, P. S., Elango, L., James, E. J. (2014). Assessment of hydrochemistry and groundwater quality in the coastal area of South Chennai, India. Arabian Journal of Geosciences, 7(7), 2641-2653.

[4] Appelo, C. A. J., Postma, D. (2005). Geochemistry, Groundwater and Pollution, 2nd edition. Boca Raton London New York. CRC Press, Taylor & Francis Group.

[5] Abdelshafy, M., Saber, M., Abdelhaleem, A., Abdel-razek, S. M., Seleem, E. M. (2019). Hydrogeochemical processes and evaluation of groundwater aquifer at Sohag City, Egypt. Scientific African, 6, e00196.

[6] Bouteldjaoui, F., Kettab, A., Bessenasse, M. (2017). Identification of the Hydrogeochemical Process in Zahrez Basin, Algeria. Algerian Journal of Environmental Science and Technology, 3(1).

[7] MIME. (2004). Kingdom of Cambodia Drinking Water Quality Standards. In Drinking Water Quality Standards.

[8] World Health Organization (2011). Guidelines for drinking-water quality, 4th ed. Geneva: World Health Organization.

Comparison Of Modelling of Soil Water Dynamic In Two Distinct Soils

Kim Sreang DY [1*], Pinnara KET[2] Seum MAO[1], Channtola SOT[1], Mengheak PHOL[1], Sophanith THA[1], Makara SOY[1], Somnang SRIM[1], Vouchleang SREANG[1], Chantha OEURNG[1]

[1] *Faculty of Water and Environmental Engineering, Institute of Technology of Cambodia, Russian Federation Blvd., P.O. Box 86, 12156 Phnom Penh, Cambodia*
[2]*Faculty of Hydrology and Water Resources Engineering, Institute of Technology of Cambodia, Russian Federation Blvd., P.O. Box 86, 12156 Phnom Penh, Cambodia*

* *dykimsreang168@gmail.com*

Abstract

Understanding the performance of soil water dynamic is important for agricultural and water resources management. Dealing with the infiltration process and its prediction is an important topic for current research. The objective of the study is to characterize water dynamic in two distinct soils in urban garden by using HYDRUS 1D. Infiltration experiment loam and sandy soils was conducted at Soil laboratory at Institute of Technology of Cambodia. Mini-tension infiltrometer was used to measure the soil infiltration process. The data from experiment was used to test the Hydrus 1D model. The result of simulation of infiltration shown that Hydrus 1D has capability to simulate the infiltration well.

Key words: *Soil degradation, soil water flow, HYDRUS-1D*

I. Introduction

In Cambodia, irrigation is a significant water-related activity, especially in urban area where agriculture cannot exist without adequate irrigation. To manage efficient water use irrigation, infiltration is crucial part to be defined. For studying water movement Characteristics in infiltration process, numerical simulation has become an important technique. The HYDRUS model can simulate water infiltration in the variable saturated zone with the term source and sink considered and manage different boundary conditions flexibly (Simunek et al. 2008). It has been used worldwide and achieved a great deal of valuable research results.
There is still the need of understa
nding of infiltration process from different soil especially in urban garden.

In this research, we conducted a field infiltration experiment of sandy soil and loam soil of greenhouse garden at soil laboratory of Institute of technology of Cambodia. The ability of applying Hydrus 1D to simulate the infiltration process is our research question.

II. Methodology

2.1 Study site and experimental set up

The infiltration experiment was conducted at Institute of Technology in October 2020 (Figure 1&2). There were two types of soil, such as loam soil (for growing vegetables) and sand soil, which were used for this experiment. The data was gathered from 10 crop cultivation boxes, which have 1.3m ×1.9m in one box. And with a 317mm emitter, the lateral space is 325mm.

Figure 1. Experimental design

2.2 Mini-disc infiltrometer

Mini-disc infiltrometer is an device used to measure the rate of water infiltration into soil or other porous media.

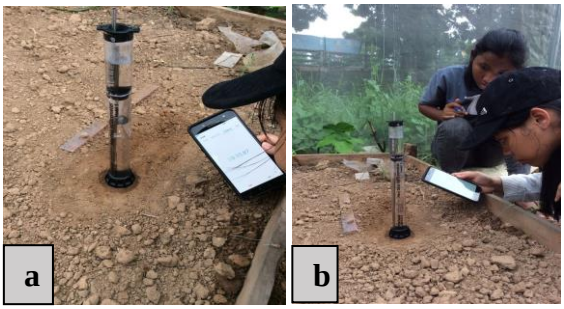

Figure 2. Infiltration on loam soil at greenhouse

2.3 HYDRUS-1D Model Setup

The HYDRUS-1D code was based on the one-dimensional Richards equation to simulate water movement in variably saturated media, and the equation was solved by numerical method (Sim ˚unek et al., 2005). The basic water movement equation was described as:

$$\frac{\partial \theta(h,t)}{\partial t} = \frac{\partial}{\partial z}\left[K(h)\left(\frac{\partial h}{\partial z}+1\right)\right]$$

The soil physical properties were estimated using the equation of van Genuchten et. al 1991.

$$\frac{\theta-\theta_r}{\theta_s-\theta} = (1+|\propto h|^n)^{-m} \qquad h>0$$

$$\theta = \theta_s \qquad h \le 0$$

Where h is the soil water pressure head (cm), is the water content (cm^3/cm^3), **r** and **s** are the residual and saturated water contents (cm3/cm3), respectively, ¸, m and n are empirical parameters and m=1 − 1/n.

$$\frac{\theta-\theta_r}{\theta_s-\theta} = \left(\frac{h_a}{h}\right)^{\lambda} = \left(\frac{1}{\acute{\alpha}h}\right)^{\lambda} \qquad \acute{\alpha}\, h>1$$

Where h is the soil water pressure head, θ is the volumetric water content, t is time, z is the vertical coordinate with the origin at the soil surface (positive upward), and K(h) is the unsaturated hydraulic conductivity. For the experiment studied, the initial condition and upper boundary condition were:

$h(z, 0) = hi(z)$

$h(0, t) = h0$

Where hi(z) is the initial soil water pressure head through the soil column, and h0 is the soil water potential at soil surface.

The free drainage was to be considered as lower boundary condition: $\partial h/\partial z=0$.

The soil profile was 20 cm depth.

$$\alpha' h \leq 1$$

contents of the two different soils, e.g. loam and sand. This is the first proposition. However, this result needs to be calibrated by the oven dry to confirm this properties. It is reasonable that Ks suggested by model proposed the small value from loam soil and high value from sand soil with Ks f 0.0029 mm/s and 0.0825 mm/s respectively.

Where α' is an empirical parameter (1/cm) and it is the reciprocal of **ha**, **ha** is often referred to as the air entry value (cm), and is the pore-size distribution parameter affecting the slope of the retention function.

The unsaturated hydraulic conductivity of each soil layer can be expressed as (van Genuchten et al., 1991):

$$K(h) = \frac{Ks\{1 - (h)mn\,[1 + (h)n]-m\}2}{[1 + (h)^{n}]^{m}}$$

III. Results

1. Physical hydraulic properties simulated

The results of estimation of hydraulic properties from the experimentation were shown in the Table 2. The model proposed the same soil moisture contents of the two different soils, e.g. loam and sand. This is the first proposition. However, this result needs to be calibrated by the oven dry to confirm this properties. It is reasonable that Ks suggested by model proposed the small value from loam soil and high value from sand soil with Ks f 0.0029 mm/s and 0.0825 mm/s respectively.

Table 2: Water Flow of Sandy and Loam Soil

Soil types	θr	θs	α (1/mm)	n	Ks (mm/sec)	l
Sand	0.045	0.43	0.0145	2.68	0.0825	0.5
Loam	0.078	0.43	0.0036	1.56	0.0029	0.5

Values of soil hydraulic parameters as obtained from the HYDRUS-1D (θr is the residual water content, θs s the saturated water content, α, n, and l are empirical parameters, and Ks is the saturated soil hydraulic conductivity).

1. Infiltration process simulated

- **Loam Soil**

  Cumulative infiltration increased from 0sec to <250 (figure 3).

  The Loam Soil Pressure Head concentration was drop down slowly from h > 75 mm to nearly 250 sec. And the data for Loam Flux Loam Soil decreased from >0.00 mm/sec at time 0 sec to >-0.00000025 mm/sec at time > 250 sec (figure 4&5).

Cum. Infiltration

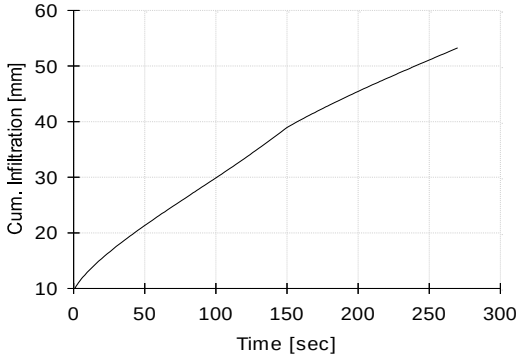

Figure 3. Cum. Infiltration of Loam soil

Surface Pressure Head

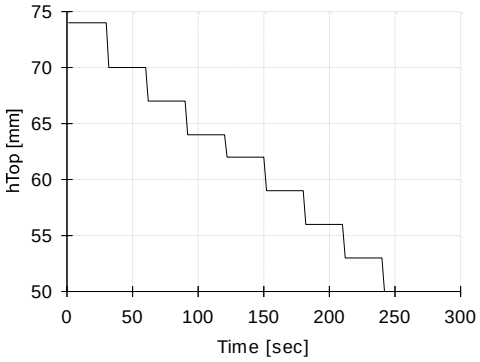

Figure 4. Pressure Head of Loam Soil

Bottom Flux

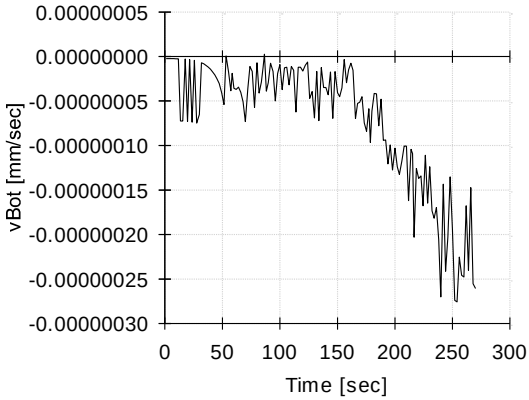

Fig.5. Bottom Flux of loam Soil

- **Sandy Soil**

Cum. Infiltration of Sand Soil was increased fatly from 0 mm to <22mm at time from <0 sec to 60 sec (figure 6). However, at the time of 0 sec >30 sec, the Bottom Flux of Sand Soil was decreed that 0.00000001mm/sec to >-0.00000008mm/sec, but at the time of 30 sec to 60 sec, the bottom flux was slowly distressed (figure 7).

For Surface Pressure Head of was drop down from the h > 75 mm at almost 60sec (figure7).

Cum. Infiltration

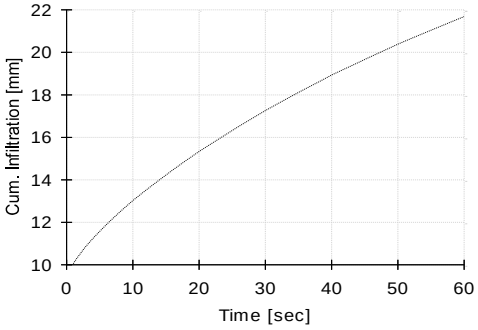

Figure.6 Cum. Infiltration of Sand Soil

This saturation persisted less than 60mm. Very slight changes in soil water pressure head during storms effected relatively large changes in both magnitude and direction of water flux.

The results of this experiment differed significantly between Sand soil and Loam Soil.

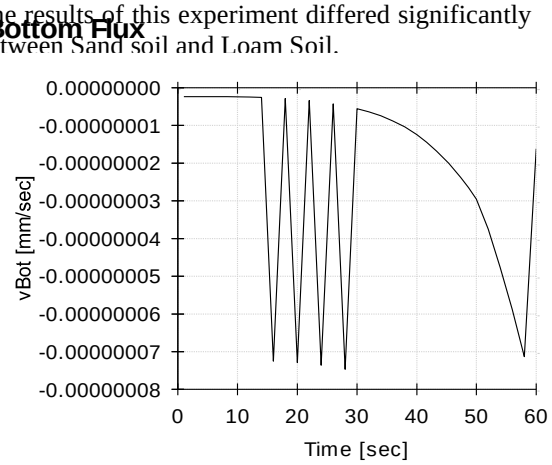

Fig8: Bottom Flux of Sand Soil

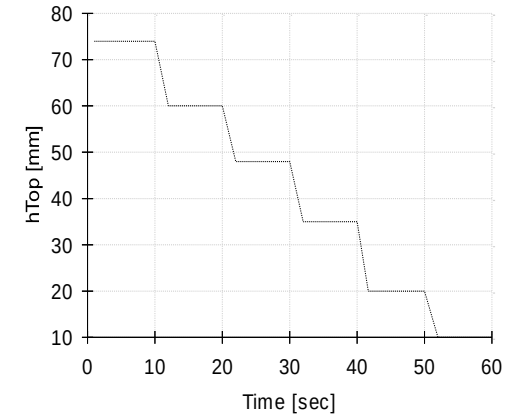

Fig.7. Surface Pressure Head of Sand Soil

IV. Conclusion

In this study, the infiltration process has been conducted at institute of technology of Cambodia. Hydrus 1D has been used to simulate the water dynamic of the process. The result proposed that saturated conductivity simulated for sandy soil was 28 time of the loam soil with a value of 0.0825 and 0.002 respectively.

The sandy soil pressure head decreased sharply with time compared to the loam soil. However, our further work is to calibrate and validate the performance of the model with statistical analysis.

Acknowledgement

We are thankful to the Science and Technology Research Partnership for Sustainable Development (SATREPS), the Japan Science and Technology Agency (JST)/Japan International Cooperation Agency (JICA) for their financial support.

References

Bouwer, H., 1986. Intake rate: cylinder infiltrometer. *Methods of Soil Analysis: Part 1 Physical and Mineralogical Methods*, *5*, pp.825-844

http://www.fao.org/3/r4082e/r4082e03.htm#2.2.1%20the%20infiltration%20process

https://www.sciencedirect.com/topics/earth-and-planetary-sciences/infiltrometer.

Šimůnek, J., M. Šejna, H. Saito, M. Sakai, and M. Th. van Genuchten, The HYDRUS-1D software package for simulating the one-dimensional movement of water, heat, and multiple solutes in variably-saturated media, Version 4.0, Hydrus Series 3, Department of Environmental Sciences, University of California Riverside, Riverside, CA, USA, 2008.

Šimůnek, J., M. Th. van Genuchten, and M. Šejna, Development and applications of the HYDRUS and STANMOD software packages, and related codes, Vadose Zone Journal, doi:10.2136/VZJ2007.0077, Special Issue "Vadose Zone Modeling", 7(2), 587-600, 2008.

Van Genuchten, M.V., Leij, F.J. and Yates, S.R., 1991. The RETC code for quantifying the hydraulic functions of unsaturated soils.

The 13th AUN/SEED-Net Regional Conference on Chemical Engineering 2020 (RCChE-2020)
Jointly held with
The 5th International Symposium on Conservation and Management of Tropical Lakes
"Insights and Challenges toward Achieving SDGs"

Comparison of Coral Bleaching Hotspot Mapping in Southeast Asia (Thailand, Cambodia and Vietnam) based on Sea Surface Temperature Modelling by National Oceanic and Atmospheric Administration Coral Reef Watch before and during Covid-19 Pandemic

Rajendra Khanal [1*], Pham Quy Giang [2], Binaya Kumar Mishra [3], Ratino Sith [4], Soly Siev [5], Varinthorn Boonyaroj [6]. Vannak Ann [7], Vengsong Khov [8], Jorge Garcia-Hernandez [1]

[1] *Department of Civil and Environmental Engineering, School of Environment and Society, Tokyo Institute of T echnology, 2-12-1-M1-4, Ookayama, Meguro-ku, Tokyo, 152-8552, Japan;* [2] *Faculty of Environment, Ha Long University, Vietnam;* [3] *Faculty of Science and Technology, Pokhara University, Nepal;* [4] *Faculty of Hydrology a nd Water Resources Engineering, Institute of Technology of Cambodia, Phnom Penh, Cambodia;* [5] *Department of Science, Technology & Innovation Policy, Ministry of Industry, Science, Technology and Innovation, Cambo dia;* [6] *Faculty of Science and Technology, Rajamangala University of Technology, Bangkok, Thailand;* [7] *Water and Environment Unit, Institute of Technology of Cambodia, Phnom Penh, Cambodia;*[8] *Tonle Sap Authority, Mi nistry of Water Resources and Meteorology, Cambodia*

* *Corresponding author: khanal.r.aa@m.titech.ac.jp*

Abstract

Due to Covid-19 pandemic in the year 2020, international travel and hence the tourism was down by more than 95% globally. Influx of tourism has been regarded as one of the reasons for coral bleaching. In this study, attempt has been made to compare the coral bleaching hotspot (CBH) mapping in the year 2019 (pre-pandemic) and 2020 (during pandemic) based on sea surface temperature (SST) modelled data by National Oceanic and Atmospheric Administration Coral Reef Watch (NOAA-CRF). The NOAA 7-day maximum SST database is compared for the Coral Triangle region – with a focus on gulf of Thailand and south China sea covering Thailand, Cambodia and Vietnam in southeast Asia – for the first day of the month in Jan, Mar, June, Sep, and Nov both in 2019 and 2020. The CBH is taken as the measure of the difference between observed SST and monthly maximum mean temperature, and was measured in the range 0 to 5 ^{O}C. No visual (< 0 ^{O}C) CBH was observed in the region for the month January and March pre-pandemic and during pandemic. In the month of May, CBH (1 - 2 ^{O}C) was dominant in the gulf of Thailand covering mostly Thailand and Cambodia, and was higher during pre-pandemic period. During July, CBH (1 - 2 ^{O}C) was dominant in the south China sea covering Vietnam, and was also higher during pre-pandemic period. Surprisingly, CBH was higher during pandemic along the Vietnam in south China sea, the reason of which is still a matter of further investigation. In general, with an exception in September 2020, CBH was higher during pre-pandemic period. A detailed study covering daily, and monthly average SST would provide better understanding of impact of covid-19 pandemic on CBH.

Keywords: *Coral bleaching hotspot, covid-19 pandemic, sea surface temperature, National Oceanic and Atmospheric Administration, Coral Reef Watch, gulf of Thailand, south China sea*

Acknowledgement

Authors would like to express gratitude to Asia-Pacific Network for Global Change Research for funding this project - "Collaborative Research Platform to Manage Risk and Enhance Resilience of Coral Reef in Southeast Asia, CRRP2019-08MY-Khanal". Acknowledgements also goes to National Oceanic and Atmospheric Administration, Coral Reef Watch for the data

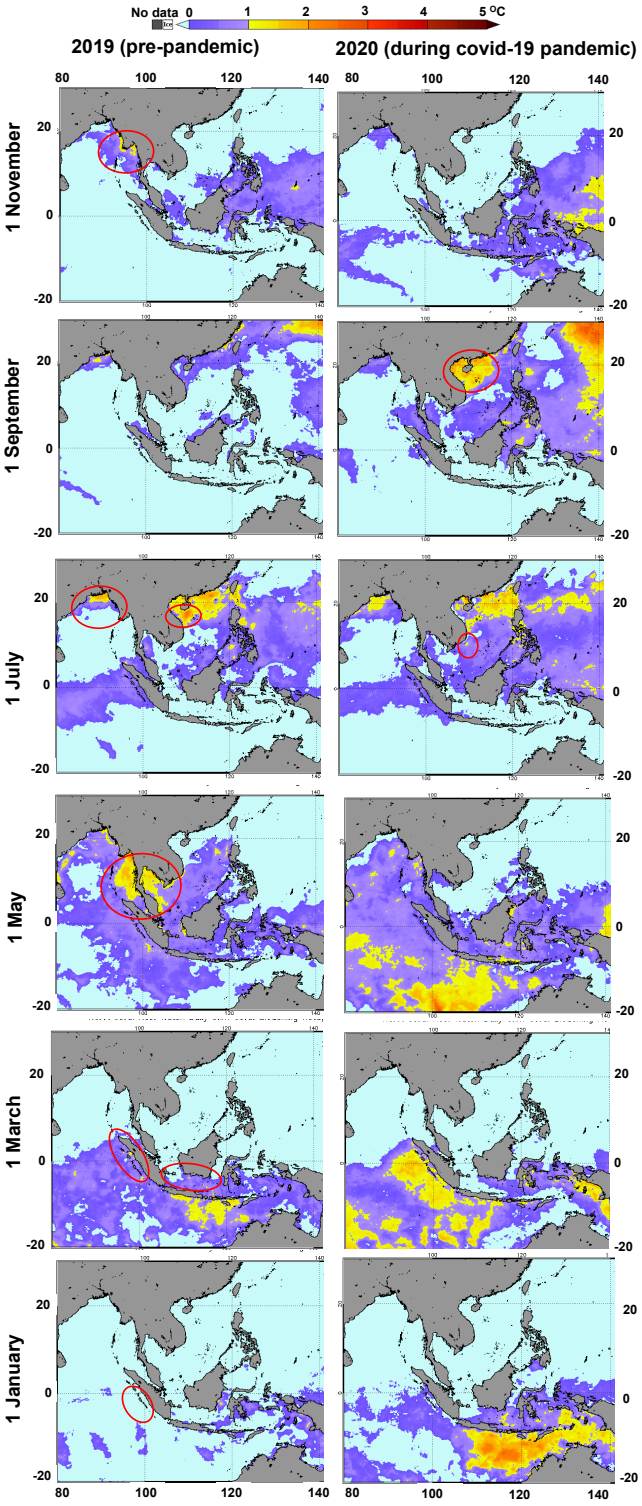

Fig. 1. Coral bleaching hotspot mapping in the year 2019 (pre-pandemic) and 2020 (during pandemic) based on sea surface temperature modelled data by National Oceanic and Atmospheric Administration Coral Reef Watch.

The 13th AUN/SEED-Net Regional Conference on Chemical Engineering 2020 (RCChE-2020)
Jointly held with
The 5th International Symposium on Conservation and Management of Tropical Lakes
"Insights and Challenges toward Achieving SDGs"

Paradox of over-tourism, income opportunities and coral degradation: A case of Maya bay, Thailand

Rajendra Khanal [1*], Varinthorn Boonyaroj [2], Jorge Garcia-Hernandez [1]

[1] *Department of Civil and Environmental Engineering, School of Environment and Society Tokyo Institute of Technology, 2-12-1-M1-4, Ookayama, Meguro-ku, Tokyo, 152-8552, Japan*
[2] *Department of Environmental Science and Technology, Faculty of Science and Technology, Rajamangala University o f Technology Phra Nakhon, 1381 Pracharat 1 Road, Wongsawang, Bang Sue, Bangkok, Thailand 10800*

* *Corresponding author: khanal.r.aa@m.titech.ac.jp*

Abstract

Tourism plays an important role in the economic development of the country. Tourism contributes to as much as 7% of Thailand national GDP. Pristine beaches in Thailand attracts millions of tourists every year. On one hand, local economy is booted with tourism. Contract to that, over-tourism may lead to stress on the local environment. One of the classical examples of impact of over tourism on the environment is the degradation of pristine beach and coral communities in the Maya bay, Phi Phi Leh, southern Thailand. This paper, aims to analyze the paradox of over-tourism, income opportunities and the impact on coral community in Maya bay, based on the literatures. Ever since, Maya bay was known to the world in early 2000's, the number of tourists visiting there every day increased by close to 3000-fold in the last 20 years. Though, tourism helped to increase the local economy dramatically, later, due to impact of probably over exploitation of corals from snorkeling and diving, and wash-off of the toxic UV-filters led to bleaching of the corals. Most of the corals were dead in 20 years of tourism exploitation by 2017. Government of Thailand came up with the strategy to ban Maya bay as a tourist hotspot, and promoted coral recovery. Because of the solid policy, and action plan of the multiple stakeholders, in the last three years, corals has been significantly recovered. This paper discusses about the strength, weakness, challenges, opportunities and threat of the action plan in restoring coral community in Maya bay.

Keywords: *Maya bay, UV-filters, coral planting, bleaching, over-tourism, stakeholder management*

I. Introduction

Over-tourism is defined as a stage whereby the excessive visit by the tourists in a particular confined space leads to overcrowding and stress on the ecosystem services. A number of tourist hotspots has reported over-tourism in recent years, which includes, Barcelona - Sagrada Familia, Indonesia - Bali, India - Taj Mahal, Nepal – Everest, etc. Over-tourism occurs as a result of certain boom in unique specialty of the particular area, so called a viral status in today's digital world. Over-tourism can be short term, or long-term. Over-tourism is a shared responsibility, and can be managed by sustainable tourism. Prioritization of the welfare of the local diversity, income opportunities, and consideration to the restoration of ecosystem services are the important framework for sustainable tourism.

Tourism serves as the significant backbone of Thailand economy, contributing to as much as 10% of national GDP. Coral reefs along the gulf of Thailand and Andaman sea are one the pristine corals in the world. These corals are the marine invertebrates, which vary in shape, size, softness,

and fluorescence. The unique fluorescence of the corals, and the huge diversity of aquatic flora and fauna are depended on the reef build by the corals. Some of these corals grow at a very slow rate, about 5mm per year, and it takes hundreds and thousands of years to build the reefs. These reefs made by the corals supports ecosystem both in land and water. With an urbanization, unplanned growth, discharge of municipal solid waste and wastewater, marine plastics, coupled with climate change has brought tremendous stress to the coral community

One of the most popular tourism spots in Thailand is the pristine white sandy beaches. May bay in Phi Phi island lies in the Krabi Province, southern part of Thailand lies at 7° 40' 44.0004" N and 98° 45' 53.9964" E. The economic value of coral tourism in Phi Phi island amounts to as much as USD 300 mil (approximate value in 2020, based on 110 mil in 2003) [1].

The main factors that led to destruction of corals in Maya bay are, i) pollutants from wash-off of UV-filters used to prevent sunburn, ii) leakage of the boat gasoline, iii) recreational activities including jetski, boat, yachts, speedboats, and iv) mechanical destruction of corals during diving, anchors, and propellers.

The main objective of this paper is to review the policies behind promotion of tourism, over-tourism impact on environment and the economy, and critical analysis of restoration policies in conservation of corals in Maya bay.

II. Discussions

2.1. Over-tourism in Maya bay

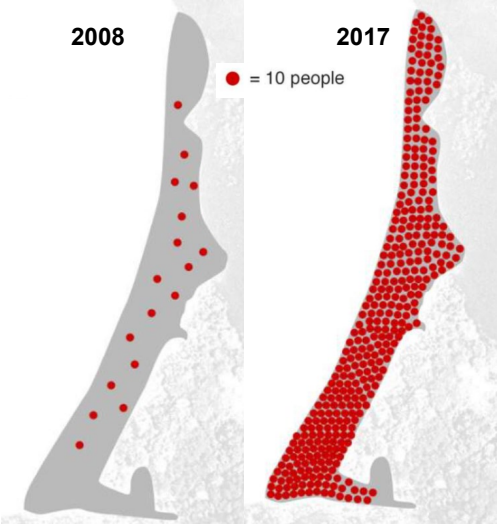

Fig. 1. Representation of the number of people visiting May bay (Adapted from [2], Saira Asher, the beach nobody can touch, BBC, 20 February 2019)

The representative figure for the over-tourism in Maya bay is shown in Fig. 1. Prior to 2000s, Maya bay was pristine. During early 2000s, by 2008, around 30% of the coral were bleached. The number of tourists in early 2000 used to be less than 10, it rose to around 170 by 2008, and by 2017, number of tourists rose to as much as 4000. The beach in itself is around 200m. As much as 18 million tourists were reported to visit Maya bay, Phi Phi Island in 2017 [3]. This huge number of people in such a confined area exerted tremendous pressure on the coral environment. The increase in tourism, though significantly led to increase in local economy, however also led to some serious problems like, disposal of solid waste at the beach, degradation of water quality, and coral bleaching. The rate of coral bleaching, and haphazard waste along the Maya bay beach continuously increased, as a result, close to 90% of the corals were degraded by early 2010. Still, due to popularity of the beach, led to increase in number of tourists. By 2015, almost all corals were bleached. This send an alarming message, as a result, Government of Thailand proposed a policy to completely banned tourism in Maya bay in 2018. Slowly and steadily corals are being restored. However, recovery is a slow process.

2.2. Economic aspects of tourism

According to the data of Ministry of Tourism and Sports, Thailand, the number of tourists visiting Thailand has increased dramatically in the last 50 years. It used to be less than 100,000 in 1960, and has increased to 10 million by 2000. Furthermore, with intensive tourism marketing, Thailand welcomed close to 40 million tourists in 2018. This makes Thailand one of the most popular tourist spots in the world. Most of the tourists do visit the white sandy Thai beach - railway beach, Koh Phi Phi, Tonsai beach, etc. At Maya bay, local government charges ~ 14 USD per person to visit the beach, and with close to 4000 people visiting Maya bay every day, the amount of revenue generated per day is quite huge ~ 56,000 USD. Tourism can have multiple impact on environment, economic, local community, infrastructure including hotel, transportations, transportation, ecosystem services, all of which are again interrelated and interdependent.

2.3. Coral restoration and conservation strategy

Thai government was aware about the impact of over-

tourism on ecosystem services in Maya bay. The steps taken by the Thai government in preserving corals in Maya bay includes, initiation of fine by the local environmental authorities of ~ 18 USD to boat operators who throw anchors into the water, waste collection bin, banning on fishing and construction. It was however difficult to follow the implementation, due to lack of manpower on monitoring, and also ignorance from the tour operators. Even, some tour operators, who used to bring lots of tourist, continued to pay fine and breached the directives. Following a series of campaigns by the environmentalist, Thai government banned a visit to Maya bay by judicatory order in June 2018, firstly for a period of 6 month, and later from Oct 1, 2018 has been closed indefinitely [3].

2.3.1 Engineering aspects of coral restoration

A number of reports are available on the coral restoration strategies, among them a study by Boström-Einarsson et al., (2020) seems quite comprehensive [4]. One of the biggest problems in coral restoration is that, each restoration is seen as a project lasting 6 to 24 months. A restoration of up to 12 years has been done in Caribbean coral reefs, which was though successful but was not a solution to restore coral community. The restoration methods can be divided into physical, biological and structural restoration. Some of the restoration strategies as proposed by Boström-Einarsson et al., (2020) includes direct transplantation of coral, coral gardening, micro-fragmentation, genetic diversity in asexual propagation, larval enhancement, artificial reefs, and substratum stabilization.

2.3.2 Japan experience on coral restoration

In Japan, the action plan to conserve coral reef ecosystem [5] has been focused on three priority issues, i) measures against negative impact from runoff, ii) promotion of regional economy through sustainable tourism, and iii) promotion of harmonic relationship between community and ecosystem. The basic action to realize above three priority issues includes, information sharing, awareness training, communication outreach, capacity development, restoration projects, planned urbanization and coastal reconstruction, water quality conservation, surveillance and monitoring, treatment of effluents, sustainable use of marine ecosystem services, and follow up and review.

2.4. Sustainable tourism

It is really quite complex to define the indicator for sustainable tourism. Qualitatively, it can be said as the maximum number of tourists that can be handled by operating sites, without hampering the aesthetic tourism quality. Koh and Fakfare (2019) recently proposed the unique strategy for the stakeholder management for the restoration of Maya bay – the BRAVE framework consisting of business, residents, authorities, visitors and environmentalists [6]. The interests of different stakeholders are different. Since, a beach area is quite open. It is nearly impossible to restrict the number of people entering such kind of open area, it all depends on concept of "responsible tourism", whereby the BRAVE framework proposes the integrated action plan to limit the number of visitors at a particular site, perhaps alternate spots of tourism sites, proper waste collection strategy, and promoting the use of non-toxic UV-filters.

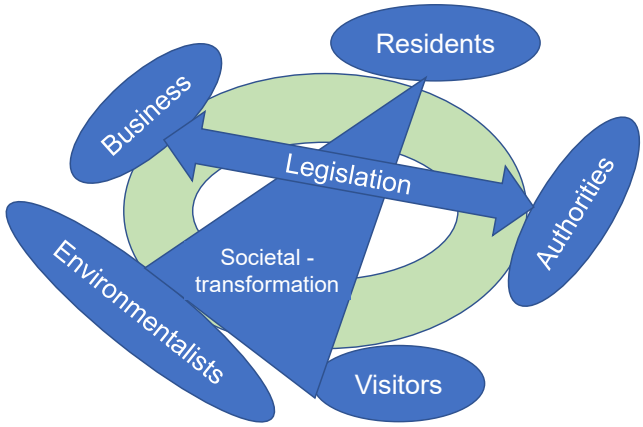

Fig. 2. Conceptual framework for achieving sustainable tourism (Adapted from [6], Koh and Fakfare (2019). (Unscaled / qualitative figure)

The framework for the sustainable tourism is shown in **Fig. 2.** The concept is adapted from BRAVE framework proposed by Koh and Fakfare, 2019. The green circle represents the interdependency of the BRAVE stakeholders. The tourism business can be checked by the authorities by the legislation. The aim of this legislation should not be to grip business, but provide the competitive access for business opportunities to all the interested one. The three other players, residents, visitors and environmentalists sole depend on the societal-transformation strategy, which means to take responsibility for the conservation of environment, without unduly compromising on one's wish, to promote responsible tourism.

2.5. SWOT analysis

The SWOT analysis of the conservation strategy taken by the Thai authorities is given in **Table 1.** The strong government approach in conservation, and availability of plenty of alternative tourist spots are the strength and opportunities of the project. Training of the tour operators, and maintaining database on spatio-temporal variation of tourist visit, frequency, time period is a challenge and a weakness. However, definition of sustainable tourism in terms of quantitative variables is really complicated. The proper balance between SWOT will lead in success of the conservation strategy.

Table 1. SWOT analysis of coral restoration strategy in Maya bay, Thailand

Strength	**Weakness**
• Strong government and local people support • Funding opportunities for the restoration, • Alternate tourism opportunities	• Quantitative parameters to define sustainable tourism • Qualitative and quantitative measure to define pollution, and economy
Opportunities	**Threat**
• As a model site for studying case of over-tourism • Multiple stakeholder engagement • Consensus between government, tourism operators, and local people	• Poacher tourism • Continuity of the preventive measures • Change in policy due to socio-economic pressure • Lack of trainings on sustainable tourism

III. Conclusion

There are 11 strategies proposed by the United Nations World Tourism Organization to manage over-tourism, some of which includes, promotion and dispersion on a time and location basics, visitor segmentation, review of the policies, and establishment of the surveillance and monitoring mechanism [7].

Impact of restoration policies are promising, and significant improvement in coral community and water quality has been observed in two years in Maya bay. However, it is still early days of coral restoration, which is a time-consuming process. Hence, all the stakeholders should be patient, and the decision to resume tourism in Maya bay should be supported by the quantitative evidence-based policies, and quantitative indicators. Maya bay is just one of the beaches affected by over tourism. Conservation strategy should be extended to all the beaches, in the form of sustainable and responsible tourism.

Acknowledgement

Authors would like to express gratitude to Asia-Pacific Network for Global Change Research for funding this project - "Collaborative Research Platform to Manage Risk and Enhance Resilience of Coral Reef in Southeast Asia, CRRP2019-08MY-Khanal".

References

[1] Christiernsson, A. 2003. An Economic valuation of the coral reefs at Phi Phi Island, master's thesis, Department of business administration and spocial sciences, Lulea university of Technology,

[2] Saira Asher, the beach nobody can touch, BBC, 20 February 2019) assessed December 10, 2020 and available at https://www.bbc.co.uk/news/resources/idt-sh/the_beach_nobody_can_touch

[3] SeATM, 2018. South east asia tourism monitor, briefing on tourism, development and environment, Vol. 9, No.3, May – June 2018

[4] Boström-Einarsson L, Babcock RC, Bayraktarov E, Ceccarelli D, Cook N, Ferse SCA, et al. (2020) Coral restoration – A systematic review of current methods, successes, failures and future directions. PLoS ONE 15(1): e0226631

[5] MOE, 2017. The Action Plan to Conserve Coral Reef Ecosystems in Japan 2016 – 2020. Biodiversity Policy Division, Nature Conservation Bureau, Ministry of the Environment, Japan

[6] Koh, E., & Fakfare, P. (2019). Overcoming "over-tourism": The closure of Maya Bay. International Journal of Tourism Cities, 6, 2, pp. 279-296

[7] World Tourism Organization (UNWTO); Centre of Expertise Leisure, Tourism & Hospitality; NHTV Breda University of Applied Sciences; and NHL Stenden University of Applied Sciences (2018), 'Overtourism'? – Understanding and Managing Urban Tourism Growth beyond Perceptions, Executive Summary, UNWTO, Madrid

The 13th AUN/SEED-Net Regional Conference on Chemical Engineering 2020 (RCChE-2020)
Jointly held with
The 5th International Symposium on Conservation and Management of Tropical Lakes
"Insights and Challenges toward Achieving SDGs"

Development of a Package Containing PAC and $Ca(OCl)_2$ for Drinking Water Treatment of Lake Water

Sereyvathana SOK[1], Phary THACH[1], Kazuhiko MIYANAGA[2] and Reasmey TAN[1,3,*]

[1] *Faculty of Chemical and Food Engineering, Institute of Technology of Cambodia, Russian Federation Blvd., P.O. Box 86, 12156 Phnom Penh, Cambodia*
[2] *School of Life Science and Technology, Tokyo Institute of Technology, 4259 J3-8 Nagatsuta-cho, Midori-ku, Yokohama, 226-8501, Japan*
[3] *Food Technology and Nutrition Research Unit, Research and Innovation Center, Institute of Technology of Cambodia, Russian Federation Blvd., P.O. Box 86, 12156 Phnom Penh, Cambodia*
* *Corresponding author: rtan@itc.edu.kh*

Abstract

The conventional treatment practices by villagers of usage alum can cause overdosing of concentration of alum since it can cause the water taste to be sour and is considered as the health risk in drinking water such as vomiting, diarrhea, mouth and skin ulcers, and so on. Therefore, the objective of this study was conducted by comparing the effects of yellow PAC and white PAC in removing turbidity, changing pH value, and settling time and the effects of using $Ca(OCl)_2$ in removing bacteria in lake water to develop a package containing PAC and $Ca(OCl)_2$. To achieve these objectives, the lake water sample was treated with the yellow PAC and white PAC. Two methods were used in bacteria removal, sole using of $Ca(OCl)_2$ and dual using of $Ca(OCl)_2$ with PAC. As a result, the highest efficiency of turbidity removal was within 97.66–99.89% and 91.55–99.88% for yellow and white PAC, respectively between the settling time of 60–120 mins. The changed of pH for yellow PAC complied with the standard for drinking water which is 6.5–8.5, while the pH for white PAC did not comply with the standard. For the results of bacteria removal, 100 % of *E. coli* was removed in both methods and 98.8–99.4% for the first method and 96.3–99.4% for the second method of total coliform removal were achieved. Overall, yellow PAC showed the better performance in removing turbidity, subsequently the second method of bacteria removal showed the best settling time is 60–120 mins. Moreover, yellow PAC has gradually changed in pH and adjusting pH was not need. Finally, It was conducted the net contents of one package are 12.75g which is contained yellow PAC and $Ca(OCl)_2$ for treating 100 L of lake water.

Keywords: *Bacteria removal, E. coli, Settling time, Total coliform, Turbidity removal.*

I. Introduction

Turbidity is a degree measurement of water clarify [1]. It is used as an indicator of water property that is based on purify and total suspended solids contained in the water [2]. The high amount of these small solid particles that is existed

in the water, the greater turbidity of the water will be high. The familiar pollutant to turbidity is organic matter which is a major cause of the quality of surface water. Turbidity is generally source from the small discrete mass of solids in the water which is connected with muddiness and color. Turbidity is commonly indicated by using turbidity meter. Turbidity is described in the united that called a Nephelometric Turbidity Unit (NTU) or a Jackson Turbidity Unit (JTU) [3].

Coagulation and flocculation are utilized to remove the organic matter from the water [4]. Coagulation and flocculation are taken place in serial steps that permit particle collision and growth into floc, then followed by sedimentation. The serial steps are connected, if coagulation is incomplete, the following steps are also incomplete and will be unsuccessful.

Total coliform bacteria refer to a broad span of facultatively anaerobic and aerobic, a large group of Gram-negative, non-spore-forming bacilli have an ability for developing in the presence of a comparatively high concentration of bile salt with the process of fermenting of lactose and a product of acid/ aldehyde in the limit of 24 hours at 35-37 °C [5]. Total coliform was presented in nature such as soil, vegetation, and water. Normally, they are located in fecal-polluted water and usually connected with a disease outbreak. *Escherichia coli* is a type of gram-negative bacilli of family Enterobacteriaceae [6]. In most water, the greater in number genus is Escherichia, and yet some species of Citrobacter, Klebsiella, and Enterobacter are also thermotolerant. *Escherichia coli* can be distinguished from the other thermotolerant coliforms by the capability to create indole from tryptophan or the creation of the enzyme β-glucuronidase [5].

II. Materials and Methods

2.1. Sampling sites

Lake water was collected from Boeung Choeung Ek with coordinate 11.466076, 104.914543 which is located Sangkat Choeung Ek, Khan Dangkor, Phnom Penh during the rainy season. The sample was collected in plastic bottles of 1.5 L. After sampling, the sample was transported immediately to ITC laboratory to analyze within a day.

2.2. Preparation of stock solution

2.2.1. Polyaluminum chloride (PAC)

1 g of PAC powder was suspended in 99 mL of distilled water to produce a PAC stock solution of 1% and stirred at room temperature until it homogenizes. 1 mL of 1% stock solution was contained 10 mg, therefore, the added 1 % solution to 1 L of water is 10 mg/L.

2.2.2. Calcium hypochorite ($Ca(OCl)_2$)

0.1 g of calcium hypochlorite granule was suspended in 100 mL of distilled water to produce Ca(OCl)2 stock solution and stirred at room temperature until it homogenizes. 1 mL of stock was contained 1 mg. 1 ppm of free chlorine was obtained by diluted 5 mg (5 mL) of $Ca(OCl)_2$ stock in 1 L of water (5 mg/L). This value was obtained by an actual measurement using the N, N-diethyl-ρ-phenylenediamine (DPD) method using the Free/Total Chlorine Colorimeter.

2.3. Experimental procedures

2.3.1. Coagulation and flocculation experiments

The lake water sample was priority treated with coagulants (yellow PAC and white PAC) to find the optimal dose in removing turbidity. High turbidity with 943 NTU of lake water sample was diluted with distilled water to obtained new initial turbidity 753 NTU, 558 NTU, and 341 NTU randomly. 500 mL of the sample of each condition of initial turbidity was filled in 3 beakers and were treated with two types of PAC products such as yellow and white to indicate one suitable product to make the package for lake water treatment.

2.3.2. Disinfection experiments

2.3.2.1. Sole using of $Ca(OCl)_2$

The 500 mL of lake water sample was primarily treated with 120 mg/L of yellow PAC for 60 mins. 250 mL of water sample after treatment was taken into a new bottle and treated with three different doses of $Ca(OCl)_2$. The sample was stirred for 1 min within 200 rpm and set for the contact time for 60 mins.

2.3.2.2. Dual using $Ca(OCl)_2$ with PAC

500 mL of lake water sample was filled in 3 sterilized bottles and treated with 120 mg/L of yellow PAC and stirred for 1min within 200rpm and then three different concentrations of $Ca(OCl)_2$ were added to the samples and continuously stirred for 2 min at the same stirring speed and set for the contact time for 60 min.

2.4. Analytical methods

2.4.1. Turbidity measurement

In each settling time, 10 mL of sample were collected at 3 cm below the surface level. The turbidity measurement of treated water was measured by using HANNA-HI 98703 Portable Turbidimeter in three replicates for accuracy. The turbidity removal efficiency was calculated by using Eq.1.

$$Turbidity\ removal(\%) = \frac{(T_i - T_f)}{T_i} \times 100 \qquad \text{(Eq.1)}$$

where T_i and T_f are the initial and final turbidity, respectively

2.4.2. pH measurement

At the end of the experiment, the sample was taken to measure the change of pH in using yellow and white PAC. The measurement was done by using WM-32EP EC/pH meter.

2.4.3. Microbiological analysis

After each performed treatment, the samples were taken for total coliform and *E. coli* count. 100 mL of sample was filtered by using Whatman® sterile membrane filters without absorbent pads with diameter 47 mm and pore size 0.45 µm and was cultured on each Chromocult® Coliform agar plate which was then incubated at 36 ± 2 ℃ for 21-24 h.

The number of colony-forming unit (CFU) of 100 mL water sample was expressed in the formula:

$$\text{CFU/100mL} = \left(\frac{\text{number of colony counted}}{\text{sample volume filtered in mL}}\right) \times 100 \qquad \text{(Eq.2)}$$

The bacteria removal efficiency was calculated by :

$$\text{Bacteria removal (\%)} = \frac{Bac_i - Bac_f}{Bac_i} \times 100 \qquad \text{(Eq.3)}$$

where Bac_i and Bac_f are the initial and final bacteria that were counted.

2.5. Statistical analysis

All data were subjected to analysis of variance (ANOVA). P-value lower than 0.05 indicates that the data are considered to be statistically significant.

III. Results and Discussion

The physicochemical characteristics of the lake water sample such as turbidity, pH, and bacteria (total coliform and *E. coli*) were analyzed. After the measurement, the parameter of turbidity was 943 NTU and pH was 7.72, while the parameter of bacteria was 4.03×10^3 of total coliform and 2.37×10^2 of *E. coli* as illustrating in **Table 1.**

Table 1. Physicochemical characteristics of lake water

Parameter	Value
Turbidity (NTU)	943
Total coliform (CFU/100ml)	4.03×10^3
E. coli (CFU/100ml)	2.37×10^2
pH	7.72

3.1. Effect of PCA on turbidity removal

Figure 1 expresses in the effect of yellow PAC and white PAC on turbidity removal in various conditions of turbidity after treated for 120 min. For each figure, it was clearly shown that each dose of yellow PAC is more effective than the dose of white PAC. Therefore, yellow PAC was chosen due to its high effectiveness in turbidity removal comparing to white PAC. Alternately, the comparison of all concentration dosages of yellow PAC was significant, thus the amount of yellow PAC between 60-120 mg/L can completely remove the turbidity with a range from 300-1000 NTU to below 5 NTU.

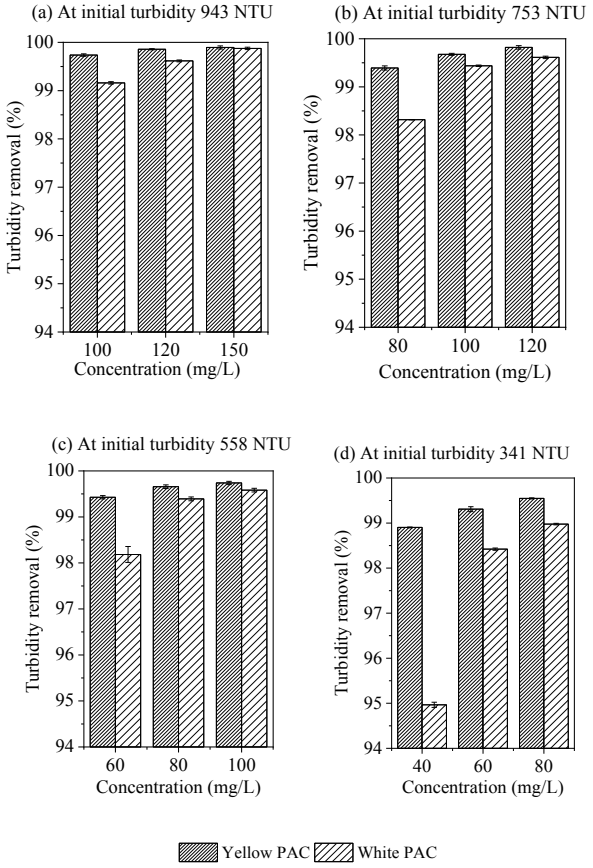

Figure 1. Effect of yellow PAC and white PAC dosage on turbidity removal in varies condition of turbidity after treated for 120 mins

3.2. Effect of PAC on changing pH value

As a result, in each initial turbidity, the change of pH in using each dose of yellow PAC was fallen into the standard for drinking water 6.5-8.5. In contrast, th e change of pH when using each dose of white PAC was fallen out from standard that was allowed for dri nking water except some doses of 100 mg/L, 80 mg/L, 60 mg/L, and 40 mg/L. Therefore, using yellow PAC

has gradually changed in pH and it did need to adjust pH before or after treatment and it is suitable for the small scale of drinking water treatment.

3.3. Effect of settling time in turbidity removal

the percentage of turbidity removal of using yellow PAC and white PAC gradually increased from low to high dose from 15 min to 120 min of settling time. at the settling time 60-120 min, the average of high re moval of turbidity is more than 99% in using yellow PAC and 98% of using white PAC.

3.4. Effect of $Ca(OCl)_2$ on bacteria removal

The comparison of both conditions of using $Ca(OCl)_2$was clearly shown that the first method of using only $Ca(OCl)_2$ is more effective than the second method of using $Ca(OCl)_2$with PAC. However, the second method of using $Ca(OCl)_2$ with PAC with a dosage of 7.5 mg/L had the same effect in reducing bacteria to the first method where 99.4% in removing total coliform, and 100% in removing *E. coli*.

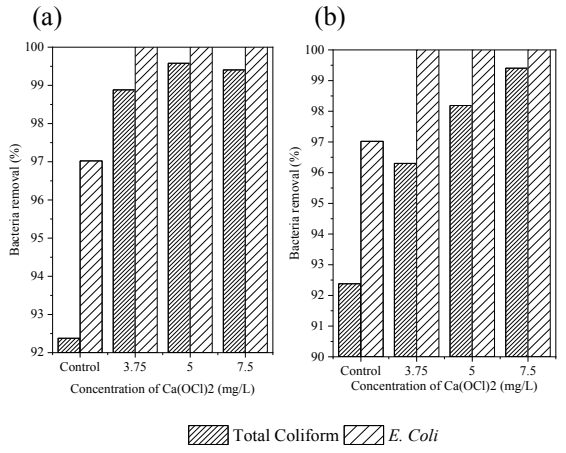

Fig. 2. Effect of $Ca(OCl)_2$on bacteria removal at the contact time for 60 mins:(a). The first method of using only $Ca(OCl)_2$ and (b).the second method using $Ca(OCl)_2$ with PAC.

3.5. The packages of yellow PAC with $Ca(OCl)_2$

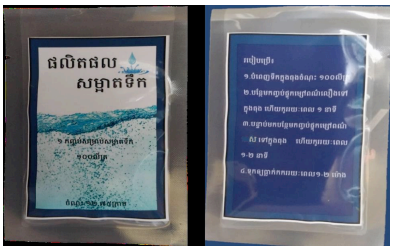

Fig. 3. Package containing yellow PAC and $Ca(OCl)_2$

IV. Conclusion

The development of a package containing yellow PAC and $Ca(OCl)_2$ was made after this study. The package was forming where the net contents of one package are 12.75g and capable for treating 100L of water. Additionally, yellow PAC displayed the better performance comparing to white PAC in removing turbidity with more than 99% owing to the various raw materials and producing methods. Thus, this made yellow PAC more suitable for drinking water process. Also, the two methods of using $Ca(OCl)_2$ showed a slight difference in removing bacteria with more than 98% in removing total coliform and 100% of *E. coli*.

Acknowledgement

We are thankful to the Science and Technology Research Partnership for Sustainable Development (SATREPS), the Japan Science and Technology Agency (JST)/Japan International Cooperation Agency (JICA) for their financial support.

References

[1] Environmental Protection Agency, 2012. 5.5 Turbidity. InWater:Monitoring&Assessment,https://archive.epa.gov/ water/archive/web/html/vms55.html (Consulted on April 01, 2020).

[2] Perlman, H., 2014. Turbidity. In the USGS Water ScienceSchool,http://ky.gov/nrepc/water/ramp/rmtss.htm (Consulted on April 01, 2020).

[3] Fondriest Environmental, Inc, 2014. "Turbidity, Total Suspended Solids and Water Clarity." Fundamentals of EnvironmentalMeasurements,https://www.fondriest.com/environmentalmeasurements/parameters/water-quality/turbidity-total-suspended-solids-water-clarity/ (Consulted on March 29, 2020).

[4] Prakash, N.B., 2015. Waste Water Treatment by Coagulation and Flocculation. *International Science and Innovative Technology (IJESIT)*, 3, 479.

[5] World Health Organization, 2011. Guidelines for drinking-water quality-4th ed. WHO Library Cataloguing-in-Publication Data, 1–564.

[6] Bhavsar, S., and Krilov, L., 2015. Escherichia coli Infections. Pediatrics in review/American Academy of Pediatrics, 36, 167–71.

The 13th AUN/SEED-Net Regional Conference on Chemical Engineering 2020 (RCChE-2020)
Jointly held with
The 5th International Symposium on Conservation and Management of Tropical Lakes
"Insights and Challenges toward Achieving SDGs"

Assessment of Particle Size Fraction Distribution of Surface Sediment of Tonle Sap Lake, Cambodia: A Case Study in Chhnok Tru.

Vibol CHEM[1], Rina HEU[3,4,*], May Phue WAI[1], Sochetra SEN[2], Kimheang THAI[2], Khy Eam EANG[3] and Sokly SIEV[2, 4]

[1]*Graduate School of Water and Environmental Engineering, Institute of Technology of Cambodia, Russian Federation Blvd, P.O. Box 86, 12156 Phnom Penh, Cambodia*
[2]*Faculty of Chemical and Food Engineering, Institute of Technology of Cambodia, Russian Federation Blvd., P.O. Box 86, 12156 Phnom Penh, Cambodia*
[3]*Faculty of Hydrology and Water Resource Engineering, Institute of Technology of Cambodia, Russian Federation Blvd., P.O. Box 86, 12156 Phnom Penh, Cambodia*
[4]*Water and Environmental Research Unit, Research and Innovation Center, Institute of Technology of Cambodia, Russian Federation Blvd, P.O. Box 86, 12156 Phnom Penh, Cambodia*
*heu.rina@itc.edu.kh

Abstract

Tonle Sap Lake (TSL), located in the center of Camboida, is the largest productive freshwater lake in Southeast Asia regions. TSL gives a huge benefit to Cambodians, especially for riparian settlements along the lake. However, changes in hydrology and water depth in the lake appear to be the main factors affecting the variability in the particle size distribution in sediment and its properties. Thus, this study aims to evaluate the D_{50} of particle size distribution and understand the compostioins of surface sediment as an ecological function of the lake. The extensive sampling survey was conducted to collect samples of surface sediment from 18 sampling sites around Chhnok Tru. The particle size distribution (PSD) was analyzed by using Laser Diffraction Particle Size Analyzer. A synthetic analysis showed that particle size fraction of surface sediment was a sensitive and effective mechanism to understand climatic and environmental changes of the lake around Chhnok Tru. Netherless, changes in PSD between different varve types were relatively small indicated that they have a similar source for the material deposition. The result also showed that the median fraction (D_{50}) of surface sediment was ranged from 164µm to 694µm consisted of 83.32% sand, 1.22% silt, and 15.46% clay. Therefore, the smaller sediment fractions and variation may attribute to the location of the flow affected by the current in the turbulence area. Besides, smaller fractions appear to carry out most of the photosynthesis around Chhnok Tru, while larger fractions are responsible for seasonal trends in sedimentation. Overall, PSD showed from poor to very poor sorting, and generally sorting deteriorated with increasing mean grain-size. The output information about particle size distribution is essential for the characterization of mineral components of biogenic lake sediments leading to understanding the changes in physical and biological trends in the lake around Chhnok Tru.

Keywords: *Assessment, Chhnok Tru, Particle size distribution, Surface sediment, and Tonle Sap Lake*

I. Introduction

Tole Sap Lake (TSL) is the largest productive lake in South-East Asia in which it covers land areas of approximately 3,000 km^2 in the dry season to more than 15,000 km^2 in the rainy season [1]. For the water depth of TSL, it is varied from 0.8 to 1 meters of water level in the dry season, while in the wet season, the water level is varied from 10 to 12 meters [2]. TSL has provided a huge benefit to Cambodian people especially for the riparian settlements along the lake. Unfortunately, scientific information about its productivities as natural resources is not well understood. In an aquatic environment, different compounds are incorporated within or absorbed on mineral matter depending on the physical, chemical, and biological processes that may change substantially the sediment texture [3].

Sediments in lakes play an important role in elemental cycling in the aquatic environment, and they are responsible for transporting a significant proportion of many nutrients and contaminants [4]. The sediments also mediate their uptake, storage, release, and transfer between environmental compartments. Most sediment on the surface of the bottom of the lake derives from surface erosion and comprises a mineral component, arising from the erosion of bedrock, and an organic component arising during soil-forming processes included biological and microbiological production and decomposition, and the additional organic component may be added by biological activity within the water body [5]. Besides, the grain-size analysis is useful for more than the characterization of the mineral component of biogenic lake sediments, and particle size distribution is important for understanding the physical and chemical properties of a material [6]. The median of 50% particle size fraction in sediment is the practical understanding of the distribution of particle; based on size fraction. On top of that, the importance of the D_{50} is to understand the dynamics and other geomorphological behaviors of the lake. Particle size and mineralogy are directly related because individual minerals tended to form within characteristic size ranges. Sediments may thus be described in terms of discrete compositional fractions, the overall characteristics of which are due to the variation in the proportions of these fractions, and the consequent changes in particle size [7]. However, there is much not known or understood about the productive ecological systems of the aquatic ecosystem of TSL, and how they interact between surface sediment and the productive systems.

II. Materials and Methods

2.1. Sampling sites

The sampling points of the study were taken randomly based on geological features around Chhnok Tru of Tonle Sap Lake; Kampong Chhnang province, by applying the mapping waypoints of coordinated system. In addition, there were 18 samples were collected on 5th March 2020 during dry season as shown in **Fig. 2.1**.

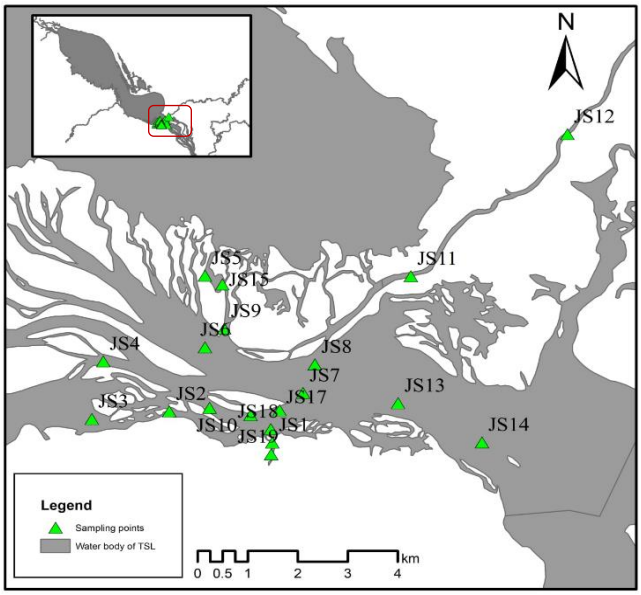

Fig.2.1: Mapping of sampling sites in TSL

The grab sampler was used to sample the surface sediment of the lake, and the sediment samples were transferred into plastic zip-locks then kept in an ice-box to maintain the quality of samples and transported to the laboratory for analysis. Critically, we assumed that the constant temperature in an ice-box is 4°C which prevents bacterial activity that could modify their properties [8].

2.2. Laser Diffraction Particle Size Analyzer

Laser diffraction particle size analyzer (SALD-2300, SHMADZU, Japan) was used to measure the size fraction of particles of 18 samples. The particle size was calculated by measuring the angle of light scattered by the particles as they pass through a laser beam through the dispersion of particles [9]. The light that is scattered at various angles by different particle sizes was measured by a multi-element detector, and the magnitude of scattered light intensities was recorded [10]. Moreover, sediment samples were analyzed for particle size fractions using the light intensity of cumulative percentages

of the ranging size of particles in micrometer. The D_{50} of particle size fraction were studied to understand 50% distribution of particle fractions of samples.

2.3. Analytical methods

The categorization of particle size fraction was based on the diameter of the particle in micrometer (**Table 2.1**) [5,11]. Thus, the size fraction was summarized into types of sediment such as sand fraction, silt fraction, and clay fraction which was in ranges of their diameters from mean of 18 points, based on percentages.

Table 2.1: Sediment types based on particle size diameter

Sediment types	Diameter	Unit
Sand	smaller than 2000	µm
Silt	smaller than 63	µm
Clay	smaller than 20	µm

Overall, the median of 50% particle size fraction was studied to understand the distribution of surface sediment around Chhnok Tru, and its critical associations to physical and biological changes of the lake.

The PSD of sediment samples was found in arithmetic means of cumulative percentage of each sampling site. Furthermore, they was plotted by means of its cumulative percentages with the particle diameter in micrometer. For graphical analysis, Origin Pro-2021 program was used.

III. Results and Discussion

The sediment types and their mean percentages from 18 sampling points as a summary of surface sediment samples around Chhnok Tru were shown in **Table 3.1**.

Table 3.1: Mean composition from 18 sampling sites

Sediment	Diameter	Percentage (%)
Sand	< 2000 µm	83.32
Silt	< 63 µm	1.22
Clay	< 20 µm	15.46

In **Table 3.1**, it revealed that the particle size fraction of sand fraction showed the highest composition in surface sediment samples of Chhnok Tru with 83.23%, while it was followed by clay fraction and silt fraction of 15. 46% and 1.22%, respectively. Moreover, the standard deviation (SD) of sand fraction showed in higher value of 13.12 followed by clay of 12.08, while silt was the lowest of 1.88 as shown in **Fig.3.1**. Therefore, the higher value of SD the higher error of sand, clay and clay, accordingly.

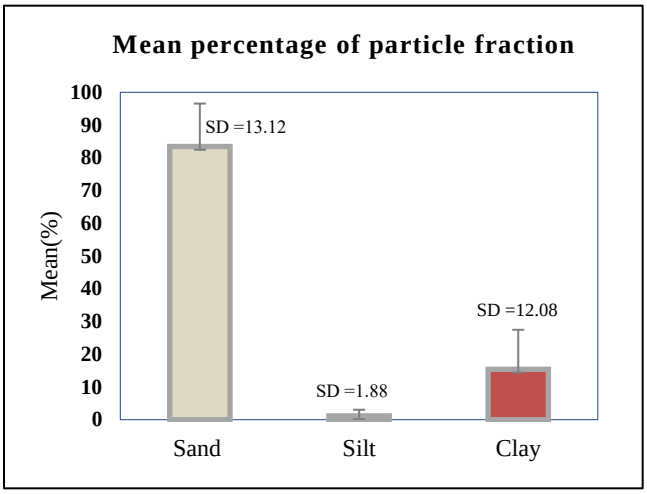

Fig.3.1: Mean of each particle fraction

The analytical measurement of PSD by particle size analyzer showed the quantitative value of particle size in range with its cumulative percentage which is based on light intensity as shown in **Fig. 3.2**. In addition to the PSD curve, the result showed about D_{10}, D_{50} and D_{90} of sediment distribution. Thus, the 50% of median fraction (D_{50}) of surface sediment was ranged from 164µm to 694µm with its mean of 300µm from each sampling site. This was meant that the 50% of particle size was sand fraction in which it showed the biggest diameters among other fractions.

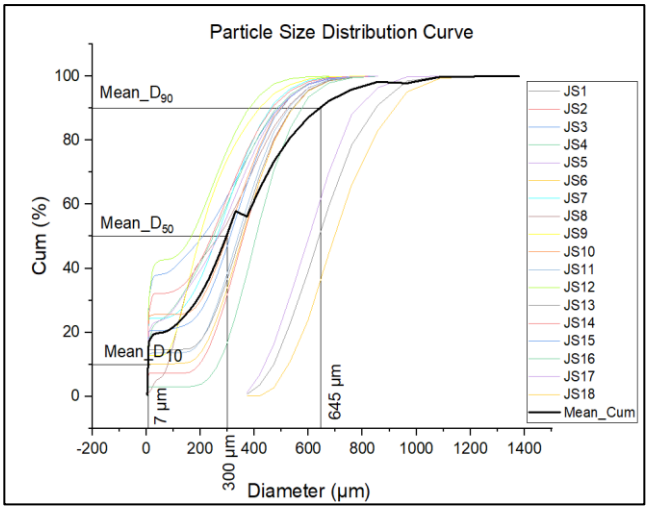

Fig.3.2: PSD curve of surface sediment of TLS

Therefore, smaller sediment fractions and variation may attribute to the location of the flow affected by the current in

the turbulence area. Besides, smaller fractions appear to carry out most of the photosynthesis in the lake, while larger fractions are responsible for seasonal trends in sedimentation. Also, there was a study that showed a similar result that sediments from lake expressed that biological and chemical content accumulated on the particles from 100 to 1000 μm in which there was a tendency associated with increasing basic content as far as decreasing particle size [12].

IV. Conclusion

Tonle Sap Lake (TSL) is the most productive lake in South-East Asia. Thus, understanding the pattern of the ecosystem of the lake around Chhnok Tur is the crucial benefit to estimate the interaction between sediment and its potential influents on the physical and biological condition of the lake. According to the result of the study, the surface sediment around Chhnok Tru was a sand fraction with the highest composition of 83.23%. In addition, the mean of D_{50} of PSD was also a sand fraction which came up with the mean of D_{50} of 300μm. Therefore, it could be concluded that the smaller sediment fractions, and the variation may attribute to the location of the flow affected by the current in the turbulence area. Moreover, PSD of surface sediment around Chhnok Tru might strongly interact with productivities in the lake as macronutrients for the growth for higher productivities.

Acknowledgment

We are thankful to the Science and Technology Research Partnership for Sustainable Development (SATREPS, Grant No: JPMJSA1503), the Japan Science and Technology Agency (JST)/Japan International Cooperation Agency (JICA), and French Developmet Agency (AFD), Grant No:CKH 1236 02P) for their financial support.

References

[1] Kite, G. (2001). Modelling the Mekong: Hydrological simulation for environmental impact studies. Journal of Hydrology, 253(1), 1–13. https://doi.org/10.1016/S0022-1694(01)00396-1

[2] Somony, T., & Schmidt, U. (2004). Aquatic Resources Management: The Tonle Sap Great Lake, Cambodia. 19.

[3] Vaasma, T. (2008). Grain-size analysis of lacustrine sediments: A comparison of pre-treatment methods. Estonian Journal of Ecology, 57(4), 231. https://doi.org/10.3176/eco.2008.4.01

[4] Uk, S., Yoshimura, C., Siev, S., Sophal, T., Yang, H., Oeurng, C., Li, S., & Hul, S. (2018). Tonle Sap Lake: Current status and important research directions for environmental management. Lakes & Reservoirs: Research & Management, 23. https://doi.org/10.1111/lre.12222

[5] Bartram. (1996). (PDF) Water quality monitoring: A practical guide to the design and implementation of freshwater quality studies and monitoring programmes. ResearchGate. https://www.researchgate.net/publication/253953121_Water_quality_monitoring_a_practical_guide_to_the_design_and_implementation_of_freshwater_quality_studies_and_monitoring_programmes

[6] Żarczyński, M., Szmańda, J., & Tylmann, W. (2019). Grain-Size Distribution and Structural Characteristics of Varved Sediments from Lake Żabińskie (Northeastern Poland). Quaternary, 2(1), 8. https://doi.org/10.3390/quat2010008

[7] Chapman, D. V., Organization, W. H., Unesco, & Programme, U. N. E. (1996). Water quality assessments: A guide to the use of biota, sediments and water in environmental monitoring. London : E & FN Spon. https://apps.who.int/iris/handle/10665/41850

[8] Eadie, B J, and S J Lozano. (1999). Grain Size Distribution of the Surface Sediments Collected during the Lake Michigan Mass Balance and Environmental Mapping and Assessment Programs. 42.

[9] Hackley, V. A., Gintautas, L., & Lum, L.-S. (2004). (PDF) Particle Size Analysis by Laser Diffraction Spectrometry: Application to Cementitious Powders. ResearchGate. https://www.researchgate.net/publication/238669156_Particle_Size_Analysis_by_Laser_Diffraction_Spectrometry_Application_to_Cementitious_Powders

[10] Lawrence, J. (2017). Particle Size and Distribution Analysis. Chemical Engineering.

[11] Blair, T. C., & McPherson, J. (1999). Grain-size and textural classification of coarse sedimentary particles. Journal of Sedimentary Research, 69, 6–19. https://doi.org/10.2110/jsr.69.6

[12] Maslennikova, S., Larina, N., & Larin, S. (2012). The effect of sediment grain size on heavy metal content. Lakes Reservoirs and Ponds, 6, 43–54.

The 13th AUN/SEED-Net Regional Conference on Chemical Engineering 2020 (RCChE-2020)
Jointly held with
The 5th International Symposium on Conservation and Management of Tropical Lakes
"Insights and Challenges toward Achieving SDGs"

Occurrence, Transportation, Regulation and Treatment Methods of Organic Pollutants in Surface Water: A Review on Case of Tonle Sap Lake, Cambodia

Mardi Meas [1], Rina Heu [2,4,*], Laty Ma [1], KhyEam Eang[2], and Sokly Siev[3,4]

[1]*Graduate School of Water and Environmental Engineering, Institute of Technology of Cambodia, Russian Federation Blvd, P.O. Box 86, 12156 Phnom Penh, Cambodia*
[2]*Faculty of Hydrology and Water Resource Engineering, Institute of Technology of Cambodia, Russian Federation Blvd., P.O. Box 86, 12156 Phnom Penh, Cambodia*
[3]*Faculty of Chemical and Food Engineering, Institute of Technology of Cambodia, Russian Federation Blvd., P.O. Box 86, 12156 Phnom Penh, Cambodia*
[4]*Water and Environmental Research Unit, Research and Innovation Centre, Institute of Technology of Cambodia, Russian Federation Blvd., P.O. Box 86, 12156 Phnom Penh, Cambodia*
*heu.rina@itc.edu.kh

Abstract

Tonle Sap Lake (TSL), the largest freshwater lake in Southeast Asia, plays an important role in the economy of Cambodia. It supports the population around it through fishery productivity, water supply and variety of biodiversity. Currently, regional residents around TSL purchase clean water for their daily consuming from private water supply facility that use raw water from TSL. However, there are growing concerns related to degradation of the quality of lake water. Even though, TSL is invaluable by its ecosystems, lake water was polluted by organic pollutants that have been discharged by various disposal through agriculture, aquaculture and human activities into the lake, and threaten local people's drinking water supply. Hence, this research aims to review on researches of occurrence, source, regulation and treatment methods of organic pollutants in TSL water. Some organic pollutants including aliphatic hydrocarbons, ether, ketone, phenol, phthalate, fatty acid ester, other oxygenated compounds, benzene and polycyclic hydrocarbons, nitrogenous, sulfur-containing, phosphorus-containing, pharmaceuticals and personal care product and pesticide were found in lake's surface water because of agriculture, aquaculture and human activities . Among them, plasticizers and pesticides are over allowable standard for drinking water and also the most toxic compounds. The biological method, adsorption, advanced oxidation process, membrane filtration, and membrane bioreactor are effective whereas coagulation and flocculation are ineffective to remove organic pollutant. The result of this study will provide the people around TSL the awareness about present of pollutants in lake water and its quality. Furthermore, it will be used as a recommendation and reference for TSL residents about using treatment method for pollutant removal.

Keywords: *Organic pollutants, occurrence, transportation, regulation, treatment methods, Tonle Sap lake*

I. Introduction

Tonle Sap Lake (TSL) is the largest freshwater water body in Cambodia (Figure 1), and its watershed extending over 43% (approximately 85,786 km2) of the national land [17]. Lake's surface area varies between the wet and the dry season [5]. During the dry season, the lake is about 120 km long and 35 km wide with an area of about 2500 km2,and maximum depth of about 3.3 m. Lake surface enlarges during the flood phases to about 250 km long and 100 km wide with an area of about 17,500 km2, and the depth reaches 8-10 m [29]. The climate in TSL region is control by two monsoon periods characterized by two distinct seasons, namely the rainy season (May-October) and dry season (December-April) [17]; and the water temperature of lake varies between 28 and 33˚C [22].

TSL provides various ecosystem services consider as a basic environmental key for nurturing the local culture

associated with it. It is estimated that more than one million people living on and around TSL. Their living is mainly depended on water resources for domestic use, irrigation and industry, adjustment of the local climate, fish production, aquaculture, transportation and tourism [17]. Lake water supports regional population through water supply [26]. Even though, TSL is significant by its value but the lake and its ecosystems are under threat due to anthropogenic activities occurring inside and outside its basin. Currently, the lake water was polluted by chemical disposal through agricultural production, aquaculture and human activities. Water pollution in TSL threatens the drinking water supply of local people, and lead to the explosive development of harmful invasive plant species, such as water hyacinth, and impact biodiversity in and around the lakes, as well as food quality and finally human health [41]. Therefore, this study aims to review occurrence of organic pollutants in lake water, understanding its sources and transportation, regulation and technologies to treat pollutants. The result from this review will be used to aware local people living around TSL about the lake water quality and give recommendation to its resident about pollutants treatment method in order to obtain clean water that ensure safe consuming.

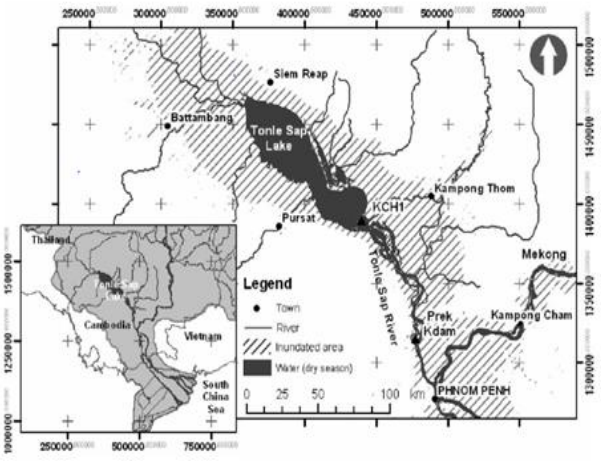

Figure 1: Tonle Sap Lake and its floodplains [9]

2. Occurrence and Transportation of Pollutants

2.1. Occurrence of Pollutants

Degradation of water quality in TSL has been growing concerns [6], which water quality is indicated as a key factor to determine the environmental health and quality of the ecosystem [6]. To Understand the importance of water quality role of lake, many researchers conducted study on contaminants occurred in the lake water. Thus, the chemical contamination, which obtained from intensive agricultural production, aquaculture and human activities within catchment area in Tonle Sap Lake of Cambodia was investigated [19, 25]. The studies found chemical contaminants in TLS such as aliphatic hydrocarbons, ether, ketone, phenol, phthalate, fatty acid ester, other oxygenated compounds, benzene and polycyclic hydrocarbons, nitrogenous, sulfur-containing, phosphorus-containing, pharmaceuticals and personal care product (PPCPs) and pesticide such as insecticides, herbicide (atrazine-i.e.) and disinfectant (Table 1).

Table 1: Concentration of compounds of organic pollutants in surface water of TSL during rainy season and dry season [19, 25]

Category	Rainy Season		Dry Season	
	Min (µg/L)	Max (µg/L)	Min (µg/L)	Max (µg/L)
Aliphatic hydrocarbons	0.0003	6.203	-	-
Benzene	0.0029	0.8703	-	-
Polycyclic hydrocarbons	0.0021	0.3036	-	-
Ether	0.181	1.854	-	-
Ketone	0.0265	3.830	-	-
Phenol	0.001	3.800	-	-
Plasticizer (Phthalates)	0.020	74.340	-	-
Fatty acid ester	0.0037	0.7308	-	-
Other compounds	0.01	27.100	-	-
Nitrogenous	0.0015	5.570	-	-
Sulfur	0.0287	1.730	-	-
Phosphorus	0.0161	8.423	-	-
PPCPs	0.0065	0.4766	-	-
Pesticide	0.001	1.0600	0.0510	2.3168

2.2. Transportation of Pollutants

The TSL ecosystem has experienced major changes over the past few decades as a result of anthropogenic activities both inside and outside of its basin (e.g., water infrastructure development; land use change, agriculture, aquaculture) [17]. Also, TSL is surrounded by the most densely populated region of Cambodia [39] with approximately 5 million people living around the lake [43, 17]. The average annual population growth was 1.4% between 1998 and 2008 [40, 17]. There is extraordinary growth in the city of Siem Reap, the city from which tourists visit Angkor. The annual increases in hotel rooms is 112% between 2003 and 2004 [5]. The city at present has no waste treatment facilities, so hotels build their own package treatment plants or septic systems, so there is increasing concern about contamination of the Siem Reap River which drains to the lake [5]. Deforestation and land use changes in the TSL basin and its inundation area are substantial. The area affected by deforestation in the TSL

basin is equal to 15% of the basin total land area, indicating a higher sediment load into TSL and its floodplain is anticipated because of erosion in its catchments. Then, the sediment could carry the organic pollutant and nutrients from upland into the lake.

The pollution from agricultural chemicals is also potentially substantial in the TSL basins [17]. A study in six provinces surrounding TSL indicated a high level of trade of prohibited pesticides still exists, despite the 1998 Sub-Decree on Standards and Management of Agricultural Materials [50]. In TSL basins, there are about 67% of farmers in the TSL region used pesticides for agricultural activities [32, 17] and the households around TSL also applied pesticides, herbicides and fungicides which was dominant in the plains zone [44]. After raining, the runoff from those agriculture and household was connected to the rivers and could potentially contaminate Tonle Sap Lake [19]. It has been found that large communities within floating villages relied mainly on fishing, rice cultivation and trading while their economic opportunity depended on zones they are living, e.g., land-base, water-base or semi-land-water base [13, 19]. The existence of communities living at floating village on the lake further induced eutrophication, small-scale-aquaculture, boat transportation within the area and solid waste/wastewater contamination not only from household, but also small factories, e.g., ice-making factory or fish processing [19].

3. Toxicity and Standard Regulation of Organic Pollutants in Drinking Water

Most chemicals arising in drinking water are health concern due to their extended exposure of years, rather than months [28]. The organic pollutants cause toxic, teratogenic, mutagenic and carcinogenic effects in aquatic environment as summarized in Table 2. To ensure a safe drinking water for public health, the Royal Government of Cambodia has established a comprehensive policy on National Water Supply and Sanitation and set the Drinking Water Quality Standard (DWS) for Cambodia (Table 3) Drinking Water Quality Standards were prepared based on standard of the latest WHO drinking water quality guidelines (2003) [27]. These standards are developed by an inter-ministerial process initiated by Ministry of Industry, Mines and Energy (MIME) and concerned ministries with support from the World Health Organization (WHO) (Table 3).

Table 2: Human-Toxicological maximum permissible risk level evaluation [1,3,16,30,31,33,34,35,36,37,38,45,48,49]

Category	Toxicity	Effect
Aliphatic hydrocarbons	100 (μg/kgbw/day)	Liver, kidney and hematologic effects
Benzene	4.3 (μg/kg bw/day)	Decreased lymphocyte and Group A (human carcinogen)
Polycyclic hydrocarbons	6.3 (μg/kg bw/day)	Carcinogenicity
Ether	23.6 (μg/day)	Increase in liver weight
Ketone	100 (μg/kg bw/day)	Skin irritation and transient, hypnotic or sedative effects,
Phenol	40 (μg/kg bw/day)	Diarrhea, salivation, urine, and blood and liver effects
Plasticizer (Phthalates)	4 (μg/kg bw/day)	Cancer, or reproductive harm, disrupt the endocrine
Nitrogenous	10 (μg/kg/day)	Carcinogenicity, neural tube defects, and diabetes
Phosphorus (White)	0.02 (μg/kg bw/day)	Gastrointestinal, kidneys, liver, cardiovascular system, and nervous system effect
PPCPs	40 (mg/kg/bw/da)	Rat study: tendency of transiently suppressed body weight and transiently decreased motor activity
Pesticide	0.1-50 (μg/kg bw/day)	Carcinogenic, oncogenic, genotoxic and teratogenic effect

Table 3: Standard regulation of drinking water

Pollutants	MIME (μg/L)	Others (μg/L)
Polychlorinated biphenyls	0.5	-
Trihalomethanes	250	-
Aliphatic hydrocarbons	-	-
Benzene	10	10[a]
Polycyclic hydrocarbons	-	0.1[b]
Ether (Methyl terrt-butyl ether)	-	13[c]
Ketone (2-butanone (methyl ethyl ketone))	-	16[d]
Phenol	-	50[b]
Plasticizer (Phthalates)	-	3[b]-6[b]-8[b]
Fatty acid ester(methyl ester of fatty acid)	-	42[b]
Nitrogenous (Nitrite)	-	100[a]
Sulfur (sulfate)	-	250000[a]
Phosphorus	-	0.1[b]
PPCPs	-	0.05[a]
Individual Pesticide	0.2-30	0.1[e]
Total Pesticides	-	0.5[e]

[a] : World Health organization(WHO)
[b] : Environmental Protection Agency(EPA)
[c] : State Water Resource Control Board(SWRCB)
[d] : Indiana Department of Environmental Management(IDEM)
[e] : European Council Directive(ECD)

4. Treatment Methods of Organic Pollutants

Currently, there are some methods to removal those organic pollutants from water such as coagulation and flocculation, biological methods, Chlorination, Activated carbon adsorption, ozonation and advanced oxidation process (AOPs), membrane process and membrane bioreactor (MBR) (Table 4). Coagulation and flocculation, biological methods, chlorination are ineffective process for organic micropollutant (OMP) removal. Advanced treatment processes including adsorption, advanced oxidation process, membrane process and membrane bioreactors can achieve higher and more consistent OMP removal [12].

Based on our interview with the Chhnok Tru Water Suppl (CTWS) in November 2020, CTWS is utilizing the conventional water treatment method through addition of Polyaluminum Chloride or Alumn in coagulation, flocculation, sedimentation, sand filtration and disinfection by chlorination. Base on this review on OMP removal methods, this conventional water treatment method (coagulation-flocculation and chlorination) are ineffective to remove OMPs.

Table 4: Treatment methods for OMP removal [12,15,18,20,46]

Treatment methods	Advantages	Disadvantages
Coagulation – flocculation	Process simplicity, Low cost	Ineffective MP/OMP removal, Large amount of sludge, Introduction of coagulant salts in the aqueous phase
Biological methods	Low cost, Significant removal	Slow process, low biodegradation
Chlorination	Significant removal	Ineffective removal at lower chemical dose, High dose of chemical Requirement, toxic by-product
Adsorption	Effective removal	Relatively high financial costs, Lower efficiency in the presence of natural organic matters (NOMs), Need for regeneration, Disposal of used adsorbent
Advanced Oxidation	Effective removal, High degradation	High energy consumption, Formation of by products, Interference of radical scavengers
Membrane processes	Removal efficiency process	High energy demand, Membrane fouling, Disposal of concentrate
Membrane Bioreactor	Effective removal, Less sludge, Small scale	Moderately high energy consumption, Inconsistent removal of polar and resistant compounds, Membrane fouling, Less sorption of on the aged MBR sludge

5. Conclusion and Future Work Need

Organic micro-pollutants were found in Tonle Sap Lake such as aliphatic hydrocarbons, ether, ketone, phenol, phthalate (plasticizer), fatty acid ester, other oxygenated compounds; benzene and polycyclic hydrocarbons; nitrogenous, sulphur-containing, phosphorous-containing, pharmaceuticals and personal care product (PPCPs) and pesticide. Their sources are derived from various disposal through agriculture, aquaculture and human activities. Base on study of chemical contaminants, plasticizer (bis (2-ethylhexyl) phthalate) and pesticide (DDT, Mefenoxam, Triadimefon and Chloroneb) are over allowable of drinking water quality standard of EPA. Benzene, polycyclic hydrocarbons, plasticizer (phthalates), Nitrogenous and pesticide, are significant toxic as their toxicities screen values are small but could cause human carcinogenicity.

The biological method, adsorption, AOPs, membrane filtration, and MBR are effective to remove OMP whereas coagulation and flocculation are ineffective for OMP removal. Thus, water treatment methods are currently used at TSL region such as CTWS, is ineffective for OMPs removal. This study will be used as recommendation and reference for TSL resident to assess the water quality and removal method of OMPs. However, further investigation is necessary to monitor the chemical pollutants during dry season.

Acknowledgement

The authors would like to acknowledge financial support from French Agency for Development –European Union (AFD-EU scholarship) with research grant number CKH 1236 02P.

References

[1] Ahmed, M., Rauf, M., Mukhtar, Z., & Saeed, N. A. (2017). Excessive use of nitrogenous fertilizers: An unawareness causing serious threats to environment and human health. Environmental Science and Pollution Research, 24(35), 26983–26987. https://doi.org/10.1007/s11356-017-0589-7

[2] Bonheur, N., & Lane, B. D. (2002). Natural resources management for human security in Cambodia's Tonle Sap Biosphere Reserve. *Environmental Science & Policy*, *5*(1), 33–41. https://doi.org/10.1016/ S1462-9011(02)00024-2

[3] Burdock, G. A., & Ford, R. A. (1992). Safety evaluation of dibenzyl ether. *Food and Chemical Toxicology*, *30*(7), 559–566. https://doi.org/10.1016/0278-6915(92)90189-R

The 13th AUN/SEED-Net Regional Conference on Chemical Engineering 2020 (RCChE-2020)
Jointly held with
The 5th International Symposium on Conservation and Management of Tropical Lakes
"Insights and Challenges toward Achieving SDGs"

Bioaccumulation of heavy metals and trace elements in six fish species from Tonle Sap Lake, Cambodia

Sokneang IN [1, 2*], Sovannmony NGET [1, 2], Soukim HENG [1,2], Dung Viet PHAM[3], MasateruNISHIYAMA[3], Hasika MITH [1, 2] and Toru WATANABE [3]

[1] *Faculty of Chemical and Food Engineering, Institute of Technology of Cambodia, Russian Federation Blvd., P.O. Box 86, 12156 Phnom Penh, Cambodia*
[2] *Food Technology and Nutrition Research Unit, Research and Innovation Center, Institute of Technology of Cambodia , Russian Federation Blvd., P.O. Box 86, 12156 Phnom Penh, Cambodia*
[3] *Faculty of Agriculture, Yamagata University, Japan*
* *in@itc.edu.kh*

Abstract

This study aimed to observe the accumulation of heavy metals and trace elements in six fish species sampled from four locations in Tonle Sap Lake. The amount of three kilograms of each fish sample was randomly collected from fishermen at ChhnokTrou commune (Kampong Chhnang Province), Phat Sanday commune (Kampong Thom Province), Kbal Tor commune (Battambang Province) and Kampong Plouk commune (Siemreap Province) between 2017 and 2018. The level of Zn, Pb, Cr, Cu, Cd and As in the fish samples were below the Maximum Permissible Limit (MPL) set by FAO/WHO. The contents of Mn and Ni in the six studied fish species ranged from 0.8 to 10.1 mg/kg in wet weight and 0.18 to 0.79 mg/kg, respectively. The mean concentration of Mn and Ni were higher than the respective MPL. The highest concentration of Mn was found in *Anabas testudineus* (10.1 mg/kg), and the highest concentration of Ni was found in *A. testudineus* (0.79 mg/kg). Among studied fish species, *A. testudineus* accumulated all of heavy metals and other trace elements most effectively. *A. testudineus* is the predatory fish (carnivorous fish) and this may be resulted from the bioaccumulation.

Keywords: *Fish species, accumulation, trace elements and heavy metals*

I. Introduction

Tonle Sap Lake, the largest freshwater lake in Southeast Asia, is surrounded by five provinces: Kampong Thom, Siem Reap, Battambang, Pusat and KampongChhnangand its surface area stretch to 2500 – 3000 km^2 during dry season and 10 000 – 16 000 km^2 during rainy season [1]. Due to the immense size of Tonle Sap Lake, this lake is the main supply of local fish consumption and exported fishproduct, which is the fifth largest freshwater fish capturing in the world after China, India and Bangladesh and Myanmar [2].

Heavy metals (HMs) are the element, which have a high atomic weight and a density at least 5 times greater than water [3, 4]. In recent year, the increasing of pollution is risen which caused by agricultural, domestic, industrials andtechnological applications. HMs sources in theenvironment are included agriculture waste, pharmaceutical, domestic effluents, industrial activities [5, 6]. Moreover, heavy metals penetrate into the water reservoirs via atmosphere, drainage of the waste, soil erosion and human activities [7, 8]. Those polluted of heavy metals was contaminated to the live in the water, especially fishes. The quality of water was contaminated by heavy metals and continued accumulate in organisms, which are consumed by fish or penetrate into fish directly through skin and gill later [8].

Due to the increasing of development of area surrounding

Tonle Sap Lake and poor wastewater management these is raising the concern of heavy metal presence in Tonle Sap lake ecosystem. Moreover, there are more than 900 000 people live on floating village.Most of the people, who live on the floating village, are lacking waste management, so they throw their daily wastes including plastic and also human waste directly into the lake, in order to make the water and soil pollution [9]. These activities also raise even more concern about the heavy metal contamination in the fish and aquatic live in the lake. Consequently, fish in Tonle Sap Lakemight have high chance of accumulation of heavy metals by the absorption of contaminated water. Therefore, the heavy metals effect on human health after consumption of the fishes, which contain the heavy metals. The main objective of this study is to quantify several heavy metals such as As, Fe, Cu, Hg, Pb, Zn, Cr, Mn, Co, Ni, and Cd in the muscle of six fish species, were collected from Chhnuk Tru village (Kampong Chhnang), Phat Sandai (Kompong Thom), Kampongs Phlork (Siem Reap) and KbalTorl (Battambang).

II. Materials and Methods

2.1. Fish Sampling

Six fish species in Tonle Sap lake were randomly collected from fishermen at Chhnok Trou commune (Kampong Chhnang Province), Phat Sanday commune Kampong Thom, Kbal tor commune Battambang and Kampong plouk commune Siemreap Province (see in Figure 1 and Table 1) between September 2017 to December 2018. 3 kg of each sample contained variable numbers of fish of uniform size were bought and coolimmediately; and transferred in icebox to laboratory of Chemical and Food Engineering Faculty, of Institute of Technology of Cambodia. Uniform fish size was divided into three categories big, medium and small size and then weight and length of these fishes were recorded. When arrived at laboratory, fish samples were frozen at about -20^{o}C and stored until analyses.

2.2. Sample preparation and Analytical methods

Samples of raw fish were cleaned with tap water before the edible part and non-edible part were separated by using the knife, and were washed in distilled water for further process. Fish muscles were freeze dried at -50^{o}C, pressure 0.04mbar for 24h in freeze dryer machine model ALPHA 1-2 LD plus. After freeze-dry, the sample was broken into small pieces, and then passed through a nylon sieve (0.5 mm) and storage at -20^{o}C for further analysis.

The digestion of fish sample for trace elements and heavy metals (except As) analysis was adapted from Ministry Environment of Japan, 2001 [10].2 g of freeze dried sample was digested 20 ml with hydrochloric acid concentrate (1mol/L) and heated at 150^{o}C, and then with 20 ml of nitric acid concentrate (1mol/L) and heated at 170^{o}C,. After finished digestion, the final volume was adjusted to 100ml with ultra-pure water for analysis (Ministry Environment of Japan, 2001) with inductively Coupled Plasma-Mass (ICP-MS) (Model Elan DRCII of PerkinElmer Japan Co., Ltd., Japan).

As analysis was adopted from Ministry Environment of Japan, 2001[10], 1g of sample was added with 10ml o HNO3 and heated at 100^{o}C-150^{o}C) covered by cap, and then 5ml of concentrated H_2SO_4 (98%) and 5ml of concentrated HNO3 (65%) were added to solution with and heated at 200^{o}C. The solution was filtered through filter paper ADVANTEC 5B (4µm) into 100ml flask. The concentration of arsenic and mercury in the solution was analyzed by using atomic absorption spectroscopy (AAS) machine Model AA7000 with hydride vapor generator HVG-1 (Shimadzu, Kyoto, Japan).

2.3 Statistical analysis

The results were statistically analyzed using the SPSS 20.0 package (IBM Corp., Armonk, NY, USA). ANOVA followed by Tukey's test, correlation analysis, and multivariate analysis was also employed. Results of principle component analysis (PCA) were visualized using RStudio.

III. Results and Discussion

Table 1. Trace element (loid) content (in wet weight) of fish species from Tonle Sap Lake (unit mg/kg)

Scientific name	Zn	Pb	Cr	Cu
Boesemaniamicrolepis	14.32	0.02	0.12	0.22
Channamicropeltes	7.77	0.06	0.07	0.17
Hampaladispar	11.53	0.05	0.04	0.30
Anabas testudineus	20.27	0.06	0.16	0.44
Channa striata	10.86	0.10	0.08	0.22
Notopterusnotopterus	6.68	0.07	0.08	0.21
MPL*	100[a]	1[a]	2[b]	20[a]

* MPL: Maximum Permissible Limit

a Thailand. Ministry of Public Health. Notification of Ministry of Public Health, No. 98, B.E. 2529, Re: Prescribing Standards of Contaminated Substances. R. Thai Gov. Gazette 1986, 103, 98. (In Thai)

b Food and Agricultural organization (FAO). Compilation of Legal Limits for Hazardous Substances in Fish and Fishery Products; Fisheries circular No. 764; Food and Agricultural Organization: Rome, Italy, 1983.http://www.fao.org/3/q5114e/q5114e.pdf (accessed on 7 July 2020).

Table 2. Heavy metal(loid) content (in wet weight) of fish species from Tonle Sap Lake (unit mg/kg)

Scientific name	Cd	As	Mn	Ni
Boesemaniamicrolepis	ND*	0.006	4.07	0.36
Channamicropeltes	ND	0.005	1.19	0.41
Hampaladispar	0.004	0.003	0.85	0.18
Anabas testudineus	0.006	0.017	10.11	0.79
Channa striata	0.006	0.002	1.10	0.22
Notopterusnotopterus	ND	0.009	0.80	0.21
MPL**	0.5[a]	1[b]	0.5[b]	0.05[c]

**ND: Not Detected; **MPL: Maximum Permissible Limit*
a Thailand. Ministry of Public Health. Notification of Ministry of Public Health, No. 98, B.E. 2529, Re: Prescribing Standards of Contaminated Substances. R. Thai Gov. Gazette 1986, 103, 98. (In Thai)
b Food and Agricultural organization (FAO). Compilation of Legal Limits for Hazardous Substances in Fish and Fishery Products; Fisheries circular No. 764; Food and Agricultural Organization: Rome, Italy, 1983.http://www.fao.org/3/q5114e/q5114e.pdf (accessed on 7 July 2020).
c U.S. Department of Health and Human Services. ATSDR Toxicology Profile for Nickel. 2005. Available online: http://www.atsdr.cdc.gov/toxprofiles/tp15.pdf (accessed on 7 July 2020).

The mean trace element and heavy metal concentrations in muscle of all six fish species was presented in Table 1 and 2. The concentrations of different trace elements and heavy metal varied within species and location. The level of Zn, Pb, Cr, Cu, Cd and As were below the Maximum Permissible Limit (MPL). However, the contents of Mn and Ni ranged from 0.8 to 10.11 mg/Kg in wet weight and 0.18 to 0.79 mg/Kg wet weight, respectively. The mean concentrations of Mn and Ni were higher than the Maximum Permissible Limit. The highest concentration of Mn and was found in *Anabas testudineus* (10.11 mg/Kg wet weight) follow by *Boesemaniamicrolepis* (4.07 mg/Kg wet weight), and the highest concentration of Ni was found in *Anabas testudineus* (0.79 mg/Kg wet weight)follow by *Channamicropeltes* (0.41 mg/Kg wet weight) and *Boesemaniamicrolepis* (0.36 mg/Kg wet weight).

The distribution of concentration of different trace elements and heavy metal, especially Mn and Ni were highly accumulated in fish from Kampong Thom Province, follow by Battambang province. Trace element and heavy metals bioaccumulations were affected by the aquatic ecosystem environmental conditions such as industrial, municipal and agricultural wastes in the water [11,12].

The accumulation of individual trace elements in fish (all species combined) collected Battambang, Kampong Chhnang, Kampong Thom and Siemreap was presented in Table 3 and 4. The results showed that the accumulation of trace elements and heavy metal was varied among the studied location. However, the distribution of concentration of different trace elements and heavy metal, especially Mn and Ni were highly accumulated in fish from KampongThom Province and Battambang province.

Table 3. Trace elements(loid) content in fish muscle in difference location

Location	Zn	Pb	Cr	Cu
Battambang	10.91	0.02	0.07	0.19
Kampong Chnag	7.68	0.10	0.07	0.24
Kampong Thom	20.89	0.06	0.17	0.43
Siemreap	8.54	0.07	0.06	0.19

Table 4. Heavy metal (loid) content in fish muscle in difference location

Location	Cd	As	Mn	Ni
Battambang	ND*	0.005	1.87	0.33
Kampong Chnag	0.006	0.013	1.32	0.29
Kampong Thom	ND	0.010	7.17	0.52
Siemreap	0.004	0.010	1.80	0.30

*ND: Not Detected

Pb level was higher in Trey Ptouk origin from Siemreap and Kampong Chnag province. Cr was detected higherconcentration in Trey Bromaand Trey Kranh from KampongThom province. Cu was more accumulating in Trey Kranh and Trey Khman from Kampong Thom province. Cad was mostly ND in the studied fish samples. The level of As was found higher concentration in Trey Kranh from Kampong Chnang, Kampong Thom and Siemreap, and in Trey Slat from Battambang. Mn was highly accumulated in Trey Kranh from Kampong Thom. According to many studies in literatures, trace elements and heavy metal bioaccumulation by fish can influence by and living environment (geographical location, contamination sources in water), fish type (predator or non predator), sex, age, size, reproductive cycle, swimming patterns, feeding behavior (demersal fish, neritic or pelagic fish) [13,14,15,16].

IV. Conclusion

Trace elements content varies depending on the zone, environmental conditions, the contamination level of the fishing area, and the characteristics of the fish (size,

endurance, and diet) constitute relevant factors, being some fish more prone to accumulating higher concentrations of these metals in the muscle.

Acknowledgement

We are thankful to the Science and Technology Research Partnership for Sustainable Development (SATREPS), the Japan Science and Technology Agency (JST)/Japan International Cooperation Agency (JICA) for their financial support.

References

[1] FAO., 2004. *Flooded Forest and Fishing Villages. pdf* (1st ed.; P. T. Evan, M. Marschke, & K. Paudyal, Eds.). *Siem reap: Asia forest network.*

[2] Baran, E., & Gallego, G., 2015. Cambodia's fisheries: a decade of changes and evolution. *Catch and Culture, Vol. 21, pp. 28–31.*

[3] Tchounwou, P. B., Yedjou, C. G., Patlolla, A. K., & Sutton, D. J., 2012. Heavy Metals Toxicity and the Environment. *EXS, 101, 133–164.*

[4] Zhenli He, Xiaoe E Yang, Peter J Stoffella., 2005. Trace Eelements in Agroecosystems and Impacts on the Environment. *Journal of Trace Elements in Medicine and Biology 19(2-3):125-40.*

[5] Kh. M. El-MoselhyKh. M. El-Moselhy a, A.I. Othman b, H. Abd El-Azem a, M.E.A. El-Metwally., 2014. Bioaccumulation of heavy metals in some tissues of fish in the Red Sea, Egypt. *egyptian journal of basic and applied sciences, 97-105.*

[6] Jan AT, Azam M, Siddiqui K, Ali A, Choi I, Haq QM., 2015. Heavy Metals and Human Health: Mechanistic Insight into Toxicity and Counter Defense System of Antioxidants. *Int J Mol Sci*;16(12):29592-29630.

[7] P. Part, O. Svanberg and A. Kiessling, "The Availability of Cadmium to Perfused Rainbow Troutgills in Different Water Qualities. *Water Research, Vol. 19, No. 2, 1985, pp. 427-434.*

[8] B. Staniskiene, P. Matusevicius1, R. Budreckiene , K.A. Skibniewska., 2006. Distribution of Heavy Metals in Tissues of Freshwater Fish in Lithuania. *Polish J. of Environ. Stud. Vol. 15, No. 4, 585-591*

[9] Johnstone Gareth, PuskurRanjitha, Declerck Fabrice, Mam Kosal, Il Oeur (ADIC), MakSithirith, PechBunna, SeakSophat, CHAN Sokheng, HakSochanny, Lov Samnang, SuonSokheng, ProumKimhor, Rest Sameth., 2013. Tonle Sap scoping report. CGIAR Research Program on Aquatic Agricultural Systems. *Penang, Malaysia.Project Report: AAS-2013-28.*

[10] Ministry of Japan, T.E (2001). Methode of sediment quality.

[11] Thiyagarajan D, Dhaneesh K V, Kumar TTA, Kumaresan S, Balasubramanian T., 2012. Metals in fish along the southeast coast of India. *Bull Environ Contam Toxicol; 88(4):582–8.*

[12] Nicole Colin, Alberto Maceda-Veiga, Núria Flor-Arnau, Josep Mora, Pau Foruno, Cristiana Vieira, Narci s Prat, Jaume Cambra and Adolfode Sostoa., 2016. Eco logical impact and recovery of a Mediterranean river af ter receiving the effluent from a textile dyeing industry. *Ecotoxicology and Environmental Safety*, Volume 132, Pages 295-303.

[13] Zhao S, Feng C, Quan W, Chen X, Niu J, Shen Z., 2012. Role of living environments in the accumulation characteristics of heavy metals in fishes and crabs in the Yangtze River Estuary, China. *Mar Pollut Bull, 64:1163e71.*

[14] Mustafa C, Guluzar A., 2003. The relationships between heavy metal (Cd, Cr, Cu, Fe, Pb, Zn) levels and the size of six Mediterranean fish species. *Environ Pollut, 121:129e36.*

[15] M Al-Busaidi, P Yesudhason, S Al-Mughairi, W A K Al-Rahbi, K S Al-Harthy, N A Al-Mazrooei, S H Al-Habsi., 2011. Toxic metals in commercial marine fish in Oman with reference to national and internationalstandards. *Chemosphere, 85(1):67e73.*

[16] Khaled A., 2004. Seasonal determination of some heavy metals in muscle tissues of *Siganusrivulatus* and *Sargussargus* fish from El-Mex Bay and Eastern Harbor, Alexandria, Egypt. *Egypt J Aquat Biol Fish, 8(1):65e81.*

The 13th AUN/SEED-Net Regional Conference on Chemical Engineering 2020 (RCChE-2020)
Jointly held with
The 5th International Symposium on Conservation and Management of Tropical Lakes
"Insights and Challenges toward Achieving SDGs"

Difference in Basic Water Quality Before and After Moving Floating Houses to Upland in Chhnok Tru Village, Tonle Sap Lake, Cambodia

May Phue WAI[1], Rina HEU[3,4,*], Vibol CHEM[1], Sochetra SEN[2], Kimheang THAI[2], Khy Eam EANG[3], Sokly SIEV[2,4]

[1]*Graduate School of Water and Environmental Engineering, Institute of Technology of Cambodia, Russian Federation Blvd, P.O. Box 86, 12156 Phnom Penh, Cambodia*
[2]*Faculty of Chemical and Food Engineering, Institute of Technology of Cambodia, Russian Federation Blvd., P.O. Box 86, 12156 Phnom Penh, Cambodia*
[3]*Faculty of Hydrology and Water Resource Engineering, Institute of Technology of Cambodia, Russian Federation Blvd., P.O. Box 86, 12156 Phnom Penh, Cambodia*
[4]*Water and Environmental Research Unit, Research and Innovation Center, Institute of Technology of Cambodia, Russian Federation Blvd, P.O. Box 86, 12156 Phnom Penh, Cambodia*
*Corresponding author: heu.rina@itc.edu.kh

Abstract

The ecosystem of Tonle Sap Lake (TSL) is widely nominated as a biosphere reserve by UNESCO in October 1997. Approximately five million people live around TSL; the discharges of sewages and wastes from the households into the lake also concern with the water quality of the lake. Government declared to move floating houses in Chhnok Tru to upland and some of the floating houses in Chhnok Tru had been already moved according to Government's plan. Thus, this paper aims to investigate water quality parameters such as temperature, pH, dissolved oxygen (DO), oxidation-reduction potential (ORP), conductivity, chlorophyll before and after moving floating houses Chhnok Tru. The water quality parameters of TSL were measured in 19 sampling sites around Chhnok Tru by using EXO sensor. The result showed that, before moving floating houses, the average temperature was 32.24 °C, pH was 6.96, conductivity was 166.9 µS/cm, salinity was 0.0673 psu (Practical Salinity Unit), DO was 4.33 mg/l, ORP was 135.5 mV and total dissolved solid was 93.92 mg/l. After moving floating houses, the average temperature was 30.9 °C, pH was 8.69, DO was 5.24 mg/l, conductivity was 203.67 µS/cm, chlorophyll was 4.39 and ORP was 81.5 mV. The average pH and DO after moving floating houses were higher than those before moving floating houses because of the less discharging of wastes from floating houses, while the average ORP was lower than that before moving floating houses because one sampling site that is close to the Chhnok Tru port had a negative ORP value showing that only high contamination in this site. The output from this study is expected to provide the information about water quality of TSL before and after moving floating houses for the support of water quality management to sustain the TSL ecosystem.

Keywords: *Ecosystem, Floating houses, Tonle Sap Lake, Water quality*

I. Introduction

Tonle Sap Lake (TSL) is the socio-economic dependency of the Cambodian communities and an important reservoir for Mekong system [1][2]. Approximately 1.7 million people in six provinces around the lake rely mainly on water for drinking and domestic uses. In this regard, Chhnok Tru is one of the busiest communities, the discharging of sewage from households causes water quality degradation [3]. According to government plan, floating houses in Chhnok Tru village had been already removed. As a consequence, the comparison and correlation between basic water quality parameters before and after moving floating houses still need to understand for knowing the effect of moving houses in Chhnok Tru village. Thus, this study aims to evaluate water quality after moving floating houses in Chhnok Tru village by comparing them with the water quality before moving the floating houses in Chhnok Tru village. Besides, the Student's t-test, Pearson's correlation test, and Principal component analysis (PCA) were used for statistical analysis. In addition, inverse distance weighted (IDW) interpolation was applied for the distribution of water quality in both 2018 and 2020.

II. Materials and Methods

2.1. Sampling sites

This study was conducted in the Chhnok Tru village, TSL. Water samples were collected in 19 sites of the Chhnok Tru village on both 7th March 2018 and 5th March 2020. The floating houses distribution in 2018 was approximately 1881 houses from one study of Chhnok Tru village [4]. Based on government plan, the floating houses were supposed to move to upland about 90% by 2020. The sample location map is shown in **Fig. 1.**

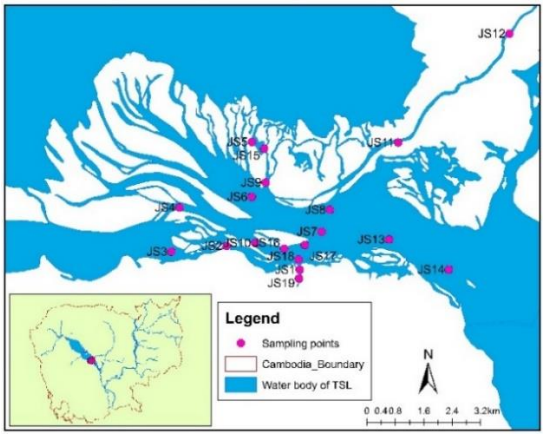

Fig. 1. Map of sampling locations

2.2. Water quality measurement

Water quality analysis in both 2018 and 2020 was performed by using Multi- Exo Sondes (YSI Incorporated, USA). In situ measurement of water quality parameters such as temperature, pH, dissolved oxygen (DO), oxidation-reduction potential (ORP), conductivity (Cond), were measured. The Multi-EXO Sondes was set to 5 minutes and repeated at least 10 times for every measurement and it was washed with sampled water before running to prevent contamination from one sample to another.

2.3 Inverse Distance Weighted (IDW) Method

A simple interpolation method, IDW method has been applied in environmental modelling. In this study, IDW was used to interpolate water quality parameters distribution in 2018 and 2020 by ArcMap (10.5).

2.4. Statistical analysis

2.4.1 Student's t-test

T-test for independent samples is used for comparison of mean values of results. Risk possibility level of 5% was taken into account in defining the statistical significance of obtained results, t value must be at least 1.96. In this study, a t-test was performed with MS excel 2019 to test the significance between before moving floating houses and after moving floating houses for the water quality parameters.

2.4.2 Correlation analysis

Correlation is the way of assessing to find the strength of the association. The Pearson product-moment correlation coefficient is the most widely used in testing correlation between two variables. The correlation coefficient is expressed by r that is ranged from -1 to +1. In this study, Pearson's correlation test was performed by R program (3.6.1).

2.4.3 Principal component analysis (PCA)

PCA is used to identify the most important components among the large variable numbers in the entire original data set. The outputs of biplot were interpreted to be a better understanding of the water quality in the sampling locations for 2018 and 2020. In this study, PCA was performed using Origin pro-2021.

III. Results and Discussion

From the graph of **Fig 2**, the results revealed that temperature was slightly decreased in 2020. For pH, the values in pH were increased in 2020 with DO was also higher than in 2018. Conductivity (Cond) in 2020 was

higher than in 2018. Meanwhile, the oxidation-reduction potential (ORP) was so much different in both 2018 and 2020.

The comparative graph of water quality in both 2018 and 2020 is shown in **Fig 2**.

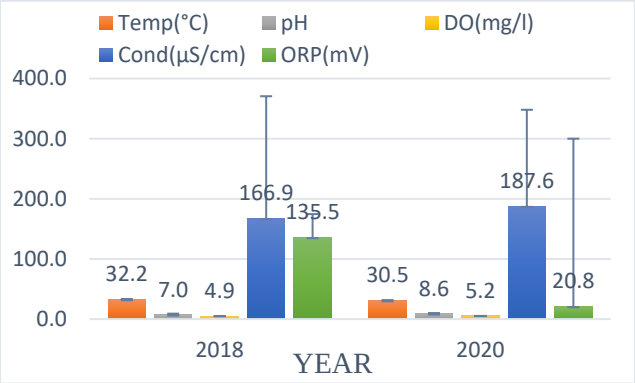

Fig. 2. Water quality in 2018 and 2020

According to water quality distribution maps shown in **Fig 3** and **Fig 4**, minimum DO value in 2018 is 0.6 while in 2020, the minimum DO value is 0.5. Maximum pH value in 2020 has become higher than in 2018. In 2018, conductivity distribution in both 2018 and 2020 is a similar distribution. But for ORP values, in 2018, most sites show low ORP values while in 2020, only some parts have low ORP values.

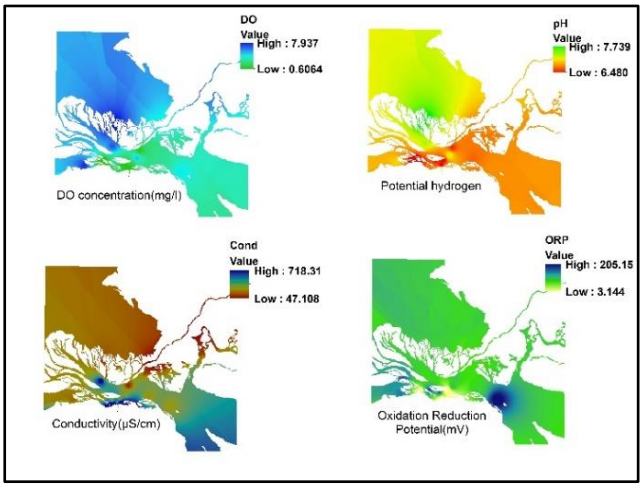

Fig. 3. Water quality distribution map in 2018

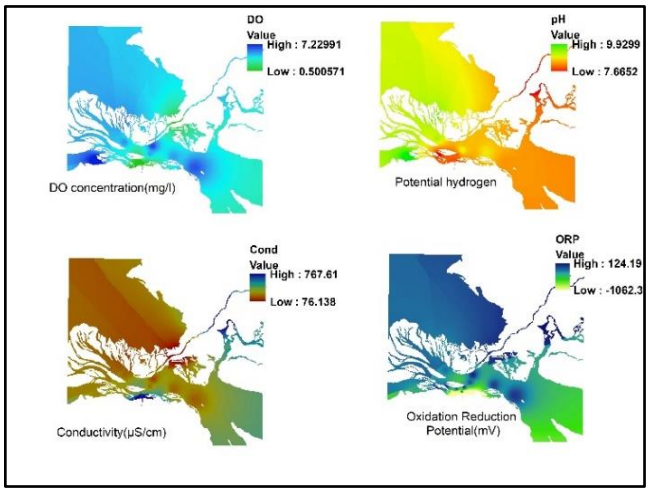

Fig. 4. Water quality distribution map in 2020

The independent t-test was performed and the results were shown in **Table 1**. According to results of t-test, as shown in **Table 1**, values of temperature were statistically significant at significance level $p<0.05$, confirming that the values of temperature were lower in 2020. Besides, pH values were higher in 2020 with the significance level $p<0.05$. As far as DO, Conductivity, and ORP were concerned, they were not statistically significant by the results of t-test.

Table 1: t-test analysis for water quality parameters in 2018 and 2020

Parameters	Year	Mean	T-test	p-value
Temperature (°C)	2018	32.24	4.45	<0.001*
	2020	30.51		
pH	2018	6.96	-10.40	<0.001*
	2020	8.59		
DO (mg/l)	2018	4.90	-0.44	0.662
	2020	5.17		
Conductivity (µS/cm)	2018	166.91	-0.34	0.732
	2020	187.62		
ORP (mV)	2018	135.53	1.73	0.1016
	2020	20.82		

Correlation analysis was performed for each specific parameter between 2018 and 2020 as shown in **Table 2**, the results showed that temperature values in both 2018 and 2020 were not correlated with each other ($r=0.1$, $p>0.05$). but for pH values in both 2018 and 2020 were positively correlated ($r=0.5$, $p<0.05$) while DO values in both 2018 and 2019 were positively correlated with $r=0.66$ and $p<0.01$.

Meanwhile, conductivity was strongly correlated in both 2018 and 2020. But for ORP values in both 2018 and 2020, these values were not correlated with each other (r= -0.1, p>0.05).

Table 2: Correlation analysis for water quality parameters in 2018 and 2020

Parameters	Year	r	p-value
Temperature (°C)	2018 2020	0.0905	0.721
pH	2018 2020	0.5437	0.01972*
DO (mg/l)	2018 2020	0.6638	0.00267*
Conductivity (µS/cm)	2018 2020	0.8805	<0.001*
ORP (mV)	2018 2020	-0.1805	0.488

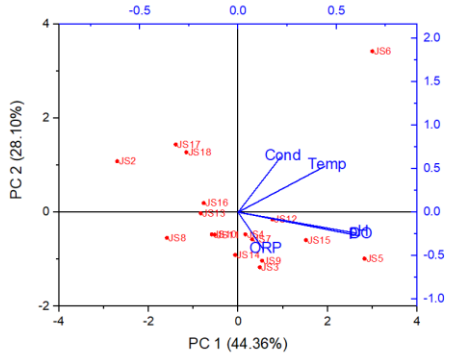

Fig.5. Biplot of water samples in 2018

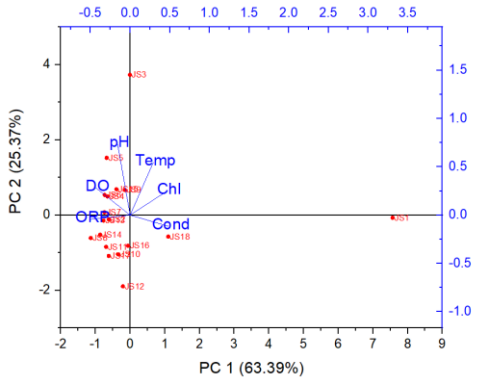

Fig. 6. Biplot of water samples in 2020

According to the results of the biplot, as shown in **Fig 5**, in 2018, Cond, temp, DO, pH and ORP had a positive score with PC1 on the sites of JS3, JS4, JS5, JS6, JS7, JS9, JS12, JS14, JS15. This showed that these sites were mainly controlled by water quality parameters in 2018. From the results of biplot, as shown in **Fig 6,** temp, Chl and Cond had a positive score with PC1 on the sites of JS1, JS3, JS18 while temp, DO, pH Chl had the positive score with PC2 on the sites of JS3, JS5, JS4, JS6, JS7, JS8, JS15.

IV. Conclusion

From the results of this study, t-test revealed that temperature and pH were significantly different between 2018 and 2020, and the correlation of pH, DO Conductivity, and ORP between 2018 and 2020 were also found out. By biplot results, in 2018, JS3, JS4, JS5, JS6, JS7, JS9, JS12, JS14, and JS15 were the main influenced sites by the water quality parameters. JS1, JS3, JS4, JS5, JS6, JS7, JS8, JS15, and JS18 were the main influenced sites by water quality parameters in 2020. Moreover, the distribution of each water quality in both 2018 and 2020 can be seen clearly by IDW method showing that some parts of study area of Chhnok Tru village still need to consider for lake ecosystem management.

Acknowledgment

We are thankful to the Science and Technology Research Partnership for Sustainable Development (SATREPS, Grant No: JPMJSA1503), the Japan Science and Technology Agency (JST)/Japan International Cooperation Agency (JICA), and French Development Agency (AFD, Grant No: CKH 1236 02P) for their financial support.

References

[1] Campbell, I. C., Say, S., Beardall, J. (2009). Tonle Sap Lake, the Heart of the Lower Mekong. The Mekong, 251–272. https://doi.org/10.1016/B978-0-12-374026-7.00010-3

[2] Sarkkula, J., Kiirikki, M., Koponen, J., & Kummu, M. (2003). Ecosystem processes of the Tonle Sap Lake. *The 1st Workshop of Ecotone Phase II*, 1–14. https://doi.org/10.2307/171246

[3] Shivakoti, B. R., Bao, P. N. (2020). Environmental Changes in Tonle Sap Lake and its Floodplain: Status and Policy Recommendations. In Institute for Global Environmental Strategies, Tokyo Institute of Technology, Institute of Technology of Cambodia. https://www.iges.or.jp/en/pub/tonlesapsatreps/en

[4] Chem, V., Hieav, S., Kim, C.(2019). Assessment of Seasonal Nutrient Loads from Floating Community of Chhnok Tru at Tonle Sap Lake, Cambodia. A Senior Project Report Presented to the Academic Member of the Faculty of Mathematics, Science, and Engineering (Bachelor's degree thesis). Pañhāsāstra University of Cambodia

The 13th AUN/SEED-Net Regional Conference on Chemical Engineering 2020 (RCChE-2020)
Jointly held with
The 5th International Symposium on Conservation and Management of Tropical Lakes
"Insights and Challenges toward Achieving SDGs"

The effectiveness of different types of polyaluminum chloride (PAC) and aluminum sulfate (alum) with $Ca(OCl)_2$ dosing for treatment surface water of Tonle Sap River

Theara YANN [1], Kazuhiko MIYANAGA[2] and Reasmey TAN [1,3,*]

[1] *Faculty of Chemical and Food Engineering, Institute of Technology of Cambodia, Russian Federation Blvd., P.O. Box 86, 12156 Phnom Penh, Cambodia*
[2] *School of Life Science and Technology, Tokyo Institute of Technology, 4259 J3-8 Nagatsuta-cho, Midori-ku, Yokohama, 226-8501, Japan*
[3] *Food Technology and Nutrition Research Unit, Research and Innovation Center, Institute of Technology of Cambodia, Russian Federation Blvd., P.O. Box 86, 12156 Phnom Penh, Cambodia*
* *Corresponding author: rtan@itc.edu.kh*

Abstract

As a treatment of water, coagulation of minute particles and disinfection of microbes are the most commonly used. The aim of this study is to optimize the appropriate condition of two different kinds (yellow and brown) of polyaluminum chloride (PAC), and alum with $Ca(OCl)_2$ for the treatment of surface water of Tonle Sap River. The optimum dosage of coagulants was obtained based on residual turbidity and pH change. The optimum dosage of $Ca(OCl)_2$ was obtained based on efficiency of removal bacterial cells and residual free chlorine. The series experiment was conducted to study the impact of dosing of (yellow and brown) polyaluminum chloride and alum with $Ca(OCl)_2$ on Tonle Sap River within high turbidity, The result of experiment showed that the highest efficiency of turbidity removal within 97.1%, 95.6% and 95.6% of 60 mg/L of yellow PAC, brown PAC and alum respectively, while pH was changed from 7.45 to 7.08, 6.88 and 6.77 respectively. As a result of using those optimum coagulant with $Ca(OCl)_2$, 100% of *E.coli* removal was obtained at 1.0ppm and 1.7ppm of free chlorine dosing, while the residual of free chlorine was range from 0.21-0.35ppm. Therefore, the amount of those coagulants and free chlorine are good for water treatment to get high quality by following the standard Ministry of Industry Mines and Energy, and World Health Organization guideline.

Keywords: *Alum, pH change, polyaluminum chloride (PAC), turbidity removal, residual of free chlorine.*

I. Introduction

Nowadays, due to many factors such as population growth, domestic wastes, agriculture wastes, sewage, and urbanization, the water source was contaminated by inorganic and organic matter. Livelihood surrounding Tonle Sap River and lake confront with serious health risks due to use this water source, especially people who is living in floating communities on Tonle Sap River and lake [1]. The fractions of natural organic matter (NOM) contained in surface water are humic acid and fulvic acid, hydrophobic, hydrophilic, carbohydrate, carboxylic acid, an amino acid. The characteristic and amount of NOM depend on the origins of the water. It comes from the degradation of plant and animal, bacterial, algae [2, 3]. NOM is not only the cause taste, odor, color and bacterial growth, but also result in the formation of disinfection by-products during disinfection process [4]. Reducing the cloudiness and

particle substance as well as turbidity was needed before disinfection process [5].

Turbidity is one of the important physical parameters of environmental water which presenting the amount of particle suspended and colloidal matters such as clay, silt, finely divided organic and inorganic, and other microorganisms [6, 7]. These particles can scatter the light creating muddily and cloudy in water [8]. Colloidal particles are normally carry negative charge on their surface which lead to the stabilization of the suspension [9]. Turbidity itself does not represent a direct risk to public health, nevertheless, it indicates the possibilities to include hazardous chemicals and/or pathogenic microorganisms. The high turbidity leads to impair the disinfection of water which acts as a barrier between disinfectant and microbial, and the cause of forming the disinfection by-products which may have long-term health effects. Therefore, the turbidity was needed to be reduced before disinfection [7, 10]. As Ministry of Industry Mines and Energy reported that to prevent any contamination of water, water system needs to go through four stages such as the storage reservoir, coagulation-flocculation, filtration and disinfection and based on standard quality within turbidity below 5 nephelometric turbidity unit (NTU) [11].

Coagulation and flocculation are utilized to remove the organic matter from the water, which are taken place in serial steps that permit particle collision and growth into floc, then followed by sedimentation. The serial steps are connected, if coagulation is incomplete, the following steps are also incomplete and will be unsuccessful [12]. In coagulation process, colloidal or particles were destabilized by charge neutralization a coagulant or flocculant with a high positive charge is adsorbed on to the surfaces of negatively charged colloids to form the small aggregate of particle, while in flocculation, aggregation particles are gathered into larger [13].

Coagulation and disinfection are the most commonly used for removing turbidity, color, algae and kill or inactivate infective microorganisms from surface water. Chemical coagulant was used to form floc for removal of those impurities [14]. Chlorine was used as a chemical disinfectant due to its effectiveness, low cost, and easy to manage. Chlorine can be used in the form of calcium hypochlorite, sodium chlorite, or chlorine gas. When chlorine undergo with water, it produced hypochlorous acid ($HOCl$) and hypochlorite (OCl^-) [15]. Hypochlorous acid act as a prime disinfection agent and its dominance is at pH below 7.5 and is a more disinfectant, while hypochlorite ions are more effective at pH above 7.5 [16]. Aluminum coagulant are aluminum sulfate (Alum), polyaluminum chloride (PAC), poly aluminum silicate sulfate (PASS), polyaluminum silicate sulfate chloride (PASC) are widely used in water treatment, using these coagulant are associated with series problem due to over amount of residual aluminum cause by overdose of coagulant [17]. The different color of polyaluminum chloride have different in application and production technology. Yellow polyaluminum chloride (Y. PAC) was mainly used for sewage disposal and drinking water treatment. Brown polyaluminum chloride (B. PAC) was used for waste water. The characteristic of yellow and brown PAC waw showed in **Table 1.** The main objective of this study is to optimize the treatment condition of yellow PAC, Brown PAC and alum with $Ca(OCl)_2$ for removal of contaminants from the water of Tonle Sap River.

II. Materials and Methods

2.1. Sampling sites

Raw water in this study was collected from Tole Sap River at Phnom Penh (with coordinate 11.5787626, 104.9249167) on Sept. 9, 2020 at 6:30am.

2.2. Experimental set-up

2.2.1. Prepare of stock solution

1% of coagulants stock were prepared by 1 g of coagulant was suspended in 99 ml of distilled water and stirring in room temperature. Therefore, added 1ml of stock solution to 1L of water is 10 mg/L. 0.1g of calcium hypochlorite granule was suspended in 100 ml of distilled water to produce $Ca(OCl)_2$ stock solution and stirring at room temperature. The concentration of free chlorine was obtained by an actual measurement using N,N-dimethyl-ρ-phenylenediamine (DPD) method.

2.2.2. Coagulation and flocculation process

250 ml of raw water was filled in 4 bottles and were treated with three types of coagulant such as yellow PAC, brown PAC and alum with various dosing 20, 40, 60 and 80 mg/l were performed stirring 3 mins with 300 rpm and settling time for 60 mins.

2.2.3. Coagulation and disinfection process

250 ml of raw water was filled in 4 bottles and were treated with optimize coagulants with 300 rpm stirring speed for 1 min before added $Ca(OCl)_2$, after added $Ca(OCl)_2$ within 0.84, 1.0 and 1.7ppm of chlorine concentration were

continue stirring for 2 mins and settle for 60 mins.

2.3. Analytical methods

10 ml of samples were collected at 3 cm below the surface level. The turbidity was measured by using HANNA-HI 98703 Portable Turbidimeter in three replicates. WM-32EP/pH meter was used to measure pH. The turbidity removal efficiency was calculated by using **Eq.1**.

$$\%Tur\ removal = \frac{(Tur_i - Tur_f) \times 100}{Tur_i} \qquad \textbf{(Eq.1)}$$

where Tur_i and Tur_f are the initial and final turbidity, respectively.

Table 1. The characteristic of yellow and brown polyaluminum chloride

Item	Y.PAC	B.PAC
Al_2O_3 (%)	≥30	≥30
Basicity (%)	70-85	50-90
pH Value(1% aqueous solution)	3.5-5.0	3.5-5.0
Water insoluble (%)	≤0.1	≤1.5

After each performed treatment, the sample were taken for total coliform and *E.coli* count. 20 ml of sample was filtered by using Whatman® sterile membrane filters without absorbent pads with 47 mm and pore size 0.45 μm and was cultured on each Chromocult® Coliform agar plate which was then incubated at 36 ±2℃ for 21-24h. The number of colony-forming unit (CFU) of 100ml was expressed in **Eq.2**. and the bacterial removal efficiency was calculated by using **Eq.3.**

$$CFU/100 = \frac{(number\ of\ colony) \times 100}{sample\ valume\ filtered\ in\ ml} \qquad \textbf{(Eq.2)}$$

$$Bacteria\ removal = \frac{(Bac_i - Bac_f) \times 100}{Bac_i} \qquad \textbf{(Eq.3)}$$

where Bac_i and Bac_f are the bacteria of raw sample and treated sample, respectively. The characteristics of source water were shown in **Table 2.**

Table 2. Physicochemical characteristics of river water

Parameter	Value
Turbidity (NTU)	83.53
Coliform (CFU/100ml)	1.33×10^5
E. coli (CFU/100ml)	2.19×10^5
pH	7.45

III. Results and Discussion

3.1. Effective of dosing coagulants on turbidity removal

The effective of yellow PAC, brown PAC and Alum dose on turbidity removal were shown in **Fig. 1.** For figure was shown clearly that each dose of yellow PAC is more effective than each dose of Alum. The percentage turbidity removal of yellow PAC was reached; 95.2%, 95.8%, 97.1% and 97.5% at the dose of 20 mg/L, 40 mg/L, 60 mg/L and 80 mg/L, respectively. Whereas, the removal of turbidity of alum was obtained; 89.9%, 94.6%, 95.6% and 95.5% at the dose of 20 mg/L, 40 mg/L, 60 mg/L and 80 mg/L, in turn. In case, 20 mg/L of those coagulants were used for water treatment, brown PAC has efficiency lower than yellow PAC, while the effective turbidity removal of brown PAC is more effective than yellow PAC with 96.8% at 40 mg/L and its efficiency was decrease where the dosage is more than 40 mg/L. Hence the highest effective of brown PAC is 40 mg/L.

Alternately, the comparation of all dose of coagulants was significant, the amount of yellow PAC ranges from 40-80mg/L, brown PAC between 40-60mg/L and the amount of alum between 40-80mg/L can completely remove turbidity from 83.5 NTU to below 5 NTU. According to Zouboulis et al., 2008 reported that polyaluminum chloride proved to be more effective coagulant than alum in water treatment plan [18]. In addition, Wang et al., 2011 illustrated that the effectiveness turbidity removal of polyaluminum chloride was slighly low that alum but it has highest effective on cloudness water with algae compare with alum. Hence the ability of polyaluminum depend on the condictional of water [19].

3.2. Effective of dosing coagulants on pH change

Fig. 2 illustrates the change of pH by using yellow PAC, brown PAC and alum. As a result, the change of pH in using each dose of coagulant were decrease as the dosage of coagulant was increased. When yellow PAC and brown PAC were used, the pH of water were slightly change from 7.5 to 7.2-7.0 and 7.2-6.8. while the high pH change (range from 7.1-6.5) was occurred by using alum. Base on **Table 1**, the basicity of yellow PAC is between 70-85% and brown PAC

is between 50-90%, while the basicity of alum is zero due to it has no OH ions in its structure [20]. High concentration dosage of PAC to be used, the consumption of pH value is also changed. Accordingly, the optimal pH for removing humic acid and clay is between 5-6 and 6.5-7.5 [21]. Also, the treatment of using PAC, the optimum pH is 7.5 for its

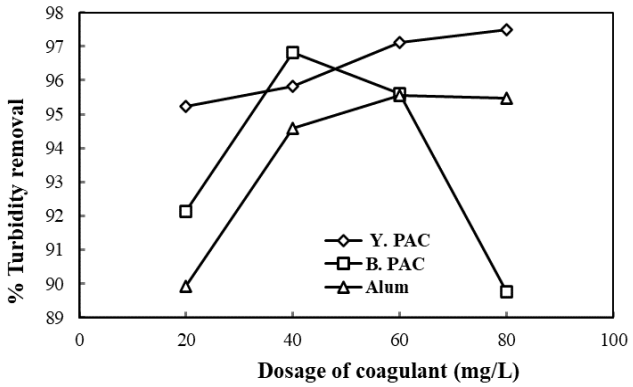

Fig. 1. Effects of yellow PAC, Brown PAC and alum dose on turbidity

high effectiveness in removing turbid water [22]. Therefore, using yellow PAC has gradually changed in pH and it did not need to adjust pH before or after treatment and it is suitable for the small scale of drinking water treatment. According to the guideline of drinking water-quality of WHO [15] and the Ministry of Industry Mines and Energy [11] reported that pH range for drinking water is 6.5-8.5. Therefore, the amount of these coagulants can be used for treatment water.

3.2. Effective of dosing $Ca(OCl)_2$ on bacterial removal and residual free chlorine

As **Fig. 3** shows the effectiveness of bacteria removal of $Ca(OCl)_2$ with various coagulants. The percentage of bacteria removals by optimum coagulant alone (control) achieved 99.9% of *E.coli* removal and 97.9% of coliform removal of 40mg/L of brown PAC, while the percentage of *E.coli* removal achieved 99.4%, 99.6%, coliform removal achieved 97.8%, and 98.2% with turns of 60mg/L of yellow PAC and alum, respectively. Besides, the efficiency removal of bacteria of $Ca(OCl)_2$ with coagulant was obtained, the percentage of *E.coli* and Coliform, 99.99%;99.84%, 100%;99.91%, 100%;99.97% of yellow PAC within the concentration of free chlorine, 0.84ppm, 1ppm, and 1.7ppm, respectively. Whereas the percentage of *E.coli* and Coliform of brown PAC with free chlorine was 100%;99.9%, 100%;99.9%, 100%;99.9% at 0.84ppm, 1.0ppm, and 1.7ppm, respectively. When the highest percentage of *E.coli* and Coliform removal of alum with free chlorine was 100%;99.9% at 1.7ppm.

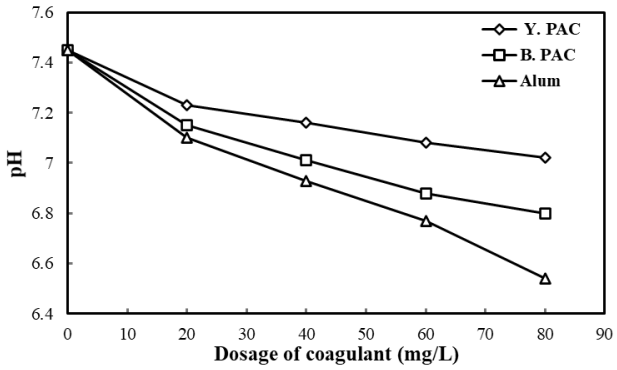

Fig. 2. Effects of coagulant dosage on pH

After each performed of experiment, the sample were taken for analysis the residual free chlorine. As in **Table 3** shows the residual free chlorine after treated by using yellow PAC, brown PAC and alum with $Ca(OCl)_2$. The residual of free chlorine was obtained 0.12ppm, 0.005ppm, and 0.04ppm at using alone yellow PAC, brown PAC and alum, respectively. While yellow PAC was used with $Ca(OCl)_2$ at 0.84ppm, 1ppm and 1.7ppm of free chlorine were increased to 0.17ppm, 0.22ppm and 0.29ppm, respectively. In case using brown PAC with $Ca(OCl)_2$, the residual free chlorine was almost same as yellow PAC with $Ca(OCl)_2$. When the residual free chlorine of alum with $Ca(OCl)_2$ 0.84ppm, 1ppm and 1.7ppm achieved 0.16ppm, 0.19ppm and 0.34ppm, respectively.

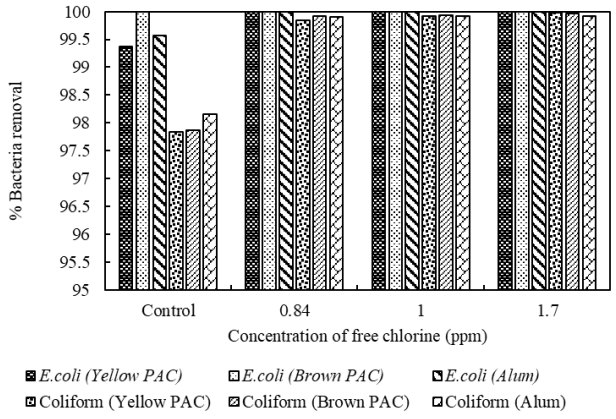

Fig. 3. Effects of yellow PAC, brown PAC and alum with $Ca(OCl)_2$ on bacteria removal

Table 3. Residual free chlorine of treated water by using yellow PAC, Brown PAC and alum with $Ca(OCl)_2$

Residual of free chlorine of treated water (ppm)			
$Ca(OCl)_2$ (ppm of free chlorine)	**Yellow PAC**	**Brown PAC**	**Alum**
Control	0.12	0.05	0.04
0.84	0.17	0.17	0.16
1.0	0.22	0.23	0.19
1.7	0.29	0.26	0.34

Coagulant coupled with chlorination has efficiency for NOM chemical structure removal which was proposed the formation of aggregates during the coagulation process inhibits the reaction between chlorine and organics that have been entrapped in the aggregates [23]. In contrast, the effective disinfection level of residual concentration of available chlorine to disinfected is below or equal to 0.5 mg/L for at least 30 mins at pH lower than 8.0. The minimum residual concentration of available chlorine should be 0.2 mg/L [15]. And according to Roy *et al,* 2016, the use of 2 mg/L of chlorine was obtained the residual free chlorine below 0.5 ppm which is within the prescribed limit. Therefore, the concentration of free chlorine that suitable for treatment water is 1.7ppm with those amount coagulants.

IV. Conclusion

The effective of different dosage of coagulant and $Ca(OCl)_2$ were studied experimentally. The efficiency of coagulant operation in coagulation and the efficiency of $Ca(OCl)_2$ operation disinfection. The highest turbidity removal was obtained at 40 mg/L of brown PAC within 96.8%, 60 mg/L of yellow PAC and alum within 97.1% and 95.6%, respectively. In addition, the highest bacteria removal and appropriate residual free chlorine were achieved when using the optimum dose of coagulant couple with $Ca(OCl)_2$ at 1.7ppm of chlorine concentration.

Acknowledgement

We are thankful to the Science and Technology Research Partnership for Sustainable Development (SATREPS), the Japan Science and Technology Agency (JST)/Japan International Cooperation Agency (JICA) for their financial support.

References

[1] J. Brown, S. Cairncross, and J. H. J. Ensink, "Water, sanitation, hygiene and enteric infections in children," *Arch. Dis. Child.*, vol. 98, no. 8, pp. 629–634, 2013, doi: 10.1136/archdischild-2011-301528.

[2] A. Matilainen, E. T. Gjessing, T. Lahtinen, L. Hed, A. Bhatnagar, and M. Sillanpää, "An overview of the methods used in the characterisation of natural organic matter (NOM) in relation to drinking water treatment," *Chemosphere*, vol. 83, no. 11, pp. 1431–1442, 2011, doi: 10.1016/j.chemosphere.2011.01.018.

[3] F. U. Kac, M. Kobya, and E. Gengec, "Removal of humic acid by fixed-bed electrocoagulation reactor: Studies on modelling, adsorption kinetics and HPSEC analyses," *J. Electroanal. Chem.*, vol. 804, no. October, pp. 199–211, 2017, doi: 10.1016/j.jelechem.2017.10.009.

[4] M. Yan, D. Wang, J. Yu, J. Ni, M. Edwards, and J. Qu, "Enhanced coagulation with polyaluminum chlorides: Role of pH/Alkalinity and speciation," *Chemosphere*, vol. 71, no. 9, pp. 1665–1673, 2008, doi: 10.1016/j.chemosphere.2008.01.019.

[5] J. McClean, "Disinfecting drinking water," *Water Wastes Dig.*, vol. 55, no. 2, pp. 34–35, 2015.

[6] P. Hayden, "Water resources," *Fire Risk Manag.*, no. MAY, pp. 39–42, 2009.

[7] M. J. Allen and R. Copes, "Turbidity and microbial risk in drinking water. Prepared by : Martin J . Allen , Ronald W . Brecher , Ray Copes , Steve E . Hrudey (Chair), and Pierre Payment Ministerial Technical Advisory Committee Prepare," no. May, 2014.

[8] W. Quality, "Turbidity: Description, Impact on Water Quality, Sources, Measures -," *Water Qual.*, vol. 3, no. March, p. 2.4, 2008.

[9] T. Tripathy and B. R. De, "Flocculation: A new way to treat the waste water," *J. Phys. Sci.*, vol. 10, pp. 93–127, 2006.

[10] World Health Organization, "Water Quality and Health- Review of Turbidity: Information for regulators and water suppliers," *Who/Fwc/Wsh/17.01*, p. 10, 2017, [Online]. Available: https://www.who.int/water_sanitation_health/publications/turbidity-information-200217.pdf%0Ahttp://www.who.int/water_sanitation_health/publications/turbidity-information-200217.pdf.

[11] MOIMAE, "Kingdom of Cambodia Drinking Water Quality Standards," *Drink. Water Qual. Stand.*, pp. 1–20, 2004.

[12] N. B. Prakash, V. Sockan, and P. Jayakaran, "Waste Water Treatment by Coagulation and Flocculation," *Certif. Int. J. Eng. Sci. Innov. Technol.*, vol. 9001, no.

2, pp. 2319–5967, 2014, [Online]. Available: http://www.ijesit.com/Volume 3/Issue 2/IJESIT201402_61.pdf.
[13] T. Suopaj, *Functionalized nanocelluloses in wastewater treatment applications*, no. April. 2015.
[14] DEFRA, "Water Treatment Processes - Drinking Water Inspectorate," *Water Treat. Process*, pp. 1–36, 2018.
[15] W. H. Organization, "Guidelines for Drinking-water Quality 4th ed," *Who Libr. Cat. Data.*, pp. 1–564, 2011, doi: 10.1007/978-1-4020-4410-6_184.
[16] World Health Organization, "Chapter 1 - Summary and Evaluation," pp. 1–499, 2000.
[17] X. Huang *et al.*, "Effect of dosing sequence and raw water pH on coagulation performance and flocs properties using dual-coagulation of polyaluminum chloride and compound bioflocculant in low temperature surface water treatment," *Chem. Eng. J.*, vol. 229, pp. 477–483, 2013, doi: 10.1016/j.cej.2013.06.029.
[18] A. Zouboulis, G. Traskas, and P. Samaras, "Comparison of efficiency between poly-aluminium chloride and aluminium sulphate coagulants during full-scale experiments in a drinking water treatment plant," *Sep. Sci. Technol.*, vol. 43, no. 6, pp. 1507–1519, 2008, doi: 10.1080/01496390801940903.
[19] Y. Wang, S. Zhuo, N. Li, and Y. Yang, "Influences of various aluminum coagulants on algae floc structure, strength and flotation effect," *Procedia Environ. Sci.*, vol. 8, no. November, pp. 75–80, 2011, doi: 10.1016/j.proenv.2011.10.014.
[20] R. E. Pieroni, "Dosage Calculation," *Arch. Intern. Med.*, vol. 140, no. 12, p. 1673, 1980, doi: 10.1001/archinte.1980.00330230119026.
[21] G. Annadurai, S. S. Sung, and D. J. Lee, "Optimization of Floc Characteristics for Treatment of Highly Turbid Water," *Sep. Sci. Technol.*, vol. 39, no. 1, pp. 19–42, 2005, doi: 10.1081/ss-120027399.
[22] S. Ghafari, H. A. Aziz, and M. J. K. Bashir, "The use of poly-aluminum chloride and alum for the treatment of partially stabilized leachate: A comparative study," *Desalination*, vol. 257, no. 1–3, pp. 110–116, 2010, doi: 10.1016/j.desal.2010.02.037.
[23] D. Ghernaout, "Coagulation and Chlorination of NOM and Algae in Water Treatment: A Review," *Int. J. Environ. Monit. Anal.*, vol. 2, no. 6, p. 23, 2014, doi: 10.11648/j.ijema.s.2014020601.14.

The 13th AUN/SEED-Net Regional Conference on Chemical Engineering 2020 (RCChE-2020)
Jointly held with
The 5th International Symposium on Conservation and Management of Tropical Lakes
"Insights and Challenges toward Achieving SDGs"

Occurrence, Transportation, Regulation and Treatment Methods of Heavy Metals in Groundwater: A Review on Case of Well Water around Tonle Sap Lake

Laty Ma [1], Rina Heu [2, 4,*], Mardi Meas [1], Khy Eam Eang[2], and Sokly Siev[3, 4]

[1]*Graduate School of Water and Environmental Engineering, Institute of Technology of Cambodia, Russian Federation Blvd, P.O. Box 86, 12156 Phnom Penh, Cambodia*
[2]*Faculty of Hydrology and Water Resource Engineering, Institute of Technology of Cambodia, Russian Federation Blvd., P.O. Box 86, 12156 Phnom Penh, Cambodia*
[3]*Faculty of Chemical and Food Engineering, Institute of Technology of Cambodia, Russian Federation Blvd., P.O. Box 86, 12156 Phnom Penh, Cambodia*
[4]*Water and Environmental Research Unit, Research and Innovation Centre, Institute of Technology of Cambodia, Russian Federation Blvd., P.O. Box 86, 12156 Phnom Penh, Cambodia*
*Corresponding author: heu.rina@itc.edu.kh

Abstract

Tonle Sap Lake (TSL), the largest natural freshwater lake in Southeast Asian area with rich endowment biodiversity and various ecosystems, provides a huge potential on agriculture and aquaculture to Cambodians who live on the floating villages and around the floodplain area. The lake and its ecosystems, however, are widely under threat due to anthropogenic activities occurring inside and outside of its basin such as activities by agricultures, water infrastructure development and land use change. Currently, one of the most concerns in this watershed is lack of clean water for consumption. While the surface water is being polluted from various human activities (e.g., fishing, navigation, using pesticide & herbicide for plant, and floating village), the groundwater was being utilized along the TSL for domestics, small industrials, and agricultural purposes. Most of shallow groundwater in Cambodia has been contaminated by heavy metals including arsenic (As), manganese (Mn), and iron (Fe). The exposure of the heavy metal substances will affect the environment and human health when its concentration is over the limitation threshold of the Drinking Water Quality Standard in Cambodia and WHO. This study aims to review the state knowledge on the well water, as well as the essential research approach by focusing on several topics including the occurrences, transportation, monitoring and treatment method of heavy metals. The findings of this review paper will propose and apply for the water treatment technologies on heavy metal removal of contaminated groundwater along the TSL. More efforts will spread the awareness of water quality for citizen surrounding the TSL area to understand the impact of utilizing well water with the presence of heavy mental that can affect their health in the long-term.

Keywords: *Heavy metals, Occurrences, Tonle Sap Lake, Treatment methods, Well water*

I. Introduction

Tonle Sap Lake (TSL), the largest permanent freshwater body in Southeast Asia, is an important natural reservoir with the total watershed extending over 43% ~ 86,786 km^2 of the national land. The lake surface area, which underpins its uniqueness not only in hydrology, but also in water quality, production, and biodiversity [1]. Unfortunately, the lake and its ecosystems are widely under threat due to anthropogenic activities occurring inside and outside its basin. The surface water in TSL was concerned and being polluted from the various activities such as fishing, navigation, using pesticide/ herbicide, and floating houses. Outside the basin, citizen living along the TSL faced with lack of clean water for common use and for drinking.

As a result, numerous dug/tube wells along in the floodplain zone have been installed and abstracted for myriad purposes such as domestic, drinking, irrigation and small-scale industries (Fig. 1). According to Ministry of Rural Development (MRD, 2014), groundwater is major source for drinking water supply in Cambodia [5]; 53% of Cambodian households drink water from groundwater sources in the dry season and ~270,000 tube-wells with hand pump are functioning. The previous studies have shown that most of tube and drill well around the TLS area have contaminated by heavy metals [6, 7]. The existence of heavy metals with high concentration in water sources and drinking water is a most concerning problem to human health.

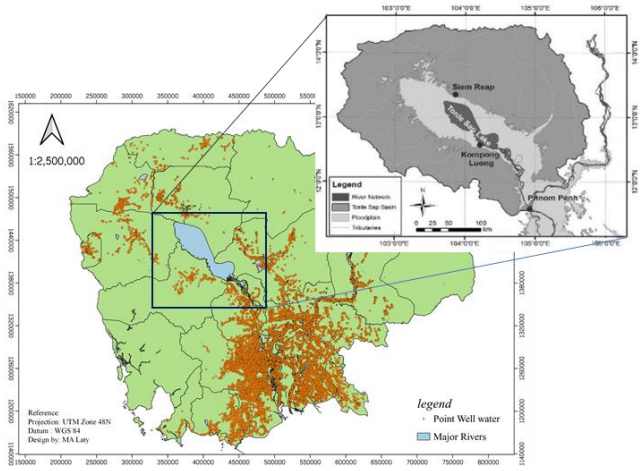

Figure1: Location of well water around the TSL, Cambodia [5]

In this paper, several major categories focusing on the occurrences and transportation of heavy metals in the groundwater were reviewed; a case study of well water along the TSL, the regulation for monitoring the water quality, and the treatment methods of heavy metals, which were applied as conventional water treatment at those areas. In addition, the review had summarized and gave the recommendation for research required.

2. Occurrence and Transportation of Heavy Metals

Heavy metal is general collective term, which applies to the group of metals and metalloids with atomic density greater than 5g.cm^{-3} or 5 times more than water [38], and they are the natural earth's crust components. A variety of reactions in soil environment, e.g., acid/base precipitation/ dissolution, oxidation/reduction, and sorption/iron exchange process can influence the speciation and mobility of metal contaminants. The rate and extent of these reactions will depend on factors such as pH, oxidation potential (Eh), complexation with other dissolved constituents, sorption and ion exchange capacity of the geological materials and organic matter content [3].

Groundwater plays a dominant role in purposing of domestic, water supply, irrigation and small scale industries for both rural and urban due to polluted surface water and lacking of usable water in dry season[3]. Many dug/tube wells have installed as the water resource for people live in the floodplain area along the TSL. A study found the major issues and challenges threatening of groundwater resource; groundwater quality problems with high arsenic (As) and iron (Fe) contents in Mekong and Tonle Sap River basin [5]. Based on [5,8,9,11], the chemical distribution assessment of well water in the floodplain areas along the TSL shows that the present of arsenic (As), manganese (Mn), and iron (Fe) with high contaminants. Some provinces along the Mekong River Basin and TSL Basin have (As) problem in groundwater. About 38% of tube-wells in those provinces area contaminated with arsenic above 50ppb [5]. This review has shown the significant chemical contamination occurred in well water in the floodplain areas around the TSL (Table 1) [8-11]. Previous data analyses from 2007 to 2020 have confirmed that the major concentration of heavy metals in well water such as As, Mn, and Fe with high concentration comparing to the standard of drinking water quality regulated by Ministry of industrial and handicraft [13] and standard for drinking water by World Health Organization [14].

Surface water naturally interacts with the groundwater system noticeably shallow groundwater [7]. Therefore, the seasonal fluctuation of surface water in TSL may contribute to the change of groundwater composition in the aquifer system. Well water quality in floodplain areas will affect by the geochemical evolution comparing to other well water areas. During the rainy season, the elemental composition of lake water appeared to greatly influence by the intrusion of water from the Mekong River through the Tonle Sap River. During the dry season, the type of lake water shifted, suggesting that the lake water stored during the rainy season replaced by inflow from other tributaries and groundwater in its vicinity [8]. The past study showed that the seasonal changes in the elemental composition of the lake water were largely controlled by surface water and groundwater circulation. However, potential risks of As and other heavy metal poisoning in the lake water system are growing, which depend on the changes in the upper reaches of Mekong River and material inputs into the lake. Therefore, we need to monitor the status of the surface water and groundwater, simultaneously, in TSL and its tributary rivers.

Table 1: Major chemical concentration in well water along the TSL area.

Parameters	®	TDS (mg/l)	As^{+} (µg/l)	Mn^{2+} (mg/l)	Mg^{2+} ((mg/l)	Ca^{2+} (mg/l)	K^{+} (mg/l)	Fe^{2+} (mg/l)	SO_4^{2-} (mg/l)	HCO_3^{-} (mg/l)	Cl^{-} (mg/l)
References											
C.Savan, 2014 (1)	Max.		*101*	-	7.81	12.24	0.23	0.1	-18.71	-0.17	-0.02
	Min.		0.1	-	0.02	0.04	0.0	0.0	0.02	-13.3	-6.43
	Mean.		*10.4*	-	1.0	2.4	0.0	0.0	-1.5	-5.5	-1.0
P.Feldman,2007 (2)	Max.	*2340*	*326*	*4.08*	97	297	143	*13.6*	177	-	*1060*
	Min.	16.7	< 0.5	0.001	0.07	0.09	0.07	0.012	0.1	-	1.1
	Mean	463	8.9	*0.29*	15.3	40.8	4.18	*1.4*	12.7	-	56
K.Ratana,2020 (Wet Season) (3)	Max.	*1251*	-	*2.2*	33.1	60.9	37.9	*24.2*	*316.8*	391.6	68.2
	Min.	21.0	-	0.0	0.1	0.0	0.0	0.0	0.0	0.0	0.0
	Mean	386.3	-	0.4	10.4	18.8	8.6	*3.3*	63.8	113.3	17.7
K.Ratana,2020 (Dry season) (3)	Max.	*1390*	-	*2.7*	34.7	39.6	167.1	0.2	*267.2*	614.9	60.1
	Min.	23.0	-	0.0	0.0	0.0	0.0	0.0	0.0	0.0	0.0
	Mean	360.3	-	*0.4*	9.2	14.4	12.2	0.2	32.9	191.4	11.7
MRD,WSP, 2014 (4)	Max.		*250*					*13*			
	Min		0.0					0.0			
	Mean		*20.76*					2.03			
DWS, Cambodia (2014)	St.d	800	50	0.1	150	200	-	0.3	250	-	250
WHO, 2005	St.d	-	10	0.5	-	-	-	-	500	-	250

Data noted:
(1). Converting from meq/l to mg/l
(2). Re-arrange to find Max, min, mean by authors
(3). Data was summed all samples, find wet/dry (max, min, mean) by authors
(4). Select the location around the TSL from the well map, and then find max, min, mean.

3. Toxicity and Standard Regulation of Heavy Metals in Drinking Water

Studies reported various effects of heavy metals in drinking water [39, 38]. The chemical contamination such as arsenic, fluoride, nitrate, and manganese presented in groundwater might pose human health and environmental issues. Among the heavy metals, As, Cd, Pb, Cr, Cu, Hg, and Ni are the major concern (Table 2), mainly due to their presence at relatively high concentrations in drinking water and their effects on human health [2]. The most toxic effect of these metals in their ionic species are the most stable oxidation state (Cd, Pb, Hg, and As) which react with the body's bio-molecules to form extremely stable bio toxic compounds [11].

Table2: Typical of heavy metals, their effect on Human Health

Heavy Metals	Permissible Level (mg/l)	Effects on Human Health
Arsenic(As)	0.01*	Skin manifestations, visceral cancers, vascular disease.
Cadmium(Cd)	0.003*	Kidney damage, renal disorder, human carcinogenic.
Chromium(Cr)	0.05***	Headache, diarrhea, nausea, vomiting, carcinogenic.
Copper(Cu)	0.25**	Liver damage, Wilson disease, insomnia.
Iron(Fe)	0.3***	Liver disease, heart disease, arthritis and osteoporosis.
Nickel(Ni)	0.2**	Dermatitis, nausea, chronic asthma, coughing, carcinogen.
Lead(Pb)	0.006**	Liver damage the fatal brain, kidney, circulatory system
Manganese(Mn)	0.1***	Weakness, muscle pain, and dizziness.
Mercury(Hg)	0.001***	Rheumatoid arthritis, kidneys, and nervous system
Nickel(Ni)	0.2**	Dermatitis, nausea, coughing, chronic asthma, carcinogen
Sodium(Na)	250***	High blood pressure, stroke and heart, stomach cancer, kidney stones osteoporosis,
Zinc(Zn)	0.8**	Depression, neurological signs, lethargy, and increased thirst

Note sources: (*) WHO, (**) USEPA, (***) MIH, Cambodia [12-16]

To protect human health, regulatory agencies have recommended the maximum concentrations of few heavy metals in drinking water (e.g., USEPA, 2015; WHO, 2011) [34]. The royal government of Cambodia has enacted the national drinking water quality standard to ensure safe drinking water for everybody by adapting to WHO. Some parameters are different in values from the WHO (Table 3).

Table 3: Drinking water quality standard (MIH, WHO) [13, 14]

Parameters	Unit	Cambodia	WHO
pH	-	6.5-8.5	6.5-8.5
Turbidity	NTU	5	≤ 5
TDS	mg/l	800	-
EC	µS/cm	-	250
Hardness	mg/l	300	
Calcium (Ca)	mg/l	200	-
Cadmium (Cd)	mg/l	0.003	0.003
Chloride (Cl)	mg/l	250	250
Chromium (Cr)	mg/l	1	0.05
Copper (Cu)	mg/l	0.3	2
Iron (Fe)	mg/l	0.3	-
Magnesium(Mg)	mg/l	150	-
Sodium (Na)	mg/l	200	200
Manganese(Mn)	mg/l	0.1	0.5
Lead (Pb)	mg/l	0.01	0.01
Sulfate (SO_4)	mg/l	250	500
Arsenic (As)	mg/l	0.05	0.01

4. Treatment Methods of Heavy Metal

Removal of heavy metals is an important step toward safe drinking water. About 71% of rural Cambodia households reported always treat their drinking water prior consumption [20]. Traditional methods were used for water treatment in Cambodian such as boiling, filtration, sedimentation and solar radiation, which is discussed in table 4. Our field survey on 15 November 2020 at the Chhnok Tru Commune located along the TSL area reported that the local residents use raw water for common utilities and 20-litre plastic jugs for drinking. Some of them also used water treatment products including ceramic water filters, bio-sand filters and mineral pot filter.

Table 4: Comparison of traditional treatment methods [21]

Methods	Advantages	Disadvantages
Filters	To eliminate microbes No particles in water Ease use for large family No need to boil water Produce clean, clear water	Not affordable for poor households Water still contains some microbes
Boiling	Most effective way to eli minate microbes Produces clean, safe water Easy method for community.	Time-consuming Requires fuel Slow Poses risk of fire
Tablets & powders	Effective in eliminating microbes Ease to use No need to boil water.	Chemical substance maybe harmful.

There is no data or research to confirm that the classical product treatment could remove contaminants of heavy metals in water, but [20] shows some effectiveness of traditional methods. The above treatment methods, which are being practiced in the community and rural household, cannot remove the heavy metals with high efficiency. The water treatment methods for removal heavy metals with efficiency are discussed in Table 5. Adsorption is considered as a suitable method for removal As, Fe, Mn because it is easy to operate, less sludge production and low cost. This is the best water treatment for rural.

5. Conclusion and Future Research need

To sum up, some significant reviews about the occurrences, transportation, toxicity, regulation, and treatment method for removal heavy metals in groundwater around the TSL were found as summarized:

- The contaminations of heavy metals in well water along the TSL area were detected includes As, Fe, Mn with high concentration comparing to the standard.
- The most toxic heavy metals that is harm to human health is As. Another toxic heavy metal is Fe, which can also risk to human body for long-term daily consuming. A standard for drinking water regulated to protect public health.
- The conventional water treatment method is important for communities at TSL area, but there are no data shown the effectiveness of heavy metals removal.

Thus, this paper encourages the future research to develop the water treatment method to remove the contaminant of heavy metal from well water with high efficiency in order to protect people and improve human health around the TSL area.

Table 5: Summary of treatment methods of heavy metals [23-33]

Treatment Methods	*Advantages*	*Disadvantage*
Ion exchange (As, Fe, Mn, Pb)	High transformation of components. High removal efficiency, fast kinetic reaction, Less sludge production.	Removes only limited metal ions Operational cost is high. Not handle concentrated metal solution as the matrix as fouled by organics and solids.
Coagulation (As, Ni, Zn, F, Cd)	Cost effective, Dewatering qualities. Cost effective, high removal efficiency.	Generation of sludge, Utilization of chemicals is high. Jar test, sludge and hardness production, and pH dependence.
Membrane Filtrations (As, Fe, Mn, Cu, Cd, Zn, Pb,)	High removal efficiency of heavy metals. Lower space requirement Reusable heavy metals,	Very expensive, Membrane fouling, Complex process. High cost membrane fouling, scaling, High-energy consumption. Sludge production.
Adsorption (As, Fe, Mn)	Easy operation, Less sludge production, Low cost adsorbents. High removal efficiency Flexibility and simplicity of design & insensitivity to toxic pollution	Desorption
Electrochemical Treatment (Cu, Cr, and Ni)	Efficient for the removal of important metal ions, low chemical usage. High removal Efficiency, reusable heavy metals, space saving.	Initial investment is high, need high electrical supply High initial investment and electricity requirement

Acknowledgement

The authors would like to acknowledge financial support from French Development Agency (AFD) with research grant number CKH 1236 02P and the Ministry of Education, Youth and Sport through Higher Education Improvement Project (HEIP) Credit No 6221-KH at Institute of Technology of Cambodia.

References

[1] Campbell, I. C., Poole, C., Giesen, W., & Valbo-Jorgensen, J. (2006). Species diversity and ecology of Tonle Sap Great Lake, Cambodia. Aquatic Sciences, 68(3), 355-373.

[2] Duruibe, J. O., Ogwuegbu, M. O. C., & Egwurugwu, J. N. (2007). Heavy metal pollution and human biotoxic effects. International Journal of physical sciences, 2(5), 112-118.

[3] Hashim, M. A., Mukhopadhyay, S., Sahu, J. N., & Sengupta, B. (2011). Remediation technologies for heavy metal contaminated groundwater. Journal of environmental management, 92(10), 2355-2388.

The 13th AUN/SEED-Net Regional Conference on Chemical Engineering 2020 (RCChE-2020)
Jointly held with
The 5th International Symposium on Conservation and Management of Tropical Lakes
"Insights and Challenges toward Achieving SDGs"

Lake Water Temperature Characteristics and Long-Term Variations in Water Temperature in the Tonle Sap Lake

Yoichi Fujihara [1,*], Keisuke Hoshikawa [2], Hideto Fujii [3], Takashi Nakamura [4], Sokly Siev [5], and Sambo Lun [5]

[1] *Ishikawa Prefectural University, 1-308, Suematsu, Nonoichi, Ishikawa 921-8836, Japan*
[2] *Toyama Prefectural University, 5180, Kurokawa, Imizu, Toyama 939-0398, Japan*
[3] *Yamagata University, 1-23, Wakaba, Tsuruoka, Yamagata 997-8555, Japan*
[4] *Tokyo Institute of Technology, 4259-G5-3, Nagatsuta, Midori, Yokohama 226-8501, Japan*
[5] *Institute of Technology of Cambodia, Russian Federation Blvd., P.O. Box 86, 12156 Phnom Penh, Cambodia*
* *Corresponding author: yfuji@ishikawa-pu.ac.jp*

Abstract

Water temperature is an important parameter for lake management because it has a major impact on material circulation and the local ecosystems. In addition, various regions have witnessed increased lake water temperatures owing to the increased air temperatures caused by the recent climate changes. However, there is little information on the water-temperature characteristics and long-term water-temperature trends for Tonle Sap Lake, Cambodia, as there are no regular, long-term water-temperature observations, and little is known about the changing lake water environment. Therefore, we investigated the characteristics of and trends in surface water temperatures of the Tonle Sap Lake from 2000 to 2019 using MOD11A1, a MODIS product to obtain daily land surface temperature data using Google Earth Engine. Moreover, the relationship between water temperature fluctuations and hydrological–meteorological conditions (e.g., air temperature, precipitation, and lake water level) were analyzed. The maximum and minimum water temperatures were recorded as 30.7 ℃ and 24.6 ℃ in May and January, respectively, indicating that these trends were one month behind those of the air temperatures. One of the spatial characteristics of this lake is that the northern part is cooler than the southern part. With respect to the water temperature trends, the maximum value increased at the rate of 0.20 ℃ in 10 years, minimum value decreased at the rate of 0.78 ℃ in 10 years, and difference between the maximum and minimum temperatures is increasing. There was a significant correlation between the maximum water temperature and lake water level. The lake water level has declined recently, with the maximum water level for 2000–2009 being 9.3 m (maximum: 10.4 m, minimum: 9.3 m) and that for 2010–2019 being 8.2 m (maximum: 10.5 m, minimum: 6.0 m). This indicates that the declining water levels are causing higher maximum water temperatures with increasing air temperatures. Conversely, the correlation between the minimum water temperature and lake water level was not strong. Factors contributing to the lower minimum water temperatures were not identified and must be studied in more detail in the future.

Keywords: *Surface water temperature, MODIS, Climate change, Lake water level, Google Earth Engine*

I. Introduction

Water temperature is an important parameter for lake management because it has a major impact on material circulation and ecosystems. In addition, various regions

have witnessed a rise in lake water temperature due to the rise in air temperature caused by recent climate change. However, there is little information on long-term water temperature trends for Tonle Sap Lake, as there are no regular, long-term water temperature observations. Although Oyagi et al. (2017) reported intensive observations of water temperature and no thermocline in the lake, little is known about the changes in the lake's water environment.

II. Materials and Methods

We investigated the trend in surface water temperature of Tonle Sap Lake from 2000 to 2019 using MOD11A1, which is a MODIS data product, and there are 365/366 images per year. The R-square between the observed water temperature and MODIS-derived temperature was approximately 0.54 in Tonle Sap Lake. We used the Google Earth Engine, a cloud-based platform for global-scale geospatial analysis that uses Google's computational capabilities for various high-impact societal applications, including water management, climate monitoring, and environmental protection. It is an integrated platform designed to empower traditional remote sensing scientists and a much wider audience lacking the technical capacity required to use conventional supercomputers or large-scale cloud computing (Gorelick et al., 2017).

We investigated the lake water temperature fluctuations for open water areas throughout the year. The data tended to be influenced by clouds. The median image for the year was obtained for each pixel from 365/366 land surface temperature values to remove this influence. In addition, the median surface temperature within the lake boundary was obtained to calculate the annual and lake average water temperatures. The trend of this median surface temperature was analyzed for data spanning 20 years. We also analyzed the yearly median air temperature of ERA5. In addition, as the maximum water level of the lake has been shown to affect water quality (e.g., Hoshikawa et al., 2019), its relationship with water temperature was also analyzed.

III. Results and Discussion

As a result, the northwestern part of the lake was found to have lower water temperatures than the southeastern part, with a difference of 1.5 °C. The annual water temperature data for the 2000–2019 period and the annual maximum water level variation of the lake are shown in Figure 1 and Figure 2. We determined that the annual mean water temperature for the 2000–2009 period was 26.0 °C (maximum 26.5 °C, minimum 25.7 °C), while for the 2010–2019 period it was 25.9 °C (maximum 26.7 °C, minimum 25.2 °C). We found that the annual fluctuation of water temperature has been increasing since 2009. Moreover, the surface temperature showed a decreasing trend of 0.78 °C /10 years, and there was no trend for the air temperature of Phnom Penh city. Considering that the temperature rise due to global warming has shown an upward trend of 0.34 °C /10 years worldwide (O'Reilly et al., 2015), the decrease in temperature of Tonle Sap Lake is an interesting phenomenon.

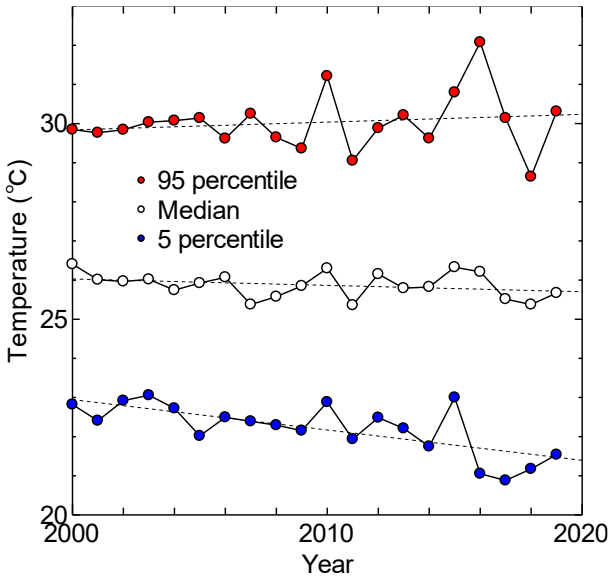

Fig. 1 Trends of water temperature (maximum, minimum, and mean)

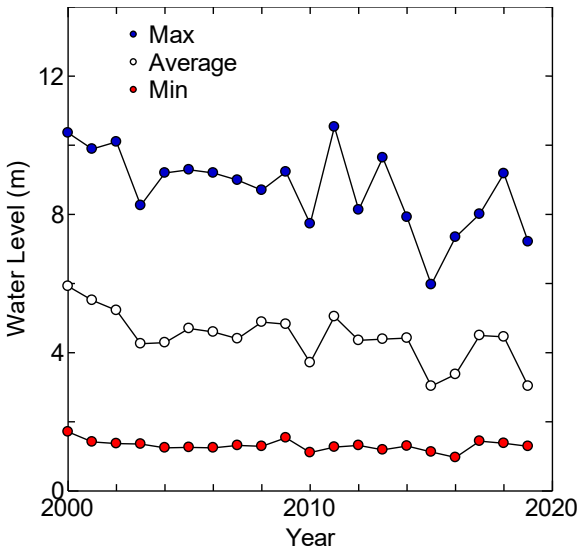

Fig. 2 Trends of water level

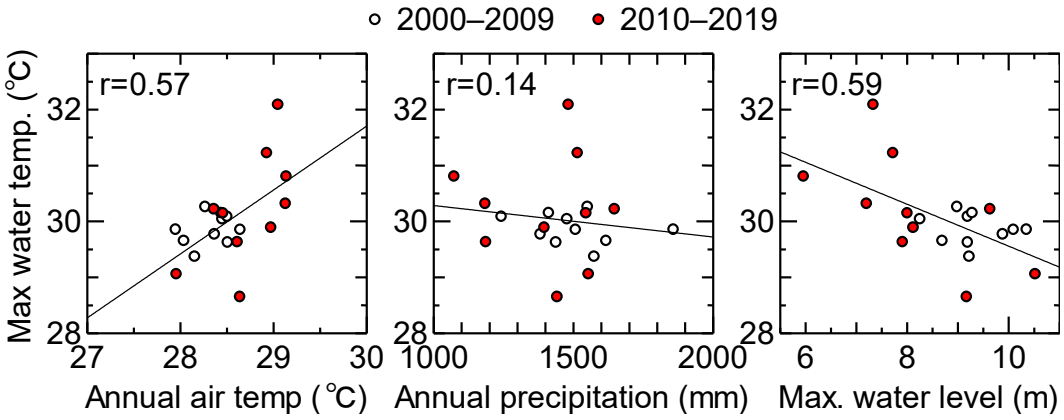

Fig.3 Factors of maximum surface water temperature

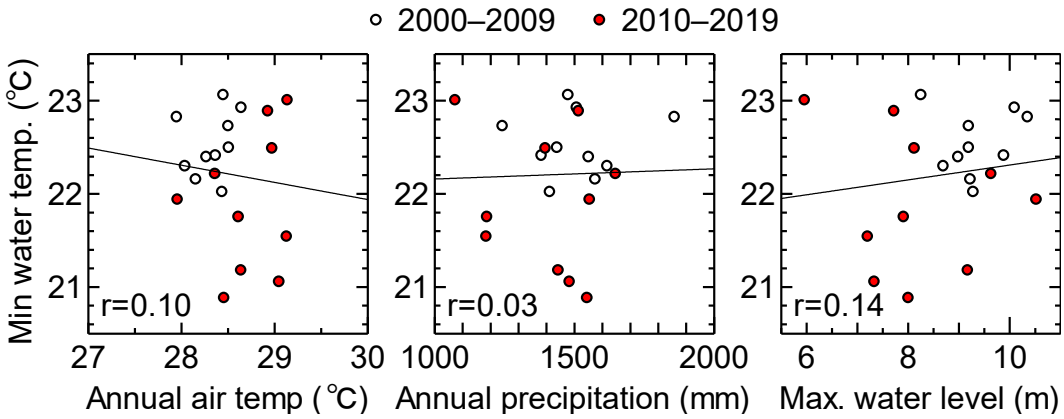

Fig.4 Factors of minimum surface water temperature

For the 2000–2009 period, there was a positive correlation between annual water temperature and annual maximum water level. However, after 2009, it changed to a negative correlation, and the variability between annual water temperature and annual maximum water level increased. It appears that both annual water temperature and annual maximum water level have fluctuated more since 2009. There was a significant correlation between the maximum water temperature and lake water level (Figure 3). The lake water level has declined recently, with the maximum water level for 2000–2009 being 9.3 m (maximum: 10.4 m, minimum: 9.3 m) and that for 2010–2019 being 8.2 m (maximum: 10.5 m, minimum: 6.0 m). This indicates that the declining water levels are causing higher maximum water temperatures with increasing air temperatures. Conversely, the correlation between the minimum water temperature and lake water level was not strong (Figure 4). Factors contributing to the lower minimum water temperatures were not identified and must be studied in more detail in the future.

The construction of a group of large dams is currently underway in the up-stream area, and it has been suggested that this will change the hydrological environment in the Mekong River (for example, Hecht et. al., 2019). While the relationship between water temperature fluctuation and dam construction cannot be accurately established in our study, such an investigation is necessary in the future. Due to the lack of hydrological data on Tonle Sap Lake, there has been no regular water quality monitoring, including water temperature, but water temperatures have definitely begun to change since 2009.

IV. Conclusion

We investigated the characteristics of and trends in surface water temperatures of the Tonle Sap Lake from 2000 to 2019 using MOD11A1, a MODIS product to obtain daily land surface temperature data using Google Earth Engine. Google Earth Engine is an effective tool for satellite image

analysis. The maximum and minimum water temperatures are recorded in May and January, respectively, indicating that these are one month behind those of the air temperatures. One of the spatial characteristics is that the northern part is cooler than the southern part. Maximum water temperature increased at the rate of 0.20℃/10-year, minimum water temperature decreased at the rate of 0.78℃/10-year.

There was a significant correlation between the maximum water temperature and lake water level. The lake water level has declined recently. This indicates that the declining water levels are causing higher maximum water temperatures. The correlation between the minimum water temperature and lake water level was not strong. Factors contributing to the lower minimum water temperatures were not identified and must be studied in more detail in the future.

Acknowledgement

We are thankful to the Science and Technology Research Partnership for Sustainable Development (SATREPS), the Japan Science and Technology Agency (JST)/Japan International Cooperation Agency (JICA) for their financial support.

References

[1] Gorelick N, Hancher M, Dixon M, Ilyushchenko S, Thau D, Moore R (2017) Google Earth Engine: Planetary-scale geospatial analysis for everyone, Remote Sensing of Environment, 202: 18-27, doi:10.1016/j.rse.2017.06.031

[2] Hecht JS, Lacombe G, Arias ME, Dang TD, Pimanh T (2019) Hydropower dams of the Me-kong River basin: A review of their hydrological impacts, Journal of Hydrology, 568: 285-300, doi:10.1016/j.jhydrol.2018.10.045

[3] Hortle KG (2007) Consumption and the yield of fish and other aquatic animals from the Low-er Mekong Basin. MRC Technical Paper No. 16, Mekong River Commission, Vientiane, Lao PDR

[4] Hoshikawa K, Fujihara Y, Siev S, Arai S, Nakamura T, Fujii H, Sok T, Yoshimura C (2019) Characterization of total suspended solid dynamics in a large shallow lake using long-term daily satellite images, Hydrological Processes, 33(21): 2745-2758, doi:10.1002/hyp.13525

[5] O'Reilly CM., Sharma S, Gray DK, Hampton SE, Read JS, Rowley RJ et al. (2015) Rapid and highly variable warming of lake surface waters around the globe, Geophysical Research Letters, 42, 2015GL066235, doi:10.1002/2015GL066235

[6] Oyagi H, Endoh S, Ishikawa T, Okumura Y, Tsukawaki S (2017) Seasonal changes in water quality as affected by water level fluctuations in Lake Tonle Sap, Cambodia, Geographical Review of Japan Series B, 90(2): 53-65, doi:10.4157/geogrevjapanb.90.53

The 13th AUN/SEED-Net Regional Conference on Chemical Engineering 2020 (RCChE-2020)
Jointly held with
The 5th International Symposium on Conservation and Management of Tropical Lakes
"Insights and Challenges toward Achieving SDGs"

Meta-analysis of Photocatalytic Degradation of Pharmaceuticals and Personal Care Products in Water

Cui LI [1], and Chihiro Yoshimura [1*]

[1] *School of Environment and Society, Tokyo Institute of Technology, 2-12-1-M1-4 Meguro-ku, Tokyo, 152-8552, Japan*
** yoshimura.c.aa@m.titech.ac.jp*

Abstract

Pharmaceuticals and personal care products (PPCPs) are a unique group of emerging environmental contaminants which are widely found in water environment in the world. An increasing number of studies has confirmed the presence of various PPCPs in different environmental compartments, which raises concerns about the potential adverse effects to humans and wildlife. To overcome this issue of PPCPs, heterogeneous photocatalysis, for example using TiO2, is an emerging and viable treatment technology. Its combination with carbonaceous materials (e.g., activated carbon, carbon nanotubes and graphene nanosheets) has been found to significantly improve the performance. In this study, meta-analysis with random effects model was applied to literature data from more than fifty series of experiments. As a result, the pooled mean removal efficiency of PPCPs by carbonaceous/TiO_2 materials was 89.5% (95 % CI = 83.4 – 94.4%, k= 64). Subgroup analysis expounded the important and influential variables (e.g., different carbon-based TiO_2 photo-catalysts, process parameters and PPCPs characteristics) in the degradation processes. Furthermore, artificial neural network models were applied to modeling the performance (removal efficiency) of these carbonaceous/TiO2 photocatalytic experiments.

Keywords: *artificial neural network modeling, carbonaceous/TiO_2 composites, heterogeneous photocatalysis, meta-analysis, modified kinetic modeling*

I. Introduction

Pharmaceuticals and personal care products (PPCPs) are emerging environmental contaminants and have attracted the world's attention since the late 1990s. PPCPs are essential in maintaining high human health and well-being, has been reported that more than 50,000 PPCPs are produced[1]. An increasing number of studies has confirmed the presence of various PPCPs in different environmental compartments, including lakes, waste water effluents and even drinking tap waters. Heterogeneous photocatalysis was considered as a promising alternative for degrading various toxic organic pollutants in water, which is drawing increasingly attention due to its ability to mineralize the pollutants into water and carbon dioxide[2]. Compared with pure TiO_2, the modification of TiO_2 with carbonaceous

nanomaterials is an innovative approach for the enhancement of photocatalytic activity.

The study of carbonaceous/TiO_2 has now focused on synthesis and optimization of the photocatalysts and treatment of single PPCP compounds[3].There are rare models which combined element reaction and operation conditions together for prediction of photocatalytic performance. Similar photocatalytic processes showed a variation in degradation performance for the same PPCP compound . For instance, the removal efficiency of Ibuprofen by AC/TiO_2 photocatalytic system, varied from 78.2% to 99%[4].This fragmented information makes it difficult to compare the removal of a certain pollutant and to investigate the influential parameters, operation settings and the technique application in actual industry. In addition, present study only focused on one or several PPCPs in one study. While the understanding of removal performance of multiple PPCPs under different reaction condition is needed to support the real application step.

Thus, it is helpful to optimize bias and variation between studies and utilize results from multiple PPCPs and reaction conditions. In addition, effort could be taken to build a model based on the existing experimental results, which could be applicable for future prediction of photodegradation performance of PPCPs. The specific objectives of this study are:

(1) To statistically understand the removal efficiency of PPCPs by carbonaceous/TiO_2 photocatalytic treatment;

(2) To identify the important variables in causing the difference in removal performance, getting insight into the degradation process;

(3) To build a model based on the data collected from literature, addressing both the element reaction and operation conditions.

II. Materials and Methods

2.1. Data source, searching strategy and data processing

A systematic search of the peer-reviewed literature was carried out in the Web of Science database for articles that evaluated the PPCPs photodegradation processes in aqueous solution. The literature search was limited to peer-reviewed publications written in English between 2010 until June, 2020.

The inclusion criteria were applied to each publication and they included scope, study quality, and data availability. Scope criteria is the evaluation of titles and abstracts of the retrieved articles. The quality of a study was evaluated by the criteria of clarity, for instance, the associated methodologies. The availability of the data was analyzed by whether the study implied the mean and standard deviation of data. After these assessments, papers will be compiled as the primary dataset, including the first author, year of publication, the type of PPCPs, composition and dosage of photocatalysts, initial concentration of experiment, source and intensity of light irradiation, reaction time, temperature, removal efficiency (RE) and apparent rate constant (K_{app}). The other properties recorded from pubmed.com, and they were: molecular weight (MW), topological polar surface area (TPSA), complexity, pKa and octanol/water partitioning coefficient (logKow). The total data points included in each analysis are shown in Table 1.

Table 1. Data points included in each analysis

Category	Data points (k)
Total	64
Meta-analysis	64
Artificial neural network modeling	49

2.2. Description of statistical approaches

(a) Meta-analysis

Meta-analysis is a statistical procedure for combining results from multiple studies which originated from medical research. A meta- analytical approach can access the drivers of the variability relating to the inherent properties of the chemicals and operations parameter of a treatment. process. In the field of environmental research, for the effect of interest is removal efficiency, correspondingly proportion meta-analysis is applied[5]. Unless otherwise specified, R program (version 3.6.3) was used for statistical analysis. Meta-analysis was conducted using ‘metafor’ and ‘meta’ packages. Random effects model was assumed to accommodate the anticipated heterogeneity.

(b) Artificial neural network modeling

Artificial neural network modeling (ANN) is used to recognize the relationship between variables and degradation performance[6]. The input variables were set as molecular related variables (molecular weight of compounds, $logK_{OW}$, pK_a, complexity and TPSA) and

process related variables (concentration, dosage of photocatalyst, TiO_2 content of photocatalyst, light source and intensity). And the output variables were set as removal efficiency. MATLAB 2019a (ANN toolbox) is used for the development of ANN model. A supervised learning technique called Levenberg-Marquardt was used for the training of the network. The total number of hidden neurons was decided by the mean square error (MSE) and the performance of the ANN model was evaluated by correlation coefficient (R). The settings of ANN model are shown in Table 2.

Sensitivity analysis was conducted by Garson's method[6].Each weight decides which proportion of the incoming signal will be transmitted into the neuron's body . It is based on partitioning of connection weights and expressed as the follow equation:

$$I_j = \frac{\sum_{m=1}^{m=N_h}((|W_{jm}^{ih}|/\sum_{k=1}^{N_i}|W_{km}^{ih}|)\times|W_{mn}^{ho}|}{\sum_{k=1}^{k=N}\{\sum_{m=1}^{m=N_h}(|W_{km}^{ih}|/\sum_{k=1}^{N_i}|W_{km}^{ih}|)\times|W_{mn}^{ho}|\}}$$

where I_j is the relative importance of the j^{th} input variable on output variable; N_i and N_h are the number of input and hidden neurons; Ws are connection weights; the superscripts i, h, and o refer to input, hidden and output layers, respectively; and subscripts k, m, and n refer to input, hidden and output neurons, respectively.

Table 2. Parameters of ANN model

Parameters	Value
Input Variables	10
Output Variables	1 (RE)
Number of Neurons	1-10
Transfer Function	TANSIG (tangent sigmoid)
Learning Cycle	9 epochs
Performance function	MSE
Data division functoin	dividerand
Data division	70%-15%-15% (35-8-8)
Training functions	Levenberg Marquardt

III. Results and Discussion

In total, 64 experiments of 32 PPCPs treatment were included in the analysis, among which more data points were available in the CNT/TiO_2 photocatalytic system (k = 29) compared with Graphene/TiO_2 treatment (k = 8). The reported removal efficiency ranged from 54% to 100% with irradiation time from 1 to 4 hours. The pooled average RE for PPCPs degradation by the carbonaceous/TiO_2 photocatalysis was 89.5% (95 % CI = 83.4 – 94.4%, k= 64). The results of subgroup parameters analysis were shown in Table 3.

The highest removal efficiency was obtained from CNT/TiO_2 subgroup with an average percentage of 94.6% (95% CI = 89.8 – 98.0%, k= 29), followed by AC/TiO_2 (79.6%, k= 11) and Graphene/TiO_2 (78.9%, k= 8). Regarding light source, UVC has the highest pooled average removal efficiency (93.2%,95%CI=86.4–97.9%, k=28). Most PPCPs were persistent under visible photocatalytic process (RE < 10%), while the graphene/TiO_2 has appeared to improve the overall degradation.

Table 3. Results of meta-analysis

Moderator	Subgroup	k	RE%	95% C.I.
Photocatalyst	AC/TiO_2	11	79.6	56.8~91.3
	CNT/TiO_2	29	94.6	89.8~98.0
	Graphene/TiO_2	8	78.9	23.1~89.7
Light Source	Visible	14	27.1	10.0~48.6
	Sunlight	5	56.3	40.0~95.1
	UVA	17	82.3	64.8~96.0
	UVC	28	93.1	64.8~97.1
Category	NAIDs	14	73.2	52.2~89.7
	AEDs	6	85.1	56.0~99.3
	PCPs	6	83.8	46.1~100
	Antibiotics	14	60.1	46.1~81.1

NAIDs: Nonsteroidal anti-inflammatory drugs;
AEDs: Antiepileptic and anti-anxiety drugs;
PCPs: Personal Care Products.

The performance of established ANN model was depicted in Fig.1. The X-axis "Target" indicates the observed value which the model targets to reach, and the Y-axis "Output" means the output of the predicted value from the model. Two lines in the graph were used to show the success of the prediction. The solid line is the line that best fits on the data of the scatter plot which is obtained by regression analysis. In a perfect fit, when the predicted value equals to the observed value, the solid line would lay on the

dotted line. For the overall model performance, the correlation coefficient (R) is 0.94.

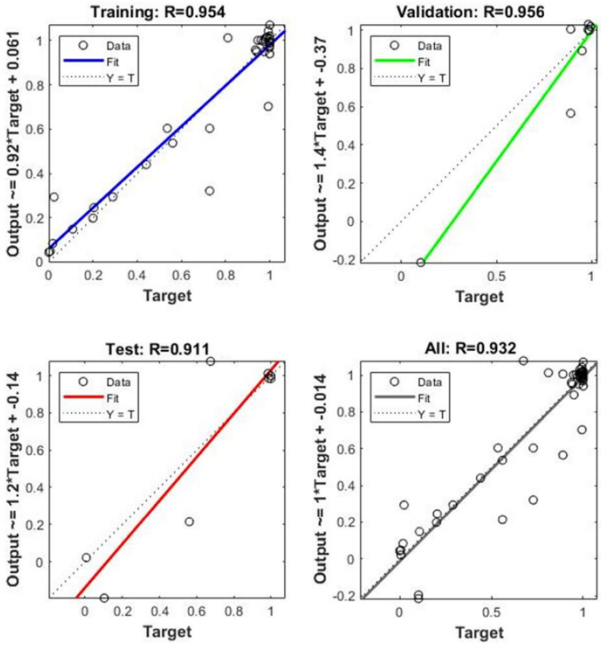

Fig. 1 Plot of the performance of the build ANN model. (Target: the observed value; Output: the predicted value by ANN model; R: correlation coefficient)

By Garson's sensitivity analysis method, we obtained the importance of each input variable (Table 4). There is no particularly noticeable difference between the importance of each variable, but process related variables have more relative importance to the model output (RE) than molecular related variables, counting to 61.2% of the total importance.

Table 4. Relative importance of input variables on RE

Input variables	Importance
Light source	14.2
Dosage	14.0
Concentration	12.3
Light intensity	12.1
pK_a	9.9
MW	9.1
Composition	8.6
Complexity	7.7
logKow	6.8
TPSA	5.3

IV. Conclusion

This study collected photocatalytic process parameters and performance of PPCPs degradation in carbonaceous/TiO_2 system published in literatures from 2010 to 2020, applying both statistical and modelling method to characterize and model the process. The results from meta-analysis found out the pooled average removal efficiency at 60-minutes' reaction time of PPCPs by carbonaceous/TiO_2 photocatalysis is 89.5%, and CNT/TiO_2 composites have the best removal performance of 94.6%. Artificial neural network with good prediction performance was built based on both molecular related features and process related parameters. A better ANN model may be realized by combing quantum structural features of molecular and process parameters, for prediction of multiple PPCPs under different reaction conditions[7]. However, model over-fitting is a problem needed to be discussed in the future studies.

Acknowledgement

We are thankful to the Science and Technology Research Partnership for Sustainable Development (SATREPS), the Japan Science and Technology Agency (JST)/Japan International Cooperation Agency (JICA) for their financial support.

References

[1] Daughton, C. G. & Ternes, T. A. Pharmaceuticals and personal care products in the environment: Agents of subtle change? Environ. Health Perspect. 107, 907–938 (1999).

[2] Awfa, D., Ateia, M., Fujii, M., Johnson, M. S. & Yoshimura, C. Photodegradation of pharmaceuticals and personal care products in water treatment using carbonaceous-TiO2 composites: A critical review of recent literature. Water Res. 142, 26–45 (2018).

[3] Gu, Y. et al. Adsorption and photocatalytic removal of Ibuprofen by activated carbon impregnated with TiO2 by UV–Vis monitoring. Chemosphere 217, 724–731 (2019).

[4] Xu, X. & Li, X. QSAR for photodegradation activity of polycyclic aromatic hydrocarbons in aqueous systems. J. Ocean Univ. China 13, 66–72 (2014).

[5] Mikolajewicz, N. & Komarova, S. V. Meta-analytic methodology for basic research: A practical guide. Front. Physiol. 10, (2019).

[6] López, M. E., Rene, E. R., Boger, Z., Veiga, M. C. & Kennes, C. Modelling the removal of volatile pollutants under transient conditions in a two-stage bioreactor using artificial neural networks. J. Hazard. Mater. 324, 100–109 (2017).

[7] Huang, X. et al. Mechanistic QSAR models for interpreting degradation rates of sulfonamides in UV-photocatalysis systems. Chemosphere 138, 183–189 (2015).

The 13th AUN/SEED-Net Regional Conference on Chemical Engineering 2020 (RCChE-2020)
Jointly held with
The 5th International Symposium on Conservation and Management of Tropical Lakes
"Insights and Challenges toward Achieving SDGs"

Application of Multivariate Techniques in the Evaluation of Spatial Surface Water Quality in an Urbanized Floodplain Area in Cambodia

Vinhteang Kaing, Ilan Ich, Lieng Thoun, Chantharath Yos, Chan Rathborey, Chan Rathboren, Layheang Song, Marith Mong, Chantha Oeurng, Ty Sok*

Faculty of Hydrology and Water Resources Engineering, Institute of Technology of Cambodia
Russian Federation Blvd., P.O. Box 86, 12156 Phnom Penh, Cambodia
**sokty@itc.edu.kh*

Abstract: Lakes and rivers are important multi-usage components, particularly lakes are not only important sources of surface water and livelihood for both rural and urban communities but they are also functioning as water retention receiving stormwater and wastewater from the urban area. Located in the northern part of Phnom Penh capital city of Cambodia, Tamouk Lake receives discharges from combined sewer systems by which a mixture of industrial wastewater, urban surface runoff, domestic wastewater, and sewer deposits from the drainage system of Phnom Penh. The water quality of Tamouk Lake has become more concern due to the pollutant load in wastewater discharge. This study aims to assess the spatial variation of water quality parameters and to determine the main contamination sources in the Tamouk Lake by using multivariate techniques. This study focuses on seven target water parameters (Total suspended solid (TSS), pH, Electrical conductivity (EC), Dissolved oxygen (DO), Chemical Oxygen Demand (COD), Phosphate (PO_4), and Nitrate (NO_3)) from 11 sampling points. The analysis was employed individually of lake conditions; normal condition and receiving storm; for understanding the effect of storm water to the water quality of the lake. The principle component analysis (PCA) was used to identify the sources of contaminant that effected the lake water quality and cause degradation. In lake normal condition, the first three principle componence explained 78.5% of the total variance in the water quality data set, while in receiving storm water condition, the first two principle componence explained for 83.15%. Overall, the study showed that most of factors determine the water quality of Tamouk lake is associated with the anthropogenic pollution sources from urban wastewater and biogenic sources in the lake. The study suggested that the management of wastewater discharge from Phnom Penh City is required to lower the accumulation of pollutants and minimize lake water quality degradation.

Keywords: *floodplain urbanized area, multivariate techniques, principal component analysis, urban wastewater*

I. Introduction

Lakes and rivers are important multi-usage components, particularly lakes are not only important sources of surface water and livelihood for both rural and urban communities but they are also functioning as water retention receiving stormwater and wastewater from the urban area. In urban area, the water quality is such a key factor which is hard to identify as its characteristic vary based on numerous factors such as street sweeping, stormwater, wastewater from domestic and small to medium industrial activity [1, 2]. These pollutants were pathogenic microorganisms, phosphorus and nitrogen, hydrocarbons, heavy metals, endocrine disruptors, and organic matter [3]. It is becoming the pressure to waterbodies (lake and reservoirs located near the urban area) as they function as the storage in biological treatment to collect the wastewater from the drainage system [4]. Thus, the deterioration of lake water quality is unavoidable. The declining water quality in freshwater lakes is an increasing problem that threatens the ecosystem services to the riparian communities, especially in developing countries [5].

Located in Cambodia, Tamouk Lake is in the northern

part of Capital Phnom Penh and has been selected as one site of wastewater treatment by JICA since 2015 [6] and to be constructed in years due to the fact that this lake is the largest lake in the northern part of Phnom Penh and has the low level of the population density in the area. Additionally, the developing status in the area is still immature [6]. It interesting to note that Tamouk Lake receiving discharges from combined sewer systems, by which a mixture of industrial wastewater, urban surface runoff, domestic wastewater and sewer deposits are discharged into receiving waters. Since the lake functions as the storage to receive storm water and wastewater from the drainage system in the northern part of Phnom Penh, the water quality in Tamouk Lake has become more concerning due to the pollutant load in wastewater discharge. Moreover, the study on water quality of Tamouk Lake is normally looked over.

As mentioned about the advantage of urban lake, the water quality concerning and lacking of study, the study on water quality in the lake and identification major pollution source of lake is crucial required. Therefore, this study is to assess the spatial variation of water quality parameters (Total suspended solid (TSS), pH, Electrical conductivity (EC), Dissolved oxygen (DO), Chemical Oxygen Demand (COD), Phosphate (PO_4), and Nitrate (NO_3)) and to determination the main contamination sources in the Tamouk Lake, a floodplain Urbanized Area in Cambodia, by using multivariate technique.

II. Materials and Methods

2.1. Sampling sites

The study was conducted in Tamouk Lake (or Kob Srov Lake) situated in Prek Pnov district of Phnom Penh, Cambodia. Tamouk Lake is the largest natural lake and the major reservoir of wastewater treatment in the northern area of Phnom Penh city. This lake is surrounded by 2 inlets, 2 outlets, and three water gates as shown in the map (Figure 1). As reported by [6], this lake covers 3270 ha and the depth water is 3.0-4.5 m in the dry season and accumulate 2-3 m more in the rainy season. Moreover, the Tamok sewage system is a separate system that covers the treatment area of 6,019.2 ha with the population of around 481,000 (population projection to 2035). The total length of trunk sewer is 66.1 km (diameter from 200 mm to 1,650 mm), and the pumping stations were installed at nine locations, seven of which were pumping stations were manhole type and two were installed at the inlet of Tamouk Lake [6].

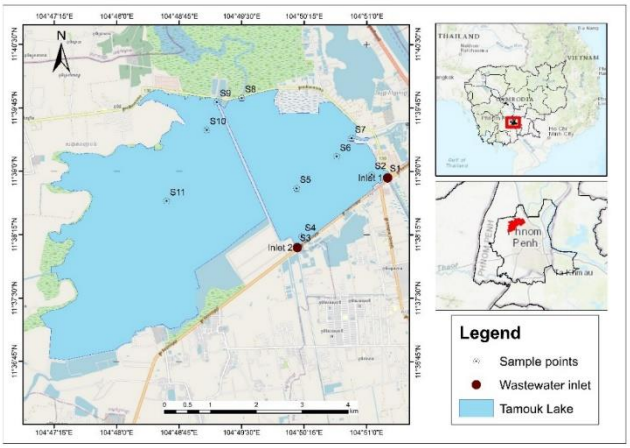

Figure 1. Location map and sampling points of Tamouk lake

2.2. Water Quality Variables Selection

The field monitoring was conducted two times: the pre-storm event called 'normal condition' and post-storm event call 'receiving storm water' at 11 sampling points (**Figure1 &Table 1**). The field survey was conducted during the pre-storm event on 28 May 2019. After that, the second field survey was conducted during the post-storm event on 7 June 2019. The 11 sampling points from the depth of 10 cm in Tamouk Lake were established for both field surveys.

Table 1. Water quality variable and site location consider in Tamouk Lake

Date	Variables	Site location
28/05/2019	EC, DO, pH, COD, PO_4, NO_3, TSS	Inlet, outlet, and middle of the lake
07/06/2019	EC, DO, pH, COD, PO_4, NO_3, TSS	Inlet, outlet, and middle of the lake

2.4. Principal component analysis (PCA)

Principal Components Analysis (PCA) was used to provide information on the most meaningful parameters which describe the whole data set interpretation and data reduction, and summarize the statistical correlation among constituent in the water with minimum loss of original information [7]. PCA data are mainly reflected by the variance of data variables. The greater the variance, the more information is included as measured by the cumulative variance contribution ratio. PCA were performed on standardized data with z-scale of mean zero and standard deviation of one in order to have an equal weight to every variable, this is for minimizing the influence of variable whose variance is large and adjusting for the disparity in the variable sizes, in the units of measurement and renders the

data dimensionless [8-10].

III. Results and Discussion

3.1. Water quality characteristic

From spatial location, pH decreased (7.7 to 9.6) at the inlet of the lake and slightly increase at the downstream as the middle of lake and outlet (9.2 to 9.5, 9.6 to 9.7). However, the DO level in the water is opposite with pH value due to the increasing the anoxic in the surface runoff from the urban area at the receiving storm water. TSS is dramatically increased at the post-storm event due to the erosion and sediment that washed from the road surface by the runoff. Additionally, EC is a bite increase in the lake at the post-rainfall event due to the additional ion and salt that picked from the road surface during the storm event. Although, EC of sample 2 and 3 are very high at the pre-storm event due to the level of ion and salinity in wastewater discharge. Furthermore, the different level of PO_4 and NO_3 in the lake due to the correlation of NO_3 with PO_4 [11, 12]. Then, COD at the inlet is drop-down, but it rises a bite near the outlet at the post-storm event. This comes from the positive correlation between COD and pH [12].

Table 2. Range of surface water quality parameters in Tamouk Lake

	Parameters	Min	Mean	Max	SD
Normal condition	pH	7.90	8.93	9.63	0.62
	DO	9.14	11.01	11.69	0.68
	EC	224.00	387.27	763.00	194.93
	TSS	1.00	28.64	97.50	27.43
	COD	10.20	38.95	112.00	38.84
	PO_4	2.90	6.26	14.50	4.01
	NO_3	2.80	5.13	9.20	1.81
Receiving storm water	pH	7.75	8.72	9.65	0.81
	DO	4.13	7.77	11.35	1.98
	EC	231.00	377.91	567.00	120.61
	TSS	10.00	59.01	152.00	49.11
	COD	9.01	22.32	49.00	15.83
	PO_4	1.80	4.79	8.00	1.84
	NO_3	2.00	6.45	15.30	4.12

Description and characteristic values of 7 key indicators of surface water quality parameters in Tamouk Lake are shown in Table 2. EC, COD, and TSS have larger standard deviations, the Tamouk Lake water quality shows obvious differences among the above 4 indicators both normal condition and receiving storm water. Thus, different condition should be treated individually in the next stage of water pollution control and water environmental conservation planning. It is affordable for us to take water quality conservation measures to the condition with good water quality while take positive counter measures to condition with poor water quality.

3.2. Identification of potential sources of monitored variables

The PCA was performed to understand the relationship between the water quality variables of all sampling points and to identify their characteristics. Factor analysis of the present data set of Tamouk lake further reduced the contribution of less significant variables obtained from PCA. The two lake conditions; normal condition and receiving storm water; were individually examined to see the effect of storm water to the lake's water quality. The PCs with the eigenvalue greater than 1 were extracted entire PCs of data set to be the retained PCs and the components with eigenvalues lower than 1 were removed due to their low significance [13]. The PC loadings of the water quality variables were categorized as 'strong', 'moderate', and 'weak' corresponding to the absolute loading values of >0.75, 0.75–0.50 and 0.50–0.30, respectively [10].

In lake normal condition, the first three PCs explain 78.5% of the total variance in the water quality data set (**Table 3**). The first factor (PC1) has moderate negative loading on EC and COD and weak negative loading with PO_4. This factor can be attributed to biogenic and anthropogenic from urban wastewater pollution sources. The second factor (PC2) showed moderate negative loading on TSS and weak positive loading on pH. This factor could be associated with the physical and chemical properties of the water, and to natural weathering of the basin. These two originated primarily from run-off with high load of solids from point sources of pollution like domestic areas, agricultural fields [14]. The third factor (PC3) showed strong positive loading on DO and weak positive loading on NO_3. The PC3 should attribute the chemical and biological process in the lake and can be associated the low level of dissolved organic matter that lead to consume less amount of oxygen.

During receiving storm water condition, the first two PC with eigenvalue>1 explained for 83.15% of the total variance (**Table 3**). The PC'1 has weak positive loading on pH and DO, and weak negative loading with EC and COD. This PC represents the physiochemical source of variability. The PC'2 has strong positive loading with TSS and NO_3. These two elements originated primarily from run-off with high load of solids and wastes from point sources of pollution like domestic areas, agricultural fields [14]. For

Tamouk lake, the main point source should be from wastewater with storm discharge from the Phnom Penh City.

The results from PCA suggested that most of factor determine the water quality of Tamouk lake is associated with the anthropogenic pollution sources from urban wastewater and its biogenic sources in the lake.

Table 3. Factor loadings of principle components of individual water quality variables in normal condition and receiving storm water of the Tamouk Lake

Variable	Principle components				
	Normal condition			Receiving storm water	
	PC1	PC2	PC3	PC'1	PC'2
pH	0.313	**0.482**	0.164	**0.465**	-
DO	-	-0.310	**0.732**	**0.425**	0.229
EC	**-0.595**	0.003	-	**-0.471**	-
TSS	-	**-0.637**	-0.332	-0.218	**0.648**
COD	**-0.536**	0.237	-0.261	**-0.487**	-0.146
PO_4	**-0.445**	0.359	0.311	-0.255	-0.160
NO_3	-0.229	-0.284	**0.401**	-0.177	**0.687**
Eigen-value	2.413	1.894	1.188	3.921	1.900
PV(%)	34.47	27.05	16.97	56.01	27.14
CPV(%)	34.47	61.52	78.49	56.01	83.15

Note: The variables with bold values of loading are variables which most explain or represent the principal components.

IV. Conclusion

The study assessed the spatial variation of water quality and identified the sources of contamination base on water quality variables (TSS, pH, EC, DO, COD, PO_4, and NO_3) in the Tamouk Lake, a floodplain Urbanized Area in Cambodia. Multivariate technique included Pearson's correlation, PCA, and CA were applied to understand spatial variation of lake water quality. The PCA was used to identify the sources or factor of contaminant that effected the Tamouk Lake water quality and cause degradation. Result from PCA suggested that the lake water quality was control by the anthropogenic pollution sources (urban waste water), and biogenic sources in the lake. The study suggests that the management of wastewater discharge from Phnom Penh City is required to lower the accumulation of pollutants and minimize environmental degradation.

Acknowledgement: We are thankful to the Agence Française de Développement (AFD) No. CKH 1236 02P for financial support of the study.

References

1. Samsudin MS, Juahir H, Zain SM, Adnan NH: Surface river water quality interpretation using environmetric techniques: Case study at Perlis River Basin, Malaysia. *International Journal of Environmental Protection* 2011, 1(5):1-8.
2. Vaze J, Chiew FH: Experimental study of pollutant accumulation on an urban road surface. *Urban Water* 2002, 4(4):379-389.
3. Akpor O, Otohinoyi D, Olaolu D, Aderiye B: Pollutants in wastewater effluents: impacts and remediation processes. *International Journal of Environmental Research and Earth Science* 2014, 3(3):050-059.
4. Verma M, Negandhi D: Valuing ecosystem services of wetlands—a tool for effective policy formulation and poverty alleviation. *Hydrological sciences journal* 2011, 56(8):1622-1639.
5. Ndungu J, Augustijn DC, Hulscher SJ, Fulanda B, Kitaka N, Mathooko JM: A multivariate analysis of water quality in Lake Naivasha, Kenya. *Marine and freshwater research* 2015, 66(2):177-186.
6. JICA: The Study on Drainage and Sewerage Improvement Project in Phnom Penh Metropolitan Area. *Final Report* 2016, II.
7. Helena B, Pardo R, Vega M, Barrado E, Fernandez JM, Fernandez L: Temporal evolution of groundwater composition in an alluvial aquifer (Pisuerga River, Spain) by principal component analysis. *Water research* 2000, 34(3):807-816.
8. Simeonov V, Stratis J, Samara C, Zachariadis G, Voutsa D, Anthemidis A, Sofoniou M, Kouimtzis T: Assessment of the surface water quality in Northern Greece. *Water research* 2003, 37(17):4119-4124.
9. Liu W, Li X, Shen Z, Wang D, Wai O, Li Y: Multivariate statistical study of heavy metal enrichment in sediments of the Pearl River Estuary. *Environmental pollution* 2003, 121(3):377-388.
10. Liu C-W, Lin K-H, Kuo Y-M: Application of factor analysis in the assessment of groundwater quality in a blackfoot disease area in Taiwan. *Science of the Total Environment* 2003, 313(1-3):77-89.
11. Alsaqqar AS, Khudair BH, Hasan AA: Application of water quality index and water suitability for drinking of the Euphrates river within Al-Anbar province, Iraq. *Journal of Engineering* 2013, 19(12):1619-1633.
12. Tripathi B, Pandey R, Raghuvanshi D, Singh H, Pandey V, Shukla D: Studies on the physico-chemical parameters and correlation coefficient of the river Ganga at Holy Place Shringverpur, Allahabad. *IOSR Journal of Environmental Science, Toxicology and Food Technology* 2014, 8(10):29-36.
13. Kim J-O, Mueller CW: Factor analysis: Statistical methods and practical issues: sage; 1978.
14. Gazzaz NM, Yusoff MK, Ramli MF, Aris AZ, Juahir H: Characterization of spatial patterns in river water quality using chemometric pattern recognition techniques. *Marine Pollution Bulletin* 2012, 64(4):688-698.

The 13th AUN/SEED-Net Regional Conference on Chemical Engineering 2020 (RCChE-2020)
Jointly held with
The 5th International Symposium on Conservation and Management of Tropical Lakes
"Insights and Challenges toward Achieving SDGs"

Effect of Water and Land Based Villages on Phosphorus Dynamics in a Lake-Floodplain System, Tonle Sap Lake

Vouchlay Theng[1]*, Hashimoto Kana[1], Sovannara Uk[1], Sophanna Ly[1], Tanaka Tomohiro[2], Yoshioka Hidekazu[3], Yoshimura Chihiro[1]

[1] *Department of Civil and Environmental Engineering, Tokyo Institute of Technology, 2-12-1 Ookayama, Meguro-ku, Tokyo, 152-8552, Japan*

[2] *Graduate School of Global Environmental Studies, Kyoto University, Kyotodaigaku-Katsura, Nishikyo-ku, Kyoto, 615-8540, Japan*

[3] *Graduate School of Natural Science and Technology, Shimane University, 1060 Nishikawatsu-cho, Matsue-shi, Shimane, 690-8504, Japan*

**Corresponding author: vouchlaytheng@gmail.com*

Abstract

The objective of this study is to develop a phosphorus (P) dynamic model by integrating the load from water and land based villages at Tonle Sap Lake's floodplain to investigate spatiotemporal changes of total P (TP) dynamics in the lake. A two-dimensional local inertial model describing hydrostatic shallow surface water dynamics was applied to simulate horizontal hydrodynamics of the lake. The processes such as advection-dispersion and internal and external loadings of TP were considered in the developed model. The model application result in 1999-2003 showed that at least 240 villages permanently stayed in the water from September 1999 to December 2003. The total input of TP from the tributary rivers was estimated to be 137 ton/month in the dry season and 692 ton/month in the rainy season. On average, the estimated TP loads from the villages were approximately 21 ton/month in the dry season and 47 ton/month in the rainy season, equivalent to 15% and 7% of the total TP load from the tributaries, respectively. More than 83% of the lake area was in mesotrophic state and some locations reached eutrophic state. The locations around the villages reached eutrophic state at the beginning of flooding periods due to the release of TP mass from land to water. Increasing TP load from the villages will increase the eutrophication problem in the rainy season which should be considered for water quality management.

Keywords: *Floodplain, phosphorus dynamics, trophic state, water and land based villages, water quality model*

I. Introduction

Phosphorous (P) is a limiting nutrient in most of the freshwater lakes [1]. Excessive phosphorus could change tropic states of the lakes to be eutrophic, which is considered as a major stress for lake ecosystems. Tonle Sap Lake (TSL) is one of such examples being excessive nutrients and likely P-limited [2]. More than 1.7 million people living in TSL's ecosystem depend directly on the lake's resources and directly discard wastes into the lake [3]. Raw domestic wastewater generally contains high concentration of P, ranging between 0.2–2.0 g/day/capita [4, 5]. Therefore, the effect of these villages to P dynamics in TSL should be investigated to understand the anthropogenic impact on the ecosystem and solve such water environmental problems.

Many process-based P models were developed to estimate total P (TP) dynamics for freshwater lakes. However, those models have not been applied to a tropical lake- floodplain system (i.e., TSL), which has a seasonal reversal flow and villages on and around the lakes. The objective of this study is, therefore, to develop a process-based dynamic model by integrating the load from the villages to analyze TP dynamics in TSL.

II. Methodology

2.1. Description of study area

TSL is a tropical lake-floodplain system in Cambodia. During the dry season, the lake's surface area is 2500 km^2 and expands up to 15 000 km^2 in the rainy season, extending the lake over the vast floodplain [6]. The villages on and around TSL were categorized into three types: land based, land-water based, and floating (water based) [7]. The TP load from these villages were included in this study.

2.2. Mathematical model

The developed model is governed by horizontal advection-dispersion and processes of sedimentation, internal loading, and input of TP from tributaries, atmosphere, and the villages on the lake in two dimensions. The dynamic mass balance of TP can be expressed as

$$\frac{\partial(hC)}{\partial t} = \frac{\partial}{\partial x}\left(D_x h \frac{\partial C}{\partial x} - v_x hC\right) + \frac{\partial}{\partial y}\left(D_y h \frac{\partial C}{\partial y} - v_y hC\right) - v_{sed}C + k_i + k_a \quad \text{(Eq.1)}$$

where, C is the TP concentration; t is the time; v_x and v_y are the water velocity in x- and y-directions, respectively; h is the water depth; v_{sed} is the settling velocity; k_a is atmospheric loading rate; k_i is the internal loading rate; $D_x = 0.6 h_x v_x^*$ and $D_y = 0.6 h_y v_y^*$ are the dispersion coefficients in x- and y-directions, respectively [8]; h_x and h_y are the respective water depths in x- and y-directions. The friction velocities, v_x^* and v_y^* are calculated by the Manning's equation. The internal loading rate is the total loading rate from resuspension and diffusional flux of sediment pore water phosphorus to overlying water column.

As shown in the conceptual framework (**Fig. 1**), the major components of the model are numerical discretization, computational domain, and input data. A finite volume method is employed and the mass conservation is locally preserved by using the total variation diminishing (TVD) scheme in spatial discretization and 1st-order Euler-forward method in temporal discretization. The monotonic upstream-centered scheme for conservation laws approach is applied into the TVD scheme as it is one of the most successful high-resolution schemes for hyperbolic conservation laws, which has second-order accuracy in space [9].

Daily water flow discharges from the boundary tributary rivers in TSL were obtained from hydrological models,

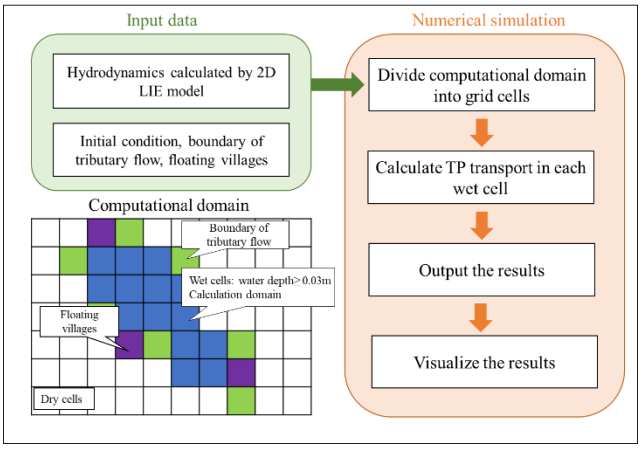

Fig. 1. The framework of the P dynamic model

Geomorphology-Based Hydrological Model and 1D hydraulic model Mike 11. Hydrodynamic data was obtained from the two-dimensional local inertial model, 2D-LIE [10]. The observed TP concentration was obtained from the Mekong River Commission's database and Water Utilisation Programme. The villages and population data in 2008 were obtained from National Institute of Statistic [11]. Then, the population of villages were converted based on the annual population growth rate of 1.54%/year. Most of floating villages moved to nearby flooded forest. Therefore, we assumed that each village area stayed within 1 km^2. The TP load from the villages was assumed to be 0.9 g/day/capita. All TP mass from the villages was assumed to accumulate on land whenever dried and be immediately released to the lake water whenever inundated. The spatial resolution was set to be 500 m.

III. Results and Discussions

3.1. Numerical accuracy and model calibration

The evaluation of the numerical accuracy of advection-dispersion was performed against 2D benchmark tests of the rotating Gaussian pulse where an exact solution is available. The mass conservation rates of the tests were higher than 99%. The preliminary test with the case of TSL also confirmed reasonable mass conservation and an assumed bell shape distribution of the concentration was not fluctuated after 1-month transport. The accumulated relative error was ranged from 0% to 1% in mass from 1999 to 2003.

The model was manually calibrated for the period from September 1999 to December 2001 at Kampong Loung (KGL1) and validated for the period from January 2002 to December 2003 at 2 locations of Kampong Loung (KGL1

and KGL2), Peam Bang (PBA), and 3 locations of Phnom Krom (PNK1, PNK2, and PNK3) (**Fig. 2**). The root mean square error of TP in the calibration was 17 µg/L (13 µg/L in the validation) while the observed TP concentration ranged from 5 µg/L to 69 µg/L. The calibrated settling velocity was 0.4 m/day, and the summation of internal loading and atmospheric loading was 8.0 mg/m^2/day.

3.3. Phosphorus dynamics in Tonle Sap Lake

The total input of TP from the tributary rivers was estimated to be 137 ton/month in the dry season and 692 ton/month in the rainy season. On average, only 14 ton/month of TP flowed out from TSL during the dry season and 28 ton/month during the rainy season. During the study periods at least 240 villages stayed permanently on the water. The average numbers of villages on the water and inundated were 405 and 608 in the dry and the rainy seasons, respectively. The estimated TP loads from the villages into the lake were approximately 21 ton/month in the dry season and 47 ton/month in the rainy season, equivalent to 15% and 7% of the total TP load from the tributaries, respectively. Most of the time, the TP settling was higher than internal and atmospheric loading. The total of net settling and atmospheric flux was 350 ton/month in the dry season and 509 ton/month in the rainy season.

On average, the TP mass stored in the lake was 492 ton and 828 ton in the dry and the rainy seasons, respectively. The water surface was observed to be mostly mesotrophic (11 µg/L ≤ TP ≤ 30 µg/L), and its surface coverage was 86% in the dry season and 83% in the rainy season. The concentration of TP in the lake in the dry season was almost higher than that in the rainy season (**Figs. 2. a & b**). The eutrophic area expanded from 4% in November to 9% in May and contracted during the rainy season. This shift was possibly caused by the low net settling flux in the low-water period and the high concentration of external input from the tributaries in such a period. Furthermore, approximately 49% of the wet cells were dried out during the dry season which contained TP mass about 30 ton or 6% of total TP mass and was released back to the lake due to the annual flood pulse. Around the villages, water became eutrophic (TP > 30 µg/L) at the beginning of flooding periods due to the release at accumulated TP mass on the land to water. Then, the lake was recovered by sedimentation process.

During the dry season, the model simulated eutrophication near the outlets of the tributaries and at the bank line along KGL1, PBA, and the outlet of the TSL

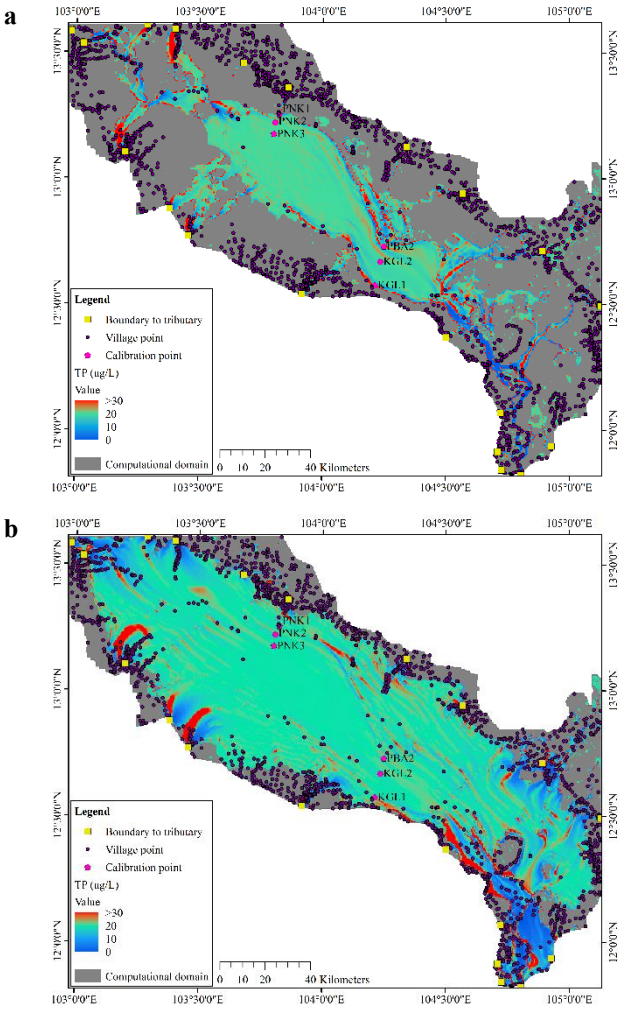

Fig. 2. Distribution of simulated TP concentration in TSL during: **a)** the dry season in March 15, **b)** the rainy season in October 15, 2001.

downstream part (e.g., **Fig. 2. a**). The eutrophic area was 7% of the lake area in March 2001. In July, TP influx via TSR quickly flowed into the middle of the lake causing eutrophication along that way. In the late rainy season, the lake water was diluted by rainwater and lowered the concentration of most tributaries input. The eutrophic area in October 2001 was 3% of the lake area due to high TP concentration from few tributaries and villages (**Fig. 2. b**).

3.4. Impact assessment of water and land based villages on eutrophication

Population in Cambodia increases rapidly. Sewages are usually discharged into the water sources without any treatment due to the lack of wastewater treatment facility [3].

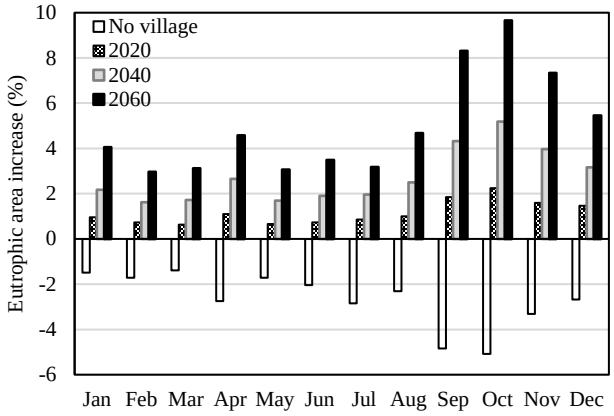

Fig. 3. Effect of water and land based villages on eutrophication area compared to the baseline of TSL in 2000

Thus, the amount of TP load from the villages will also increase. By assuming the population growth rate keeps constant, 1.54%/year, the impact of the villages in 2020, 2040, 2060; and no village loading on eutrophic area is found by comparing to the baseline of TSL in 2000 using model calibration result (**Fig. 3**). The results show that the villages are highly effect on eutrophication in rainy season due to the inundation at the lake flood-plain area. The highest increases of eutrophic area are 2%, 5%, and 10% in October in 2020, 2040, and 2060, respectively. However, if there is no TP load from the villages (e.g., people move to the land or the wastewater treatment facility is developed), the eutrophic area will be reduced from 1% to 5%.

IV. Conclusion

The developed P dynamic model is useful for describing mass balance of TP processes, the spatiotemporal changes of P, and the effect of the villages on eutrophication in TSL. However, the biological process of phytoplankton uptake and release and speciation of P (e.g., dissolved and particulate P) were not explicitly included. The uncertainty of data should be considered in further work.

Acknowledgement

We are thankful to the Science and Technology Research Partnership for Sustainable Development (SATREPS), the Japan Science and Technology Agency /Japan International Cooperation Agency for their financial support, and the Mekong River Commission and Water Utilisation Programme of Finland Component Project for the provision of the observed data of phosphorus in Tonle Sap Lake.

References

[1] Schindler, D.W., Hecky, R.E., Findlay, D.L., Stainton, M.P., Parker, B.R., Paterson, M.J., Beaty, K.G., Lyng, M., Kasian, S.E.M., 2008. Eutrophication of lakes cannot be controlled by reducing nitrogen input: Results of a 37-year whole-ecosystem experiment. *Proceedings of the National Academy of Sciences of the United States of America* 105, 11254–11258.

[2] Burnett, W.C., Wattayakorn, G., Supcharoen, R., Supcharoen, R., Sioudom, K., Kum, V., Chanyotha, S., Kritsananuwat, R., 2017. Groundwater discharge and phosphorus dynamics in a flood-pulse system: Tonle Sap Lake, Cambodia. *Journal of Hydrology* 549, 79–91.

[3] Ung, P., Peng, C., Yuk, S., Tan, R., Ann, V., Miyanaga, K., Tanji, Y., 2019. Dynamics of bacterial community in Tonle Sap Lake, a large tropical flood-pulse system in Southeast Asia. *Science of the Total Environment* 664, 414–423.

[4] Okada, M., Sudo, R., 1986. Per Capita Loadings of Domestic Wastewater. *Research Report from the National Institute for Environment Studies* 95, 7-20.

[5] Mesdaghinia, A., Nasseri, S., Mahvi, A.H., Tashauoei, H.R., Hadi, M., 2015. The estimation of per capita loadings of domestic wastewater in Tehran. *Journal of Environmental Health Science & Engineering* 13, 1–9.

[6] Keskinen, K., 2006. The Lake with Floating Villages : Socio- economic Analysis of the Tonle Sap Lake. *Water Resources Development* 22, 463-480.

[7] Binaya, R.S., Pham, N.B., 2020. Environmental Changes in Tonle Sap Lake and Its Floodplain: Status and Policy Recommendations. Institute for Global Environmental Strategies, Tokyo Institute of Technology and Institute of Technology of Cambodia.

[8] Huang, L., Fang, H., He, G., Jiang, H., Wang, C., 2016. Effects of internal loading on phosphorus distribution in the Taihu Lake driven by wind waves and lake currents. *Environmental Pollution* 219, 760–773.

[9] Bai, F., Yang, Z., Zhou, W., 2017. Study of total variation diminishing (TVD) slope limiters in dam-break flow simulation. *Water Science and Engineering* 11, 68–74.

[10] Tanaka, T., Yoshioka, H., Siev, S., Fujii, H., Fujihara, Y., Hoshikawa, K., Ly, S., Yoshimura, C., 2018. An integrated hydrological-hydraulic model for simulating surface water flows of a shallow lake surrounded by large floodplains. *Water (Switzerland)* 10, 1–23.

[11] National Insitute of Statistics (NIS), 2010. Census Map Layer and Databases 2008. National Institute of Statistic, Phnom Penh, Cambodia.

The 13th AUN/SEED-Net Regional Conference on Chemical Engineering 2020 (RCChE-2020)
Jointly held with
The 5th International Symposium on Conservation and Management of Tropical Lakes
"Insights and Challenges toward Achieving SDGs"

Groundwater Quality Assessment in the Floodplain Area around the Tonle Sap Lake, Cambodia

Bunhuot Ruos[1], Ratana Kheang[1], Sreyleang Ya[2], Vuthy Chork[2], Kong Chhuon[2], Ratha Doung[2], Ratino Sith[2], Sokly Siev[3], Boreborey Ty[3], Khy Eam Eang[2*]

[1] *Master of UWE, Graduate School, Institute of Technology of Cambodia, Russian Federation Blvd., P.O. Box 86, Phnom Penh, Cambodia*
[2] *Faculty of Hydrology and Water Resources Engineering, Institute of Technology of Cambodia, Russian Federation B lvd., P.O. Box 86, Phnom Penh, Cambodia*
[3] *Faculty of Chemical and Food Engineering, Institute of Technology of Cambodia, Russian Federation Blvd., P.O. Box 86, Phnom Penh, Cambodia*

**Corresponding author: khyeam_eang@yahoo.com*

Abstract

This study attempted to evaluate the groundwater quality in the floodplain area around the Tonle Sap lake. Thirty-six and forty well water samples were collected from the study area in the wet and dry season, respectively and analyzed for major physicochemical properties. As a result, temperature, pH, TDS (total dissolved solids), and EC (electrical conductivity) varied considerably between both seasons and among the sampling sites. The major concentrations of cations and anions were in the respective order of Ca > Na+K > Mg and HCO_3 > SO_4 > Cl > NO_3. Three major hydro-chemical facies (Ca-HCO_3, Ca-Cl, and Na-HCO_3) were identified using a Piper trilinear diagram. The value of pH, K, Mn, and Fe, nearly 50% of water samples were unsuitable for drinking purposes within both seasons, except Fe in the dry season, probably due to high precipitation of iron-hydroxide. The total hardness (TH) indicated that the well water more than 50% were defined as soft water for both seasons. Residual sodium carbonate (RSC) revealed that 40% samples of dry season were unsuitable for irrigation purposes. However, Wilcox and USSL (US salinity laboratory) classified that the groundwater was suitable for irrigation. The overall quality of groundwater in both seasons could be considered as moderately higher than drinking standard, but adequate for irrigation.

Keywords: *Drinking water, Floodplain area, Groundwater quality assessment, Irrigation purpose*

I. Introduction

Cambodia groundwater regarded as a widely available supplemental source to support 53% of Cambodian households in the dry season [1] . Until now, groundwater quality concern is still being doubtful for Cambodian people particularly, the part of floodplain area around the Tonle Sap lake. The groundwater from this area is being used without knowing whether it satisfied with drinking and irrigation standards. Some researches were conducted in this area, but it was rarely related to groundwater quality. Additionally, the water depth of the lake varied seasonally with an average depth less than 2 m in dry season and increased to 10 m in flood season. This unique phenomenon could change the chemical distribution in groundwater over time. It is very beneficial to be known all these mentioned problems. Therefore, this study aims to carry out the evaluation of groundwater quality in floodplain area of Tonle Sap lake which focus on the current status of water quality and the suitability in drinking and irrigation purpose.

II. Materials and Methods

2.1. Sampling sites

The present study was conducted in floodplain area around the Tonle Sap lake as shown in **Fig. 1**. Thirty-six and

forty samples from selected locations were collected in wet season (August, 2019) and dry season (December,2019), respectively.

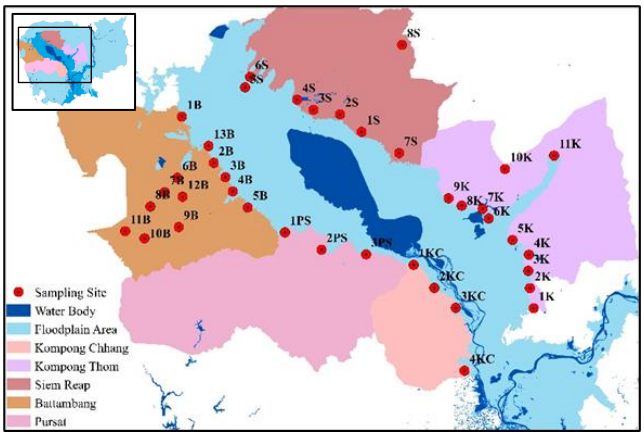

Fig. 1. Study area and sampling site

2.2. Experimental set-up

The physicochemical parameters included pH, temperature, TDS, EC were analyzed in-situ by using Multi-EXO Sondes. Seven of major ions: Ca^{2+}, Mg^{2+}, K^{+}, Na^{+}, Cl-, NO_3^{-}, and SO_4^{2-} were analyzed by ion chromatography (IC) while, six heavy metals such as Mn, Fe, Cu, Pb, Cd, and Cr were analyzed via atomic adsorption spectrophotometry (AAS). IC and AAS analyses were conducted at SATREPs laboratory and chemical laboratory of Institute of Technology of Cambodia (ITC).

2.3. Analytical methods

To study on current status of water quality, three parameters such as pH, EC, and temperature were carried out by using Box and Whisker plot while ion components were plotted in piper diagram [2] .

Instantly, to assess to drinking water this study has used the current data to compare with Cambodia Drinking Water Standard (DWS) by Ministry of Industry, Mining and Energies and World Health Organization [3] [4] . The total hardness (TH) was classified for domestic purpose based on Environmental Protection Agency (1976) [5] . In terms of irrigation purpose, sodium adsorption ratio (SAR), residue sodium carbonate (RSC), and sodium percentage (%Na) were calculated based on US salinity laboratory (USSL), Food Agriculture Organization (FAO), and Wilcox (1948), respectively [6] -[8] .

III. Results and Discussion

3.1. Current status of water quality

The pH ranged from 4.12 to 7.65 in rainy season and 3.1 to 7.86 in dry season. The downing pH would be result in buffering calcium minerals but high in dissolved carbon dioxide (H_2CO_3) [9] . EC has reached 3.6 mS/cm in dry season. Higher EC when its depth downs to 30m and pH greater than 8. Temperature in both seasons ranges from 28ºC to 32ºC excepting the dry season in Battambang (35ºC). Higher temperatures can reduce oxygen and dissolve more minerals to higher electrical conductivity. The pH, EC, and Temperature are provided in **Table 2**.

The platform hydro-chemical facies use to describe characteristic chemical composition, **Table 1**. It is observed that water samples in both seasons are influenced by cation: Ca > Na+K > Mg and anion: HCO_3 > SO_4, > Cl but, HCO_3 increased to 75%. The majority of the water samples fall in calcium-bicarbonate type (Ca-HCO_3) and calcium-chloride type (Ca-Cl) field, in rainy season. In rainy, it is apparent that the total hydrochemistry is dominated by bicarbonate (HCO_3). In the dry season, the majority of waters defined as Ca-HCO_3 type and following by sodium-bicarbonate type (Na-HCO_3).

Table 1. Result from piper diagram

Ions	% Sample	
	Rainy (34 Samples)	Dry (40 samples)
Ca^{2+}	33%	34%
Mg^{2+}	23%	20.5%
Na^{+}+ K^{+}	32%	30.5%
No dominant	12%	15%
HCO_3^{-}	56%	75%
SO_4^{2-}	20%	10%
Cl^{-}	15%	10%
No dominant	9%	5%
Water Type	Ca-HCO_3 Ca-Cl	Ca-HCO_3 Na-HCO_3

3.3. Suitability in drinking and irrigation purpose

The results in **Table 2** showed that EC, TDS, pH, K, Fe, and Mn are slightly out of the standard range for both seasons except for Fe in the dry season. The pH is not desirable for drinking when smaller than 6.5. Fe within 50% is detected more than the permissible limit (PL) of 0.3 mg/l in the rainy period, while Mn also exceeded the PL more than 40% in both seasons. K^{+} has reached more than a thousand mg/l which surpassed the permissible limit of 12

mg/l. The highest K would be provoked by the leaching from fertilizer use in agriculture. Some ions in well water such NO_3, SO_4, HCO_3 also found to overtake the PL with a few sites but HCO_3 is higher in the dry season. TH showed that 3% in rainy and none in dry samples, which are considered as very hard (**Table 4**), exceeding 300 mg/l and may lead to the incidence of parental mortality and some types of cancer.

The RSC stretches from -2.8 to 12.6 in rainy season and -2.5 to 21.5 in dry season (**Table 3**). Based on RSC, water can be classified as safe, marginally suitable, and unsuitable. It is observed that RSC was 40% in dry season and was not suitable for irrigation and agriculture. RSC greater than 5meq/l are considered harmful to the growth of plants. In **Fig. 4**, it is revealed that most samples low in sodium and high in SAR. Most sample is located in C1S1, C2S1, and C3S1 which is suitable for all crops. The classification Wilcox 1948 is applied for the study as given in **Fig. 5**. Samples ranged from excellent to poor category. The graph showed that 4 samples in the rainy and 1 sample in the dry are unsuitable while 6 samples from both seasons are still doubtful to unsuitable condition. However, samples are most likely in good condition based on zone 1 and zone 2.

Table 2. Ranges of physicochemical parameters and their comparison with drinking water standards of MIME (2004) and WHO (2017)

Parameter	Range		Permissible limit (PL)	Percentage of sample exceeded PL	
	Rainy	Dry	MME, WHO	Rainy (n=34)	Dry (n=40)
pH	4.12-7.65	3.1-7.86	6.5-8.5	41%	40%
EC	36-3697	37-3032	1500	21%	15%
TDS	21-2209	23-1826	800	21%	18%
K^+	0-1247	0-1108	12	35%	40%
HCO_3^-	0-827	0-1396	600	3%	20%
NO_3^-	0-146	0-94	50	6%	5%
SO_4^{2-}	0-503	0-296	250	6%	5%
Mn	0-2.23	0-2.7	0.1	41%	45%
Fe	0-23.92	0-0.31	0.3	50%	2.5%

*Ca, Mg, Na, Cl are all under permissible limit (PL), while Cu, Pb, Cr, Cd are under detected limit

Table 3. Classification of well water for agricultural purposes

Parameter	Sample Range		Range	Classification	% of Sample	
	Rainy	Dry			Rainy (n=34)	Dry (n=40)
RSC (meq/l)	-2.8-12.6	-2.5-21.5	<1.25	Good (G)	67.5%	60%
			1.25-2.5	Medium (M)	15%	0%
			>2.5	Bad (B)	17.5%	40%

Table 4. Classification of groundwater in term of hardness

Parameter	Sample Range		Range	Classification	% of Sample	
	Rainy	Dry			Rainy (n=34)	Dry (n=40)
Hardness (mg/l)	0.8-307	0-286	<75	Soft	53%	55%
			75-150	Moderated hard	18%	25%
			150-300	Hard	26%	20%
			>300	Very hard	3%	0%

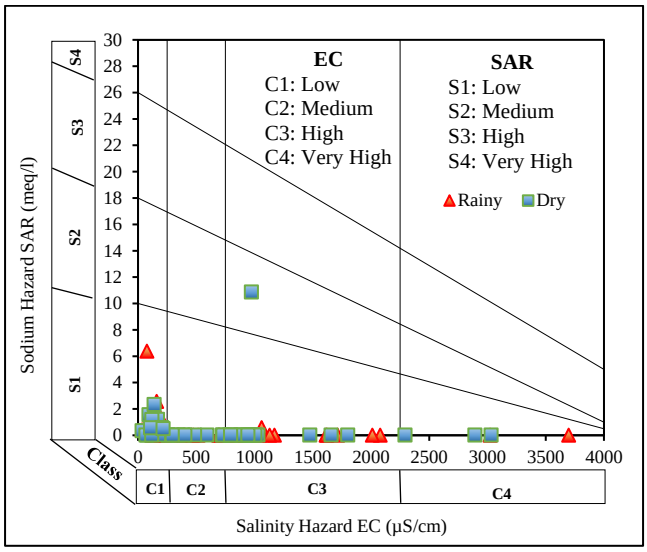

Fig. 4. Diagram rating of well water samples in relation to salinity hazard and sodium hazard

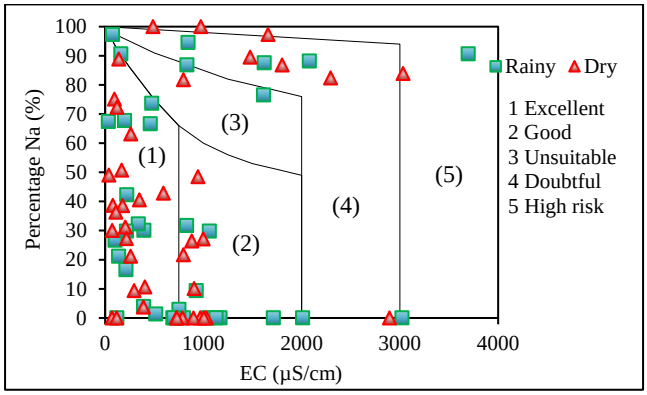

Fig. 5. Rating of well water samples on the basis of electrical conductivity and percent sodium

IV. Conclusion

Higher values of EC, TDS, Mn, and Fe were observed in rainy season while higher HCO_3^- was recorded in dry season. The groundwater quality of the study area had a principal issue of low pH. The water should be treated before consumption such concern parameters of HCO_3, Fe, Mn, and K while the salt water should be checked before irrigated on soil or plants. For a better interpretation and clarification on geochemistry controlling the well water quality, Saturation Index (SI) may be needed and geological formation of the well profile are one of the important information to be suggested for the future study.

Acknowledgement

We are thankful to the Science and Technology Research Partnership for Sustainable Development (SATREPS), the Japan Science and Technology Agency (JST)/Japan International Cooperation Agency (JICA) for their financial support.

References

[1] Sok, S. (2011). *Groundwater Research in Cambodia*. https://archive.iges.or.jp/en/natural-resource/groundwater/PDF/activity20110602/S1-3_Mr.Sok-Sophally_GW_Cambodia.pdf. Accessed 15 December 2020.

[2] Piper, A. M. (1944). A graphic procedure in the geochemical interpretation of water-analyses. *Eos, Transactions American Geophysical Union*, *25*(6), 914–928. https://doi.org/10.1029/TR025i006p00914

[3] MIME. (2004). Kingdom of Cambodia Drinking Water Quality Standards. In *Drinking Water Quality Standards*.

[4] WHO. (2017). *Guideline for Drinking-water Quality* (4th Editio). Word Health Organization.

[5] EPA, U. S. E. P. A. (1976). *Quality Criteria for Water. Office of Water Planning and Standards*.

[6] Ayers, R. S., & Westcot, D. W. (1976). Water Quality for Agriculture. FAO Irrigation and Drainage Paper 29 Rev.1. In *FAO Irrigation and Drainage Paper: Vol. No.29*.

[7] USSL. (1954). Diagnosis and Improvement of Saline and Alkaline Soils. *Soil Science Society of America Journal*, *18*(3), 348. https://doi.org/10.2136/sssaj1954.03615995001800030032x

[8] Wilcox, L. V. (1948). Classification and use of irrigation water. *Agricultural Circular No. 969,Washington, DC: USDA.*, *969*, 1–19. https://doi.org/USDA

[9] Appelo, C. A. . and D. P. (2005). Geochemistry, Groundwater and Pollution, 2nd Edition. In *A.A. BALKEMA PUBLISHERS*.

The 13th AUN/SEED-Net Regional Conference on Chemical Engineering 2020 (RCChE-2020)
Jointly held with
The 5th International Symposium on Conservation and Management of Tropical Lakes
"Insights and Challenges toward Achieving SDGs"

Analytical Studies on Water Quality Index of Prek Te River, A Mekong River Tributary in Cambodia

Kong Chhuon [1,*], Alpy Math [1], Hua Lin [2], Yu Guo [2]

[1] *Faculty of Hydrology and Water Resources Engineering, Institute of Technology of Cambodia Russian Federation Blvd., P.O. Box 86, 12156 Phnom Penh, Cambodia*
[2] *College of Environmental Science and Engineering, Guilin University of Technology, Guilin 541004, China*
* *Corresponding author: chhuon.k@itc.edu.kh*

Abstract

Prek Te river is a tributary of Mekong river in Cambodia. It is of particular importance to start studying on this river water quality because of the concern on the impact due to the agricultural development, land cover change and water uses inside its catchment. Water quality is needed to evaluate the physical, chemical, biological state. The Water Quality Index (WQI) reduces the number of parameters to a simple expression in order to facilitate the interpretation of the data. This study is to analysis Prek Te river water quality in 2018 and 2020 using WQI method to express the average quality of water at a time, based on analytical values of physico-chemical parameters. The 13 water samples were collected to analyze physico-chemical and heavy metal. In dry season of 2018, the WQI was 128 which made it fell into the moderate water quality, but the value decreased to only 88 in wet season of 2020 which corresponded to the good quality. The high value of WQI is influenced mainly from the high concentration of TDS and COD. TDS and COD were found to be higher with 153mg/L and 42mg/L respectively, at the tributary of Prek Te. Cr, Fe, Mn, and Arsenic were found to be below the standard WHO. The pesticide is also analyzed in this study at five sites but it turned out only detectable of some molecules. It can be concluded that, water in Prek Te has good quality in wet season, while moderate quality in dry season. This study showed the current situation of water quality in Prek Te which will be served as the baseline for future impact evaluation. It is recommended to do regularly monitoring for identifying any changes and further study is needed.

Keywords: *Prek Te, WQI, physico-chemical, heavy metal, pesticide*

I. Introduction

A tributary of the Mekong River in Cambodia, Prek Te River is draining water via valleys and falls from the mountainous area in Mundul Kiri province and crossing alluvial plains before flowing into the Mekong River in Kratie province with a total area of 11.094 km^2 with 81.42% of the population are farmers. The crops such as rice, corn, and bean are along the Mekong river of the southwest segment and agro-industry plantations such as rubber, pepper, and cashew nuts are at the northeast plateau region. Prek Te River is the main water source for farmers in both domestic and agricultural purposes. The water quality from the rivers has considerable importance for the reason that these water resources are generally used for multiple matters.

Typically, water quality is determined by comparing the physical and chemical characteristics of a water sample with water quality guidelines or standards. One of the simplest methods to assess water quality conditions is by using a water quality index. It is a tool that provides meaningful summaries of water quality data that are useful to both technical and non-technical individuals interested in water quality results. This study is to analysis Prek Te river water quality in 2018 and 2020 using WQI method to express the

average quality of water at a time, based on analytical values of physico-chemical parameters.

II. Materials and Methods

2.1. Sampling sites

A tributary of Mekong River in Cambodia, Prek Te watershed (**Fig 1)** is situated in Kratie province which lays from the eastern plateau in Mondulkiri province at an altitude of around 900 m to the Mekong River flood plain south of Kratie town at an elevation less than 14 m. Its basin area is 4,372 km2 which equals to 2.41% of Cambodia total land area.

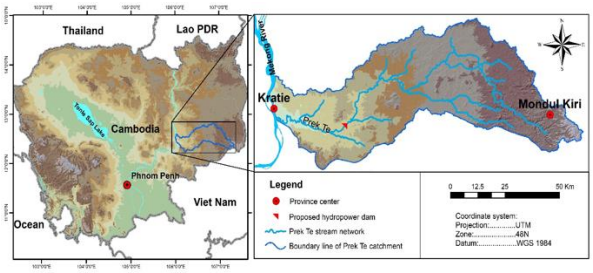

Fig. 1. Map of Prek Te river catchment of the study area

2.2. Experimental set-up

On-site Analysis: Temperature, pH, turbidity, EC, DO, and TDS were carried out at the site of sample collection by using EXO2 Multiparameter Sonde YSI. The polyethylene bottles were rinsed with sampled water at least three times before being filled and stored.

Laboratory Analysis: The heavy metal (Cr, Mn, Fe and cyanide), Alkalinity, COD, As, TS and pesticides will be analyzed in the laboratory at the Institute of Technology of Cambodia. The quality of water will be classified following the Cambodia water pollution standards and the WHO standards.

2.3. Analytical methods

Water Quality Index (WQI): The WQI was calculated using the Weighted Arithmetic Index method. The quality rating scale for each parameter *qi* was calculated by using this expression:

$$q_1 = \left(\frac{C_i}{S_i}\right) \times 100 \qquad \text{(Eq.1)}$$

Each of the 10 parameters was assigned a weight (wi) according to its relative importance in the overall quality of water for drinking purposes. The weight was assigned between 1 and 5 based on their relative significance in the water quality. The overall Water Quality Index was calculated by aggregating the quality rating (Q) with unit weight (Wi):

$$\text{Overall WQI} = \frac{\sum q_i w_i}{\sum w_i} \qquad \text{(Eq.2)}$$

Principle Component Analysis: The PCA is a descending dimension algorithm, in which the complex raw data are replaced by several unrelated variables (Wu et al. 2014). Only the components with the high eigenvalues (> 1) were extracted (Wang et al. 2017). All the results are conducted by using the analysis unit in software Origin 2018 .

III. Results and Discussion

Concentrations of Water Quality Parameter

pH is a crucial indicator that can be used for assessing water quality and degree of contamination in water bodies. The variation of pH values in 2018 showed not different values between site 1, 2, and 4. However, the pH value in which higher average values of 8.10 are obtained at site 5 during the wet season, whereas the lower average values of 7.22 are obtained at site 1. In 2020, the pH values recorded in the Prek Te river from 6.95 to 7.21.

EC is another useful water quality indicator observed by this study. Except for site 4, which had values of the high conductivity of 573.35 µS/cm and 270.56 µS/cm during in 2018 and 2020, respectively, all EC levels for site 1, 2, 3, and 5 were recorded to fall outside the recommended range of the WHO standard.

DO is one of the most important indicators of water quality. To maintain acceptable or good water quality. The highest DO value in the Prek Te River was observed at site 3 (7.78 mg/L) at the end of the wet season in 2018, while the lowest was observed at site 4 (4.17 mg/L). In 2020, DO data along the river that on average concentrations tended to be higher in the upper stream of the river, the highest DO concentration was recorded in site 4 at 7.62 mg/L.

Turbidity measures the relative clarity of the water by the presence of organic and mineral suspended particles and color producing substances. The mean turbidity readings of the samples at all sampling sites were in the range of 10.51 to 78.02 NTU. The results indicate that the turbidity of all the samples studied was higher the maximum standard limit

of 5 NTU.

TDS is usually estimated by EC and there is a strong relationship between EC and TDS. The values found from the Prek Te water samples are all within the maximum limit of 800 mg/L. The TDS ranged from 35 mg/L at site 5 to 153 mg/L at site 4 during the end of dry season. These higher TDS values could be due to the natural weathering of certain sedimentary rocks or a certain anthropogenic source, e.g., irrigation discharge, domestic effluents, and sewage effluent.

TS, the TS concentrations in analyzed samples ranged from 54 mg/L to 186 mg/L during the end of dry season in 2020. The TS values of all the water samples were far below the prescribed limit (500 mg/L) as per WHO standards.

Alkalinity refers to the capability of water to resist changes in pH. Carbonate and bicarbonate alkali substances represent the major forms of alkalinity in natural waters. Alkalinity values for the water samples in the study ranged from 48.8 mg/L to 146.84 mg/L during the end of dry season. According to the WHO standards for the river, the total alkalinity values of all water samples below the permissible limit of 200 mg/L.

COD concentrations of water samples were fluctuating between minimum 24.6 mg/L at site 4 and the maximum COD concentration was recorded at 42 mg/L at site 3 in the middle stream, this is higher than the recommended WHO guidelines. In 2020, COD showed that 5 water quality monitoring sites reported COD values water samples exacted the permissible limit of 5 mg/L.

Heavy Metals and Pesticides

Fe, the values of all water samples below the permissible limit of 0.3 mg/L, while the Chromium values below the permissible limit of 0.05 mg/L.

Cyanide (CN^-): In 2020, samples were analyzed for total cyanides at five sites. Results were all below the detection limit. Unfortunately, the detection limit used in this study is higher than those values.

As, the arsenic concentration in the five sampled water located in Prek Te River were below the permissible limit (0.05 mg/L). The same concentration of As (0.005 mg/L) was observed at site 2, site 3, and site 5, where, the concentration of site 1 and site 4 not detected. The variation of concentration of heavy metal from locations to locations may be correlated with the flow of the rivers and the location of industries.

Pesticides: Pesticides are chemical compounds used to control or eradicate pests. At the end of wet seasons, the analysis of 2018 showed that all 5 water quality monitoring sites have only detectable some molecules.

Water Quality Index (WQI)

The WQI in 2018 and 2020 has been calculated which has been applied also for 5 sampling sites, along the Prek Te River. For computing WQI three steps are followed. In the first step, each of the 11 parameters (pH, EC, turbidity, TDS, TS, Alkalinity, DO, COD, Fe, Cr, and Mn) has been assigned a weight (wi) according to its relative importance in the quality of water for drinking purposes. In 2018, except for site 4, located on the upstream, the water quality status is poor quality (128.18), which are influenced by the nutrients, as a result of the agricultural practices, municipal and industrial, manure from farms. In **Fig. 2** the five study sites located in the Prek Te River, four study sites were rated as good water (79.58-80.90).

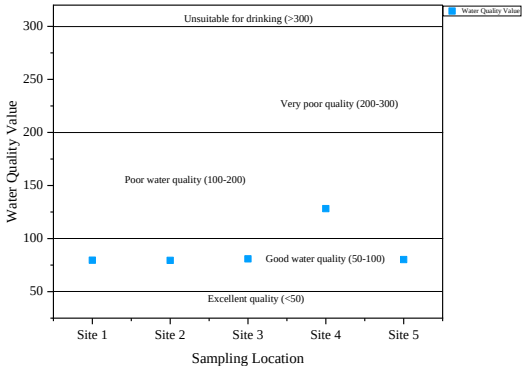

Fig. 2. Water quality classification based on WQI in 2018

An analysis of the 2020 water quality data, using the WQI showed that water quality of the Prek Te River is still of good quality, with all sites rated as either “good”. Of the five sites located in the Prek Te Rive, poor water quality (136.19) is noted at site 4 a tributary of Prek Te River.

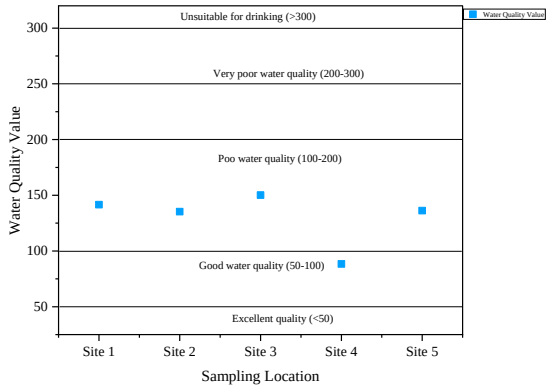

Fig. 3. Water quality classification based on WQI in 2020

Principal Component Analysis

PC1 and PC2 was selected to plot in biplot in order to indicate the influence parameters link to the sample sites (**Fig 4**). The result of biplot in 2018 shown that site 3, 4 and 5 was influenced by PC1 under pH and DO while site 1 and 2 were controlled by PC2, temperature and pH.

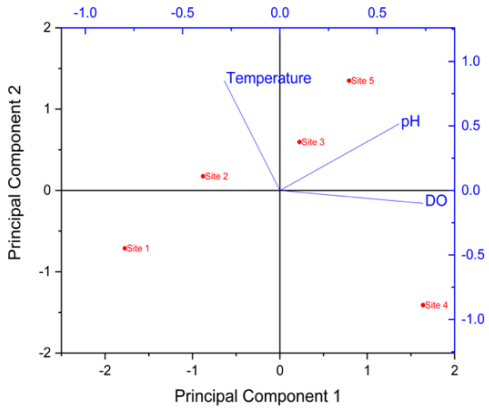

Fig. 4. Bivariate plot of the scores of PCs 1 and 2 in 2018

In 2020, result shown that there are 61.79% of total variance were captured by PC1 which strong influenced by temperature, TDS, TS, pH, and DO at site 4 and 5 in the upstream while 24.43% was controlled by PC2, under controlled by Fe at site 3 in the middle stream. The result of biplot shown that site 1 and 2 was influenced by PC3 under Alkalinity and COD.

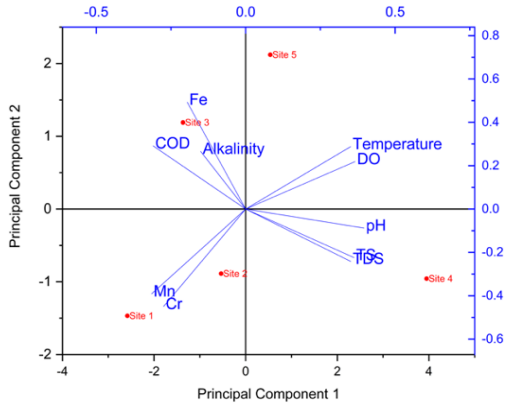

Fig. 5. Bivariate plot of the scores of PCs 1 and 2 in 2020

IV. Conclusion

The water quality of Prek Te Rivers is still of good quality. There were only a small number of measurements exceeding the standard. The value of water quality parameters of heavy metals and Arsenic from all sample collection in the end of dry season were also measure and found to be well below the standard of WHO, while Cyanides are not detected at 5 sampling sites. Therefore, the results of pesticides have only detectable some molecules. Furthermore, at site 4 a tributary of Prek Te River has strongly influenced by TS, temperature, TDS, pH, and DO. The overall WQI showed that, by including all physico-chemical parameters, all water samples were classified as good quality at the end of wet season while it has poor quality at end of dry season.

Based from the results of this study, the water quality of Prek Te Rivers is generally still be considered as in good quality for domestic use.

Acknowledgement

This work is supported by Guangxi science and technolo gy program (Guike AD17195023 ; 2018AD16013-04).

References

[1] Chhuon, K., Herrera, E., Nadaoka, K,. 2016. Application of Integrated Hydrologic and River Basin Management Modeling for the Optimal Development of a Multi-Purpose Reservoir Project. Water Resources Management, 30(9), 3143–3157. https://doi.org/10.1007/s11269-016-1336-4

[2] Wang J, Liu G, Liu H, Lam, PKS,. 2017. Multivariate statistical evaluation of dissolved trace elements and a water quality assessment in the middle reaches of Huaihe River, Anhui, China. Sci Total Environ 583:421–431. https://doi.org/10.1016/j.scitotenv.2017.01.088

[3] Wu, J., Li, P., Qian, H., Duan, Z., Zhang, X., 2014. Using correlation and multivariate statistical analysis to identify hydrogeochemical processes affecting the major ion chemistry of waters: case study in Laoheba phosphorite mine in Sichuan China. Arab J Geosci 7(10):3973–3982. https://doi.org/10.1007/s12517-013-1057-4

The 13th AUN/SEED-Net Regional Conference on Chemical Engineering 2020 (RCChE-2020)
Jointly held with
The 5th International Symposium on Conservation and Management of Tropical Lakes
"Insights and Challenges toward Achieving SDGs"

Pesticide Distribution in the Hydrological Compartment in Koh Thum

Nalin Hak[1], Sombath Keo[1], Chhovin Long[1], Melvin Frick[1], Sylvain Massuel[2], Chanvorleak Phat[3], Chhuon Kong[4], Sambo Lun[4], Sokly Siev[3], Ratha Doung[4], Jean-Philippe Venot[2], Khy Eam Eang[4*]

[1] *Master of UWE, Graduate School, Institute of Technology of Cambodia, Russian Federation Blvd., P.O. Box 86, Phnom Penh, Cambodia*
[2] *UMR G-EAU, IRD, Institute of Technology of Cambodia, Russian Federation Blvd., P.O. Box 86, Phnom Penh, Cambodia*
[3] *Faculty of Chemical and Food Engineering, Institute of Technology of Cambodia, Russian Federation Blvd., P.O. Box 86, Phnom Penh, Cambodia*
[4] *Faculty of Hydrology and Water Resources Engineering, Institute of Technology of Cambodia, Russian Federation Blvd., P.O. Box 86, Phnom Penh, Cambodia*
**Corresponding author: khyeam_eang@yahoo.com*

Abstract

This study aimed to make an investigation of the environmental state with regards to pesticides during the dry season after 10 years of intensive use in Koh Thum. Water from irrigation canal (Prek) and crop field and groundwater from mango farm were sampled and pesticides were detected by semi-quantitative analysis using gas chromatography coupled to mass-spectrometry (GC-MS). Firstly, 77 pesticides were inventoried through interviews of farmers and resellers in Kandal province. Next, among the MS database of 451 molecules, 167 pesticides were detected including 21 which were part of the inventoried pesticides from interviews while other 146 detected pesticides were off-list. The major types of biocides were insecticides (33%), fungicides (25%) and herbicides (21%) and the major chemical families were carbamates (14%), organophosphates (13%), triazoles (12%), organochlorines (11%), and pyrethroids (11%). Most of pesticides detected were moderately hazardous (40%). Otherwise, 119 pesticides detected were not allowed in European Union while 10 were banned in Cambodia. Chloroneb was detected in every water sample, with particularly high concentrations in groundwater (3.4010 ± 0.3644 µg/L) and in water in the middle of Prek Touch (3.8314 ± 0.0826 µg/L). The Bassac river was the least contaminated (54 molecules), the rice field water appeared to be the source of pesticides with 99 molecules, while 84 molecules were detected in the middle of Prek Touch and 71 molecules were detected at Prek Chann drainage gate. Furthermore, 26 pesticides were common to every compartment, suggesting water exchanges occurring between all compartments at the same time, probably during the wet season. Almost twice as many pesticides were detected in the Preks than in the Bassac river and the Prek Touch West. The pesticides would accumulate by remaining locally in the water near the treated locations while the flush effect would remain limited. The unrehabilitated prek - the most hydrologically isolated - counted the greatest number of pesticides.

Keywords: Pesticides, hazardous pesticides, gas chromatography coupled to mass-spectrometry (GC-MS)

I. Introduction

Pesticides are natural or chemical, organic or inorganic, substances or mixtures intended to prevent, destroy populations of insects, weeds, rodents, fungi or other harmful pests [1]. Pesticides consist of different products with different functions. The extensive use of pesticides has impacted seriously on environmental, human, animal, and ecosystem. The classification of pesticide is dependent on the intended target they control including herbicides, insecticides, fungicides, rodenticides and many others [2]. Furthermore, the four main groups of toxicity pesticides are including organochlorine, organophosphorus, carbamates, and nitrogen based pesticides; they are persistent in the environment. However, these banned pesticides are still

used in the developing countries [3]. The classification toxicity hazard of each pesticide based on the acute oral and dermal toxicity followed the WHO: Ia (extremely hazardous), Ib (highly hazardous), II (moderately hazardous) and III (slightly hazardous) (see **Table 1**) [4].

The use of pesticides in Cambodia started in the early 60s. Between 2002 and 2012, the import of pesticides increased by seventeen times, while most of pesticides in Cambodia were imported from neigbour countries such as Vietnam, Thailand and China since no factories were reported in Cambodia. Based on the different survey studied, Cambodia is the first range among other 13 countries with the highest pesticide residue on vegetables, especially leaf of vegetables from Kandal province [5]. On the other hand, many Cambodian farmers have experienced health problem by pesticide poisoning. Those chemicals have been extensively misused in term of time, strength and way of use because of insufficient understanding and the lack of relevant instruction manual written in the native Khmer language [6]. Three main challenges to pesticide risk reduction were identified such as the rapid spreading of pesticide trade associated with a weak regulatory, the strong satisfaction of pesticides associated with insufficient awareness of risks and a lack of knowledge in the use of pesticides, and the non-regular monitoring of pesticide risks [7].

Table 1. Classification of hazards followed by WHO (2006)

Class	LD_{50} for the rat (mg/Kg body weight)			
	Oral		Dermal	
	Solids	Liquids	Solids	Liquids
Ia Extremely Hazardous	< 5	< 20	< 10	< 40
Ib Highly hazardous	5-50	20-200	10-100	40-400
II Moderately hazardous	50-500	200-2000	100-1000	400-4000
III Slightly hazardous	Over 500	Over 200	Over 1000	Over 4000

II. Materials and Methods

2.1. Sampling sites

The samples were collected on March 20th, 2020 in the Prek system (Prek Chan and Prek Touch) and Bassac river which located in Koh Thum district, Kandal province (see **Fig.1**). The Prek system is a canal perpendicular to the Bassac river which was used for irrigating the crop located on the high bank of the alluvial plain called "Chamcar". Five surfaces water and one groundwater sample were collected in triplicate, which were as representative as possible in the Prek system. 1000 mL of each sample were collected and directly filtrated at the field site through 2µm multilayered glass microfiber in order to remove debris and suspended materials, and then transported in iced box (around 4˚C) to SATREPS lab in the Institute of Technology of Cambodia.

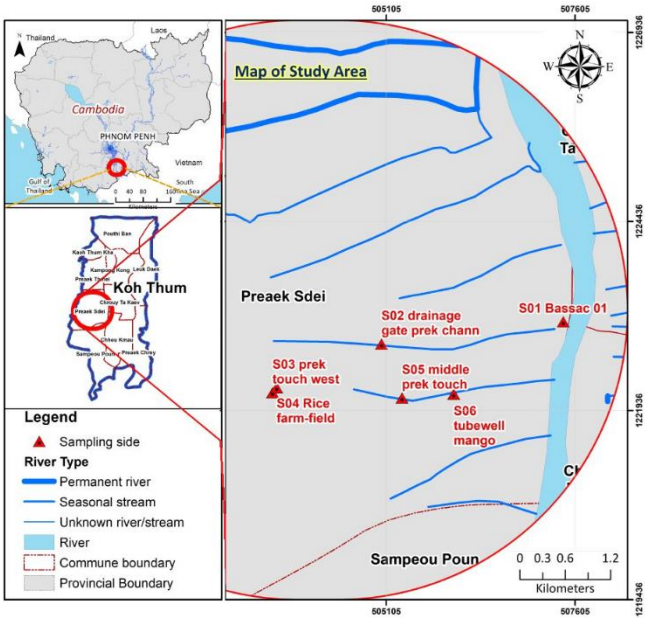

Fig. 1. Prek system in Koh Thum district, Kandal province

2.2. Clean-up procedure

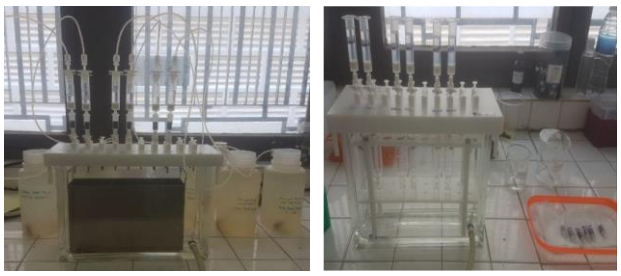

Fig. 2. SPE: Sample Elution & PLS3 Sorbent Washing

The samples were proceeded to purity by solid-phase extraction (SPE) method following the method of Jinya, 2013 [8]. Sodium phosphate buffer solution (pH=7, 1mol/L) was added to the water samples and left for rest for 1h. The sorbents PLS3 and AC in their respective cartridges were activated by conditioning with 5 mL of dichloromethane, 5 mL of acetone and two-time 5 mL of distilled water. The samples were next passed through the cartridges at the flow rate of about 15 mL/mn (see **Fig.2**). The cartridges were dried using nitrogen gas stream for 30 mn. After that, the dried cartridges were disassembled and washed: 2 mL of acetone followed by 5 mL of dichloromethane for the PLS3 cartridge, while both of the cartridge PLS3 and AC were washed with 5 mL of acetone. The mixed eluted solvent was collected and concentrated to approximately 1 mL, using nitrogen gas stream. Then, 10 mL of hexane were added to the previous concentrated solution of 1 mL, to be then

dehydrated by elution through sodium sulfate. The solution obtained was concentrated to 1 mL using nitrogen gas stream, transferred into vial, and finally stored at -20 ˚C.

2.3. Calibration for Analysis

A 1ppm mixture of standard pesticides containing about 950 molecules similar to those to be detected was added to the samples. In addition, an external calibration was performed with 1ppm, 0.5ppm, 0.125ppm, 0.1ppm, 0.05ppm, and 0.025ppm solution containing 24 target pesticides; to which was also added 10ppm mixture of standard pesticides containing the other similar pesticides. A quality analysis could be performed on the 24 target pesticides (see **Table 1**) while other pesticides could be detected in a semi-quantitative way.

Table 1. Target pesticides for an external calibration of quantitative analysis

No.	Name	No.	Name
1	Methamidophos	13	Terbacil
2	O,p'-DDT	14	Methyl-parathion
3	Metalaxyl	15	Parathion
4	Isoxathion	16	Pyroquilon
5	Hexachlorobenzene	17	Anilofos
6	Heptachlor	18	Azaconazole
7	Aldrin	19	Isazofos
8	Dieldrin	20	Mefenoxam
9	Endrin	21	BHC/HCH
10	Chlordane		(α, β, γ, δ)
11	Chloroneb	22	Lindane
12	Atrazine	23	Malathion
		24	Triadimefon

2.4. Detection procedure

The detection procedures were inspired from Jinya (2013), and analyzed by using GC-MS device, model TQ8040 series. The column was DB-5ms, whose length was 30m, thickness 0.25µm and diameter 0.25mm. Injection was splitless with volume 1µL. The temperature of the oven containing the column was maintained for 2mn at 40˚C, and then reached 310˚C for 5mn at a speed of 8˚C/mn. The flow rate of the carrier gas, ultra-pure helium, was 50mL/mn, and the GC column flow rate was 1.23 mL/mn. The MS ion source temperature was 200˚C, and the MS interface temperature was 300˚C. The detection threshold for every compound was 0.0001 µg/L. The identification of pesticides was performed by the data treatment system and the computer, which calculated the monoisotopic mass, predicted the structural formula of compounds, and compared them using the MS database.

2.5. Database software for simultaneous analysis

GC-MS (GC-MSTQ8040, Shimadzu, Japan) is equipped with automated identification and quantification system with database. The database containing the mass spectra, retention time and calibration curves about 1000 substances included 451 pesticides compound, 194 compounds of CH, 150 compounds of CHO, 113 compound of CHN (O), 14 compounds of PPCPs, 12 compounds of CHS (NO), and 8 compounds of CHP (NOS), which permitted simultaneous identification and quantification of about 1000 plus substances without the use of chemical standards. Maximizing the performance of this database required high-sensitivity instrument together with feature-rich quantitative soft.

2.6. Statistical analysis

All essays were carried out three times and the results were expressed as mean (±) standard deviation. Single-factor analysis of variance (ANOVA) were performed to test the differences between mean concentrations of pesticides, for completely randomized design (CRD) using Excel Data analysis software. A p-value < 0.05 was considered statistically significant for every sample location.

III. Results and Discussion

3.1. General profile of pesticides detected in Koh Thum

In the area of Koh Thum, 167 pesticides were detected, the majority of which were insecticides (32%), then fungicides (25%) and herbicides (21%). Acaricides represented 14%, nematicides were 3% and a further minority included bactericides, molluscicides and plant growth regulators. Carbamates (14%), organophosphate (13%), triazoles (12%), organochlorines (11%), and pyrethroids (11%) were the most present chemical family of the pesticides detected. Furthermore, pesticides moderately hazardous were detected as predominant (40%), slightly hazardous (16%) and unlikely to present acute hazard (16%); highly hazardous pesticides (8%) and extremely hazardous pesticides 1%.

3.2 Pesticide detection and its regulation

Various pesticide molecules were detected in Koh Thum district through semi-quantitative analysis, including 119 molecules either no approved or not registered in the European Union, while 10 were banned in Cambodia since

Table 2. Target pesticides detected at the sample location

Pesticide	Concentrations detected at the sample locations						EU water drinking standard (µg/L)
	Bassac (µg/L)	D.Gate PC(µg/L)	Mango F (µg/L)	Middle PT (µg/L)	PT West (µg/L)	Rice F (µg/L)	
Methamidophos	-	-	-	0.0019±0.0032	-	-	0
O,P'-DDT	-	-	0.0029±0.0051	-	-	-	0
Metalaxyl	-	-	0.2319±0.2452	-	-	-	0.1
Isoxathion	-	-	-	-	-	0.0055±0.0096	0
Dieldrin	-	0.0278±0.0254	-	-	-	0.0035±0.0061	0
Endrin	-	0.0114±0.0197	-	-	-	-	0
Chloroneb	0.9449±0.8682	1.1099±0.1544	3.4010±0.3644	3.8314±0.0826	0.4282±0.0491	0.5231±0.0061	0
Pyroquilon	-	-	-	0.0018±0.0031	-	-	0
Azaconazole	-	-	0.0123±0.0213	-	-	0.0011±0.0019	0
Mefenoxam	-	-	0.3121±0.3293	-	-	-	0.1
Triadimefon	0.0283±0.0184	0.0176±0.0155	0.0158±0.0137	0.0197±0.0134	0.0331±0.0119	0.0225±0.0295	0

***Note:** (-) is not detected, (0) not allowable to present in drinking water; D: Drainage; F: Farm; PT: Prek Touch

2012 [5]; namely, o,p'-DDT, isozathion, dieldrin and endrin. Moreover, 11 molecules were detected among the 24 targeted pesticides through a quantitative analysis. Among those 11 molecules, only 2 were authorized in European Union, namely metalaxyl and mefenofam, whose water drinking standards were 0.1 µg/L (see **Table 2**).

3.3. Pesticide distribution, its persistence and toxicity

Among the 167 pesticides detected in the hydrological compartments, Bassac river was observed to be contaminated with the least number of pesticides than the Preks, the Prek Touch West, and the rice field. Most of pesticides detected in Bassac river were moderately hazardous (22 molecules) followed by slightly hazardous (11 molecules), and 11 molecules of unknown toxicity. Rice field is the highest contaminated (99 pesticides), among of these pesticides 5 highly hazardous, 42 moderately hazardous, 20 slightly hazardous and 14 molecules were not listed in WHO classification. Mango farm and Prek Touch West were showed the similar number of pesticides (60 and 57 pesticides). In Mango farm, no highly hazardous pesticides were detected while 1 extremely hazardous, 33 moderately hazardous, and 7 slightly hazardous. Prek Touch West the number of pesticides were detected including 4 highly hazardous, 26 moderately hazardous, 8 slightly hazardous, and 8 pesticides of unknow toxicity. In Middle of Prek Touch, there were 84 number of pesticides were detected including 1 extremely hazardous, 7 highly hazardous, 41 moderately hazardous and 13 slightly hazardous and 6 molecules unknown toxicity. In addition, 71 pesticides were detected in the drainage gate of the Prek Chan including 4 highly hazardous, 30 moderately

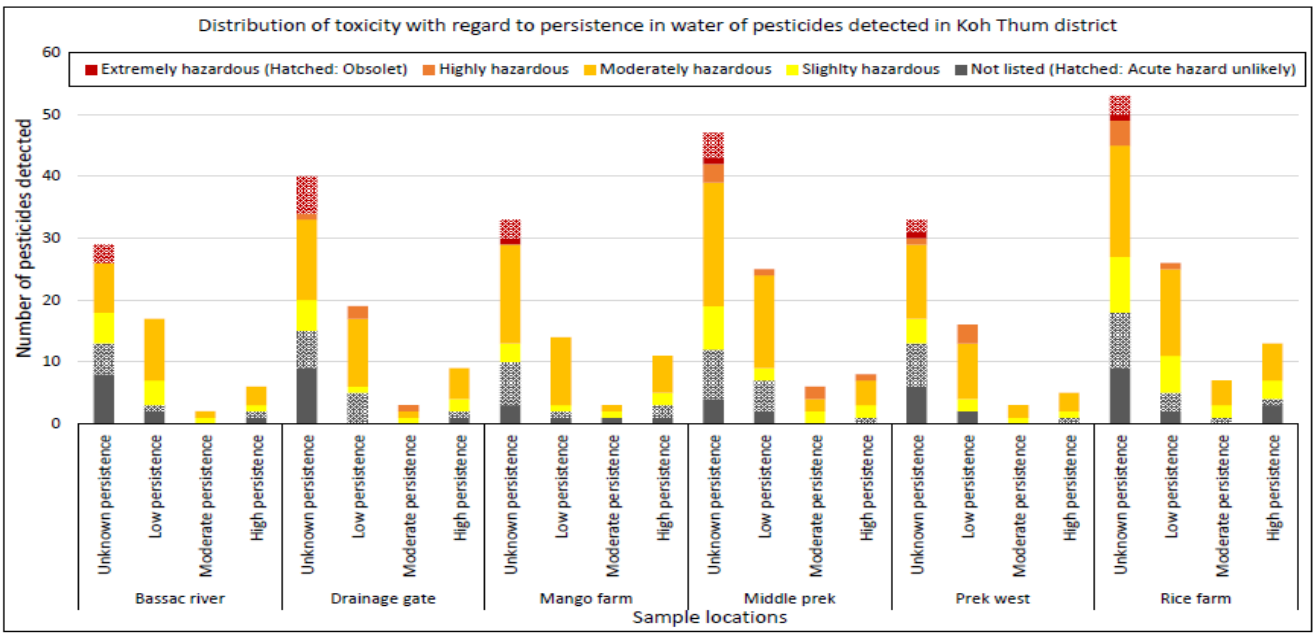

Fig 3. Distribution of toxicity with regard to persistence of pesticides detected in the Koh Thum district

hazardous, 9 slightly hazardous and 10 unknown toxicities (see **Fig. 3**).

3.4 Hydrological flows and pesticide movement

Firstly, in dry season, potential exchanges may happen between the Bassac river and the rehabilitated Prek Chan since they shared 37 pesticides in common (52.1% of the pesticides detected in Prek chan and 68.5% of the pesticides detected in the Bassac river. At this stage, it was impossible to determine if the source of pesticide came from the prek, the river, or both of them. The presence of pesticide in Prek Chan could either come from the neighboring treated plots by excess irrigation return flow and by leakage drainage, or come from exchange with groundwater. Secondly, we have known that the water flow was very limited in Prek Chan. Prek Touch was isolated from the Bassac and the Prek Touch West. We could determine that the pesticide found in the preks were mostly tied to the presence of pesticides in the surrounding treated plots in dry season. The detection of pesticide in non-rehabilitated Prek Touch (84 pesticides) more than in the rehabilitated Prek Chan (71 pesticides) could be explained either by the spatial variability that would imply poor mixing of prek water or by limited exchanges with the Bassac river and Prek Touch West for Prek Chan. Compare to the prek, the Bassac river and the Prek Touch West clearly showed lower and similar numbers of pesticides detected (54 and 57 pesticides). The Prek Touch west, running from north toward the south collected water from the Bassac river through other preks upstream and flow directly to the boeung. Compare to the groundwater 60 pesticide were detected and 41 pesticides were found in Prek Touch (48.8% of the pesticides detected in Prek Touch and 68.3% of pesticides detected in the groundwater). This would suggest possible exchanges even in dry season with groundwater where pesticides could be stored, but it was difficult to draw any conclusion with a single groundwater sample.

IV. Conclusion

The result obtains from this study indicated that the three major types of biocides were insecticides, fungicides and herbicides, and most of pesticides were moderately hazardous. The Bassac river was the least contaminated and the least hazardous water in term of potency of toxicity. However, the rice field appeared to be the source of pesticide application, which accumulated mostly in waters of the rehabilitated and non-rehabilitated Preks. The water in middle Prek Touch was the most hazardous, while captafol which was banned in Cambodia was detected in the groundwater, the rice field water, the water of the Prek Touch West and the water in middle of the Prek. Moreover, 26 pesticides were common to every hydrological compartment. A separation between Prek and Bassac river and the Prek Touch West on the other hand seemed to emerge in the dry season. The surface water flow from the Bassac river connected to the Prek Touch West seemed to maintain a lower number of pesticides while these numbers tended to build up in the Preks. Those conclusions should be confronted to analysis in raining season to confirm the pesticides transport during the flood period.

Acknowledgement

We are thankful to the COSTEA project for the financial support under the management of Institut de Recherche pour le Développement (IRD).

References

[1] Mahmood, I., Imadi, S. R., Shazadi, K., Gul, A., Hakeem, K. R. (2016). Effects of pesticides on environment. In Plant, Soil and Microbes. Springer, Cham, 253-269.

[2] Uqab, B., Mudasir, S., Nazir, R. (2016). Review on bioremediation of pesticides. *J Bioremed Biodeg*, 7, 343.

[3] Saravi, S. S. S., Shokrzadeh, M. (2011). Role of pesticides in human life in the modern age: a review. Pesticides in the modern world-risks and benefits, 3-12.

[4] WHO-UNEP *(*2006). Sound management of pesticides and diagnosis and treatment of pesticide poisoning: a resource tool. Geneva: Inter-organization Programme for the Sound Management of Chemicals.

[5] FFTC Agricultural Policy Platform (FFTC-AP) (2015). Current Use of Pesticides in the Agricultural Products of Cambodia. https://ap.fftc.org.tw/article/986. Accessed 25 December, 2020.

[6] Matsukawa, M., Ito, K., Kawakita, K., Tanaka, T. (2016). Current status of pesticide use among rice farmers in Cambodia. *Applied Entomology and Zoology*, 51(4), 571-579.

[7] Schreinemachers, P., Afari-Sefa, V., Heng, C. H., Dung, P. T. M., Praneetvatakul, S., Srinivasan, R. (2015). Safe and sustainable crop protection in Southeast Asia: status, challenges and policy options. *Environmental Science & Policy*, 54, 357-366.

[8] Jinya, D. (2012). Development of solid-phase extraction method for simultaneous analysis of semi-volatile organic compounds using a GC-MS database system. SHIMADZU Technical Report. https://www.shimadzu.com.cn/solution/green/pdf/jjfa/s19.pdf. Accessed 25 January, 2021.

The 13th AUN/SEED-Net Regional Conference on Chemical Engineering 2020 (RCChE-2020)
Jointly held with
The 5th International Symposium on Conservation and Management of Tropical Lakes
"Insights and Challenges toward Achieving SDGs"

Assessment of Pesticide Residues in Surface Water and Fish from Chhnok Tru, Kampong Chhnang

Chanvorleak Phat [1,2,*], Kearakvattey Kun [1], Voleak Pheap [1], Sereyvath Yoeun [1], Eden G. Mariquit [3], Winarto Kuriniawan [3] and Hirofumi Hinode [3]

[1] *Faculty of Chemical and Food Engineering, Institute of Technology of Cambodia, Russian Federation Blvd., P.O. Box 86, 12156 Phnom Penh, Cambodia*
[2] *Food Technology and Nutrition Research Unit, Research and Innovation Center, Institute of Technology of Cambodia, Russian Federation Blvd., P.O. Box 86, 12156 Phnom Penh, Cambodia*
[3] *School of Environment and Society, Tokyo Institute of Technology, Japan*
* *Corresponding author: phatchanvorleak@itc.edu.kh*

Abstract

Surface water from 5 different sites and 4 types of fish from the Cyprinidae family were collected from Chhnok Tru, floating community of Tonle Sap Lake. Those samples were subjected to pesticide residues analysis using gas chromatography mass spectrometry. Qualitative results showed that water samples were detected with fungicides fluquinconazole and fenpropimorph. Insecticides such as lenacil and mevinphos were also found in some studied sites. For fish samples, two active compounds of fungicides were detected in muscle part of fish from Cyprinidae family. Quantitative results could be drown only from water samples as targeted compounds were not found in fish samples. Three fungicides including azaconazole, chloroneb, and pyroquilon were detected with the concentrations of 16.46 µg/L in CT3, 0.28 µg/L in CT5, and 0.51 µg/L in CT2, respectively. Four active compounds of insecticides were found in CT3 and CT5, which CT3 were detected with chlordane and CT5 were contaminated with three compounds such as HCHs, isazofos, and parathion. The presences of these pesticides in water and fish sample pose a high risk to human as well as to the lake environment.

Keywords: *Pesticides, Chnhnok Tru, Tonle Sap Lake, Qualitative analysis, Quantitative analysis*

I. Introduction

The Tonle Sap Lake (TSL), or the Great Lake of Cambodia, is located in the central plains of Cambodia. The lake is known for its rich biodiversity and outstanding water regime, with vast seasonal variations in water levels and volumes [1]. Fishing and agricultural activities in the TSL basin benefited from abundant freshwater, nutrients and rich soils contributed by seasonal flood pulse and rainfall; together, these ecosystem services have preserved the region's livelihoods for centuries [2].

Agriculture is the economic foundation of Cambodia, where more than 70% of the population engage in agricultural activities [3, 4]. However, agriculture sectors face some constrain such as crop losses due to pest infestication making the application of pesticides crucial for plant protection and increase crop yield. A number of global monitoring studies have shown the ability of pesticides to contaminate surface and ground water by runoff, groundwater leaching and spray drift [4–6]. Each year, over 3 million cases of pesticide poisoning with an estimated 220,000 deaths occur globally especially in developing

countries.

Scientific evidence is required to raise public awareness of the adverse effects of pesticides on all stakeholders, including farmers and policy makers. However, there is limited information on pesticide contamination in Cambodia. Therefore, this study aims to identify the presence of commonly used pesticides and evaluate the levels of some banned pesticides in surface water and fish from Chhnok Tru, Kampong Chhnang, Cambodia. Chhnok Tru is one of TSL's floating communities. With its unique characteristics, the majority of the village is submerged during the rainy season, while broad cultivated land is accessible during the dry season. This contributes to the abundance of rice and other crop cultivation in this region, making it important to study on pesticide contamination levels from agriculture to water and aquasystem.

II. Materials and Methods

2.1. Sample collection

Surface water were collected in March 2020 from 5 site at Chhnok Tru community (**Fig.1**). Water samples were stored in cleaned 1 L plastic bottles and transported to the laboratory at Institute of Technology of Cambodia for analysis.

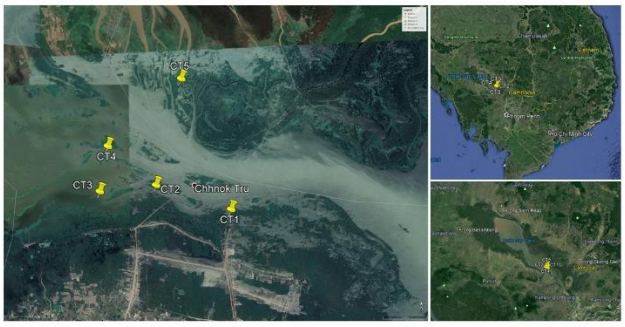

Fig.1. Water sampling points at Chhnok Tru

Freshwater fish samples of the Cyprinidae family (Trey Chhkork (*Cyclocheilichthys enoplos*), Trey Chhpin (*Hypsibarbus suvattii* spp), Trey Chrakaing (*Puntioplites falcifer*), and Trey Khmann (*Hampala macrolepidota*)) were collected from fishermen at the various sites in Chhnok Tru, Kompng Chhnang Province.

2.2. Water sample preparation

Sample preparation has been adopted from Jinya (2013) in which 1 L of surface water sample has been adjusted with 1 mL of phosphate buffer solution (1 mol/L, pH 7.0) [7]. Water samples were then filtered using 0.45 µm fiber glass filter (Whatman GMF 150) to remove suspended solids. Suspended solids retained by the filters were eluted with 5 mL of acetone and 5 mL of dichloromethane to dissolve potentially adsorbed compounds. Filtered samples were subjected to extraction process by using solid-phase extraction method (SPE) as described by Jinya (2013).

2.3. Fish sample preparation

Fish muscles were then grind and freeze-dried. Five grams of freezed dry fish muscle in powder form was homogenized with 50 mL of distilled water and 100 mL of acetone/hexane mixture (50/50, v/v) was added to the suspension and stirred for 15 min. After that, this mixture was filtered with Whatman filter paper (pore size of 2 µm). Then, ten grams of sodium chloride and 1 mL of phosphate buffer solution (1 mol/L, pH 7.0) were added into the filtrated solution and stirred again for 10 min. After that, the decanter was used to separate the layer of organic solvent from fish fat part. Then, anhydrous sodium sulfate was used to remove any remaining water and impurities from the solution. Lastly, the solution was applied to SPE following the method of Jinya (2013).

2.4. GC-MS analysis

The pesticide compounds were analyzed using gas chromatograph and mass spectrometer (GC-MS), model TQ8040 series (Shimadzu, Japan). The column used was DB-5ms with the length of 30 m. One microliter of sample was injected to GC-MS by auto injector using spitless mode. After that, the column oven temperature was programmed from 40 to 310°C by holding for 2 minutes at 40°C, increased the temperature to 310°C with a rate of 8°C/min, and then held for 5minutes. The carrier gas was ultra-pure helium at the total flow of 50 mL/min while the column flow was 1.23 mL/min. The ion source temperature was 200°C and the temperature of the interface was 300°C. All pesticides were both qualitatively and quantitatively analyzed by retention time and specific ions, and quantified by the external standard method.

III. Results and Discussion

3.1. Qualitative analysis of pesticides

Qualitative analysis was carried out by scanning method to identify the presences of pesticides in tested samples. The results showed that water samples were detected with fungicides fluquinconazole and fenpropimorph in CT3 and

CT2, respectively (Table1). Fungicides have been greatly used for the control of pathogen fungi in crops; however, it can exhibit undesirable effects on non-target plant-beneficial microorganisms [8]. Besides, fenpropimorph has a very negative impact on the plant root development which lead to growth deduction in some cereal seedlings [8]. Insecticides such as lenacil and mevinphos were also found in some studied sites (CT1 and CT2). Lenacil is an odorless herbicide employed for selective weed control. The detection of this compound in water sample might be from agricultural application and its solubility and stability in water [9].

Table 1. Presences of pesticides in surface water from Chhnok Tru

Category	Active compounds	CT1	CT2	CT3	CT4	CT5
Insecticide	Lenacil	-	+	-	-	-
	Mevinphos	+	-	-	-	-
Fungicide	Fenpropimorph	-	+	-	-	-
	Fluquinconazole	-	-	+	-	-

For fish samples, two active compounds (biphenyl and fluquinconazole) of fungicides were detected in muscle part of fish from Cyprinidae family (Table 2). Biphenyls are important structural analog, which are used considerably in synthesis of various compounds. Earlier, biphenyl derivatives were widely used as pesticides in the form of polychlorinated biphenyls (PCBs). Biphenyl is a chemical fungicide used in agricultural application to kill or inhibit the growth of fungi. Biphenyl is insoluble in water and vapor are heavier than air cause a persistent in environment, could absorbed through the skin, the mucous membrane and pulmonary system of organism. Fish can accumulate of biphenyl by direct absorption through the gills, exposure to contaminated sediments, and consumption of insects and smaller fish [10]. Fish were contaminated with biphenyl and fluquinconazole in their muscle due to the accumulation of pollutant from their surrounded environment include live in contaminant water or consume the contaminant food.

Table 2. Presences of pesticides in fish from Chhnok Tru

Fish species	Fungicide	
	Biphenyl	Fluquinconazole
Trey Chhkork (*Cyclocheilichthys enoplos*)	-	+
Trey Chhpin (*Hypsibarbus suvattii spp*)	+	-
Trey Chrakaing (*Puntioplites falcifer*)	+	-
Trey Khmann (*Hampala macrolepidota*)	-	+

3.2. Quantitative analysis of pesticides

Among 23 target pesticides (fungicides include azaconazole, chloroneb, hexachlorobenzen, mefenoxam, metalaxyl, pyroquilon, and triadimefon; herbicides include anilofos, atrazine, and terbacil; insecticides include Aldrin, chlordane, dieldrin, endrin, HCHs, heptachlor, isazofos, isoxathion, malathion, methamidophos, methyl parathion, o,p'-DDT, and parathion), seven active compounds were detected in water sample from Chhnok Tru. CT5, which is surrounded by rice and crop field was the most contaminated sites with four pesticide compounds (Table 3). Some banned pesticides such as chlordane, HCHs, and parathion were detected in this study with the concentrations of 9.64 µg/L in CT3, 0.50 µg/L in CT5, and 0.36 µg/L in CT5, respectively. The presences of these compounds might be due to their highly persistence in environment or their illegal application. For instance, chlordane may remain in soils for 20 years and travel long-distances to higher latitudes through repeated deposition and evaporation [11]. The levels of pesticides detected in this study were highly over the WHO single pesticide limit of 0.1 µg/L for drinking water [12]. As Chhnok Tru is a floating community, most of populations there use lake water as the main source for drinking, cooking, and household uses. This elaborate the primary route of exposure of those pesticides to human which can cause severe health issues as chlordane initially accumulates in the kidney and liver, and it is then redistributed to adipose tissue, where it can be stored for several years due to its high lipophilicity [11].

Table 3. Levels of target pesticides in surface water from Chhnok Tru

Compounds	CT1	CT2	CT3	CT4	CT5
Azaconazole	-	-	16.46±0.03	-	-
Chloroneb	-	-	-	-	0.28±0.01
Pyroquilon	-	0.51±0.01	-	-	-

Chlordane	-	-	9.64±0.15	-	-
HCHs	-	-	-	-	0.50±0.03
Isazofos	-	-	-	-	0.61±0.01
Parathion	-	-	-	-	0.36±0.00

The residues of pesticide in aquatic system can be from a historic or recently used around the study area. For our study, all of 23 target compounds were not detected in all of fish samples include muscle, gill and inner part of the four fish species in Cyprinidae family. Base on the previous studies, most of organochlorine compounds were detected in fish, where the agriculture area using large amount of pesticides around the lake or river. Most of the compounds were detected in a low or high level depend on the environment they lived [13].

IV. Conclusion

In this study, surface water samples from 5 sites and four fish species were collected from Chhnok Tru floating community and evaluated the levels pesticide contamination. The results showed that 80% of water samples and 100% of fish samples were contaminated with at least one of pesticide compound. Among 23 target compounds, azaconazole, chloroneb, pyroquilon, chlordane, HCHs, isazofos, and parathion were detected in surface water from Chhnok Tru area. Routine monitoring studies should be conducted to raise public awareness of pesticide contamination and to prevent the worsening of pesticide pollution issues.

Acknowledgement

This research was financially supported by SATREPS - JST/JICA: grant-number JPMJSA1503 - Establishment of Environmental Conservation Platform of Tonle Sap Lake.

References

1. Keskinen M (2006) The Lake with Floating Villages: Socio-economic Analysis of the Tonle Sap Lake. Int J Water Resour Dev 22:463–480. https://doi.org/10.1080/07900620500482568
2. Lin Z, Qi J (2017) Hydro-dam – A nature-based solution or an ecological problem: The fate of the Tonlé Sap Lake. Environ Res 158:24–32. https://doi.org/10.1016/j.envres.2017.05.016
3. FAO (2014) Country fact sheet on food and agriculture policy trends. Fapda 6
4. Jensen HK, Konradsen F, Jørs E, et al (2011) Pesticide use and self-reported symptoms of acute pesticide poisoning among aquatic farmers in phnom penh, cambodia. J Toxicol 2011:. https://doi.org/10.1155/2011/639814
5. Kapsi M, Tsoutsi C, Paschalidou A, Albanis T (2019) Environmental monitoring and risk assessment of pesticide residues in surface waters of the Louros River (N.W. Greece). Sci Total Environ 650:2188–2198. https://doi.org/10.1016/j.scitotenv.2018.09.185
6. Papadakis EN, Vryzas Z, Kotopoulou A, et al (2015) A pesticide monitoring survey in rivers and lakes of northern Greece and its human and ecotoxicological risk assessment. Ecotoxicol Environ Saf 116:1–9. https://doi.org/10.1016/j.ecoenv.2015.02.033
7. Jinya D (2013) Report Development of Solid-Phase Extraction Method for Simultaneous Analysis of Semi-Volatile Organic Compounds Using a GC-MS Database System. Shimadzu Tech Rep 1–8
8. Campagnac E, Fontaine J, Sahraoui AL-H, et al (2008) Differential effects of fenpropimorph and fenhexamid, two sterol biosynthesis inhibitor fungicides, on arbuscular mycorrhizal development and sterol metabolism in carrot roots. Phytochemistry 69:2912–2919. https://doi.org/10.1016/j.phytochem.2008.09.009
9. Worden AN, Noel PRB, Mawdesley-Thomas LE, et al (1974) Feeding studies on lenacil in the rat and dog. Toxicol Appl Pharmacol 27:215–224. https://doi.org/10.1016/0041-008X(74)90192-6
10. Kampire E, Rubidge G, Adams JB (2015) Distribution of polychlorinated biphenyl residues in sediments and blue mussels (Mytilus galloprovincialis) from Port Elizabeth Harbour, South Africa. Mar Pollut Bull 91:173–179. https://doi.org/10.1016/j.marpolbul.2014.12.008
11. Singh K, Nong A, Feeley M, Chan HM (2019) Development of Biomonitoring Equivalents for chlordane and toxaphene with application to the general Canadian population. Regul Toxicol Pharmacol 106:262–269. https://doi.org/10.1016/j.yrtph.2019.05.015
12. WHO (1993) WHO-Guidelines for Drinking Water Quality, Chemical Aspects. https://www.who.int/water_sanitation_health/dwq/GDW8rev1and2.pdf
13. Kafilzadeh F (2015) Assessment of Organochlorine Pesticide Residues in Water, Sediments and Fish from Lake Tashk, Iran. Achiev Life Sci 9:107–111. https://doi.org/10.1016/j.als.2015.12.003

The 13th AUN/SEED-Net Regional Conference on Chemical Engineering 2020 (RCChE-2020)
Jointly held with
The 5th International Symposium on Conservation and Management of Tropical Lakes
"Insights and Challenges toward Achieving SDGs"

Optimization of Young Mango Fermentation and Effect of Different Preservation Methods on its Shelf-life

Kimleang NGOUN [1], Guechleang CHHUN [1], Reasmey TAN [1,2,*]

[1] *Faculty of Chemical and Food Engineering, Institute of Technology of Cambodia, Russian Federation Blvd., P.O. Box 86, 12156 Phnom Penh, Cambodia*
[2] *Food Technology and Nutrition Research Unit, Research and Innovation Center, Institute of Technology of Cambodia, Russian Federation Blvd., P.O. Box 86, 12156 Phnom Penh, Cambodia*
* *Corresponding author: rtan@itc.edu.kh*

Abstract

Fermented young mango is one of the most famous mango based products in Cambodia and it is particularly popular among teenagers. However, even if this were to be the case, we observe that the quality of this product is considerably low and has a short shelf-life. The objectives of this study were to produce a fermented young mango that is well-received by consumers and study on the effect of two food preservation methods on its shelf life. The optimization of young mango fermentation in this study focused on the mango's preparation (mango fermented as whole fruit and peeled fruit), blanching temperature and time (65 °C for 15 min and 70 °C for 10 min), fermentation conditions (ferment at room temperature and 4 °C), salt concentrations (2% and 5%) and sugar concentrations (20 °Brix, 23 °Brix, and 25 °Brix). The sensory evaluation was conducted in each step except for blanching temperature and time and the duration of soaking in cold water by using 9 points hedonic scale. For the study of shelf life, the vacuum packaging was utilized and two food preservatives (sodium benzoate and sodium metabisulfite) were used individually on the fermented young mango that was fermented after one day at the concentration of 0.1%. During the three weeks' observation on its shelf life, it was revealed that the sample treated with sodium benzoate stored at 4 °C was the best condition as in the final week of observation, it attained the highest pH (2.41±0.04), lowest acidity (1.35±0.00), lowest total soluble solids (13.55±0.07), lowest salt content (0.59±0.00) and yeast and mold was not detected in the sample.

Keywords: *Sodium benzoate, Sodium metabisulfite, Lactic acid bacteria, Titratable acidity*

I. Introduction

Mangoes are fruits with high valuable nutritional properties but like other fruits, they are perishable and have a short shelf-life. Not to mention, they are seasonal, therefore, they are not available all year long in the shops which were the reason processes are developed to extend their shelf-life. After collecting, mango ripe rapidly since it is classified as a climacteric fruit. Problems with the disease, vulnerability to low temperature, and perishable nature of the fresh fruit limit the transport of the product from the location to farther areas. This issue can be illuminated by utilizing green fresh fruits to turn them into pickle or chutney or sundried acidifying condiment (Amchur is a fruity spice powder made from dried unripe green mangoes and is used as a citrus seasoning), whereas ripe mangoes are utilized for the preserve, jam, sauces and so on [1]. Fermented mangoes are prepared with high sugar content and a low salt

concentration to help the lactic acid fermentation. Since the sugar is the main ingredient and raw mangoes were utilized, the prepared mangoes taste sweet and sour and it also provides energy [2]. Nevertheless, due to it being a low-salt fermentation, it has a lot of risks in contaminating by other spoilage bacteria which end up with a short shelf-life. That is why the current study was conducted to find a food preservation method to prolong its shelf-life.

II. Materials and Methods

2.1. Sampling sites

A type of mangoes as known as Keo Romeat in Cambodian. The selected mangoes were small in size not fully ripe nor mature with bright green color skin indicating that they were still young. Mangoes were stored in ambient temperature overnight before bringing to the work area to process the fermented young mango.

2.2. Analytical methods

2.2.1.pH

STARTER300 was used to measure the pH value of fermented young mango. The pH meter was calibrated at 25 ºC using buffer solutions of acidic and basic values of 4 and 7, respectively. The sample of each condition was put into a small beaker around 20 ml then immerse the electrode of pH meter enough to submerge. Each sample was done in triplicate.

2.2.2. Total soluble solids (TSS)

Brix value was measured by a refractometer (ATAGO, Japan) to determine the total soluble solids in the liquid. Only a few drops of the sample were required to drop on the prism surface. Each sample was done in triplicate.

2.2.3. Acidity

The acidity of fermented young mango was determined through an analytical method adopted by AOAC (Association of Official Analytical Chemists). Bring 10 ml of sample to titrate with NaOH (0.1N) using phenolphthalein as an indicator for 2-3 drops. Keep the titration going until the solution turned a light pink color. Each sample was done in triplicate.

$$\%TA = \frac{V_s \times N \times 90 \times 100}{V \times 1000} \qquad \text{(E.q. 2.1)}$$

2.2.4. Salt

The salt content was determined by using a salt meter, ATAGO ES-421, Japan. Firstly, click start to power on then drop a few drops of distilled water onto the titanium electrode and click 'zero'. Each sample was done in triplicate.

2.3. Yeast and Mold

Potato dextrose agar (PDA), a selective media for the growth of yeast and media was used. Using the spread plate method, 0.1 ml of the sample was dropped onto the solid media then using the spreader to gently and evenly distribute the sample. Finally, bring it to incubate 5 days at 25-30 ºC. Yeasts will grow creamy to white colonies and mold will grow as filamentous colonies, black spores.

$$N = \frac{\sum C}{V[(1 \times n_1)+(0.1 \times n_2)] \times d} \qquad \text{(E.q. 2.2)}$$

2.4. Sensory analysis

The sensory evaluation of the two fermented young mangoes that participated by 12 panelists using 9 points Hedonic scale.

2.5. Statistical analysis

The data are expressed as mean ± standard deviation ($X \pm SD$). Statistical test one-way ANOVA was applied to find a significant difference between the value of various parameters recorded for the effect of different preservation methods on the fermented young mango's shelf life, p-value ≤ 0.05 was considered statistically significant.

III. Results and Discussion

3.1.Sensory Evaluation

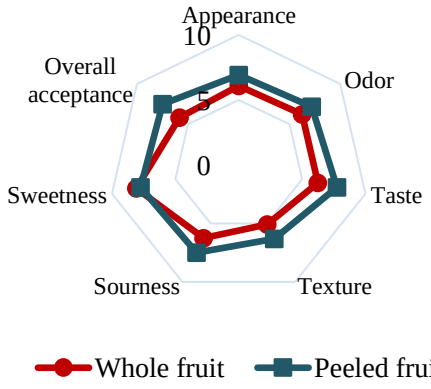

Fig. 1. Sensory evaluation of mango's preparation

. There was a significant difference (p-value ≤ 0.05) in the appearance of the two fermented mango of which the fermented mango with a whole fruit without peeling and cutting received 6.08±1.16 due to its drastic change in skin color which was visible to the eyes and the coagulated sap that stuck on the surface of the skin resulting in a negative response from the panelist. Meanwhile, the fermented mango with peeled skin and cut into thin strips obtained a higher score which was 6.92±1.16 receiving some positive comments from the consumer due to its hygienic and good looking appearance.

3.2. Effect of sodium benzoate, sodium metabisulfite and vacuum packaging on pH

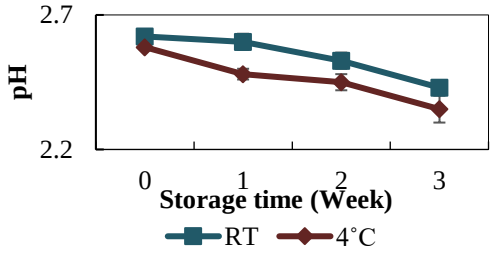

Fig. 2. pH of vacuum packaging samples stored in both conditions

Regardless of any conditions, pH value of the samples decreased for 3 weeks of which after one-week fermentation the pH dropped quickly in comparison to two-weeks and three-weeks fermentation. For, fermented young mango with the addition of E211 and E223 stored at room temperature, it dropped significantly from 2.95±0.03 to 2.56±0.02 and 2.77±0.02 to 2.54±0.03 respectively after one-week fermentation with no significant difference to be found in week 1 but there was a significant difference between Con, 2.45±0.02 and the two preservatives in week one. However, it had to be noted that the pH for every sample stored at 4ºC was higher than that of room temperature. The reason for the decrease in pH can be attributed to the increase in acidity which due to lactic acid fermentation in which LAB converted carbohydrates into lactic acid. Another reason that contributed to the strong acidity was due to the Ascorbic acid content contained in the young mango.

3.3.Effect of sodium benzoate, sodium metabisulfite and vacuum packaging on total soluble solids (TSS)

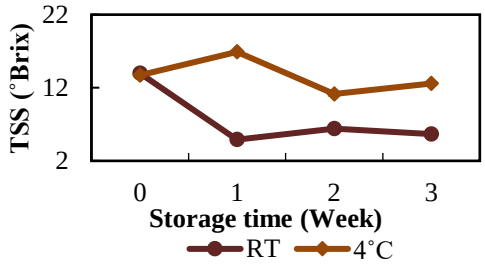

Fig. 3. TSS of vacuum packaging samples stored in both conditions

For vacuum packaging, fermented young mango for both conditions had its TSS fluctuated throughout the observation with the one stored at room temperature greatly changed from 13.97±0.35 to 5.65±0.70 unlike when it was stored at 4 °C which varied from 13.7±0.14 to 12.6±0.14. During the fermentation, LAB converted sugars into lactic acid which caused a decline in TSS [3] and at the same time, there were also three simultaneous mass transfer phenomena occurred; water flows from the product to the solution, a solute transfer from the solution to the product and a minor transfer of product's own solutes (sugars, organic acids, minerals, and vitamins) to the concentrated solution [2].

3.4.Effect of sodium benzoate, sodium metabisulfite and vacuum packaging on acidity

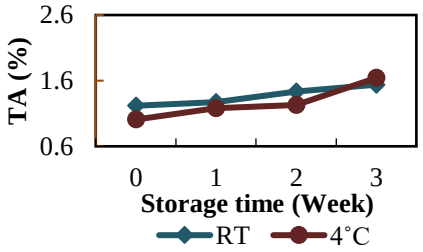

Fig. 4. TA of vacuum packaging samples stored in both conditions

The acidity for vacuum packaging stored at room temperature was lower than the one stored at 4 °C possibly due to the Ascorbic acid degradation with the exposure to the sunlight because it was well-known that Normally, the fermentation started with Leuconostoc mesenteroides as they produced lactic acid until it reached 0.25 to 0.3%. As the acidity increased Leuconostoc species started to die off, the Lactobacilli species (plantarum and cucumeris) took over as they continued until the acidity was 1.5 to 2.0%. The last bacteria in the chain was the Lactobacilli pentoaceticus that continued until the acidity was 2-2.5% [3]. The highest acidity in this study was 1.64±0.03% of fermented mango with vacuum packaging stored at 4 °C while others were around 1.5% showing that the fermentation hasn't reached the end yet.

3.5.Effect of sodium benzoate, sodium metabisulfite and vacuum packaging on salt content

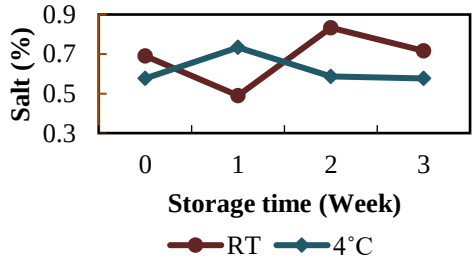

Fig. 5. Salt content of vacuum packaging samples stored in both conditions

Salt decreased over time for every sample regardless of with or without the addition of preservatives. For both conditions and no significant difference was found for each sample in different storage conditions. Salt allowed water and needed sugars to be pulled from the product [4]. For vacuum packaging, fermented young mango stored at room temperature is no longer safe to be consumed after 3 days-storage as it exhibited an unpleasant appearance and odor this spoilage was caused by excess lactic acid fermentation and other spoilage bacteria present due to the fermented young mango's high sugar content and low salt concentration which is a favorable condition for them to grow [4].

3.6. Effect of sodium benzoate, sodium metabisulfite and vacuum packaging on yeast and mold

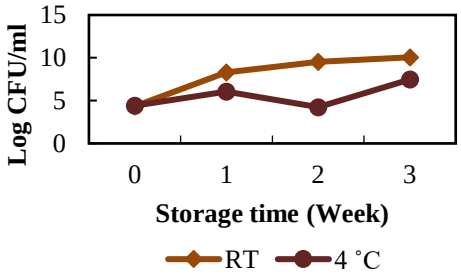

Fig. 6. Yeast and mold present in vacuum packaging samples stored in both conditions

Due to the high acidity of the product, it inhibited the growth of spoilage bacteria, therefore, only LAB, yeast, and mold were able to grow in an acidic environment. Also, this was a low-salt concentration which promoted the growth of more types of fermenting organisms, especially in natural fermentation, leading to faster acid production and a more acidic product. However, the lower salt concentrations can allow for mold and other contaminant growth resulting in a softer texture or off-flavored final product [4]. As it is shown in Figure 6. at room temperature, it was found that yeast was present in the Con sample with 4.49 log CFU/ml in week 0 then rose dramatically to 10.72 log CFU/ml in week 2 and finally showed a slight decline in week 3, 9.53 log CFU/ml possibly due to the increase in acidity which hindered the growth of yeast and the decrease in sugar and salt content which were considered to be their nutrients. Meanwhile, on the other hand, the effect of preservatives on the shelf-life could be seen with the naked eye. Antimicrobial activity of E211 is deeply related with the pH as most of its activity occurred at low pH and it was also deemed as an effective deterrent force against yeast and mold that were able to grow in an acidic environment [5].

IV. Conclusion

In the young mango's fermentation, it was found that fermented mango tasted better if it was to be peeled and cut into thin strips and the ideal blanching temperature and time was at 65 °C for 10 min. After the mild-heating process, bringing it to ferment for one day. According to the sensory evaluation, it was discovered that young mango fermented at room temperature worked better than the fermentation process at 4°C as it had a more desirable odor, texture, and taste. Besides, young mango fermented with a salt concentration of 2% and sugar content of 23 °Brix received a positive response from the panelists. Regarding the study of shelf life, in consideration of the slower fermentation process, fermented young mango added with sodium benzoate stored at 4 °C was the best condition as it had highest pH and lowest acidity among the studied conditions. For further study, it is recommended to do a more detailed preliminary study on the blanching temperature and time, salt concentration and study the effect of the combination between the two preservatives (sodium benzoate and sodium metabisulfite), the addition of preservatives should be done while processing the fermented young mango and it is also highly suggested to choose another preservative that has an antimicrobial effect against LAB in the future study.

References

[1] Saroj, Kumar, A., Singh, A., Sharma, M., 2010. Standardization of recipe and method for mango chutney. *Haryana Journal of Horticultural Sciences*. 39, 247–249.

[2] Khan, S., Ali, W., Kamal, T., Usman Khan, M., Gul, S., 2016. Preservation of mango slices in sucrose solution with various concentrations. *Journal of Food: Microbiology, Safety & Hygiene. 1, 1–7.*

[3] Food and Agriculture Organization., 2012. Pickles. *General information*. 4, 15–16.

[4] Eifert, J.A., Safety, F., Agent, E., Extension, V.C., Boyer, R.R., Science, F., Tech, V., Williams, R.C., 2015. Vegetable fermentation. *Fermentation*. 3, 10–11.

[5] Shahmohammadi, M., Javadi, M., Nassiri-Asl, M., 2016. An overview on the effects of sodium benzoate as a preservative in food products. *Biotechnology and Health Sciences*. 3, 44–49.

The 13th AUN/SEED-Net Regional Conference on Chemical Engineering 2020 (RCChE-2020)
Jointly held with
The 5th International Symposium on Conservation and Management of Tropical Lakes
"Insights and Challenges toward Achieving SDGs"

The effect of blanching on curcumin content and chemical composition of essential oils of dried Turmeric (*Curcuma longa*)

Chhanthyda Nong[1], Sokneang In[1,*]

[1] *Faculty of Chemical and Food Engineering, Institute of Technology of Cambodia, Russian Federation Blvd., P.O. Box 86, 12156 Phnom Penh, Cambodia*
* *in@itc.edu.kh*

Abstract

Turmeric is normally dried and grind into powder prior to storage and usage, and the conditions of blanching is one of important factors that can affect on the quality of dried turmeric. The objective of this study was to observe the impact of blanching on total phenolic content (TPC), antioxidant activity, curcuminoids content and essential oil composition of dried turmeric. Fresh turmeric rhizome was processed with blanching in boiling water for 0, 15, 30 and 45 minutes before oven dried at 55°C for 16 hours. The curcuminoids content and essential oil composition was determined by HPLC and GC-MS, respectively. The highest content of TPC (107.62 ± 6.46 mg GAE/g dried turmeric) and the total of antioxidants activity (9.58 ± 0.11 mg VCE/g dried turmeric) were found in the sample blanching for 30 minutes. The curcumin content of all blanching condition was ranged from 1.78 ± 0.12% to 2.20 ± 0.07% for bisdemethoxycurcumin, 1.00 ± 0.08% to 1.24 ± 0.05% for demethoxycurcumin and 2.24 ± 0.06% to 2.62 ± 0.14% for curcumin. The essential oil was ranged from 4.44 ± 0.55% to 4.96 ± 0.30% and the non-blanching sample and blanching sample for 30 minutes (37 and 31 compounds of essential oils, respectively) could detect more compounds than the other blanching conditions. Among detected compounds in essential oil, there were three main compounds, Ar-turmerone (33.37 ± 0.08%), Turmerone (32.27 ± 0.11%) and Curlone (20.66 ± 0.15%) in the essential oils of turmeric. Blanching turmeric before drying did affected on the quality of turmeric, especially curcumin content and essential oil yield and essential oil composition.

Keywords: *blanching, phenolic content, curcuminoids, essential oils*

I. Introduction

As one of the important spices, turmeric known as *Curcuma longa* and belong to *Zingiberaceae* family is an indigenous plant of India. This spice has been used as a seasoning, coloring agent, preservative, flavouring as well as folk medicine to treat many types of disease since ancient time and also noted to be used as cosmetic application. The special color from turmeric is yellow and it came from the presence of the compound which is named "Curcuminoids" [7]. In like manner, about 400,000 tone of turmeric were produced by India in fresh weight per year and it was about 80% of the world's supply of commercial turmeric. Between this, the rhizomes have been harvested then dried before distributing to the world [2]. Regarding to this, Cambodia is one among the Asian countries that cultivated and used turmeric since ancient time for any cooking recipe such as curry, amok and other Khmer foods to give the aroma and beautiful yellow color to the dishes.

Based on the potential application of turmeric due to its bioactive compounds, especially curcumin compound and the huge amount of the turmeric plants in Cambodia, hence turmeric rhizomes became a potential spice for apply in different important sectors. Between this, the drying and

blanching process have both positive and negative effect on the quality and the content of those bioactive compounds, therefore the studying of the effect of blanching on quality of turmeric with different blanching condition of dried turmeric have been investigated.

II. Materials and Methods

2.1. Sample preparation

Fresh turmeric rhizome was obtained from a farm at Kampong Cham province, Cambodia. After blanching in boiling water for 15, 30 and 45 minutes and then transferred to oven, the samples were packed with aluminum paper and stored in freezer at -20°C for further analysis.

2.2. Materials

Folin-Ciocalteu (Sigma, USA), gallic acid (Himedia. India) and sodium bicarbonate (Merck, Germany) are phenolic's reagents. Ascorbic acid(Merck,Germany) and DPPH (sigma, USA) were used for Total antioxidant activity analysis. Curcumin, bisdemethoxycurcumin and demethoxycurcumin (sigma, USA, purity ≥ 98%) were use as standard of curcuminoids analysis. Acetonitrile (Merck, Germany), acetic acid (Sigma,USA) and water grade (Merck, USA) were used for HPLC analysis of curcuminoids. Methanol (Merck, Germany) was used as solvent for extraction and dilution in this experiment.

2.3. Analytical methods

2.3.1. Total phenolic content

The determination of Total phenolic compounds was done by followed Wijaya, [10] with slightly modification by using Folin-ciocalteu assay. The mixture was measured with UV-Vis spectrophotometer at 765 nm. Result was expressed as mg gallic acid equivalent/g of dried turmeric (mgGAE/gDT).

2.3.2. Antioxidants activity of the extracts

The radical scavenging activity of the extracted turmeric was determined by using the DPPH free radical activity (2,2-diphenyl-1picrylhydrazyl) according to Choi *et al.,* [3]. The mixture of reagents and sample was then measured with the absorbance 517nm by using the spectrophotometer. The result was as expressed mg VCE/g DT.

2.3.3. Curcumin analysis by HPLC

HPLC was used for quantification the curcuminoids from turmeric and the method was modified from Hirun *et al.*[4]. A Shimadzu LC-20AT HPLC system connected to a Shimadzu SPD-M20A UV-VIS detector and apHera C18 – Polymer (25cm x 4.6mm,5µm) column was use in this experiment. (60:40 of acetonitrile and acidified water with acetic acid 1%) were used as mobile phase with 0.7ml/min and 25min, 5µL of curcuminoids were detected at 425nm.

2.3.4. Essential oil and composition analysis

Essential Oils were extracted from dried turmeric rhizomes by hydro-distillation in Clevenger's type apparatus and the results were expressed as % of Essential Oils yield (AOAC 2012).

The method was modified from Tran *et al.*[9] for GCMS analysis. In chromatographic system, the polar phase capillary column, TG-5MS (acid-deactivated polyethylene glycol) with the size of 30 m length × 0.25 mm internal diameter × 0.25µm film thickness (Thermo Fisher Scientific, USA) were performed on a GC-2010 Plus chromatograph (Shimadzu, Japan) with AOC-20i autosampler (Shimadzu, Japan). GC-MS were operated under the following conditions : Carried gas He; flow rate 1.0ml/min; split 1:50, injection volume 1.0 µl; injection temperature 250°C; oven temperature progress included an initial hold at 50°C for 2 min, a rise to 80°C at 2°C/min, a rise to 150°C at 5°C/min, a rise to 200°C at 10°C/min and a rise to 300°C at 20°C/min for 5 min. Total running time is 46 min.

III. Results and Discussion

3.1. Total phenolic content of the extract

Table.1 were presented the total phenolic of dried turmeric. The highest value of total phenolic content was recorded in dried turmeric at 55°C with blanching 30 minutes. Moreover, the results shown a different number but not significantly different between the results of TPC for these 4 conditions in this study ($p>0.05$). Bamidele *et al.*[1] stated that there might be some increasing of total phenolic content while increasing the blanching time. The increasing in the total phenolic content were attributed to the reduction of enzyme-mediated polyphenol degradation (complete inactivation of native polyphenol oxidase) and might due to the release of bound phenolic acids from the breakdown of cellular constituents of cell wall.

3.2. Antioxidant activity of the extract

Antioxidant activities of dried turmeric in this study have shown a different number (**Table 1.**) but there are not significantly different ($p>0.05$) among the studied condition. Not far from total phenolic content, 30 minutes was a good condition among 3 blanching condition which could remain higher of antioxidants activity. This meant that blanching process could prevent the major loss of antioxidant activity, but it should be performed with the minimal heat treatment. The other publication has said that, it is possible to believe that total phenolic group are highly responsible for antioxidants activity of plants, that is why both of them have strongly correlation. [6].

Table 1. Total phenolic content and antioxidant activity of the extract from dried turmeric

Sample	TPC (mg GAE/g DT)	Antioxidant activity (mgVCE/g DT)
NB	105.47±5.37[a]	9.60±0.18[a]
B15	93.42±4.53[a]	9.44±0.08[a]
B30	107.62±6.46[a]	9.58±0.11[a]
B45	96.28±5.35[a]	9.37±0.18[a]

Values are presented as mean (n=3). Means with different superscripts alphabets in the same column are significantly different ($p<0.05$).

3.3. Curcuminoids content by HPLC

Table2. Curcuminoids content in dried turmeric rhizomes

Sample	Curcumin (%)	Bisdemethoxy-curcumin (%)	Demethoxy-curcumin (%)
NB	2.62 ± 0.14[a]	2.20 ± 0.07[b]	1.24 ± 0.05[b]
B15	2.24 ± 0.06[a]	1.89 ± 0.13[a]	1.03 ± 0.01[a]
B30	2.33 ± 0.20[a]	1.90 ± 0.03[a]	1.05 ± 0.07[a]
B45	2.25 ± 0.24[a]	1.78 ± 0.12[a]	1.00 ± 0.08[a]

Mean with different small letters (a-b) in the same column are significantly different at $p<0.05$. Number of replicated = 3.

The result was showed that the curcumin, bisdemethoxy-curcumin and demethoxycurcumin was the highest in non-blanching condition and dried at 55°C while the lowest one was found in blanching 45 minutes (**Table. 2).** The result revealed the significantly different among non-blanching and blanching condition of bisdemethoxycurcumin and demethoxycurcumin in dried turmeric. From the results of this current study, it could be indicated that blanching has affected on the amount of bisdemethoxycurcumin and demethoxycurcumin as it decreased while the blanching time increased to 45 minutes. Non-blanching condition could remain the high value of curcuminoids and blanching 15 to 30 minutes could preserve the curcuminoids with higher amount if compared to blanching 45 minutes.

3.4. Essential oils of dried turmeric rhizomes and its composition

The highest value of essential oil from turmeric was found in dried turmeric at 55°C with blanching 30 minutes (4.96 ± 0.30 %) while the lowest one was found in blanching 45 minutes condition (4.04 ± 0.05 %). The result of these 4 conditions showed in **Table 3**. was not significantly different (p value > 0.05).

Table 3. Percentage of essential oils yield

Condition	% yield of EOs
NB	4.82 ± 0.25[a]
B15	4.84 ± 0.53[a]
B30	4.96 ± 0.30[a]
B45	4.44 ± 0.55[a]

Mean with different small letters (a,b) in the same column are significantly different.. Number of replicates = 2

A studying has done on the seed and plants, and it has been claimed that blanching the oil seeds could be a promising technique to improve the yield and quality of the oil. It is an inexpensive technique that disintegrates the seed's cell walls and increases the extractability of the intracellular material and the extraction method could be the most effect factor of essential yield [5]. Link with this result, blanching 30 minutes has been noticed as the optimum condition which could maintain the essential oil with higher amount if compared to other studied conditions. Around 46 compounds were detected in turmeric oil for this study among 4 conditions, and the similarity of the compounds were compared with compound library NIST11s which percentage was higher than 90%. **Table 4** only shows the main compounds in dried turmeric oil with 4 condition of studying.

Table 4. Percentage of main compounds of essential oils yield

N	Compounds	RI (Cal.)	NB %	B15 %	B30 %	B45 %
1	β-Caryophellene	1326	1.04	0.96	0.81	0.67
2	α-Terpinolene	987	1.94	0.93	1.05	1.37
3	α-Curcumene	1388	1.87	1.91	2.26	1.72
4	Zingiberene	1400	2.30	2.51	2.96	2.44
5	β-Sesquiphellandrene	1433	3.28	3.57	4.12	3.25
6	Curlone	1614	19.31	20.51	20.28	20.66
7	Turmerone	1582	29.03	30.64	27.87	32.27
8	Ar-Tumerone	1578	30.33	31.47	33.37	30.34
9	Other composition	-	10.9	7.5	7.28	7.28
	Total compounds		37	28	31	30

RI (Cal): Retention Index, identify based on the calculation of RI value which relative to C7-C31n-alkanes on TG-5MS Column, % are given by the mean of two determinations. (-) None detected and not found.

The differences number of compositions may due to some factors such as method of blanching and parameters that are characteristic of the product subjected to blanching. For blanching, in some case of formation new compounds after blanching or cooking process has been recorded probably because of oxidation reactions, hydrolysis of glycosylated forms, or the release of compounds by the rupture of cell walls [8].

IV. Conclusion

The study on determination of bioactive compounds in dried turmeric rhizomes from Kampong Cham province with different conditions of blanching (NB, B15, B30 and B45) prior to oven drying at 55°C has been investigated. Blanching turmeric before drying did affected on the quality of turmeric, specially curcumin content and essential oil composition. Among 3 blanching conditions, dried turmeric with blanching 30 minutes is the optimum condition which could preserve yield of crude extracts, total phenolic content, antioxidants activity, yield of essential oils and its compositions and curcuminoids content close to non-blanching condition.

Acknowledgement

Thank to my advisor Dr. IN Sokneang for all the supporting and thankful to the world bank (HEIP Project) for their financial support.

References

[1] Bamidele, O., Fasogbon, M., Adebowale, O., Ade yanju, A., 2017. Effect of blanching time on total Phenolic content. *Current Journal of Applied Scie nce and Technology*. 24, 1–8.

[2] Borah, A., Hazarika, K., Khayer, S.M., 2015. Dr ying kinetics of whole and sliced turmeric rhizom e in a solar conduction dryer. *Information Process ing in Agriculture*. 2, 85–92.

[3] Choi, Y., Ban, I., Lee, H., Baik, M.Y., Kim, W., 2019. Puffing as a novel process to enhance the a ntioxidant and anti-inflammatory properties of *Cu rcuma longa L.* (turmeric). *Antioxidants MDPI*. 8, 2–4.

[4] Hirun, S., Utamaang, N., Roach, P.D., 2014. Tur meric (*Curcuma longa L.*) drying: an optimization approach using microwave-vacuum drying. *Journ al of Food Science and Technology*. 51, 2127 – 2 133.

[5] Kaseka, U.L.O., 2006. Physicochemical attributes. *Bioactive Compounds*. 6, 234–289.

[6] Oboh, G., 2005. Effect of blanching on the antiox idant properties of some tropical green leafy vege tables. *LWT - Food Science and Technology*. 38, 513–517.

[7] Osorio-Tobón, J.F., Carvalho, P.I.N., Barbero, G.F. ,Nogueira, G.C., Rostagno, M.A., Meireles, M.A. D.A., 2016. Fast analysis of curcuminoids from t urmeric (*Curcuma longa L.*) by high-performance liquid chromatography using a fused-core column. *Food Chemistry*. 200, 167 – 174.

[8] Ratseewo, J., Tangkhawanit, E., Meeso, N., Kaew seejan, N., Siriamornpun, S., 2016. Changes in an tioxidant properties and volatile compounds of kaf fir lime leaf as affected by cooking process. *Inter national Food Research Journal*. 23(1), 188–196.

[9] Tran, T.H., Ha, L.K., Nguyen, D.C., Dao, T.P., N han, L.T.H., Nguyen, D.H., Nguyen, T.D., Vo, D. V.N., Tran, Q.T., Bach, L.G., 2019. The study on extraction process in essential oils of black peppe r *(Piper nigrum L.)* seeds harvested in Gia Lai Pr ovince, *Vietnam. Processes*. 7(2), 56.

[10] Wijaya, C., 2018. Optimization of Extraction time and temperature for Java tea. Food and Nutrition Open Access. 2, 1-8.

The 13th AUN/SEED-Net Regional Conference on Chemical Engineering 2020 (RCChE-2020)
Jointly held with
The 5th International Symposium on Conservation and Management of Tropical Lakes
"Insights and Challenges toward Achieving SDGs"

Production of White Pepper from Ripe Pepper Berries (*Piper nigrum* L.)

Seanghai Hoeun [1], Sreyleak Meas [1], Elen Morm [1] and Sokneang In [1,*]

[1] *Faculty of Chemical and Food Engineering, Institute of Technology of Cambodia, Russian Federation Blvd., P.O. Box 86, 12156 Phnom Penh, Cambodia*
* *in@itc.edu.kh*

Abstract

White pepper (*Piper nigrum* L.) is commonly produced from ripe pepper berries by removing the outer skin before drying. This spice is preferred using by consumers due to its light color, milder flavour and pungency. White pepper exists in the market as the whole and ground form. It is commonly used in food products such as sauces, soups, salad dressing and mayonnaise. The main purpose of this study is to determine the suitable conditions for white pepper production from ripe pepper berries. The study was conducted in different blanching times (0, 1, 3, and 5 min), soaking in water for 24 hours and drying at 65ºC for 16 hours. Drying kinetic, color measurement and bioactive compounds including total phenolic compound, total antioxidant capacity, essential oils and an alkaloid (piperine) content were evaluated. According to the results, soaking at 24 hours within non blanching and drying at 65°C for 12 hours, was considered as a suitable condition for white pepper production However, total phenolic content and total antioxidant capacity decreased in overall for white pepper after processing due to the skin removed while the piperine content and total essential oil remained stable.

Keywords: *Blanching, color, Piper nigrum L., piperine and white pepper*

I. Introduction

In general, white pepper is produced from fully ripe berries by removing their pericarp before drying. This spice could provide economical, nutritional, and medicinal benefits [1]. Also, it is used in food industries and pharmaceutical industries for medicinal purposes. In European countries, white pepper is commonly used in light-colored sauces, soups, salad dressing, mayonnaise, balsamic tomatoes and mostly used as a flavoring agent [2]. As for processing technique, it is quite different from area to area and from country to country. For instant in Malaysia, the pepper berries were soaked in water one or two weeks to remove the skin before drying, while in Cambodia, the berries were boiled in water for a certain period, subsequently soaked in water to remove the skin prior drying. According to Aziz *et al.* [3], blanching time should be from 3 to 10 min to restrain the loss of color, aroma, and essential oil components of pepper. However, blanching for less than 1 minute is insufficient to remove the outer skin. Even though, the process of white pepper has been studied and a lot of study has been done in other countries. Therefore, white pepper processing techniques should be developed, improved and optimized to obtain better white pepper quality and provide information to the local farmer.

II. Materials and Methods

2.1. Sample preparation

The ripe pepper berries (Khmer cultivate) were collected from Rosemoric farm in Ratanakiri province in April 2020 and transported by storing in the icebox. The pepper berries

were washed with distilled water thrice to remove the foreign matters. Then, the ripe berries were pretreated in boiling water for 1, 3, and 5 min and soaked for 24 hours. The soaking condition was also applied to non-boiling peppers. Next, they were rubbed manually to remove pericarp and rested. Eventually, the white pepper was weighted prior drying.

2.2. Drying kinetic

All the samples were oven-dried and compared to un-pretreated pepper berries. The amount of 100 g of green pepper berries were oven-dried at the optimum condition of 65ºC for 16 hours. The samples were taken out and weighted for every one hour.

2.3. Crude extraction

An amount of 0.5 g of ground pepper was extracted with 10 ml of methanol then placed in the ultrasonic tank 120 W (VWR International bvba/sprt, Malaysia) for 20 min. After extraction, the solvent was centrifuged (Rotofix 32A, Germany) at 2000 rpm for 15 min. The clear supernatant was poured out by putting in the evaporated flask and the extraction was repeated 3 times with 10 ml of methanol added. The rotary evaporator (IKA RV-10 Control, IKA, Germany) was performed to evaporate the solvent until the sample was dried. The extract was diluted with 10 ml of methanol and stored at -20ºC for further analysis.

2.4. Initial moisture content, color, and bioactive compounds analysis

The initial moisture content of peppercorns was determined by followed an analytical method AOAC (Association of Official Analytical Chemists) with a slight modification [4]. The fresh pepper was oven-dried at 105ºC for 24 hours. Color of white pepper after peeling and drying process was measured by using Chroma meter (CR-400, Konica Minolta). The total phenolic content (TPC) of the pepper was determined by the Folin-Ciocalteu's reagent test [5, 6]. The antioxidant activity was determined by using DPPH (2,2-diphenyl-1-picrylhydrazy) radical scavenging capacity assay with the slight modifications [7]. Piperine content was detected by HPLC (High Performance Liquid Chromatography, Shimadzu, LC 2010A, Japan) coupled with UV detector [8].

III. Results and Discussion

3.1. Drying kinetic of white pepper

The effect of pretreatment and soaking on drying kinetic of white pepper produced from ripe pepper berries in different pretreatment conditions (0, 1, 3, and 5 min) after drying at 65 ºC for 16 hours was shown in **Fig. 1**.

D65-NB, D65-1B, D65-3B, and D65-5B represented pepper berries after drying at 65ºC for 16 hours at different pretreatment conditions including without pretreatment, pretreatment for 1, 3 and 5 min, respectively.

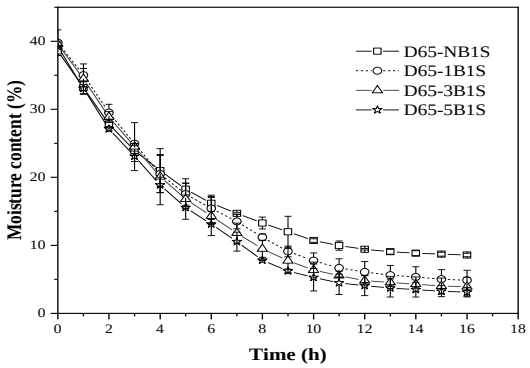

Fig. 1. Drying kinetic of white pepper

The drying kinetic indicated that drying from the early stage to 8 hours, each moisture content went down similarly. After drying for 8 hours, pretreated sample for 5 min declined sharply and followed by pretreated sample for 1 and 3 min, respectively. Meanwhile, the unpretreated sample moderately decreased. The results showed that the longer the pretreatment in boiling water improved the drying kinetic of white pepper. All moisture content of all conditions remained stable after 12 hours drying. The pretreated sample for 1, 3 and 5 min could reduce the moisture content to lower than 10-13 % for 8 hours, while the unpretreated sample was about 15%. In general, the moisture content of white pepper is around 12 to 13% [9]. Additionally, the yield of white pepper obtained from ripe pepper ranged from 35 to 37%. The obtained results showed higher yield than the study Aziz *et al.* [3] that found the mature berries were able to yield about 25-28 % of white pepper.

3.2. Color

The result of the chromatic coordinates L^*, a^*, b^*value of peeled pepper and pepper after drying at 65 ºC for 16 hours were indicated in **Fig. 2**.

RP represented fresh ripe pepper berries. PNB, P1B, P3B, and P5B represented the peeled pepper berries in different pretreatment conditions including without pretreatment, pretreatment for 1, 3 and 5 min, respectively.

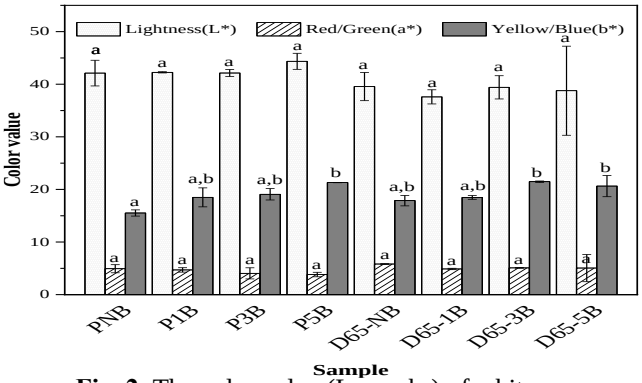

Fig. 2. The color value (L*, a*, b*) of white pepper

The lightness L* value was found 42.12 ± 2.44, 42.27 ± 0.12, 42.13 ± 0.68, and 44.37 ± 1.52 on peeled pepper berries PNB, P1B, P3B, and P5B, respectively. For dried pepper berries, lightness L* value was 39.56 ± 2.68, 37.60 ± 1.35, 39.42 ± 2.21, and 38.77 ± 8.47 of D65-NB, D65-1B, D65-3B, and D65-5B, accordingly. The lightness L* value of all the conditions of peeled pepper and dried pepper were similar. The redness/greenness a* value of peeled pepper and dried pepper conditions were not significantly different. Furthermore, the yellowness b* value of peeled pepper condition were increased slightly. For dried pepper berries, the yellowness b* value of D65-NB and D65-1B showed lower than the one of D65-3B and D65-5B. It seems that drying condition has no influence on the color of white pepper. According to Mey [10] found that drying below 70ºC did not affect the color of pepper because it could not deactivate the enzymes responsible for browning reaction of color.

3.3. Total phenolic compound and total antioxidant capacity

The results of TPC and total antioxidant capacity (TAC) were described in **Table 2** and expressed as milligram of gallic acid equivalent (GAE) in gram of dried pepper and milligram of vitamin C equivalent (Vit.CE) in gram of dried pepper.

Table 2. The amount of TPC and TAC

Sample	TPC (mg GAE/g DW)	TAC (mg Vit.CE/g DW)
RP	6.75 ± 0.45^{d}	3.71 ± 0.26^{e}
PNB	$2.60 \pm 0.27^{a,b,c}$	1.08 ± 0.15^{a}
P1B	3.35 ± 0.32^{c}	$1.64 \pm 0.06^{b,c,d}$
P3B	3.12 ± 0.54^{c}	2.05 ± 0.40^{d}
P5B	$2.95 \pm 0.39^{b,c}$	2.06 ± 0.18^{d}
D65-NB	1.96 ± 0.04^{a}	$1.17 \pm 0.09^{a,b,c}$
D65-1B	1.90 ± 0.06^{a}	$1.23 \pm 0.05^{a,b,c}$
D65-3B	$2.14 \pm 0.07^{a,b}$	$1.17 \pm 0.11^{a,b}$
D65-5B	1.91 ± 0.15^{a}	$1.70 \pm 0.06^{c,d}$

The lowercase letter represents a significant different for each condition (*p-value* < 0.05)

The TPC of fresh ripe pepper berries was found the highest value compared to peeled pepper and dried white pepper. The obtained results were similar to the study of Aziz *et al.* [3] that found the TPC of white pepper contained around 3-6 mg GAE/g dried pepper. However, the TPC of dried white pepper was not significantly different, but lower than peeled and fresh pepper. The loss of TPC was probably due to the fact that the phenolic compounds are mostly located in the mesocarp of pepper berries [11]. Therefore, the TPC lost while the skin of pepper berries was removed to produce white pepper.

The TAC of ripe pepper berries (RP) was greater value than peeled and dried pepper berries samples. Both TAC results of PNB and D65-NB were found similarly and lower than the one of peeled and dried pepper berries condition. For the dried pepper conditions, the TAC of D65-5B showed higher compared to D65-NB, D65-1B, and D65-3B. It was demonstrated that the pretreatment could be increased the amount of antioxidant capacity except drying slightly effects on antioxidant capacity in white pepper after processing.

Comparison between TPC and TAC, there showed that TPC and TAC had a positive strong correlation (0.929) in white pepper. From the previous study, Eyenga *et al.* [12] stated that all of the antioxidant activities were positively and strongly (> 90%) correlated with TPC. It makes sense that antioxidant activity was declined if the TPC was decreased.

3.4. Essential oil and piperine

As shown in **Table 3**, the amount of essential oil and piperine in pepper were expressed as percentage (% w/w).

Table 3. The percentage of essential oil and piperine in white pepper

Sample	Essential oil (%)	Piperine (%)
RP	2.22 ± 0.08[a]	3.58 ± 0.24[a]
PNB	2.21 ± 0.01[a]	5.37 ± 0.61[b]
P1B	3.02 ± 0.37[a]	5.68 ± 0.18[b,c]
P3B	3.11 ± 0.19[a]	6.08 ± 0.16[b,c]
P5B	2.86 ± 0.02[a]	5.39 ± 0.25[b]
D65-NB	2.44 ± 0.38[a]	6.29 ± 0.15[c]
D65-1B	2.63 ± 0.16[a]	4.33 ± 0.18[a]
D65-3B	2.26 ± 0.41[a]	3.62 ± 0.35[a]
D65-5B	2.57 ± 0.19[a]	3.86 ± 0.26[a]

According to **Table 3**, the essential oil yield of all samples were not significantly different. The study of Weil *et al*. [13] mentioned that blanching caused the structure of the peppercorn may protect the volatile compounds from transfer during processing. However, pretreatment in boiling water and soaking for one day had no effects on the yield of essential oil from white pepper. Moreover, the essential oil cells were mainly in the inner portion of the skin [11]. According to Jayatunga and Amarasinghe [14], drying pepper at 65ºC obtained the highest yield of essential oil. Therefore, there was no impact of pretreatment, soaking and drying on the essential oil content of white pepper produced from ripe pepper berries. Based on FAO (Food and Agriculture Organization) [9] the essential oil contained 1.5 % was classified in grade I and II and 1.0 % of essential oil was classified in grade III. Thus, the percentage of essential oil results was about 2-3 % which classified in grade I white pepper.

In term of piperine content, ripe pepper berries was found the piperine content (3.58 ± 0.24 %) and there was not significantly different for piperine value in peeled pepper berries. For peeled pepper berries, the piperine was found greater than dried pepper berries. However, the D65-NB contained the highest piperine among of those from dried pepper condition. Based on these obtained results, there was no impact of pretreatment and soaking on piperine content, while the drying that had a very slight influence. It could be explained that the piperine molecule located in the inner core of pepper grain. As a result, this molecule did not much effect when the pepper skin removed during processing [11]. The study of Weil *et al*. [13] showed that piperine contents were not affected by the wet process as blanching. The piperine of those dried pepper berries was around 3-6 %. 4.0% of piperine and it was classified in grade I, 3.5 % classified in grade II and 3.0% classified in grade III [9].

IV. Conclusion

White pepper produced from ripe pepper berries with soaking at 24 hours without pretreatment and drying at 65°C for 16 hours, was considered as a suitable condition for white pepper production because it obtained higher production yield, better color, high amount of bioactive compounds. The total phenolic content and antioxidant activity decreased after processing while the piperine content and total essential oil remained stable.

ACKNOWLEDGMENTS

This research has been partially supported by funds from the ARES-CCD.

REFERENCES

[1] Olalere, O.A., Abdurahman, N.H., Alara, O.R., Habeeb, O.A., 2017. Parametric optimization of microwave reflux extraction of spice oleoresin from white pepper (*Piper nigrum*). *Journal of Analytical Science and Technology*. 8, 1–7.

[2] Azam Ali., 2007. Pepper processing. *Technology challenging poverty*. 44, 1–8. Om, C., Daily, F., Vlieghe, E., MaLaughlin, J.C., Mclaws, M.L., 2017.

[3] Aziz, N.S., Sofian Seng, N.S., Razali, N.S.M., Lim, S.J., Mustapha, W.A.W., 2019. A Review on Conventional and Biotechnological Approaches in White Pepper Production. *Journal of Science of Food and Agriculture*. 99, 2665–2676.

[4] AOAC, 2000. Official methods of Analysis. 4th ed. Association of Official Analytical Chemist, Washington DC, USA.

[5] Chan, E.W.C., Lim, Y.Y., Wong, S.K., Lim, K.K., Tan, S.P., Lianto, F.S., Yong, M.Y., 2009. Effects of different drying methods on the antioxidant properties of leaves and tea of ginger species. *Food Chemistry*. 113, 166–172.

[6] Rabeta, M.S., Vithayia, M., 2013. Effect of different drying methods on the antioxidant properties of Vitex negundo Linn. tea. *International Food Research Journal*. 20, 3171–3176.

[7] Bopitiya, D., Madhujith, T., 2014. Antioxidant potential of rice bran oil prepared from red and white rice. *Tropical Agricultural Research*. 26, 1–11.

[8] Sharma, N., Joshi, H.M., Malik, A., Mishra, M., Singh, B.P., Tripathi, S., Upadhyay, V., 2013. Development and Validation of Rapid RP- HPLC Method for Estimation of Piperine in Piper nigrum L.

International Journal of Herbal Medicine IJHM. 1, 6–9.

[9] FAO, 2017. Standard for Black, White and Green Peppers Cxs 326-2017. *Codex Alimentarius*.

[10] Mey, P., 2017. Effects of blanching temperature on quality of black pepper (*Piper nigrum* L.). *International Journal of Environmental and Rural Development*. 8, 1–6

[11] Attokaran, M., 2011. Natural Food Flavors and Colorants. 1st ed. Blackwell, Wiley.

[12] Eyenga, M., Youovop, J., Ngondi, J., Sindic, M., 2020. Temperature dependent studies on nutritional, total polyphenols, flavonoids content and antioxidant activities of Aframomum citratum (C.Pereira) K.Schum and Tetrapleura tetraptera (Schum. & Thonn.) Taub. fruits. *Biotechnol. Agron. Soc. Environ. 2020*. 24, 207–220.

[13] Weil, M., Shum Cheong Sing, A., Méot, J.M., Boulanger, R., Bohuon, P., 2017. Impact of blanching, sweating and drying operations on pungency, aroma and color of Piper borbonense. *Food Chemistry*. 219, 274–281.

[14] Jayatunga, G.K., Amarasinghe, B.M.W.P.K., 2019. Drying kinetics, quality and moisture diffusivity of spouted bed dried Sri Lankan black pepper. *Journal of Food Engineering*. 263, 38–45.

The 13th AUN/SEED-Net Regional Conference on Chemical Engineering 2020 (RCChE-2020)
Jointly held with
The 5th International Symposium on Conservation and Management of Tropical Lakes
"Insights and Challenges toward Achieving SDGs"

Development of Fermented Small Cucumbers with Different Tastes Using Isolated Lactic Acid Bacteria

Marinich NET [1], Daly DIM[1] and Reasmey TAN [1,2,*]

[1] *Faculty of Chemical and Food Engineering, Institute of Technology of Cambodia, Russian Federation Blvd., P.O. Box 86, 12156 Phnom Penh, Cambodia*
[2] *Food Technology and Nutrition Research Unit, Research and Innovation Center, Institute of Technology of Cambodia, Russian Federation Blvd., P.O. Box 86, 12156 Phnom Penh, Cambodia*
* *Corresponding author: rtan@itc.edu.kh*

Abstract

Young cucumber is a popular vegetable in Cambodia and the preservation of this vegetable by fermentation is widely practiced. However, the methodology of the fermentation process is not specified yet and the quantity of lactic acid bacteria was not determined clearly and the sensory evaluation was also not remained the same. Regarding this, pure isolated LAB is the best way to provide the best quality, prolong shelf life and the taste is remained stable. The objective of this study was the development of fermented cucumber by using pure isolated LAB and shelf life determination by the addition of food preservatives including sodium metabisulphite and sodium benzoate. To achieve this purpose, the brine solution of fermented cucumbers was purchased in local markets in Phnom Penh and yogurt was bought from supermarket. Then, culture and isolated in three times to purified it, and 10 pure isolated LAB were collected to fermented. For physicochemical characteristics and sensory evaluation were analyzed after fermentation for two days. Acidity value was in range 0.22% to 0.32%, pH was 3.82 to 4.14, salt concentration was 1.62% to 1.75%, and TSS was 2.5 to 3-degree brix of LAB S1, S2 and S3. They were collected to continue fermentation with the addition of sugar 4% and without sugar addition to choosing fermentation by blanching at 75℃ in 5min. According to sensory evaluation and physicochemical analysis again, only one pure isolated lactic acid bacteria was conducted on shelf life base on physicochemical value including total acidity 0.22%, pH 4.14 and reducing sugar value 0.85% and sensory evaluation. To sum up, sodium metabisulphite is the best one to preserve shelf life and provide good quality depends on physicochemical analysis and microbial count.

Keywords: *Young cucumber, sodium metabisulphite, sodium benzoate, Total plate count, Yeasts, Molds*

I. Introduction

Food is one of our basic needs that all humans have been recognized in the world. Be a part of the food, vegetables play an important role in maintaining proper health and provide our body a lot of nutritional [7]. Cambodia is a developing country where has less industrial activities, it is hard to transform or to preserve vegetables by any modern methods besides fermentation because fermentation is the cheap and easy process to conserve the vegetables, which can be afforded by most of the Cambodian people [1]. Similarly, the principal of the fermentation process is to preservation, shelf life-extending, other effects such as the improvement of safety, nutritional value, and organoleptic quality of the food. Therefore, the best method to store those products healthily and economically is lactic acid fermentation. Fermentation

process needs less energy simple for handling and storage without cooling and easy method for handling of raw material before further processing. Based on the benefits of vegetable, fermented products become the common foods which were utilized in the local [8]. The object of this study was the development of fermented small cucumbers with different tastes using isolated LAB by selecting the pure isolated LAB from brine solution of fermented cucumber and yogurt in cucumber fermentation and to observe the shelf life in cucumber fermentation with addition food preservative base on physicochemical analysis and number of microbial count.

II. Materials and Methods

2.1. Sampling sites

Raw materials were used in cucumber fermentation including fresh cucumber, salt, and sugar were purchased from Kilo Lekh buon market.

2.2. Analytical methods

2.2.1. Total acidity

The total acid produced during fermentation is determined by the method acid-base titration. At each sampling time, 10ml of brine is placed in Erlenmeyer and 3 drops of phenolphthalein are added. Then the titration with NaOH 0.1N is going until the light pink color persisted [6].

2.2.2. Determination of pH

The pH of the fermented liquors was determined at the specified interval by a pH meter (Model HI2020, HANNA instruments Woonsocket, Romania) [5].

2.2.3. Salt concentration

The salt concentration is determined by using a salt meter (Model ES-421, ATAGO Co., Ltd, Japan). The value of salt concentration is indicated in percent [5].

2.2.4. Total soluble solid

Brix value was measured by a refractometer to determine the total soluble solids in the liquid [5]. Only a few drops of the sample were required to drop on the prism surface.

2.2.5. Determination of moisture content

To determine moisture, samples were weighed 5g and dried for 3 hours in an oven at 105±2°C and it is rested in a desiccator for 15mn then the dried sample is weighed [2].

2.2.6. Determination of yeast mold count

Appropriately 15 to 20ml of agar was poured in the sterile Petri dishes and allows them to solidify. The marked sterile Petri dishes were inoculated with 100µl of appropriate tenfold serial dilution of the samples by using brine. Place the bent portion of the glass rod on the agar surface and spin for 30s to distribute the 0.1ml of dilution evenly over the entire agar surface. The plates were incubated in aerobic at 37°C for a period of 48h. After a 48h incubation period, the colonies were counted in the range 30-300 CFU/ml.

2.3. Sensory evaluation

A sensory evaluation test using descriptive test was evaluated by 16 panelists and affective tests was evaluated by 30 panelists participate using 9 points Hedonic scale.

2.4. Statistical data analysis

All data were subjected to determine the significant difference among mean on those samples by one way ANOVA analysis of variance in SPSS version 16.0. The predetermined acceptable level of probability was 5% for all comparisons ($p \leq 0.05$).

III. Results and Discussion

3.1. The influence of food preservative on total acidity

The total acidity value store in room temperature and 4C were shown in Figure 1. In week 0, sodium metabisulphite was the highest quantity of total acidity came behind by control and sodium benzoate respectively 0.14%, 0.07%, and 0.06%. In contrast, sodium metabisulphite was the lowest amount of total acidity in week 1 and week 3, whereas, Sodium benzoate and control contained a similar value around 0.40% and 0.39% respectively.

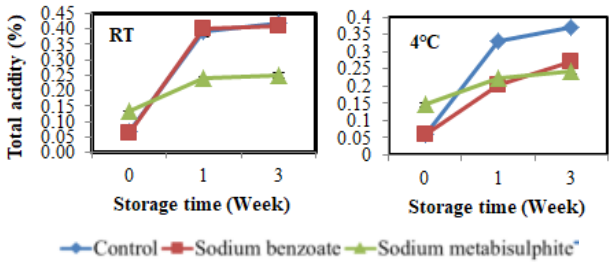

Fig 1. Total acidity store in room temperature and 4°C

For storage condition 4C, sodium metabisulphite is the best food preservative because it is the lowest quantity of total acidity, and it is small amount of microorganism contain in this brine solution.

3.2. The influence of food preservative on pH Value

Figure 2 illustrates pH value store in room temperature and at 4°C. In week 0, control, sodium benzoate and sodium metabisulphite had pH value 3.88, 4.62, and 3.91 respectively. Furthermore, these 3 samples were also significantly different with p-value ($p \leq 0.05$) in

respectively 3.27, 3.41, and 3.61 of control, sodium benzoate and sodium metabisulphite.

According to the result at 4°C, pH value of these two preservatives and control samples were declined significantly from week 0 to week 1 despite they dropped slightly from week 1 to week 3. As a consequence, sodium metabisulphite was the preservative that was the best one to preserve cucumber fermentation and prolong longer shelf life in storage conditions in 4°C.

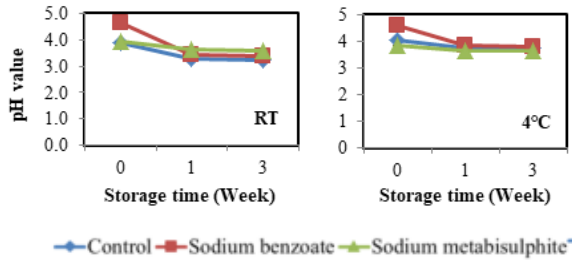

Fig 2. pH value store in room temperature and 4°C

3.3. Food preservative influence on salt concentration

The salt concentration value in brine solution by addition of food preservative and store in room temperature and refrigerator at 4°C show in Figure 3. Depending on this figure, it was noted that salt concentration was declined dramatically from week 0 to week 3 both in room temperature and 4°C storage condition. It is agreed with this study that salt extracts liquid from the vegetable which serves as a substrate for the growth of lactic acid bacteria [4]. In addition, control was the lowest amount of salt concentration each week for 4°C but RT was only in week1 and week 3. However, sodium benzoate was the highest quantity in week 1 and week 3 both in RT and 4°C too. Especially, sodium metabisulphite was the food preservative that contained a large quantity of salt concentration 1.44% and 1.41% in week 1 and week 3 respectively in RT and 1.37%, 1.31% in week1, and week 3 in 4°C.

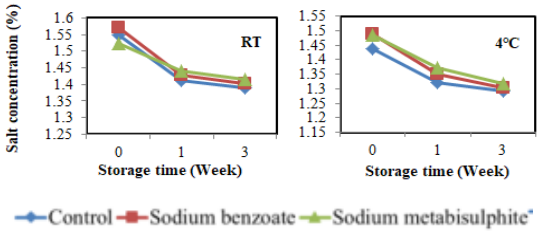

Fig 3. Salt concentration store in room temperature and 4°C

3.4. Food preservative influence on total soluble solid

The total soluble solid value of brine solution in room temperature condition was proved in Figure 4. It noticed sodium metabisulphite and control had the same total soluble solid value in week 0 in value 1.7 degrees Brix and sodium benzoate was the biggest value in week 0 2 degrees Brix. As well as to this, sodium benzoate and sodium metabisulphite were in the same value from week 1 to week 3 in 3 degrees Brix while control was also stable in 2-degree Brix from week 1 to week 3. In assumption, sodium benzoate and sodium metabisulphite were considered as adding into cucumber fermentation to prolong shelf life at room temperature. However, for condition 4°C, it was pointed out that sodium benzoate and sodium metabisulphite were in the same value each week, and they were rose quickly from week 0 to week 1 but they were remained stabled from week 1 to week 3.

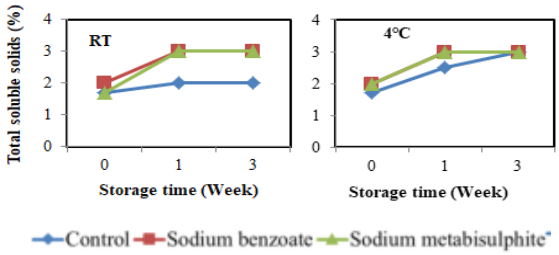

Fig 4. Total soluble solid store in room temperature and 4°C

3.5. Food preservative influence on moisture content

Figure 5 was observed about the moisture content value of brine solution in cucumber in room temperature and 4°C storage condition. In obviously, sodium metabisulphite was the lowest amount of moisture content from week 1 to week 3 both in RT and 4°C conditions in respectively 95.03% to 97.04% and 94.78 to 95.23%. Besides, control had the largest amount around 99.78% and came after by sodium benzoate in week 3 for RT condition in respectively. Apart from this, sodium benzoate was the highest amount in wee1 and week 3 by approximately 95.08% and 97.05%.

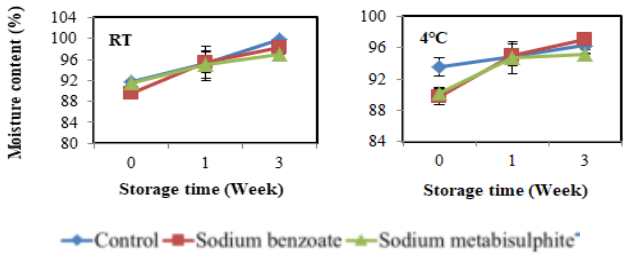

Fig 5. Moisture content store in room temperature and 4°C

3.6. Result of yeast and mold count

Figure 6 shown yeast mold count of brine solution with the addition of 2 different preservatives. It displayed that sodium benzoate and sodium metabisulphite were declined considerably from week 0 to week3 both in RT and 4℃. On the other hand, control increased massively from week 0 to week 3 not only in RT but also at 4℃. Control was the highest amount of yeast mold count both in RT and 4℃ from week 1 to week 3 in respectively 4.39 log CFU/ml to 4.67 log CFU/ml and for 4℃, they were 4.18 log CFU/ml to 4.52 log CFU/ml. In contrast, sodium metabisulphite was the lowest quantity of yeast mold count from week 0 to week 3 in respectively 2.54 log CFU/ml, 1.69 log CFU/ml, and 1.39 log CFU/ml for 4℃. Along with this, they were 2.81log CFU/ml, 2.35log CFU/ml, and 2.35 log CFU/ml in respectively in each week in RT condition.

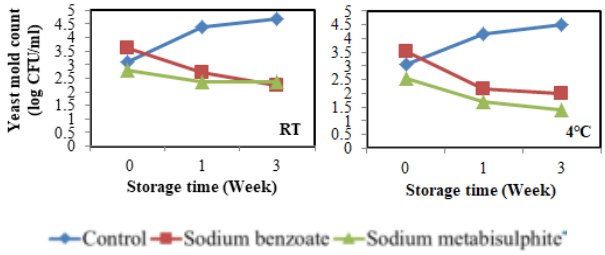

Fig 6. Yeast mold count

3.7. Result of sensory evaluation

Figure 7 was represented of sensory evaluation in 10 different isolated lactic acid bacteria of cucumber fermentation on the second day. According to running one way ANOVA, all attributes were significantly different with p-value ($p \leq 0.05$) in these 10 LAB except the color. Following running one-way ANOVA, it was assumed that pure isolated lactic acid bacteria S1, S2, and S3 were picked up to confirm fermentation again by adding sugar 4%.

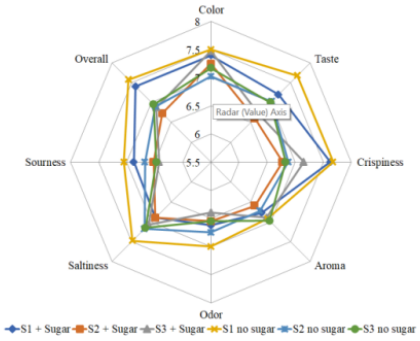

Fig 7. Sensory of cucumber fermentation in second day

IV. Conclusion

According to the result, LAB S1, S2, and S3 were chosen for studying the shelf life. To prolong the shelf life of cucumber fermentation, sodium benzoate and sodium metabisulphite 0.1% were added into the brine solution compare to the control sample. Following this experiment, it was found that sodium metabisulphite is the food preservative that can prolong longer shelf life than sodium benzoate depending on data of physicochemical parameters including total acidity 0.22%, pH 4.14 and reducing sugar value 0.85% and the number of microorganisms count.

References

[1] Chrun, R., Hosotani, Y., Kawasaki, S., Inatsu, Y., 2017. Microbioligical hazard contamination in fermented vegetables sold in local markets in Cambodia. *Biocontrol Science*. 22, 181–185.

[2] Defrise, M., Grangeat, P., 2010. Analytical methods. *Tomography*. 79 , 21–62.

[3] Egbe, J., Lennox, J., Rao, P., Anitha, Umoafia, G., 2017. Lactic acid bacteria profile of fermenting cucumber in 7% brine solution. *Journal of Advances in Microbiology*. 3, 1–8.

[4] Khanna, S., 2019. Effects of salt soncentration on the physicochemical properties and microbial safety of spontaneously fermented cabbage. *Food Science and Human Nutrition*. 48 , 67–74.

[5] Nations, U., 2001. Food and agriculture organization of the United nations. *Vegetable product*. 26, 98–104.

[6] Niro, G.E.A., 2006. A 19 a - Titratable acidity. Interlaboratory testing of methods for assay. 39 , 1–2.

[7] Pe, I.M., Ferna, A.G., Gallego, J.B., Yoon, S.S., Johanningsmeier, S.D., 2013. *Fermented and acidified vegetables*. 29, 59–65.

[8] Zhai, Y., 2017. Fermentation cover brine reformulation for cucumber processing with low salt to reduce bloater defect. *Cucumber Fermentation*. 55, 78-81.

The 13th AUN/SEED-Net Regional Conference on Chemical Engineering 2020 (RCChE-2020)
Jointly held with
The 5th International Symposium on Conservation and Management of Tropical Lakes
"Insights and Challenges toward Achieving SDGs"

Development of Fermented Young Melon using Isolated Lactic Acid Bacteria

Tetoutdam KONG[1], Sreyleang HEAN[1] and Reasmey TAN[1,2*]

[1] *Faculty of Chemical and Food Engineering, Institute of Technology of Cambodia, Russian Federation Blvd., P.O. Box 86, 12156 Phnom Penh, Cambodia*
[2] *Food Technology and Nutrition Research Unit, Research and Innovation Center, Institute of Technology of Cambodia, Russian Federation Blvd., P.O. Box 86, 12156 Phnom Penh, Cambodia*
* *Corresponding author: rtan@itc.edu.kh*

Abstract

The young melon is a popular crop for Cambodian people. Some of them eat it as a vegetable while others as a pickle. Inoculation with a pure culture with lactic acid bacteria (LAB) is known a large-scale method for vegetable fermentation. Therefore, the purpose of this study was to produce high quality and delicious young melon fermented using pure varieties of different acidic bacteria. Initially, lactic acid bacteria were isolated from four samples of young melon sold on different markets in Phnom Penh. The isolated LAB were applied for young melon fermentation for 2 days. The analysis physicochemical parameters, sensory tests for 2 times and microbials were also conducted. Sodium benzoate and sodium metabisulfite were used as preservatives in the products and their effects were investigated for 2 weeks. Based on the results obtained, fresh young melon used in this study had a pH of 6.30, a moisture content of 93.74%, a total acidity of 0.25%, reducing sugar of 1.97% and an ash content of 0.53%. Moreover, four strains of LAB were found; S1, S2, S3 and S4. After the first sensory test, fermented young melon products with S2, S3 and S4 were selected to be tested again to select the best one that give good quality in term of crunchiness and flavor. Consequently, S4 which was isolated from a sample of 7 Makara market; was considered as the best LAB since the fermented young melon with this LAB got the highest score of flavor and crunchiness attributes. For long-term preservation of fermented young melon, both sodium benzoate and sodium metabisulfite could prevent the microbial growth but sodium benzoate is more beneficial than sodium metabisulfite.

Keywords: *Young melon, Fermentation, Lactic acid bacteria*

I. Introduction

Young melon is a kind of hybrid melon that belongs to the family of Cucurbitaceae and in scientific name called *Cucumis melo Linnaeus*. These young fruits are occasionally harvested and eaten as a vegetable either raw or cooked and they are available year-round. Young melon is a kind of vegetables in Cambodia. The fermentation of vegetables is an important method for vegetable preservation, especially for rural communities, as it gives products with organoleptic traits that can add variety to the diet and is a means of extending the availability of vegetables beyond their season [1]. The traditional process usually gives lower organoleptic quality and the fermented vegetables cannot be stored for a long period. To guarantee the consistent quality of fermentation of vegetables for large-scale production, inoculation with a pure culture of lactic acid bacteria (LAB) should be done. LAB are defined as beneficial bacteria of which the main metabolites from carbohydrate metabolism is lactic acid. For the food application, LAB is used in the

industry of fermented vegetables where they contribute to the preservation of organoleptic quality. Therefore, the aim of this study is to make fermented young melon products with different tastes using isolated LAB. Moreover, the quality of the products would be also investigated.

II. Materials and Methods

2.1. Materials

The ingredients for fermentation were fresh young melon, salt without iodine and sugar bought from the local markets. Young melons selected were fresh with lower than 27mm diameter and no injuries; and prepared at ambient temperature in the laboratory before fermentation. Furthermore, 4 commercially fermented young melon were also purchased for LAB isolation. Sodium benzoate and sodium metabisulfite were used as preservatives. There was still other modern equipment which was further described.

2.2. LAB isolation

The samples were first serially diluted with brine 5% from 10^{-1} to 10^{-7}; and then spread on MRS agar and incubated at 37°C for 24 h. The colonies (LAB) were chosen to isolate on MRS agar and incubate at 37°C for 24h, then picked up, and stood overnight in 1ml of broth. Next, 700 ml of sterilized glycerol was mixed up with broth; and the mixture was stored in the fridge of -81°C. Finally, LAB were harvested.

2.3. Fermentation process of young melon

Young melon was first washed with tap water at least three times. The bloom in the bottom of the melon should be removed. Young melon was then cut in half and first blanched at a temperature at 75 °C for 5 minutes. Then, it was fermented in brine 4% with ratio 1:1 including with adding 4% of sugar. Obviously 10% of each isolated LAB was added to the mixture with different containers. The fermentation process was done for 2 days. Finally, 0.1% of both preservatives were added exclusively and the final products were stored with two temperature condition; at room temperature and 4°C for 2 weeks for further analysis.

2.4. Sampling

Brine solution, fresh and processed young melon would be used to conduct some experiment such as physicochemical and microbial analysis and sensory evaluation.

III. Results and Discussion

3.1. Physicochemical characteristics of young melon

The physicochemical characteristics of young melon is shown in **Table 3.1**.

Table 3.1. Physicochemical characteristics of young melon

Parameters	Value
pH	6.30 ± 0.02
Moisture content (%)	93.74 ± 0.74
Total acidity (%)	0.25 ± 0.52
Reducing sugar (%)	1.97 ± 0.10
Ash (%)	0.53 ± 0.18

3.2. LAB isolated from fermented young melon

Four different strains were isolated from commercially fermented young melon; S1, S2, S3 and S4. S1 and S2 were from Orussey market and S3 and S4 were from 7 makara market; Phnom Penh; Cambodia.

3.3. Physicochemical characteristics while fermentation

3.3.1. Changes of pH

According to **Figure 3.3.1 (a)**. The initial pH in the brine solution was 6.29 and then the pH dropped significantly to less than 4 and approximately 3.5 at day 1 and day 2; respectively.

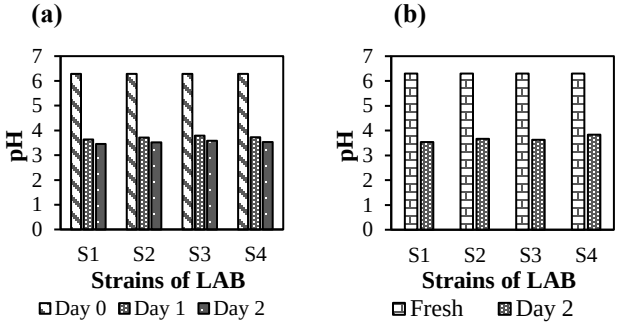

Figure 3.3.1. Changes of pH in (a) brine solution and (b) fermented young melon

Based on **Figure 3.3.1 (b),** the initial pH of fresh young melon was 6.30 but it ranged from 3.54 to 3.83 at day 2. When LAB was inoculated at the beginning of fermentation, it caused a decrease in pH in short period due to the production of lactic acid from fermentable sugar.

3.3.2. Changes of salt concentration

Depending on **Figure 3.3.2 (a)**, the salt concentration was 4% at day 0 while those ranged between 1.11 to 1.70% at day 1.

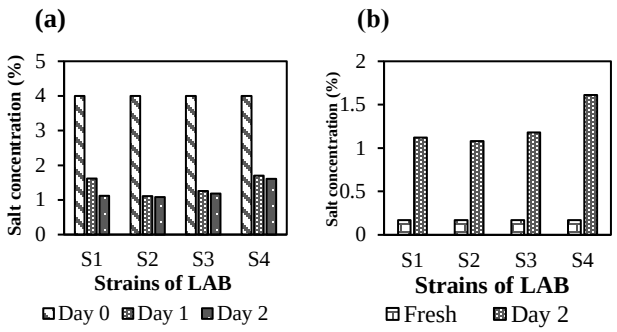

Figure 3.3.2. Changes of salt concentration in (a) brine solution (b) fermented young melon

During fermentation, some amount of salt in the brine solution absorbed into young melon through osmosis. And then the salt was slightly decreased in day 2. The higher NaCl concentration in salt solution resulted a rapid salt penetration into young melon while the rate of changes in pH and the total acidity were reduced [2]. According to the result in **Figure 3.3.2 (b)**, different types of LAB had influence on the final concentration of fermented young melon. The lowest salt concentration was found in S2 while the highest one was found in S4 at day 2.

3.3.3. Changes of total soluble solids

The changes of total soluble solids in fermented young melon during fermentation are shown in **Figure 3.3.3**. Therefore, fresh young melon had a sugar content of 3 ºBrix, and then at day 2 fermentation, it fell to 2.4-2.7 ºBrix. According to metabolism of lactic acid bacteria [3], they convert sugar to lactic acid.

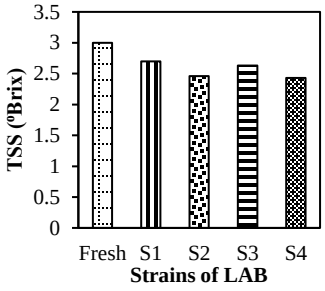

Figure 3.3.3. Changes of TSS in fermented young melon at day 2

So, that means the losses of sugar content in fresh young melon are because sugar is converted to lactic acid. So, S2 and S4 are the resented the high amount of LAB.

3.4. Sensory evaluation

According to **Figure 3.4.1**. All the strains of LAB had a similar result of color and sourness. S4 was the most popular one according to panelists due to its highest score of 6.17 for flavor. Regarding the firmness, S2 got the highest score of 6.05. For saltiness attribute, S4 had the highest score of 4.35 while S2 got the highest score; 5.64 of sourness. In this case, the gap of sourness between these four strains of LAB were not much different, so the results would get variable from the sensory evaluation. Therefore, to reduce this kind of problem, there was a preference from the panelists who likely to eat pickle or fermented products and the best score of acceptance of sourness was found around 4.5 to 5.

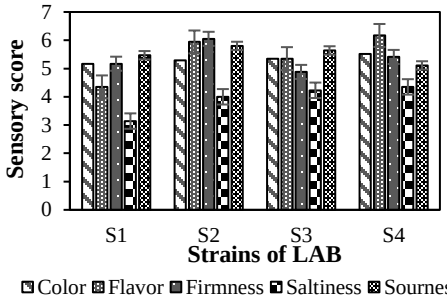

Figure 3.4.1. Sensory evaluation of fermented young melon

The 3 selected LAB after the first sensory test, gave similar results to all parameters except crunchiness and overall acceptance (**Figure 3.4.2**). The crunchiness score ranged from 6.48, 7.15 and 7.18 for S3, S2 and S4; respectively. For overall acceptance, S4 got highest score of 7.33 and was followed by S2 and S3. The flavor and crunchiness could make a big difference for the 33 panelists.

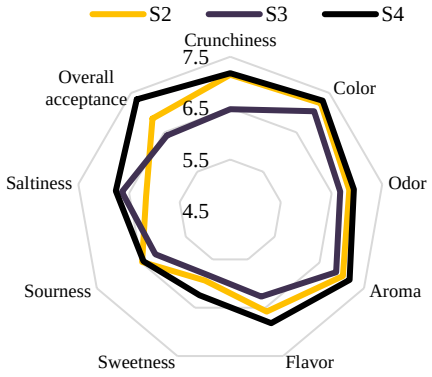

Figure 3.4.2. Sensory evaluation of 3 selected fermented young melon

3.5. Effect of preservatives on fermented young melon during storage

Adding preservatives was done for the best fermented young melon chosen, the fermented young melon with S4 of lactic acid bacteria after the sensory tests.

3.5.1. Physicochemical characteristics

Based on **Table 3.5.1**, the pH decreased slightly for all

conditions at day 7 and day 14.

Table 3.5.1. Physicochemical characteristics of fermented young melon using food preservatives

Sample	Day	pH	Salt (%)
Control	0	3.36	1.43
	7	3.24	1.50
	14	3.15	1.49
With S. Meta	0	3.63	1.47
	7	3.37	1.54
	14	3.15	1.52
With S. Ben	0	3.78	1.41
	7	3.19	1.50
	14	2.62	1.50

In this case, it could be because of replacement of brine solution. In the low salt concentration, the growth of lactic acid bacteria occurred [4]. Thus, a change of brine including with using low salt concentration enhanced lactic acid bacteria growth. So, that was why the pH decreased.

The salt concentrations were approximately 1.45% at day 0 for all samples. But at day 7, they increased slightly to about 1.50%. At day 14, the salt concentration of the sample with sodium metabisulfite was nearly stable but it decreased a little for that with sodium benzoate. This might due to the osmosis process during storage. It may be that added brine was not equivalent with the salt content in the fermented young melon.

3.5.2. Total plate count

At day 0, it was detected in all samples based on **Figure 3.5.2 (a)** and **(b)**. But there was no total plate count for samples with preservatives at day 7 and day 14 at both temperatures.

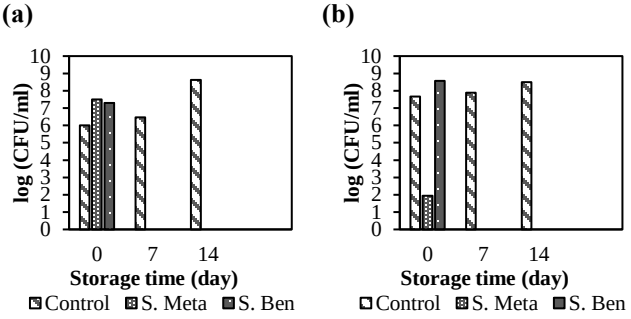

Figure 3.5.2. Effect of preservatives on total plate count at (a) room temperature and (b) 4℃

3.5.3. Yeast and mold

Based on **Figure 3.5.3 (a),** they were both detected in all samples at room temperature. However, yeasts and molds were not detected in all samples at 4℃ based on **Figure 3.5.3 (b)**. Then, none of them was present at day 7 and day 14 at both temperature conditions for the preservative-containing samples. For the control samples investigated at both temperature conditions, it was observed that yeasts and molds grew normally at day 7 and day 14.

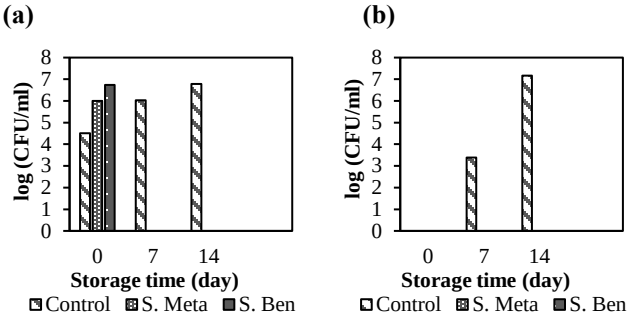

Figure 3.5.3. Effect of preservatives on yeasts and molds at (a) room temperature and (b) 4℃

IV. Conclusion

The fermented young melon using S4 isolated from a commercially fermented young melon sold at 7 makara market was considered as the best one due to its highest score of flavor and crunchiness after the sensory tests. Sodium benzoate and sodium metabisulfite both could prevent microbial growth during storage time and preserve the products for a long time, but sodium benzoate had a more beneficial health effect than sodium metabisulfite. However, the shelf-life study should be done by doing more research about its characteristics and methodology in the future.

References

[1] Yamani, M.I., Hammouh, F., 1999. Production of fermented cucumbers and turnips with reduced levels of sodium chloride.

[2] K. Jong-Goon; Hee-Sook, Choi; Sang-Song, Kim; Woo-Jung, K., 1989. Changes in Physicochemical and Sensory Qualities of Korean Pickled Cucumbers during Fermentation.pdf., 838–844.

[3] Liu, S., 2003. Practical implications of lactate and pyruvate metabolism by lactic acid bacteria in food and beverage fermentations. 83, 115–131.

[4] Mcmurtrie, E.K., Johanningsmeier, S.D., Jr, F.B., Price, R.E., 2019. Effect of Brine Acidification on Fermentation Microbiota, Chemistry, and Texture Quality of Cucumbers Fermented in Calcium or Sodium Chloride Brines.

The 13th AUN/SEED-Net Regional Conference on Chemical Engineering 2020 (RCChE-2020)
Jointly held with
The 5th International Symposium on Conservation and Management of Tropical Lakes
"Insights and Challenges toward Achieving SDGs"

Determination of Antibiotic Resistance of *Enterococcus* spp. Isolated from Drinking Water Collected from Stoung District

Chanchakriya SAM [1], Sovannmony NGET [1, 2], Soukim HENG [1,2], Sokneang IN [1, 2], Msateru NISHIYAMA [3], Toru WATANABE [3] and Hasika MITH [1, 2,*]

[1] *Faculty of Chemical and Food Engineering, Institute of Technology of Cambodia, Russian Federation Blvd., P.O. Box 86, 12156 Phnom Penh, Cambodia*
[2] *Food Technology and Nutrition Research Unit, Research and Innovation Center, Institute of Technology of Cambodia, Russian Federation Blvd., P.O. Box 86, 12156 Phnom Penh, Cambodia*
[3] *Faculty of Agriculture, Yamagata University, Japan, 1-23 Wakaba-machi, Tsuruoka, Yamagata 997-8555, Japan*

* *hasika@itc.edu.kh*

Abstract

The rapid evolution of antibiotic resistant bacteria is occurring worldwide, threatening the efficacy of antibiotics. Antibiotic resistance becomes the main problem for public health in developing countries including Cambodia that suffers from poverty and poor access to safe water in rural areas, especially at the areas around the Tonle Sap Lake. Therefore, the purpose of the current study was to detect the presence of *Enterococcus* spp. in drinking water collected from Stoung District in Kampong Thom province, and to determine their antibiotic susceptibility. The samples of drinking water were collected from three communes, Trea (land based), Msa Krang (water-land based) and Peam Bang (water based) in Stoung District. The detection and isolation of *Enterococcus* spp. were carried out, followed by antibiotic susceptibility test. Out of 145 samples, 83 samples were found contaminated with *Enterococcus* spp. The results showed that, among the 257 isolated strains of *Enterococcus* spp., 23% were resistant to tetracycline (TC), 20% to erythromycin (EM), 11% to vancomycin (VCM), 7.39% to doxycycline (DOX), 4.3% to ciprofloxacin (CIP), 2.7% to levofloxacin (LVX), and 1.2% ampicillin (AMP). In addition, 38% of isolated strains were resistant to at least one antibiotic agent as resulting in high-risk contamination of *Enterococcus* spp. from different water samples. The results also revealed that 11 isolated strains of enterococci were multidrug-resistant. Remarkably, two strains of enterococci isolated from Msa Krang commune showed high multiple antibiotic resistance to LVX-AMP-DOX-CIP-VA-TC-EM corresponding to five antibiotic categories. Nevertheless, the presence of antibiotic resistant enterococci in drinking water at Kampong Thom province could potentially be a serious harm for public health, particularly the communities in those area.

Keywords: *drinking water, Enterococcus spp., antibiotic resistance*

I. Introduction

The quality of drinking water is the main crucial factor that could cause infection and diseases [1]. The microbiological quality in drinking water was interested by worldwide because of implied public health impacts [2]. Contaminated water and inadequate sanitation are involved in the pathogenesis transmission, such as cholera, dysentery, hepatitis A, typhoid and polio. Water and sanitation facilities that are deficient, insufficient, or poorly handled expose individuals to preventable health danger [3]. The bacteria

can be the reasons of infection in human being when it enters blood, urine, or wound [4]. Antimicrobial resistance is a measure of an antimicrobial agent's decreased ability to kill or inhibit the growth of a microorganism. This is determined practically by testing a bacterial isolate in an in vitro system against various antimicrobials. There are many pathogenic bacteria that might contaminate in drinking water. But the purpose of the current study was to focus on identification of antibiotic resistance of *Enterococcus spp.* potentially present in drinking water. There are several types of antibiotics used in study namely ampicillin, ciprofloxacin, levofloxacin, tetracycline, doxycycline, vancomycin and erythromycin.

II. Materials and Methods

2.1. Sampling sites

The current study was carried out at three communes, Trea (land-based), Msa Krang (water land-based), and Peam Bang (water-base area) located in Stoung district, in Kampong Thom province. The samples were collected in three different villages per commune (**Fig. 1)** and kept cooled and sent to laboratory for microbiological analysis. The water sample were analyzed within 24h to 48h as they keep in 1℃ to 4℃ in the dark [5].

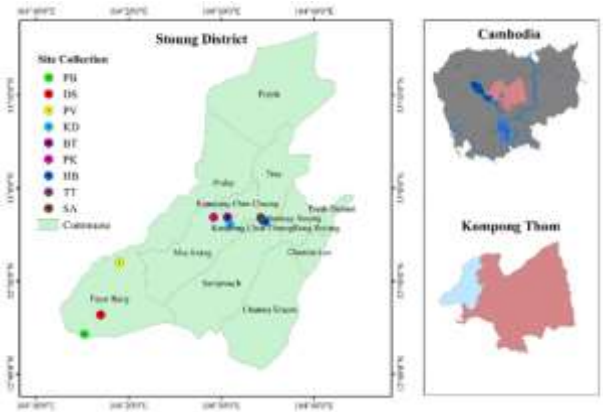

Fig. 1. Sampling sites areas in Kampong Thom

2.2. Detection and isolation of *Enterococcus* spp.

Enterococci were isolated using membrane filtration method, considered as "gold standard" for quality assessment in drinking water by culturing on mEnterococcus agar (Bacton, Le Pont de Claix, France). A volume of 100 mL of drinking water sample were filtered through a membrane filter (0.45 µm pore size, 47 mm diameter, sterile membrane filters without absorbent pads, Whatman), then incubated for 24 h – 48 h at 37 °C (Standard Methods 9230C). After incubation, the colonies were identified as enterococci with light and dark red colonies. The colonies assumed to be enterococci were picked and transferred into Enterococcosel broth and incubated for 24 h at 37 °C, the broth changed into black when the enterococci are present and then a loop of inoculated broth was streaked on Todd Hewitt agar (TH, Becton, Le Pont de Claix, France) and incubated for 24 h at 37 °C. Then enterococci stains were picked and transferred into TH broth with presence 15 percent of glycerol. Finally, all isolated strains of enterococci were stored at -80 °C.

2.3. Antibiotic susceptibility test

The antibiotic susceptibility testing of enterococci was conducted by using the disk diffusion method recommended by CLSI (2017). The enterococci strains were grown on Todd Hewitt agar to culture the bacteria for 16 h – 24 h from -80 °C. Then, the colonies were picked into 10 mL of saline water (0.85%) and compare with 0.5 MacFarland standard which contains the concentration of standardized 10^8 CFU/mL [6]. After that, a sterile cotton swap was dipped into bacteria suspension and transfer into Mueller Hinton agar (MH, Himedia, Mumbai, India) by streaking the over the surface of MH agar. The streaking method of bacteria suspension three times at a different angle of 60˚ on MHA and then, let the plate dry 3 - 5 minutes. The concentration of antibiotics contains in disks were chosen according to recommend from CLSI (2017). The diameter of each zone was measured in millimeter by using digital Caliper and the interpretation of measurement results as sensitive, intermediate resistance and resistance was made by CLSI (2017) that demonstrated in **Table 1.**

Table 1. CLSI diameter of inhibition zone

Antibiotics	Diameter of inhibition zone (mm)		
	Susceptible (S)	Intermediate (I)	Resistance (R)
Ampicillin	≥17	-	≤16
Ciprofloxacin	≥21	16-20	≤15
Doxycycline	≥16	13-15	≤12
Erythromycin	≥23	14-22	≤13
Levofloxacin	≥17	14-16	≤13
Tetracycline	≥19	15-18	≤14
Vancomycin	≥17	15-16	≤14

III. Results and Discussion

3.1. Detection and isolation of *Enterococcus* spp.

The presence of *Enterococcus* spp. was observed from different commune Trea, Msa Krang, and Peam Bang. In comparison, drinking water sample in Msa krang and Trea are mostly contaminated compare to Peam bang commune. The concentration of *Enterococcus* spp. in Msa Krang have a wide range of 1 to 867 CFU/100mL while Peam Bang have concentration range of 0.5 to 776 CFU/100mL. In the previous study of [7], the concentration of enterococci increase range from 32 to 82× 10^4 CFU/100mL. The most contaminated site was from water-land based and most of the sample detected were filtered water sample. Therefore, the contamination of enterococci might be because people in those area are lack of knowledge of changing filter regularly

3.2. Detection and isolation of *Enterococcus* spp.

Out of the 145 samples tested, which were collected from three different communes in Stoung district in Kampong Thom province, 83 samples 57% were found to be contaminated with enterococci in drinking water sample. In these 83 samples 57%, 40% (n=33) were collected from Msa Krang commune which is the water-land based communities, 36% (n=30) were from land base area in Trea commune, and 24% (n=20) were collected from Peam Bang commune; water based or floating communities. In this study, 257 strains of *Enterococcus* spp. were isolated from 83 samples with seven different types of samples such as rain water, bottle water (20L), filter, boiling water, water supply, well water, and lake water as shown in **Fig.2**.

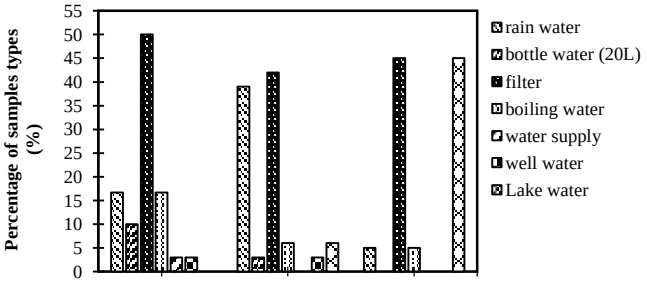

Fig. 2. Percentage of samples types collected from St oung district.

3.3. Antibiotic resistance of *Enterococcus* spp. in drinking water

The isolated *Enterococcus* spp. from drinking water samples in Stoung district were conducted antibiotic susceptibility test with seven antibiotics agent in five antibiotic classes. Those antibiotic classes are β-lactam, fluoroquinolone, tetracycline, macrolides, and vancomycin. 257 isolated colonies from 83 samples were conducted disk diffusion test. As the **Fig. 3** show the variation of sensitivity degree to the test antibiotic in Stoung district. Most strains are sensitive to ampicillin 96% (n=247), doxycycline 77%, ciprofloxacin 77%, tetracycline 73%, levofloxacin 71%, vancomyci 33% and erythromycin 13% (n=34). There are still have some strains are resistant to those antibiotics mostly resistant to tetracycline 24% (n=62) and erythromycin 19.84% (n=51).

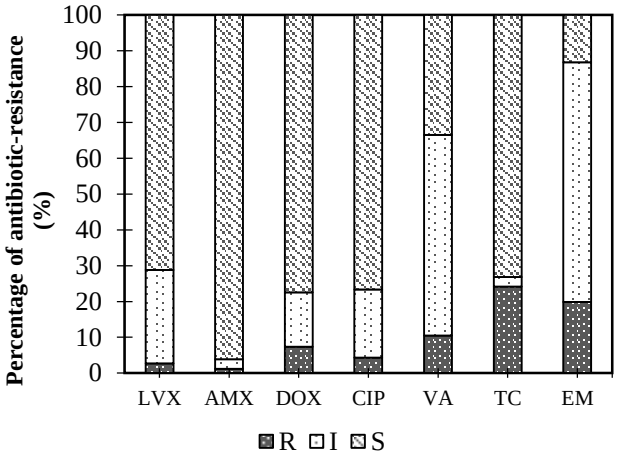

Fig. 3. Percentages of antibiotic-resistance *Enterococcus* spp. in Stoung District

Enterococci, which are found in many aquatic compartments, have an advantage in terms of persistence and multiplication because of their tolerance to various environmental factors, such as alkaline pH, increased temperature, and sodium chloride concentration. Because long-term survival is possible in the aquatic environment, antibiotic resistant enterococci present a higher risk of spreading antibiotic resistance genes than other bacteria [8]. According to [6], more than 45% of the enterococci studied were resistant to ciprofloxacin, erythromycin and tetracycline, antibiotics are often used by humans and in animals as therapeutic agents

3.4 Multi-antibiotic resistance of *Enterococcus* spp.

In antibiotic susceptibility test, 51% of colonies is susceptible and intermediate resistant to the antimicrobial agent. Whereas, 38% were resistance to the at least one antimicrobial agent, while 11% (n=11) were multidrug-

resistant strains. Only two strains (2.0%) were resistance to all type of antibiotic resistance LVX-AMP-DOX-CIP-VA-TC-EM in different five antimicrobial categories as demonstrated in **Fig 4**.

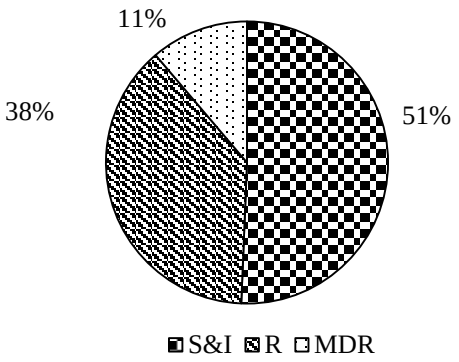

Fig. 4. Percentage of antibiotic resistant of *Enterococcus* spp. in drinking water indicated as S&I: susceptible and intermediate resistant, R: resistant, MDR: multidrug-resistance.

Poor hygiene and infection control, lack of sanitation, weak or unenforced medicines regulation, and sub-standard quality drugs have been suggested as some of the main drivers of AMR in SE Asia [9]. In Cambodia, the behavior of people using antibiotics in rural areas including trained and untrained pharmacists, drugstores and nurses are provided drugs to patients without go through any diagnose. Moreover, the villagers in the communities mostly purchasing antibiotic by self-prescription.

IV. Conclusion

In conclusion, more than 50 percent of drinking water, mostly filtered water, were contaminated with pathogenic enterococci and could be a health risk for the communities living in those area. in order to reduce the multiple antibiotic resistance, the authorities should educate people to strengthen the hygienic practice including cleaning and boiling water consumption, especially cleaning regularly the water containers with clean water to reduce recontamination and filter change. Moreover, proper use of antibiotics should be considered based on doctor's prescription. Moreover, wastewater from health care should be treated to ensure absence of pathogenic bacteria before discharge to environment since microorganisms will continue to adapt to environment by developing resistance to new drugs and to cause serious infection.

Acknowledgement

We are thankful to the Science and Technology Research Partnership for Sustainable Development (SATREPS), the Japan Science and Technology Agency (JST)/Japan International Cooperation Agency (JICA) for their financial support.

References

[1] Emad Abada, Zarraq Al-Fifi, Abdul Jabbar Al-Rajab, M.M. and M.S., 2019. Molecular identi fi cation of biological contaminants in different drinking water resources of the Jazan region , Saudi Arabia. , 622–632.

[2] Abdelrahman, A.A., 2011. Bacteriological quality of drinking water in Nyala , South Darfur , Sudan. , 37–43.

[3] WHO., 2019. Drinking-water. *World Health Organization*., 1.

[4] CLSI., 2012. Methods for Dilution Antimicrobial Susceptibility Tests for Bacteria That Grow Aerobically.

[5] Water, department of., 2009. Surface water sampling methods and analysis — technical appendices Standard operating procedures for water sampling-.

[6] Macedo, A.S., Freitas, A.R., Abreu, C., Machado, E., Peixe, L., Sousa, J.C., Novais, C., 2011. International Journal of Food Microbiology Characterization of antibiotic resistant enterococci isolated from untreated waters for human consumption in Portugal. *International Journal of Food Microbiology*. 145, 315–319.

[7] Lata, P., Ram, S., Agrawal, M., Shanker, R., 2009. Enterococci in river Ganga surface waters : Propensity of species distribution , dissemination of antimicrobial-resistance and virulence-markers among species along landscape. 10, 1–10.

[8] Nishiyama, M., A.I.& Y.S., 2015. Journal of Environmental Science and Health , Part A : Toxic / Hazardous Substances and Environmental Identification of Enterococcus faecium and Enterococcus faecalis as vanC-type Vancomycin-Resistant Enterococci (VRE) from sewage and river water in th. , 37–41.

[9] Reed, T.A.N., Krang, S., Miliya, T., *et al.*, 2019. International Journal of Infectious Diseases Antimicrobial resistance in Cambodia : a review. 85, 98–107.

The 13th AUN/SEED-Net Regional Conference on Chemical Engineering 2020 (RCChE-2020)
Jointly held with
The 5th International Symposium on Conservation and Management of Tropical Lakes
"Insights and Challenges toward Achieving SDGs"

Investigation on Antibiotic Resistance of *Escherichia coli* Isolated from Drinking Water Collected in Stoung District

Boren BUN [1], Sovannmony NGET [1, 2], Soukim HENG [1,2], Sokneang IN [1, 2], Nishiyama MASETERU [3], Toru WATANABE [3] and Hasika MITH [1, 2,*]

[1] *Faculty of Chemical and Food Engineering, Institute of Technology of Cambodia, Russian Federation Blvd., P.O. Box 86, 12156 Phnom Penh, Cambodia*
[2] *Food Technology and Nutrition Research Unit, Research and Innovation Center, Institute of Technology of Cambodia, Russian Federation Blvd., P.O. Box 86, 12156 Phnom Penh, Cambodia*
3 Faculty of Agriculture, Yamagata University, Japan
** Corresponding author: hasika@itc.edu.kh*

Abstract

Escherichia coli has been known as key indicator of fecal contamination for drinking water. Even most of *E. coli* were not pathogenic but some of them could be a threat in causing serious illness and outbreaks in many countries. Misuse of antibiotics is currently becoming a major concern in relation to increase of antibiotic resistance of *E. coli* and prolongation of hospitalization. Therefore, the current study was carried out to determine antibiotic resistance of *E. coli* isolated from drinking water collected from three communes, Trea, Msa Krang and Peambang, in Stoung District, Kampong Thom province. The drinking water samples were subjected for detection and isolation of *E. coli*, followed by antibiotic susceptibility test with seven antibiotics. Among the 145 collected samples, there were 48 samples from Trea, 50 samples from Msa Krang and 47 samples from Peambang. The results showed that the presence of *E. coli* was detected in 54 out of 145 samples with 94 isolated strains. In terms of antibiotic susceptibility, *E. coli* were found to be resistant to the tested antibiotics as following: 67% to ampicillin, 52.31% to ticarcillin, 49.98% to tetracycline, 13.45% to ciprofloxacin, 10.46% to fosfomycin, 3.19% to gentamicin, and 1.06% to ceftazidime. In addition, 44.68% were identified as multi-drug resistant (MDR) with MAR index value > 0.2 and remarkably 2.12% were resistant to six antibiotics corresponding to six classes of antibiotics. These findings could be an indicator showing a concern in terms of health risk for the communities living in those areas.

Keywords: *antibiotic resistance, Escherichia coli, drinking water*

I. Introduction

For infectious diseases, antibiotics are the main therapeutic strategy for bacterial infection [1]. In Cambodia, with general frost, diarrhea and even general unwellness, antibiotics are found to be used [2]. *Escherichia coli* is an opportunistic pathogenic bacterium found in water [3], and more than five million people suffer from diseases associated with contaminated drinking water, unclean domestic conditions, and inappropriate disposal of excreta [4]. More fundamentally, resistance to antibiotics is associated with overuse and abuse of antibiotics. As well as the lack of production of new medicines from the pharmaceutical industries [5]. It is impossible to quantify the

real value of bacterial resistance to antibiotics since bacterial antibiotic resistance is the natural process that happens after the bacteria are exposed to it [6]. Consequently, there is uncertainty about post-antibiotics about the issue of antibiotics in the future and the broader effect on the health system in emerging and developed countries, and even basic infections would be unmanageable and potentially fatal [7].

II. Materials and Methods

2.1. Sampling sites

145 samples were taken from three communes in Stoung District, Kampong Thom Province, Cambodia (Figure 3.1). Trea (land-based) 48 samples, Msa Krang (water-land-based) 50 samples, and Peambang (water-based) 47 samples were such communities. Sterilized bottles of 500 ml of drinking water (rain water, purified water, bottled water, lake water, well water and water supply) per household were dispensed and then sent to the microbial laboratory of the Institute of Technology of Cambodia.

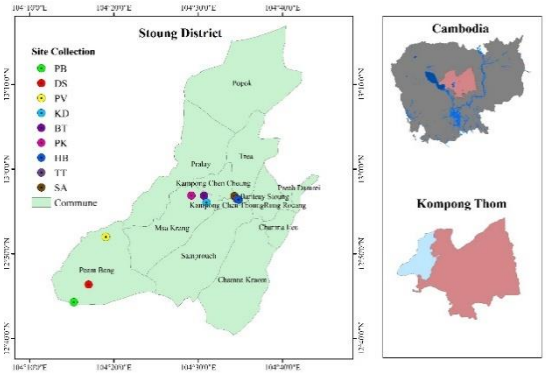

Fig. 1. Map of sampling locations

2.2. Detection and isolation of *Escherichia coli*

Using the membrane filtration for detection of *Escherichia coli* from the samples in 24 h after collection. The Chromocult coliform agar was used as the selective media, and incubation was at 37 ℃ for 18-24 h. The dark-blue or violet formed colonies were considered as *Escherichia coli* and would then be picked by loop to another Chromocult coliform agar plate for isolation. This process would be continued until all the colonies form on the plates are purple or only dark-blue colonies appeared. Then the colonies were ready for stock culture storage. Using the LB broth for the media to grow the isolated strains, prepared in the Eppendorf, picking the colonies strains to the Eppendorf and incubated at 37 ℃ for 24 h. After incubation, adding the glycerol to make the glycerol concentration is 15-20%, vortex then keeping in the -80 ℃ freezer.

2.3. Antibiotics susceptibility test

Susceptibility test was done by using the disc diffusion method and following the categories of Clinical laboratory standard institute (CLSI) for determining the susceptibility or resistance. Muller Hinton agar was used as the media for the test. Only the fresh culture can be used for susceptibility test, using the LB agar to subculture the colonies. Prepare the 0.5 McFarland concentration of colonies in 10 ml saline solution. Placing antibiotics discs with on the media surface, make sure they are well touched the media. The position of disk on the inoculated plate, the center-center distance is 24 mm and from edge to edge is 10 to 15 mm, then incubated in the optimum temperature of 37 ℃ for 16-18 h. In interpretation of result, measured the diameter of zone inhibition and report the result as Resistant (R), Intermediate (I) and Susceptible (S) by comparing the reference in CLSI, as shown in **Table 1**.

Table 1. Diameter of inhibition zone [8].

Antibiotics	Diameter of inhibition (mm)		
	Susceptible (S)	Intermediate (I)	Resistance (R)
AMP	≥17	14-16	≤13
CAZ	≥21	18-20	≤17
CIP	≥21	16-20	≤15
GEN	≥15	13-14	≤12
FOS	≥16	13-15	≤12
TE	≥15	12-14	≤11
TIC	≥20	15-19	≤14

III. Results and Discussion

3.1. Detection of *Escherichia coli*

Among 145 samples in three communes, there are 54 samples were found positive *of Escherichia coli*, with 17 samples in Trea commune, 20 samples in Msa Krang commune and 17 samples from Peambang. The total of isolated strains from these three locations are 94 samples which then be tested for antibiotics susceptibility.

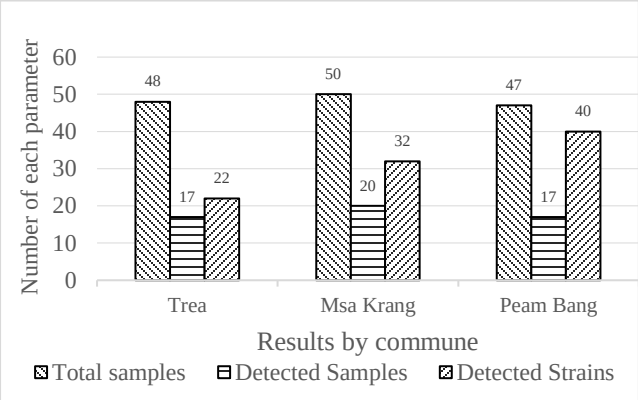

Fig.2. Results of detected samples.

3.2. Antibiotics resistance of *Escherichia coli*

3.2.1. Antibiotics susceptibility test in Trea

With 22 strains for conducting on study of antibiotic susceptibility of *E. coli*, 59.09% of isolated strains were resistant to TE, 54.55% were resistant to AMP, 50% to TIC, 9.09% to CIP and 4.55% to FOS. Predictably, AMP, TE [7] and TIC [9] resistance is common in E. coli. AMP and TE is used as common treatment among Cambodians [2]. There are up to over 200 βlactamase genes that responds for antibiotics resistance to that used to be detected [10], and also TE, it is used for growth promoter in animal husbandry [11], animal feed contains antibiotics, is to stimulate growth becomes a global practice [12], antibiotic is widely used in agriculture [10]. As it is available freely in the region [2], this might be the cause reason that make bacteria becomes resistant to drugs.

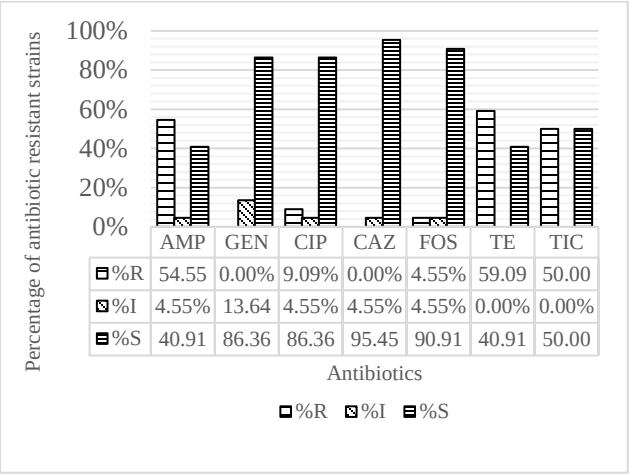

Fig. 3. Percentage of R, I, S in each antimicrobial agent in Trea commune.

3.2.2. Antibiotics susceptibility test in Msa Krang

There are 32 strains of *E. coli* were conducted with antibiotics susceptibility study. The resistance result of E. coli strains contributed to AMP with 37.5%, TE with 34.38% and TIC with 28.13%. While, only 12.5% are resistant to CIP and Following by GEN and CAZ with 6.25% of total strains. In Cambodia, the level of understanding about antibiotics is still low. They lack of education about drug consumption and the potential impacts [2]. Using drug freely, discharging to the environment without treatment, bacteria can evolve their gene to be resistant to antibiotics [11]. While, waste water treatment plant is currently not specifically tasked with the removal of antibiotics resistance gene yet [13]. With presence of antibiotics in the environment, it may create selective pressure which antibiotic resistance, in consequence [14].

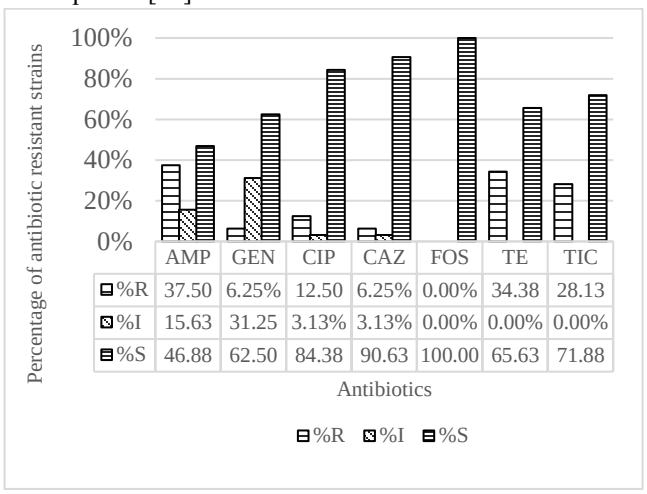

Fig.4. Percentage of R, I, S in each antimicrobial agent in Msa Krang commune.

3.2.3. Antibiotics susceptibility test in Peambang

AMP and TIC in the study of *E. coli* strains from Peambang commune, are the noteworthy ones which 80% and 70% among 40 strains are resistant to them, respectively. Moreover, TE is still in high level, with 55% of all strains are resistant to this drug. While, as shown in Figure 4.3, following by with 15%, CIP with 12.5% and GEN with just 5%. Related factors associated with location as aquatic environment, usage of antimicrobials in humans or terrestrial food animal, sewage contamination or run-off from agricultural areas with grazing animals to aquaculture operations [15] are the great cause for antibiotics resistant among microbiota. There is also a suggestion that fish consumption that contain resistant bacteria can contribute to resistant bacteria [16]. Also, in Peambang, people tend to have fish farming under or nearby their floating houses, the drinking water source and the fish farm is almost the same one. Some of them use the feed from the market. This may create another factor to bacterial resistance. The animal feed contains antibiotics as growth promoter and disease prevention [14], and will then push antibiotics resistance

among the microbiota as antibiotics exposure to bacteria [2], and antimicrobial resistance is accelerated when overexposure of bacteria to antibiotics [17].

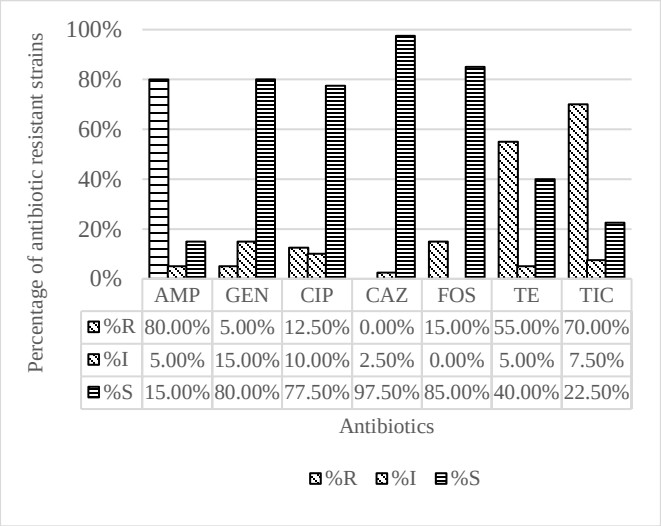

Fig. 5. Percentage of R, I, S in each antimicrobial agent in Peambang commune.

IV. Conclusion

In conclusion, among such sampling area, Trea, Msa Krang and Peambang, there is a high contamination of drinking water with *E. coli* with 94 strains of *E. coli* isolated from 54 out of 145 collected drinking water samples, E. coli is mostly contaminated in the rain water source as the container was exposed to the surrounded environment, lack of hygiene and there is no proper treatment. The antibiotic susceptibility study revealed that the isolated *E. coli* were found to be more resistant to AMP, TIC and TET as in order. There were 44.68% of total strains found to be MAR. Particularly, some strains (2.12%) could be resistant to six groups of antibiotics, such as AMP-GEN-CAZ-CIP-TIC-TE.

References

[1] Rayner, C., Munckhof, W.J., 2005. Antibiotics currently used in the treatment of infections caused by Staphylococcus aureus. *Internal medicine journal*. 35, 1–16.

[2] Om, Chhorvoin, Daily, F., Vlieghe, E., McLaughlin, J.C., McLaws, M.L., 2017. Pervasive antibiotic misuse in the Cambodian community: Antibiotic-seeking behaviour with unrestricted access. *Antimicrobial Resistance and Infection Control*. 6, 1–8.

[3] Gorchev, H.G., Ozolins, G., 2004. Guidelines for Drinking-water Quality, 3rd Edition. *Who*. 1, 564.

[4] Peter., 2002. Dirty Water: Estimated Deaths from Water-Related Diseases 2000-2020 Pacific. *Dirty Water: Estimated Deaths from Water-Related Diseases 2000-2020 Pacific*., 1–12.

[5] Mobarki, N., Almerabi, B., Hattan, A., 2019. Antibiotic Resistance Crisis. *International Journal of Medicine in Developing Countries*. 40, 561–564.

[6] Prestinaci, F., Pezzotti, P., Pantosti, A., 2015. Antimicrobial resistance: A global multifaceted phenomenon. *Pathogens and Global Health*. 109, 309–318.

[7] Li, X., Watanabe, N., Xiao, C., Harter, T., McCowan, B., Liu, Y., Atwill, E.R., 2014. Antibiotic-resistant E. Coli in surface water and groundwater in dairy operations in Northern California. *Environmental Monitoring and Assessment*. 186, 1253–1260.

[8] Dolinsky, A.L., 2017. M100 Performance Standards for Antimicrobial Susceptibility Testing.

[9] Li, X., Watanabe, N., Xiao, C., Harter, T., McCowan, B., Liu, Y., Atwill, E.R., 2014. Antibiotic-resistant E. Coli in surface water and groundwater in dairy operations in Northern California. *Environmental Monitoring and Assessment*. 186, 1253–1260.

[10] Alm, E.W., Zimbler, D., Callahan, E., Plomaritis, E., 2014. Patterns and persistence of antibiotic resistance in faecal indicator bacteria from freshwater recreational beaches. *Journal of Applied Microbiology*. 117, 273–285.

[11] Karami, N., Nowrouzian, F., Adlerberth, I., Wold, A.E., 2006. Tetracycline resistance in escherichia coli and persistence in the infantile colonic microbiota. *Antimicrobial Agents and Chemotherapy*. 50, 156–161.

[12] Chattopadhyay, M.K., 2014. Use of antibiotics as feed additives: A burning question. *Frontiers in Microbiology*. 5, 1–3.

[13] Kraemer, S.A., Ramachandran, A., Perron, G.G., 2019. Antibiotic pollution in the environment: From microbial ecology to public policy. *Microorganisms*. 7, 1–24.

[14] Manyi-Loh, C., Mamphweli, S., Meyer, E., Okoh, A., 2018. Antibiotic use in agriculture and its consequential resistance in environmental sources: Potential public health implications.

[15] Alday, V., Guichard, B., Smith, P., Uhland, C., 2006. Joint FAO / WHO / OIE Expert Consultation on Antimicrobial Use in Aquaculture and Antimicrobial Resistance Towards a risk analysis of antimicrobial use in aquaculture. , 29 pp.

[16] Petersen, A., Andersen, J.S., Kaewmak, T., Somsiri, T., Dalsgaard, A., 2002. Impact of integrated fish farming on antimicrobial resistance in a pond environment. *Applied and Environmental Microbiology*. 68, 6036–6042.

[17] Smith, G.L., 2018. Infectious Diseases and Nanomedicine III. Springer Singapore.

The 13th AUN/SEED-Net Regional Conference on Chemical Engineering 2020 (RCChE-2020)
Jointly held with
The 5th International Symposium on Conservation and Management of Tropical Lakes
"Insights and Challenges toward Achieving SDGs"

Antibiotic Resistance along Kopsrov Lake Impacted By Domestic Wastewater

Sopheavattey MONIROTH [1], Sornpisey KHUT [2], Rithineth TORTH [2], Monychot Tepy CHANTO[2,3] and Chanthol PENG [2,4,*]

[1] *Faculty of Hydrology and Water Resource Engineering, Institute of Technology of Cambodia, Russian Federation Blvd., P.O. Box 86, 12156 Phnom Penh, Cambodia*

[2] *Faculty of Chemical and Food Engineering, Institute of Technology of Cambodia, Russian Federation Blvd., P.O. Box 86, 12156 Phnom Penh, Cambodia*

[3] *Food Technology and Nutrition Research Unit, Research and Innovation Center, Institute of Technology of Cambodia, Russian Federation Blvd., P.O. Box 86, 12156 Phnom Penh, Cambodia*

[4] *Water and Environment Research Unit, Research and Innovation Center, Institute of Technology of Cambodia, Russian Federation Blvd., P.O. Box 86, 12156 Phnom Penh, Cambodia*

**peng@itc.edu.kh*

Abstract

The emerging of Antibiotic Resistant Bacteria (ARB) in wastewater and freshwater systems is a severe health problem and water quality concern. Thus, the monitoring and assessment of ARB in the water system are essential for public health protection. This study aims to assess the water quality in term of physicochemical, total bacteria and ARB concentration at Kopsrov lake (KL) that is impacted by domestic wastewater. Three different sites at KL, including upstream, middle, and downstream, were chosen. The physicochemical properties such as pH, temperature, turbidity, dissolved oxygen (DO), conductivity, and oxidation-reduction potential (ORP) were analyzed. Moreover, culture-dependent methods were used to determine the concentration of total bacteria and ARB (*Escherichia coli* and Coliform) that are resistant to ampicillin (AMP), kanamycin (KAN) and ciprofloxacin (CIP). The result showed that the physicochemical properties (pH and DO) were followed the national effluent standard for pollution sources while Coliform concentration were higher than the standard. The concentration of total bacteria at the upstream site of KL showed the highest concentration (4.04E+05 CFU/ml) which contained coliform (7.90E+04 CFU/ml) that was higher than national standard (<1.0E+01 MPN/ml). While at the downstream, the concentration of total bacteria was reduced to 3.23E+04 CFU/ml where coliform concentration (2.60E+03 CFU/ml), but remained higher than standard. Notably, the middle lake water showed the lowest concentration (3.91E+03 CFU/ml) while Coliform (1.33E+03 CFU/ml) was still higher than compared standard. Similarly, the antibiotic-resistant *E. coli* and Coliform at upstream showed the highest, followed by the downstream site. The antibiotic resistant *E. coli* was not detected in the middle lake water sample. *E. coli* and Coliform had the highest resistant to AMP, followed by CIP and minor resist to KAN at each sampling site. This finding implies that, (KL) is constituted of some significant ARB which are considered as a potential threat to humans and/or animal health since they may lead to more cases of difficult-to-treat infections. Moreover, part of the ARB released from wastewater will not only be able to cause disease in humans or animals, the risk of worsening the environmental problem which results in contributing to the emergence of resistant pathogenic bacteria.

Keywords: *Antibiotic Resistance Bacteria, E. coli, Coliform, Wastewater*

I. Introduction

Wastewater Treatment Plants (WWTPs) have a crucial role in the protection of the environment, in particular – the natural water bodies. In order to remove chemical pollutants and photogenic microorganisms from sewage and wastewater, technological combinations of physicochemical and biological treatments are needed to achieve for allowing the return of good quality water to the environment [1]. Antibiotics, either are cytotoxic or cytostatic to the

microorganisms, allow the body's natural defenses, the immune system, to eliminate them by inhibiting the synthesis of a bacterial cell, synthesis of proteins, deoxyribonucleic acid (DNA), ribonucleic acid (RNA) [2]. In fact, antibiotics are widely used in many applications such as for the treatment of infectious diseases to protection of human health and added into feed to promote animal growth which is partially leaded to emerge of antibiotic-resistant bacteria (ARB) [3]. Antibiotics has become an emerging micropollutant and their presence in the water lead bacteria to develop resistant gene which is often transferred from bacterial cells to other cells, occasionally from commensal bacteria to pathogenic ones, promote ARB and antibiotic resistance genes (ARGs) in the environment. Thus, environment can promote the development and dissemination of ARGs, which have been identified as a global public health crisis [4].

Currently, wastewater released from households contains 234 tons of feces, 2,335 m^3 of urine and 8,154 m^3 of grey water per day. There are 14 pumping stations in Phnom Penh's 732-kilometer drainage system and 44,807 converted-holds in Phnom Penh for wastewater management. Kopsrov water treatment facility on the lake became the 14th pumping station, with the construction of a water treatment facility that covers about 500-hectares, the lake is now being used to discharge sewage and flood water from Phnom Penh [5]. Since Kopsrov Lake (KL) has received many sources of wastewater which may contained high concentration of pollutant and various bacteria. Thus, the monitoring and assessment of bacteria, especially ARB are essential for public health protection. This study investigates the current status of water quality of KL that is impacted by the flow of untreated wastewater.

II. Materials and Methods

2.1. Sampling sites

Samples were collected on 07th October, 2020, during rainy season from three different sites as surface water and wastewater discharging point in KL including upstream (US), middle stream (MS), and downstream (DS). 1000 mL of each sample was collected and stored in sterilized polyethylene bottle, and placed in ice box while transporting to ITC laboratory for analysis.

2.2. Physicochemical analysis

Physicochemical properties such as pH, temperature (Tem), turbidity, dissolved oxygen (DO), conductivity (Cond), and oxidation-reduction potential (ORP) were analyzed by using YSI EXO2 multi-parameter instrument.

2.3. Quantification of Total Bacteria and ARB

Culture-dependent methods were used to determine of total bacteria and ARB (*Escherichia coli* and Coliform) that are resistant to ampicillin (AMP), kanamycin (KAN) and ciprofloxacin (CIP).

Lysogeny Broth agar was used to culture Total Bacteria (TPC) which colonies appeared in white colour with Pour Plate Method. For *Escherichia coli* (*E. coli*) and Coliform were done by Pour Plate technique with Chromocult® Coliform Agar by Merck Millipore. Bacteria was distinguished by colonies color which can be known as dark blue or violet is *E. coli* while pink represented Coliform.

Three antibiotics were added into culture media. Stock solution was prepared by dissolving antibiotics powder into sterilized pure water and diluting it into culture media to achieve the concentration of 50 µg/mL for AMP and KAN, and 5 µg/mL for CIP. Antibiotic-resistant bacteria enumerated by using spread plate technique. All sampled plates were done triplicate and control plate contained no antibiotic. The concentration of bacteria was calculated by using the following equation

$$N = \frac{\sum C}{n \times d \times v} \quad \text{(Eq.1)}$$

Where N is the concentration of bacteria (CFU/ml), ΣC is the sum of counted colonies, n is the amount of plates, d is the dilution factor, and V is the inoculated volume.

III. Results and Discussion

The physicochemical characteristics at each site, are shown in Table 1. It can be seen that Tem, DO, turbidity, Cond and ORP of UP site were 22.72^{o}C, 7.36, 2.92 mg/l, 102.00 NTU, 312.33 µs/cm, and 209.50 mV respectively. At MS site, the Tem, pH, DO, turbidity, Cond and ORP were 22.13 ^{o}C, 7.89, 5.93 mg/l, 18.27 NTU, 278.93 µs/cm, and 357.17 mV while at DS were 20.98^{o}C, 7.74, 6.61 mg/l, 22.03 NTU, 270.73 µs/cm, and 423.53 mV respectively. Moreover, pH and DO value at each site were ranged within national standard (pH: 6.5-8.5) and DO (7.5-2.0), according to sub-degree on water pollution control [6].

Table 1. Physicochemical characteristics of lake water

Parameter	UP	MS	DS	SD
Tem (ºC)	22.72	22.13	20.98	-
pH	7.36	7.89	7.74	6.5-8.5
DO (mg/l)	2.92	5.93	6.61	7.5-2.0
Tur (NTU)	102.00	18.27	22.03	-
Cond (µs/cm)	312.33	278.93	270.73	-
ORP (mV)	209.50	357.17	423.53	-

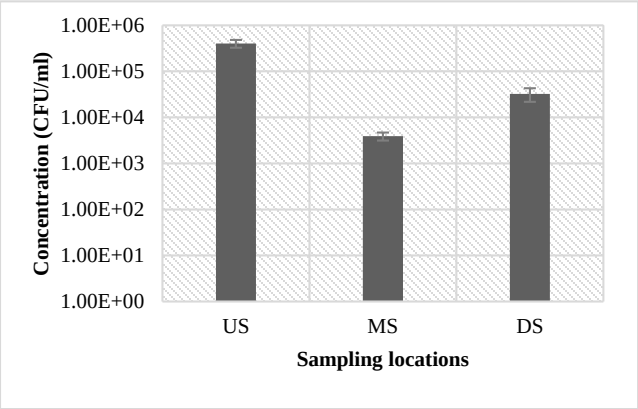

Fig. 1. Concentration of Total Plate Count

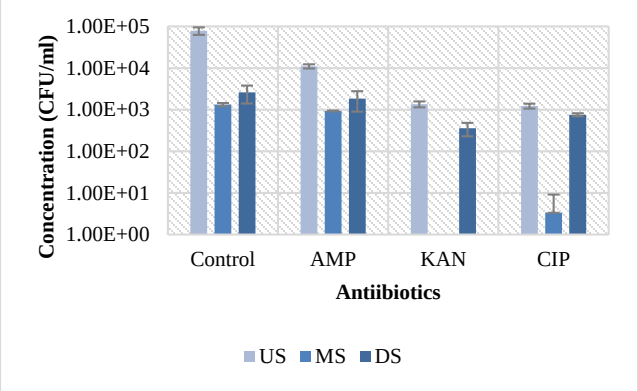

Fig. 2. Antibiotic Resistance in Coliform

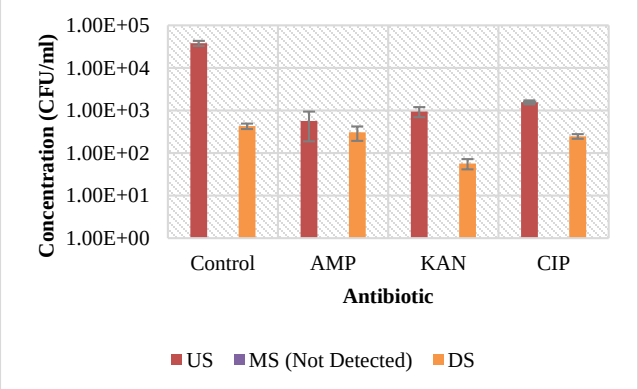

Fig. 3. Antibiotic Resistance in *E. coli*

Concentration of Total Plate Count (TPC), Antibiotic Resistance of Coliform and antibiotic resistance of *E. coli* which expressed in CFU/ml were shown in **Fig. 1**, **Fig. 2** and **Fig. 3**. respectively. In **Fig. 1**, concentration TPC at UP (4.04E+05 CFU/ml) was higher than those at DS (3.23E+04 CFU/ml) and MS (3.91E+03 CFU/ml). Out of TPC in US, MS and DS contained Coliform (7.90E+04, 1.33E+03 and 2.60E+03 CFU/ml) which equaled to 19.55%, 34.02% and 8.05% while *E. coli* (3.82E+04, 0.00E+00 and 4.30E+02 CFU/ml) that equaled 9.46%, 0.00% and 5.72% respectively. Coliform concentration at all three sites were higher than given standard on water pollution control (<1.0E+01 MPN/ml) which meant that those sample were not complied with national standard [6]. Coliform, primary indicator of fecal contamination that found at three sites could be brought into aquatic environment through treated or untreated wastewater release. In **Fig. 2** suggested that, the highest antimicrobial resistance of Coliform that compared to control, at DS tolerant to AMP (70.77%), followed by CIP (29.12%) and KAN (13.73%). At UP, antimicrobial resistance of Coliform for AMP (13.92%), followed by KAN (1.72%) and CIP (1.55%) while at MS for AMP (69.92%), followed by CIP (0.25%) and KAN (0.00%). In **Fig. 3**, antimicrobial resistance of comparing to control, the highest resistance of *E. coli* is at DS for AMP (71.40%), followed by CIP (57.44%) and KAN (13.19%). At UP, antimicrobial resistance of *E. coli* for CIP (4.08%), followed by AMP (1.48%) and KAN (0.50%) while at MS *E. coli* was not detected.

The frequency of antibiotic resistance among Coliform and *E. coli* bacteria varied from sample to sample, and this is probably dependent upon the sources of contamination of the water. The highest concentration of TPC is located at UP which is correlate to Coliform and *E. coli*. For UP samples were taken at the surface of discharging flow from various sources to KL where water flow from sewage system that may contain high pollution. Additionally, DO value at UP is quite low as there are many bacteria or aquatic animals in that area. They may be overpopulated which resulting consuming great amount of DO At the same time, that site presented the lowest value of ORP (209.50 mV) which indicated the high amount of presented reducing agent and pollution than the other two sites as water pollution levels tended to increase with low ORP readings [7].

Concentration of Coliform in control, plate without antibiotic at each site are higher than antibiotic plates which is respected to the theory of antibiotic's action whether

killing or decreasing growth of bacteria. Even though Coliform was not fully removed, its concentration at DS is still highly resistant to all three drugs as shown in **Fig. 2** comparing to control. The percentage of antibiotic resistance at DS, MS, or UP to AMP is higher than other two drugs. For MS site is clearly indicated that Coliform is highly tolerant to AMP (69.92%) while resistance level is less for CIP (0.25%) and KAN (0.00%), so Coliform growth were inhibited by KAN and CIP at MS site. Coliform is an indicator microorganism which subdivided into total and fecal coliforms *(E. coli*, *Klebsiell*a, and *Enterobacter*) while total coliform includes both soil intermediates and fecal forms, fecal coliforms confines to those from fecal origin, used as standard microbial indicators of water quality. Because some pathogenic microorganism also known as Coliform group, so its highly resistant to specific drugs appeared as a serious concern of multi-drug resistant of pathogenic one [9]. *E. coli* at MS site was not detected while the highest concentration is at UP which can be expressed in higher contaminated from human activities. This result paralleled to Coliform which the most contaminated site known as UP. Since MS sample is absent of *E. coli*, so this site could not use to express antibiotic resistance while the other two have shown. Each studied site shown the percentage of resistance where at DS known as highly resistant one. Detected *E. coli* (5.72%) from total bacteria indicated the highest tolerance to AMP (71.40%), followed by CIP (57.44%) and KAN (13.19%). This result indicated that *E. coli* resisted to AMP. *E. coli* were not killed and it continued to grow even the presence of AMP. *E. coli* too had developed ability and defeated the drug which were usually applied to kill them [8]. Moreover, from resistance percentage, it is indicated that *E. coli* was not resistant to KAN as it showed small resistant percentage, so KAN is the most effective one among studied drugs. *E. coli* is the most common cause of uncomplicated and community acquired urinary tract infection [8]. According to **Fig.2**. and **Fig.3**. both *E. coli* and Coliform are highly resistant to AMP and minor resistant to CIP and KAN. AMP which is considered as a resistance drug to either Coliform or *E. coli* could not use to treat infected human. The reason for this is common practice of prescribing ampicillin in the tract infections, and the fact that ampicillin was the most commonly prescribed antibiotics in developing countries. World Health Organization donated large doses of these antibiotics in the treatment of many infectious diseases [9]. Concentration of KAN (50µg/L) and CIP (5µg/L) indicated their minimal inhibitory concentration (MIC) which is varied by depending on antibiotic group [10]. Even if low concentrations of CIP, a group of fluoroquinolones could promote resistance for both detected *E. coli* and Coliform. This might be from overuse of one of the fluoroquinolone leads to the development of resistance to the whole group of quinolone antibiotics. Fluoroquinolones which are mostly added to the animal feed and used to treat humans caused selected *E. coli* strains resistant to these drugs [9]. However, *E. coli* also known as less resistance to KAN which located in aminoglycosides group that used to treat serious bacterial infections. These group are poorly absorbed by orally, so they are usually injected into a vein [10].

IV. Conclusion

Results of our research have shown that TPC is a contained Coliform and *E. coli*. Also frequency of TPC at UP was the highest. *E. coli* showed major resistance to AMP and CIP, and minor resistance to KAN. Emerging of these resistance while a growing of common infection such as waterborne and foodborne disease are becoming harder, and sometime impossible, to treat as antibiotic become less effective.

Acknowledgement

This research was supported by the Science and Technology Research Partnership for Sustainable Development (SATREPS), the Japan Science and Technology Agency (JST)/Japan International Cooperation Agency (JICA) with the grant-number JPMJSA1503, and AFD/EU.

References

[1] Manaia, C.M., Rocha, J., Scaccia, N., Marano, R., Radu, E., Biancullo, F., Cerqueira, F., Fortunato, G., Iakovides, I.C., Zammit, I., Kampouris, I., Vaz-Moreira, I., Nunes, O.C., 2018. Antibiotic resistance in wastewater treatment plants: Tackling the black box. Environ. Int. 115, 312–324

[2] Zaman, S.B., Hussain, M.A., Nye, R., Mehta, V., Mamun, K.T., Hossain, N., n.d. A Review on Antibiotic Resistance: Alarm Bells are Ringing. Cureus 9.

[3] Qadir, M., Wichelns, D., Raschid-Sally, L., McCornick, P.G., Drechsel, P., Bahri, A., Minhas, P.S., 2010. The challenges of wastewater irrigation in developing countries. Agric. Water Manag. 97, 561–568.

[4] Liu, X., Guo, X., Liu, Y., Lu, S., Xi, B., Zhang, J., Wang, Z., Bi, B., 2019. A review on removing antibiotics and antibiotic resistance genes from wastewater by constructed wetlands: Performance and microbial response. Environ. Pollut. 254, 112996.

[5] Pumping station pollution plagues community, 2018. . Khmer Times. URL https://www.khmertimeskh.com/528735/pumping-station-pollution-plagues-community/ (accessed 12.15.20).

[6] Royal Government Concil of Minister, n.d. Sub-Degree-27-on-Water-Pollution-Control_990406.pdf. [7] Marín Galvín, R., Rodríguez Mellado, J.M., Ruiz Montoya, M., Jiménez Gamero, C., 2001. OXIDATION-REDUCTION POTENTIAL (ORP) IN PREPARED AND INDUSTRIALLY TREATED WATERS. Bol. Soc. Chil. Quím. 46, 387–397.

[8] Cooke, M.D., 1976. Antibiotic resistance in coliform and faecal coliform bacteria from natural waters and effluents. N. Z. J. Mar. Freshw. Res. 10, 391–397.

[9] Vranic, S.M., Uzunovic, A., 2016. ANTIMICROBIAL RESISTANCE OF ESCHERICHIA COLI STRAINS ISOLATED FROM URINE AT OUTPATIENT POPULATION: A SINGLE LABORATORY EXPERIENCE. Mater. Socio-Medica 28, 121–124.

[10] Brain J., W., n.d. Aminoglycosides - Infections.MSD Man. Consum. Version. URL https://www.msdmanuals.com/home/infections/antibiotics/aminoglycosides (accessed 12.8.20).

The 13th AUN/SEED-Net Regional Conference on Chemical Engineering 2020 (RCChE-2020)
Jointly held with
The 5th International Symposium on Conservation and Management of Tropical Lakes
"Insights and Challenges toward Achieving SDGs"

Study on Antibiotic Resistance of *Pseudomonas aeruginosa* Isolated from Drinking Water Collected from Three communes in Kampong Thom Province

Seab SAT [1], Sovannmony NGET [1, 2], Soukim HENG [1,2], Sokneang IN [1, 2], Masateru NISHIYAMA [3], Toru WATANABE [3] and Hasika MITH [1, 2,*]

[1] *Faculty of Chemical and Food Engineering, Institute of Technology of Cambodia, Russian Federation Blvd., P.O. Box 86, 12156 Phnom Penh, Cambodia*
[2] *Food Technology and Nutrition Research Unit, Research and Innovation Center, Institute of Technology of Cambodia, Russian Federation Blvd., P.O. Box 86, 12156 Phnom Penh, Cambodia*
[3] *Faculty of Agriculture, Yamagata University, Japan 1-23 Wakaba-machi, Tsu Yamagata 997-8555, Japan*
* *hasika@itc.edu.kh*

Abstract

The opportunistic pathogenic *Pseudomonas aeruginosa* has been categorized as the critical prioritized pathogen for research and development of new antibiotics according to the World Health Organization. However, the awareness of *P. aeruginosa*'s antibiotic resistance is still not widely and specifically studied in developing countries. The current study was conducted to determine antibiotic resistance of *P. aeruginosa* isolated from drinking water collected in Kampong Thom province. The enumeration of *P. aeruginosa* was carried out using filtration method, followed by isolation and antibiotic susceptibility test. The results showed that out of 145 samples, 35 drinking water samples were detected with presence of *P. aeruginosa*. Furthermore, a total number of 123 strains were isolated prior to antibiotic susceptibility test. As a result, only nine isolated strains were found to be resistant to ticarcillin among the tested antibiotics. Even though no single strain showed its resistance to meropenem and fosfomycin, but 2 and 17 strains of *P. aeruginosa* were observed to be intermediate to the two antibiotics, respectively. However, colistin, gentamicin, and ciprofloxacin showed a good effectiveness against these isolated *P. aeruginosa*. Based on this study, the prevalence of antibiotic-resistance of *P. aeruginosa* is not high in the drinking water collected from the three communes in Stoung District.

Keywords: *Antibiotic resistance, drinking water, Pseudomonas aeruginosa*

I. Introduction

The antibiotic resistance is considered a potential global threat for food safety and development, since it sharply rose the mortality of population [1]. According to the World Health Organization, *P. aeruginosa* is classified as "Critical" priority pathogen for research and development of new antibiotics. Moreover, the potable water is defined as consumable water and safety for lifetime [2], meanwhile the population in developing country is still suffering from waterborne diseases [3]. As a result, the study of antibiotic resistance in developing country on *P. aeruginosa* was conducted in order to assess this problem in drinking water. To deeply investigate this issue, the study area was located in Kampong Thom with three different sites including land-based, water- and land-based, and water-based.

II. Materials and Methods

2.1. Sampling sites

A total number of 145 drinking water samples were col-lected, located in Kampong Thom province along To nle Sap Lake. The sampling was carried out in three co mmunes such as Trea, Msa Krang and Peam Bang with three villages from each commune, and the map of sam pling sites was shown in **Fig. 1** The samples were imm ediately sent to the laboratory to analyze within 24 h [4].

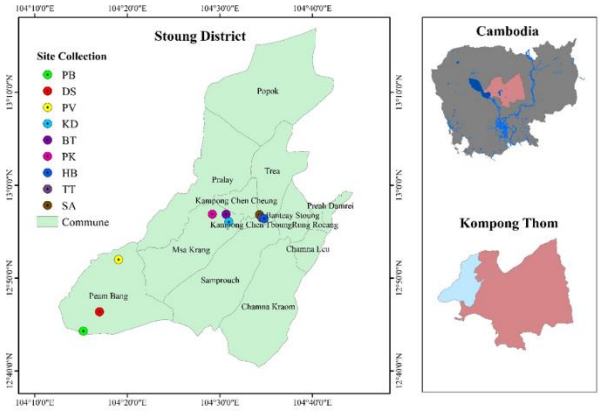

Fig. 1. Sampling sites areas in Kampong Thom.

2.2. Detection of *P. aeruginosa* by filtration method

The collected drinking water samples were enumerated for *P. aeruginosa* using filtration method. A volume of 100 ml of samples was filtrated using 0.45 µm mixed cellulose ester filters (Merck Millipore, Germany). The filters were placed onto the prepared Pseudomonas CFC/CN agar (Merck KGaA, Darmstadt, Germany) with CN supplement and incubated at 37 ˚C for 24 h, the blue/green colonies were detected and considered as *P. aeruginosa*.

2.3. Isolation of *P. aeruginosa* from water samples

The grown colonies were selected continuously for isolation to ensure the purity of each strain out of diverse bacterial population. The colonies were looped and streaked on another agar plate (Pseudomonas agar base CN supplement) for few times in order to obtain the same morphology and color indicator of colonies. The collected strains were then stored in Luria-Bertani broth (LB, Difco, Franklin Lakes, United State) with 15% glycerol in cryogenic tubes.

2.4. Antibiotic susceptibility test

In the current study,), the disk diffusion method was used to determine the susceptibility of the isolated *P. aeruginosa* following the Clinical and Laboratory Standard Institute (CLSI). Six antibiotics from different categories were gentamycin (10 µg/disk), meropenem (10 µg/disk), ciprofloxacin (5 µg/disk), colistin (10 µg/disk), Fosfomycin (200 µg/disk) and ticarcillin (75 µg/disk). The antibiotic containing disks were placed on the Mueller Hinton agar (MH, Himedia, Mumbai, India). The diameters of inhibitory zone (mm) were measured and compared to the reference to determine whether the isolated strains were susceptible, intermediate or resistant, as shown in the **Table 1**.

Table 1. CLSI diameter of inhibition zone

Antibiotics	Diameter of inhibition zone (mm)		
	Susceptible (S)	Intermediate (I)	Resistance (R)
Ticarcillin	≥24	16-23	≤15
Meropenem	≥19	16-18	≤15
Colistin	≥11	-	≤10
Gentamicin	≥15	13-14	≤12
Fosfomycin	≥16	13-15	≤12
Ciprofloxacin	≥21	16-20	≤15

III. Results and Discussion

3.1. Detection and isolation of *P. aeruginosa*

In overall 145 samples were taken from nine villages in three different communes in Kampong Thom province to detect the presence of *P. aeruginosa*. As the result, the presence of *P. aeruginosa* was found in 35 samples among those 14, 11, 10 samples were from Trea, Msa Krang, and Peam Bang respectively. They were originated from various resources including rain water, bottle water (20L), lake water, filter, and boiling in 23%, 11%, 14%, 43%, 9% respectively.

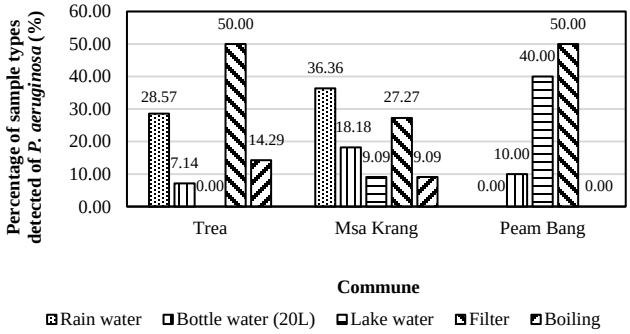

Fig. 2. Different sample types detected of *P. aeruginosa* from each commune in Kampong Thom province.

As shown in **Fig. 2**, the presence of *P. aeruginosa* was found in filtered, boiling drinking water which could be an explanation of water being stored inappropriately that could cause contamination from the container or lack of effectiveness of the filtration method.

3.2. Antibiotic susceptibility of isolated *P. aeruginosa*

3.2.1. Trea Commune

The sampling sites in Trea commune are located in t hree different villages such as SA, TT, and HB that are full of villagers. There are 48 isolated strains in Trea co mmune that have to be applied with disc diffusion meth od, and in order to determine its resistance, zone measur ements were compared to the reference in CLSI (2017) [5].

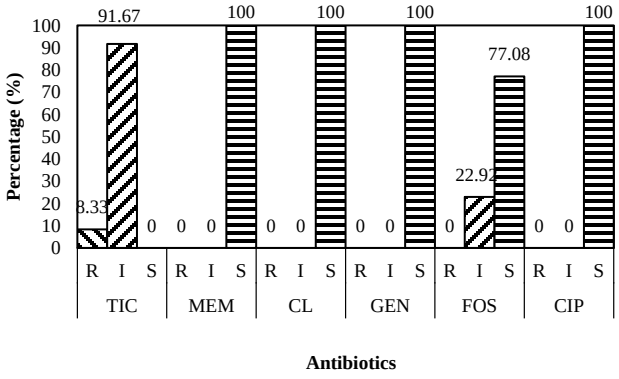

Fig. 3. Antibiotic resistance of *P. aeruginosa* in Trea commune. "R" means "Resistant", "I" means "Intermediate", and "S" means "Susceptible".

As shown in **Fig. 3**, four strains of *P. aeruginosa* were resistant and 44 strains were susceptible to TIC, meanwhile 11 strains were also intermediate to FOS. However, MEM, CL, GEN, and CIP were highly effective against this bacterium. Another study of [6] also showed similar result as above one, antibiotic resistance was often resistant to TIC, FOS whereas there were no resistant strains to CIP, GEN, and MEM. According to this observation, the occurrence of antibiotic resistance could be an evidence of environmental antibiotic resistance genes because of extensive use of antibiotic in agricultural purpose and therapy [7] that lead to selective pressure in environmental bacteria and was found in a populated commune.

3.2.2. Msa Krang Commune

Three villages of sampling sites in Msa Krang commune were done in PK, BT, and KD. There are 31 isolated strains that have to be tested with disk diffusion method and zone measurement to determine its resistance.

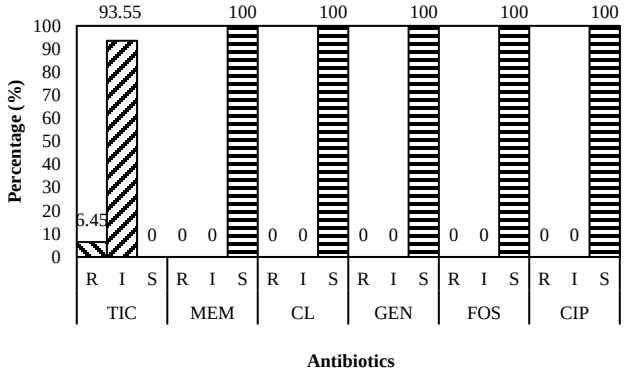

Fig. 4. Antibiotic resistance of *P. aeruginosa* in Msa Krang Commune.

As shown in **Fig. 4**, the antibiotic resistance of *P. aeruginosa* is quite similar to the previous result that two *P. aeruginosa* strains were resistant and 29 strains were susceptible to TIC, whereas MEM, CL, GEN, FOS, and CIP were still highly effective. In this scenario, TIC was considered a concern for clinical treatment because in another investigate with 40 isolates of *P. aeruginosa* were resulted in 85% of TIC resistance [8].

3.2.3. Peam Bang Commune

Three villages in Peam Bang commune were chosen as the sampling sites including PV, DS, and PB that are alongside the Tonle Sap Lake. Total 44 isolated strains were also tested with disk diffusion method.

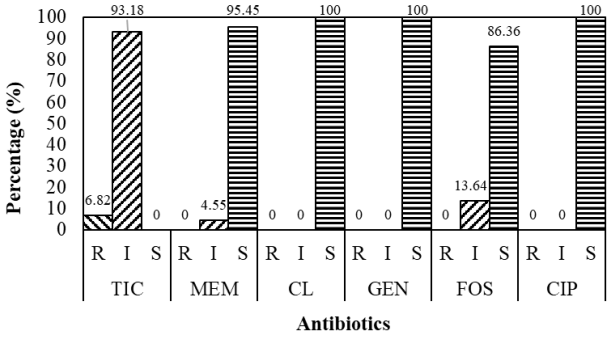

Fig. 5. Antibiotic resistance of *P. aeruginosa* in Peam B ang commune.

As shown in **Fig. 5**, TIC is still a less effective drug against *P. aeruginosa* with 41 intermediate-strains, three resistant-strains. Moreover, MEM notably consists two intermediate-strains which is an interesting result compare to previous two communes, and FOS also contains six intermediate-strains. Meanwhile CL, GEN and CIP continue

to play a strong role to inhibit this pathogen. This result could be evidence of a possible presence of antibiotic resistance genes (ARGs) contamination from Tonle Sap Lake along with Peam Bang commune, and the occurrence and transfering of ARGs could be caused by pollution from human activities [9].

IV. Conclusion

In conclusion, a high concentration of *P. aeruginosa* was found in drinking water that originated from home-collected boiling and rain water. The prevalence of antibiotic-resistant *P. aeruginosa* is not high in drinking water for those sampling sites while the presence of multi-drug resistance is not detected for any isolated strain.

Acknowledgement

We are thankful to the Science and Technology Research Partnership for Sustainable Development (SATREPS), the Japan Science and Technology Agency (JST)/Japan International Cooperation Agency (JICA) for their financial support and Institute of Technology of Cambodia for their laboratory cooperation.

References

[1] Jasovský, D., Littmann, J., Zorzet, A., Cars, O., 2016. Antimicrobial resistance—a threat to the world's sustainable development. *Upsala Journal of Medical Sciences*. 121, 159–164.

[2] Alam, M.J.B., Islam, M.R., Muyen, Z., Mamun, M., Islam, S., 2007. Water quality parameters along rivers. *International Journal of Environmental Science and Technology*. 4, 159–167.

[3] Brander, N., 2003. Drinking water in schools. *Nursing times*. 99, 50–51.

[4] WHO., 1997. Guidelines for Drinking-water Quality. *World Health*. 1, 104–8.

[5] CLSI., 2017. M100 Performance Standards for Antimicrobial Susceptibility Testing.

[6] Vaz-Moreira, I., Nunes, O.C., Manaia, C.M., 2012. Diversity and antibiotic resistance in Pseudomonas spp. from drinking water. *Science of the Total Environment*. 426, 366–374.

[7] Martinez, J.L., 2009. Environmental pollution by antibiotics and by antibiotic resistance determinants. *Environmental Pollution*. 157, 2893–2902.

[8] Pitondo-Silva, A., Martins, V.V., Fernandes, A.F.T., Stehling, E.G., 2014. High level of resistance to Aztreonam and Ticarcillin in Pseudomonas aeruginosa isolated from soil of different crops in Brazil. *Science of the Total Environment*. 473–474, 155–158.

[9] Ash, R.J., Mauck, B., Morgan, M., 2002. Antibiotic resistance of gram-negative bacteria in rivers, United States. *Emerging Infectious Diseases*. 8, 713–716.

Detection of Antibiotic-Resistant Bacteria in Water Environment of Tonle Sap Area and Wastewater

Sovathana PHUONG[1], Monychot Tepy CHANTO[1,3], Chanthol PENG[1,3], Kazuhiko MIYANAGA[2] and Reasmey TAN [1, 3,*]

[1] *Faculty of Chemical and Food Engineering, Institute of Technology of Cambodia, Russian Federation Blvd., P.O. Box 86, 12156 Phnom Penh, Cambodia*
[2] *School of Life Science and Technology, Tokyo Institute of Technology, 4259 J3-8 Nagatsuta-cho, Midori-ku, Yokohama, 226-8501, Japan*
[3] *Food Technology and Nutrition Research Unit, Research and Innovation Center, Institute of Technology of Cambodia, Russian Federation Blvd., P.O. Box 86, 12156 Phnom Penh, Cambodia*
** Corresponding author: rtan@itc.edu.kh*

Abstract

Use, misuse, and overuse of antibiotic have led to the emergence of antibiotic-resistant bacteria. However, the prevalence of such bacteria in water environment of Cambodia is still less studied. Thus, this study was done in order to detect antibiotic-resistant bacteria in water environment of Tonle Sap area (Tonle Sap River and Tonle Sap Lake) and wastewater. Enumeration and isolation of antibiotic-resistant *Klebsiella pneumoniae*, *Escherichia coli*, and *Staphylococcus aureus* were done by spread plate method and streaking on selective media supplemented with antibiotics. The isolated strains were then used in antibiotic susceptibility experiment by disc diffusion method in order to confirm its resistance. The result shows that highest concentration of antibiotic-resistant bacteria was found in wastewater, and a few sites of Tonle Sap area where influence of anthropogenic pollution may cause promotion of gene transfer and acquisition of resistance genes. From this study, it could be said that now antibiotic-resistant bacteria is highly prevalent in all sample sites which are in close proximity with human population of water environment of Tonle Sap area.

Keywords: *antibiotic-resistant bacteria, disc diffusion method, Tonle Sap area, wastewater*

I. Introduction

Pollution of antibiotics from usage in medicine, livestock, and aquaculture into water environment in combination with wastewater discharge containing antibiotics residues in environment lead to occurrence of antibiotic resistance in environmental bacteria [12, 15]. However, little is known about antibiotic-resistant bacteria that represent environmental isolates. As a result, this study is conducted in order to detect antibiotic-resistant bacteria in the water environment and wastewater in order to contribute to lack of data prevalence of drug resistance in environment. Recently, with the finding that there is a high concentration of *Proteobacteria* and *Firmicutes* in the water environment of Tonle Sap area especially near the floating villages [16], *K. pneumoniae*, *E. coli*, and *S. aureus* are selected to study its antibiotic resistance.

II. Methodology

2.1. Sampling sites and enumeration of antibiotic-resistant bacteria

Seven sampling sites which were chosen in this study are located in Phnom Penh city (one from Tonle Sap River and one from Cheung Ek wastewater), Kampong Chhnang province (four from around Chnok Trou floating village) and Pursat province (one from Kampong Luong floating village). Antibiotic-resistant bacteria was enumerated by using viable plate count method with spread plate technique on DHL Agar (for *K. pneumoniae*), Chromocult Agar (for *E. coli*), and Mannitol Salt Agar (for *S. aureus*).

The selective media were supplemented with antibiotics such as ampicillin, ciprofloxacin, kanamycin, meropenem, and vancomycin at breakpoint concentration.

2.2. Disc diffusion method for confirmation of resistance

Four colonies with different size and morphology were isolated from different media with different antibiotics by streak plate method. Then, the isolated single colony was used to prepare the overnight culture using LB broth. Culture from LB broth was used for disc diffusion method, in which six antibiotics discs (disc content: ampicillin 25 µg, kanamycin 30 µg, vancomycin 30 µg, ciprofloxacin 5 µg, meropenem 10 µg , and tetracycline 30 µg) were applied. The diameter of the zone of inhibition was measured and interpreted by using CLSI standard.

III. Results and Discussions

3.1. Concentration of antibiotic-resistant bacteria

Viable plate count of *K. pneumonia, E. coli,* and *S. aureus* shows that high concentration of these bacteria resistant to antibiotic used were found abundantly in wastewater site since wastewater provides good condition for proliferation of bacteria and transferring of resistance genes [2]. For Tonle Sap area, the highest concentration of antibiotic-resistant *K. pneumonia* and *E. coli* were found in Tonle Sap river site, followed by Port site, Lake Water site, and Kampong Luong site which could indicate fecal contamination in these area as well as influence of anthropogenic pollution [3, 11]. However, high concentration of antibiotic-resistant *S. aureus* are also found in Port site, UP site, and KL site which could be sue to shedding from users of water for recreational purpose

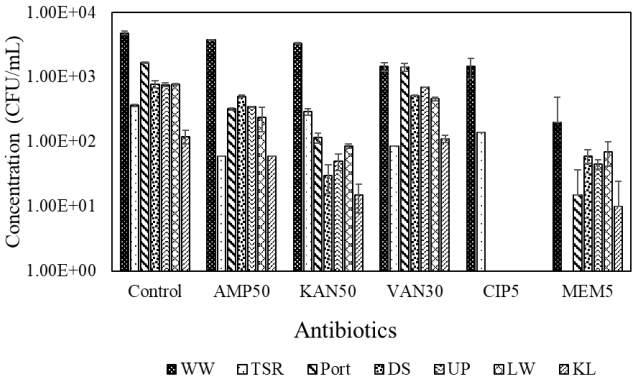

(a)

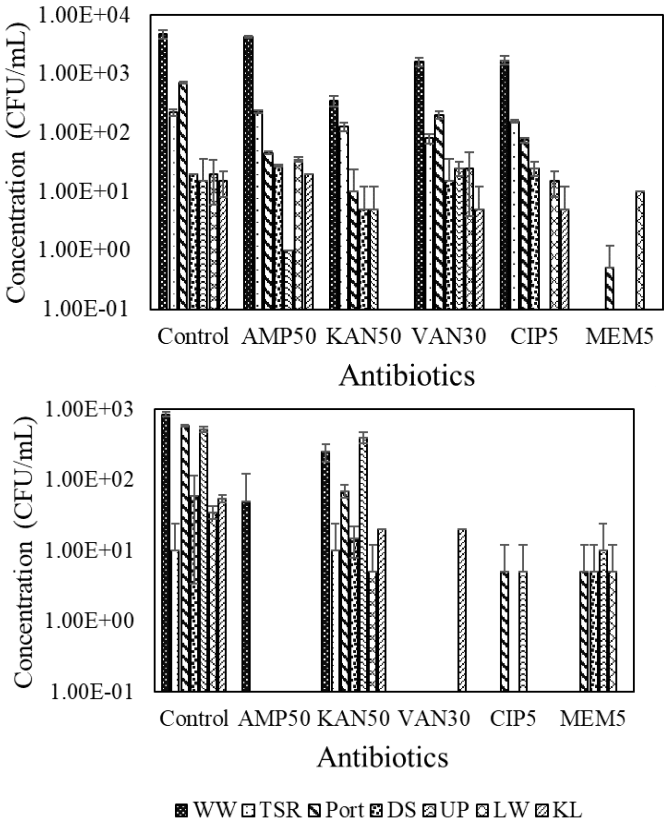

(c)

Fig. 1. (a). Concentration of antibiotic-resistant *K. pneumoniae*, (b). Concentration of antibiotic-resistant *E. coli*, (c). Concentration of antibiotic-resistant *S. aureus* (AMP: ampicillin, KAN: kanamycin, VAN: vancomycin, CIP: ciprofloxacin, MEM: meropenem, WW: Wastewater, TSR: Tonle Sap river, DS: Downstream, UP: Upstream, LW: Lake Water, KL: Kampong Luong)

in addition to human and animal waste and waste disposal [4, 5, 10]. Overall, the prevalence of antibiotic-resistant bacteria in Phnom Penh sample sites was more than that in sample sites of Kampong Chhnang and Pursat as the pollution activity in the capital is much higher than in province [8].

3.2. Resistance of isolated strains to antibiotics

Measuring of the diameter of the zone of inhibition for each antibiotics yields the following result. From 73% to 100% of isolated strains of antibiotic-resistant *K. pneumoniae* are resistant to ampicillin and vancomycin which are intrinsic resistant of this bacteria [13] while high resistance to tetracycline could be due to possession of *tetB* or *tetD* gene that encode efflux pump [9]. For *E. coli*, high resistance to vancomycin is also due to intrinsic resistant to this antibiotic. However, high percentage of ampicillin-resistant strain is expected as ampicillin is a drug that was introduced in 1961 and has been used for a long time [14]. In addition, high resistance to tetracycline could be due to the use of this antibiotic in aquaculture as prophylactics which then lead to selection of resistant bacteria [7]. For production of staphylococcal β-lactamase [6] and dissemination of *aacA* genes in the water environment [1].

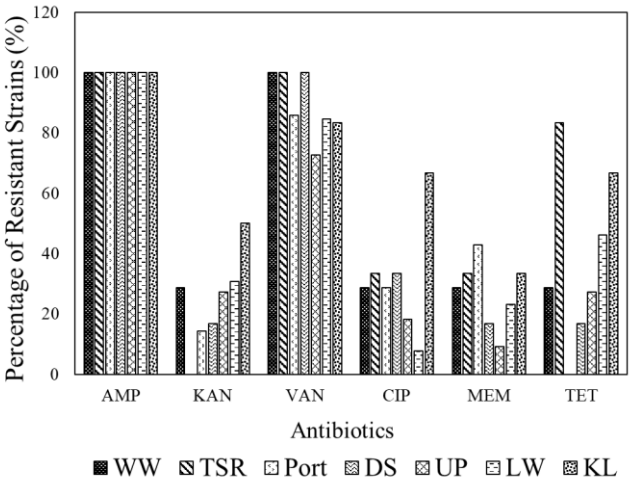

(a)

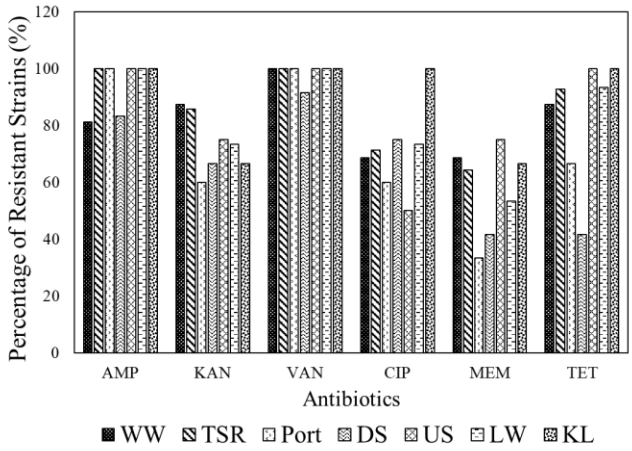

(b)

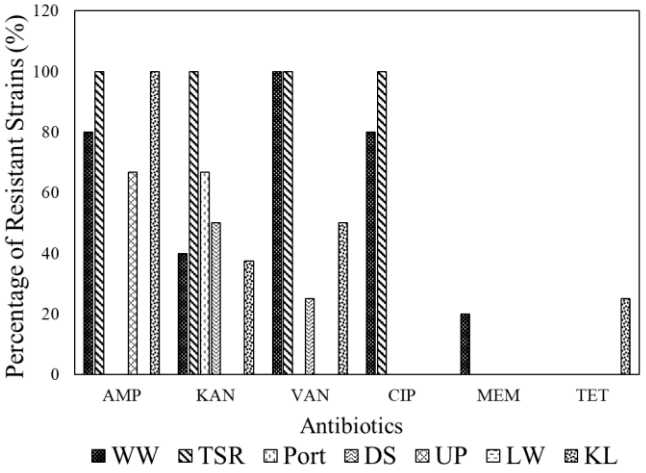

(c)

Fig. 2. (a). Resistance of *K. pneumoniae* to antibiotics, (b). Resistance of *E. coli* to antibiotics, (c) Resistance of *S. aureus* to antibiotics (AMP: ampicillin, KAN: kanamycin, VAN: vancomycin, CIP: ciprofloxacin, MEM: meropenem, WW: Wastewater, TSR: Tonle Sap river, DS: Downstream, UP: Upstream, LW: Lake Water, KL: Kampong Luong)

IV. Conclusion

In conclusion, high concentration of these antibiotic-resistant bacteria was found in Wastewater site and in sampling sites of water environment of Tonle Sap area such as Tonle Sap river site, Port site, Lake Water site, and Kampong Luong site where their locations are in close proximity to human population.

Acknowledgement

We are thankful to the Science and Technology Research Partnership for Sustainable Development (SATREPS), the Japan Science and Technology Agency (JST)/Japan International Cooperation Agency (JICA) for their financial support.

Reference

[1] Baquero, F., Martínez, J. L., and Cantón, R., 2008. Antibiotics and antibiotic resistance in water environments. *Current Opinion in Biotechnology*, 19, 260–265.

[2] Bouki, C., Venieri, D., and Diamadopoulos, E., 2013. Detection and fate of antibiotic resistant bacteria in wastewater treatment plants: A review. *Ecotoxicology and Environmental Safety*, **91**, 1–9.

[3] Czekalski, N., Sigdel, R., Birtel, J., Matthews, B., and Bürgmann, H., 2015. Does human activity impact the natural antibiotic resistance background? Abundance of antibiotic resistance genes in 21 Swiss lakes. *Environment International*, 81, 45–55.

[4] El-Shenawy, M., 2005. Staphylococcus aureus and fecal indicators in Egyptian coastal waters of Aqaba Gulf, Suez Gulf, and Red Sea. *Egypt Journal of Aquatic Research*, 31, 113–124

[5] Hatcher, S. M., Myers, K. W., Heaney, C. D., Larsen, J., Hall, D., Miller, M. B., and Stewart, J. R., 2016. Occurrence of methicillin-resistant Staphylococcus aureus in surface waters near industrial hog operation spray fields. *Science of the Total Environment*, 565, 1028–1036.

[6] Kesharwani, A. K. and Mishra, J., 2019. Detection of β-lactamase and antibiotic susceptibility of Clinical Isolates of Staphylococcus aureus. *Biocatalysis and Agricultural Biotechnology*, 17, 720–725.

[7] Li, D., Yu, T., Zhang, Y., Yang, M., Li, Z., Liu, M., and Qi, R., 2010. Antibiotic resistance characteristics of environmental bacteria from an oxytetracycline production wastewater treatment plant and the receiving river. *Applied and Environmental Microbiology*, 76, 3444–3451.

[8] MOE, 2009. Cambodia Environment Outlook. 1st ed. Ministry of Environment, Phnom Penh.

[9] Nawaz, M., Khan, S. A., Tran, Q., Sung, K., Khan, A. A., Adamu, I., and Steele, R. S., 2012. Isolation and characterization of multidrug-resistant Klebsiella spp. isolated from shrimp imported from Thailand. *International Journal of Food Microbiology*, 155, 179–184.

[10] Plano, L. R., Garza, A. C., Shibata, T., Elmir, S. M., Kish, J., Sinigalliano, C. D., Gidley, M. L., Miller, G., Withum, K., Fleming, L. E., and Solo-Gabriele, H. M., 2011. Shedding of Staphylococcus aureus and methicillin-resistant Staphylococcus aureus from adult and pediatric bathers in marine waters. *BMC Microbiology*, 11, 1-10.

[11] Pruden, A., Arabi, M., and Storteboom, H. N., 2012. Correlation between upstream human activities and riverine antibiotic resistance genes. *Environmental Science and Technology*, 46, 11541–11549.

[12] Rozman, U., Duh, D., Cimerman, M., and Turk, S. Š., 2020. Hospital wastewater effluent: hot spot for antibiotic resistant bacteria. *Journal of Water, Sanitation and Hygiene for Development*, 1–8.

[13] Sarkar, P., Yarlagadda, V., Ghosh, C., and Haldar, J., 2017. A review on cell wall synthesis inhibitors with an emphasis on glycopeptide antibiotics. *MedChemComm*, 8, 516–533.

[14] Simon, H. J. and Miller, R. C., 1966. Ampicillin in the Treatment of Chronic Typhoid Carriers. *New England Journal of Medicine*, 274, 807–815.

[15] Suzuki, S. and Hoa, P. T. P., 2012. Distribution of quinolones, sulfonamides, tetracyclines in aquatic environment and antibiotic resistance in Indochina. *Frontiers in Microbiology*, 3, 1–8.

[16] Ung, P., Peng, C., Yuk, S., Tan, R., Ann, V., Miyanaga, K., and Tanji, Y., 2019. Dynamics of bacterial community in Tonle Sap Lake, a large tropical flood-pulse system in Southeast Asia. *Science of the Total Environment*, 664, 414–423.

The 13th AUN/SEED-Net Regional Conference on Chemical Engineering 2020 (RCChE-2020)
Jointly held with
The 5th International Symposium on Conservation and Management of Tropical Lakes
"Insights and Challenges toward Achieving SDGs"

Isolation of Bacteriophages from Water Environment and Their Infectivities on Multidrug Resistant Bacteria

Chakrya Theap[1], Chanthol Peng*[2)], Monychot Tepy Chantho[1], Kazuhiko Miyanaga[3]

[1] *Faculty of Chemical and Food Engineering, Institute of Technology of Cambodia, Russian Federation Blvd., P.O. Box 86, 12156 Phnom Penh, Cambodia*
[2] *Water and Environment Research Unit, Research and Innovation Center, Institute of Technology of Cambodia, Russian Federation Blvd., P.O. Box 86, 12156 Phnom Penh, Cambodia*
[3]*School of Life Science and Technology, Tokyo Institute of Technology, 4259 J2-15 Nagatsuta-cho, Midori-ku, Yokohama, 226-850 1, Japan*
* peng@itc.edu.kh

Abstract

The increasing of antibiotics resistance bacteria becomes a current critical problem which has to be solved as soon as possible. Bacteriophage is found as an alternative treatment to antibiotic to treat the bacterial infection with its high specificity to their host. The seven bacteriophages were screened from wastewater and used to treat with the six resistance strains of Escherichia coli such as *E. coli* 09-02E, *E. coli* E302, *E. coli* papRG-06-5, *E. coli* Mt1B1, *E. coli* STEC711 and *E. coli* ECCRA-119 which were isolated from river water and wastewater in the previous study. The host range of 7 phages were determined by performing spot test with 6 primary hosts which mentioned above, and one phage was eventually selected for further study due to its high infectivity. Phage ΦW1El had the widest host range, producing clear plaques on two hosts, *E. coli* 09-02E and *E. coli* E302. The measurement of optical density at the wavelength of 660 nm (OD660) of ΦW1El treated with both strains was confirmed the infectivity of phage and indicated that phage activity against both strains of bacterial was obtained within 3 h to 9 h. However, the phage began to lyse at 3 h but then the phage-resistant bacteria appeared after 9h.

Keywords: *Escherichia coli; multidrug-resistant bacteria; phage-antibiotic combination; phage therapy; the infectivity of phage*

I. Introduction

The inappropriate use of antibiotics occurred from agricultural and hospitalized were considered as the biggest major of increasing multi-drug resistant bacterial (MDR) [3, 4]. Bacteriophage (phage) was considered as an alternative way to antibiotics [2, 5, 6]. Phages are viruses that can infect and kill bacteria without any negative effect on human or animal cell. The phage pathway involves in several steps including bacteriophage attach to the susceptible host bacterium then infects the bacterial and insert its DNA into bacterial chromosome, assembled the phage protein and then the process of phage lysis is started [2]. By the reason of some antibiotics became less effective, this study aims to isolate phage from aquatic environment and detect their infectivity on multidrug resistance bacteria through their host range and also the phage infection in culturing by

observation of optical density at the wavelength of 660nm.

II. Materials and Methods

2.1. Sampling sites, *E. coli* strains, isolation of bacteriophages

Three different samples were collected from Tonle Sap River, Trabek Chanel and Cheoung Ek Lake. Pure strains *E. coli* k12 and *E. coli* 0157 and the multidrug strains which were isolated from surface water and wastewater were used for phages isolation. Initially, host cell of the bacterial was cultured in 2ml Luria-Bertani (LB) overnight. After getting host cell overnight culture, phage solution had to be diluted by Sodium-magnesium buffer (SM buffer) (5.8g of NaCl, 2.0g of MgSO4, 50ml of 1M Tris-HCl (pH7.5), 0.1g of gelatin and 1L of distilled water). LB soft agar (10g of tryptone, 5g of yeast extract, 5g of NaCl, 5g of agar granule and 1L of distilled water with 5ml of MgSO4 1M, 0.5% (w/v) and 5ml of CaCl2 1M, 05% (w/v)) in the glass tubes were melt by boiling water and cooling down to 45 to 46℃ in heating block. Then, the plaque assay method was conducted. All of the LB plates were incubated at 37℃ upside down overnight. Thus, after overnight incubation, the plaques appeared and individual plaque was picked up by truncated plastic tip then transfer the isolation phage with its host to the 2ml fresh LB medium and then shaking for several hours. After incubation, the solution was centrifuged at 10000×g, 10mn, 4℃ and use the supernatant as an isolated phage solution.

2.2. Phage purification

To obtain the pure phage, different dilution of previous phage solution was used with different host bacterium by repeated plaque assay until getting the uniform plaques and picking a single plaque. After that, 5ml of SM buffer was added directly to the plate surface followed by plate lysate and the PEG [#6000]-NaCl precipitation method (10%(w/v) of PEG [#6000], 4% (w/v) of NaCl) to collect phage.

2.3. Spot test

A spot test method is a quick way to check whether a phage sample can infect a bacterium by dropping a small spot of phage titer onto a plate inoculated with the bacterium. The spot test method was mentioned in [7]. The positive spot test will show up as total pulverization of the whole drop area, whereas a negative spot test will result within the bacterial lawn growing normally in the region of the spot. The lytic ability of phages was considered by the plaques clarity which was observed as clear, turbid, and faint.

2.4. Optical density of bacterial

The effect of phage was observed by using the optical density at the wavelength of 660nm (OD_{660}) measurement. Initially, 60µl of bacterial overnight culture with the concentration of 10^7 CFU/ml was added into glass tube containing 6ml of LB broth and shaking at 120rpm, 37℃ in Bio-shaker. After an hour incubating of bacterial culture, phages concentration was 10^7 PFU/ml were added at the MOI=1 to each glass tubes and the OD was measured every one hour. This process was conducting until 24h.

III. Results and Discussion

3.1. Isolation of bacteriophages from aquatic environment and host range

Phages were screened from three different sources of water such as from surface water and wastewater which resulted in the isolation of lytic phages against *E. coli* K12 and *E. coli* 0157. Phages isolated from three different water samples were tested using plaque method. In an effort to determine the most hopeful applicant for lysis of the widest range of *E. coli* strains, each of the 7 phage types was spotted onto the bacterial lawns. As the result we found only one phage ΦW$_1$El showed high infectivity against 50% of all representative strain of *E. coli* (**Figure 1**). There are only two multidrug resistant strains of *E. coli*, 09-02E, E302 that were able to get infected by ΦW1El. None of the phages were able to produce clear plaques Mt1B1 resistance cell of *E. coli*, although some phages did produce turbid plaques. For multi-drug strain ECCRA-119, only one ΦW2P2 was able to produce turbid plaques. One phage, classified W1EL, produced the clearest plaques on two resistance cells such as *E. coli* 09-02E, *E. coli* E302, and another two pure strains *E. coli* K12 and *E. coli* 0157. To be the most promising candidate, host range and the clarity of plaques which is considered as lytic ability are required. Among of seven phages, there is only one phage, ΦW1EL was found to be the most auspicious candidate. ΦW1EL produced clear

plaques on two resistance strains whereas another six phages only produce turbid plaques are judged as less infection.

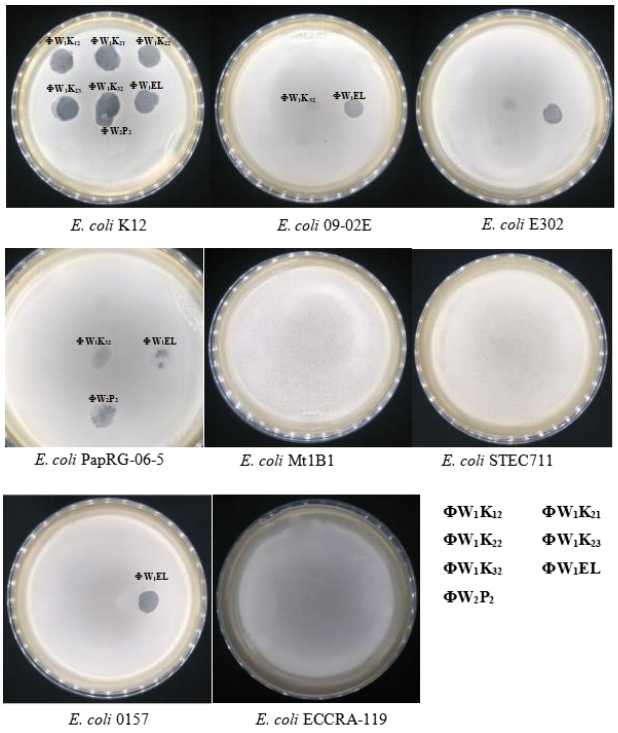

Figure 1. Spot tests for the 7 phages with the widest host ranges and representative *E. coli* lawns in 0.5% agar LB medium. The host bacterial strain is indicated at the bottom of each plate. A key for the phage spots is shown in the bottom right panel.

3.2. Optical density of bacterial

By the reason of phage W1EL which was the only one phage that show the widest host range and much activities against two primary hosts that already mentioned from above, it was considered to choose for the further study. In order to identify the effects of ΦW1El on *E. coli*, each phage was cultured in the LB liquid medium. The reduction in the OD_{660} was considered as a consequence of the lytic activity of a phage on its host. A following decrease in the OD_{660} was considered to be the reduction in the nutrients available as the OD_{660} of the bacterium-only control also declined. The obtained results illustrate that a phage ΦW_1El infect strongly against on two primary hosts, *E. coli* 09-02E and *E. coli* E302 (**Figure 2**). The decreasing of turbidity in bacterial was notified during 3h as the phage began to lyse its host and then the bacterial start steadily recover after 3h. From 3h until 9h, the OD_{660} remained almost steady. After 9h, it was observed that the OD_{660} slightly increase as the number of phage resistant bacteria increased in both strains. However, the four other strains did not show any differences even with or without phage added which means that phage W1EL was not able to infect those bacteria hosts. The increasing of bacterial density might be caused by lysis from without. The lysis from without described an early bacterial lysis induced by high multiplicity virion adsorption and that occurs without phage production simply say, lysis does not depend on phage infection but instead is influenced directly by extracellularly contributed agents [1]. A large amount of phage particles is adsorbed to the host bacterium, the decreasing turbidity of bacterial is considered as phage lysis. Lysis from without is different from normal lysis which occurs at the end of the phage latent period with release of new phage [8].

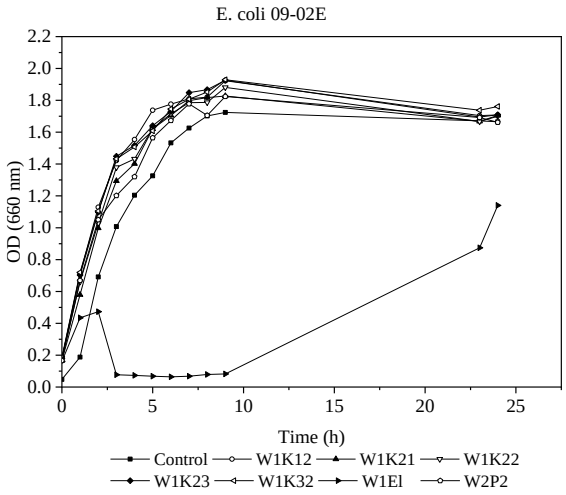

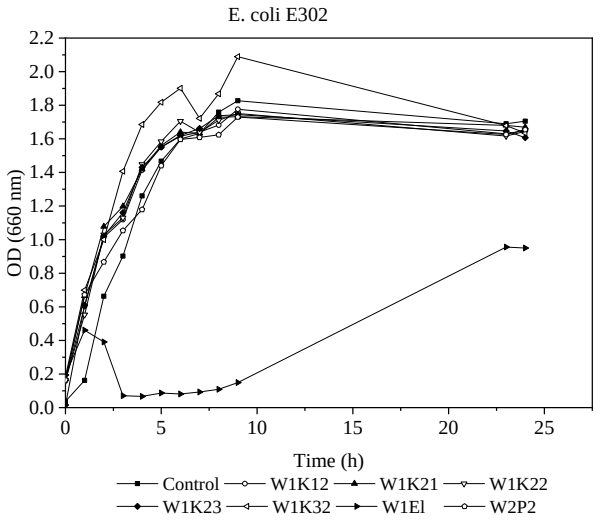

Figure 2. The culture of bacteriophage and *E. coli* resistance strains in LB medium. The bacterial strain was indicated in each graph.

IV. Conclusion

In conclusion, only ΦW1EL showed infectivity on multidrug resistant strains of *E. coli*. However, the infectivity was obtained within 3 h to 9 h. After that, the phage resistant appeared, yet lower than the bacterial control. Therefore, the phage infection with the same concentration of bacterial is not sufficient to use in this case.

Acknowledgement

This research was supported by the Science and Technology Research Partnership for Sustainable Development (SATREPS), the Japan Science and Techonolgy Agency (JST)/Japan Internation Cooperation Agency (JICA) with the grant-number JPMJSA1503.

References

[1] Abedon, S. T., 2011. Lysis from without. *Bacteriophage*, 1, 46–49

[2] Azam, A. H. and Tanji, Y., 2019. Bacteriophage-host arm race: an update on the mechanism of phage resistance in bacteria and revenge of the phage with the perspective for phage therapy. *Applied Microbiology and Biotechnology*, 103, 2121–2131

[3] Cantón, R., Horcajada, J. P., Oliver, A., Garbajosa, P. R., and Vila, J., 2013. Inappropriate use of antibiotics in hospitals: The complex relationship between antibiotic use and antimicrobial resistance. *Enfermedades Infecciosas y Microbiologia Clinica*, 31, 3–11

[4] Khachatourians, G. G., 1998. Agricultural use of antibiotics and the evolution and transfer of antibiotic-resistant bacteria. *Cmaj*, 159, 1129–1136

[5] Lin, D. M., Koskella, B., and Lin, H. C., 2017. Phage therapy: An alternative to antibiotics in the age of multi-drug resistance. *World Journal of Gastrointestinal Pharmacology and Therapeutics*, 8, 162.

[6] Nilsson, A. S., 2019. Pharmacological limitations of phage therapy. *Upsala Journal of Medical Sciences*, 124, 218–227.

[7] Synnott, A. J., Kuang, Y., Kurimoto, M., Yamamichi, K., Iwano, H., and Tanji, Y., 2009. Isolation from sewage influent and characterization of novel Staphylococcus aureus bacteriophages with wide host ranges and potent lytic capabilities. *Applied and Environmental Microbiology,* 75, 4483–4490

[8] Visconti, N., 1953. Resistance to lysis from without in bacteria infected with T2 bacteriophage. *Journal of bacteriology*, 66, 247–253

The 13th AUN/SEED-Net Regional Conference on Chemical Engineering 2020 (RCChE-2020)
Jointly held with
The 5th International Symposium on Conservation and Management of Tropical Lakes
"Insights and Challenges toward Achieving SDGs"

Price Evaluation and Quality Control of Different Soy Sauces Sold in the Markets

Luka LY [1], Monychot Tepy CHANTO[2,3], Chanthol PENG[2,3], Reasmey TAN [2,3*]

[1] *Graduate School, Institute of Technology of Cambodia, Russian Federation Blvd., P.O. Box 86, Phnom Penh, Cambodia.*
[2] *Food Technology and Nutrition Research Unit, Institute of Technology of Cambodia, Russian Federation Blvd., P.O. Box 86, Phnom Penh, Cambodia.*
[3] *Faculty of Chemical and Food Engineering, Institute of Technology of Cambodia, Russian Federation Blvd., P.O. Box 86, Phnom Penh, Cambodia.*
* *rtan@itc.edu.kh*

Abstract

This study is aimed to evaluate the price and quality control of different soy sauces sold in the markets. Four local markets and five supermarkets were selected to survey the price and collecting samples. To analyze the quality of soy sauce, pH, salt content, soluble salt - free solid, reducing sugar, total nitrogen, amino acid nitrogen, halophilic yeast and total bacteria were selected in determining soy sauce quality. As a result, Cambodian soy sauce, Vietnamese, and Thai soy sauce were abundant in the local markets, and Chinese soy sauce, Malaysian soy sauce, Taiwanese and Indonesian soy sauces were found mostly in supermarkets. Within 42 soy sauce brands found, the price was between 400 riel/100mL and 12000 riel/100mL. Within the physiochemical analysis of the 42 soy sauce samples, their pH was between 3.79 to 4.62, Salt was between 4.7 g/100 mL to 23.40 g/100mL, Reducing sugar was between 0.21 g/100 mL and 9.57 g/100 mL, soluble salt-free solid content was between 1.21 g/100mL and 38.65 g/100 mL, Total nitrogen was between 0.08 g/100 mL and 2.2 g/100 mL and Amino acid nitrogen was between 0.01 g/100mL and 1.2 g/100mL. For microbiological quality, there were 3 soy sauces that had the presence of halophilic yeasts and Total plate count was detected in 50% of soy sauces but they were lower than standard limits. By comparing the results in the physicochemical analysis and microbiological quality, there were 11 samples that were within the specifications of Cambodia's national soy sauce standards. For further study, 3-MCPD and the volatile compounds of 42 soy sauces will be analysed.

Keywords: *Soy sauce, brand, Cambodia, physicochemical parameters, microbiological analysis*

I. Introduction

Soy sauce has been a liquid condiment originated from China since approximately 2200 years ago. It is produced by mixing the steamed soybeans with roasted and grided wheat, and Koji mold spores and incubate for 3 to 5 days followed by fermentation in brine for about 3 to 6 months [1]. People in Asian countries such as China, Japan, Korea, Thailand, the Philippines, Indonesia, and more than 90% of Cambodian people consumed soy sauce [2]. Soy sauce is normally used in cooking, such as in soups, frying, roasting, marinating, and also for dipping. It is widely used in the purpose of food, for improving the taste, flavour and aroma, as it is the main source of natural umami taste [3]. Not only that, scientists found that soy sauce also contains bioactive compounds with anticarcinogenic, antimicrobial, antioxidative, and antiplatelet activities [4] and also antiallergenic activity [5]. There are many different soy sauces sold in Cambodia; however, the study of their quality is unknown. The price and quality are essential for attracting the consumers. The main objective of this study was to know the price and quality of soy sauces currently sold in Cambodia's markets by providing awareness to the consumers and providing information to the manufacturers to be more careful with the quality of soy sauce production.

II. Materials and Methods

2.1. Survey of soy sauce price

The survey was conducted in 2 weeks from 26 February to 03 March 2020. Market survey was divided into 2 sections in the local markets and supermarkets around and in the middle of Phnom Penh city. First section was local markets such as Psa Thom Thmey, Samaki, Tu Tum Pung, and Ou Reusey. In local markets, 4 sellers were selected in Psa Thom Thmey, 3 sellers were selected in Psa Samaki, 4 sellers were selected in Psa Tu Tum Pung, and 6 sellers were selected in Psa Ou Reusey. The distance between each seller was 3 to 4 shops. And the second section was in supermarkets such as: Lucky Olympic, Lucky Steung Mean Chey, Aeon I and II, and Macro supermarket. Data were collected by recorded the volume of soy sauce bottles, price and country of production origin.

2.2. Physicochemical analysis of soy sauces

Soy sauce samples were bought from the markets to analyze their physicochemical characteristics. The salt concentration was analysed using salt-meter (Atago model ES-421), pH measurement was analysed by using pH meter (OHAUS, Starter300), soluble salt free solid content and amino nitrogen was analysed as described in GB/T 18186-2000 [14], and total nitrogen was analysed as described in AOAC. (2000) [15] The soy sauce samples were analysed in triplicate and data was represented in the form of mean ± standard deviation (SD). Analysis of variance (ANOVA) with Tukey's test was performed to evaluate significant difference in the physicochemical parameters from different samples, and a significant difference was defined as $p < 0.05$, and one-way ANOVA was conducted using SPSS software.

2.2. Microbiological analysis of soy sauces

Halophile yeasts were cultured by using Potato Dextrose Salt agar. Media was made by weighting 24 g of potato Dextrose Broth powder and 15 g of agar powder together into a 1000 mL bottle with 100g of sodium chloride, then stir and Autoclave 15 minutes at 121 ℃ after autoclaved keep it until 45 ℃ in the water bath and add 10 mL of 10% tartaric acid solution, then media was poured (about 25 to 30 mL) to the plate and keep it until cool, 0.1 mL of soy sauce sample was pipetted to the hard agar media, then a spreader was used to spread the sample over the agar until dried [6]. Plate Count Agar was used to grow and count the total number of aerobic microbial contaminants in samples. 23.5 g of PCA was added and 1000 mL of distilled water, and then stirred until becoming a homogenous solution, sterilized in an autoclave set at 121°C for 15 minutes. Sample was tested 3 times by taking 1 ml of soy sauce diluted with buffer sodium chloride, after that pouring 15-20ml of PCA at 45°C ±1°C into the Petri and put it into the incubator at 36°C ± 1°C for 2 days.

III. Results and Discussion

There are 42 different soy sauce brands that were collected from local markets and supermarkets. Price of each soy sauce brand sold in local markets and supermarkets is shown in **Fig. 1.**. Within a price from 400 riel to 4000 riels per 100 mL in local markets, Cambodian soy sauces were the same price or cheaper than Thai and Vietnamese soy sauces, except the C7 that has high price of 2,000 riels and, there were 38 brands of soy sauces sold in the supermarkets. Soy sauces imported from Japan, Hong Kong, Taiwan, Korea and France can be found in the supermarkets with the high price varying from 550 to 12,000 Riels per 100 mL among soy sauces sold in markets, the price of J2 soy sauce was the highest.

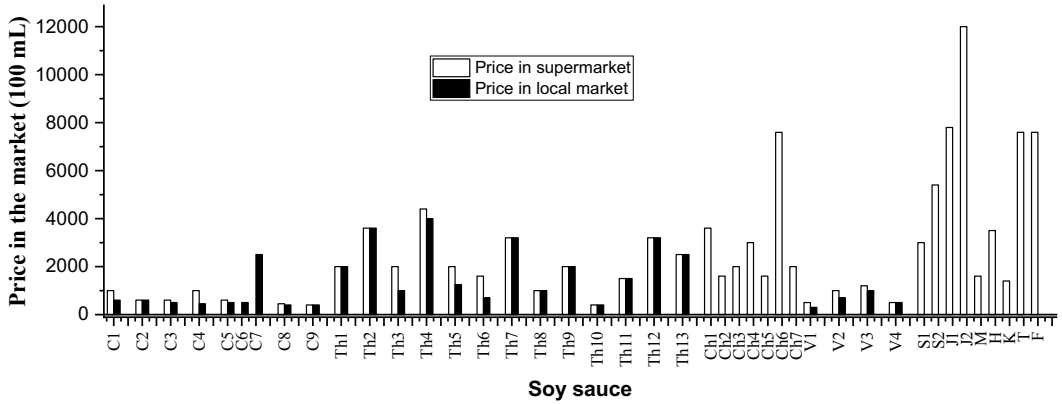

Fig. 1. Price of soy sauce sold in super markets compared with local market, The alphabet codes (C, Th, Ch, V, S, J, M, H,

K, T, and F) are represented: (Cambodia, Thailand, China, Vietnam, Singapore, Japan, Malaysia, Hong Kong, Korea, Taiwan and French), respectively.

According to the institute of standard of Cambodia, soy sauce's pH should be between 4.2 and 4.8 [8]. As shown in **Fig 2.** The pH of the soy sauce samples was between 3.79 ± 0.02 and 4.62 ± 0.01, soy sauce C4, C5, C6, C8, TH3, Ch6, V1, V4 were lower than the standard.

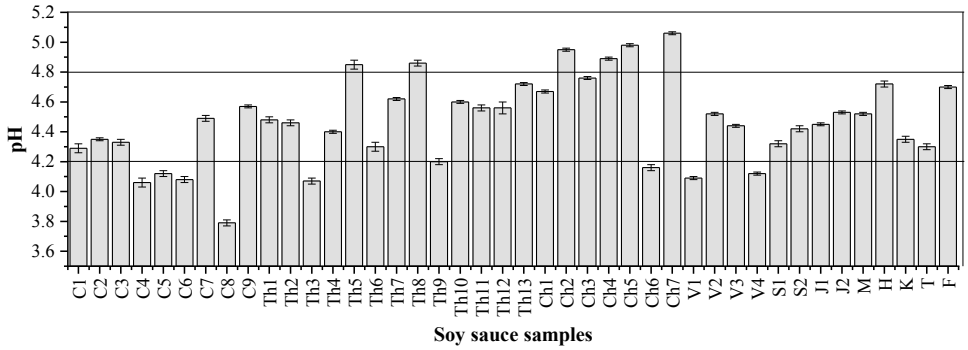

Fig.2. pH of soy sauce samples. The alphabet codes (C, Th, Ch, V, S, J, M, H, K, T, and F) are represented: (Cambodia, Thailand, Vietnam, Singapore, Japan, Malaysia, Hong Kong, Korea, Taiwan and French), respectively.

Salt is an important ingredient used in soy sauce fermentation, a good fermented soy sauce should have 18% to 20% of salt [6]. Out of 42 soy sauce samples, soy sauce code M has a salt content of only 4.7 g/100 mL, with an amount so low, this product needs to add a food preservative to ensure safety and a longer shelf life.

While Ch6 has salt content 23.40 g/100mL this amount is very high over the Cambodian soy sauce standard [8], consumption of too much sodium is not good for the health, especially for someone who suffers from heart disease, hypertension and kidney disease [9]. Based on the national institute of standards of Cambodia, the maximum amount of salt allowed in soy sauce is 20%. Amount of 42 soy sauce samples, there are only 7 soy sauce simples had high amount of salt over 20%. Reducing sugar is very important for making a good taste and quality of soy sauce, and had about 2 to 5% in a good quality of soy sauce [6]. Within 42 soy sauce samples the lowest reducing sugar was found in "C8" has the total amount 0.21 ± 0.01% while the highest of reducing sugars was found in sample "S2" has the total amount 9.57 ± 0.06% by the way there were only 12 samples found in the range of 2 to 5. The lowest amount of soluble salt free solid content was found in "C8" sample (1.21±0.09 g/100mL) while the highest was found in "M" sample (38.65 ± 0.14 g/100ml) the main reason that made sample "M" has the soluble salt free solid greater than other samples it could be from adding sugar [11] and it also described in soy sauce ingredient on soy sauce "M" about the adding of sugar in the ingredient. There are 18 samples having an amount of soluble salt free solid content bigger than 15. According to the Institute of standards of Cambodia, soy sauce was divided into 2 parts, such as dark soy sauce and light soy sauce. Light soy sauce had a soluble salt free solid content about (15 to 18 g/100 mL) and dark soy sauce has soluble salt free solid content about (22 to 44 g/100 mL). Total nitrogen is another parameter indicating the quality in soy sauce [6]. According to the national institute of standards in Cambodia, soy sauce must have at least total nitrogen 0.8%. There are 22 soy sauce samples having the total nitrogen greater than 0.8 g/100mL. Total nitrogen and total amino nitrogen was used as an indicator to show the effect of fermentation too, by the way in sample C8 (0.08 ±0.02 g/100mL) total nitrogen so low it could be from poor fermentation, short period of time or the digestion of soy beans was not done well, moreover this soy sauce could be make from excessive dilution [10]. Amino nitrogen is one of the testing parameters showing us the quality and effective of soy sauce fermentation. Amount of 42 soy sauce samples, there are 23 soy sauces having the amino nitrogen bigger than 0.26 g/ 100 mL, Th13 sample had amino nitrogen 1.18 ± 0.17 (g/100 mL) greater than other samples, by the way "C8" samples had amino nitrogen only 0.01 ± 0.00 (g/100 mL) lower than the other samples. According to institute of standard of Cambodia the amino nitrogen in soy sauce must be equal or bigger than 0.26 g/100 mL [7].

Within the experiments there were 3 samples found having halophilic yeast inside. TH5 has halophilic yeast more than other samples followed by C6 and C2.as shown in **Table 1.** The presence of halophilic yeasts in the samples should be from the lack of hygienic practice in the production,

pasteurize or sterilize not well. The halophile yeasts could deteriorate soy sauce quality; it could be given off an offensive odour and forming the thin pellicle during long term storage [12].

Table 1. Halophilic yeast detected in the soy sauce samples.

Samples	Halophilic yeast colony (CFU/mL)
C2	$1.1\pm 1.00\times10^{2}$
C6	$2.2\pm 2.64\times10^{1}$
Th5	$2.35\pm 8.02\times10^{2}$

Based on the Nation Institute of Standard of soy sauce in Cambodia, Halophilic yeasts much be absence in the soy sauce. According to the nation food safety soy sauce standard in China, the total number of bacterial colony should be lower than 5000 CFU/mL [13]. The highest bacteria grown on "S1" sample about 1.6×10^{3} CFU/mL, all of samples had total bacteria lower than 5×10^{3} CFU/mL or not detected in the samples.

IV. Conclusion

From the market survey on 42 soy sauce samples, the price was between 400 riel/100mL to 12000 riel/100mL, For the physiochemical tests, and microbiological tests, as the results, 11 samples has found to have high quality as shown in Institute of Standard of Cambodia such as one of Cambodia soy sauce (C7), 2 of Thai's soy sauce (Th6, Th12), one of China's soy sauce (Ch3), a Singapore's soy sauce (S2), two of Japan's soy sauce (J1, J2), a Hong Kong's soy sauce (H), a Malaysia's soy sauce (M), a Taiwan's soy sauce (T) and a French's soy sauce (F).

For further research, volatile compounds, 3-MCPD, development of high-quality soy sauce with the benefits for the human health and price competition should be conducted.

Acknowledgements

We would like to acknowledge the Ministry of Education, Youth and Sport for financial support through Higher Education Improvement Project (HEIP) Research Grant.

References

[1] Leboffe, M.J. & Pierce, B.E. (2006). Microbiology: Laboratory Theory and Application, Essentials - Michael J. Leboffe, Burton E. Pierce - Google Bøker. Morton Publishing Company.

[2] Theary, C., Panagides, D., Laillou, A., Vonthanak, S., Kanarath, C., Chhorvann, C., Sambath, P., Sowath, S. & Moench-Pfanner, R. (2013). Fish sauce, soy sauce, and vegetable oil fortification in Cambodia: where do we stand to date? Food Nutr. Bull. 34.

[3] Marcus, J.B. (2019). Flavor Enhancement Ingredients, in: Aging, Nutrition and Taste. Elsevier, pp. 173–206.

[4] Murooka, Y. & Yamshita, M. (2008). Traditional healthful fermented products of Japan. J. Ind. Microbiol. Biotechnol. 35: 791 –798

[5] Kobayashi, M. (2005). Immunological functions of soy sauce: Hypoallergenicity and antiallergic activity of soy sauce. J.

[6] Food and Agriculture Organization, 1984. Manuals of food quality control. 1st ed. Rome, Italy.

[7] Luh, B. S., 1995. Industrial production of soy sauce. Journal of Industrial Microbiology, 14, 467–471.

[8] CS 066:2011. (2012)., Institute of standards of Cambodia., Soy sauce standard**.**

[9] He, F.J., MacGregor, G.A., 2010. Reducing Population Salt Intake Worldwide: From Evidence to Implementation. Prog. Cardiovasc. Dis. 52, 363–382.

[10] Röling, W.F.M., Van Verseveld, H.W., 1996. Characterization of Tetragenococcus halophila populations in Indonesian soy mash (kecap) fermentation. Appl. Environ. Microbiol. 62, 1203–1207.

[11] Garnida, Y., Taufik, Y., 2014. Fermentation in Salt Solution to Produce Jack Beans (Canavalia ensiformis L) SAUCE, International Congress on Challenges of Biotechnological Research in Food and Health. Slamet Riyadi University.

[12] Lee, Y. T.-S., Chu, Y.-H., Shin, B.-K., and and Ju-Hyun, 1975. Study on Preservation of Soy Sauce. , 7, 200–207

[13] GB/T GB 2717-2018. (2000)., Nation standard of the people's republic of china., Soy sauce. Chinese Standard Publishing House.

[14] GB/T 18186-2000. (2000)., Nation standard of the people's republic of china., Fermented soy sauce. Chinese Standard Publishing House.

[15] AOAC. (2000). Official Methods of Analysis 17th Ed., AOAC IN-TERNATIONAL, Gaithersburg, MD, Method 991.20.